frontiers | Research Topics

Microbial roles in caves

Edited by
Valme Jurado, Diana Eleanor Northup and
Cesareo Saiz-Jimenez

Published in
Frontiers in Microbiology

ISSN 1664-8714
ISBN 978-2-8325-5188-2
DOI 10.3389/978-2-8325-5188-2

About Frontiers

Frontiers is more than just an open access publisher of scholarly articles: it is a pioneering approach to the world of academia, radically improving the way scholarly research is managed. The grand vision of Frontiers is a world where all people have an equal opportunity to seek, share and generate knowledge. Frontiers provides immediate and permanent online open access to all its publications, but this alone is not enough to realize our grand goals.

Frontiers journal series

The Frontiers journal series is a multi-tier and interdisciplinary set of open-access, online journals, promising a paradigm shift from the current review, selection and dissemination processes in academic publishing. All Frontiers journals are driven by researchers for researchers; therefore, they constitute a service to the scholarly community. At the same time, the *Frontiers journal series* operates on a revolutionary invention, the tiered publishing system, initially addressing specific communities of scholars, and gradually climbing up to broader public understanding, thus serving the interests of the lay society, too.

Dedication to quality

Each Frontiers article is a landmark of the highest quality, thanks to genuinely collaborative interactions between authors and review editors, who include some of the world's best academicians. Research must be certified by peers before entering a stream of knowledge that may eventually reach the public - and shape society; therefore, Frontiers only applies the most rigorous and unbiased reviews. Frontiers revolutionizes research publishing by freely delivering the most outstanding research, evaluated with no bias from both the academic and social point of view. By applying the most advanced information technologies, Frontiers is catapulting scholarly publishing into a new generation.

What are Frontiers Research Topics?

Frontiers Research Topics are very popular trademarks of the *Frontiers journals series*: they are collections of at least ten articles, all centered on a particular subject. With their unique mix of varied contributions from Original Research to Review Articles, Frontiers Research Topics unify the most influential researchers, the latest key findings and historical advances in a hot research area.

Find out more on how to host your own Frontiers Research Topic or contribute to one as an author by contacting the Frontiers editorial office: frontiersin.org/about/contact

Microbial roles in caves

Topic editors

Valme Jurado — Institute of Natural Resources and Agrobiology of Seville, Spanish National Research Council (CSIC), Spain

Diana Eleanor Northup — University of New Mexico, United States

Cesareo Saiz-Jimenez — Institute of Natural Resources and Agrobiology of Seville, Spanish National Research Council (CSIC), Spain

Citation

Jurado, V., Northup, D. E., Saiz-Jimenez, C., eds. (2024). *Microbial roles in caves*. Lausanne: Frontiers Media SA. doi: 10.3389/978-2-8325-5188-2

Table of contents

frontiers | Frontiers in Microbiology

TYPE Editorial
PUBLISHED 29 May 2024
DOI 10.3389/fmicb.2024.1411535

OPEN ACCESS

EDITED AND REVIEWED BY
Jeanette M. Norton,
Utah State University, United States

*CORRESPONDENCE
Valme Jurado
✉ vjurado@irnase.csic.es
Diana E. Northup
✉ dnorthup@unm.edu
Cesareo Saiz-Jimenez
✉ saiz@irnase.csic.es

RECEIVED 03 April 2024
ACCEPTED 17 May 2024
PUBLISHED 29 May 2024

CITATION
Jurado V, Northup DE and Saiz-Jimenez C (2024) Editorial: Microbial roles in caves. *Front. Microbiol.* 15:1411535. doi: 10.3389/fmicb.2024.1411535

Editorial: Microbial roles in caves

Valme Jurado[1]*, Diana E. Northup[2]* and Cesareo Saiz-Jimenez[1]*

[1]Instituto de Recursos Naturales y Agrobiologia, Consejo Superior de Investigaciones Cientificas (IRNAS-CSIC), Seville, Spain, [2]Department of Biology, University of New Mexico, Albuquerque, NM, United States

KEYWORDS

subsurface microbiology, geomicrobiology, biomineralization, biogeochemical cycles, speleothems, microbiota, *Bacteria*, *Archaea*

Editorial on the Research Topic
Microbial roles in caves

Subsurface ecosystems (caves) are a window into hidden niches of the Earth where microorganisms adapt to live in hostile environmental conditions that could be analogs to Mars, particularly volcanic caves and extremely acidic environments. Caves have attracted the attention of NASA and ESA, as the search for life on other Solar System bodies is a major stimulus for planetary exploration. Thus, cave research is useful in astrobiology for searching/identifying extraterrestrial life.

Some caves show high carbon dioxide and radon concentrations throughout the year. In these cases, caves have been considered extreme environments characterized by harsh environmental conditions and low nutrient inputs where microorganisms are forced to adapt their metabolism to survive in extreme conditions, in which the low input of carbon, nitrogen, and phosphorus, as well as the chemical composition of the rock, has a direct impact on the community diversity.

The colonization of cave rocks and speleothems provides complex communities active in the main biogeochemical cycles of the biosphere. Current research shows that microorganisms are involved in the formation of stalactites, moonmilks, and other mineral formations. However, the interactions of microbes with the air–water–rock interfaces in subterranean ecosystems and the biological mechanisms by which microorganisms adjust to new environments or changes in their current environment are poorly understood.

This Research Topic includes 16 articles that provide some clues to understand the *Microbial roles in caves*, and describes a broad range of microbial activities in subsurface environments.

The global biogeochemical cycles, and particularly the carbon, nitrogen, sulfur, and phosphorus cycles, are essential for life in caves. Zhu et al. discussed in their review the dissolution and deposition of carbonate minerals, the roles of cave microbes in the C, N, S, and Fe cycles, and the production of bioactive compounds and antimicrobials by cave microorganisms. Of particular importance is the involvement of methane-oxidizing bacteria in the consumption of cave methane. Bogdan et al. studied the diversity and distribution of microbial communities in a Romanian cave with low anthropic impact. Interestingly, the cave was largely dominated by the phyla *Pseudomonadota* and *Actinomycetota*, the same phyla frequently found in disturbed caves. A study of the potential functional role of these communities revealed the presence of genes involved in the C and N cycles.

Mondini et al. investigated the total and active prokaryotic and eukaryotic communities of millennium-old ice accumulated in Scarisoara Cave, Romania. The initial microbial community on cave ice was dominated by potentially active *Bacteria*, with a minor presence of *Archaea* and a low relative abundance of *Eukaryota*. Heat shock cycles had a strong impact on the composition of the ice microbiome, leading to important decreases of the relative abundance of *Archaea* and *Eukaryota*, while the bacterial community appeared to be more stable, prevailing in the ice community exposed to temperature fluctuations. The ice community was dominated by copiotrophic taxa that were able to quickly use the carbon sources released after ice thawing, with the *Pseudomonadota* and *Bacteroidota* taxa prevailing after thermal stress. This article offers a glimpse of the environmental impacts of climate change that lead to glacier retreat.

The microbiomes of three types of caves: limestone, sulfidic, and volcanic so far frequently studied were compared by Turrini et al.. These caves have different genesis, rock, and chemical composition which can determine diverse colonization patterns. A literature search identified the most prevalent bacterial taxa and the authors discussed the microbial diversity and their functional roles in the three cave types. Limestone and volcanic caves presented *Pseudomonadota* and *Actinomycetota* as primary colonizers, while sulfidic caves revealed the predominance of sulfur-oxidizing *Campylobacterota*. Good practices in future cave microbiome studies were discussed.

Prescott et al. studied the ecological drivers that structure the diversity and assemblies of the bacterial community in volcanic ecosystems in Hawai'i and compared the oldest lava tubes (500–800 years) to the more variable and extreme conditions of the younger geothermally active caves and fumaroles (<400 years old). Data showed that lava caves and geothermal sites harbor unique microbial communities, with very little overlap between caves or sites. Additionally, older lava tubes hosted greater phylogenetic diversity than geothermally active or younger sites. Most ASVs were not able to be assigned to a named genus or species; therefore, volcanic caves and fumaroles represent underexplored ecosystems. In this context Gonzalez-Pimentel et al. investigated the microbial communities of volcanic caves in La Palma Island (Canary Islands, Spain) and described a new species of *Streptomyces*, *S. benahoarensis*, isolated from two different samples, a speleothem and a microbial mat on the walls of *Fuente de la Canaria* lava tube. The genes predicted involved in antimicrobial mechanisms for resistance and biosynthesis of these two strains emphasized this *Streptomyces* as a biological reservoir for bioactive compounds, both described and not discovered yet.

Castañar Cave (Caceres, Spain) is an extreme environment with very high concentrations of radon (^{222}Rn) in air with an annual average >30 kBq/m^3. In 2008, a vomit caused a fungal outbreak that was initiated by *Mucor circinelloides* and *Neocosmospora solani* and contaminated sediments. The cave sediments were cleaned and visits resumed in 2014. Martin-Pozas et al. analyzed the fungal community in the cave after 12 years of the fungal outbreak and the prevalence and spatio-temporal evolution of the fungi caused by the vomit over the years under the conditions of relative isolation and high radiation that characterize this cave. The occurrence of *N. solani* in all samplings from 2008 to 2020 is notable, as it has been widely reported in relation to outbreaks in other caves. Fungi previously reported in highly radioactive environments were also found in Castañar Cave, but the effect of high ^{222}Rn on these fungi was not conclusive because the diversity was similar to that found in other caves with relatively low concentrations of ^{222}Rn.

Fungal outbreaks also occur in other subsurface environments, as exemplified in the Roman Catacombs. De Leo et al. investigated the sudden fungal outbreak that occurred after 1 year of restoration treatment in the Catacombs of SS. Marcellino and Pietro in Rome (Italy). The restored marble pieces were colonized by a complex fungal biofilm consisting mainly of *Coniophora* sp. and other genera, such as *Hypomyces, Purpureocillium, Acremonium, Penicillium*, and *Alternaria*, many of which are well known for the biodeterioration of stone surfaces. The article features the first finding of a strain of the genus *Coniophora* (order *Boletales*), reported as one of the causes of wood wet-rot decay, in association with the evident phenomena of stone biodeterioration.

Ghezzi et al. reported that Imawarì Yeuta Cave (Venezuela) is composed of 98% silica in the form of α-quartz and minor amounts of amorphous silica. Microbial communities that inhabit caves in quartz-rich rocks are poorly known. A set of 19 biofilm samples in water ponds, quartzite host rocks, sediments and speleothems on pavement, walls, and ceiling at different sites within the cave was classified into three groups according to the water content: <89%, 4%−20% and <1%, and the dominant groups in each case were *Pseudomonadota* (*Gammaproteobacteria*), *Acidobacteriota,* and *Actinobacteriota*, respectively. Oligotrophy probably in association with the geochemistry of silica/quartz low pH buffering activity and alternative energy sources led to colonization of specific silica-associated microorganisms.

Wang et al. hypothesize that microbial communities living in cave rocks vary with zones, and mineral substrates contribute significantly to the variation. To test the hypothesis, the authors collected weathered rock samples from the entrance to the end in the Heshang Cave, China. The rocks were mainly composed of dolomite, calcite, Mg-calcite, quartz, and phosphate minerals (hydroxyapatite and fluorapatite). The bacterial communities were significantly affected by hydroxyapatite, and fluorapatite positively impacted the fungal communities, while the co-occurrence network showed that the bacterial and fungal communities formed a close organization through cooperation among different species. The effect of phosphate-rich deposits on the bacterial community in Muierilor Cave, Romania, was also studied by Haidău et al.. They found genera involved in the P, N, Fe, and Mn cycles, as such elements are usually found in guano, located in the upper level of the cave. Several genera were related to bats and guano, while others were related to humans derived from the impact of visits.

Microbially induced calcite precipitation (MICP) is defined as the formation of carbonate minerals from a solution due to the presence of cells, microbial products, or metabolic activity. Precipitation can be due mainly to modulation of the environmental pH, nucleation sites on cell surfaces, or by the action of enzymatically driven processes involving carbonic anhydrase, urease, etc. Koning et al. studied the MICP potential of cave bacteria isolated from the Iron Curtain Cave in Canada. Ninety-nine bacterial strains were isolated from popcorn and soda straw speleothems. These isolates were screened for urease enzymatic

activity, with 11 candidates found to be positive for urease, including *Sphingobacterium* sp. and *Pseudarthrobacter* sp. which were found to produce the highest crystal production with varying morphologies. *Pseudarthrobacter* sp. encoded a single and complete urease pathway, whereas *Sphingobacterium* sp. showed two urease pathways encoded in the genome, with an unknown gene in the middle of the sequence.

Anglés et al. reported the formation of biospeleothems during the early Holocene in caves from the Uyuni Salar, Bolivia. The caves show bizarre speleothems framed by large fungal buildings (>1 m) covering the older mineralized structures of algae. The abundance and size of the preserved fungal structures suggest that they were sustained by a constant supply of organic matter and stable hydrological activity. The analysis of the lipids recorded in the samples also provided some insight into the paleoenvironmental conditions accompanying the formation of biospeleothems. It is worth noting the appearance of biomarkers from cyanobacteria and eukaryotes. The authors stated that the search for biomarkers in caves can answer questions about the limits of life and allow the recognition of the geochemical signatures of life.

In recent years, much attention has been paid to fungal infections that affect amphibians. Zalar et al. studied the cultivable skin mycobiota of healthy and diseased *Proteus anguinus*, the blind cave salamander, endemic to the Dinaric Karst, Slovenia, one of the priority species of the EU in need of strict protection. Symptomatic animals were colonized by a variety of fungal species, most of them represented by a single isolate, including genera known for their involvement in chromomycosis, phaeohyphomycosis, zygomycosis, and saprolegniosis in amphibians: *Acremonium, Aspergillus, Cladosporium, Exophiala, Fusarium, Mucor, Ochroconis, Phialophora*, *Penicillium*, and *Saprolegnia*. The article represents the first comprehensive report on the cultured skin mycobiome of this unique amphibian in nature and in captivity, with an emphasis on potentially pathogenic fungi and oomycetes.

Diverse gut bacteria are potentially involved in many physiological processes of insects, which contribute to the adaptation of host insects to the environment. Dong et al. studied the gut microbiota of the orthopteran *Diestrammena japanica*, a keystone species in the karst cave in China, and reported that individuals of different light strengths along the cave exhibit different morphological features. The gut bacteria of *D. japonica* exhibit low diversity but strong cooperation interactions in the dark region. These results indicated that intestinal bacteria may help *D. japanica* adapt to the poor nutrient cave environment.

Electrical lighting enhances the growth of photosynthetic communities known as lampenflora in cave entrances and speleothems. Djebaili et al. screened the cyanobacteria isolated from green biofilms in Stiffe caves, Italy, for the production of poly-β-hydroxybutyrate (PHB). The high production of PHB could be related to the lack of light for an extended period of closure in caves linked to COVID-19, as the accumulation of PHB allows coping with unfavorable environmental conditions.

This selection of articles should be viewed as a snapshot of the multiple biogeochemical processes and provide evidence that microbes play significant roles in caves.

Author contributions

VJ: Writing—original draft, Writing—review & editing. DN: Writing—original draft, Writing—review & editing. CS-J: Writing—original draft, Writing—review & editing.

Funding

The author(s) declare financial support was received for the research, authorship, and/or publication of this article. VJ and CS-J were supported by the Spanish Ministry of Science and Innovation through project PID2020-114978 GB-I00.

Acknowledgments

This is a contribution from CSIC Interdisciplinary Thematic Platform Open Heritage: Research and Society (PTI-PAIS).

Conflict of interest

The authors declare that the research was conducted in the absence of any commercial or financial relationships that could be construed as a potential conflict of interest.

Publisher's note

frontiers in Microbiology

ORIGINAL RESEARCH
published: 10 March 2022
doi: 10.3389/fmicb.2021.809076

Heat Shock Response of the Active Microbiome From Perennial Cave Ice

Antonio Mondini[1†], Muhammad Zohaib Anwar[2,3†], Lea Ellegaard-Jensen[2], Paris Lavin[4,5], Carsten Suhr Jacobsen[2] and Cristina Purcarea[1]*

[1] Department of Microbiology, Institute of Biology, Bucharest, Romania, [2] Department of Environmental Science, Aarhus University, RISØ Campus, Roskilde, Denmark, [3] Center for Infectious Disease Genomics and One Health, Faculty of Health Sciences, Simon Fraser University, Burnaby, BC, Canada, [4] Centre of Biotechnology and Bioengineering (CeBiB), Universidad de Antofagasta, Antofagasta, Chile, [5] Departamento de Biotecnología, Facultad de Ciencias del Mar y Recursos Biológicos, Universidad de Antofagasta, Antofagasta, Chile

OPEN ACCESS

Edited by:
Julia Kleinteich, Bundesanstalt für Gewässerkunde (BFG), Germany

Reviewed by:
Dongwei Hou, Sun Yat-sen University, China
Marika Pellegrini, University of L'Aquila, Italy
Cesareo Saiz-Jimenez, Institute of Natural Resources and Agrobiology of Seville, Spanish National Research Council (CSIC), Spain

***Correspondence:**
Cristina Purcarea
cristina.purcarea@ibiol.ro

[†] These authors have contributed equally to this work

Specialty section:
This article was submitted to Extreme Microbiology, a section of the journal Frontiers in Microbiology

Received: *04 November 2021*
Accepted: *28 December 2021*
Published: *10 March 2022*

Citation:
Mondini A, Anwar MZ, Ellegaard-Jensen L, Lavin P, Jacobsen CS and Purcarea C (2022) Heat Shock Response of the Active Microbiome From Perennial Cave Ice. Front. Microbiol. 12:809076. doi: 10.3389/fmicb.2021.809076

Ice caves constitute the newly investigated frozen and secluded model habitats for evaluating the resilience of ice-entrapped microbiomes in response to climate changes. This survey identified the total and active prokaryotic and eukaryotic communities from millennium-old ice accumulated in Scarisoara cave (Romania) using Illumina shotgun sequencing of the ribosomal RNA (rRNA) and messenger RNA (mRNA)-based functional analysis of the metatranscriptome. Also, the response of active microbiome to heat shock treatment mimicking the environmental shift during ice melting was evaluated at both the taxonomic and metabolic levels. The putatively active microbial community was dominated by bacterial taxa belonging to Proteobacteria and Bacteroidetes, which are highly resilient to thermal variations, while the scarcely present archaea belonging to Methanomicrobia was majorly affected by heat shock. Among eukaryotes, the fungal rRNA community was shared between the resilient Chytridiomycota and Blastocladiomycota, and the more sensitive Ascomycota and Basidiomycota taxa. A complex microeukaryotic community highly represented by Tardigrada and Rotifera (Metazoa), Ciliophora and Cercozoa (Protozoa), and Chlorophyta (Plantae) was evidenced for the first time in this habitat. This community showed a quick reaction to heat shock, followed by a partial recovery after prolonged incubation at 4°C due to possible predation processes on the prokaryotic cluster. Analysis of mRNA differential gene expression revealed the presence of an active microbiome in the perennial ice from the Scarisoara cave and associated molecular mechanisms for coping with temperature variations by the upregulation of genes involved in enzyme recovery, energy storage, carbon and nitrogen regulation, and cell motility. This first report on the active microbiome embedded in perennial ice from caves and its response to temperature stress provided a glimpse into the impact of glaciers melting and the resilience mechanisms in this habitat, contributing to the knowledge on the functional role of active microbes in frozen environments and their response to climatic changes.

Keywords: ice caves, metatranscriptome, heat-shock response, active microbiome, microbial resilience, bioinformatics, meta-omics

INTRODUCTION

Ice can be considered as a storage matrix for microorganisms, representing a source of genomic diversity and a reservoir of new microbial species (Priscu et al., 1998; Miteva et al., 2009; Anesio and Laybourn-Parry, 2012; Anesio et al., 2017; Zhong et al., 2021). Recently, investigations of the microbial communities from a series of frozen environments have been performed, including permafrost (Schostag et al., 2019), Antarctic ice sheets (Abyzov et al., 2005; Weisleitner et al., 2019), Arctic ice (Ma et al., 2000), sea ice (Deming, 2002; Nichols, 2005), mountain glaciers (Garcia-Lopez et al., 2021), and subglacial lakes (Rogers et al., 2013). Meanwhile, very limited data regarding the microbiome embedded in perennial ice deposits accumulated in caves are available to help understand the resilience and ecological role of microbial communities from these secluded underground frozen habitats (Purcarea, 2018).

The Scarisoara ice cave (Romania) harbors the oldest and largest perennial ice block accumulated in a cave worldwide (Holmlund et al., 2005), representing a model habitat for studying paleoclimate processes (Perşoiu et al., 2011, 2017; Persoiu and Pazdur, 2011; Perşoiu and Onac, 2012; Rimbu et al., 2012) and the role and response to environmental stress factors of microbiomes preserved in underground ice from caves (Purcarea, 2018). The presence of ice-contained microorganisms in Scarisoara cave was first mentioned in the ice stalagmites formed in the Little Reserve area (Hillebrand-Voiculescu et al., 2013), followed by studies of the cultured/uncultured microbial communities from the perennial ice block (Hillebrand-Voiculescu et al., 2015) and the chronological distribution of cultured bacteria in ice layers up to 900 years old (Itcus et al., 2016). A series of psychrotrophic and psychrophilic bacterial strains were isolated from the 13,000-year-old ice core of this cave, confirming the microbial viability in this old icy habitat (Paun et al., 2021). Although the culturing method provided a step forward in microbial screening, scientists became aware of the limitations of culture-dependent techniques due to microbial uncultivability in describing the diversity of microbiomes (Hug et al., 2016). To overcome this problem, studies were conducted using denaturing gradient gel electrophoresis (DGGE) to unravel fungal diversity (Brad et al., 2018), while a more advanced sequence identification was achieved with the application of molecular techniques, including 454 pyrosequencing of the prokaryotic community (Itcus et al., 2018) and Illumina sequencing of the fungal communities along the 1,500-year-old ice based on ITS2 Illumina sequencing (Mondini et al., 2018).

These reports based on DNA sequencing provided information on the total communities, while no data on the metabolically active microbiome from this habitat have been provided so far. Recently, the total and potentially active bacterial communities from a 13,000-year-old ice core from Scarisoara have been determined using 16S ribosomal RNA (rRNA) Illumina sequencing (Paun et al., 2019), suggesting the existence of an active microbial community in this habitat. In this context, the current study focused on investigating the active microbiome from the Scarisoara cave ice using RNA Illumina shotgun sequencing and metatranscriptomic analysis of the total and active prokaryotic and eukaryotic microbial communities. Ice sample 900-O, previously collected from a sediment-rich ice layer accumulated 900 years ago in Scarisoara cave (Persoiu and Pazdur, 2011; Itcus et al., 2016), was selected considering the high diversity of prokaryotic and uncultured fungal communities found in this cave ice deposit (Itcus et al., 2018; Mondini et al., 2018).

Although reports on metatranscriptomes from frozen habitats revealed the presence of active microorganisms in ice (Rogers et al., 2013), the occurrence of an active microbiome in perennial ice from caves and its taxonomic and functional profiles are still unknown. Also, studies of the heat shock response of microbiomes from cold environments have been limited to soil (Schostag et al., 2019), while the mechanisms of coping with temperature shifts in the case of microbial communities from ice habitats are still not investigated.

In this context, the current survey represents the first investigation unraveling active prokaryotic and eukaryotic microbial communities in millennium-old underground perennial ice accumulated from caves based on total RNA [rRNA and messenger RAN (mRNA)] Illumina sequencing. Moreover, our data report the changes occurring at the taxonomic and metabolic levels in the total and active microbial communities in response to a 3-day cycle treatment followed by incubation at 4°C up to 14 days, which were done in order to understand the impact of glacier melting on the ice-embedded microbiome.

MATERIALS AND METHODS

Site Description and Ice Sample Collection

The Scarisoara ice cave located in the Apuseni Mountains (NW Romania) (**Figure 1A**) harbors one of the largest and oldest underground perennial ice blocks, ^{14}C-dated to more than 10,500 years before present (BP) (Holmlund et al., 2005; Hubbard, 2017). The particular climate of the cave due to local temperate conditions and the large size of the entrance (**Figure 1B**) ensure underground constant negative temperatures, thus favoring the formation of a stable ice deposit (Racovita and Onac, 2000; Rimbu et al., 2012). The accumulated ice resulted from the annual freezing of precipitation and infiltration water constitute the alternating ice layers of organic-rich and clear ice deposits, with recent strata forming the floor of the Great Hall area and with an exposed side wall of up to 1,000 years BP ice in the Little Reserve sector (**Figure 1C**).

Previously (Hillebrand-Voiculescu et al., 2015; Itcus et al., 2016), ice samples of different ages were collected from the surface and side wall areas of the cave ice block to investigate the microbial diversity from this habitat. Among these, ice samples collected from the 900-year-old layer of high organic sediment content (Itcus et al., 2016) were used in this study (sample 900-O). The samples were obtained from the ice block side in the Little Reserve area (**Figure 1C**) by horizontal drilling using a modified PICO electric drill (Koci and Kuivinen, 1984) manufactured by Heavy Duties S.R.L (Cluj Napoca, Romania). Ice collection was carried out under aseptic conditions using 5-s flame sterilization

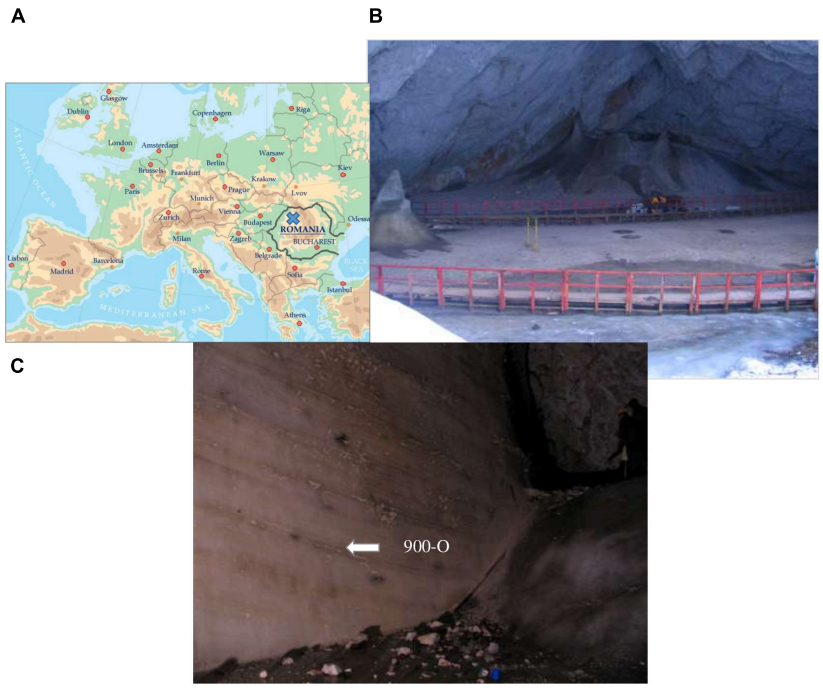

FIGURE 1 | Scarisoara ice cave. **(A)** Map of the cave location. **(B)** The Great Hall area (photo by C. Purcarea). **(C)** The Little Reserve area (photo by C. Purcarea).

of the auger and ice block surface before each step. The ice was harvested under aseptic conditions in 1-L sterile flasks, transported under stable frozen state monitored by an H-B Durac Bluetooth thermometer data logger (Sigma-Aldrich, Steinheim, Germany), and stored at −20°C until use (Itcus et al., 2016).

Heat Shock Experimental Design

The combined cave ice core samples were transferred in a 20-L autoclaved glass bottle under aseptic conditions using a microbiological biosafety cabinet to avoid contamination. After slow thawing at 4°C, the melted ice was equally distributed (1.7 L per sample) in 12 sterile 5-L bottles and submitted to thermal treatment (**Figure 2**). The process comprised three daily heat shock steps at 25°C for 8 h, followed by 16 h at 4°C and subsequent incubation at 4°C up to 14 days. Melted ice samples were analyzed prior to incubation (T0) and at 3 days (T3), 7 days (T7), and 14 days (T14) post-thermal stress (**Figure 2**). Three replicates were used for each analyzed step. In addition, a triplicate control was used by incubation of melted ice at 4°C for 14 days in the absence of thermal shock. After each step, the cells were collected by filtration and used for total RNA extraction.

RNA Extraction, cDNA Library Preparation, and Illumina Shotgun Sequencing

The protocol for the preparation of RNA extraction and complementary DNA (cDNA) Illumina shotgun libraries (Mondini et al., 2019) was adapted from Schostag et al. (2019) and Bang-Andreasen et al. (2020). Triplicate ice samples were submitted to heat shock treatment and analyzed. After each heat shock step, the microbial cells from individual treated ice samples were immediately collected under aseptic conditions using a vacuum-driven stainless steel filtering system (Merck Millipore, Darmstadt, Germany) and sterile 0.22-μm microfiltration (MF) membranes (Merck Millipore, Darmstadt, Germany). Filters containing microbial biomass were placed in 15-mL sterile tubes with 2 ml G2 DNA/RNA Enhancer (Ampliqon, Odense, Denmark) and snap frozen for 15 s in liquid nitrogen. Total RNA extraction was carried out for each triplicate of the T0, T3, T7, and T14 samples using the RNeasy® PowerSoil® Total RNA Kit (Qiagen, Valencia, CA, United States) according to the manufacturer's protocol. DNA contaminants were removed from the resulted RNA (50 μl) with the DNeasy Max® Kit (Qiagen, Valencia, CA, United States), and the purity and yield were determined by fluorometry using a Qubit 2.0 (Thermo Fisher Scientific, Roskilde, Denmark) in the presence of a Qubit DNA HS Assay Kit (Thermo Fisher Scientific, Roskilde, Denmark) and Qubit RNA HS Assay Kit, respectively. The RNA integrity number (RIN) was determined using a Bioanalyzer 2100 (Agilent Technologies, Glostrup, Denmark).

To perform the Illumina shotgun sequencing, a specific cDNA library was prepared for each of the 12 samples using 100 ng RNA and the NEBNext® Ultra II Directional RNA Library Prep Kit for Illumina® (New England Biolabs, Frankfurt am Main, Germany). The subsequent indexing process was carried out using the NEBNext Multiplex Oligos for Illumina and Index Primers Set 1 and the final cDNA library then purified using Sample Purification Beads (both from New England Biolabs, Frankfurt am Main, Germany). All the reactions were performed

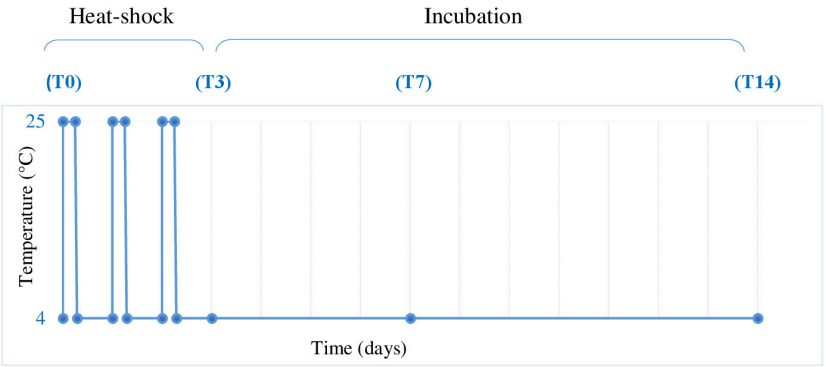

FIGURE 2 | Heat shock experimental design. Melted ice samples stored at 4°C were submitted to 3 daily heat shock cycles (4–25°C) by incubation at 25°C for 8 h, followed by 4°C for 16 h and further incubation at 4°C for up to 14 days. The samples were collected before heat shock treatment (T0) and after 72 h (3 days, T3), 168 h (7 days, T7), and 336 h (14 days, T14), in triplicate, and analyzed as described in Section "Materials and Methods."

according to the manufacturer's protocol in a dedicated PCR clean room. The cDNA library was quantified using a Qubit 2.0 spectrophotometer (Thermo Fisher Scientific, Roskilde, Denmark) and Qubit DNA HS Assay Kit (Qubit, New York, NY, United States). Library quantification was carried out using the KAPA Biosystems Library Quantification Kit for Illumina® Platforms (Merck, Søborg, Denmark) performing a series of 10-fold dilutions according to the manufacturer's instructions. The final library quality control (QC) and the fragment size distribution were assessed using an Agilent Bioanalyzer 2100 and DNA Chips (Agilent Technologies, Glostrup, Denmark).

The resulting equimolar metatranscriptomic libraries obtained from each T0, T3, T7, and T14 triplicate were pooled and sequenced (150 bp paired-end) using a NextSeq 500/550 high-throughput kit v2.5 and the Illumina NextSeq platform (both from Illumina, San Diego, CA, United States) at the Department of Environmental Sciences, Aarhus University, Denmark.

Bioinformatics and Statistical Analyses

The generated Illumina sequences (see *Data Availability Statement* for access code) were processed to assess the bioinformatics quality control and downstream analysis. Adapters and reads with an average quality score less than q20 and shorter than 60 bp were filtered using fastp (Chen et al., 2018). Reads were then sorted into small subunit (SSU) rRNA, large subunit (LSU) rRNA, and non-rRNA sequences using SortMeRNA v.2.1 (Kopylova et al., 2012).

SSU rRNA sequences were assembled into longer SSU rRNA contigs using MetaRib (Xue et al., 2020). Contigs were taxonomically classified using CREST (Lanzén et al., 2012), and the rRNA reads were mapped to the resulting MetaRib contigs using BWA (Li and Durbin, 2009), as performed in Bang-Andreasen et al. (2020), resulting in a table of taxonomically annotated read abundance across samples. In the case of the T3-3 sample (**Table 1**), the number of QC-rRNA reads was low (<10%), thus inconclusive for taxonomic assignment. Consequently, the metatranscriptome of this heat shock step was further represented only by duplicate samples.

CoMW (Anwar et al., 2019a,b) was used on a combined pool of non-ribosomal sequences from all samples. It uses trinity v.2.0.6 (Grabherr et al., 2011) for *de novo* assembly. CoMW filters non-coding RNA from the assembled contigs by aligning contigs to the Rfam database v.12.0 (Griffiths-Jones et al., 2003) with a significant *e*-value threshold of $<10^{-3}$. CoMW also normalizes the contigs by removing those with relative expression lower than 1 out of the number of sequences in the dataset with the least number of sequences. The remaining contigs were then aligned against the M5nr protein database (Williams et al., 2013) and annotated using eggNOG annotation. Contigs were also aligned against specialist databases such as the Carbohydrate–Active Enzymes (CAZy) database (Cantarel et al., 2009) and the nitrogen cycling genes database (NCycDB) (Tu et al., 2019) to assess specific functions. Using CoMW, all alignments were filtered by keeping hits with a minimum *e*-value of 10^{-5} as the threshold. The scores indicated the abundance of number of reads from each sample assigned to groups of different functional genes from each database.

To identify the genes from eggNOG, CAZy, and NCycDB, gene families or functional subsystems that were significantly differentially expressed at different heat shock times, the DESeq2 (Love et al., 2014) module of the SarTools pipeline (Varet et al., 2016) was deployed using parametric mean–variance and independent filtering of false discoveries with the Benjamini–Hochberg procedure ($p > 0.05$) to adjust for type 1 error.

RESULTS AND DISCUSSION

Community Composition and Thermal Response of the Potentially Active (rRNA) Ice Microbiome From Scarisoara Cave

Illumina shotgun sequencing of the total rRNA extracted from the untreated and thermal-treated cave ice microbiome generated a total of 414,992,189 paired-end reads assigned to potentially active bacterial, archaeal, and eukaryotic taxa.

TABLE 1 | Paired-end read number and percentage of taxonomically assigned rRNA sequences from the Scarisoara ice microbiome submitted to heat shock.

Sample	Kingdom	Phyla	Class	Order	Family	Genus	Species
Prokaryotes (paired-end reads)							
T0-1	26,708,245	26,703,774	26,580,617	26,160,037	25,175,013	15,372,387	232,719
T0-2	27,836,047	27,831,490	27,705,786	27,265,799	26,228,364	16,033,779	236,871
T0-3	23,651,606	23,647,680	23,542,953	23,190,627	22,316,316	13,650,325	205,351
T3-1	28,282,664	28,282,278	28,213,325	28,011,200	27,349,501	15,875,298	250,887
T3-2	30,048,507	30,047,903	29,974,055	29,773,531	29,049,227	16,525,904	259,987
T7-1	28,597,318	28,596,970	28,524,035	28,237,593	27,581,953	15,576,993	275,193
T7-2	29,166,257	29,165,875	29,096,425	28,797,811	28,144,191	15,880,847	276,760
T7-3	28,056,523	28,056,226	27,986,377	27,828,392	27,184,407	14,488,376	234,245
T14-1	29,164,367	29,163,781	29,050,244	28,743,795	28,039,857	14,320,030	225,376
T14-2	23,308,066	23,307,516	23,252,628	23,055,747	22,457,392	11,849,106	176,860
T14-3	26,724,309	26,724,094	26,663,320	26,535,498	25,894,839	12,242,956	202289
Total	301,543,909	301,527,587	300,589,765	297,600,030	289,421,060	161,816,001	2,576,538
%	100	99.99	99.68	98.69	95.97	53.66	0.85
Eukaryotes (paired-end reads)							
T0-1	763,980	760,414	737,076	479,751	274,840	251,622	24,239
T0-2	871,593	866,740	831,435	502,818	272,033	245,268	26,419
T0-3	526,254	523,460	506,911	307,312	170,213	154,424	17,606
T3-1	86,733	86,430	81,668	75,446	39,425	32,040	6,868
T3-2	100,642	100,308	95,297	83,791	42,895	37,103	6,748
T7-1	275,448	275,341	251,498	247,971	92,595	56,769	6,426
T7-2	159,704	159,636	151,830	149,714	48,531	30,998	9,126
T7-3	555,313	555,133	545,029	534,363	102,128	91,387	23,573
T14-1	1,883,481	1,883,239	1,792,711	1,764,124	412,826	348,384	109,120
T14-2	985,865	985,791	911,617	895,093	235,039	205,225	47,561
T14-3	1,740,762	1,740,618	1,711,716	1,677,803	333,685	309,978	58,931
Total	7,949,775	7,937,110	7,616,788	6,718,186	2,024,210	1763,198	33,6617
%	100	99.84	95.81	84.5	25.46	22.17	4.23

Taxonomic assignment of the putatively active microbiome from the cave ice deposit (**Table 1**) led to the identification of a complex prokaryotic community composed of 42 bacterial phyla assigned to 103 classes and 182 orders, and 4 classes belonging to 1 archaeal phylum, in addition to a diverse eukaryotic community composed of 46 phyla, 76 classes, and 80 orders. The rRNA reads after each thermal treatment step could be assigned to a large extent to order (98.69%) and family (95.97%) ranks for prokaryotes and to class (95.81%) for eukaryotes, while only 0.85 and 4.23% of the corresponding communities could be identified at the species level (**Table 1**). Therefore, the profile variations of the heat-exposed ice microbiome were evaluated at the subsequent high taxon levels.

The initial cave ice microbial community (T0) was dominated by potentially active Bacteria (95.66 ± 0.76%), with a minor presence of Archaea (0.18 ± 0.02%) and low relative abundance of Eukarya (4.16 ± 0.43%) representatives (**Table 2**).

Application of the heat shock cycles (T3) had a strong impact on the composition of the ice microbiome, leading to 9- and 8-fold decreases of the relative abundance of Archaea (0.02%) and eukaryotes (0.53 ± 0.02%), respectively, while the bacterial community appeared more stable prevailing (99.45 ± 0.02%) in the ice community exposed to temperature fluctuations (**Table 2**). Among the microbial eukaryotes, the strongest decline (12.5-fold) was observed in the case of the Metazoa taxon (from 0.25 to 0.02%). Thermal shock also induced an 8-fold decrease in relative content of both fungal

TABLE 2 | Microbiome composition of the 900-O ice sample from the Scarisoara ice cave submitted to heat shock resulted from rRNA Illumina shotgun sequencing.

	Relative abundance (%)			
	T0	T3	T7	T14
Bacteria	95.66 ± 0.76	99.45 ± 0.02	98.68 ± 0.71	94.49 ± 1.17
Archaea	0.18 ± 0.02	0.02 ± 0.00	0.01 ± 0.00	0.02 ± 0.01
Eukaryotes	4.16 ± 0.43	0.53 ± 0.02	1.40 ± 0.72	5.49 ± 1.17
Algae	0.97 ± 0.20	0.07 ± 0.00	0.92 ± 0.69	4.58 ± 1.17
Metazoa	0.26 ± 0.10	0.05 ± 0.02	0.01 ± 0.01	0.01 ± 0.01
Fungi	0.24 ± 0.11	0.041 ± 0.00	0.02 ± 0.01	0.03 ± 0.01
Plantae	1.27 ± 0.23	0.19 ± 0.00	0.18 ± 0.01	0.22 ± 0.03
Protista	0.78 ± 0.12	0.15 ± 0.01	0.17 ± 0.01	0.63 ± 0.22
Protozoa	0.02 ± 0.00	0.01 ± 0.00	0.002 ± 0.00	0.005 ± 0.00

Relative abundance was calculated based on the number of paired-end reads of the rRNA Illumina shotgun sequences of the untreated 900-O ice sample (T0), after 3-day heat shock treatment (T3), and after 7 days (T7) and 14 days (T14) incubation, as described in Section "Materials and Methods." The average and standard deviation values were calculated for triplicate samples.

(from 0.23 to 0.03%) and protozoan (from 0.8 to 0.01%) communities (**Table 2**).

Further incubation at 4°C for 2 weeks led to a partial recovery of the eukaryotic community, with relative content increases of up to 1.40 ± 0.72% (T7) and 5.49 ± 1.17% (T14) (**Table 2**). This trend appeared to be related to a slight decrease of bacterial presence after 7 days (98.68%) and 14 days (94.49%) incubation at 4°C post-treatment. Meanwhile, the composition of the archaeal taxon was very little affected, up to a relative abundance varying from 0.01% (T7) to 0.05 ± 0.01% (T14).

Overall, the response of the ice microbiome to heat shock treatment indicated a high resilience and a faster recovery of the bacterial taxon compared to the archaeal and eukaryotic taxa (**Table 2**).

Heat Shock Response of the Ice Prokaryotic Community

Microbial composition at the phylum level of the untreated (T0) cave ice potentially active (rRNA) bacteria indicated the presence of 53% Proteobacteria, 17.4% Chlorobi, 10.8% Actinobacteria, 8% Bacteroidetes, and 5% Firmicutes (**Figure 3A**). The higher relative abundance of Actinobacteria and the equal representation of Proteobacteria and Firmicutes in the 900-O ice sample compared to the ice core millennium-old strata (Paun et al., 2019) could be due to the different locations of the samples in the ice block. Major changes in the prokaryotic community composition were observed after the heat shock step (T3), resulting in a relative content decrease of Firmicutes by 10-fold (from 5 to 0.5%), Actinobacteria by 5-fold (from 10.6 to 2.6%), and Chlorobi by 5-fold (from 10.6 to 2.6%), while the representation of Proteobacteria and Bacteroidetes increased up to 71 and 27%, respectively (**Figure 3A**). A reduced effect was further observed after incubation at 4°C (T7 and T14), with a slight increase for Proteobacteria of up to 80%, whereas Bacteroidetes content showed a moderate decline to 15% after prolonged incubation (**Figure 3A**).

At the class level, Proteobacteria was mostly represented by Betaproteobacteria (68%), also containing Alphaproteobacteria (18%), Gammaproteobacteria (10%), and Deltaproteobacteria (3%) prior to heat shock exposure (T0) (**Figure 3B**). Within the Proteobacteria group, heat shock (T3) shaped the community by

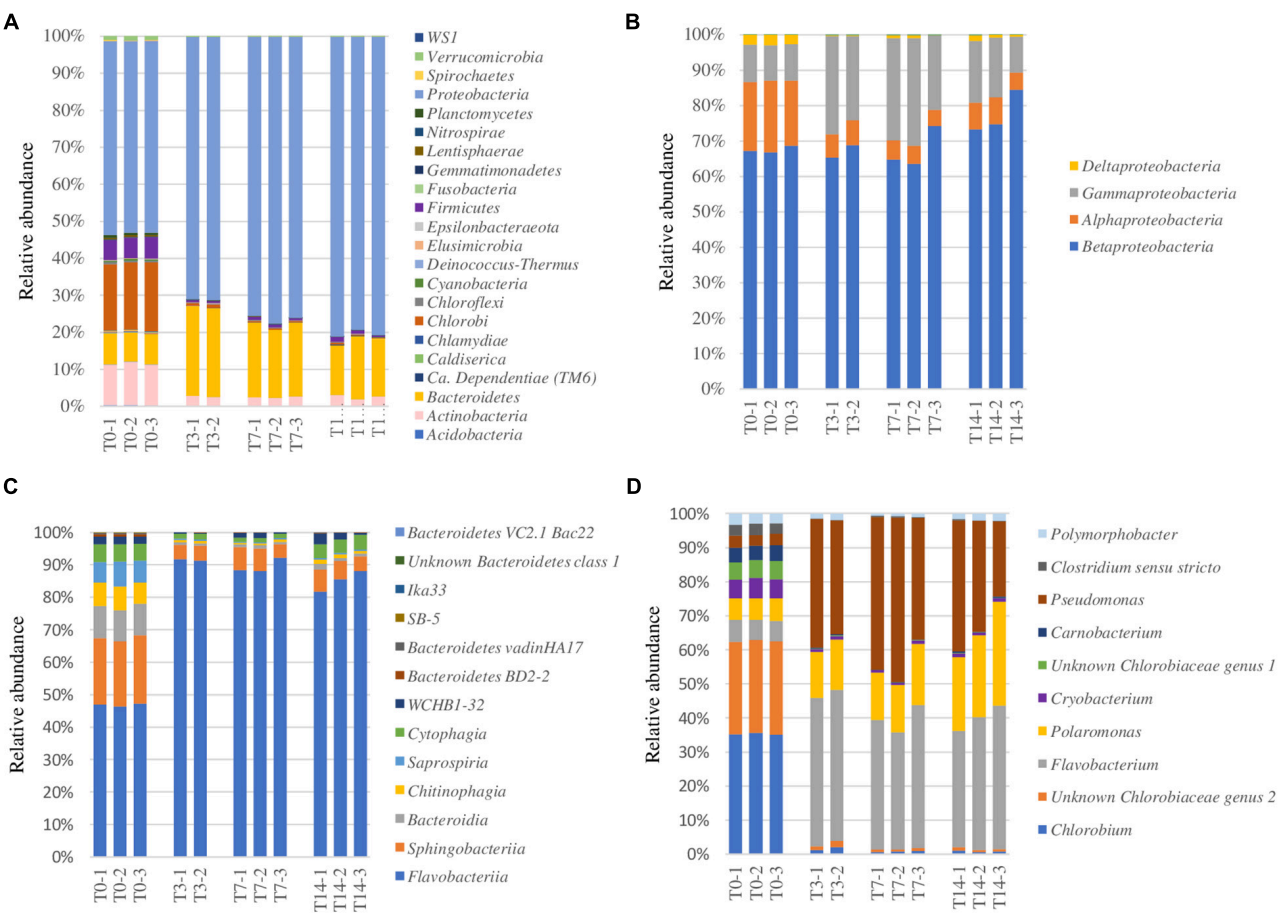

FIGURE 3 | Heat shock effect on the potentially active bacterial taxa (rRNA) from the 900-O cave ice sample. **(A–D)** Relative abundance of bacterial phyla **(A)**, Proteobacteria classes **(B)**, Bacteroidetes classes **(C)**, and the most abundant 10 genera **(D)** of the ice microbiome before heat shock (*T0*) and after 3 days (*T3*), 7 days (*T7*), and 14 days (*T14*) of thermal treatments indicating variations in the bacterial community structure at specified taxonomic levels.

reducing the content of Alphaproteobacteria (6%) and increasing that of Gammaproteobacteria (25%), while maintaining an invariable (65%) Betaproteobacteria relative abundance. Prolonged incubation led to an increase of Betaproteobacteria (75%) alongside a reduction of Gammaproteobacteria (16%) and a slight increase in Alphaproteobacteria (7%) representation (**Figure 3B**).

The primarily represented classes of phylum Bacteroidetes (**Figure 3C**) from the untreated ice microbiome (T0) were Flavobacteriia (47%) and Sphingobacteriia (20%), with important representation of Bacteroidia (10%), Chitinophagia (8%), Saprospiria (7%), and Cytophagia (6%). The response to thermal treatment revealed a drastic drop of the relative abundance of most Bacteroidetes classes, while Flavobacteriia became the dominant group, constituting up to 90% of this phylum after heat shock (T3), and minor recovery of *Cytophagia* after 14 days (T14), indicating the high resilience of Flavobacteriia phylotypes to thermal stress (**Figure 3C**).

The Flavobacteriia, Betaproteobacteria, and Gammaproteobacteria classes responded positively to thermal treatment, outlining their advanced resilience coupled with their copiotrophic metabolism (Ho et al., 2017) and their quick response to a sudden nutrient increase (Fox et al., 2017). The associated increase of the relative abundance of these bacterial classes after thermal treatment might be a result of a multifactorial combination considering the high organic-rich composition of the 900-O sample (Itcus et al., 2016) and the metabolism of each specific taxon (Ramirez et al., 2012; Bastida et al., 2015). The reduced presence of Firmicutes phylotypes could be explained by their capacity to cope with environmental stressors by producing resistance cells, as proven by the presence of *Paenibacillus* sp., known for their ability to form endospores (Onyenwoke et al., 2004). The decrease of the relative content of Actinobacteria might have been due to their high sensitivity to temperature changes, as observed in the case of the soil microbiome (Schostag et al., 2019).

Among the 10 most abundant bacterial genera assigned in the T0 sample (**Figure 3D**), *Chlorobium* (35%) and *Chlorobiaceae genus 2* (28%) were the dominant ones, suggesting an important autotrophic activity. The initial microbiome structure also revealed an important (5–8%) presence of the genera *Polymorphobacter*, *Clostridium sensu stricto*, *Pseudomonas*, *Carnobacterium*, *Unknown Chlorobiaceae genus 1*, *Cryobacterium*, *Polaromonas*, and *Flavobacterium*. Heat shock treatment induced a redistribution of the major bacterial genera in the T3, T7, and T14 samples, leading to relative content increases from 6 to 15% (T7) and 20% (T14) of *Polaromonas* spp., a psychrophilic genus ubiquitous in glacial systems (Darcy et al., 2011), from 4% to 40–45% of *Pseudomonas* species widely present in Scarisoara ice block (Paun et al., 2019), and from 8 to 45% of *Flavobacterium* species commonly found in freshwater (Bernadet et al., 1996; **Figure 3D**).

The putatively active archaeal phylotypes identified in the cave ice samples were assigned to class Methanomicrobia (Euryarchaeota) and showed a strong drop in relative abundance after thermal treatment, from 0.16 ± 0.01% (T0) to 0.02 ± 0.00% (T3) and 0.01 ± 0.00% in both T7 and T14 samples. Other archaeal reads were identified only at *p*-values below the threshold ($p < 0.005$).

Ice Fungal Community Response to Heat Shock

This rRNA-based survey constituting the first report on the potentially active fungal community structure in ice caves showed the presence of a complex community representing 0.23% of the Scarisoara ice microbiome (**Table 2**) assigned to 6 phyla and 14 classes (**Figure 4**).

At the phylum level (**Figure 4A**), the initial (T0) fungal community was shared among Chytridiomycota (40%), Ascomycota (30%), and Basidiomycota (20%), a highly spread taxon in frozen environments (Butinar et al., 2007), with a small (4%) relative content of Blastocladiomycota. The applied thermal treatment induced slight increases in the relative abundance of Chytridiomycota of up to 55% after 7 days of incubation (T7) and of Blastocladiomycota of up to 15% immediately after the 3-day treatment (T3), which was reduced to 10% after 14 days incubation at 4°C (T14). The relative abundance of both Basidiomycota and Ascomycota was reduced by heat shock (T3) to 8 and 20%, respectively, with preservation during the incubation at low temperature (T14) (**Figure 4A**).

At the class level (**Figure 4B**), the initial putatively active fungal community from cave ice (T0) was dominated by Chytridiomycetes (40%) and Agaricomycetes (20%). Eurotiomycetes was also highly represented in one of the T0 triplicates (50%), but only 5% in the other duplicates. The applied heat shock treatment (T3) shaped the fungal distribution by reducing the relative content of Agaricomycetes (4%) by 5-fold and increasing that of Chytridiomycetes phylotypes up to 50% (T3) and 58% (T14). Blastocladiomycetes, constituting 7% of the potentially active fungal community, also showed an increase in relative abundance of up to 20% (T3) immediately after heat shock, followed by a decline to 12% (T14). A similar trend was observed in the case of Microbotryomycetes, showing a slight increase in relative abundance (from 3 to 8%) in T3 that was stabilized after a longer incubation (T14) (**Figure 4B**).

The high relative abundance of Chytridiomycetes could be associated with the wide spread of this phylum in freshwater, marine habitats, and in soil (Money, 2016), according to their parasitic activity on planktonic algae (order Chytridiales) and their capacity to degrade chitin and keratin (McConnaughey, 2014). Moreover, this taxon is known as highly resistant to heat shock. The relative abundance of Blastocladiomycetes, a recently assigned phylum derived from Chytridiomycota (James et al., 2006), also increased (from 5 to 20%) after heat shock (T3) and remained at 11% after 7 days (T7) of incubation at 4°C. The resilience of these fungi, also present in freshwater, soil, and mud, could be related to their ability to decompose plant and animal debris and to parasitize arthropods (Money, 2016). Interestingly, the total fungal community from the 900-O ice sample based on DNA ITS2 Illumina sequencing (Mondini et al., 2018) indicated a dominant Ascomycota representation of uncultured taxa, unlike our data where Chytridiomycota was the

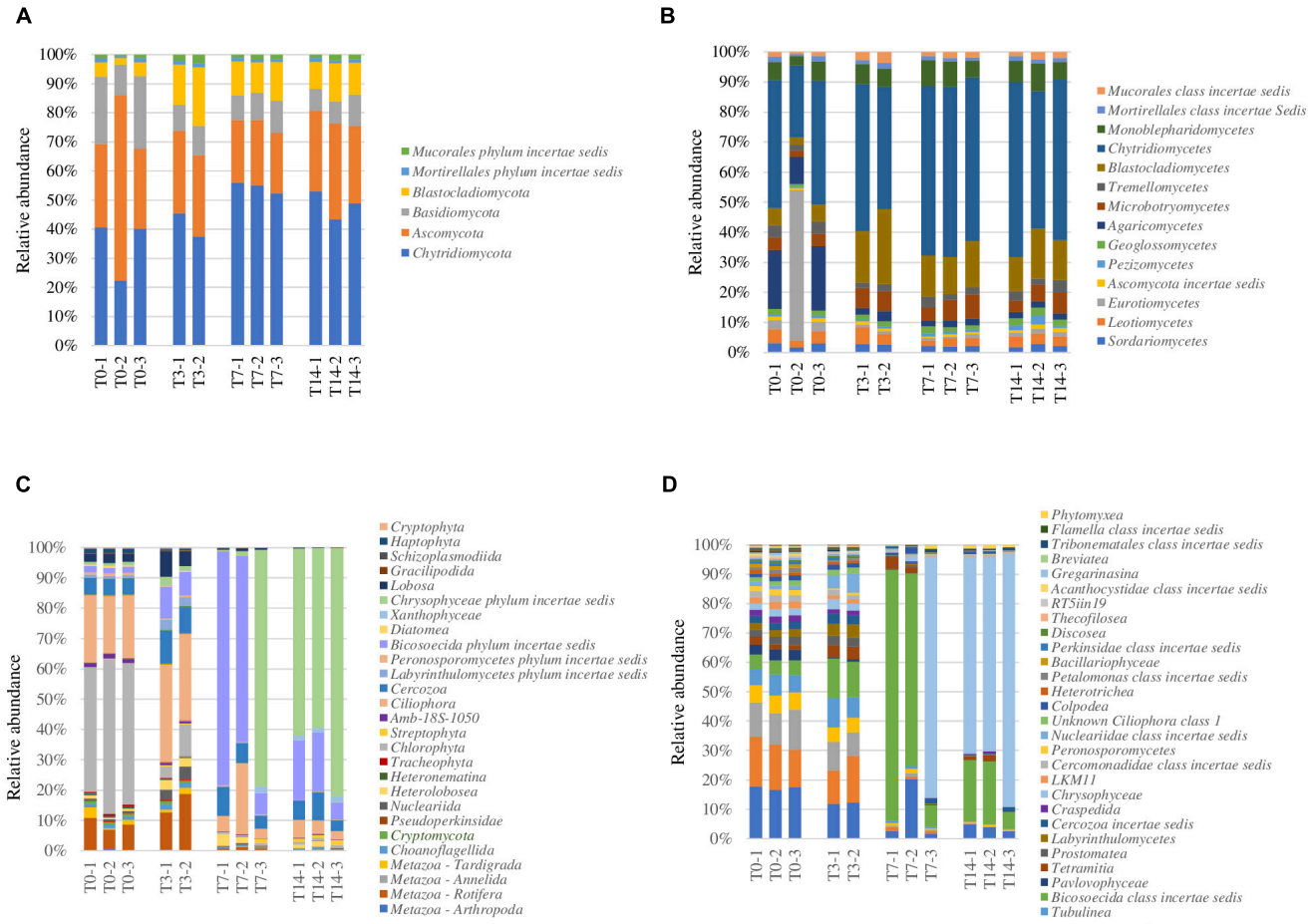

FIGURE 4 | Analysis of the response of the potentially active eukaryotic community from the Scarisoara cave ice to thermal treatment before (*T0*) and after exposure to thermal stress (*T3*, *T7*, and *T14*), as described in Section "Materials and Methods." **(A,B)** Relative fungal abundance at the phylum **(A)** and class **(B)** levels. **(C,D)** Relative abundance of eukaryotic phyla **(C)** and Protozoa classes **(D)**.

main class found in the potentially active fungal community of this ice deposit.

At the genus level (**Supplementary Figure 1**), the potentially active fungal reads from the T0 sample could be assigned to the *Rhizophydium* (Chytridiomycota), *Geoglossum* (Ascomycota), and *Ochroconis* (Ascomycota) taxa, with relatively similar representation. *Rhizophydium* species belonging to *Rhysophydiales* are parasites of invertebrates, chytrids, and algae, assuming a possible role in the control of aquatic populations, and are also common in soil, primarily as saprobes, with a possible role in nutrient recycling (Powell, 1993; Nieves-Rivera, 2003; Ibelings et al., 2004; van der Wal et al., 2013; Burow et al., 2019). *Ochroconis* is a fungal genus reported in caves (Novakova, 2009; Martin-Sanchez et al., 2012b; Martinez-Avila et al., 2021), guano, and bats (Cunha et al., 2020). A few novel species were described in cave habitats, such as *Ochroconis anellii*, *Ochroconis lascauxensis*, and *Ochroconis anomala* (de Hoog and von Arx, 1973; Martin-Sanchez et al., 2012a). *Geoglossum* species are saprophytic fungi found in pastures and grassy forests (Kučera and Lizoň, 2012). Interestingly, no major effect was observed on the relative abundance of the identified fungal genera after heat shock (**Supplementary Figure 1**).

Microeukaryotic Community Response to Heat Shock

The microeukaryotic group identified in the cave ice samples, representing the eukaryotic community mRNA without the fungal and plant assemblies, comprise 0.26% of the potentially active microbiome (T0) (**Table 2**). After the heat shock step (T3), the relative abundance of this microbial fraction was drastically reduced to 0.06%, followed by an increase of up to 5% after 14 days (T14).

Analysis of the taxonomic distribution of the microeukaryotes in the untreated T0 microbiome (**Figure 4C**) revealed the dominance of the phyla Tardigrada (4%) and Rotifera (10%), belonging to Metazoa, and the presence of more complex Protozoa group mainly assigned to the phyla Ciliophora (21%), Cercozoa (6%), and Bicosoecida (3%), in addition to Chlorophyta (Plantae) representatives (40%) (**Figure 4D**). In

response to thermal treatment, the microeukaryotic group displayed an altered composition after each step, affecting various taxon compositions within the T0–T3, T3–T7, and T7–T14 intervals (**Figure 4C**).

Heat shock treatment (T3) reduced the relative content of Chlorophyta (5%) and increased those of the taxa belonging to Metazoa (15%), Ciliophora (30%), Cercozoa (10%), and Bicosoecida (12%). After a week of incubation at 4°C (T7), the microeukaryotic community was dominated by Bicosoecida (80%), with a severe representation loss in the Metazoa group (1%). The prolonged incubation (T14) of ice samples induced further changes in the distribution of microeukaryotes, leading to a clear dominance of Chrysophyceae (62%) and a reduction of the relative content of Bicosoecida to 20% (**Figure 4C**).

Potentially active Protozoa community from the 900-O untreated (T0) cave ice samples occupied 0.8% of the rRNA identified microbiome (**Table 2**). Assessment of Protozoa at the class level outlined a high diversity with virtually equal distributions of the classes Spirotrichea (19%), Oligohymenophorea (16%), and Litostomatea (10%) (**Figure 4D**). For this community, heat shock (T3) had no major effect, except for a slight drop of the relative abundance of Spirotrichea (12%) and Oligohymenophorea (11%) and a corresponding increase for class Bicosoecida (from 4 to 12%). Prolonged incubation outlined a diverse distribution coupled with varied class abundance between samples T7 and T14. After a week of incubation (T7), Bicosoecida was the dominant protozoan (80%), but after 14 days of incubation, its relative abundance dropped to 20% on behalf of Chrysophyceae (62%) representatives (**Figure 4D**).

The Metazoa group from the Scarisoara 900-O ice sample (T0) constituted 0.26% of the potentially active (rRNA) cave ice microbiome (**Table 2**), mainly composed of taxa belonging to the classes Bdelloidea ($81.6 \pm 3.5\%$) and Eutardigrada ($14.3 \pm 9.08\%$) (**Supplementary Figure 2**). While heat shock (T3) induced a 5-fold drop in the overall Metazoa content (**Figure 4A**), no major changes in the relative abundance of these classes were observed, where Bdelloidea represented up to 95% of the community after 7 and 14 days of incubation at 4°C (**Supplementary Figure 2**).

Prolonged incubation at a low temperature over 14 days delineated an increase of the relative abundance of the microeukaryotic community, highlighting the prospect of predation on the prokaryotic cluster (**Figures 4C,D**). Among the assigned reads, genera belonging to the Stramenopiles group, such as *Oikomonas*, *Spumella*, and *Bicosoeca*, displayed an increase in T7, with the highest representation after 14 days. The very high abundance of these genera could be explained considering a combination of the characteristics of Stramenopiles and the decline of the relative contents of prokaryotes in this sample. Stramenopiles are characterized by a smaller cell size compared to other protozoa (Ekelund and Rønn, 1994), corresponding to a faster duplication as colonizers, as proven in soil communities (Altenburger et al., 2010). The reduced occurrence of prokaryotes could be related to the ecological role of Protozoa and Metazoa as predators in bacterial communities (Rønn et al., 2012) enhanced in liquid environments. The latter assumption was corroborated by the observation of the correlated relative abundance of prokaryotes and protozoa (**Table 2**), suggesting an increase in the relative content of microeukaryotes based on the reduction of the bacterial community. In this view, the active participation of the Protozoa group in regulating bacterial abundance (Porter et al., 1985; Berninger et al., 1991) could play a role in the control of the fast growth of copiotrophic bacteria in organic-rich environments. Contrarily, representation of the Metazoa group could be restrained by the presence of Chytridiomycota, known for their parasitic endeavor on arthropods (Money, 2016).

Heat Shock Impact on Gene Transcription (mRNA) of the Active Ice Microbiome

The mRNA analysis of the 900-O cave ice Illumina shotgun sequence highlighted the presence of an active microbial community in the Scarisoara ice cave, a groundbreaking result for this habitat. The gene transcriptional pattern of the T3, T7, and T14 thermal-treated ice communities compared to that of the untreated microbiome (T0) was modeled by both the increased temperature and prolonged incubation at 4°C, with the subsequent activation of different processes corroborated by the upregulation of specific gene clusters (**Figure 5** and **Supplementary Table 1**).

Functional annotation using the eggNOG database revealed 639 differential functions. The impact of thermal shock and prolonged incubation on the metabolism of the active microbial community harbored in the Scarisoara millennium-old ice was deciphered by evaluating the gene expression profile of this microbiome belonging to different groups and after each thermal step (**Figure 6** and **Supplementary Table 1**).

While the T0 sample showed a reduced general transcription, the T3 microbiome revealed the highest increase in mRNA overall transcripts (**Table 3**, **Supplementary Figures 3, 4**, and **Supplementary Table 1**). Thermal shock induced the transcription of genes involved in energy production and conversion (level 2, category C); amino acid transport and metabolism (level 2, category E); lipid transport and metabolism (level 2, category I); translation, ribosomal structure, and biogenesis (level 2, category J); transcription (level 2, category K); replication, recombination, and repair (level 2, category L); cell wall/membrane/envelope biogenesis (level 2, category M); signal transduction mechanisms (level 2, category T); and intracellular trafficking, secretion, and vesicular transport (level 2, category U). Moreover, the T7 sample displayed a comparable gene expression profile to that produced after 3 heat shock cycles (T3), but at a reduced level, whereas incubation for 14 days (T14) revealed a discrete reduction in the relative abundance of the C, J, K, L, and U genes.

Analysis of the differential gene expression between the thermal treatment steps of various functional genes from the eggNOG database (**Figure 6** and **Table 3**) showed an overall transcript increase substantiated by the upregulation of the genes involved in translation, ribosomal structure, transcription, replication, and repair (level 2, categories J, K, and L)

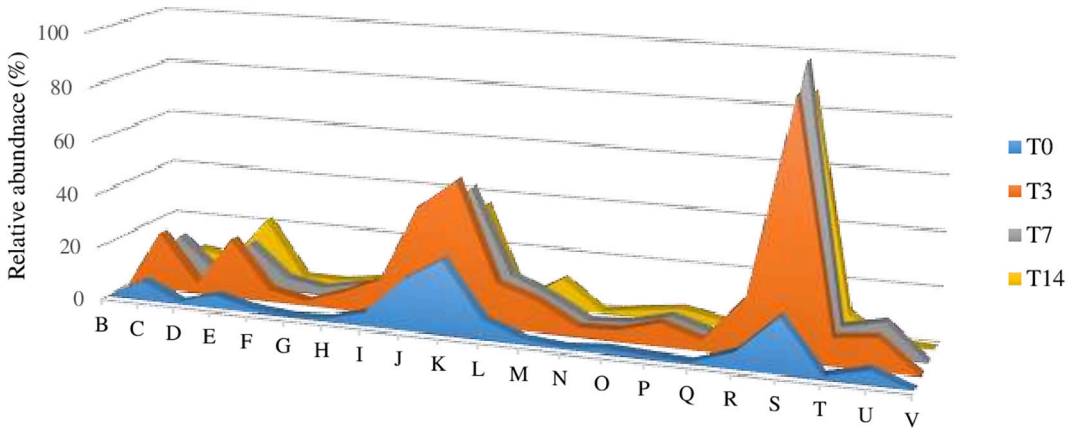

FIGURE 5 | (A) Impact of heat shock on gene expression (mRNA) variations of the Scarisoara cave active ice microbiome. (B–V) Relative abundance values of the genes assigned by eggNOG gene annotations (level 2) involved in chromatin structure and dynamics (B); energy production and conversion (C); cell cycle control, cell division, and chromosome partitioning (D); amino acid transport and metabolism (E); nucleotide transport and metabolism (F); carbohydrate transport and metabolism (G); coenzyme transport and metabolism (H); lipid transport and metabolism (I); translation, ribosomal structure, and biogenesis (J); transcription (K); replication, recombination, and repair (L); cell wall/membrane/envelope biogenesis (M); cell motility (N); posttranslational modification, protein turnover, and chaperones (O); inorganic ion transport and metabolism (P); secondary metabolites biosynthesis, transport, and catabolism (Q); general function prediction only (R); function unknown (S); signal transduction mechanisms (T); intracellular trafficking, secretion, and vesicular transport (U); and defense mechanisms (V) calculated for the T0, T3, T7, and T14 untreated and treated samples, as described in Section "Materials and Methods."

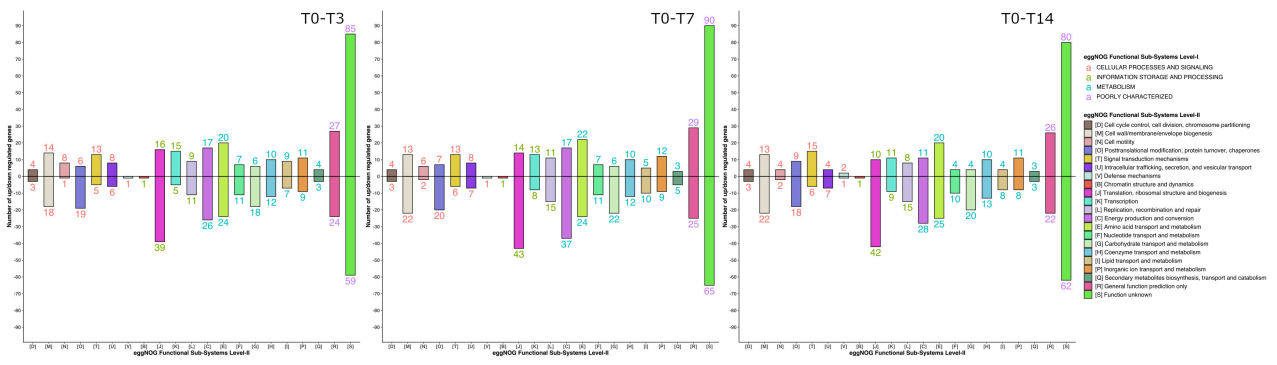

FIGURE 6 | Gene expression shifts in response to the different thermal treatment steps. The profiles of the gene expression and number of upregulated and downregulated genes from different gene families (see **Figure 5**) during the T0–T3, T0–T7, and T7–T14 heat shock steps were determined as indicated in Section "Materials and Methods."

processes, with the higher presence of transcripts for DNA and RNA helicases (level 3, category COG0513_1), threonyl-tRNA synthetase (level 3, category COG0441), DNA-directed RNA polymerase (level 3, category COG0202), and predicted transcriptional regulator (level 3, category COG1959). Increased transcriptional and translational activities were visible after thermal treatment and following 14 days of incubation (**Figure 6** and **Table 3**).

A pronounced increase in the transcripts associated with the tricarboxylic acid (TCA) cycle (level 3, categories COG0114, COG0567, COG1894, and COG0045) was visible after the thermal shock step (T3), while a distinct reduction was evident after 7 and 14 days of incubation (**Table 3**). The increase in gene transcription involved in the TCA cycle substantiated the dominance of the copiotrophic taxa in the T3 and T7 samples, where the carbon sources are fully available after ice thawing, hence the need to release the stowed energy through oxidative processes. According to this hypothesis, the microbiome submitted to the 2-week thermal treatment (T14) mimicking putative natural daily phenomena after glacier melting displayed a declined transcription of these genes associated with reduced carbon sources for oxidative processes and a reduced presence of copiotrophic bacteria exposed to protozoa predation. Interestingly, the transcripts for the Phasin family proteins, such as polyhydroxyalkanoates (PHAs) (level 3, category NOG45042), were upregulated, in accordance with the energy storage by the microbial community after prolonged incubation at low temperatures. The increased energy storage could explain the dominance of copiotrophic bacterial cells also after a prolonged (14 days) heat shock incubation necessary for a composition shift in the copiotrophic–oligotrophic microbial community.

TABLE 3 | Differential functional gene expression of cave ice microbiome submitted to heat shock.

COG_ID	COG_Category_lvl_2	COG_Category_lvl_3	T0	T3	T7	T14
COG0513_1	[J] Translation, ribosomal structure, biogenesis	Superfamily II DNA and RNA helicases	745	1,408	1,376	–
COG0441	[J] Translation, ribosomal structure, biogenesis	Threonyl-tRNA synthetase	207	400	329	334
COG0202	[K] Transcription	DNA-directed RNA polymerase, alpha subunit/40-kDa subunit	1,048	1478	–	–
COG1959	[K] Transcription	Predicted transcriptional regulator	1,069	1,718	2,589	3,449
COG0114	[C] Energy production and conversion	Fumarase	52	368	202	171
COG0567	[C] Energy production and conversion	2-Oxoglutarate dehydrogenase complex, dehydrogenase (E1) component, and related enzymes	107	403	309	195
COG1894	[C] Energy production and conversion	NADH:ubiquinone oxidoreductase, NADH-binding (51 kDa) subunit	189	561	458	294
COG0045	[C] Energy production and conversion	Succinyl-CoA synthetase, beta subunit	173	450	311	–
NOG45042	[S] Function unknown	Phasin family protein	469	1,688	1,662	2,317
COG0683	[E] Amino acid transport and metabolism	ABC-type branched-chain amino acid transport systems, periplasmic component	169	432	–	347
COG0174	[E] Amino acid transport and metabolism	Glutamine synthetase	168	662	499	623
COG0459	[O] Posttranslational modification, protein turnover, chaperones	Chaperonin GroEL (HSP60 family)	2,718	788	663	710
COG0605	[P] Inorganic ion transport and metabolism	Superoxide dismutase	83	416	268	179
COG1344	[N] Cell motility	Flagellin and related hook-associated proteins	72	141		
COG2804_2	[N] Cell motility	Type II secretory pathway, ATPase PulE/Tfp pilus assembly pathway, ATPase PilB	12	145	85	45
COG0577	[V] Defense mechanisms	ABC-type antimicrobial peptide transport system, permease component	–	–	–	14
COG1619	[V] Defense mechanisms	Uncharacterized proteins, homologs of microcin C7 resistance protein MccF	–	–	–	28

The mRNA reads of the untreated (T0) 900-O ice sample and after 3 (T3), 7 (T7), and 14 days (T14) of thermal treatment were assigned to different functional gene groups using the eggNOG database, as indicated in Section "Materials and Methods."

Transcripts involved in amino acid transport (level 3, category COG0683) and related to carbon and nitrogen metabolism using amino acids as intermediates (level 3, category COG0174) were also upregulated after the application of thermal treatment (**Table 3**). The transcripts for processes of amino acid transport were found associated with Proteobacteria (Suzuki et al., 2014), in accordance with the high relative abundance of this bacterial taxa in all To-T14 samples. Upregulation of the glutamine synthetase (GS) coding gene indicated the enhancement of nitrogen metabolism and the synthesis of glutamine (Hosie and Poole, 2001; Joo et al., 2018) of the ice microbiome submitted to thermal stress.

A direct response of the ice microbiome to temperature increase was also present after the ice thawing step, substantiated by the presence of transcripts involved in protein folding during thermal stress, such as GroEL (HSP60 family; level 3, category COG0459). Although the level of GroEL transcripts increased right after the ice thawing (T0), a significant decrease of this gene expression was observed (**Table 3**), which suggested a short response time for producing molecular chaperones to protect the microbial cells from the effects of high temperature. Another direct microbial response to the temperature increase consisted in the upregulation of transcripts coding for superoxide dismutase (level 3, category COG0605) in T3 samples (**Table 3**). This phenomenon, also described in *Escherichia coli,* indicated a direct correlation with the production of reactive oxygen species (ROS) in response to heat treatment (Marcén et al., 2017). Furthermore, the gene coding for alternative SigmaE factor, which controls the stress response at high temperatures (De Las Peñas et al., 1997), was highly upregulated after the thermal shock (T3), followed by a reduction in T7 and T14 samples. A slight increase in the relative abundance of cell motility genes (level 3, categories COG1344 and COG2804_2) was visible in T0 and T3 samples (**Table 3**), suggesting an increased motility associated with the water environment.

In addition, prolonged incubation for 14 days resulted in an increase in the defense mechanisms (level 3, categories COG0577 and COG1619) gene expression (**Figure 6** and **Table 3**), suggesting the start of shortage of food sources and the competition among active microbes to outcompete the taxa utilizing similar substrates for community sustenance.

Elevated temperatures also accelerated fungal decomposition, resulting in increased carbon dioxide emission from the soil, which can lead to a faster temperature rise. A more detailed analysis could help in identifying the differential expression of genes involved in microbial respiration. Therefore, these genes could also be considered as potential markers for identifying specific microbial taxa adapted to higher temperatures that could contribute to global CO_2 emissions as a primary driver of climate change.

Although development of the investigated system in the long run remains an open question, the short-term temperature changes (heat shock applied by environmental temperature shift on melted ice microbiome exposed on the soil surface)

appeared to shape the active microbial community embedded in the Scarisoara cave ice. Extended investigations on long-term temperature variations will help deepen the knowledge on the microbial role in the global climate change.

CONCLUSION

To date, this study provides the first evidence of an active microbiome and putatively active microeukaryotic taxa in perennial ice from caves, in addition to initial data on the thermal treatment response of the total and active ice-entrapped microbiomes using Illumina shotgun sequencing of rRNA and mRNA shift analysis. Temperature changes are known to disturb the microbial homeostasis alongside an altered taxon distribution, while little is known about the transcriptomic response to thermal stress. This overview of the structural and functional shifts in the ice microbial community induced by heat shock cycles and prolonged incubation contributed to increasing our understanding on changing environments and their ecological impacts due to ice melting.

The taxonomic profile of the potentially active microbiome from this icy environment was primarily modeled by heat shock, meanwhile revealing resilience mechanisms and specific functional responses to thermal stress. The ice community dominated by copiotrophic taxa was able to quickly use the carbon source released after ice thawing, with the Proteobacteria and Bacteroidetes taxa prevailing after thermal stress, unlike Archaea showing no recovery after incubation at a low temperature and the highly affected fungal community structure. Meanwhile, microeukaryotes exhibited fast recovery based on the putative predation process on bacteria. The resilience strategies of the active ice microbiome after heat shock exposure involved refolding, oxidative stress, and DNA synthesis-related gene upregulation. An increase in energy production and storage occurred during thermal stress, in accordance with the distribution of the dominant bacterial classes endowed with a copiotrophic lifestyle. Boosted carbon and nitrogen regulation and cellular motility appeared to respond to requirements for the water environment after ice melting, while the activation of defense mechanisms suggested a start of competition for similar food sources. The reported structural and functional modifications of the active microbial community from the Scarisoara cave ice due to thermal variations offered a glimpse of the environmental impacts of climate change leading to glacier retreat. In-depth analyses of the reconstructed metagenomes could contribute to unraveling the evolutionary patterns of metabolic pathways in this secluded cold habitat, subtle molecular adaptation mechanisms to icy environments, and novel cold-active biomolecules of applicative potential. Meanwhile, this first report on a critical shift of the active microbiomes from melting ice habitats represents a warning for possible major changes of the environmental biogeochemistry associated with late accelerated ice loss.

DATA AVAILABILITY STATEMENT

The sequencing datasets presented in this study are publicly available at Sequence Read Archive (SRA) under the BioProject ID PRJNA777283 (https://www.ncbi.nlm.nih.gov/bioproject/PRJNA777283).

AUTHOR CONTRIBUTIONS

AM and CP wrote the manuscript. AM performed the sample filtration, heat shock experiment, RNA extraction, and cDNA library preparation. LE-J and CJ designed the thermal treatment experiment and carried out the Illumina shotgun sequencing with contributions from AM and MZA. MZA performed the bioinformatics and statistical analyses. AM and PL contributed to the sequence analyses. CP performed the experimental design and coordinated the project. All authors contributed to data interpretation and revised the manuscript.

FUNDING

This study was financially supported by the European Union's H2020 Research and Innovation ITN MicroArctic Program under the Marie Skłodowska-Curie grant (Agreement No. 675546) and the H2020 UEFISCDI ERANet-LAC ELAC2014/DCC0178 Joint Program.

ACKNOWLEDGMENTS

We thank Christian A. Ciubotarescu, Vlad Murariu, Corina Itcus, Aurel Persoiu, Alexandra Hillebrand-Voiculescu, Traian Brad, and Madalina D. Pascu for ice sampling support and Dinu Pasca and Iuliana Pasca for field trip assistance. We also express our gratitude to Toke-Bang Andreasen and Morten Schostag for their valuable feedback on the experiment protocol and Tina Thane and Tanja Begovic for laboratory assistance.

SUPPLEMENTARY MATERIAL

The Supplementary Material for this article can be found online at: https://www.frontiersin.org/articles/10.3389/fmicb.2021.809076/full#supplementary-material

REFERENCES

Abyzov, S. S., Poglazova, M. N., Mitskevich, J. N., and Ivanov, M. V. (2005). "Common features of microorganisms in ancient layers of the Antarctic ice sheet," in *Life in Ancient Ice*, eds J. D. Castello and S. O. Rogers (Princeton: Princeton University Press), 240–250.

Altenburger, A., Ekelund, F., and Jacobsen, C. S. (2010). Protozoa and their bacterial prey colonize sterile soil fast. *Soil Biol. Biochem.* 42, 1636–1639. doi: 10.1016/j.soilbio.2010.05.011

Anesio, A. M., and Laybourn-Parry, J. (2012). Glaciers and ice sheets as a biome. *Trends Ecol. Evol.* 27, 219–225. doi: 10.1016/j.tree.2011.09.012

Anesio, A. M., Lutz, S., Chrismas, N. A. M., and Benning, L. G. (2017). The microbiome of glaciers and ice sheets. *NPJ Biofilms Microbiomes* 3:10. doi: 10.1038/s41522-017-0019-0

Anwar, M., Lanzén, A., Bang-Andreasen, T., and Jacobsen, C. S. (2019a). *Comparative Metatranscriptomics Workflow (CoMW)*. Computer Programme. CodeOcean. doi: 10.24433/CO.1793842.v1

Anwar, M., Lanzén, A., Bang-Andreasen, T., and Jacobsen, C. S. (2019b). To assemble or not to resemble - a validated comparative metatranscriptomics workflow (CoMW). *Gigascience* 8, 1–10. doi: 10.1101/642348

Bang-Andreasen, T., Anwar, M. Z., Lanzen, A., Kjoller, R., Ronn, R., Ekelund, F., et al. (2020). Total RNA sequencing reveals multilevel microbial community changes and functional responses to wood ash application in agricultural and forest soil. *FEMS Microbiol. Ecol.* 96:fiaa016. doi: 10.1093/femsec/fiaa016

Bastida, F., Selevsek, N., Torres, I. F., Hernández, T., and García, C. (2015). Soil restoration with organic amendments: linking cellular functionality and ecosystem processes. *Sci. Rep.* 5:15550. doi: 10.1038/srep15550

Bernadet, J.-F., Segers, P., Vancanneyt, M., Berthe, F., Kersters, K., and Vandamme, P. (1996). Cutting a Gordian Knot: emended Classification and Description of the Genus Flavobacterium, Emended Description of the Family Flavobacteriaceae, and Proposal of Flavobacterium hydatis nom. nov. (Basonym, *Cytophaga* aquatilis Strohl and Tait 1978). *Int. J. Syst. Evol.* 46, 128–148. doi: 10.1099/00207713-46-1-128

Berninger, U.-G., Finlay, B. J., and Kuuppo-Leinikki, P. (1991). Protozoan control of bacterial abundances in freshwater. *Limnol. Oceanogr.* 36, 139–147. doi: 10.4319/lo.1991.36.1.0139

Brad, T., Itcus, C., Pascu, M. D., Persoiu, A., Hillebrand-Voiculescu, A., Iancu, L., et al. (2018). Fungi in perennial ice from Scarisoara Ice Cave (Romania). *Sci. Rep.* 8:10096 . doi: 10.1038/s41598-018-28401-1

Burow, K., Grawunder, A., Harpke, M., Pietschmann, S., Ehrhardt, R., Wagner, L., et al. (2019). Microbiomes in an acidic rock–water cave system. *FEMS Microbiol. Lett.* 366:fnz167. doi: 10.1093/femsle/fnz167

Butinar, L., Spencer-Martins, I., and Gunde-Cimerman, N. (2007). Yeasts in high Arctic glaciers: the discovery of a new habitat for eukaryotic microorganisms. *Antonie van Leeuwenhoek* 91, 277–289. doi: 10.1007/s10482-006-9117-3

Cantarel, B. L., Coutinho, P. M., Rancurel, C., Bernard, T., Lombard, V., and Henrissat, B. (2009). The Carbohydrate-Active EnZymes database (CAZy): an expert resource for Glycogenomics. *Nucleic Acids Res.* 37, D233–D238. doi: 10.1093/nar/gkn663

Chen, S., Zhou, Y., Chen, Y., and Gu, J. (2018). fastp: an ultra-fast all-in-one FASTQ preprocessor. *Bioinformatics* 34, i884–i890. doi: 10.1093/bioinformatics/bty560

Cunha, A. O. B., Bezerra, J. D. P., Oliveira, T. G. L., Barbier, E., Bernard, E., Machado, A. R., et al. (2020). Living in the dark: bat caves as hotspots of fungal diversity. *PLoS One* 15:e0243494. doi: 10.1371/journal.pone.0243494

Darcy, J. L., Lynch, R. C., King, A. J., Robeson, M. S., and Schmidt, S. K. (2011). Global distribution of Polaromonas phylotypes–evidence for a highly successful dispersal capacity. *PLoS One* 6:e23742. doi: 10.1371/journal.pone.0023742

de Hoog, G. S., and von Arx, J. A. (1973). Revision of *Scolecobasidium* and *Pleurophragmium*. *Kavaka* 1, 55–60.

De Las Peñas, A., Connolly, L., and Gross, C. A. (1997). SigmaE is an essential sigma factor in *Escherichia coli*. *J. Bacteriol.* 179, 6862–6864. doi: 10.1128/jb.179.21.6862-6864.1997

Deming, J. W. (2002). Psychrophiles and polar regions. *Curr. Opin. Microbiol.* 5, 301–309. doi: 10.1016/S1369-5274(02)00329-6

Ekelund, F., and Rønn, R. (1994). Notes on protozoa in agricultural soil with emphasis on heterotrophic flagellates and naked amoebae and their ecology. *FEMS Microbiol. Rev.* 15, 321–353. doi: 10.1111/j.1574-6976.1994.tb00144.x

Fox, B. G., Thorn, R. M. S., Anesio, A. M., and Reynolds, D. M. (2017). The in situ bacterial production of fluorescent organic matter; an investigation at a species level. *Water Res.* 125, 350–359. doi: 10.1016/j.watres.2017.08.040

Garcia-Lopez, E., Moreno, A., Bartolomé, M., Leunda, M., Sancho, C., and Cid, C. (2021). Glacial Ice Age Shapes Microbiome Composition in a Receding Southern European Glacier. *Front. Microbiol.* 12:714537. doi: 10.3389/fmicb.2021.714537

Grabherr, M. G., Haas, B. J., Yassour, M., Levin, J. Z., Thompson, D. A., Amit, I., et al. (2011). Full-length transcriptome assembly from RNA-Seq data without a reference genome. *Nat. Biotechnol.* 29, 644–652. doi: 10.1038/nbt.1883

Griffiths-Jones, S., Bateman, A., Marshall, M., Khanna, A., and Eddy, S. R. (2003). Rfam: an RNA family database. *Nucleic Acids Res.* 31, 439–441. doi: 10.1093/nar/gkg006

Hillebrand-Voiculescu, A., Itcus, C., Ardelean, I., Pascu, D., Persoiu, A., Rusu, A., et al. (2015). Searching for cold-adapted microorganisms in the underground glacier of Scarisoara Ice Cave, Romania. *Acta Carsol.* 43, 319–329. doi: 10.3986/ac.v43i2-3.604

Hillebrand-Voiculescu, A., Rusu, A., Itcus, C., Persoiu, A., Brad, T., Pascu, D., et al. (2013). Bacterial 16S-rRNA gene clone library from recent ice stalagmites of Scarisoara cave. *Rom. J. Biochem.* 50, 109–118.

Ho, A., Di Lonardo, D. P., and Bodelier, P. L. E. (2017). Revisiting life strategy concepts in environmental microbial ecology. *FEMS Microbiol. Ecol.* 93:fix006. doi: 10.1093/femsec/fix006

Holmlund, P., Onac, B. P., Hansson, M., Holmgren, K., Mörth, M., Nyman, M., et al. (2005). Assessing the palaeoclimate potential of cave glaciers: the example of the Scărişoara ice cave (Romania). *Geogr. Ann. A Phys. Geogr.* 87, 193–201. doi: 10.1111/j.0435-3676.2005.00252.x

Hosie, A. H. F., and Poole, P. S. (2001). Bacterial ABC transporters of amino acids. *Res. Microbiol.* 152, 259–270. doi: 10.1016/S0923-2508(01)01197-4

Hubbard, J. (2017). *3D Cave and Ice Block Morphology from Integrated Geophysical Methods: A Case Study at Scarisoara Ice Cave, Romania*. Ph.D. thesis. Florida: University of South Florida.

Hug, L. A., Baker, B. J., Anantharaman, K., Brown, C. T., Probst, A. J., Castelle, C. J., et al. (2016). A new view of the tree of life. *Nat. Microbiol.* 1:16048. doi: 10.1038/nmicrobiol.2016.48

Ibelings, B. W., De Bruin, A., Kagami, M., Rijkeboer, M., Brehm, M., and Donk, E. V. (2004). Host parasite interactions between freshwater phytoplankton and chytrid fungi (Chytridiomycota) 1. *J. Phycol.* 40, 437–453. doi: 10.1111/j.1529-8817.2004.03117.x

Itcus, C., Pascu, M., Brad, T., Pet Oiu, A., and Purcarea, C. (2016). Diversity of cultured bacteria from the perennial ice block of Scarisoara Ice Cave, Romania. *Int. J. Speleol.* 45:89–100. doi: 10.5038/1827-806X.45.1.1948

Itcus, C., Pascu, M. D., Lavin, P., Persoiu, A., Iancu, L., and Purcarea, C. (2018). Bacterial and archaeal community structures in perennial cave ice. *Sci. Rep.* 8:15671. doi: 10.1038/s41598-018-34106-2

James, T. Y., Letcher, P. M., Longcore, J. E., Mozley-Standridge, S. E., Porter, D., Powell, M. J., et al. (2006). A molecular phylogeny of the flagellated fungi (Chytridiomycota) and description of a new phylum (Blastocladiomycota). *Mycologia* 98, 860–871. doi: 10.1080/15572536.2006.11832616

Joo, H. K., Park, Y. W., Jang, Y. Y., and Lee, J. Y. (2018). Structural Analysis of Glutamine Synthetase from *Helicobacter pylori*. *Sci. Rep.* 8:11657. doi: 10.1038/s41598-018-30191-5

Koci, B. R., and Kuivinen, K. C. (1984). The PICO lightweight coring auger. *J. Glaciol.* 30, 244–245. doi: 10.3189/S0022143000006018

Kopylova, E., Noé, L., and Touzet, H. (2012). SortMeRNA: fast and accurate filtering of ribosomal RNAs in metatranscriptomic data. *Bioinformatics* 28, 3211–3217. doi: 10.1093/bioinformatics/bts611

Kučera, V., and Lizoň, P. (2012). Geoglossaceous fungi in Slovakia III. The genus Geoglossum. *Biologia* 67, 654–658. doi: 10.2478/s11756-012-0053-6

Lanzén, A., Jørgensen, S. L., Huson, D. H., Gorfer, M., Grindhaug, S. H., Jonassen, I., et al. (2012). CREST–classification resources for environmental sequence tags. *PLoS One* 7:e49334. doi: 10.1371/journal.pone.0049334

Li, H., and Durbin, R. (2009). Fast and accurate short read alignment with Burrows–Wheeler transform. *Bioinformatics* 25, 1754–1760. doi: 10.1093/bioinformatics/btp324

Love, M. I., Huber, W., and Anders, S. (2014). Moderated estimation of fold change and dispersion for RNA-seq data with DESeq2. *Genome Biol.* 15:550. doi: 10.1186/s13059-014-0550-8

Ma, L.-J., Rogers, S. O., Catranis, C. M., and Starmer, W. T. (2000). Detection and Characterization of Ancient Fungi Entrapped in Glacial Ice. *Mycologia* 92, 286–295. doi: 10.1080/00275514.2000.12061156

Marcén, M., Ruiz, V., Serrano, M. J., Condón, S., and Mañas, P. (2017). Oxidative stress in E. coli cells upon exposure to heat treatments. *Int. J. Food Microbiol.* 241, 198–205. doi: 10.1016/j.ijfoodmicro.2016.10.023

Martinez-Avila, L., Peidro-Guzman, H., Perez-Llano, Y., Moreno-Perlin, T., Sanchez-Reyes, A., Aranda, E., et al. (2021). Tracking gene expression, metabolic profiles, and biochemical analysis in the halotolerant basidiomycetous yeast Rhodotorula mucilaginosa EXF-1630 during benzo[a]pyrene and phenanthrene biodegradation under hypersaline conditions. *Environ. Pollut.* 271:116358. doi: 10.1016/j.envpol.2020.116358

Martin-Sanchez, P. M., Nováková, A., Bastian, F., Alabouvette, C., and Saiz-Jimenez, C. (2012b). Two new species of the genus Ochroconis, O. lascauxensis

and O. anomala isolated from black stains in Lascaux Cave, France. *Fungal Biol.* 116, 574–589. doi: 10.1016/j.funbio.2012.02.006

Martin-Sanchez, P. M, Bastian, F., Alabouvette, C., and Saiz-Jimenez, C. (2012a). Real-time PCR detection of Ochroconis lascauxensis involved in the formation of black stains in the Lascaux Cave, France. *Sci. Total Environ.* 443, 478–484. doi: 10.1016/j.scitotenv.2012.11.026

McConnaughey, M. (2014). "Physical chemical properties of fungi," in *Reference Module in Biomedical Sciences* (Amsterdam: Elsevier). doi: 10.1016/b978-0-12-801238-3.05231-4

Miteva, V., Teacher, C., Sowers, T., and Brenchley, J. (2009). Comparison of the microbial diversity at different depths of the GISP2 Greenland ice core in relationship to deposition climates. *Environ. Microbiol.* 11, 640–656. doi: 10.1111/j.1462-2920.2008.01835.x

Mondini, A., Donhauser, J., Itcus, C., Marin, C., Perşoiu, A., Lavin, P., et al. (2018). High-throughput sequencing of fungal communities across the perennial ice block of Scărişoara Ice Cave. *Ann. Glaciol.* 59, 134–146. doi: 10.1017/aog.2019.6

Mondini, A., Schcostag, M.-D., Ellegard-Jensen, L., Bang-Andreasen, T., Anwar, M. Z., Purcarea, C., et al. (2019). *Total RNA Protocol (Extraction, Quantification and Illumina Library Preparation)*. protocols.io. doi: 10.17504/protocols.io.457gy9n

Money, N. (2016). "Fungal Diversity," in *The Fungi: Third Edition*, eds S. C. Watkinson, L. Boddy, and N. P. Money (Amsterdam: Elsevier Inc), 1–36.

Nichols, D. S. (2005). "The growth of prokaryotes in Antarctic sea ice: Implications for ancient ice communities," in *Life in Ancient Ice*, eds J. D. Castello and S. O. Rogers (Princeton: Princeton University Press), 50–68.

Nieves-Rivera, ÁM. (2003). Mycological survey of Río Camuy Caves Park, Puerto Rico. *J. Cave Karst Stud.* 65, 22–28.

Novakova, A. (2009). Microscopic fungi isolated from the Domica Cave system (Slovak Karst National Park, Slovakia). A review. *Int. J. Speleol.* 38, 71–82. doi: 10.5038/1827-806X.38.1.8

Onyenwoke, R. U., Brill, J. A., Farahi, K., and Wiegel, J. (2004). Sporulation genes in members of the low G+C Gram-type-positive phylogenetic branch (Firmicutes). *Arch. Microbiol.* 182, 182–192. doi: 10.1007/s00203-004-0696-y

Paun, V. I., Icaza, G., Lavin, P., Marin, C., Tudorache, A., Persoiu, A., et al. (2019). Total and Potentially Active Bacterial Communities Entrapped in a Late Glacial Through Holocene Ice Core From Scarisoara Ice Cave, Romania. *Front. Microbiol.* 10:1193. doi: 10.3389/fmicb.2019.01193

Paun, V. I., Lavin, P., Chifiriuc, M. C., and Purcarea, C. (2021). First report on antibiotic resistance and antimicrobial activity of bacterial isolates from 13,000-year old cave ice core. *Sci. Rep.* 11:514. doi: 10.1038/s41598-020-79754-5

Perşoiu, A., and Onac, B. P. (2012). "Ice in Caves," in *Encyclopedia of Caves (Second Edition)*, eds W. B. White and D. C. Culver (Amsterdam: Academic Press), 399–404.

Perşoiu, A., Onac, B. P., and Perşoiu, I. (2011). The interplay between air temperature and ice mass balance changes in Scărişoara Ice Cave, Romania. *Acta Carsol.* 40, 445–456. doi: 10.3986/ac.v40i3.4

Persoiu, A., and Pazdur, A. (2011). Ice genesis and its long-term mass balance and dynamics in Scarisoara Ice Cave, Romania. *Cryosphere* 5, 45–53. doi: 10.5194/tc-5-45-2011

Perşoiu, A., Onac, B. P., Wynn, J. G., Blaauw, M., Ionita, M., and Hansson, M. (2017). Holocene winter climate variability in Central and Eastern Europe. *Sci. Rep.* 7:1196. doi: 10.1038/s41598-017-01397-w

Porter, K. G., Sherr, E. B., Sherr, B. F., Pace, M., and Sanders, R. W. (1985). Protozoa in Planktonic Food Webs1,2. *J. Protozool.* 32, 409–415. doi: 10.1111/j.1550-7408.1985.tb04036.x

Powell, M. J. (1993). Looking at Mycology with a Janus Face: a Glimpse at Chytridiomycetes Active in the Environment. *Mycologia* 85, 1–20. doi: 10.1080/00275514.1993.12026239

Priscu, J. C., Fritsen, C. H., Adams, E. E., Giovannoni, S. J., Paerl, H. W., Mckay, C. P., et al. (1998). Perennial Antarctic lake ice: an oasis for life in a polar desert. *Science* 280, 2095–2098. doi: 10.1126/science.280.5372.2095

Purcarea, C. (2018). "Chapter 8 - Microbial Life in Ice Caves," in *Ice Caves*, eds A. Perşoiu and S.-E. Lauritzen (Amsterdam: Elsevier), 173–187.

Racovita, G., and Onac, B. P. (2000). "*Scarisoara Glacier Cave*," in *Monographic study*, ed. Carpatica (Cluj-Napoca), 140.

Ramirez, K. S., Craine, J. M., and Fierer, N. (2012). Consistent effects of nitrogen amendments on soil microbial communities and processes across biomes. *Glob. Change Biol.* 18, 1918–1927. doi: 10.1111/j.1365-2486.2012.02639.x

Rimbu, N., Onac, B. P., and Racovita, G. (2012). Large-scale anomaly patterns associated to temperature variability inside Scarisoara Ice Cave. *Int. J. Climatol.* 32, 1495–1502. doi: 10.1002/joc.2369

Rogers, S. O., Shtarkman, Y. M., Koçer, Z. A., Edgar, R., Veerapaneni, R., and D'elia, T. (2013). Ecology of subglacial lake vostok (antarctica), based on metagenomic/metatranscriptomic analyses of accretion ice. *Biology* 2, 629–650. doi: 10.3390/biology2020629

Rønn, R., Vestergård, M., and Ekelund, F. (2012). Interactions between Bacteria, Protozoa and Nematodes in Soil. *Acta Protozool.* 51, 223–235. doi: 10.4467/16890027AP.12.018.0764

Schostag, M., Priemé, A., Jacquiod, S., Russel, J., Ekelund, F., and Jacobsen, C. S. (2019). Bacterial and protozoan dynamics upon thawing and freezing of an active layer permafrost soil. *ISME J.* 13, 1345–1359. doi: 10.1038/s41396-019-0351-x

Suzuki, S., Kuenen, J. G., Schipper, K., Van Der Velde, S., Ishii, S. I., Wu, A., et al. (2014). Physiological and genomic features of highly alkaliphilic hydrogen-utilizing Betaproteobacteria from a continental serpentinizing site. *Nat. Commun.* 5:3900. doi: 10.1038/ncomms4900

Tu, Q., Lin, L., Cheng, L., Deng, Y., and He, Z. (2019). NCycDB: a curated integrative database for fast and accurate metagenomic profiling of nitrogen cycling genes. *Bioinformatics* 35, 1040–1048. doi: 10.1093/bioinformatics/bty741

van der Wal, A., Geydan, T. D., Kuyper, T. W., and De Boer, W. (2013). A thready affair: linking fungal diversity and community dynamics to terrestrial decomposition processes. *FEMS Microbiol. Rev.* 37, 477–494. doi: 10.1111/1574-6976.12001

Varet, H., Brillet-Guéguen, L., Coppée, J. Y., and Dillies, M. A. (2016). SARTools: a DESeq2- and EdgeR-Based R Pipeline for Comprehensive Differential Analysis of RNA-Seq Data. *PLoS One* 11:e0157022. doi: 10.1371/journal.pone.0157022

Weisleitner, K., Perras, A., Moissl-Eichinger, C., Andersen, D. T., and Sattler, B. (2019). Source Environments of the Microbiome in Perennially Ice-Covered Lake Untersee, Antarctica. *Front. Microbiol.* 10:1019. doi: 10.3389/fmicb.2019.01019

Williams, T. J., Wilkins, D., Long, E., Evans, F., Demaere, M. Z., Raftery, M. J., et al. (2013). The role of planktonic Flavobacteria in processing algal organic matter in coastal East Antarctica revealed using metagenomics and metaproteomics. *Environ. Microbiol.* 15, 1302–1317. doi: 10.1111/1462-2920.12017

Xue, Y., Lanzén, A., and Jonassen, I. (2020). Reconstructing ribosomal genes from large scale total RNA meta-transcriptomic data. *Bioinformatics* 36, 3365–3371. doi: 10.1093/bioinformatics/btaa177

Zhong, Z.-P., Tian, F., Roux, S., Gazitúa, M. C., Solonenko, N. E., Li, Y.-F., et al. (2021). Glacier ice archives nearly 15,000-year-old microbes and phages. *Microbiome* 9:160. doi: 10.1186/s40168-021-01106-w

Conflict of Interest: The authors declare that the research was conducted in the absence of any commercial or financial relationships that could be construed as a potential conflict of interest.

Publisher's Note: All claims expressed in this article are solely those of the authors and do not necessarily represent those of their affiliated organizations, or those of the publisher, the editors and the reviewers. Any product that may be evaluated in this article, or claim that may be made by its manufacturer, is not guaranteed or endorsed by the publisher.

frontiers | Frontiers in Microbiology

ORIGINAL RESEARCH
published: 27 April 2022
doi: 10.3389/fmicb.2022.869661

Diversity of Microfungi in a High Radon Cave Ecosystem

Tamara Martin-Pozas[1], Alena Nováková[2], Valme Jurado[3], Angel Fernandez-Cortes[4], Soledad Cuezva[5], Cesareo Saiz-Jimenez[3] and Sergio Sanchez-Moral[1]*

[1]Department of Geology, National Museum of Natural Sciences (MNCN-CSIC), Madrid, Spain, [2]Laboratory of Fungal Genetics and Metabolism, Institute of Microbiology of the CAS, Prague, Czechia, [3]Department of Agrochemistry, Environmental Microbiology and Soil Conservation, Institute of Natural Resources and Agricultural Biology (IRNAS-CSIC), Seville, Spain, [4]Department of Biology and Geology, University of Almeria, Almeria, Spain, [5]Department of Geology, Geography and Environment, University of Alcala, Alcala de Henares, Spain

Castañar Cave is a clear example of an oligotrophic ecosystem with high hygrothermal stability both seasonal and interannual and the particularity of registering extraordinary levels of environmental radiation. These environmental conditions make the cave an ideal laboratory to evaluate both the responses of the subterranean environment to sudden changes in the matter and energy fluxes with the exterior and also any impact derived from its use as a tourist resource under a very restrictive access regime. In 2008, a fungal outbreak provoked by a vomit contaminated the sediments which were removed and subsequently treated with hydrogen peroxide. Fungal surveys were carried out in 2008 and 2009. The visits were resumed in 2014. Here, 12 years after the outbreak, we present an exhaustive study on the cave sediments in order to know the distribution of the different fungal taxa, as well as the prevalence and spatio-temporal evolution of the fungi caused by the vomit over the years under the conditions of relative isolation and high radiation that characterize this cave.

Keywords: fungal outbreak, Castañar Cave, radon, ionizing radiation, *Ascomycota*, *Basidiomycota*

OPEN ACCESS

Edited by:
Saskia Bindschedler, Université de Neuchâtel, Switzerland

Reviewed by:
Nihal Doğruöz Güngör, Istanbul University, Turkey
Johann Leplat, Laboratoire de Recherche des Monuments Historiques, France

****Correspondence:***
Cesareo Saiz-Jimenez
saiz@irnase.csic.es

Specialty section:
This article was submitted to Terrestrial Microbiology, a section of the journal Frontiers in Microbiology

Received: *04 February 2022*
Accepted: *05 April 2022*
Published: *27 April 2022*

Citation:
Martin-Pozas T, Nováková A, Jurado V, Fernandez-Cortes A, Cuezva S, Saiz-Jimenez C and Sanchez-Moral S (2022) Diversity of Microfungi in a High Radon Cave Ecosystem. Front. Microbiol. 13:869661. doi: 10.3389/fmicb.2022.869661

INTRODUCTION

Castañar Cave (Castañar de Ibor, Caceres, Spain) was discovered in 1967, declared Natural Monument in 1997 and opened to visits in 2003. The interest of this cavity lies in its great variety of speleothems formed mainly by aragonite and calcite of low magnesium (Alonso-Zarza et al., 2011) and in its very high concentrations of radon (^{222}Rn) in air with annual average above 30 kBq/m^3 (Lario et al., 2006; Garcia-Guinea et al., 2013). These values are much higher than the average ^{222}Rn concentrations found in most caves studied around the world (0.5–8.3 kBq/m^3; Cigna, 2005; Somlai et al., 2011). ^{222}Rn was used as tracer for assessing ventilation of Castañar Cave because its variations depend only on the exchange of air with the exterior (Fernandez-Cortes et al., 2009). The slates hosting the cave contain uranium (39.2 ± 5.2 mg.kg^{-1}; Garcia-Guinea et al., 2013), so that its disintegration to radon and the subsequently ^{222}Rn exhalation from bedrock entails a continuous source of this gas to cave atmosphere. The weathering leakage processes of the bedrock also favor the remobilization of radionuclides *via* leaching and their later settlement into the cave environment associated to mineral phases of cave deposits (Garcia-Guinea et al., 2013). This favors maintaining the high ^{222}Rn activity of cave air since

there is a continuous regeneration of this gas due to the long-lived of these radionuclides of the radium radioactive decay chain.

The morning of August 26, 2008, on the cave walls and ground sediments appeared long, white fungal mycelia as the result of the vomit of a visitor, 40 h before. The vomit area was located at 17 m from the cave entrance and the ground sediments exhibited a widespread fungal colonization after the disturbance. In the following days, visitors stepped on the sediments colonized by the fungi, and detritus, mycelia and spores were distributed along the touristic trail, as evidenced by the presence of patches of fungal growth farther than the vomit area (Jurado et al., 2010). To help to control the outbreak, the entire area directly affected by vomiting was cleaned and subsequently treated with hydrogen peroxide and the visits were cancelled on September 11, 2008, 16 days after the spillage. In 2009, the cave was only visited by scientists and staff people for controlling the fungal outbreak. The cave was reopened in 2014 but the number of visitors/year was reduced from 1,500 to 1,600 in 2008, to an annual maximum of 450 visitors. Besides, since the cave re-opened, in order to minimize the entrance of external material, the visitors uses clean and uncontaminated suits and shoe covers.

In Castañar Cave, we had the opportunity to carry out extensive microbiological studies on 2008 and 2009, up to 12 months after the fungal outbreak, and again 12 years after the outbreak in a subsequent and exhaustive study carried out in 2020. Castañar Cave is a natural environment with high levels of ionizing radiation but also a low energy cave and high environmental stability throughout the annual cycle (Fernandez-Cortes et al., 2011) which make it more sensitive to the entry of matter and energy from outside. There are a few reports about the dominance of microbial communities in radioactive environments such as the International Space Station and Chernobyl reactor (Dadachova and Casadevall, 2008; Van Houdt et al., 2012; Romsdahl et al., 2018). These works give some examples of microbial species and melanized fungi with a high tolerance to radioactivity. However, research works in natural environments with high ionizing radiation and on the evolution of microbial populations in these environments are very scarce (Siasou et al., 2017).

The direct control that environmental conditions exert on the distribution of fungi in subterranean ecosystems has recently been demonstrated (Jurado et al., 2021; Sanchez-Moral et al., 2021). The objective of this study is to know the distribution of the different fungal taxa throughout Castañar Cave, as well as the prevalence and spatio-temporal evolution of the fungi caused by the vomit over the years under conditions of high isolation of the cave atmosphere from the outside and an outstanding radon activity.

MATERIALS AND METHODS

Site

Castañar Cave (SW Spain, 39°37′40′′N, 5°24′59′′W, 590 m.a.s.l.) is currently located under a natural olive grove that grows in a temperate and semi-arid climate with a rainfall regime of less than 500 mm per year, long periods of drought in summer and maximum rains in autumn. Outside, the annual average temperature is 15.9°C and the average relative humidity is 62.5%.

The cave was developed by dissolution of dolomite strata interbedded in shales and greywackes of the Precambrian Age (Alonso-Zarza and Martin-Perez, 2008). Castañar Cave is a small karstic cavity with a cumulative length of 2,135 m, distributed in six main and wider halls (e.g., Sala Nevada) and some narrow galleries connecting them, with heights of less than 3 m in any case (**Figure 1**). The cave entrance is a unique vertical access, 9 m long over an area of 1.5 m^2, with a quasi-hermetic door installed at the entrance. All these characteristics make Castañar a low energy cave with very high ^{222}Rn gas concentration and high environmental stability throughout the annual cycle (Fernandez-Cortes et al., 2011).

Environmental Surveys

Variations in ^{222}Rn concentration and air temperature are two key environmental parameters to determine the exchange rates of matter and energy and the main connection pathways between the exterior and the cavity. A set of five autonomous thermohygrometer recorders (Tinytag TGP-4500) and five nuclear track-etch passive detectors equipped with a solid state LR-115 type film (Kodak) were installed inside the cave, distributed according to the geomorphological characteristics of the subterranean galleries and the distance to the entrance (**Figure 1**). This monitoring network makes it possible to obtain monthly mean values of the ^{222}Rn concentration of the subterranean air and a continuous thermo-hygrometric record at each point.

Microbiological Analysis

On December 3, 2020, seven sediment samples (approximately 3–4 cm depth) were collected in Castañar Cave (P1-P7) and one from the exterior soil (E) near the cave entrance (**Figure 1**). All samples were collected using sterile spatulas and immediately suspended in DNA/RNA Shield™ into sterile polypropylene tubes. Then, the samples were stored at 4°C, in the dark during transportation and were kept at −80°C until processing.

Total DNA was extracted from environmental samples using the QIAGEN Power Soil Kit, following the manufacturer's instructions. Two independent DNA extractions were carried out for each sampling point, except in P1 where we only collected one sample. Extracted DNA was used as template for generating PCR-amplicons. The internal transcribed spacer 2 (ITS2) of the nuclear ribosomal DNA (about 400 bp) was amplified using the primers ITS86F (5 'GTGAATCATCGAATCTTTGAA 3′; Turenne et al., 1999) and ITS4 (5 'TCCTCCGCTTATTGATATGC 3′; White et al., 1990). Amplifications settings were as follows: 95°C for 5 min followed by 35 cycles consisting of 95°C for 30s, 49°C for 30 s, and 72°C for 30s and a 10-min elongation step at 72°C. PCR-amplicons were sequenced by high-throughput sequencing at AllGenetics Company (A Coruña, Spain) on

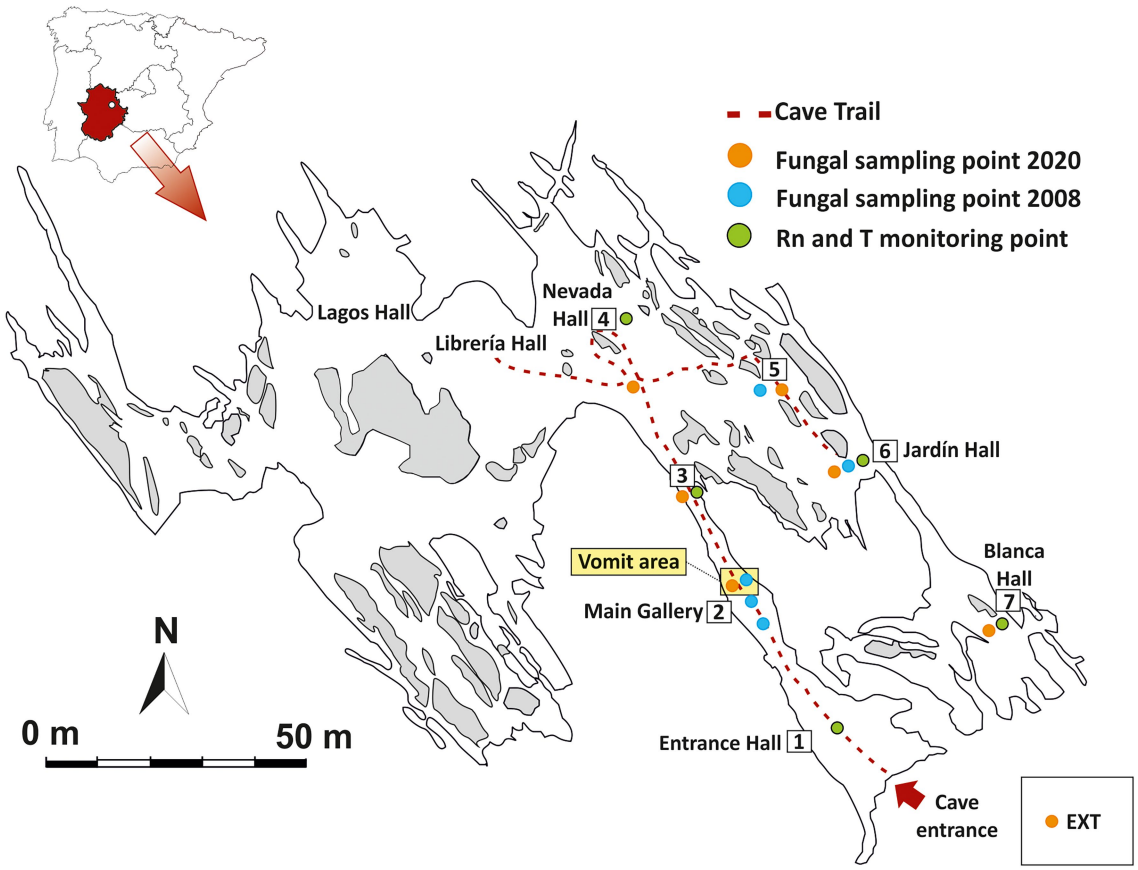

FIGURE 1 | Map of Castañar Cave with location of sampling points, passive radon dosimeters and thermohygrometer recorders for environmental monitoring. EXT: Exterior.

the Illumina MiSeq platform using the paired-end reads 2 × 300 bp reagent kit, according to the manufacturer's instructions. Extraction and PCR blanks were used.

To analyze fungal community composition, Raw fastq files were processed with QIIME2 (Bolyen et al., 2019). Briefly, DADA2 (Callahan et al., 2016) filtered the raw data according to the quality, generating an amplicon sequence variant (ASV) table. Then, taxonomic assignments were determined for ASVs using qiime2-feature-classifier classify-sklearn against the UNITE fungal ITS database (version 8.0; UNITE Community, 2019) and trained with Naive Bayes classifier on the full reference sequences. Taxa were also blasted (BlastN) against GenBank for fungal verification. All fungal names were reported according to the MycoBank Database. The sequencing data was further imported into the R environment 3.6.0 and processed using the phyloseq package (McMurdie and Holmes, 2013). Barplots and clustered heat maps by euclidean distance were prepared using ggplot and pheatmap packages to illustrate the composition of fungal communities in Castañar Cave. Alpha diversity was calculated using Shannon diversity index and Faith's Phylogenetic Diversity, directly using QIIME2. The raw reads were deposited into the NCBI Sequence Read Archive (SRA) database under accession number PRJNA802044.

RESULTS

Environmental Parameters

Figure 2 shows the annual mean values and the annual oscillation ranges of ^{222}Rn concentration of the monitored area. The spatio-temporal distribution of tracer gases is directly related to morphology and cave air circulation. The results show that the entire cave has a very high level of natural radiation throughout the year, higher than 30 kBq/m^3, ranging from 32,440 Bq/m^3 in the Jardin area (P5-P6) to 34,940 Bq/m^3 (P1-P7). The highest mean concentrations and the maximum variations (in red tones) are recorded in the area near the entrance (P1) and in Sala Blanca (P7) – Sala Final, the end of the cave. On the contrary, the most stable area throughout the year is Sala Nevada (P4) with an intra-annual variation of 19,942 Bq/m^3.

In the case of air temperature (**Figure 3**), the annual mean values range from 17.08°C in the internal zone (P5-P6) to 17.81°C in the areas near the entrance (P1). The data show the high environmental stability of the cave which annual variation ranges below 0.25°C at all measurement points except in the entrance area (P1, 0.71°C of annual amplitude, red tones), where the external direct influence is evident. These data indicate that the sectors close to the

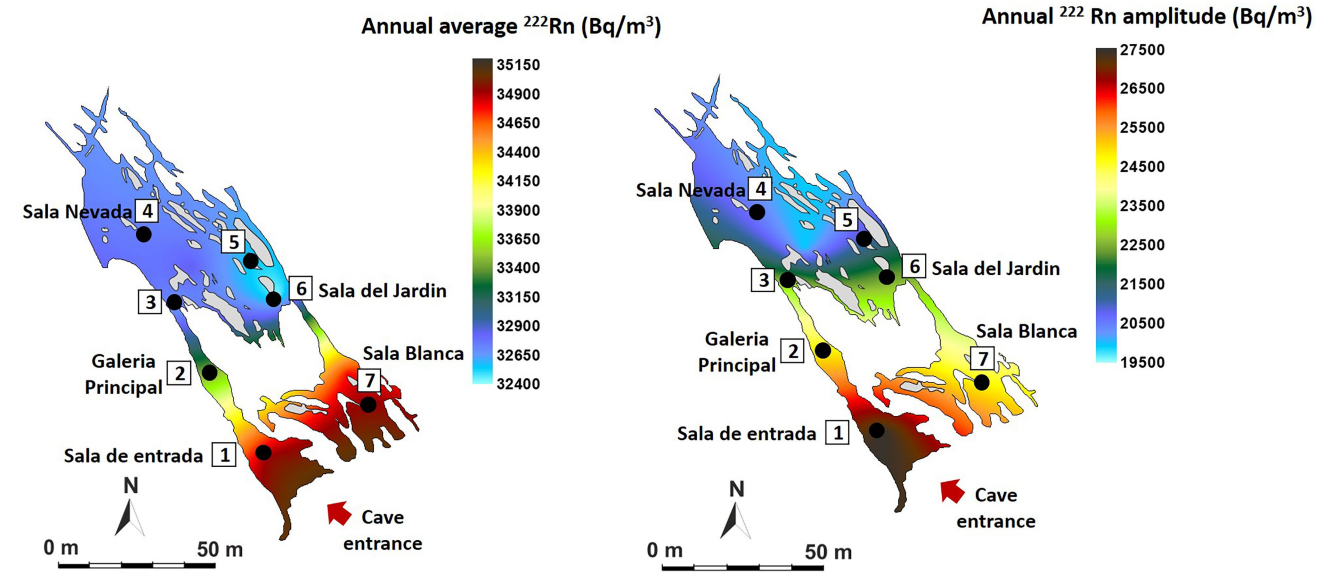

FIGURE 2 | Spatial distribution in Castañar Cave of mean annual radon concentration and maximum amplitude of annual variation expressed in Bq/m^3.

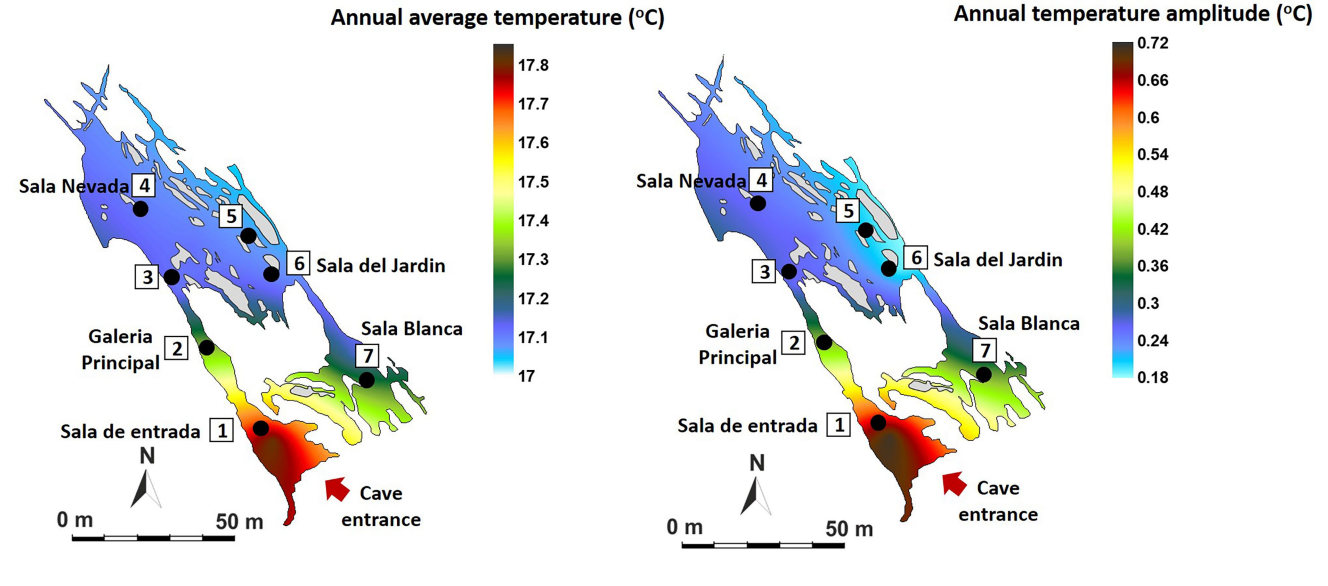

FIGURE 3 | Spatial distribution in Castañar Cave of mean annual air temperature and maximum amplitude of annual variation expressed in degrees centigrade (°C).

entrance show the highest rates of air renewal and consequently of matter and energy exchange with the outside atmosphere. On the contrary, the most stable area with the least energy exchange with the exterior is located in P5-P6 (Sala del Jardin, in light blue tones).

Fungal Communities in 2020

Six samples from the cave sediments were taken in December 2020 along the touristic trail and one soil sample outside the cave, which were used for molecular studies. Sample P-3 was not studied.

Supplementary Table S1 shows the alpha diversity indices and how fungal diversity decreased in the cave environment when compared to the topsoil. Inside the cave, the lowest fungal diversity was observed in the internal zone (P5-P6), while the highest was found in Sala de Entrada, near the cave entrance. These data indicate that fungal diversity increased with the entry of external organic matter and only a few species survive in the most oligotrophic areas (P5-P6).

Figure 4 shows phyla distribution in the different samples. In general, there is an uneven distribution between the phyla *Ascomycota* and *Basidiomycota*, with a predominance of

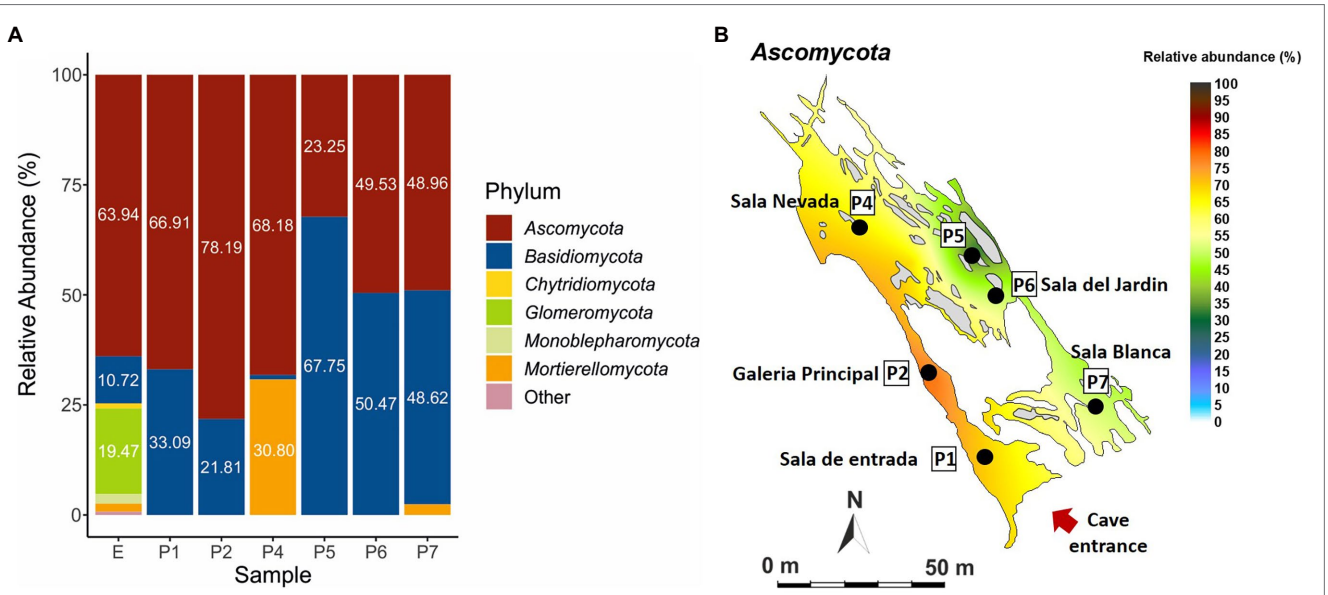

FIGURE 4 | Fungal abundance at phylum level in Castañar Cave, in the December 2020 campaign. **(A)** Barplot illustrating fungal abundance at phylum level in P1-P7, and exterior soil E. Phyla with abundances below 1% are represented as Other. **(B)** Spatial distribution of *Ascomycota* in the December 2020 campaign.

ascomycetes in the exterior soil (E) and the first part of the trail from Sala de Entrada (P1) to Sala Nevada (P4), which reversed in the last part of the trail, especially in P5 with a majority of *Basidiomycota*. At the end of the trail, Sala del Jardin (P6) and Sala Blanca (P7) the relative abundances of both phyla were equivalent. Other abundant phyla were *Mortierellomycota* in P4 and *Glomeromycota* in the soil (E). The quantities of other phyla were negligible, below 1%, except for *Monoblepharomycota* that reached 2.1% in the soil (E).

Figure 5 and **Supplementary Table S2** illustrate the relative abundance of major fungi (higher than 1% in at least one sample) at the species level. Thirty five fungi were identified at the species level, while 14 were only at genus level. The most abundant species was *Candida parapsilosis* followed by *Sistotrema oblongisporum*, *Cephalotrichum microsporum*, *Cystobasidium slooffiae*, *Mortierella alpina*, *Omphalotus olearius*, *Neocosmospora solani* (= *Fusarium solani*), *Trichophyton ajelloi*, *Stereum hirsutum*, and *Malassezia globosa*.

Other species identified, although with relative abundance below 5% were *Pseudopithomyces chartarum*, *Bahusandhika caligans*, *Aspergillus tamari*, *Conocybe ingridiae*, and *Solicoccozyma aeria*, which were only found in the soil (E), and *Penicillium simplicissimum, Pseudogymnoascus pannorum, Meyerozyma guilliermondii, Leptobacillium leptobactrum, Fusarium oxysporum, Acremonium furcatum, Skeletocutis nivea*, and *Basidioascus persicus* in different halls.

Among the unidentified members of genera and families were predominant *Buckleyzyma*, *Diaporthe*, *Preussia*, *Purpureocillium*, *Glomeraceae* and *Mortierella*. With relative abundance below 5% were members of the genera *Massarina, Paraphoma*, *Aspergillus*, *Claroideoglomus* and *Glomus* in the soil (E) and *Talaromyces* in the cave.

DISCUSSION

Fungi in Castañar Cave 12 Years After a Fungal Outbreak

Only three fungi retrieved from previous surveys in sediments (2008–2009) were found again in the 2020 campaign: *Neocosmospora solani*, *Fusarium oxysporum*, and *Mortierella alpina*. It must be noticed that the comparison was made within isolates and NGS sequences, which could create some bias. Nevertheless, their presence in the cave despite the extensive cleaning of sediments carried after the spillage suggests that these three fungi are resistant and well adapted to the oligotrophic and high radiation conditions of the cave.

The occurrence of *Neocosmospora solani* was detected in three sediment samples (Galeria Principal, Sala Nevada and Sala Blanca) and seems to be a permanent inhabitant of Castañar Cave, present in all samplings since 2008. From a point of view of cave conservation, *Neocosmospora solani* is a dangerous fungus and has been widely reported in relation to cave outbreaks (Dupont et al., 2007; Bastian et al., 2009), and particularly in Castañar Cave (Jurado et al., 2010).

In some caves *Fusarium oxysporum* was associated with *Neocosmospora solani* (Jiang et al., 2017; Popkova and Mazina, 2019), as they are in Castañar Cave. *Fusarium oxysporum* is widely found as a plant pathogen, endophyte, and soil saprobe and was isolated from Chernobyl (Urbaniak et al., 2019).

Mortierella alpina and other *Mortierella* species were usually abundant in bat dung samples collected in caves (Degawa and Gams, 2004). *Mortierella* species were reported to be present in all of the 39 samples collected across five habitats, including sediments, weathered rocks, bat guano, drip waters, and air in Heshang Cave, China (Man et al., 2018). In addition to *Fusarium*, *Mortierella* species have been isolated from bat

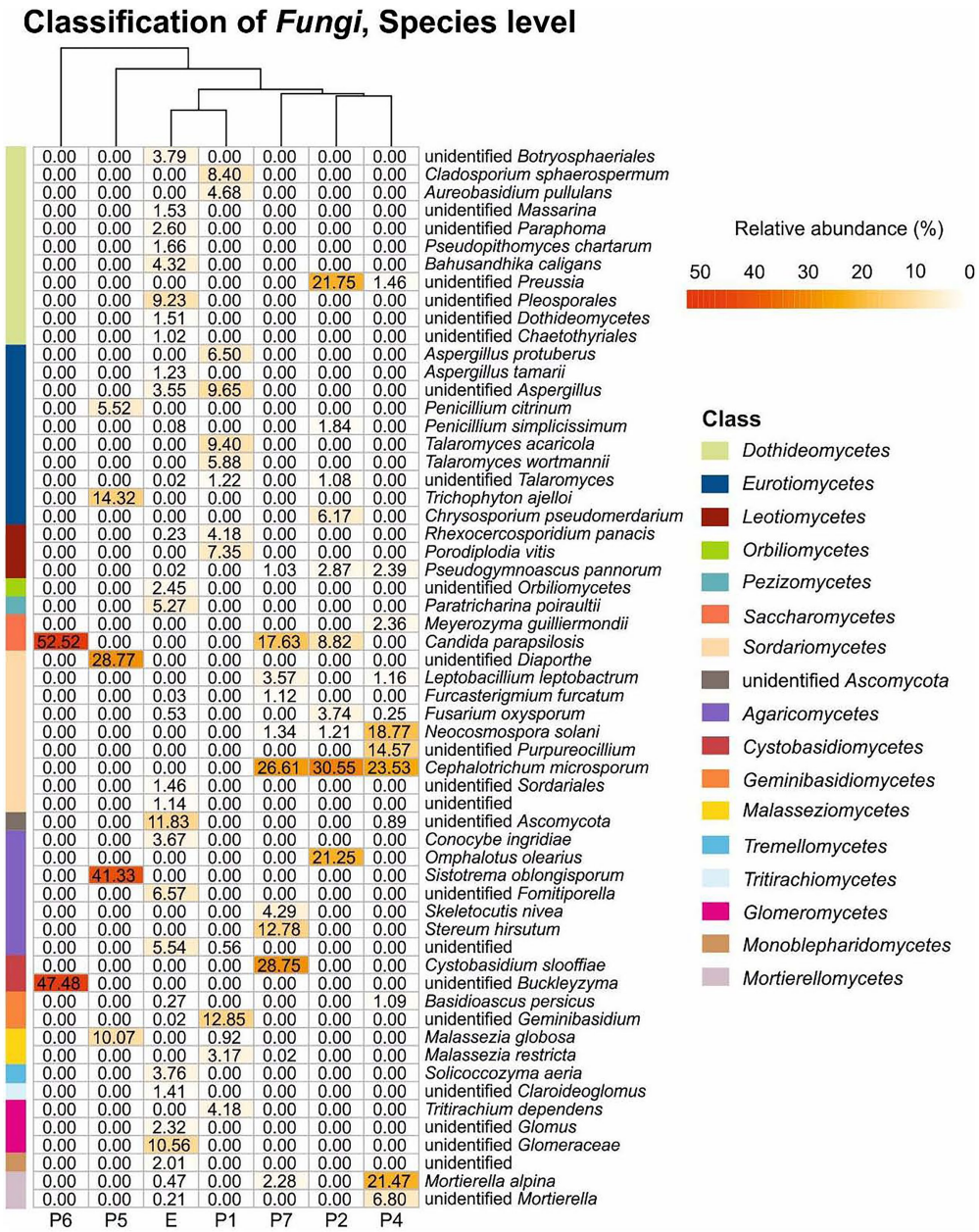

FIGURE 5 | Fungal heat map in Castañar Cave samples. Scales bar show the relative abundance at species level, white squared represents the least abundant species and red the most abundant. Branching patterns on top of each heat map group sediment samples by shared species relative abundance patterns. Bars on the left and the legend on the right indicate the classification at the class level. The species with abundances below 1% are not included.

carcasses found in caves (Karunarathna et al., 2020; Nováková, 2021). In Castañar Cave no bats have been reported, but rodents, geckos and their feces were found. We have detected brushite (hydrated calcium phosphate) in the sediments, a mineral from guano-rich caves (Hill and Forti, 1997; Giurgiu and Tamas, 2013). However, brushite is also excreted by rats (Khan, 1998).

Regarding the most abundant taxa (>10%) found in 2020 (**Figure 5**) 17 taxa stand out. *Candida parapsilosis* was previously isolated from organs and viscera of bats captured in Brazilian urban forests (Ludwig et al., 2023). Other different and abundant *Candida* spp. were isolated from guano and intestinal contents of bats captured in Mexican caves (Ulloa et al., 2006). The occurrence in Castañar Cave is likely associated with the feces of rodents inhabiting the cave.

The genus *Cephalotrichum* seems to be dominant in some caves (Nováková, 2009; Nováková et al., 2018; Vanderwolf et al., 2019). Jiang et al. (2017) isolated 30 strains of *Cephalotrichum* from a Chinese cave, and three were described as new species. *Cephalotrichum microsporum*, a fungus not detected in 2008, was

one of the most abundant in the 2020 sampling (**Supplementary Table S2**; **Figure 5**), and is a saprophytic fungus often reported from animal dung and soils (Heredia et al., 2018; **Supplementary Tables S3**, **S4**). However, its abundance represents a potential risk for the conservation of the cave. As well as *Candida parapsilosis* its presence could be associated with animal dung.

The connection from Sala Nevada to Sala del Jardin (P5) is characterized by the dominance of an unidentified species of *Diaporthe*, followed by *Trichophyton ajelloi*, and *Penicillium citrinum*, among ascomycetes. *Diaporthe* is a genus mainly composed of plant pathogens, responsible for diseases on a wide range of plants, in addition to endophytes and saprobes (Gomes et al., 2013). *Diaporthe* spp. have been isolated from the air in caves from China (Zhang et al., 2017), Brazil (Cunha et al., 2020), Spain (Sanchez-Moral et al., 2021), and from bats in Malaysian caves (Wasti et al., 2020). *Trichophyton ajelloi* (=*Arthroderma uncinatum*) is a geophilic dermatophyte that can cause infections in humans, with a preference for keratin-rich substrates (Zheng et al., 2020). Other *Trichophyton* spp. have been isolated from cave air (Nováková, 2009; Martin-Sanchez et al., 2014; Sanchez-Moral et al., 2021).

Conversely, in the connection from Sala Nevada to Sala del Jardin (P5) the basidiomycetes are composed of *Sistotrema oblongisporum* (41.33%) and *Malassezia globosa* (10.07%). *Sistotrema* spp. have been previously found in mines, always associated with timbers (Eslyn and Lombard, 1983; Held et al., 2020). The presence of these basidiomycetes in the cave could be related with a definite nutrient source, and the most common could be the presence of wood and/or branches fragments. *Malassezia globosa* is a cold-adapted yeast with the ability to survive in extreme conditions (Connell et al., 2014). This species requires lipids for growth and is common in human dandruff and seborrheic dermatitis and may be an indication of human or animal activity (Connell and Staudigel, 2013).

Sala del Jardin (P6) is characterized by the strong relative abundance of two yeasts, *Candida parapsilosis* (*Ascomycota*, *Saccharomycetes*) and an unidentified species of the genus *Buckleyzyma* (*Basidiomycota*, *Cystobasidiomycetes*), both covering 100% of the relative abundance. It has been reported that *Candida parapsilosis* and other yeasts are associated with basidiomycetes (Péter et al., 2017), as we found in Galeria Principal (P2) and Sala Nevada (P7). The genus *Buckleyzyma* comprises species previously placed in the genera *Rhodotorula, Sporobolomyces* and *Bullera* (Wang et al., 2016). Species of *Buckleyzyma* have been isolated from litter (Mašínová et al., 2017), plant leaves and soils (Li et al., 2020), as well as from floor and walls of a winery (Abdo et al., 2020). In most of these environments, *Buckleyzyma* was associated with *Candida, Solicoccozyma, Malassezia, Meyerozyma*, and other yeasts. Species of *Buckleyzyma*, *Candida, Malassezia,* and *Meyerozyma* were found in Castañar Cave and *Solicoccozyma* in the soil outside the cave.

The genus *Preussia* (*Pleosporales, Sporormiaceae*), abundant in the vomit area, Galeria Principal (P2), is widespread on different types of animal dung, and soil, decayed wood, and plant debris. Gonzalez-Menendez et al. (2017) reported that 28 out of 29 species of *Preussia* from the Iberian Peninsula were isolated from dung.

Omphalotus olearius (basidiomycetes) and *Chrysosporium pseudomerdarium* (ascomycetes) only appeared in Galeria Principal (P2). The habitat of *Omphalotus olearius* is olive trees (Castro et al., 2011) in accordance with the extensive olive grove under which the cavity is located. This basidiomycete species clearly point to an origin outside the cave and their transport inside, as it was found near the cave entrance. *Chrysosporium pseudomerdarium* was isolated from soils, caves and bat guano (Nagai et al., 1998; Larcher et al., 2003; Saxena et al., 2004). Most species of *Chrysosporium* are keratinolytic (Bohacz, 2017).

A few basidiomycete species appeared exclusively in Sala Blanca (P7): *Cystobasidium slooffiae* (28.75%), *Stereum hirsutum* (12.78%) and *Skeletocutis nivea* (4.29%). *Sistotrema oblongisporum* is a corticioid fungus, as well as *Stereum hirsutum* and *Skeletocutis nivea*. These fungi are wood-rotting species, common in forest on dead branches and logs (Korhonen et al., 2018). Conversely, *Cystobasidium slooffiae*, previous known as *Rhodotorula slooffiae*, was found on bats in Australian caves (Holz et al., 2018). Sala Blanca (P7), at the end of the trail, is rarely visited but the environmental data indicated an external direct influence. The occurrence of these basidiomycetes could be associated to the connection of Sala Blanca with the exterior. Another basidiomycete, an unidentified *Geminibasidium* occurred in Sala de Entrada with relative abundance of 12.85%, but only 0.02% in the exterior soil. The species of this genus have been isolated from forest soils and rhizosphere (Nguyen et al., 2013; Ren et al., 2021).

Other fungi (*Glomeromycota* phylum), only found in the exterior soil, but not in the cave, were the genera *Glomus*, *Claroideoglomus*, and unidentified members of the family *Glomeraceae*, which are arbuscular mycorrhizal fungi (Pagano, 2016). Their obligate association with plants precludes their presence in the cave.

With low relative abundances there are a few interesting fungi in different locations along the cavity: *Pseudogymnoascus pannorum* and *Leptobacillium leptobactrum*.

Pseudogymnoascus pannorum is a psychrophilic, keratinolytic fungus (Garzoli et al., 2019), closely related to *Pseudogymnoascus destructans*, the causative agent of white-nose syndrome in bats. This is a soil borne fungus occurring worldwide and in caves. The fungus is common in European and North American caves and is adapted to grow between 4 and 15°C (Out et al., 2016; Vanderwolf et al., 2019; Sanchez-Moral et al., 2021).

The saprotrophic fungus *Leptobacillium leptobactrum* was detected in French and German caves (Bastian et al., 2009; Porca et al., 2011; Burow et al., 2019). In Spanish caves, the abundance of *Leptobacillium leptobactrum* and *Leptobacillium symbioticum* amounted 100% of the fungi isolated from the air in some halls (Dominguez-Moñino et al., 2021). This abundance was suggested to be related to their entomopathogenic activity.

Meyerozyma guilliermondii appeared exclusively in Sala Nevada. This is a cold-adapted ascomycete yeast often recorded in Arctic and Antarctic ecosystems (Sannino et al., 2021). *Meyerozyma guilliermondii* occurred in bat guano, in some cases with high isolation frequency (Larcher et al., 2003; Dimkić et al., 2020).

Spatial Distribution of Fungal Communities in Castañar Cave in 2020

In the 2020 sampling, the distribution of 12 fungal phyla in the soil outside the cave (**Figure 4**) is similar to that of forest soils. In fact, Kujawska et al. (2021) reported that in forest soils *Ascomycota* was the most abundant phylum, followed by *Basidiomycota*, *Mucoromycota* and *Mortierellomycota*. However, this diversity was greatly reduced inside the cave, with only two phyla (*Ascomycota* and *Basidiomycota*) in samples P1, P2, P5 and P6, and three phyla (*Ascomycota*, *Basidiomycota* and *Mortierellomycota*) in P4 and P7. This loss of diversity can be attributed, among other factors, to the lack of nutrients inside the cave, as opposite to the forest soil. The loss of diversity inside the cave increased in the inner part of the trail (P5-P6), corresponding to the most stable area with the least energy exchange with the exterior.

The uneven distribution of the phyla *Ascomycota* and *Basidiomycota* across the cave is remarkable. Most ascomycetes have been found in areas well connected to the entrance: Sala de Entrada (P1) and Galeria Principal (P2) or in areas with a high impact of tourist visits such as Sala Nevada (P4; **Figure 1**). Therefore, their presence in the cave is an indirect consequence of the entry of organic matter by three ways: cave animals, human visitors, and airborne spores from outside. The second part of the trail comprises a passage between Sala Nevada and Sala del Jardin (P5), Sala del Jardin (P6), and Sala Blanca (P7; **Figure 1**), where the relative abundances of basidiomycetes increased, especially in P5. The connection from Sala Nevada to Sala del Jardin (P5) is a very narrow passage that in some way separates both trail sides and this kind of isolation could be responsible of the different niches colonized by ascomycete and basidiomycete species.

It is worth mentioning the abundance of *Mortierellomycota* (30.80%) in Sala Nevada (P4), against *Basidiomycota* (1.01%), contrarily to those found in other halls where *Basidiomycota* ranged from 67.75 to 10.72% (**Figure 4**). *Mortierellomycota* was only found in Sala Nevada (P4), in addition to Sala Blanca (P7), where reached 2.42%. Most *Mortierellomycota* are saprobic soil-inhabiting fungi and many *Mortierella alpina* strains have been isolated from agricultural soils (Wagner et al., 2011). Other species of *Mortierella* were found in soil samples near the cave. Species of the genus *Mortierella* are common in soils and occur frequently in cave sediments (Nováková, 2009; Zhang et al., 2014; Man et al., 2018; Nováková et al., 2018).

Inside the cave, the fungal diversity was greater in Sala de Entrada (P1), an ecotone area very close to the entrance, where some roots and animals are frequently observed, as well as in P2, P4 and P7, while in the inner areas (P5 and P6) was low (**Figure 5**). Members of the phyla *Basidiomycota* and *Ascomycota* were found in the soil and Sala de Entrada sediment with high relative abundances. *Glomeromycota* were only found in the soil, as correspond to symbiotic arbuscular mycorrhizal fungi (Pagano, 2016). It was worthy of note the increase of *Basidiomycota* in all cave halls and galleries with respect to the exterior soil, except for Sala Nevada (P4).

It should be noted the high presence of endophytic fungus (*Talaromyces, Porodiplodia vitis, Aureobasidium pullulans*) and fungal species associated with roots and decaying plant material (*Rhexocercosporidium panacis* and *Tritirachium dependens)* in Sala de Entrada (Lu et al., 2014; Vanam et al., 2018; Crous et al., 2019). Therefore, their presence near the entrance was related with roots and the transport of organic matter from outside.

Regarding the ascomycetes, a few fungi were noticeable for their relative abundance: *Candida parapsilosis, Cephalotrichum microsporum*, an unidentified species of the genus *Preussia* and *Neocosmospora solani* were found at different locations along the cavity, while the unidentified species of the genera *Diaporthe* and *Purpureocillium*, as well as *Trichophyton ajelloi* only appeared in Sala Nevada (P4) and/or the connection between Sala Nevada and Sala del Jardin (P5).

Ecological Traits of Fungi

Castañar Cave is a highly radioactive site with peaks above 50 kBq/m^3, but also a low-energy cave with oligotrophic conditions (before the vomit spillage) due to the high isolation level from the outdoor environment. These special conditions could affect fungal communities' development.

Fungi are highly radioresistant when subjected to high doses of ionizing radiation under experimental or accidental conditions (Dadachova and Casadevall, 2008). Chernobyl (Dighton et al., 2008) and the Nevada Test Site (Durrell and Shields, 1960) affected by atmospheric and subterranean nuclear detonations are two reference sites where fungal studies have been carried out. Recently, Fukushima Dai-ichi Nuclear Power Plant was added to the list and it was shown that fungi accumulated high amounts of radiocesium (Fuma et al., 2017). In the literature there are a few papers on the microbial diversity in high ^{222}Rn ecosystems (Anitori et al., 2002; Brugger et al., 2005; Weidler et al., 2007).

In the cave sediments the genera *Preussia*, *Aspergillus*, *Acremonium*, *Mortierella* and *Penicillium* were coincident with those found in Chernobyl as well as the species *Pseudogymnoascus pannorum*, *Neocosmospora solani*, *Fusarium oxysporum*, *Penicillium citrinum*, and *Purpureocillium lilacinum* (Zhdanova et al., 1994, 2000; Egorova et al., 2015). However, all these fungi can be considered as cave inhabitants, either in ionized caves or not, which indicates that these species are relatively tolerant to ionizing radiations.

A number of fungi have been studied in relation to the presence or activity in radioactive sites. Some of them have been found in Castañar Cave. Li et al. (2015) reported the isolation of the yeasts *Meyerozyma* (= *Candida*) *guilliermondii* and *Rhodotorula calyptogenae* from a radioactive waste repository. Shuryak et al. (2017) indicated that fungi were particularly resistant to ionizing radiation. These included *Candida parapsilosis* and *Meyerozyma guilliermondii*, in addition to a few *Aspergillus, Acremonium* and *Chrysosporium* species. The two first yeasts were found in the cave as well as different species of the three last fungal genera.

Zhdanova et al. (2000) detected fungal growth on the buildings of Chernobyl and isolated 37 fungi, from which *Penicillium citrinum*, *Pseudogymnoascus pannorum*, *Neocosmospora solani*, and *Fusarium oxysporum* were also found in the cave. All species, except *Pseudogymnoascus pannorum*, were isolated in locations severely contaminated. According to the authors,

the annual dose received by these fungi is 10^5 times the natural background radiation and they noticed that about 80% of the fungi contained melanin.

Blachowicz et al. (2019) investigated the survival of 12 fungi isolated from Chernobyl to UV-C and simulated Mars conditions. Interestingly, among the fungi were represented *Fusarium oxysporum* and different species of *Acremonium*, *Penicillium* and *Aspergillus*.

Gessler et al. (2014) reported that *Purpureocillium lilacinum* strains isolated from Chernobyl areas had a melanin content 2–2.5 times higher than strains from other areas, concluding that radionuclide contamination changed the fungal communities by increasing the amount of melanized fungi, and Egorova et al. (2015) pointed out that this fungus, was used as a bioindicator of the high level of contamination with radionuclides in Chernobyl soils.

Traxler et al. (2021) proved that non-melanized fungi, non-adapted to high ionizing radiation, can survive, grow and spread in the Chernobyl Exclusion Zone soil, with a high level of ionizing radiation. The authors inoculated a model basidiomycete *Schizophyllum commune* into the soil and confirmed that the fungus was present 1 year after inoculation and could cross 1 m distance within 6 months. The test showed that unadapted fungi can thrive in highly contaminated soils where radiation and heavy metals were present.

In light of our data, a high number of non-melanized fungi thrived in the cave sediments but melanized fungi were scarce. This can be explained because cave fungi do not need melanins to protect from UV radiation.

The ecological traits, as well the niches of the most abundant fungal species in Castañar Cave (from P2 to P7) are summarized in **Supplementary Tables S3** and **S4**. Regarding the potential danger to human health, a few species were human opportunistic fungal pathogens: *Candida parapsilosis*, *Meyerozyma guilliermondii*, *Pseudogymnoascus pannorum*, *Leptobacillium leptobactrum*, *Malassezia globosa*. Almost all the fungi in this cave were saprophytes and endophytes and were isolated from caves and soils. As opposed to that observed in other show caves (Dominguez-Moñino et al., 2021), Castañar Cave presented a low occurrence of entomopathogenic fungi: *Leptobacillium leptobactrum* and *Purpureocillium*, both in areas well connected to the outside.

Other different ecological traits were noticed with the identification of psychrophilic (*Candida parapsilosis*, *Malassezia globosa*, *Pseudogymnoascus pannorum*, *Meyerozyma guilliermondii, Buckleyzyma, Penicillium* sp., *Mortierella, Neocosmospora solani, Fusarium oxysporum, Preussia* sp.), keratinolytic (*Trichophyton ajelloi, Pseudogymnoascus pannorum*, *Chrysosporium pseudomerdarium*, *Penicillium* spp., *Neocosmospora solani*, *Candida parapsilosis*, *Penicillium citrinum*, *Talaromyces*), or coprophilous and/or guano-inhabitant taxa (*Mortierella alpina*, *Preussia* sp., *Penicillium citrinum*, *Chrysosporium pseudomerdarium*, *Meyerozyma guilliermondii*, *Candida parapsilosis, Talaromyces* spp., *Cephalotrichum microsporum*).

In general, most fungi retrieved are typical soil-borne fungi and widespread in nature (e.g., *Purpureocillium lilacinum*, *Penicillium decumbens*, *Neocosmospora solani*, *Chaetomium globosum*, *Pochonia chlamydosporia*, *Cephalotrichum stemonitis*, *Cephalotrichum microsporum*, *Penicillium citrinum*, *Cladosporium cladosporioides*, *Cladosporium sphaerospermum*, *Aspergillus ustus*, etc.; Domsch et al., 2007).

CONCLUSION

The mycobiota of Castañar Cave is defined by the input of organic matter from anthropogenic and animal sources (including dung). It is hypothesized that ecologically distinct niches were created in the cave by the input of diverse types of organic matter, under different environmental conditions and mineral substrata. These niches may account for certain fungal species being present or absent along the cave. The zones well connected to the exterior and Sala Nevada with high impact of tourist visits host copiotrophic fungal species while those thriving in the inner zones occurred under relatively oligotrophic conditions. Under these limited conditions, we observed occasional fungal inhabitants because of the entry of foreign organic matter during visits. The loss of diversity inside the cave increased in the inner part corresponding to the most stable area with the least energy exchange with the exterior.

Regarding persistence, the occurrence of *Neocosmospora solani* in all samplings from 2008 till 2020 is noteworthy since it has been widely reported in relation to cave outbreaks. In addition, this fungus is usually a very abundant soil inhabitant and is able of taking advantage of any disturbance to over develop, as it made during the vomit spillage. An additional attention merits the abundance of *Cephalotrichum microsporum* along the cave. This and other abundant taxa should be controlled.

Fungi previously reported in highly radioactive environments were also found in Castañar Cave, but the effect of high ^{222}Rn on these fungi is not conclusive taking into account that the diversity is similar to that found in other caves with relatively low ^{222}Rn concentrations.

DATA AVAILABILITY STATEMENT

The datasets presented in this study can be found in online repositories. The name of the repository and accession number can be found in the article.

AUTHOR CONTRIBUTIONS

TM-P, AN, and VJ: samplings and microbial analyses. AF-C, SS-M, and SC: environmental analyses. TM-P and CS-J: writing of the manuscript with support from SS-M and AF-C. SS-M and CS-J: research coordination and funding. All authors have contributed to the scientific discussion of the data and agreed to the submitted version of the manuscript.

FUNDING

This research was supported by the Spanish Ministry of Science and Innovation through project PID2019-110603RB-I00 and

the collaboration of PID2020-114978GB-I00 project, MCIN/AEI/FEDER, UE/10.13039/501100011033.

ACKNOWLEDGMENTS

The authors acknowledge to CSIC Open Access Publication Support Initiative through its Unit of Information Resources for Research (URICI), and CSIC Interdisciplinary Thematic Platform Open Heritage: Research and Society (PTI-PAIS) for the professional support.

SUPPLEMENTARY MATERIAL

The Supplementary Material for this article can be found online at: https://www.frontiersin.org/articles/10.3389/fmicb.2022.869661/full#supplementary-material

REFERENCES

Abdo, H., Catacchio, C. R., Ventura, M., D'Addabbo, P., Alexandre, H., Guilloux-Bénatier, M., et al. (2020). The establishment of a fungal consortium in a new winery. *Sci. Rep.* 10:7962. doi: 10.1038/s41598-020-64819-2

Alonso-Zarza, A. M., and Martin-Perez, A. (2008). Dolomite in caves: recent dolomite formation in oxic, non-sulfate environments. Castañar Cave, Spain. *Sediment. Geol.* 205, 160–164. doi: 10.1016/j.sedgeo.2008.02.006

Alonso-Zarza, A. M., Martín-Pérez, A., Martín-García, R., Gil-Peña, I., Meléndez, A., Martínez-Flores, E., et al. (2011). Structural and host rock controls on the distribution, morphology and mineralogy of speleothems in the Castañar Cave (Spain). *Geol. Mag.* 148, 211–225. doi: 10.1017/S0016756810000506

Anitori, R. P., Trott, C., Saul, D. J., Bergquist, P. L., and Walter, H. R. (2002). A culture-independent survey of the bacterial community in a radon hot spring. *Astrobiology* 2, 255–270. doi: 10.1089/153110702762027844

Bastian, F., Alabouvette, C., and Saiz-Jimenez, C. (2009). The impact of arthropods on fungal community structure in Lascaux Cave. *J. Appl. Microbiol.* 106, 1456–1462. doi: 10.1111/j.1365-2672.2008.04121.x

Blachowicz, A., Chiang, A. J., Elsaesser, A., Kalkum, M., Ehrenfreund, P., Stajich, J. E., et al. (2019). Proteomic and metabolomic characteristics of extremophilic fungi under simulated mars conditions. *Front. Microbiol.* 10:1013. doi: 10.3389/fmicb.2019.01013

Bohacz, J. (2017). Biodegradation of feather waste keratin by a keratinolytic soil fungus of the genus *Chrysosporium* and statistical optimization of feather mass loss. *World J. Microbiol. Biotechnol.* 33:13. doi: 10.1007/s11274-016-2177-2

Bolyen, E., Rideout, J. R., Dillon, M. R., Bokulich, N. A., Abnet, C., Al-Ghalith, G. A., et al. (2019). Reproducible, interactive, scalable, and extensible microbiome data science using QUIIME 2. *Nat. Biotechnol.* 37, 852–857. doi: 10.1038/s41587-019-0209-9

Brugger, J., Long, N., McPhail, D. C., and Plimer, I. (2005). An active amagmatic hydrothermal system: the Paralana hot springs, northern Flinders ranges, South Australia. *Chem. Geol.* 222, 35–64. doi: 10.1016/j.chemgeo.2005.06.007

Burow, K., Grawunder, A., Harpke, M., Pietschmann, S., Ehrhardt, R., Wagner, L., et al. (2019). Microbiomes in an acidic rock–water cave system. *FEMS Microbiol. Lett.* 366:fnz167. doi: 10.1093/femsle/fnz167

Callahan, B. J., Mcmurdie, P. J., Rosen, M. J., Han, A. W., Johnson, A. J., and Holmes, S. P. (2016). DADA2 paper supporting information: high-resolution sample inference from amplicon data. *Nat. Methods* 13, 581–583. doi: 10.1038/nmeth.3869

Castro, M. L., Barreiro, F., and Martínez, J. J. (2011). *Omphalotus olearius* (DC.: Fr.) Singer: especie alóctona da micobiota de Galicia (España)? *Mykes* 14, 7–11.

Cigna, A. A. (2005). Radon in caves. *Int. J. Speleol.* 34, 1–18. doi: 10.5038/1827-806X.34.1.1

Connell, L. B., Rodriguez, R. R., Redman, R. S., and Dalluge, J. J. (2014). "Cold-adapted yeasts in Antarctic deserts," in *Cold-Adapted Yeasts*. eds. P. Buzzini and R. Margesin (Heidelberg: Springer), 75–98.

Connell, L., and Staudigel, H. (2013). Fungal diversity in a dark oligotrophic volcanic ecosystem (DOVE) on mount Erebus, Antarctica. *Biology* 2, 798–809. doi: 10.3390/biology2020798

Crous, P. W., Schumacher, R. K., Akulov, A., Thangavel, R., Hernández-Restrepo, M., Carnegie, A. J., et al. (2019). New and interesting fungi. 2. *Fungal Syst. Evol.* 3, 57–134. doi: 10.3114/fuse.2019.03.06

Cunha, A. O. B., Bezerra, J. D. P., Oliveira, T. G. L., Barbier, E., Bernard, E., Machado, A. R., et al. (2020). Living in the dark: bat caves as hotspots of fungal diversity. *PLoS One* 15:e0243494. doi: 10.1371/journal.pone.0243494

Dadachova, E., and Casadevall, A. (2008). Ionizing radiation: how fungi cope, adapt, and exploit with the help of melanin. *Curr. Opin. Microbiol.* 11, 525–531. doi: 10.1016/j.mib.2008.09.013

Degawa, Y., and Gams, W. (2004). A new species of *Mortierella*, and an associated sporangiiferous mycoparasite in a new genus, *Nothadelphia*. *Stud. Mycol.* 50, 567–572.

Dighton, J., Tugay, T., and Zhdanova, N. (2008). Fungi and ionizing radiation from radionuclides. *FEMS Microbiol. Lett.* 281, 109–120. doi: 10.1111/j.1574-6968.2008.01076.x

Dimkić, I., Stanković, S., Kabić, J., Stupar, M., Nenadić, M., Ljaljević-Grbić, M. et al. (2020). Bat guano-dwelling microbes and antimicrobial properties of the pygidial gland secretion of a troglophilic ground beetle against them. *Appl. Microbiol. Biotechnol.* 104, 4109–4126. doi: 10.1007/s00253-020-10498-y

Dominguez-Moñino, I., Jurado, V., Rogerio-Candelera, M. A., Hermosin, B., and Saiz-Jimenez, C. (2021). Airborne fungi in show caves from southern Spain. *Appl. Sci.* 11:5027. doi: 10.3390/app11115027

Domsch, K. H., Gams, W. and Anderson, T.-H. (2007). *Compendium of Soil Fungi. 2nd Edn*. Eching: IHW-Verlag.

Dupont, J., Jacquet, C., Dennetiere, B., Lacoste, S., Bousta, F., Orial, G., et al. (2007). Invasion of the French Paleolithic painted cave of Lascaux by members of the *Fusarium solani* species complex. *Mycologia* 99, 526–533. doi: 10.1080/15572536.2007.11832546

Durrell, L. W., and Shields, L. M. (1960). Fungi isolated in culture from soils of the Nevada test site. *Mycologia* 52, 636–641. doi: 10.2307/3756096

Egorova, A. S., Gessler, N. N., Ryasanova, L. P., Kulakovskaya, T. V., and Belozerskaya, T. A. (2015). Stress resistance mechanisms in the indicator fungi from highly radioactive Chernobyl zone sites. *Microbiology* 84, 152–158. doi: 10.1134/S0026261715020034

Eslyn, W. E., and Lombard, F. F. (1983). Decay in mine timbers. Part II. Basidiomycetes associated with decay of coal mine timbers. *Forest Prod. J.* 33, 19–23.

Fernandez-Cortes, A., Sanchez-Moral, S., Cuezva, S., Benavente, D., and Abella, R. (2011). Characterization of tracer gases fluctuations on a "low energy" cave (Castañar de Ibor, Spain) using techniques of entropy of curves. *Int. J. Climatol.* 31, 127–143. doi: 10.1002/joc.2057

Fernandez-Cortes, A., Sanchez-Moral, S., Cuezva, S., Cañaveras, J. C., and Abella, R. (2009). Annual and transient signatures of gas exchange and transport in the Castañar de Ibor cave (Spain). *Int. J. Speleol.* 38, 153–162. doi: 10.5038/1827-806X.38.2.6

Fuma, S., Ihara, S., Takahashi, H., Inaba, O., Sato, Y., Kubota, Y., et al. (2017). Radiocaesium contamination and dose rate estimation of terrestrial and freshwater wildlife in the exclusion zone of the Fukushima Dai-ichi nuclear power plant accident. *J. Environ. Radioac.* 171, 176–188. doi: 10.1016/j.jenvrad.2017.02.013

Garcia-Guinea, J., Fernandez-Cortes, A., Alvarez-Gallego, M., Garcia-Antón, E., Casas-Ruiz, M., Blázquez-Pérez, D., et al. (2013). Leaching of uranyl–silica complexes from the host metapelite rock favoring high radon activity of subsoil air: case of Castañar cave (Spain). *J. Radioanal. Nucl. Chem.* 298, 1567–1585. doi: 10.1007/s10967-013-2587-7

Garzoli, L., Riccucci, M., Patriarca, E., Debernardi, P., Boggero, A., Pecoraro, L., et al. (2019). First isolation of *Pseudogymnoascus destructans*, the fungal causative agent of white-nose disease, in bats from Italy. *Mycopathologia* 184, 637–644. doi: 10.1007/s11046-019-00371-6

Gessler, N. N., Egorova, A. S., and Belozerskaya, T. A. (2014). Melanin pigments of fungi under extreme environmental conditions (review). *Appl. Biochem. Microbiol.* 50, 105–113. doi: 10.1134/S0003683814020094

Giurgiu, A., and Tamas, T. (2013). Mineralogical data on bat guano deposits from three Romanian caves. *Studia UBB Geol.* 58, 13–18. doi: 10.5038/1937-8602.58.2.2

Gomes, R. R., Glienke, C., Videira, S. I. R., Lombard, L., Groenewald, J. Z., and Crous, P. W. (2013). *Diaporthe*: a genus of endophytic, saprobic and plant pathogenic fungi. *Persoonia* 31, 1–41. doi: 10.3767/003158513X666844

Gonzalez-Menendez, V., Martin, J., Siles, J. A., Gonzalez-Tejero, M. R., Reyes, F., Platas, G., et al. (2017). Biodiversity and chemotaxonomy of *Preussia* isolates from the Iberian Peninsula. *Mycol. Prog.* 16, 713–728. doi: 10.1007/s11557-017-1305-1

Held, B. W., Salomon, C. E., and Blanchette, R. A. (2020). Diverse subterranean fungi of an underground iron ore mine. *PLoS One* 15:e0234208. doi: 10.1371/journal.pone.0234208

Heredia, G., Arias-Mota, R. M., Mena-Portales, J., and Castañeda-Ruiz, R. F. (2018). Saprophytic synnematous microfungi. New records and known species for Mexico. *Rev. Mex. Biodivers.* 89, 604–618. doi: 10.22201/ib.20078706e.2018.3.2352

Hill, C. A., and Forti, P. (1997). *Cave Minerals of the World. 2nd Edn*. Huntsville: National Speleological Society.

Holz, P. H., Lumsden, L. F., Marenda, M. S., Browning, G. F., and Hufschmid, J. (2018). Two subspecies of bent-winged bats (*Miniopterus orianae bassanii* and *oceanensis*) in southern Australia have diverse fungal skin flora but not *Pseudogymnoascus destructans*. *PLoS One* 13:e0204282. doi: 10.1371/journal.pone.0204282

Jiang, J.-R., Cai, L., and Liu, F. (2017). Oligotrophic fungi from a carbonate cave, with three new species of *Cephalotrichum*. *Mycology* 8, 164–177. doi: 10.1080/21501203.2017.1366370

Jurado, V., Del Rosal, Y., Liñan, C., Martin-Pozas, T., Gonzalez-Pimentel, J. L., and Saiz-Jimenez, C. (2021). Diversity and seasonal dynamics of airborne fungi in Nerja Cave, Spain. *Appl. Sci.* 11:6236. doi: 10.3390/app11136236

Jurado, V., Porca, E., Cuezva, S., Fernandez-Cortes, A., Sanchez-Moral, S., and Saiz-Jimenez, C. (2010). Fungal outbreak in a show cave. *Sci. Total Environ.* 408, 3632–3638. doi: 10.1016/j.scitotenv.2010.04.057

Karunarathna, S. C., Dong, Y., Karasaki, S., Tibpromma, S., Hyde, K. D., Lumyong, S., et al. (2020). Discovery of novel fungal species and pathogens on bat carcasses in a cave in Yunnan Province, China. *Emerg. Microbes Infect.* 9, 1554–1566. doi: 10.1080/22221751.2020.1785333

Khan, S. R. (1998). "Phosphate urolithiasis, rat," in *Urinary System. Monographs on Pathology of Laboratory Animals*. eds. T. C. Jones, G. C. Hard and U. Mohr (Berlin: Springer), 451–456.

Korhonen, A., Seelan, J. S. S., and Miettinen, O. (2018). Cryptic species diversity in polypores: the *Skeletocutis nivea* species complex. *MycoKeys* 36, 45–82. doi: 10.3897/mycokeys.36.27002

Kujawska, B., Rudawska, M., Wilgan, R., and Leski, T. (2021). Similarity and differences among soil fungal assemblages in managed forests and formerly managed forest reserves. *Forests* 12:353. doi: 10.3390/f12030353

Larcher, G., Bouchara, J. P., Pailley, P., Montfort, D., Behuin, H., De Bièvre, C., et al. (2003). Fungal biota associated with bats in Western France. *J. Med. Mycol.* 13, 29–34.

Lario, J., Sanchez-Moral, S., Cuezva, S., Taborda, M., and Soler, V. (2006). High ^{222}Rn levels in a show cave (Castañar de Ibor, Spain): proposal and application on management measures to minimize the effects on guides and visitors. *Atmos. Environ.* 40, 7395–7400. doi: 10.1016/j.atmosenv.2006.06.046

Li, C.-C., Chung, H.-P., Wen, H.-W., Chang, C.-Y., Wang, Y.-T., and Chou, F.-I. (2015). The radiation resistance and cobalt biosorption activity of yeast strains isolated from the Lanyu low-level radioactive waste repository in Taiwan. *J. Environ. Radioact.* 146, 80–87. doi: 10.1016/j.jenvrad.2015.04.010

Li, A.-H., Yuan, F.-X., Groenewald, M., Bensch, K., Yurkov, A. M., Li, K., et al. (2020). Diversity and phylogeny of basidiomycetous yeasts from plant leaves and soil: proposal of two new orders, three new families, eight new genera and one hundred and seven new species. *Stud. Mycol.* 96, 17–140. doi: 10.1016/j.simyco.2020.01.002

Lu, X. H., Chen, A. J., Zhang, X. S., Jiao, X. L., and Gao, W. W. (2014). First report of *Rhexocercosporidium panacis* causing rusty root of *Panax ginseng* in northeastern China. *Plant Dis.* 98:1580. doi: 10.1094/PDIS-01-14-0082-PDN

Ludwig, L., Muraoka, J. Y., Bonacorsi, C., and Donofrio, F. C. (2023). Diversity of fungi obtained from bats captured in urban forest fragments in Sinop, Mato Grosso, Brazil. *Braz. J. Biol.* 83:e247993. doi: 10.1590/1519-6984.247993

Man, B., Wang, H., Yun, Y., Xiang, X., Wang, R., Duan, Y., et al. (2018). Diversity of fungal communities in Heshang Cave of Central China revealed by mycobiome-sequencing. *Front. Microbiol.* 9:1400. doi: 10.3389/fmicb.2018.01400

Martin-Sanchez, P. M., Jurado, V., Porca, E., Bastian, F., Lacanette, D., Alabouvette, C., et al. (2014). Aerobiology of Lascaux Cave (France). *Int. J. Speleol.* 43, 295–303. doi: 10.5038/1827-806X.43.3.6

Mašínová, T., Bahnmann, B. D., Větrovský, T., Tomšovský, M., Merunková, K., and Baldrian, P. (2017). Drivers of yeast community composition in the litter and soil of a temperate forest. *FEMS Microbiol. Ecol.* 93:fiw223. doi: 10.1093/femsec/fiw223

McMurdie, P. J., and Holmes, S. (2013). Phyloseq: an R package for reproducible interactive analysis and graphics of microbiome census data. *PLoS One* 8:e61217. doi: 10.1371/journal.pone.0061217

Nagai, K., Suzuki, K., and Okada, G. (1998). Studies on the distribution of alkalophilic and alkali-tolerant soil fungi II: fungal flora in two limestone caves in Japan. *Mycoscience* 39, 293–298. doi: 10.1007/BF02464011

Nguyen, H. D., Nickerson, N. L., and Seifert, K. A. (2013). *Basidioascus* and *Geminibasidium*: a new lineage of heat-resistant and xerotolerant basidiomycetes. *Mycologia* 105, 1231–1250. doi: 10.3852/12-351

Nováková, A. (2009). Microscopic fungi isolated from the Domica cave system (Slovak karst National Park, Slovakia). A review. *Int. J. Speleol.* 38, 71–82. doi: 10.5038/1827-806X.38.1.8

Nováková, A. (2021). Výskyt hub v jeskyních a jiných podzemních prostorách Slovenské republiky (Fungal occurrence in caves and other underground spaces in the Slovak Republic). *Acta Carsologica Slovaca* 59, 5–58.

Nováková, A., Hubka, V., Valinová, S., Kolařík, M., and Hillebrand-Voiculescu, A. M. (2018). Cultivable microscopic fungi from an underground chemosynthesis-based ecosystem: a preliminary study. *Folia Microbiol.* 63, 43–55. doi: 10.1007/s12223-017-0527-6

Out, B., Boyle, S., and Cheeptham, N. (2016). Identification of fungi from soil in the Nakimu caves of glacier National Park. *UJEMI+* 2, 26–32.

Pagano, M.C. (2016). *Recent Advances on Mycorrhizal Fungi*. Cham: Springer.

Péter, G., Takashima, M., and Cadez, N. (2017). "Yeast habitats: different but global," in *Yeasts in Natural Ecosystems: Ecology*. eds. P. Buzzini, M.-A. Lachance and A. Yurkov (Cham: Springer), 39–71.

Popkova, A. V., and Mazina, S. E. (2019). Microbiota of hypogean habitats in Otap Head Cave. *J. Environ. Res. Eng. Manag.* 75, 71–82. doi: 10.5755/j01.erem.75.3.21106

Porca, E., Jurado, V., Martin-Sanchez, P. M., Hermosin, B., Bastian, F., Alabouvette, C., et al. (2011). Aerobiology: an ecological indicator for early detection and control of fungal outbreaks in caves. *Ecol. Indic.* 11, 1594–1598. doi: 10.1016/j.ecolind.2011.04.003

Ren, H., Wang, H., Yu, Z., Zhang, S., Qi, X., Sun, L., et al. (2021). Effect of two kinds of fertilizers on growth and rhizosphere soil properties of bayberry with decline disease. *Plan. Theory* 10:2386. doi: 10.3390/plants10112386

Romsdahl, J., Blachowicz, A., Chiang, A. J., Singh, N., Stajich, J. E., Kalkum, M., et al. (2018). Characterization of *Aspergillus niger* Isolated from the International Space Station. *mSystems* 3, e00112–e00118. doi: 10.1128/mSystems.00112-18

Sanchez-Moral, S., Jurado, V., Fernandez-Cortes, A., Cuezva, S., Martin-Pozas, T., Gonzalez-Pimentel, J. L., et al. (2021). Environment-driven control of fungi in subterranean ecosystems: the case of La Garma cave (northern Spain). *Int. Microbiol.* 24, 573–591. doi: 10.1007/s10123-021-00193-x

Sannino, C., Borruso, L., Mezzasoma, A., Battistel, D., Ponti, S., Turchetti, B., et al. (2021). Abiotic factors affecting the bacterial and fungal diversity of permafrost in a rock glacier in the Stelvio Pass (Italian Central Alps). *Appl. Soil Ecol.* 166:104079. doi: 10.1016/j.apsoil.2021.104079

Saxena, P., Kumar, A., and Shrivastava, J. N. (2004). Diversity of keratinophilic mycoflora in the soil of Agra (India). *Folia Microbiol.* 49, 430–434. doi: 10.1007/BF02931605

Shuryak, I., Matrosova, V. Y., Gaidamakova, E. K., Tkavc, R., Grichenko, O., Klimenkova, P., et al. (2017). Microbial cells can cooperate to resist high-level chronic ionizing radiation. *PLoS One* 12:e0189261. doi: 10.1371/journal.pone.0189261

Siasou, E., Johnson, D., and Willey, N. J. (2017). An extended dose–response model for microbial responses to ionizing radiation. *Front. Environ. Sci.* 5:6. doi: 10.3389/fenvs.2017.00006

Somlai, J., Hakl, J., Kávási, N., Szeiler, G., Szabó, P., and Kovács, T. (2011). Annual average radon concentration in the show caves of Hungary. *J. Radioanal. Nucl. Chem.* 287, 427–433. doi: 10.1007/s10967-010-0841-9

Traxler, L., Wollenberg, A., Steinhauser, G., Chyzhevskyi, I., Dubchak, S., Großmann, S., et al. (2021). Survival of the basidiomycete *Schizophyllum commune* in soil under hostile environmental conditions in the Chernobyl exclusion zone. *J. Hazard. Mater.* 403:124002. doi: 10.1016/j.jhazmat.2020.124002

Turenne, C. Y., Sanche, S. E., Hoban, D. J., Karlowsky, J. A., and Kabani, A. M. (1999). Rapid identification of fungi by using the ITS2 genetic region and an automated fluorescent capillary electrophoresis system. *J. Clin. Microbiol.* 37, 1846–1851. doi: 10.1128/JCM.37.6.1846-1851.1999

Ulloa, M., Lappe, P., Aguilar, S., Park, H., Pérez-Mejía, A., Toriello, C., et al. (2006). Contribution to the study of the mycobiota present in the natural habitats of *Histoplasma capsulatum*: an integrative study in Guerrero, Mexico. *Rev. Mex. Biodivers.* 77, 153–168.

UNITE Community (2019). UNITE QIIME release for fungi. Version 18.11.2018. 10.15156/BIO/786334.

Urbaniak, C., van Dam, P., Zaborin, A., Zaborina, O., Gilbert, J. A., Torok, T., et al. (2019). Genomic characterization and virulence potential of two *Fusarium oxysporum* isolates cultured from the International Space Station. *mSystems 4*, e00345–e00318. doi: 10.1128/mSystems.00345-18

Van Houdt, R., Mijnendonckx, K., and Leys, N. (2012). Microbial contamination monitoring and control during human space missions. *Planet. Space Sci.* 60, 115–120. doi: 10.1016/j.pss.2011.09.001

Vanam, H. P., Rao, P. N., Mohanran, K., Yegneswaran, P. P., and Rudramurthy, S. P. M. (2018). Distal lateral subungual onychomycosis owing to *Tritirachium oryzae*: A bystander or invader? *Mycopathologia* 183, 459–463. doi: 10.1007/s11046-017-0226-5

Vanderwolf, K. J., Malloch, D., and McAlpine, D. F. (2019). No change detected in culturable fungal assemblages on cave walls in eastern Canada with the introduction of *Pseudogymnoascus destructans*. *Diversity* 11:222. doi: 10.3390/d11120222

Wagner, L., Stielow, B., Hoffmann, K., Petkovits, T., Papp, T., Vágvölgyi, C., et al. (2011). Molecular characterization of airborne fungi in caves of the Mogao grottoes, Dunhuang, China. *Int. Biodeter. Biodegr.* 65, 726–731. doi: 10.1016/j.ibiod.2011.04.006

Wang, Q.-M., Yurkov, A. M., Göker, M., Lumbsch, H. T., Leavitt, S. D., Groenewald, M., et al. (2016). Phylogenetic classification of yeasts and related taxa within *Pucciniomycotina*. *Stud. Mycol.* 81, 149–189. doi: 10.1016/j.simyco.2015.12.002

Wasti, I. G., Fui, F. S., Zhi, T. Q., Mun, C. W., Kassim, M. H. S., Dawood, M. M., et al. (2020). Fungi from dead arthropods and bats of Gomantong cave, northern Borneo, Sabah (Malaysia). *J. Cave Karst Stud.* 82, 261–275. doi: 10.4311/2019MB0146

Weidler, G. W., Dornmayr-Pfaffenhuemer, M., Gerbl, F. W., Heinen, W., and Stan-Lotter, H. (2007). Communities of archaea and bacteria in a subsurface radioactive thermal spring in the Austrian Central Alps, and evidence of ammonia-oxidizing Crenarchaeota. *Appl. Environ. Microbiol.* 73, 259–270. doi: 10.1128/AEM.01570-06

White, T. J., Bruns, T., Lee, S., and Taylor, J. (1990). "Amplification and direct sequencing of fungal ribosomal RNA genes for phylogenetics," in *PCR Protocols: A Guide to Methods and Applications*. eds. M. A. Innis, D. H. Gelfand, J. J. Sninsky and T. J. White (London: Academic Press), 315–322.

Zhang, Z. F., Liu, F., Zhou, X., Liu, X. Z., Liu, S. J., and Cai, L. (2017). Culturable mycobiota from karst caves in China, with descriptions of 20 new species. *Persoonia* 39, 1–31. doi: 10.3767/persoonia.2017.39.01

Zhang, T., Victor, T. R., Rajkumar, S. S., Li, X., Okoniewski, J. C., Hicks, A. C., et al. (2014). Mycobiome of the bat white nose syndrome affected caves and mines reveals diversity of fungi and local adaptation by the fungal pathogen *Pseudogymnoascus* (*Geomyces*) *destructans*. *PLoS One* 9:e108714. doi: 10.1371/journal.pone.0108714

Zhdanova, N. N., Vasilevskaya, A. I., Lashko, T. N., Gavrilyuk, V. I., and Dighton, J. (1994). Changes in micromycetes communities in soil in response to pollution by long-lived radionuclides emitted in the Chernobyl accident. *Mycol. Res.* 98, 789–795. doi: 10.1016/S0953-7562(09)81057-5

Zhdanova, N. N., Zakharchenko, V. A., Vember, V. V., and Nakonechnaya, L. T. (2000). Fungi from Chernobyl: mycobiota of the inner regions of the containment structures of the damaged nuclear reactor. *Mycol. Res.* 104, 1421–1426. doi: 10.1017/S0953756200002756

Zheng, H., Blechert, O., Mei, H., Ge, L., Liu, J., Tao, Y., et al. (2020). Assembly and analysis of the whole genome of *Arthroderma uncinatum* strain T10, compared with *Microsporum canis* and *Trichophyton rubrum*. *Mycoses* 63, 683–693. doi: 10.1111/myc.13079

Conflict of Interest: The authors declare that the research was conducted in the absence of any commercial or financial relationships that could be construed as a potential conflict of interest.

Publisher's Note: All claims expressed in this article are solely those of the authors and do not necessarily represent those of their affiliated organizations, or those of the publisher, the editors and the reviewers. Any product that may be evaluated in this article, or claim that may be made by its manufacturer, is not guaranteed or endorsed by the publisher.

frontiers | Frontiers in Microbiology

ORIGINAL RESEARCH
published: 16 May 2022
doi: 10.3389/fmicb.2022.907816

Streptomyces benahoarensis sp. nov. Isolated From a Lava Tube of La Palma, Canary Islands, Spain

Jose L. Gonzalez-Pimentel[1], *Bernardo Hermosin*[2], *Cesareo Saiz-Jimenez*[2] *and Valme Jurado*[2*]

[1] *HERCULES Laboratory, Evora University, Evora, Portugal,* [2] *Instituto de Recursos Naturales y Agrobiologia, Consejo Superior de Investigaciones Cientificas (IRNAS-CSIC), Sevilla, Spain*

Two *Streptomyces* strains, labeled as MZ03-37^T and MZ03-48, were isolated from two different samples, a mucolite-type speleothem and a microbial mat on the walls of a lava tube from La Palma Island (Canary Islands). Phylogenetic analysis based on concatenated sequences of six housekeeping genes indicated that both strains belonged to the same species. The closest relatives for both strains were *Streptomyces palmae* CMU-AB204^T (98.71%), *Streptomyces catenulae* NRRL B-2342^T (98.35%), and *Streptomyces ramulosus* NRRL B-2714^T (98.35%). Multi-locus sequence analysis (MLSA), based on five house-keeping gene alleles (i.e., *atpD, gyrB, recA, rpoB,* and *trpB*), indicated that both isolated strains were closely related to *S. catenulae* NRRL B-2342^T. Whole-genome average nucleotide identity (ANI) scores of both strains were in the threshold value for species delineation with the closest species. Both strains presented a G+C content of 72.1 mol%. MZ03-37^T was light brown in substrate and white in aerial mycelium, whereas MZ03-48 developed a black aerial and substrate mycelium. No pigment diffusion was observed in both strains. They grew at 10°C–37°C (optimum 28°C–32°C) and in the presence of up to 15% (w/v) NaCl. MZ03-37^T grew at pH 5–10 (optimal 6–9), whereas MZ03-48 grew at pH 4–11 (optimal 5–10). LL-Diaminopimelic acid was the main diamino acid identified. The predominant fatty acids in both strains were iso-$C_{16:0}$, anteiso-$C_{15:0}$, $C_{16:0}$, and iso-$C_{14:0}$. The major isoprenoid quinones were MK-9(H6) and MK-9(H8), and the main polar lipids were aminolipid, phospholipid, and phosphoglycolipid. *In silico* analyses for functional annotation predicted the presence of gene clusters involved in resistome mechanisms and in the synthesis of described antimicrobials such as linocin-M18 and curamycin, as well as different genes likely involved in mechanisms for active compound synthesis, both already described and not discovered so far. On the basis of their phylogenetic relatedness and their phenotypic and genotypic features, the strains MZ03-37^T and MZ03-48 represented a novel species within the genus *Streptomyces*, for which the name *Streptomyces benahoarensis* sp. nov. is proposed. The type strain is MZ03-37^T (= CECT 9805 = DSMZ 8002); and MZ03-48 (= CECT 9806 = DSMZ 8011) is a reference strain.

Keywords: ***Streptomyces benahoarensis*, lava tube, polyphasic taxonomy, resistome, antimicrobials**

OPEN ACCESS

Edited by:
Rafael Rivilla, Autonomous University of Madrid, Spain

Reviewed by:
Esther Menendez, University of Salamanca, Spain
Lorena Fernández-Martínez, Edge Hill University, United Kingdom

***Correspondence:**
Valme Jurado
v.jurado@csic.es

Specialty section:
This article was submitted to Terrestrial Microbiology, a section of the journal Frontiers in Microbiology

Received: *30 March 2022*
Accepted: *20 April 2022*
Published: *16 May 2022*

Citation:
Gonzalez-Pimentel JL, Hermosin B, Saiz-Jimenez C and Jurado V (2022) Streptomyces benahoarensis sp. nov. Isolated From a Lava Tube of La Palma, Canary Islands, Spain. Front. Microbiol. 13:907816. doi: 10.3389/fmicb.2022.907816

INTRODUCTION

The genus *Streptomyces* was originally proposed by Waksman and Hinrici (1943). It is the most representative genus within the phylum *Actinobacteria* with more than 800 described species and subspecies (http://www.bacterio.net/streptomyces.html). Besides, the genus *Streptomyces* constitutes roughly 5% of all described bacteria so far. Its versatile metabolism has allowed to colonize diverse and antagonist ecosystems by different members of this group. They are fundamentally aerobics and chemoorganotrophic bacteria, with oxidative metabolism. Its vegetative development generates sporulate ramified mycelia, the reason why *Streptomyces* was considered a transition group between fungi and bacteria (Miyadoh, 1997).

Classification of *Streptomyces* has evolved in the past 100 years starting with the former and shallower morphological study of the substrate and aerial mycelia (Waksman, 1919), achieving later a deeper morphological analysis carried out by the International *Streptomyces* Project ISP (Shirling and Gottlieb, 1966), as well as the inclusion of chemotaxonomic, genetic, and more recently, genomic analyses. Amplification of the 16S rRNA gene is considered the first analysis for genetic analysis (Weisburg et al., 1991), but it is the multi-locus sequence analysis (MLSA), which provides a better resolution to species level relatedness (Guo et al., 2008; Rong and Huang, 2014). The development of platforms for next-generation sequencing has boosted the sequencing of whole genomes allowing the comparison of relative genomes that determine the degree of differentiation among compared genomes. Thus, pairwise genome comparison appeared as a robust method to replace the DNA–DNA hybridization method (Richter and Rosselló-Móra, 2009).

The genus *Streptomyces* is a well-known secondary metabolite producer. In fact, around 80% of current antibiotics are originally obtained from species of *Streptomyces* (Mast and Stegmann, 2018), and also some of them have the capacity to synthesize anti-inflammatory and antitumoral compounds (Barka et al., 2016). Former antibiotics were discovered from soil microorganisms, but new environments have been explored in the last years, as is the case of marine and subterranean environments (Gould, 2016; Tortorella et al., 2018; Rangseekaew and Pathom-Aree, 2019). *In silico* analysis focused on resistome and secondary metabolism mechanisms has been presented as a reliable tool, not only to discover new molecules and differentiate mechanisms involved in drug resistance but also to differentiate species of bacteria with identical 16S rRNA gene sequences (Antony-Babu et al., 2017) as is the case of *Streptomyces*, as well as to identify conserved specialized metabolites, supporting phylogenetic relationships (Vicente et al., 2018).

In this study, two strains, namely, MZ03-37^T and MZ03-48, were isolated from a lava tube (volcanic cave) located on La Palma Island (Canary Islands, Spain). The taxonomic position of the isolates was clarified using a polyphasic approach, which lead to the identification of a new species of the genus *Streptomyces*.

MATERIALS AND METHODS

Bacterial Isolation and Culture Conditions

Strains MZ03-37^T and MZ03-48 were isolated on nutrient agar (NA, BD, Sparks, USA) with 3% of magnesium sulfate and 2% of glycerol at 28°C for 21 days, from two different locations in the lava tube Fuente de la Canaria (latitude: 28°35'25.2"N and longitude: 17°48′01.3"W) located in La Palma Island, Canary Islands (Spain) (Gonzalez-Pimentel et al., 2021). MZ03-37^T was isolated from a light-brown mucolite and MZ03-48 from a dark-brown microbial mat, both sampling sites separated by a distance of 15 m. Morphological, chemotaxonomical, and physiological studies were carried out from cultures on yeast extract-malt extract agar (International *Streptomyces* Project medium no 2, ISP2) at 28°C, except when otherwise indicated.

Phylogenetic and Genome Annotation Analysis

Genomic DNA was extracted by implementing the Marmur method (Marmur, 1961). Amplification of the 16S rRNA gene was carried out using the method described by Laiz et al. (2009). Identification of the closest bacteria was determined using the global alignment algorithm on the EzBioCloud (Yoon et al., 2017). Additionally, the study of MLSA based on five housekeeping genes was carried out: *atpD* (ATP synthase β-subunit), *gyrB* (DNA gyrase β-subunit), *recA* (recombinase A), *rpoB* (RNA polymerase β-subunit), and *trpB* (tryptophan synthase β-subunit). The primers for amplification, PCR conditions, and sequencing of *atpD, recA, rpoB,* and *trpB* genes were described previously by Guo et al. (2008), whereas the primers for *gyrB* were redesigned by Rong et al. (2009). PCR products were sequenced by Macrogen (Seoul, Korea). The identification of closest-related strains was obtained through the BLAST algorithm (Altschul et al., 1990), in the GenBank database by the National Center for Biotechnology Information and the *Streptomyces* MLST database (http://pubmlst.org/streptomyces). Sequences of each gene and the closest-related strains were multiply aligned using MUSCLE (Edgar, 2004). Phylogenetic trees based on concatenated sequences of six housekeeping genes (16S rRNA-*atpD-gyrB-recA-rpoB-trpB*) were constructed using the maximum-likelihood (Felsenstein, 1981), neighbor-joining (Saitou and Nei, 1987), and maximum-parsimony (Kluge and Farris, 1969) methods in MEGA version 6 (Tamura et al., 2013). The tree robustness was evaluated using a bootstrap analysis of 1,000 resamplings.

The company MicrobesNG (Birmingham, UK) was responsible for sequencing genomic DNA in order to assemble the draft genome for both bacteria. Sequencing of genomic DNA of strains MZ03-37^T, MZ03-48, and *Streptomyces palmae* CMU-AB204^T and subsequent assembly was described by Gonzalez-Pimentel et al. (2021). The genome of *Streptomyces ramulosus* NRRL B-2714^T was assembled following the same procedure using the raw data (Ju et al., 2015).

Functional annotation analyses were carried out focusing on the predicted genes by Prokka (Seemann, 2014) and the contigs assembled from sequenced genomes aimed at characterizing

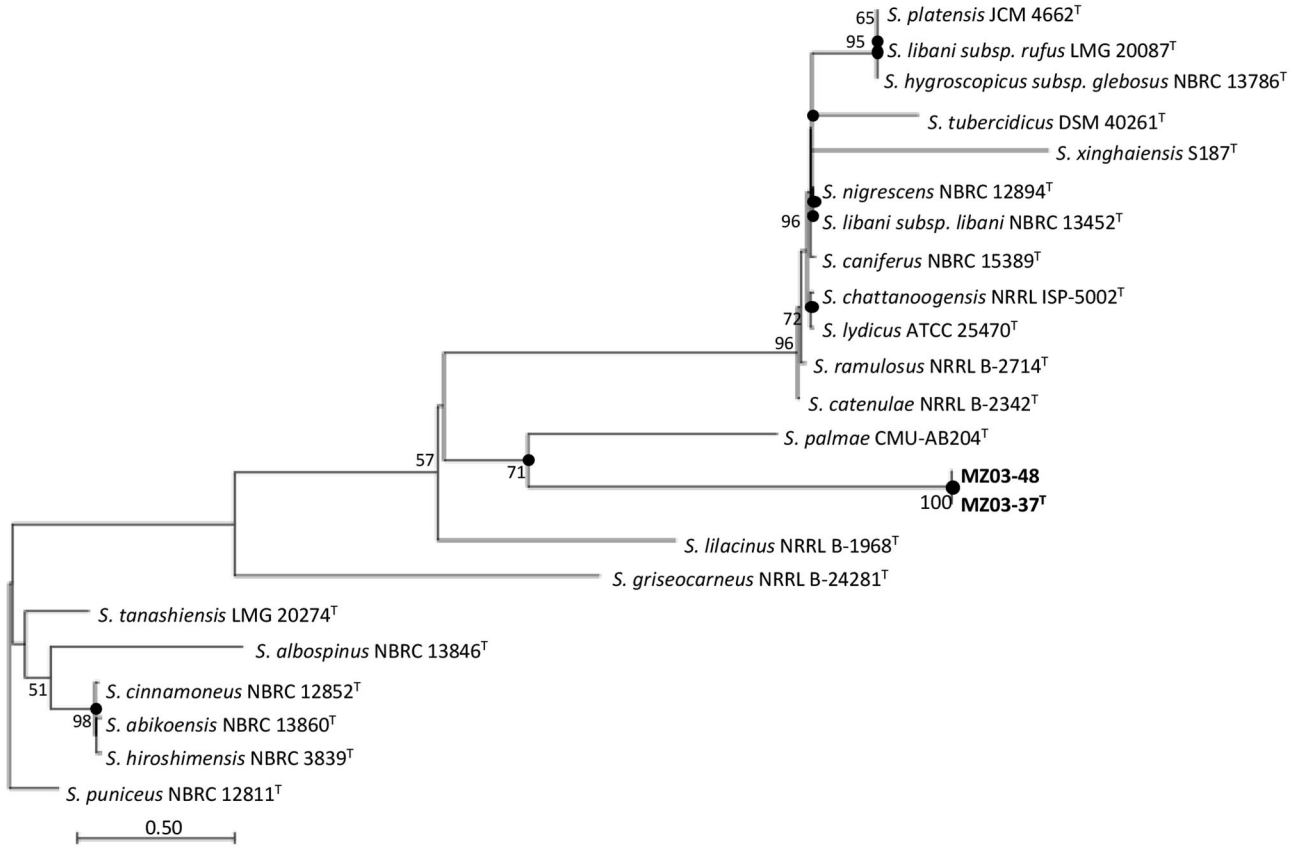

FIGURE 1 | Maximum-likelihood trees based on six-gene concatenated sequences (16S rRNA-atpD-gyrB-recA-rpoB-trpB) showing the relationship of strains MZ03-37T and MZ03-48 and other species of the genus *Streptomyces*. Bootstrap values (N50%) are expressed as percentages of 1,000 replicates. Closed circles show the nodes that were also recovered by the neighbor-joining and maximum-parsimony algorithms. *Streptomyces puniceus* NBRC 12811T was used as the outgroup. Bar, 0.50 substitutions per nucleotide position.

the function of genes and predicting the mechanisms for antimicrobial resistance, also called resistome, as well as the gene clusters involved in the secondary metabolism developed in every bacterium. The tools used for these purposes were Sma3s (Muñoz-Mérida et al., 2014) for functional annotations using the UniProt bacteria database with "uniprot" option, and antiSMASH in strict search mode (Blin et al., 2021) for secondary metabolite biosynthesis gene clusters prediction. Pairwise genome comparison between genomes of MZ03-37^T and MZ03-48 and *S. palmae* CMU-AB204^T, *S. ramulosus* NRRL B-2714^T, and *Streptomyces catenulae* NRRL B-2342^T was assessed calculating the average nucleotide identity (ANI) by means of BLAST+ (ANIb) (Camacho et al., 2008), MUMmer (ANIm) (Kurtz et al., 2004), as well as tetra-nucleotide signature algorithms through JspeciesWS web service (Richter et al., 2016) and orthoANI using EzBioCloud database (Yoon et al., 2017). ANIb, ANIm, and orthoANI establish a 95% threshold under which compared genomes belong to different bacteria, whereas the values above would suggest that compared genomes would belong to strains from the same species. TETRA is based on standardized tetrameric frequencies represented in "*z*-score" values, so fix three values to suggest genomes belong to the same (above 0.999) or different (below 0.989). When obtained *z*-score resulted between these two values, only ANIb, ANIm, and orthoANI values will be considered.

Mauve software for genome segment alignment (Darling et al., 2004) was used to analyze conserved gene clusters involved in curamycin production. R package-based visualization tools were used. Genes involved in pathways and biological processes were plotted by means of the "ggplot2" library, secondary metabolite prediction was represented through a heat map using the "gplots" library, and the "genoPlotR" library was used for genome segment comparison from MAUVE alignment.

The GenBank/EMBL/DDBJ accession numbers for MZ03-37^T, MZ03-48, *S. palmae* CMU-AB204^T, and *S. catenulae* NRRL B-2342^T are VKJP00000000, VKLS00000000, SRID00000000, and JODY00000000, respectively. *S. ramulosus* NRRL B-2714^T draft genome was assembled from the SRA file with accession number SRR7783857, following the same methodology for genome assembly used in this study.

Phenotypic, Morphological, and Chemotaxonomic Features

Comparative studies were carried out in triplicate on ISP2 medium at 28°C for all strains. Spores were observed using light microscopy after 7 days of incubation. International *Streptomyces* Project medium no. 3 (Oatmeal agar), 4 (Inorganic salt starch agar), 5 (Glycerol asparagine agar), 6 (Peptone yeast Iron agar), and 7 (Tyrosine agar) were additionally used for morphological and physiological analyses. Oxidase activity was tested using BBL^{TM}DrySlide^{TM} Oxidase (BD, Sparks, USA). The temperature range for growth was assessed at 5°C, 10°C, 20°C, 25°C, 28°C, 30°C, 32°C, 37°C, and 40°C. Salt tolerance was tested in the presence of 0–15% (w/v) NaCl with increases of 1% on nutrient agar (BD, Sparks, USA). Growth at different pH values was determined on trypticase soy broth and agar plates adjusted to pH 4.0–12.0 (at intervals of 1.0 pH unit) using HCl 1 M and NaOH 1 M solutions. The pH values were verified after autoclaving. Physiological characteristics were determined with API 20NE gallery (bioMérieux, Marcy l'Etoile, France), according to the manufacturer's instructions. The use of sugars as sole carbon sources was checked in a minimal medium containing M9 salts (Savic et al., 2007) and a 1% carbon source (w/v) (Miller, 1992). Cellular fatty acid profiles were analyzed in triplicate after collecting biomass from a culture grown for 3 days on TSA at 30°C following the methodology described by Jurado et al. (2009). Analysis of respiratory quinones and polar lipid composition were carried out by the Deutsche Sammlung von Mikroorganismen und Zellkulturen GmbH (Braunschweig, Germany).

TABLE 1 | Differential characteristics of strains MZ03-37^T, MZ03-48, and related species.

Test	1	2	3	4	5
NaCl concentration for growth:					
6 % (w/v)	+	+	−	+	+
Optimal pH for growth	6–9	5–10	6–9	5–10	5–10
Enzymatic activity:					
Urease	+	+	−	+	+
Arginine dihydrolase	+	−	−	+	−
β-glucosidase	+	+	+	−	+
β-galactosidase	−	−	+	−	+
Oxidase	−	−	+	−	−
Assimilation of:					
Arabinose	−	−	+	−	−
Mannose	+	+	−	+	+
D-mannitol	+	+	−	+	+
D-maltose	−	−	−	+	+
Adipic acid	−	−	+	−	+
Trisodium citrate	+	+	−	−	−
Nitrate reduction	−	−	+	+	−
Growth with sole carbon source (1% p/v):					
Xylose	+	+	−	(+)	+
Mannitol	+	(+)	−	+	+
Diffusible pigment	Not	Not	Not	Dark	Dark
%GC content	72.1	72.1	72.4	73	72.7

Strains: 1, MZ03-37^T; 2, MZ03-48; 3, Streptomyces palmae CMU-AB204^T; 4, Streptomyces catenulae NRRL B-2342^T; 5, Streptomyces ramulosus NRRL B-2714^T. +, positive; (+) weak positive; –, negative.

RESULTS AND DISCUSSION

Phylogenetic, Morphological, and Physiological Analyses

The 16S rRNA gene sequence analysis revealed that strains MZ03-37^T and MZ03-48 were 100% identical among them and most closely related to *S. palmae* CMU-AB204^T (98.70%), *S. ramulosus* NRRL B-2714^T (98.28%), and *S. catenulae* NRRL B-2342^T (98.28%), equal or below the threshold suggested by Yarza et al. (2014) for identifying a new species of bacterium. MLSA analysis showed that *S. palmae* CMU-AB204^T (16S rRNA gene), *S. catenulae* NRRL B-2342^T (*atpD, gyrB, recA,* and *trpB* genes), and *S. ramulosus* (*rpoB* gene) were the closest relatives to MZ03-37^T and MZ03-48. The maximum-likelihood analysis based on concatenated housekeeping genes (**Figure 1**) showed that the closest relative of both strains was *S. palmae* CMU-AB204^T in a group well supported by a 71% bootstrap value. The species *S. catenulae* NRRL B-2342^T and *S. ramulosus* NRRL B-2714^T were grouped in a reliable group (98% bootstrap value), phylogenetically nearest to other *Streptomyces* species. These three species were selected as reference strains.

Strains MZ03-37^T and MZ03-48 were aerobic and Gram-positive. Cell morphology after 7 days of incubation at 28°C in ISP2 liquid medium showed well developed and abundant hyphae as described for species affiliated to the genus *Streptomyces* (Kämpfer, 2012). Both strains grew at 37°C and up to 15% of NaCl, but also these strains showed differences between each other and with respect to the reference strains (**Table 1**). They differed in their ability to grow at different pH and in the use of arginine as a source of carbon and energy. No significant differences were observed in the use of sole sources of carbon between MZ03-37^T and MZ03-48 beyond a weak growth using distinct sugars or sugar alcohols. Using *myo*-inositol and mannitol, MZ03-37^T grew well, whereas MZ03-48 showed a low development of biomass. These two strains seemed to present more characteristics in common with *S. catenulae* and *S. ramulosus* rather than *S. palmae*. These five bacteria showed GC contents between 72.1 and 73%, in accordance with the GC-rich content of *Streptomyces* species.

Results from the International *Streptomyces* Project medium showed notable differences between the study strains. MZ03-37^T presented a light brown substrate mycelium and a white-colored aerial mycelium in ISP2 and ISP3, mustard tan in ISP5, beige in ISP6, and brown for both mycelia in IPS4 and ISP7, whereas MZ03-48 developed a light-black colored substrate and aerial mycelia in ISP2, ISP3, and ISP7 (**Supplementary Figure S1**) and a light-orange for both mycelia in ISP5, ISP6, and ISP4, but with white aerial mycelium in the last one (**Supplementary Table S1**). None of the analyzed strains produced soluble pigment on any of the tested ISP media. *Streptomyces* MZ03-37^T and MZ03-48 were also compared with the type strains grown in the same culture

TABLE 2 | Values for pairwise genome comparison with ANIb, ANIm, orthoANI (%), and TETRA (0–1).

	1	2	3	4	5
ANIb					
1	–	76.95	77.82	76.98	77.01
2	77.97	–	92.06	91.32	91.35
3	77.18	92.40	–	91.69	91.69
4	77.98	91.20	91.59	–	99.96
5	77.93	91.14	91.62	99.98	–
ANIm					
1	–	85.52	85.62	85.54	85.56
2	85.52	–	93.36	92.57	92.65
3	85.64	93.37	–	93.05	93.11
4	85.54	92.56	93.05	–	99.99
5	85.55	92.65	93.11	99.99	–
TETRA					
1	–	0.93579	0.95677	0.95066	0.95231
2	0.93579	–	0.99299	0.99246	0.99379
3	0.95677	0.99299	–	0.99534	0.99664
4	0.95066	0.99246	0.99534	–	0.99949
5	0.95231	0.99379	0.99664	0.99949	–
OrthoANI					
1	–	–	–	–	–
2	78.72	–	–	–	–
3	79.15	92.66	–	–	–
4	79.14	91.67	92.23	–	–
5	79.24	91.91	92.30	99.96	–

Strains: 1, Streptomyces palmae CMU-AB204^T; 2, Streptomyces catenulae NRRL B-2342^T; 3, Streptomyces ramulosus NRRL B-2714^T; 4, MZ03-37^T; 5, MZ03-48. –, Means that pairwise genome comparison against themselves result in 100% identity.

medium where the study bacteria were isolated, NA with 3% magnesium sulfate, and 2% glycerol (**Supplementary Figure S1**). MZ03-37^T formed a white aerial mycelium and a light brown substratum, MZ03-48 developed a light black substratum and aerial mycelium, *S. catenulae* formed a beige substratum and an aerial mycelium, *S. ramulosus* presented an aerial mycelium white-colored and a beige substrate, while *S. palmae* did not grow on this medium.

Pairwise Genome Comparison

The strains MZ03-37^T and MZ03-48 (**Table 2**) showed ANIb and ANIm, as well as OrthoANI values above the 99.9% among them, and less than 93.11% with *S. ramulosus*, the closest species observed in this analysis. Moreover, the results of TETRA calculations showed a high coefficient (>0.999) between the strains MZ03-37^T and MZ03-48 and a low coefficient (<0.999) between any of the closest species and both strains supporting the species circumscription. These values suggest that strains MZ03-37^T and MZ03-48 belonged to the same species since they showed high similarity after using referenced algorithms, whereas results obtained against the closest species point out that they could be considered as a new species within the genus *Streptomyces*.

In silico Analyses for Resistome and Secondary Metabolism

Genome characteristics are described in **Supplementary Table S2**. Sma3s resulted in 1,562 and 1,565 annotations from 6,336 and 6,410 queried sequences using UniProt – SwissProt curated database, for strains MZ03-37^T and MZ03-48, respectively. Genes predicted to a role in antimicrobial biosynthesis were the most abundant after amino acid and cofactor biosynthesis, with 65 out of a total of 652 genes predicted on pathway annotations, in MZ03-37^T, and 67 out of 654 in MZ03-48. In addition, genes involved in antibiotic biosynthesis and antibiotic resistance were significantly abundant within the biological process category, with 83 and 44 out of 1,500 annotated genes, respectively, in MZ03-37^T, and 82 and 42 out of 1,500 annotated sequences predicted in MZ03-48 (**Supplementary Figure S2**).

Predicted genes involved in antimicrobial mechanisms for resistance and biosynthesis in MZ03-37^T and MZ03-48 strains using Sma3s and UniProt-SwissProt database emphasize *Streptomyces* members as a biological reservoir for bioactive compounds, both described and not discovered yet (**Supplementary Table S3**). Genes or gene clusters associated with linocin-M18 (Valdés-Stauber and Scherer, 1994) and curamycin (Bergh and Uhlén, 1992) were predicted with a 50%-75% similarity in both strains, MZ03-37^T and MZ03-48. Monensin gene cluster (Arrowsmith et al., 1992) was predicted to get more than a 75% similarity with every aligned gene only in strain MZ03-37^T. Likewise, several annotated sequences exhibited descriptive information on antimicrobial resistance mechanisms related to transport and/or efflux systems as well as enzymes used to degrade the antimicrobials. Thus, more than 50% of sequence similarity genes were involved in resistance against cationic antimicrobial peptides (CAMPs), macrolides, β-lactam, nosiheptide, among others. With a similarity of 75% or higher, resistance for chloramphenicol and rifampicin was predicted in both strains. Also, new possible molecules not described yet could be produced by MZ03-37^T and MZ03-48 since there were predicted sequences showing high similarity with described genes which encoded to polyketide antibiotics as was the case of the putative polyketide hydroxylase (*schC*) (Blanco et al., 1993a,b) with a 69% of similarity, as well as other antibiotic-related synthases and transferases that appear in non-completed pathways in MZ03-37^T and MZ03-48 strains.

Secondary Metabolite Comparison

Beyond antimicrobial production, the genus *Streptomyces* is well known for including species being able to produce additional bioactive compounds with extensible uses in biotechnology (Goodfellow and Fiedler, 2010). The antiSMASH web tool predicted a total of 28 gene clusters involved in secondary metabolism activity in MZ03-37^T and 29 gene clusters in MZ03-48 (**Supplementary Table S4**). Both strains shared the same number of types of metabolites, with the exception of non-ribosomal peptide synthases (NRPS), having one more predicted gene cluster in MZ03-48. In summary, for MZ03-37^T, eight NRPS and nine for MZ03-48, four terpenes, four siderophores, three type 1 polyketide synthases (T1PKS), two type 2 polyketide

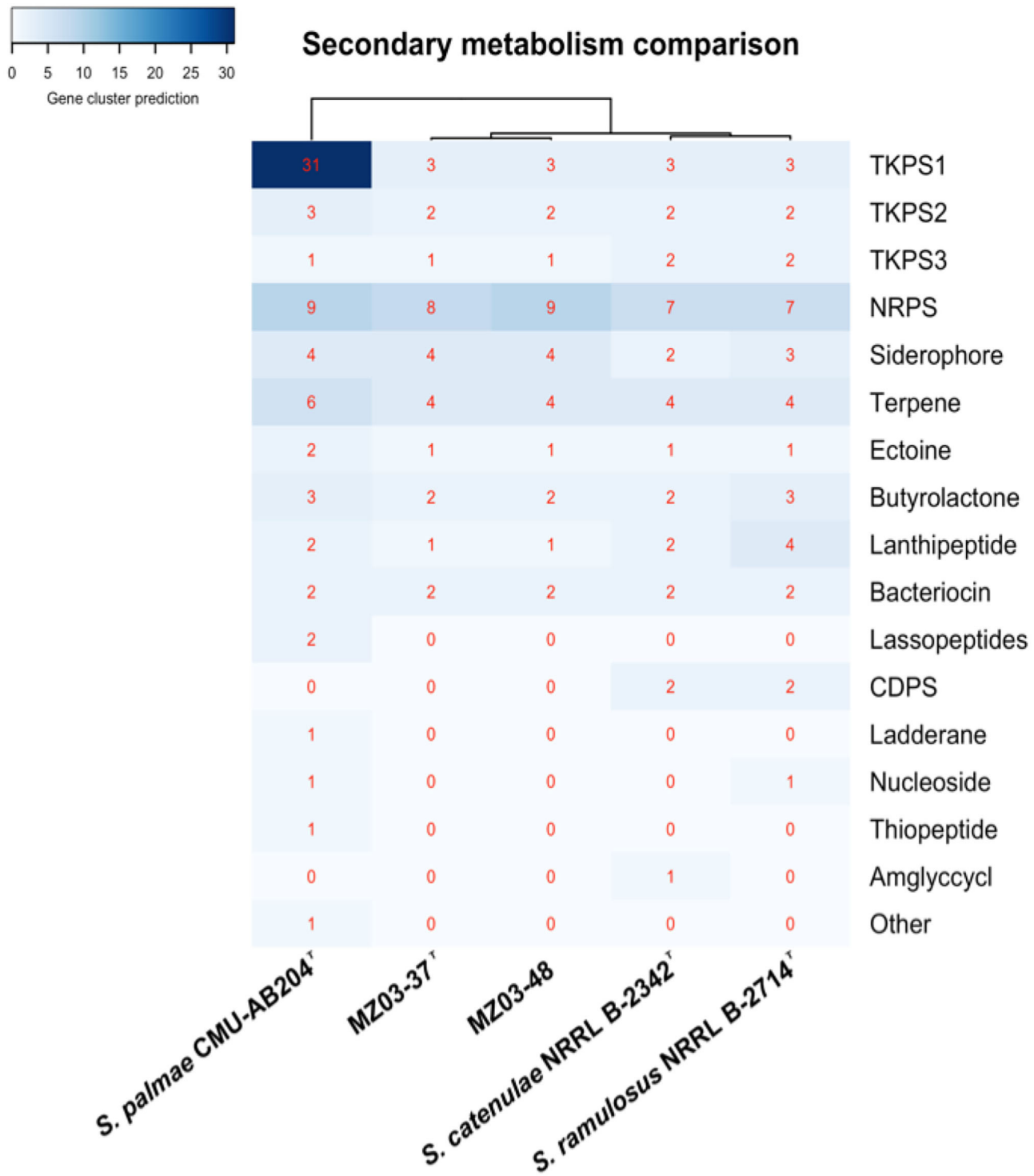

FIGURE 2 | Secondary metabolism comparison using anti-SMASH. Abundance of secondary metabolites predicted. TKPS1, type 1 polyketides synthase; TKPS2, type 2 polyketides synthase; TKPS3, type 3 polyketides synthase; NRPS, nonribosomal peptide synthase; CDPS, tRNA-dependent cyclodipeptide synthase; Amglyccycl, aminoglycoside/aminocyclitol cluster; other, cluster containing a secondary metabolite-related protein that does not fit into any other category. Cladogram built using Euclidean algorithm.

synthases (T2PKS), one type 3 polyketide synthases (T3PKS), two butyrolactone, two bacteriocins, one ectoine, and one lanthipeptide were predicted.

Likewise, additional anti-SMASH analyses were implemented for type strains for secondary metabolism comparison (**Figure 2**). Sixty-nine gene clusters were predicted for *S. palmae* which presented the most active secondary metabolism. Notably, 34 gene clusters were predicted for *S. ramulosus* and 30 for *S. catenulae*. Shared metabolites on the five strains were scarce, being present some typical molecules already described before for *Streptomyces* (Vicente et al., 2018), as it was the case of geosmin (Gerber and Lechevalier, 1965), hopene (Poralla et al., 2000), and ectoine (Malin and Lapidot, 1996), as well as the antibiotic curamycin (Bergh and Uhlén, 1992).

Naringenin gene cluster was also predicted for MZ03-48, *S. catenulae*, and *S. ramulosus*, missing in MZ03-37^T and *S. palmae*. Naringenin, along with the additional NRPS cluster

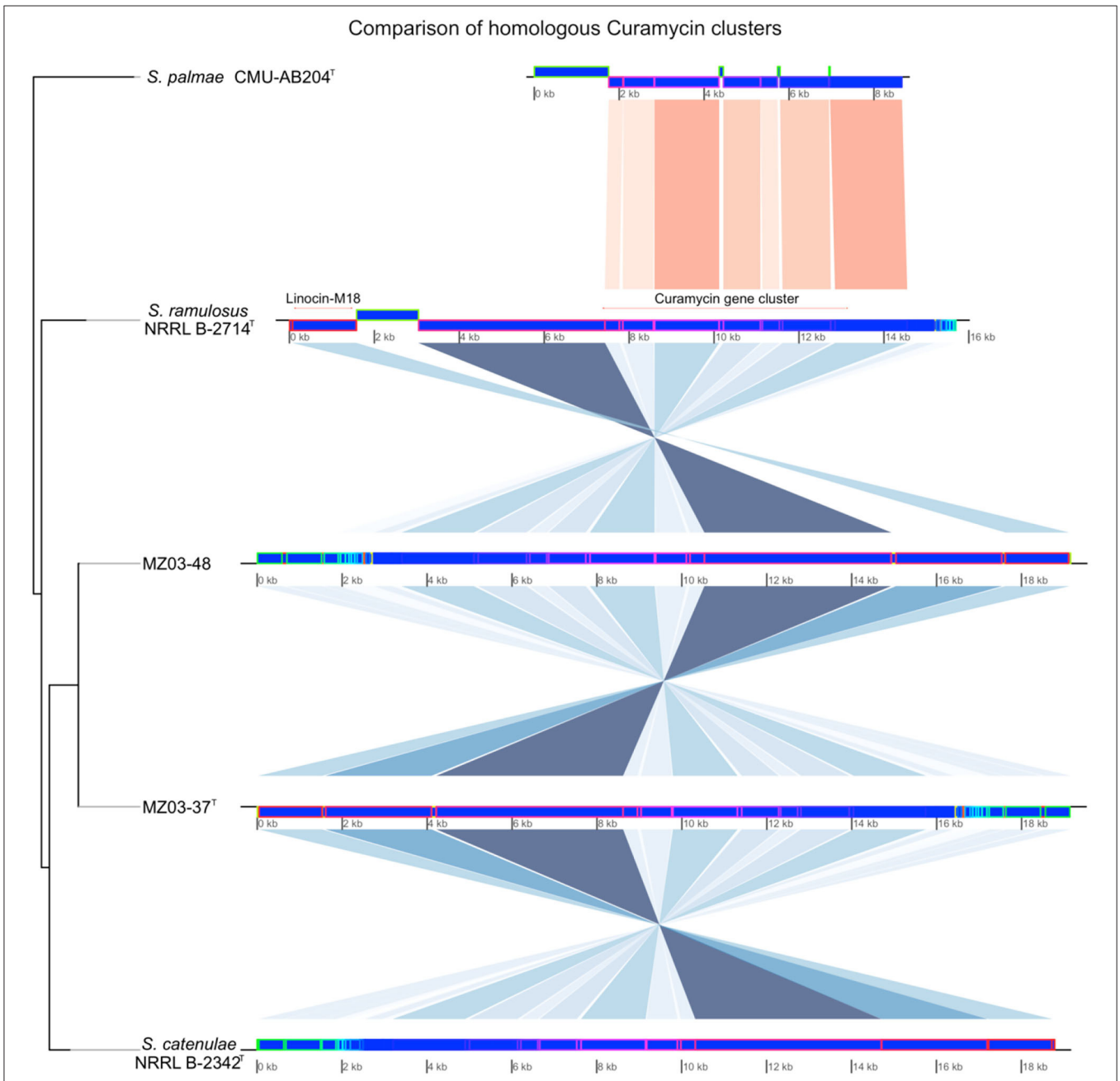

FIGURE 3 | Comparison of segments where Curamycin-Linocin-M18 gene clusters were predicted. Newick phylogenetic tree using Euclidean algorithm was built to determine the relatedness among contigs of the five bacteria. Conserved regions identified by MAUVE were represented with shades of blue and red.

predicted in MZ03-48, was supposed for the main difference between this strain and MZ03-37^T. Linocin-M18 was predicted for all analyzed strains with the exception of *S. palmae*. Linocin-M18 was located along with curamycin gene cluster in the same contig (**Figure 3**). BLAST alignment resulted in a 100% of identity in the case of strains MZ03-37^T and predicted in reverse orientation, MZ03-48. These two contigs aligned a 94.03% with the contig from *S. catenulae*, a 93.82% with *S. ramulosus,* and a 78.31% was aligned against contig where curamycin gene cluster was predicted for *S. palmae*. No Linocin-M18 gene cluster was predicted in other assembled contigs for this last bacterium.

Comparison of predicted secondary metabolites could add a new insight for differing closely related bacteria, as is the case of *Streptomyces* spp., beyond the discovery of new metabolites from microorganisms dwelling in specific environments, as is the case of caves and lava tubes (Vicente et al., 2018; Sottorff et al., 2019). Differences in the prediction of gene clusters, as well as similarities in particular segments to compare, showed a trend for bacterial relatedness which reinforces the results from the polyphasic characterization, multilocus sequence typing, and full genome sequencing analyses.

Based on all characteristics, strains MZ03-37^T and MZ03-48 represent a new species, for which we proposed the name *Streptomyces benahoarensis* sp. nov.

Description of *S. benahoarensis* sp. nov.

Streptomyces benahoarensis (be.na.hoar.en'sis. N.L. fem. adj. *benahoarensis*, originating from Benahoare, the Guanche name of La Palma, the island where both strains were isolated) is Gram-positive and aerobic, and forms rectiflexibiles spore chains. No fragmentation is developed neither aerial nor substrate mycelia. Growth was observed at 10–37°C (optimal 28–32°C), with 0–15% (w/v) NaCl (optimal 0–10%), and at pH 4.0–10.0 (optimal 6–9) for MZ03-37^T. It is oxidase-negative. Nitrate is not reduced to nitrite. Indole is produced from tryptophan, and glucose fermentation does not occur. It is positive for arginine dihydrolase, urease, β-glucosidase, and protease and negative for β-galactosidase. It shows positive assimilation for glucose, mannose, mannitol, N-acetyl-glucosamine, potassium gluconate, malate, trisodium citrate, and phenylacetic acid and negative assimilation for arabinose, maltose, capric acid, and adipic acid. It uses sacarose, maltose, mannose, glycerol, xylose, *myo*-inositol, and mannitol as carbon sources for growth but not dextran. It shows weak growth with D-galactose, lactose, fructose, and glucose, and good growth on ISP media (2, 3, 4, 5, 6, and 7). Soluble pigments are not produced, and melanin is not formed. Major cellular fatty acids are iso-$C_{16:0}$, anteiso-$C_{15:0}$, $C_{16:0}$, and iso-$C_{14:0}$. The cell wall contains LL-diaminopimelic acid in its peptidoglycan. The GC content of the type strain is 72.1 mol%.

The type strain, MZ03-37^T (=CECT 9805^T = DSMZ 8002^T), was isolated from a lava tube speleothem collected in Fuente de la Canaria (La Palma Island, Canary Islands, Spain); a reference strain, MZ03-48 (= CECT 9806 = DSMZ 8011) was isolated from a microbial mat from Fuente de la Canaria lava tube (La Palma Island, Canary Islands, Spain).

DATA AVAILABILITY STATEMENT

The datasets presented in this study can be found in online repositories. The names of the repository/repositories and accession number(s) can be found in the article/**Supplementary Material**.

AUTHOR CONTRIBUTIONS

JG-P developed the ideas and designed the experimental plans. CS-J supervised the research and provided funding support. JG-P and VJ performed experiments. JG-P, VJ, and BH analyzed the data. JG-P, VJ, and CS-J prepared the manuscript. All authors contributed to this study and approved the submitted version.

FUNDING

This study was supported by the project 0483_PROBIOMA_5_E, co-financed by the European Regional Development Fund within the framework of the Interreg V A Spain – Portugal program (POCTEP) 2014–2020. 2015 and 2016 field trips to the cave were supported by a former Spanish Ministry of Economy, Industry, and Competitiveness (MINEICO) project CGL2013-41674-P.

ACKNOWLEDGMENTS

We acknowledge CSIC Open Access Publication Support Initiative through its Unit of Information Resources for Research (URICI) and CSIC Interdisciplinary Thematic Platform Open Heritage: Research and Society (PTI-PAIS) for the professional support.

SUPPLEMENTARY MATERIAL

The Supplementary Material for this article can be found online at: https://www.frontiersin.org/articles/10.3389/fmicb.2022.907816/full#supplementary-material

Supplementary Figure S1 | Morphology of colonies MZ03-48 (A), MZ03-37^T (B), and reference strains *Streptomyces ramulosus* NRRL B-2714^T (C) and *Streptomyces catenulae* NRRL B-2342^T (D). Plates cultured on nutrient agar (NA, BD, Sparks, USA) with 3% of magnesium sulfate and 2% of glycerol at 28°C for 7 days.

Supplementary Figure S2 | Genes classified by functional categories in pathways (A) and biological processes (B) from curated UniProt-SwissProt. "Others" gathered those categories with less than 1% of total genes.

Supplementary Table S1 | Morphology and physiology observed after culturing of MZ03-37^T and MZ03-48 in International *Streptomyces* Project media.

Supplementary Table S2 | Genome characterization of *Streptomyces* strains MZ03-37^T, MZ03-48, and reference species. rRNA, ribosomal RNA; tRNA, transfer RNA; tmRNA, transfer-messenger RNA.

Supplementary Table S3 | Antimicrobial biosynthesis and resistance mechanisms identified in MZ03-37^T and MZ03-48 by Sma3s. The table differentiates identifications with similarities from 50 to 75% and from 75 to 100%. nonavailable (N/A) gene names are replaced by their protein names: (A) monensin polyketide synthase ACP; monensin polyketide synthase putative ketoacyl reductase; putative polyketide beta-ketoacyl synthase 1; putative polyketide beta-ketoacyl synthase 2; granaticin polyketide synthase bifunctional cyclase/dehydratase. (B) Putative nosiheptide resistance regulatory protein. (1)

Cationic antimicrobial Peptides. (2) Tetracyclines, macrolides, lincosamides, and aminoglycosides (Morris et al., 2005). (3) Tylosin and erythromycin (Quirós et al., 1998). (4) Only present in MZ03-37^T.

Supplementary Table S4 | Secondary metabolites predicted for MZ03-37^T and MZ03-48 by anti-SMASH. Gene clusters predicted without reference to the identified closest cluster in the database were omitted. "Similarity" pointed out the % of genes predicted that have been identified in described biosynthetic clusters. The minimum threshold used by anti-SMASH for finding homology fixed a BLAST e-value below 1E-05, a 30% minimal sequence identity, and a coverage of >25% of the sequence. [1]The query sequence covered only 25% of the closest sequence.

REFERENCES

Altschul, S. F., Gish, W., Miller, W., Myers, E. W., and Lipman, D. J. (1990). Basic local alignment search tool. *J. Mol. Biol.* 215, 403–410. doi: 10.1016/S0022-2836(05)80360-2

Antony-Babu, S., Stien, D., Eparvier, V., Parrot, D., Tomasi, S., and Suzuki, M. T. (2017). Multiple *Streptomyces* species with distinct secondary metabolomes have identical 16S rRNA gene sequences. *Sci. Rep.* 7, 11089. doi: 10.1038/s41598-017-11363-1

Arrowsmith, T. J., Malpartida, F., Sherman, D. H., Birch, A., Hopwood, D. A., and Robinson, J. A. (1992). Characterisation of actI-homologous DNA encoding polyketide synthase genes from the monensin producer *Streptomyces cinnamonensis*. *Mol. Gen. Genet.* 234, 254–264. doi: 10.1007/BF00283846

Barka, E. A., Vatsa, P., Sanchez, L., Gaveau-Vaillant, N., Jacquard, C., Klenk, H. P., et al. (2016). Taxonomy, physiology, and natural products of *Actinobacteria*. *Microbiol. Mol. Biol. Rev.* 80, 1–43. doi: 10.1128/MMBR.00019-15

Bergh, S., and Uhlén, M. (1992). Analysis of a polyketide synthesis-encoding gene cluster of *Streptomyces curacoi*. *Gene* 117, 131-136. doi: 10.1016/0378-1119(92)90501-F

Blanco, G., Brian, P., Pereda, A., Mendez, C., Salas, J. A., and Chater, K. F. (1993b). Hybridization and DNA sequence analyses suggest an early evolutionary divergence of related biosynthetic gene sets encoding polyketide antibiotics and spore pigments in *Streptomyces* spp. *Gene* 130, 107–116. doi: 10.1016/0378-1119(93)90352-4

Blanco, G., Pereda, A., Brian, P., Méndez, C., Chater, K. F., and Salas, J. A. (1993a). A hydroxylase-like gene product contributes to synthesis of a polyketide spore pigment in *Streptomyces halstedii*. *J. Bacteriol.* 175, 8043–8048. doi: 10.1128/jb.175.24.8043-8048.1993

Blin, K., Shaw, S., Kloosterman, A. M., Charlop-Powers, Z., van Wezel, G. P., Medema, M. H., et al. (2021). antiSMASH 6.0: improving cluster detection and comparison capabilities. *Nucleic Acids Res.* 49, W29–W35. doi: 10.1093/nar/gkab335

Camacho, C., Coulouris, G., Avagyan, V., Ma, N., Papadopoulos, J., Bealer, K., et al. (2008). BLAST+: architecture and applications. *BMC Bioinform.* 10, 421. doi: 10.1186/1471-2105-10-421

Darling, A. C., Mau, B., Blattner, F. R., and Perna, N. T. (2004). Mauve: multiple alignment of conserved genomic sequence with rearrangements. *Genome Res.* 14, 1394–1403. doi: 10.1101/gr.2289704

Edgar, R. C. (2004). MUSCLE: multiple sequence alignment with high accuracy and high throughput. *Nucleic Acids Res.* 32, 1792–1797. doi: 10.1093/nar/gkh340

Felsenstein, J. (1981). Evolutionary trees from DNA sequences: a maximum likelihood approach. *J. Mol. Evol.* 17, 368–376. doi: 10.1007/BF01734359

Gerber, N. N., and Lechevalier, H. A. (1965). Geosmin, an earthly-smelling substance isolated from actinomycetes. *Appl. Microbiol.* 13, 935–938. doi: 10.1128/am.13.6.935-938.1965

Gonzalez-Pimentel, J. L., Martin-Pozas, T., Jurado, V., Miller, A. Z., Caldeira, A. T., Fernandez-Lorenzo, O., et al. (2021). Prokaryotic communities from a lava tube cave in La Palma Island (Spain) are involved in the biogeochemical cycle of major elements. *PeerJ.* 9: e11386. doi: 10.7717/peerj.11386

Goodfellow, M., and Fiedler, H. P. (2010). A guide to successful bioprospecting: informed by actinobacterial systematics. *Anton. Leeuw.* 98, 119. doi: 10.1007/s10482-010-9460-2

Gould, K. (2016). Antibiotics: from prehistory to the present day. *J. Antimicrob. Chemother.* 71, 572–575. doi: 10.1093/jac/dkv484

Guo, Y., Zheng, W., Rong, X., and Huang, Y. (2008). A multilocus phylogeny of the *Streptomyces griseus* 16S rRNA gene clade: use of multilocus sequence analysis for streptomycete systematics. *Int. J. Syst. Evol. Microbiol.* 58, 149-159. doi: 10.1099/ijs.0.65224-0

Ju, K. S., Gao, J., Doroghazi, J. R., Wang, K. K., Thibodeaux, C. J., Li, S., et al. (2015). Discovery of phosphonic acid natural products by mining the genomes of 10,000 actinomycetes. *Proc. Natl. Acad. Sci. USA.* 112, 12175–12180. doi: 10.1073/pnas.1500873112

Jurado, V., Kroppenstedt, R. M., Saiz-Jimenez, C., Klenk, H.-P., Mouniée, D. and Laiz, L., et al. (2009). *Hoyosella altamirensis* gen. nov., sp. nov., a new member of the order Actinomycetales isolated from a cave biofilm. *Int. J. Syst. Evol. Microbiol.* 59, 3105–3110. doi: 10.1099/ijs.0.008664-0

Kämpfer, P. (2012). "Genus I. *Streptomyces* Waksman and Henrici 1943, 339AL emend. Witt and Stackebrandt 1990, 370 emend. Wellington, Stackebrandt, Sanders, Wolstrup and Jorgensen 1992, 159", in *Bergey's Manual of Systematic Bacteriology, vol. Five. The Actinobacteria, Part A and B*, eds. M. Goodfellow et al. *(New York: Springer)* 1455–1767.

Kluge, A. G., and Farris, F. S. (1969). Quantitative phyletics and the evolution of anurans. *Syst. Zool.* 18, 1–32. doi: 10.2307/2412407

Kurtz, S., Phillippy, A., Delcher, A. L., Smoot, M., Shumway, M., Antonescu, C., et al. (2004). Versatile and open software for comparing large genomes. *Genome Biol.* 5, R12. doi: 10.1186/gb-2004-5-2-r12

Laiz, L., Miller, A. Z., Jurado, V., Akatova, E., Sanchez-Moral, S., Gonzalez, J. M., et al. (2009). Isolation of five *Rubrobacter* strains from biodeteriorated monuments. *Naturwissenschaften* 96, 71–79. doi: 10.1007/s00114-008-0452-2

Malin, G., and Lapidot, A. (1996). Induction of synthesis of tetrahydropyrimidine derivatives in *Streptomyces* strains and their effect on *Escherichia coli* in response to osmotic and heat stress. *J. Bacteriol.* 178, 385–395. doi: 10.1128/jb.178.2.385-395.1996

Marmur, J. (1961). A procedure for the isolation of deoxiribonucleic acid from microorganisms. *J. Mol. Biol.* 3, 208–218. doi: 10.1016/S0022-2836(61)80047-8

Mast, Y., and Stegmann, E. (2018). Actinomycetes: The antibiotics producers. *Antibiotics* 8, 105. doi: 10.3390/antibiotics8030105

Miller, J. H. (1992). *A Short Course in Bacterial Genetics: a Laboratory Manual and Handbook for Escherichia coli and Related Bacteria*. Cold Spring Harbor, New York: Cold Spring Harbor Laboratory.

Miyadoh, S. (1997). *Atlas of Actinomycetes*. Tokyo: Asakura Publishing Co.

Morris, R. P., Nguyen, L., Gatfield, J., Visconti, K., Nguyen, K., Schnappinger, D., et al. (2005). Ancestral antibiotic resistance in *Mycobacterium tuberculosis*. *Proc. Natl. Acad. Sci. USA.* 102, 12200–12205. doi: 10.1073/pnas.0505446102

Muñoz-Mérida, A., Viguera, E., Claros, M. G., Trelles, O., and Pérez-Pulido, A. J. (2014). Sma3s: a three-step modular annotator for large sequence datasets. *DNA Res.* 21, 341–353. doi: 10.1093/dnares/dsu001

Poralla, K., Muth, G., and Härtner, T. (2000). Hopanoids are formed during transition from substrate to aerial hyphae in *Streptomyces coelicolor* A3(2). *FEMS Microbiol. Lett.* 189, 93–95. doi: 10.1111/j.1574-6968.2000.tb09212.x

Quirós, L. M., Aguirrezabalaga, I., Olano, C., Méndez, C., and Salas, J. A. (1998). Two glycosyltransferases and a glycosidase are involved in oleandomycin modification during its biosynthesis by *Streptomyces antibioticus*. *Mol. Microbiol.* 28, 1177–1185. doi: 10.1046/j.1365-2958.1998.00880.x

Rangseekaew, P., and Pathom-Aree, W. (2019). Cave actinobacteria as producers of bioactive metabolites. *Front. Microbiol.* 10, 387. doi: 10.3389/fmicb.2019.00387

Richter, M., and Rosselló-Móra, R. (2009). Shifting the genomic gold standard for the prokaryotic species definition. *Proc. Natl. Acad. Sci. USA.* 106, 19126–19131. doi: 10.1073/pnas.0906412106

Richter, M., Rosselló-Móra, R., Oliver Glöckner, F., and Peplies, J. (2016). JSpeciesWS: a web server for prokaryotic species circumscription based on pairwise genome comparison. *Bioinformatics* 32, 929–931. doi: 10.1093/bioinformatics/btv681

Rong, X., Guo, Y., and Huang, Y. (2009). Proposal to reclassify the *Streptomyces albidoflavus* clade on the basis of multilocus sequence analysis and DNA-DNA hybridization, and taxonomic elucidation of

Streptomyces griseus subsp. *solvifaciens*. *Syst. Appl. Microbiol.* 32, 314–322. doi: 10.1016/j.syapm.2009.05.003

Rong, X., and Huang, Y. (2014). "Multi-locus sequence analysis: Taking prokaryotic systematics to the next level," in *Methods in Microbiology, Vol. 41*, eds M. Goodfellow, I. Sutcliffe, and J. Chun (Academic Press), 221–251. doi: 10.1016/bs.mim.2014.10.001

Saitou, N., and Nei, M. (1987). The neighbor-joining method: a new method for reconstructing phylogenetic trees. *Mol. Biol. Evol.* 4, 406–425.

Savic, M., Bratic, I., and Vasiljevic, B. (2007). *Streptomyces durmitorensis* sp. nov., a producer of an FK506-like immunosuppressant. *Int. J. Syst. Evol. Microbiol.* 57, 2119-2124. doi: 10.1099/ijs.0.64913-0

Seemann, T. (2014). Prokka: rapid prokaryotic genome annotation. *Bioinformatics* 30, 2068–2069. doi: 10.1093/bioinformatics/btu153

Shirling, E. B., and Gottlieb, D. (1966). Methods for characterization of *Streptomyces* species. *Int. J. Syst. Bacteriol.* 16, 313. doi: 10.1099/00207713-16-3-313

Sottorff, I., Wiese, J., Lipfert, M., Preußke, N., Sönnichsen, F. D., and Imhoff, J. F. (2019). Different secondary metabolite profiles of phylogenetically almost identical *Streptomyces griseus* strains originating from geographically remote locations. *Microorganisms* 7, 166. doi: 10.3390/microorganisms7060166

Tamura, K., Stecher, G., Peterson, D., Filipski, A., and Kumar, S. (2013). MEGA6: molecular evolutionary genetics analysis version 6.0. *Mol. Biol. Evol.* 30, 2725–2729. doi: 10.1093/molbev/mst197

Tortorella, E., Tedesco, P., Palma Esposito, F., January, G. G., Fani, R., Jaspars, M., et al. (2018). Antibiotics from deep-sea microorganisms: Current discoveries and perspectives. *Mar. Drugs* 16, 355. doi: 10.3390/md16100355

Valdés-Stauber, N., and Scherer, S. (1994). Isolation and characterization of Linocin M18, a bacteriocin produced by *Brevibacterium linens*. *Appl. Environ. Microbiol.* 60, 3809-3814. doi: 10.1128/aem.60.10.3809-3814.1994

Vicente, C. M., Thibessard, A., Lorenzi, J. N., Benhadj, M., Hôtel, L., Gacemi-Kirane, D., et al. (2018). Comparative genomics among closely related *Streptomyces* strains revealed specialized metabolite biosynthetic gene cluster diversity. *Antibiotics* 7, 86. doi: 10.3390/antibiotics7040086

Waksman, S. A. (1919). Cultural studies of species of Actinomycetes. *Soil. Sci.* 8, 71–125. doi: 10.1097/00010694-191908000-00001

Waksman, S. A., and Hinrici, A. T. (1943). The nomenclature and classification of the actinomycetes. *J. Bacteriol.* 46, 337–341. doi: 10.1128/jb.46.4.337-341.1943

Weisburg, W. G., Barns, S. M., Pelletier, D. A., and Lane, D. J. (1991). 16S ribosomal DNA amplification for phylogenetic study. *J. Bacteriol.* 173, 697–703. doi: 10.1128/jb.173.2.697-703.1991

Yarza, P., Yilmaz, P., Pruesse, E., Glöckner, F. O., Ludwig, W., Schleifer, K. H., et al. (2014). Uniting the classification of cultured and uncultured bacteria and archaea using 16S rRNA gene sequences. *Nat. Rev. Microbiol.* 12, 635–645. doi: 10.1038/nrmicro3330

Yoon, S. H., Ha, S. M., Kwon, S., Lim, J., Kim, Y., Seo, H., et al. (2017). Introducing EzBioCloud: A taxonomically united database of 16S rRNA and whole genome assemblies. *Int. J. Syst. Evol. Microbiol.* 67, 1613–1617. doi: 10.1099/ijsem.0.001755

Conflict of Interest: The authors declare that the research was conducted in the absence of any commercial or financial relationships that could be construed as a potential conflict of interest.

Publisher's Note: All claims expressed in this article are solely those of the authors and do not necessarily represent those of their affiliated organizations, or those of the publisher, the editors and the reviewers. Any product that may be evaluated in this article, or claim that may be made by its manufacturer, is not guaranteed or endorsed by the publisher.

frontiers | Frontiers in Microbiology

ORIGINAL RESEARCH
published: 19 May 2022
doi: 10.3389/fmicb.2022.877481

A 16S rRNA Gene-Based Metabarcoding of Phosphate-Rich Deposits in Muierilor Cave, South-Western Carpathians

Catalina Haidău[1], Ruxandra Năstase-Bucur[2,3], Paul Bulzu[4], Erika Levei[5], Oana Cadar[5], Ionuţ Cornel Mirea[3,6], Luchiana Faur[3,6,7], Victor Fruth[8], Irina Atkinson[8], Silviu Constantin[3,6,9] and Oana Teodora Moldovan[2,3,9]**

[1] Department of Biospeleology and Karst Edaphobiology, Emil Racovita Institute of Speleology, Bucureşti, Romania, [2] Department of Cluj-Napoca, Emil Racovita Institute of Speleology, Cluj-Napoca, Romania, [3] Romanian Institute of Science and Technology, Cluj-Napoca, Romania, [4] Department of Molecular Biology and Biotechnology, Faculty of Biology and Geology, Babeş-Bolyai University, Cluj-Napoca, Romania, [5] Research Institute for Analytical Instrumentation Subsidiary, National Institute of Research and Development for Optoelectronics INOE 2000, Cluj-Napoca, Romania, [6] Department of Geospeleology and Paleontology, Emil Racovita Institute of Speleology, Bucureşti, Romania, [7] Faculty of Geology and Geophysics, University of Bucharest, Bucureşti, Romania, [8] Institute of Physical Chemistry "Ilie Murgulescu" of the Romanian Academy, Bucuresti, Romania, [9] Centro Nacional Sobre la Evolucion Humana, Burgos, Spain

OPEN ACCESS

Edited by:
Cesareo Saiz-Jimenez, Institute of Natural Resources and Agrobiology of Seville (CSIC), Spain

Reviewed by:
Kathleen Lavoie, State University of New York at Plattsburgh, United States
Ana Z. Miller, Spanish National Research Council (CSIC), Spain

***Correspondence:**
Catalina Haidău
haidau.catalina@gmail.com
Oana Teodora Moldovan
oanamol35@gmail.com

Specialty section:
This article was submitted to Terrestrial Microbiology, a section of the journal Frontiers in Microbiology

Received: *16 February 2022*
Accepted: *21 April 2022*
Published: *19 May 2022*

Citation:
Haidău C, Năstase-Bucur R, Bulzu P, Levei E, Cadar O, Mirea IC, Faur L, Fruth V, Atkinson I, Constantin S and Moldovan OT (2022) A 16S rRNA Gene-Based Metabarcoding of Phosphate-Rich Deposits in Muierilor Cave, South-Western Carpathians. Front. Microbiol. 13:877481. doi: 10.3389/fmicb.2022.877481

Muierilor Cave is one of Romania's most important show caves, with paleontological and archeological deposits. Recently, a new chamber was discovered in the cave, with unique yellow calcite crystals, fine-grained crusts, and black sediments. The deposits in this chamber were related to a leaking process from the upper level that contains fossil bones and a large pile of guano. Samples were taken from the new chamber and another passage to investigate the relationship between the substrate and microbial community. Chemical, mineralogical, and whole community 16S rRNA gene-based metabarcoding analyses were undertaken, and the base of the guano deposit was radiocarbon dated. Our study indicated bacteria linked to the presence of high phosphate concentration, most likely due to the nature of the substrate (hydroxyapatite). Bacteria involved in Fe, Mn, or N cycles were also found, as these elements are commonly identified in high concentrations in guano. Since no bat colonies or fossil bones were present in the new chamber, a high concentration of these elements could be sourced by organic deposits inside the cave (guano and fossil bones) even after hundreds of years of their deposition and in areas far from both deposits. Metabarcoding of the analyzed samples found that ∼0.7% of the identified bacteria are unknown to science, and ∼47% were not previously reported in caves or guano. Moreover, most of the identified human-related bacteria were not reported in caves or guano before, and some are known for their pathogenic potential. Therefore, continuous monitoring of air and floor microbiology should be considered in show caves with organic deposits containing bacteria that can threaten human health. The high number of unidentified taxa in a small sector of Muierilor Cave indicates the limited knowledge of the bacterial diversity in caves that can have potential applications in human health and biotechnology.

Keywords: cave microbiology, metabarcoding, radiocarbon, Romania, pathogens, fossil bones, bat guano

INTRODUCTION

Caves are oligotrophic subterranean environments with original biological communities consisting of species with various morphological (i.e., pigmentation and sight loss, body and appendage elongation, etc.), behavioral (i.e., loss of circadian rhythm), and physiological adaptations (i.e., low metabolism rate and tolerance to high CO_2/low O_2) (Hershey and Barton, 2018; Howarth and Moldovan, 2018; Friedrich, 2019; Hervant and Malard, 2019; Kowalko, 2019; Zhu et al., 2019). Nowadays, interest in caves has grown proportionally with the curiosity of the people, which is reflected in the growing number of visitors worldwide for the beauty of the subterranean domain and the valuable information it can provide about the past (Gascoyne, 1992; Baldini, 2010; Polyak and Denniston, 2019). Some caves are regarded as great attractions due to their unique morphology (Hill and Forti, 1995; White, 2019; Prelovšek et al., 2021), cultural value (Leroi-Gourhan, 1982; Ronquillo, 1995; Saiz-Jimenez et al., 2011; Skeates and Bergsvik, 2012), or biological diversity (Howarth and Moldovan, 2018; Culver and Pipan, 2019).

The opening of the first show cave in the early 17th century (Vilenica Cave, Slovenia) was just the beginning of the development of speleo-tourism (Cigna, 2019). Since then, more than 600 caves have been visited by tourists worldwide, receiving more than 25 million visitors per year (Cigna and Burri, 2000; Novas et al., 2017; Tièar et al., 2018). With the growing number of tourists, proper management of the caves' natural heritage is required against the impacts affecting cave habitats and microclimate (Pulido-Bosch et al., 1997; Hoyos et al., 1998; Northup and Lavoie, 2001; Mann et al., 2002; Paksuz and Özkan, 2012; Bercea et al., 2018, 2019; Debata, 2020; Constantin et al., 2021). However, the biological resources of caves can be reservoirs for pathogens and may be regarded as potential environments for pathogen transmission (Dean, 1957; Jurado et al., 2010; Igreja, 2011). Consequently, visitors must be informed of the threats, particularly where the management of show caves is rudimentary (Constantin et al., 2021).

The increasing interest in caves also encompasses the potential biotechnological applications in biological and medical sciences of the cave microbiomes (Jiang et al., 2015; Rangseekaew and Pathom-Aree, 2019; Zada et al., 2021). Already known bacteria reveal new characteristics, and the potential of pathogenicity has been found in some bacteria (Jurado et al., 2010; Moldovan et al., 2020). Alongside these discoveries, unreached sides of metabolism in organisms are starting to be discovered and understood.

Herein, we present the results of the studies on the microbiome of different deposit types in a protected sector of Muierilor Cave (Romania) to unravel the diversity of microorganisms related to the substrate chemistry and mineralogy and identify their possible sources. Muierilor Cave is one of the most important caves from paleontological, biological, and archeological points of view (Mirea et al., 2021). With more than 130,000 visitors each year, it is also one of the most visited show caves in the country (Burghele et al., 2018; Constantin et al., 2021; Mirea et al., 2021).

MATERIALS AND METHODS

Site Description and Sampling

Muierilor Cave (45°11′31.78″N and 23°45′14.07″E) is developed in limestone and located in Baia de Fier, south-western Romania, and is one of the most-visited show caves in the country (**Figure 1**). The cave is situated on the right slope of Galbenul Gorges at 650 m.a.s.l and is developed on four distinct levels. The second one has been a tourist and scientific attraction since the late 19th century. It is the first cave to be fitted with electric lights from Romania since 1963. The cave is inhabited by four species of hibernating bats, with the most abundant being *Miniopterus schreibersii* and *Rhinolophus ferrumequinum*, each forming colonies of around 1,000 individuals, especially along the touristic path.

Muierilor Cave is also known for the rich presence of hydroxyapatite [$Ca_5(PO_4)_3(OH)$] on rocks and boulders in different sectors of the cave. Hydroxyapatite is a naturally occurring mineral found in the bones and teeth of mammals, which is white when pure and yellow, green, or brown in nature. The lower level is the Scientific Reserve, from where the studied samples were collected, specifically from the Yellow Chamber.

The Yellow Chamber was resurveyed in 2019 during the paleontological excavation in the Scientific Reserve (Mirea et al., 2021). It was named after the yellow calcite crystals that cover the rock surface in some of its parts. The Yellow Chamber is situated roughly underneath the Guano Chamber (which owes its name to a big pile of guano) located along the Touristic Passage (**Figure 1**). The Touristic Passage is also known for the abundance of fossil remains (belonging mainly to *Ursus spelaeus* sensu lato) (Mirea et al., 2021). Part of the Yellow Chamber floor is covered with a black deposit of sandy clay with very sparse drips of water coming from the upper level, while two big boulders in its middle are covered with white and black crusts at a few tens of centimeters apart. The fragile crusts cover a small surface of the boulders, and at present, no water is dripping in that area. None of the other chambers or passages of the cave have such features, and they have not been seen in other Romanian caves. The ceiling of the Yellow Chamber is about 14 m at the highest point. The walls are covered with seemingly an organic deposit brought by the percolating water from the upper level.

The Yellow Chamber is a side passage with little ventilation. The geomorphological features develop on secondary faults (perpendicular to the main N–S fault) and connect with the upper levels through shafts and fissures. This feature allows the percolating water to precipitate in the lower levels. The temperature at the entrance of the Yellow Chamber (registered with a permanent data logger) was about 10°C, and the humidity was >92%. Spot measurements of CO_2 were around 560 ppm (Constantin et al., 2021).

Sediment samples were collected in sterile Falcon tubes for microbiological analysis. A sample of 10 g of sediments was taken directly from the Yellow Chamber's black, sandy clay floor in a

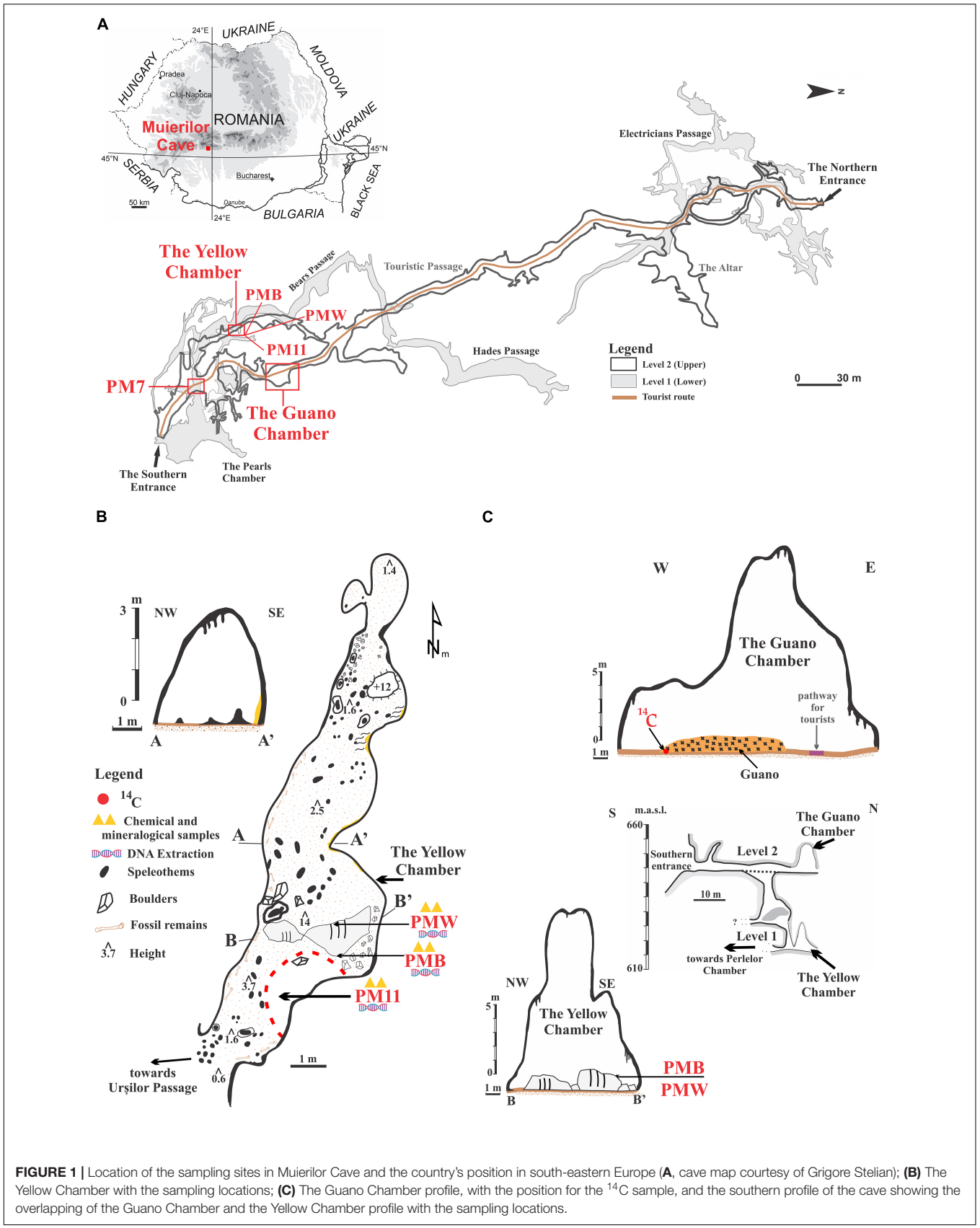

FIGURE 1 | Location of the sampling sites in Muierilor Cave and the country's position in south-eastern Europe (**A**, cave map courtesy of Grigore Stelian); **(B)** The Yellow Chamber with the sampling locations; **(C)** The Guano Chamber profile, with the position for the ^{14}C sample, and the southern profile of the cave showing the overlapping of the Guano Chamber and the Yellow Chamber profile with the sampling locations.

Falcon tube (PM11), and about 2 g of each crust was sampled with a sterilized scalpel (PMW = white crust, PMB = black crust). An additional sample of 10 g of brown sandy clay sediments was taken directly in a sterile Falcon tube from a different passage of the Scientific Reserve (PM7). The samples were transported for further laboratory analysis in an icebox and kept in the freezer at −60°C until extraction.

For the chemical and mineralogical analysis, 10 g of sediments from PM7 and PM11 and 2 g of both crusts were collected in clean plastic bags and transported to the laboratory for analysis.

Dating of Guano Deposits

A guano sample was collected with a small corer from the bottom of the guano pile in the touristic passage for radiocarbon dating. The AMS ^{14}C dating was done commercially at the Poznan Radiocarbon Laboratory (Poland), following the procedures described in Mirea et al. (2021). The calibration of AMS ^{14}C ages was performed using the program OxCal ver. 4.4.2 (Bronk Ramsey, 2009, 2020) against the INTCAL13 radiocarbon calibration curve (Reimer et al., 2020).

Chemical and Mineralogical Analysis

The pH was measured using a Seven Excellence Multiparameter (Mettler Toledo, Greifensee, Switzerland) in a 1/5 (m/v) solid to water suspension. N and C were measured using a Flash 2000 CHNS/O analyzer (Thermo Fisher Scientific, Waltham, MA, United States) by combustion of 2 mg of sample. For metal, S, and P analysis, 1 g of dried and grounded sample (<250 μm) was digested in 28 ml of 3/1 (v/v) HCl (37%)/HNO_3 (62%) mixture. The concentration of Na, Mg, K, Ca, Al, Fe, P, and S was measured by inductively coupled plasma optical emission spectrometry using a 5300 Optima DV (Perkin Elmer, Waltham, MA, United States) spectrometer. The concentration of trace elements was determined by inductively coupled plasma mass spectrometry (ICP-MS) using an Elan DRC II (Perkin Elmer, Waltham, MA, United States) spectrometer.

To preserve crust deposits as well as possible, the mineralogical analysis was performed only on sediment samples. Sampling for mineralogical analysis could lead to the destruction of crusts and subsequently could limit the possibility of further studies. Samples were analyzed using powdered X-ray diffraction method with Rigaku Ultima IV diffractometer in parallel beam geometry equipped with CuKα radiation (wavelength 1.5406 Å). The XRD patterns were collected in the 2θ range between 5 and 80 with a speed of 2°/min and a step size of 0.02°. Rigaku PDXL Software connected to the ICDD database was used for phase identification. The quantitative determination was made using the RIR (reference intensity ratio) methodology.

DNA Extraction and Sequencing

DNA from sediments (PM7 and PM11) and crusts (PMW and PMB) were extracted according to the following protocol. Sediments were extracted in duplicates, while crusts were extracted in triplicates.

Cells were disrupted using FastPrep-24TM (MP Biomedicals), and genomic DNA was extracted in duplicates from each sample using the commercial kit Quick-DNA Fecal/Soil Miniprep kit (Zymo Research, Irvine, CA, United States), according to the manufacturer's instructions. DNA was quantified using SpectraMax QuickDrop (Molecular Devices, San Jose, CA, United States) and was further used as a template to investigate the composition of microbial communities in the samples. MiSeq 16S V3–V4 Metagenome Sequencing was performed by a commercial company (Macrogen, Amsterdam, Netherlands). PCR of the V3–V4 hypervariable regions of the bacterial and archeal SSU rRNA gene was performed using primers 341F (50-CCTACGGGNGGCWGCAG-3) and 805R (50-GACTACHVGGGTATCTAATCC-30), according to Illumina's 16S amplicon-based metagenomics sequencing protocol.

Metabarcoding Analysis

Sequencing primers from both forward and reverse reads and reads containing any N characters were removed using Cutadapt v2.9 (Martin, 2011). Only reads with a minimum length of 250 nt and a maximum of 301 nt were kept for further analysis. Paired-end reads for the 10 samples were processed using the DADA2 package (Callahan et al., 2016a) implemented in R by adapting existing pipelines [Callahan et al., 2016b; DADA2 Pipeline Tutorial (1.16)]. DADA2 allows accurate differentiation between sequencing errors and true biological variation, thus avoiding the use of operational taxonomic units (OTUs). Instead, DADA2 infers amplicon sequence variants (ASVs). Following primer removal, paired reads were loaded into the DADA2 pipeline and trimmed (forward reads 3′ truncated at 280 nt, reverse reads 3′ truncated at 250 nt), filtered (max. 2 errors per read, minimum length after trimming = 200 nt), and finally merged with a minimum required overlap of 50 nt. Chimeras were removed from merged pairs (1,576 bimeras out of 7,439; 95.8% pass rate). Following filtration and chimera removal, a total of 413,539 merged reads were retained (min per sample = 29,706, max per sample = 55,460, average = 41,353). Taxonomic classification of curated ASVs was performed using the SILVA 138.1 database (Pruesse et al., 2007). From the obtained ASVs, a mean value for triplicates (crusts) and duplicates (sediments) was used in the further analysis. Sequence data generated during this study are available in the European Nucleotide Archive (ENA) as part of project PRJEB51350 with accession numbers ERR9118894–ERR9118903.

Statistical Analysis

Differences in community composition and statistics were computed using the phyloseq (McMurdie and Holmes, 2013) package in R. Bray distance-based hierarchical clustering and alpha-diversity were estimated after merging replicates by calculating their mean values. Counts and relative abundances were further generated at the genus, class, family, and phylum levels after taxonomic agglomeration using the tax_glom function provided by phyloseq (McMurdie and Holmes, 2013). Taxa merged at each taxonomic rank were considered for abundance estimations only if they were assigned a minimum of 10 counts in at least one averaged sample. Domain *Bacteria* were considered for further analysis of microbial composition. Shannon and Simpson's diversity indices provided information about the composition of samples by considering both the

number of species and the abundance of each species. Shannon's index gives a better description of a sample's diversity by considering the species richness and rare species, while Simpson's index considers evenness and common species. The Chao1 index estimates diversity from abundance data and gives more weight to low-abundance species.

Venn analysis was performed using Web software developed by Heberle et al. (2015). It was used to indicate the distribution of the genera abundances between the different samples. TBtools were used for heatmap representations (Chen et al., 2020).

We used multidimensional scaling (MDS) to represent the sediment samples in a bi-dimensional space. The MDS was done from a similarity matrix between the chemical characteristics of the samples to the coordinates of these in bi-dimensional space for easy visualization. The analysis was done in XLSTAT 2021.4.1 (Addinsoft, New York, NY, United States).

RESULTS

Chemical and Mineralogical Analysis

The chemical composition of the samples is presented in **Table 1**. The pH of both sediments and crusts was slightly alkaline, ranging from 8.3 to 7.4. The sediment sample collected in the Scientific Reserve (PM7) has a slightly higher pH (8.3) than the sediments collected in the Yellow Chamber (PM11, pH = 7.4) and the crusts (pH = 7.7). The carbon content was low (<3%) in the PM11 sediment and the crusts and much higher in PM7 sediment (11.6%), while the N content was low in all the samples (<1%).

TABLE 1 | Chemical composition of sediment (PM7 and PM11) and crust (PMW and PMB) samples in Muierilor Cave.

Elements	PM7	PM11	PMW	PMB
C (%)	11.6	2	2.84	2.73
N (%)	<0.01	0.84	0.45	0.38
S (mg/kg)	64.7	248	2997	799
Na (mg/kg)	67	397	2485	535
Mg (mg/kg)	282	1208	2275	859
K (mg/kg)	96	3390	2816	678
Ca (mg/kg)	303673	358330	360033	342288
Al (mg/kg)	2537	25183	11931	2758
Fe (mg/kg)	152	25246	8554	739
P (mg/kg)	243	22053	60656	60992
Ba (mg/kg)	44.4	363	111	66.9
Li (mg/kg)	0.96	11.9	9.84	1.87
V (mg/kg)	6.7	24.0	59.7	3.3
Cr (mg/kg)	1.0	24.7	37.7	8.1
Mn (mg/kg)	7.2	240	673	711
Co (mg/kg)	1.0	3.4	10.3	1.7
Ni (mg/kg)	17.9	10.9	93	19.5
Cu (mg/kg)	1.7	286	329	195
Zn (mg/kg)	6.1	559	2251	2387
Ga (mg/kg)	0.06	8.11	3.28	0.7
As (mg/kg)	14.3	5.5	75.3	5.6
Rb (mg/kg)	0.72	37.9	13.1	1.67
Sr (mg/kg)	49.9	138	148	171
Zr (mg/kg)	0.60	7.95	6.56	1.43
Cd (mg/kg)	0.10	2.1	4.4	5.3
Pb (mg/kg)	1.0	11.0	18.9	2.7

The MDS that uses the chemical composition of samples (**Supplementary Figure 1**) shows the similarity between the crusts separated from the sediment samples. Spatially and thus chemically, PM11 is the nearest to the crusts.

Calcium is the main element present in all the samples, accounting for 30–40% of the sample. The sediment sample collected in the Yellow Chamber (PM11) had higher major and trace element concentrations than the sediment in PM7. Except for Al, Fe, K, and Ba, the sediment in the Yellow Chamber had a lower concentration of metals than the crusts. The high P content in the samples from Yellow Chamber (about 6% in crusts and 2.5% in PM11 sediment) suggests the presence of minerals containing P, most probably hydroxyapatite (**Supplementary Figure 2**). The PM7 sediment sample has a Ca content similar to that of the crusts, but a much lower P content. The white crust (PMW) has one order of magnitude higher contents of S, Na, Mg, K, Al, and Fe and slightly higher contents of trace elements, suggesting that aluminosilicates constitute these secondary minerals. The high amount of these elements is also reflected in the different abundance of microbial composition in our samples.

X-ray diffraction patterns show that the mineralogical composition of sediments collected from the cave contains mostly primary minerals of detrital origin (**Supplementary Figure 2**). The mineralogical association is relatively similar, with both samples containing quartz, muscovite, and albite in various concentrations. In addition to the mentioned silicates, the PM11 sample collected from the Yellow Chamber includes hydroxyapatite.

Guano Deposit Age

The guano sample collected from the bottom of the deposit in the Guano Chamber (**Figure 1C**) yielded a ^{14}C age of 1,315 ± 30 years BP, which corresponds to a calibrated age between AD 654 and 775 (95.4% probability).

Analysis of Microbial Composition

A total of 5,864 ASVs belonging to *Archaea* (13) and *Bacteria* (5,850) were identified, from which a total of 45 phyla, 105 classes, 221 orders, 265 families, and 464 genera were detected in the four samples. Many ASVs were unclassified at each level, namely 43 phyla (PM7, 16; PM11, 11; PMW, 9; PMB, 7), 332 classes, 901 orders, 2,004 families, and 3,497 genera. Following taxa agglomeration and filtration, 41 phyla, 92 classes, 189 orders, 232 families, and 378 genera were detected in the four averaged samples. Thirty-nine phyla, 90 classes, 187 orders, 231 families, and 378 genera were detected in the four averaged samples.

Among all the four samples, *Proteobacteria* was the most abundant phylum (**Figure 2**), with varied percentages in each sample (PM7, 26%; PM11, 32%; PMW, 55%; and PMB, 45%), followed by *Actinobacteriota* (PM7, 21%; PM11, 17%; PMW, 12%; and PMB, 31%). The third most abundant phyla were

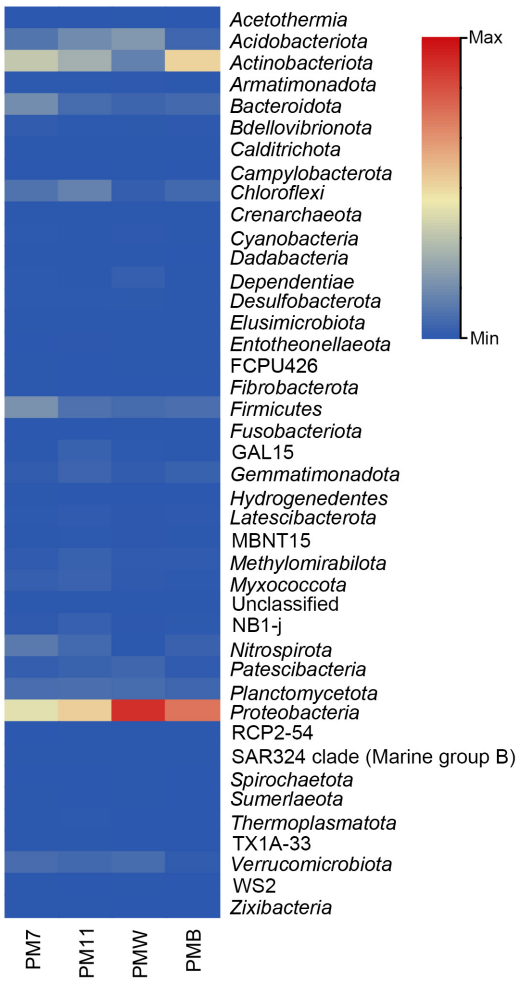

FIGURE 2 | Heatmap of the relative abundance of the different bacterial phyla in the four analyzed samples of Muierilor Cave.

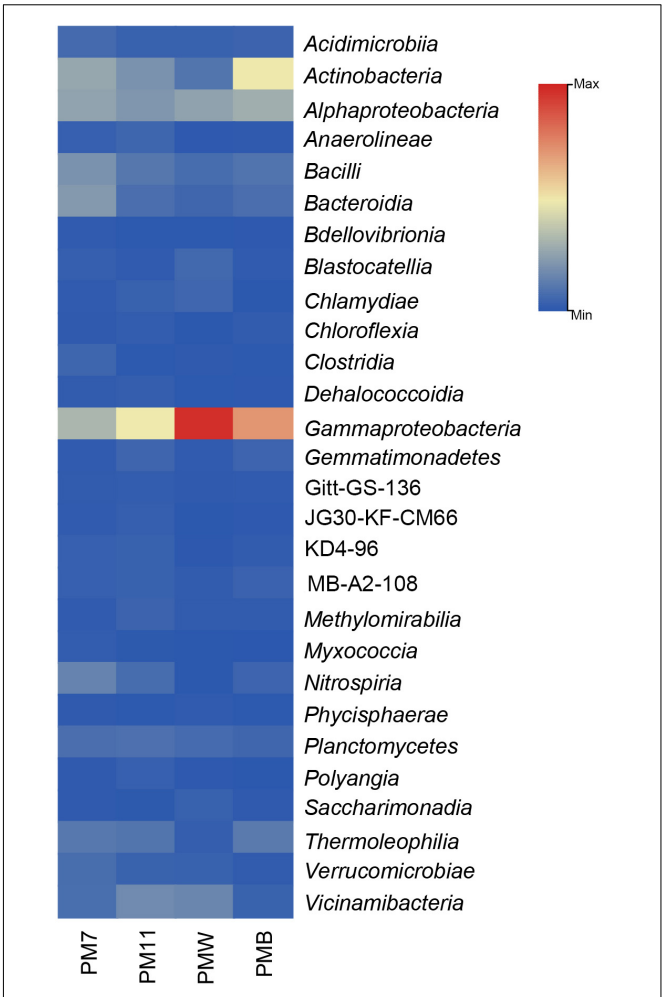

FIGURE 3 | The relative abundance (only > 1% are represented) of the bacterial classes in the four analyzed samples of Muierilor Cave.

Firmicutes in PM7 and PMB (11% and 4%) and *Acidobacteriota* in PM11 and PMW (10 and 8%).

Few differences were identified when comparing the presence and absence of phyla, with some present only in sediments or crusts and others present only in one of the samples. *Acetothermia, Campylobacterota,* and *Spirochaetota* were only identified in PMW, while *Fibrobacterota* and *Hydrogenedentes* were observed only in PM7. In addition, *Fusobacteriota* was only found in crust samples, while *Zixibacteria* and TX1A-33 were found in sediment samples.

At the class level, the relative abundance differed among the samples (**Figure 3**). In sediment sample PM7, *Gammaproteobacteria* (14%) was the most abundant class, followed by *Actinobacteria* (12%) and *Alphaproteobacteria* (11%). The most abundant class in PM11 was *Gammaproteobacteria* (22%), followed by *Alphaproteobacteria* and *Actinobacteria* (∼9%).

In the crust sample PMW, *Gammaproteobacteria* was the most abundant (∼44%), followed by *Alphaproteobacteria* (12%). In PMB, the most abundant class was also *Gammaproteobacteria* (32%), followed by *Actinobacteria* (22%) and *Alphaproteobacteria* (13%).

Families found in high abundance (**Figure 4**) in the sediment sample PM7 were *Micrococcaceae* and *Nitrospiraceae* (∼7%), *Flavobacteriaceae* and *Planococcaceae* (∼5% and 4%); in PM11 were *Micrococcaceae* (4%), *Nitrosococcaceae* (∼4%), and *Nitrospiraceae* (3%); in the crust sample PMW were *Diplorickettsiaceae* (8%), *Comamonadaceae* (7%), and *Coxiellaceae* (5%); and in PMB were *Nitrosococcaceae* (14%), *Micrococcaceae* (13%), and *Oxalobacteraceae* (6%).

The relative abundance of genera was different among the samples and even between the samples of the same type. The most abundant genera in each sample (**Figure 5**) were *Nitrospira, Flavobacterium*, and *Pseudarthrobacter* in PM7; wb1-P19, *Nitrospira*, NA ASV82, and *Pseudarthrobacter* in PM11; *Aquicella, Delftia,* and *Coxiella* in PMW; and wb1-P19, *Pseudarthrobacter*, and *Massilia* in PMB. The abundance of the total unassigned genera was significantly high (PM7, 31%; PM11,

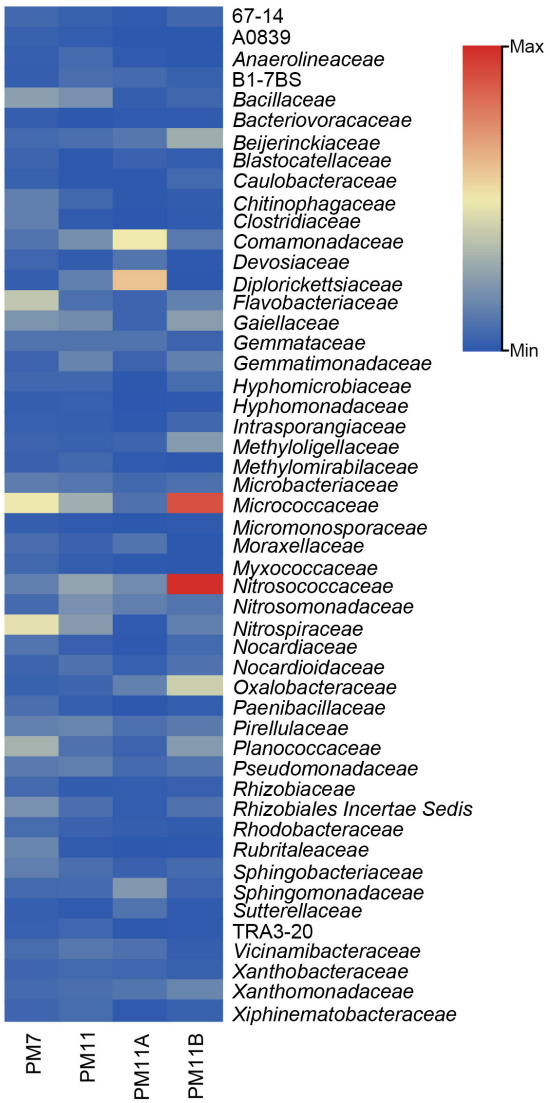

FIGURE 4 | Heatmap of the relative abundance (only > 1% are represented) of bacterial families in the sediment and crust samples of Muierilor Cave.

31%; PMW, 29%; and PMB, 25%), and representatives were found to be among the firsts (**Figure 5**).

Further analysis indicated the presence of human-related bacteria mainly in Yellow Chamber samples and some presenting potential of being pathogenic (**Supplementary Table 1**), such as *Actinomyces, Prevotella*, and *Bacteroides*. Almost half of the identified genera were not mentioned to be present in the caves or guano before, with crust samples having the higher abundance (38% in PMW and 25% in PMB).

We performed a Venn analysis to better visualize the differences at the genus level (**Figure 6**). Of the 378 assigned genera, 90 were found in all four samples. The number of genera identified in PM7 (219) was lower than that identified in PM11 (228). The number of genera identified in PMW (248) was higher than in PMB (192). The crust sample PMW (72) had the highest number of unique genera, followed by the sediment samples PM7 (26) and PM11 (24), while PMB (3) had the lowest number.

The calculated alpha diversity indices (Shannon, Chao1, Simpson's, InvSimpson; **Table 2**) showed that the bacterial diversity differed between the samples, with a higher diversity in the sediment samples than in the crust samples. Richness estimator, Chao1, showed high values in the sediment samples.

DISCUSSION

Chemical and Mineralogical Considerations

The four analyzed samples had a high content of Ca originating from other minerals in this sample, most probably from the limestone rock or calcite dissolution. Among the four samples, only the ones collected from the Yellow Chamber (crusts and PM11) had high P content, which can be attributed to the presence of hydroxyapatite as one of their main constituents. The higher contents of S, Na, Mg, K, Al, Fe, and trace elements in the white crust suggest the presence of aluminosilicates in these secondary minerals. Detrital minerals (quartz, muscovite, and albite) are related to the weathering and transport of soils and geological formations that outcrop outside the cave (Bosch and White, 2004; Kurečić et al., 2021) by running or percolating waters. Hydroxyapatite can be formed in the cave environment by interacting with phosphorus ions and the carbonate component (Audra et al., 2019). The source of phosphate in caves is usually represented either by a fossil bone deposit or a guano accumulation (Hill, 1999; Queffelec et al., 2018). Elements, such as C, P, N, S, K, Na, Cl, Ca, Mg, Fe, Al, Zn, and Ba, were usually identified in guano deposits (Miko et al., 2001; Wurster et al., 2015; Misra et al., 2019), and high concentration of these elements was also found in both the crusts of Muierilor Cave. Considering that no bat colonies or fossil bones are present in the Scientific Reserve, the mechanisms involved in the precipitation of hydroxyapatite in the Yellow Chamber could be related to the presence of organic matter in the above level (the Touristic Passage). The possible source of organic matter in the Touristic Passage is represented by a recent guano deposit (less than c. 1,400 years BP) and fossil bone remains with ages ranging between ∼20,000 and ∼50,000 ka (Mirea et al., 2021). The fossil bone deposits may represent the main source of PO_4, but the leaching of guano should also be considered. The actual source of phosphate for the Scientific Reserve is challenging to assess, and further studies are required to understand the mechanisms responsible for hydroxyapatite precipitation.

Microbial Diversity of Sediments vs. Crusts

The microbiological surveys of caves indicate that the most abundant phyla usually found in caves are *Proteobacteria* and *Actinobacteriota* in different proportions, followed by *Firmicutes, Bacteroidota*, and *Chloroflexi* (Porca et al., 2012; Kieraite-Aleksandrova et al., 2015; Oliveira et al., 2017; Dhami et al., 2018; Zhu et al., 2019; Tok et al., 2021), a fact which

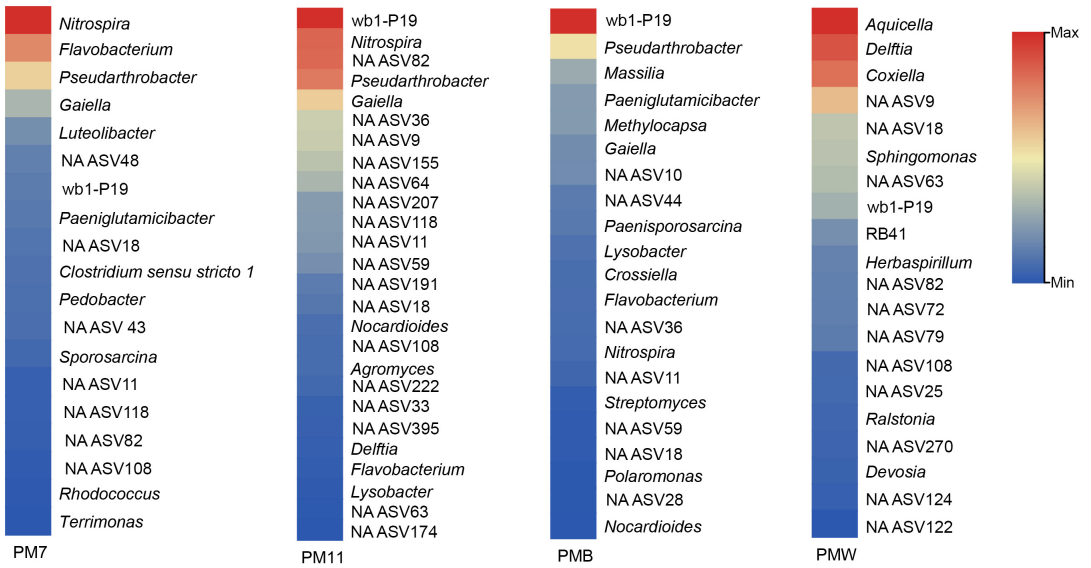

FIGURE 5 | The most abundant genera in each sample of Muierilor Cave (>1%).

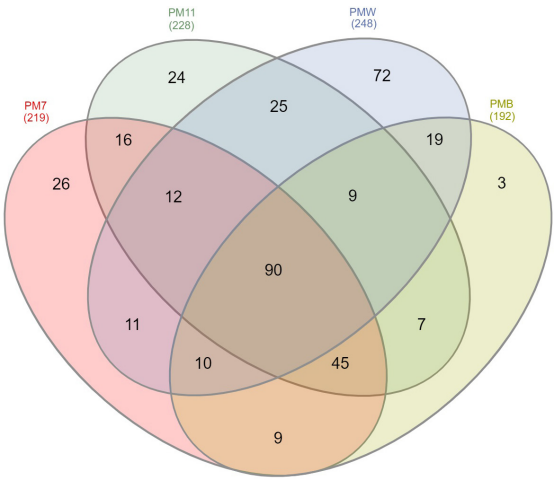

FIGURE 6 | Venn diagram showing the number of shared and unique 16S rRNA-related ASVs in the sediment (PM7 and PM11) and crust (PMW and PMB) samples of Muierilor Cave.

TABLE 2 | Diversity indices of crust (PMW and PMB) and sediment samples (PM7 and PM11) in Muierilor Cave.

Sample		PMB	PMW	PM11	PM7
Diversity indices	Chao1	1424.0887	1547	2241.0263	1870.0765
	Shannon	5.3614	6.2129	6.8254	6.4270
	Simpson's	0.9830	0.9935	0.9968	0.9954
	InvSimpson	58.8863	156.2362	320.9038	218.6732

is consistent with our results. *Proteobacteria* was the most abundant phylum in all the samples and is characterized by a vast metabolic diversity (Kersters et al., 2006; Dong et al., 2020; Tok et al., 2021). *Actinobacteria* was the second most abundant phylum in PM7, PM11, and PMB samples. Members of this phylum are a key community in soil, where they play an important role in the decomposition of organic matter (Madigan et al., 2018; Hazarika and Thakur, 2020; Scheublin et al., 2020). The members of *Acidobacteriota* (second most abundant in PMW and third in PM11) are also known for their involvement in nitrogen assimilation and metabolism of iron, a finding that coincides with the high concentration of N and Fe in our samples (Kielak et al., 2016; Dedysh and Damsté, 2018). The representatives of *Firmicutes* (third most abundant in PM7 and PMB) are commonly found in soils, particularly in the rhizosphere (Kumar et al., 2012). Their presence in caves could be justified by the highly resistant endospores, which are generally unaffected by the environmental stress factors, such as high/low temperatures, unfavorable pH, UV, and lack of water or nutrients (Parkes and Sass, 2009).

Bacterial communities found on the bat's skin represented the members of the families found in high abundance in our samples, such as members of *Micrococcaceae, Flavobacteriaceae, Comamonadaceae*, and *Planococcaceae* (González-Quiñonez et al., 2014; Lemieux-Labonté et al., 2017). In our samples, families found in high abundance were those previously mentioned in caves or related to bats. For instance, members of *Micrococcaceae* and *Planococcaceae* were sampled from cave walls (Laiz et al., 1999; Armetta et al., 2022), members of *Flavobacteriaceae* from cave water (Shabarova and Pernthaler, 2009), members of *Nitrospiraceae* from speleothem surface (Baskar et al., 2016), and members of *Nitrosococcaceae* from sediment and water (Zhu et al., 2019).

A slight correlation could be drawn when commenting on the relationship between chemistry and microbial composition, and the genera identified mirror the chemical composition of the samples. The Yellow Chamber samples (crusts and PM11) were higher in P, and the identified genera involved in the P cycle (Chen et al., 2006; Sarikhani et al., 2019) showed a higher abundance in these samples than those found in PM7. Such genera are *Chryseobacterium, Enterobacter* (PM11, PMW, and PMB), *Delftia, Stenotrophomonas* (PM11 and PMW), and *Pantoea* (PMW). Higher amounts of Fe, N, and Mn were also found in the samples collected from the Yellow Chamber when compared to the PM7 sediments. Some genera, such as *Rheinheimera* (PMW) and *Ralstonia* (PM11 and PMW), are known to be involved in the iron cycle (Swanner et al., 2011; Schröder et al., 2016), while *Aphanizomenon* NIES81 (PMW), *Herbaspirillum, Methylocella,* and *Ralstonia* (PM11 and PMW) are involved in the N cycle (Ploug et al., 2010; Dalsing et al., 2015; Dedysh and Dunfield, 2016; Waller et al., 2021). Bacteria involved in the Mn cycle (Yang et al., 2013; Bai et al., 2021; Lee et al., 2021) were identified as *Escherichia/Shigella, Halomonas, Microbacterium* (PMW), and *Cupriavidus* (PMW and PMB). Elements, such as N, Fe, and P, are usually found in guano (Miko et al., 2001; Wurster et al., 2015; Misra et al., 2019), P is also associated with bones (Audra et al., 2019), and Mn deposits are usually biogenic in caves (Northup and Lavoie, 2001).

Since we analyzed the chemical differences between PM7 and the Yellow Chamber samples, we could also consider this grouping when discussing human- and bat/guano-related genera. Most bat/guano- and human-related genera were identified in the Yellow Chamber samples (**Supplementary Table 1**). PM7 was collected from a passage without guano or other organic accumulation.

Bats are a significant reservoir of pathogens and a well-known vector for disease transmission (Ogórek et al., 2018; Agustin et al., 2019). Genera found in crusts, such as *Fusobacterium* and *Rothia*, were previously related to bats, while *Microbacterium* was previously related to guano. Some genera identified in our samples, most of them in crusts, are also found in the guano of other caves in Europe, which are habitats for the same bat species. These are *Enterococcus, Acinetobacter, Pseudomonas, Paenibacillus, Bacillus, Staphylococcus, Rahnella, Micrococcus, Enterobacter, Lysinibacillus,* and *Sphingobacterium* (Tomova et al., 2013; Vandžurová et al., 2013; Veikkolainen et al., 2014; Vengust et al., 2018; Wolkers-Rooijackers et al., 2019; Dimkić et al., 2020; Gerbáčová et al., 2020). Their abundance did not dominate the microbial composition in our samples, but their presence could indicate a possible connection to the upper Guano Chamber.

The presence of a significant number of genera never reported in a cave before (**Supplementary Table 1**) suggests the limited knowledge regarding the bacterial diversity of caves. Almost half of the genera identified in our samples were never reported in a cave or were never related to bats/guano. Some genera are known members of human microbiota: *Abiotrophia* (Rasic et al., 2020), *Gemella* (García López and Martín-Galiano, 2020), *Granulicatella* (Shailaja et al., 2013), *Treponema* (Seña et al., 2015), and *Haemophilus* (Johnson, 2018). Genera, such as *Bacillus, Escherichia*, and *Staphylococcus*, which are known as "human indicator bacteria," are usually found in high concentrations after extended cave visits (Lavoie and Northup, 2006; Bercea et al., 2018; Mudgil et al., 2018) and were identified in our samples in high abundance. Recent studies in Muierilor Cave compared the microbial composition in touristic and non-touristic sites. Based on an air survey and human exposed surfaces (Bercea et al., 2018, 2019), the touristic sector of Muierilor Cave fits in the high-risk class (500–2,000 CFU/m^3, according to the European Commission's report on Biological Particles in Indoor Environments and Commission of the European Communities, 1994). Moldovan et al. (2020) concluded a clear difference in the microbial composition of water habitats between touristic and non-touristic sites, indicating the strong impact of tourism. These studies found a high abundance of members of *Bacillus* and *Staphylococcus*, which are also abundant in our samples.

Muierilor Cave, as a touristic cave, may be considered as a reservoir of novel and allochthonous species, since animals and humans transit and use it for different purposes. Moreover, visitors play an important role in the spread of bacteria and continuously influence the composition of the microbial community.

CONCLUSION

Most of the identified ASVs in four samples, two sediments and two crusts, collected from Muierilor Cave belong to bacteria. The crusts and the nearby sediment sample in a small chamber (the Yellow Chamber) of the cave are phosphate-rich deposits, with abundant bacteria involved in the P cycle. Moreover, bacteria involved in Fe, Mn, and N cycles were found, as these elements are commonly identified in high concentrations in guano. Since no bat colonies or fossil bones were present in the chamber, a high concentration of these elements could be sourced from organic deposits (fossil bones and guano) located at the upper levels of the cave. The high diversity of human-related genera identified only in the crusts and sediment samples collected from the Yellow Chamber, such as *Capnocytophaga, Anaerococcus, Abiotrophia, Actinomyces, Alloprevotella*, and *Eikenella*, could only be related to the upper touristic sector of the cave. Tourism in caves with bat colonies and guano accumulation should benefit from continuous monitoring of the air and floor microbiomes.

Approximately 47% of non-identified bacteria in a small sector of the complex subterranean system of Muierilor Cave indicates the limited knowledge of the bacterial diversity in caves, and these bacteria have high potential in human health and biotechnology applications.

DATA AVAILABILITY STATEMENT

The datasets presented in this study can be found in online repositories. The names of the repository/repositories and accession number(s) can be found below: ENA – PRJEB51350.

AUTHOR CONTRIBUTIONS

OM and CH designed the research. OM, RN-B, CH, IM, and LF collected the field data. RN-B, CH, and PB contributed to the extraction, bioinformatic analysis, and interpretation of the molecular data. EL, OC, LF, VF, and IA contributed to the chemical and mineralogical analyses. SC and IM contributed to the geological context and radiocarbon data interpretation. CH, OM, PB, EL, IM, and LF wrote the first draft. All the authors corrected and approved the final version.

FUNDING

This research was financially supported by the Ministry of Research, Innovation and Digitization grant, CNCS/CCCDI – UEFISCDI, project no. 2/2019 (DARKFOOD), within PNCDI III, and the EEA Financial Mechanism 2014–2021 under the project contract no. 3/2019 (KARSTHIVES 2).

ACKNOWLEDGMENTS

We are grateful to the editor and the reviewers for their valuable suggestions that improved the manuscript clarity considerably.

SUPPLEMENTARY MATERIAL

The Supplementary Material for this article can be found online at: https://www.frontiersin.org/articles/10.3389/fmicb.2022.877481/full#supplementary-material

REFERENCES

Agustin, A. L. D., Atma, C. D., Munawaroh, M., Ningtyas, N. S., Legowo, A. P., and Sukmanadi, M. (2019). Bacterial pathogens from cave-dwelling bats that are a risk to human, animal and environmental health on Lombok Island, Indonesia. *Eur. J. Biosci.* 13, 1509–1513.

Armetta, F., Cardenas, J., Caponetti, E., Alduina, R., Presentato, A., Vecchioni, L., et al. (2022). Conservation state of two paintings in the Santa Margherita cliff cave: role of the environment and of the microbial community. *Environ. Sci. Pollution Res.* 29, 29510–29523. doi: 10.1007/s11356-021-17211-0

Audra, P., De Waele, J., Bentaleb, I., Chroòáková, A., Krištùfek, V., D'Angeli, I. M., et al. (2019). Guano-related phosphate-rich minerals in European caves. *Int. J. Speleol.* 48, 75–105. doi: 10.5038/1827-806X.48.1.2252

Bai, Y., Su, J., Wen, Q., Huang, T., Chang, Q., and Ali, A. (2021). Characterization and mechanism of Mn (II)-based mixotrophic denitrifying bacterium (*Cupriavidus sp*. HY129) in remediation of nitrate (NO3–N) and manganese (Mn (II)) contaminated groundwater. *J. Hazardous Mater.* 408:124414. doi: 10.1016/j.jhazmat.2020.124414

Baldini, J. U. (2010). The geochemistry of cave calcite deposits as a record of past climate. *Sedimentary Record* 8, 4–9. doi: 10.2110/sedred.2010.2.4

Baskar, S., Routh, J., Baskar, R., Kumar, A., Miettinen, H., and Itävaara, M. (2016). Evidences for microbial precipitation of calcite in speleothems from Krem Syndai in Jaintia Hills, Meghalaya, India. *Geomicrobiol. J.* 33, 906–933. doi: 10.1080/01490451.2015.1127447

Bercea, S., Năstase-Bucur, R., Mirea, I. C., Măntoiu, D. Ş, Kenesz, M., Petculescu, A., et al. (2018). Novel approach to microbiological air monitoring in show caves. *Aerobiologia* 34, 445–468. doi: 10.1007/s10453-018-9523-9

Bercea, S., Năstase-Bucur, R., Moldovan, O. T., Kenesz, M., and Constantin, S. (2019). Yearly microbial cycle of human exposed surfaces in show caves. *Subterranean Biol.* 31, 1–14. doi: 10.3897/subtbiol.31.34490

Bosch, R. F., and White, W. B. (2004). "Lithofacies and transport of clastic sediments in karstic aquifers," in *Studies of Cave Sediments*, eds I. D. Sasowsky and J. Mylroie (Boston, MA: Springer), 1–22. doi: 10.1007/978-1-4419-9118-8_1

Bronk Ramsey, C. (2009). Bayesian analysis of radiocarbon dates. *Radiocarbon* 51, 337–360. doi: 10.2458/azu_js_rc.51.3494

Bronk Ramsey, C. (2020). *OxCal Online*. Available online at: https://c14.arch.ox.ac.uk/oxcal.html (Accessed September 7, 2020).

Burghele, B. D., Cucos, A., Papp, B., Stetca, F. A., Mirea, I., and Constantin, S. (2018). Distribution of radon gas in Romanian show caves and radiation safety. *Radiation Protection Dosimetry* 181, 1–5. doi: 10.1093/rpd/ncy091

Callahan, B. J., McMurdie, P. J., Rosen, M. J., Han, A. W., Johnson, A. J. A., and Holmes, S. P. (2016a). DADA2: high-resolution sample inference from Illumina amplicon data. *Nat. Methods* 13, 581–583. doi: 10.1038/nmeth.3869

Callahan, B. J., Sankaran, K., Fukuyama, J. A., McMurdie, P. J., and Holmes, S. P. (2016b). Bioconductor workflow for microbiome data analysis: from raw reads to community analyses. *F1000Research* 5:1492. doi: 10.12688/f1000research.8986.2

Chen, C., Chen, H., Zhang, Y., Thomas, H. R., Frank, M. H., He, Y., et al. (2020). TBtools: an integrative toolkit developed for interactive analyses of big biological data. *Mol. Plant* 13, 1194–1202. doi: 10.1016/j.molp.2020.06.009

Chen, Y. P., Rekha, P. D., Arun, A. B., Shen, F. T., Lai, W. A., and Young, C. C. (2006). Phosphate solubilizing bacteria from subtropical soil and their tricalcium phosphate solubilizing abilities. *Appl. Soil Ecol.* 34, 33–41. doi: 10.1016/j.apsoil.2005.12.002

Cigna, A. A. (2019). "Chapter 108 - show caves," in *Encyclopedia of Caves*, 3rd Edn, eds W. B. White, D. C. Culver, and T. Pipan (Waltham, MA: Academic Press), 909–921. doi: 10.1016/B978-0-12-814124-3.00108-4

Cigna, A. A., and Burri, E. (2000). Development, management and economy of show caves. *Int. J. Speleol.* 29, 1–27. doi: 10.5038/1827-806x.29.1.1

Commission of the European Communities (1994). *Report no. 12: Biological Particles in Indoor Environments*. Luxembourg: Commission of the European Communities.

Constantin, S., Mirea, I. C., Petculescu, A., Arghir, R. A., Măntoiu, D. Ş, Kenesz, M., et al. (2021). Monitoring human impact in show caves. a study of four Romanian caves. *Sustainability* 13:1619. doi: 10.3390/su13041619

Culver, D. C., and Pipan, T. (2019). "Survey of subterranean life," in *The Biology Of Caves And Other Subterranean Habitats*, eds D. C. Culver and T. Pipan (Oxford: Oxford University Press), 40–74. doi: 10.1093/oso/9780198820765.003.0003

DADA2 Pipeline Tutorial (1.16). Available online at: http://benjjneb.github.io/dada2/tutorial.html

Dalsing, B. L., Truchon, A. N., Gonzalez-Orta, E. T., Milling, A. S., and Allen, C. (2015). Ralstonia solanacearum uses inorganic nitrogen metabolism for virulence, ATP production, and detoxification in the oxygen-limited host xylem environment. *mBio* 6:e02471-14. doi: 10.1128/mBio.02471-14

Dean, G. (1957). Cave disease. *Central African J. Med.* 3, 79–81.

Debata, S. (2020). Bats in a cave tourism and pilgrimage site in eastern India: conservation challenges. *Oryx* 55, 684–691. doi: 10.1017/S00306053190 0098X

Dedysh, S. N., and Damsté, J. S. S. (2018). "Acidobacteria ," in *Encyclopedia of Life Sciences*, (Chichester: John Wiley and Sons, Ltd.), 1–10. doi: 10.1002/9780470015902.a0027685

Dedysh, S. N., and Dunfield, P. F. (2016). "Methylocella," in *Bergey's Manual of Systematics of Archaea and Bacteria*, eds M. E. Trujillo, S. Dedysh, P. DeVos, B. Hedlund, P. Kämpfer, F. A. Rainey, et al. (Hoboken, NJ: John Wiley and Sons, Inc), 1–9. doi: 10.1002/9781118960608.gbm00797.pub2

Dhami, N. K., Mukherjee, A., and Watkin, E. L. (2018). Microbial diversity and mineralogical-mechanical properties of calcitic cave speleothems in natural and in vitro biomineralization conditions. *Front. Microbiol.* 9:40. doi: 10.3389/fmicb.2018.00040

Dimkić, I., Stanković, S., Kabić, J., Stupar, M., Nenadić, M., Ljaljević-Grbić, M., et al. (2020). Bat guano-dwelling microbes and antimicrobial properties of the

pygidial gland secretion of a troglophilic ground beetle against them. *Appl. Microbiol. Biotechnol.* 104, 4109–4126. doi: 10.1007/s00253-020-10498-y

Dong, Y., Gao, J., Wu, Q., Ai, Y., Huang, Y., Wei, W., et al. (2020). Co-occurrence pattern and function prediction of bacterial community in Karst cave. *BioMed. Central Microbiol.* 20:137. doi: 10.1186/s12866-020-01806-7

Friedrich, M. (2019). "Adaptation to darkness," in *Encyclopedia of Caves*, 3rd Edn, eds W. B. White, D. C. Culver, and T. Pipan (Cambridge, MA: Academic Press), 16–23. doi: 10.1016/B978-0-12-814124-3.00003-0

García López, E., and Martín-Galiano, A. J. (2020). The versatility of opportunistic infections caused by Gemella isolates is supported by the carriage of virulence factors from multiple origins. *Front. Microbiol.* 11:524. doi: 10.3389/fmicb.2020.00524

Gascoyne, M. (1992). Palaeoclimate determination from cave calcite deposits. *Quaternary Sci. Rev.* 11, 609–632. doi: 10.1016/0277-3791(92)90074-I

Gerbáčová, K., Malinièová, L., Kisková, J., Maslišová, V., Uhrin, M., and Pristaš, P. (2020). The faecal microbiome of building-dwelling insectivorous bats (*Myotis myotis* and *Rhinolophus hipposideros*) also contains antibiotic-resistant bacterial representatives. *Curr. Microbiol.* 77, 2333–2344. doi: 10.1007/s00284-020-02095-z

González-Quiñonez, N., Fermin, G., and Muñoz-Romo, M. (2014). Diversity of bacteria in the sexually selected epaulettes of the little yellow-shouldered bat *Sturnira lilium* (Chiroptera: Phyllostomidae). *Interciencia* 39, 882–889.

Hazarika, S. N., and Thakur, D. (2020). "Actinobacteria," in *Beneficial Microbes in Agro-Ecology*, eds N. Amaresan, M. Senthil Kumar, K. Annapurna, K. Kumar, and A. Sankaranarayanan (Cambridge, MA: Academic Press), 443–476. doi: 10.1016/B978-0-12-823414-3.00021-6

Heberle, H., Meirelles, G. V., da Silva, F. R., Telles, G. P., and Minghim, R. (2015). InteractiVenn: a web-based tool for the analysis of sets through Venn diagrams. *BioMed. Central Bioinform.* 16:169. doi: 10.1186/s12859-015-0611-3

Hershey, O. S., and Barton, H. A. (2018). "The microbial diversity of caves," in *Cave Ecology*, eds O. T. Moldovan, L. Kováè, and S. Halse (Cham: Springer), 69–90. doi: 10.1007/978-3-319-98852-8_5

Hervant, F., and Malard, F. (2019). "Adaptations: low oxygen," in *Encyclopedia of Caves*, 3rd Edn, eds W. B. White, D. C. Culver, and T. Pipan (Cambridge, MA: Academic Press), 8–15. doi: 10.1016/B978-0-12-814124-3.00002-9

Hill, A. C., and Forti, P. (1995). The classification of cave minerals and speleothems. *Int. J. Speleol.* 24, 77–82. doi: 10.5038/1827-806x.24.1.5

Hill, C. A. (1999). Mineralogy of Kartchner Caverns, Arizona. *J. Cave Karst Stud.* 61, 73–78.

Howarth, G. F., and Moldovan, T. O. (2018). "The ecological classification of cave animals and their adaptations," in *Cave Ecology*, eds T. O. Moldovan, L. Kovac, and S. Halse (Berlin: Springer), 41–67. doi: 10.1007/978-3-319-98852-8_4

Hoyos, M., Soler, V., Cañaveras, J. C., Sánchez-Moral, S., and Sanz-Rubio, E. (1998). Microclimatic characterization of a karstic cave: human impact on microenvironmental parameters of a prehistoric rock art cave (*Candamo Cave*, northern Spain). *Environ. Geol.* 33, 231–242. doi: 10.1007/s002540050242

Igreja, R. P. (2011). Infectious diseases associated with caves. *Wilderness Environ. Med.* 22, 115–121. doi: 10.1016/j.wem.2011.02.012

Jiang, Z. K., Guo, L., Chen, C., Liu, S. W., Zhang, L., Dai, S. J., et al. (2015). Xiakemycin a, a novel pyranonaphthoquinone antibiotic, produced by the *Streptomyces sp*. CC8-201 from the soil of a karst cave. *J. Antibiotics* 68, 771–774. doi: 10.1038/ja.2015.70

Johnson, D. I. (2018). "*Haemophilus spp*," in *Bacterial Pathogens and Their Virulence Factors*, ed. D. I. Johnson (Cham: Springer), 249–256. doi: 10.1007/978-3-319-67651-7_17

Jurado, V., Laiz, L., Rodriguez-Nava, V., Boiron, P., Hermosin, B., Sanchez-Moral, S., et al. (2010). Pathogenic and opportunistic microorganisms in caves. *Int. J. Speleol.* 39, 15–24. doi: 10.5038/1827-806x.39.1.2

Kersters, K., De Vos, P., Gillis, M., Swings, J., Vandamme, P., and Stackebrant, E. (2006). "Introduction to the proteobacteria," in *The Prokaryotes*, eds M. Dworkin, S. Falkow, E. Rosenberg, K. H. Schleifer, and E. Stackebrandt (New York, NY: Springer), 3–37. doi: 10.1007/0-387-30745-1_1

Kielak, A. M., Barreto, C. C., Kowalchuk, G. A., Van Veen, J. A., and Kuramae, E. E. (2016). The ecology of Acidobacteria: moving beyond genes and genomes. *Front. Microbiol.* 7:744. doi: 10.3389/fmicb.2016.00744

Kieraite-Aleksandrova, I., Aleksandrovas, V., and Kuisiene, N. (2015). Down into the Earth: microbial diversity of the deepest cave of the world. *Biologia* 70, 989–1002. doi: 10.1515/biolog-2015-0127

Kowalko, E. J. (2019). "Chapter 4 - adaptations: behavioral," in *Encyclopedia of Caves*, eds W. White, D. C. Culver, and T. Pipan (Waltham, MA: Academic Press), 24–32. doi: 10.1016/B978-0-12-814124-3.00004-2

Kumar, G., Kanaujia, N., and Bafana, A. (2012). Functional and phylogenetic diversity of root-associated bacteria of Ajuga bracteosa in Kangra valley. *Microbiol. Res.* 167, 220–225. doi: 10.1016/j.micres.2011.09.001

Kurečić, T., Bočić, N., Wacha, L., Bakrač, K., Grizelj, A., Tresič Pavičić, D., et al. (2021). Changes in cave sedimentation mechanisms during the Late Quaternary: an example from the Lower Cerovaèka Cave. Croatia. *Front. Earth Sci.* 9:672229. doi: 10.3389/feart.2021.672229

Laiz, L., Groth, I., Gonzalez, I., and Saiz-Jimenez, C. (1999). Microbiological study of the dripping waters in Altamira cave (Santillana del Mar, Spain). *J. Microbiol. Methods* 36, 129–138. doi: 10.1016/s0167-7012(99)00018-4

Lavoie, K. H., and Northup, D. E. (2006). "Bacteria as indicators of human impact in caves," in *Proceedings of the 17th National Cave and Karst Management Symposium*, (Albany, NY: The NCKMS Steering Committee), 40–47.

Lee, C. J., Wright, M. H., Bentley, S. R., and Greene, A. C. (2021). Draft genome sequence of *Halomonas sp*. strain KAO, a halophilic Mn (II)-oxidizing bacterium. *Microbiol. Resource Announcements* 10:e0032-21. doi: 10.1128/MRA.00032-21

Lemieux-Labonté, V., Simard, A., Willis, C. K., and Lapointe, J. F. (2017). Enrichment of beneficial bacteria in the skin microbiota of bats persisting with white-nose syndrome. *Microbiome* 5:115. doi: 10.1186/s40168-017-0334-y

Leroi-Gourhan, A. (1982). The archaeology of *Lascaux cave*. *Sci. Am.* 246, 104–113. doi: 10.1038/scientificamerican0682-104

Madigan, M. T., Bender, K. S., Buckley, D. H., Sattley, W. M., and Stahl, D. A. (2018). "Chapter 16 – diversity of bacteria," in *Brock Biology of Microorganisms*, 15th Global Edn, eds M. T. Madigan, K. S. Bender, D. H. Buckley, W. M. Sattley, and D. A. Stahl (Boston, MA: Benjamin Cummins), 530–565.

Mann, S. L., Steidl, R. J., and Dalton, V. M. (2002). Effects of cave tours on breeding *Myotis velifer*. *J. Wildlife Manag.* 66, 618–624. doi: 10.2307/3803128

Martin, M. (2011). Cutadapt removes adapter sequences from high-throughput sequencing reads. *Eur. Mol. Biol. Network J.* 17, 10–12. doi: 10.14806/ej.17.1.200

McMurdie, P. J., and Holmes, S. (2013). phyloseq: an R package for reproducible interactive analysis and graphics of microbiome census data. *Public Library Sci. One* 8:e61217. doi: 10.1371/journal.pone.0061217

Miko, S., Kuhta, M., and Kapelj, S. (2001). "Bat guano influence on the geochemistry of cave sediments from Modriè Cave; Croatia," in *Proceedings of the 13th International Congress of Speleology*, (Brazil).

Mirea, I. C., Robu, M., Petculescu, A., Kenesz, M., Faur, L., Arghir, R., et al. (2021). Last deglaciation flooding events in the Southern Carpathians as revealed by the study of cave deposits from Muierilor Cave. Romania. *Palaeogeography Palaeoclimatol. Palaeoecol.* 562:110084. doi: 10.1016/j.palaeo.2020.110084

Misra, P. K., Gautam, N. K., and Elangovan, V. (2019). Bat guano: a rich source of macro and microelements essential for plant growth. *Ann. Plant Soil Res.* 21, 82–86.

Moldovan, O. T., Bercea, S., Năstase-Bucur, R., Constantin, S., Kenesz, M., Mirea, I. C., et al. (2020). Management of water bodies in show caves – a microbial approach. *Tour. Manag.* 78:104037. doi: 10.1016/j.tourman.2019.104037

Mudgil, D., Baskar, S., Baskar, R., Paul, D., and Shouche, Y. S. (2018). Biomineralization potential of *Bacillus subtilis*, *Rummeliibacillus stabekisii* and *Staphylococcus epidermidis* strains in vitro isolated from speleothems, Khasi Hill Caves, Meghalaya, India. *Geomicrobiol. J.* 35, 675–694. doi: 10.1080/01490451.2018.1450461

Northup, D. E., and Lavoie, K. H. (2001). Geomicrobiology of caves: a review. *Geomicrobiol. J.* 18, 199–222. doi: 10.1080/01490450152467750

Novas, N., Gázquez, J. A., MacLennan, J., García, R. M., Fernández-Ros, M., and Manzano-Agugliaro, F. (2017). A real-time underground environment monitoring system for sustainable tourism of caves. *J. Cleaner Product.* 142, 2707–2721. doi: 10.1016/j.jclepro.2016.11.005

Ogórek, R., Guz-Regner, K., Kokurewicz, T., Baraniok, E., and Kozak, B. (2018). Airborne bacteria cultivated from underground hibernation sites in the Nietoperek Bat Reserve (Poland). *J. Cave Karst Stud.* 80, 161–171. doi: 10.4311/2017MB0117

Oliveira, C., Gunderman, L., Coles, C. A., Lochmann, J., Parks, M., Ballard, E., et al. (2017). 16S rRNA gene-based metagenomic analysis of Ozark cave bacteria. *Diversity* 9:31. doi: 10.3390/d9030031

Paksuz, S., and Özkan, B. (2012). The protection of the bat community in the Dupnisa Cave System, Turkey, following opening for tourism. *Oryx* 46, 130–136. doi: 10.1017/s0030605310001493

Parkes, R. J., and Sass, H. (2009). "Deep sub-surface," in *Encyclopedia of Microbiology*, 3rd Edn, ed. M. Schaechter (Cambridge, MA: Academic Press), 64–79. doi: 10.1007/978-3-642-11274-4_573

Ploug, H., Musat, N., Adam, B., Moraru, L. C., Lavik, G., Vagner, T., et al. (2010). Carbon and nitrogen fluxes associated with the cyanobacterium *Aphanizomenon sp*. in the Baltic Sea. *Int. Soc. Microbial Ecol.* 4, 1215–1223. doi: 10.1038/ismej.2010.53

Polyak, J. V., and Denniston, F. R. (2019). "Paleoclimate records from speleothems," in *Encyclopedia of Caves*, eds W. White, D. C. Culver, and T. Pipan (Waltham, MA: Academic Press), 784–793. doi: 10.1016/B978-0-12-814124-3.00095-9

Porca, E., Jurado, V., Žgur-Bertok, D., Saiz-Jimenez, C., and Pašić, L. (2012). Comparative analysis of yellow microbial communities growing on the walls of geographically distinct caves indicates a common core of microorganisms involved in their formation. *FEMS Microbiol. Ecol.* 81, 255–266. doi: 10.1111/j.1574-6941.2012.01383.x

Prelovšek, M., Gabrovšek, F., Kozel, P., Mulec, J., Pipan, T., and Šebela, S. (2021). The Škocjan Caves–UNESCO World Heritage Site. *Zeitschrift für Geomorphologie Supplementary Issues* 62, 49–64. doi: 10.1127/zfg_suppl/2021/0690

Pruesse, E., Quast, C., Knittel, K., Fuchs, B. M., Ludwig, W., Peplies, J., et al. (2007). SILVA: a comprehensive online resource for quality checked and aligned ribosomal RNA sequence data compatible with ARB. *Nucleic Acids Res.* 35, 7188–7196. doi: 10.1093/nar/gkm864

Pulido-Bosch, A., Martin-Rosales, W., López-Chicano, M., Rodriguez-Navarro, C. M., and Vallejos, A. (1997). Human impact in a tourist karstic cave (Aracena, Spain). *Environ. Geol.* 31, 142–149. doi: 10.1007/s002540050173

Queffelec, A., Bertran, P., Bos, T., and Lemée, L. (2018). Mineralogical and organic study of bat and chough guano: implications for guano identification in ancient context. *J. Cave Karst Stud. Natl. Speleol. Soc.* 80, 49–65. doi: 10.4311/2017ES0102

Rangseekaew, P., and Pathom-Aree, W. (2019). Cave actinobacteria as producers of bioactive metabolites. *Front. Microbiol.* 10:387. doi: 10.3389/fmicb.2019.00387

Rasic, P., Bosnic, S., Vasiljevic, Z. V., Djuricic, S. M., Milickovic, M., and Savic, D. (2020). Abiotrophia defectiva liver abscess in a teenage boy after a supposedly mild blunt abdominal trauma: a case report. *BioMed. Central Gastroenterol.* 20, 1–6. doi: 10.1186/s12876-020-01409-6

Reimer, P., Austin, W., Bard, E., Bayliss, A., Blackwell, P., Bronk Ramsey, C., et al. (2020). The IntCal20 Northern Hemisphere radiocarbon age calibration curve (0–55 cal kBP). *Radiocarbon* 62, 725–757. doi: 10.1017/RDC.2020.41

Ronquillo, P. W. (1995). Anthropological and cultural values of caves. *Philippine Quarterly Culture Soc.* 23, 138–150. doi: 10.1371/journal.pone.0254848

Saiz-Jimenez, C., Cuezva, S., Jurado, V., Fernandez-Cortes, A., Porca, E., Benavente, D., et al. (2011). Paleolithic art in peril: policy and science collide at Altamira Cave. *Science* 334, 42–43. doi: 10.1126/science.1206788

Sarikhani, M. R., Khoshru, B., and Greiner, R. (2019). Isolation and identification of temperature tolerant phosphate solubilizing bacteria as a potential microbial fertilizer. *World J. Microbiol. Biotechnol.* 35:126. doi: 10.1007/s11274-019-2702-1

Scheublin, T. R., Kielak, A. M., van den Berg, M., van Veen, J. A., and de Boer, W. (2020). Identification and antimicrobial properties of bacteria isolated from naturally decaying wood. *bioRxiv [preprint]* doi: 10.1101/2020.01.07.896464

Schröder, J., Braun, B., Liere, K., and Szewzyk, U. (2016). Draft genome sequence of *Rheinheimera sp*. strain SA_1 isolated from iron backwash sludge in Germany. *Genome Announcements* 4:e00853-16. doi: 10.1128/genomeA.00853-16

Seña, A. C., Pillay, A., Cox, D. L., and Radolf, J. D. (2015). "*Treponema* and *Brachyspira*, human host-associated *spirochetes*," in *Manual of Clinical Microbiology*, ed. J. H. Jorgensen, K. C. Carroll, G. Funke, M. A. Pfaller, M. L. Landry, S. S. Richter, et al. (Washington, DC: American Society of Microbiology), 1055–1081. doi: 10.1128/9781555817381.ch60

Shabarova, T., and Pernthaler, J. (2009). "Investigation of bacterioplankton communities in aquatic karst pools in Bärenschacht cave of Bernese Oberland," in *Proceedings of the 15th International Congress of Speleology, Kerrville, Texas, July 19-26, 2009*, (Huntsville, AL: National Speleological Society), 416–421.

Shailaja, T. S., Sathiavathy, K. A., and Unni, G. (2013). Infective endocarditis caused by *Granulicatella adiacens*. *Indian Heart J.* 65, 447–449. doi: 10.1016/j.ihj.2013.06.014

Skeates, R., and Bergsvik, K. A. (2012). "Chapter 1 caves in context: an introduction," in *Caves in Context: the Cultural Significance of Caves and Rockshelters in Europe*, eds S. R. Skeates and K. A. Bergsvik (Oxford: Oxbow Books), doi: 10.2307/j.ctvh1djk4

Swanner, E. D., Nell, R. M., and Templeton, A. S. (2011). *Ralstonia species* mediate Fe-oxidation in circumneutral, metal-rich subsurface fluids of Henderson mine, CO. *Chem. Geol.* 284, 339–350. doi: 10.1016/j.chemgeo.2011.03.015

Tičar, J., Tomič, N., Valjavec, M. B., Zorn, M., Markovič, S. B., and Gavrilov, M. B. (2018). Speleotourism in Slovenia: balancing between mass tourism and geoheritage protection. *Open Geosci.* 10, 344–357. doi: 10.1515/geo-2018-0027

Tok, E., Olgun, N., and Dalfes, H. N. (2021). Profiling bacterial diversity in relation to different habitat types in a limestone cave: insuyu Cave, Turkey. *Geomicrobiol. J.* 38, 776–790. doi: 10.1080/01490451.2021.1949647

Tomova, I., Lazarkevich, I., Tomova, A., Kambourova, M., and Vasileva-Tonkova, E. (2013). Diversity and biosynthetic potential of culturable aerobic heterotrophic bacteria isolated from Magura Cave, Bulgaria. *Int. J. Speleol.* 42, 65–76. doi: 10.5038/1827-806X.42.1.8

Vandžurová, A., Baèkor, P., Javorskı, P., and Pristaš, P. (2013). Staphylococcus nepalensis in the guano of bats (Mammalia). *Vet. Microbiol.* 164, 116–121. doi: 10.1016/j.vetmic.2013.01.043

Veikkolainen, V., Vesterinen, E. J., Lilley, T. M., and Pulliainen, A. T. (2014). Bats as reservoir hosts of human bacterial pathogen, *Bartonella mayotimonensis*. *Emerg. Infect. Dis.* 20, 960–967. doi: 10.3201/eid2006.130956

Vengust, M., Knapic, T., and Weese, J. S. (2018). The faecal bacterial microbiota of bats; Slovenia. *Public Library Sci. One* 13:e0196728. doi: 10.1371/journal.pone.0196728

Waller, S., Wilder, S. L., Schueller, M. J., Housh, A. B., Scott, S., Benoit, M., et al. (2021). Examining the effects of the nitrogen environment on growth and N2-fixation of endophytic *Herbaspirillum seropedicae* in maize seedlings by applying 11C radiotracing. *Microorganisms* 9:1582. doi: 10.3390/microorganisms9081582

White, B. W. (2019). "Speleothems," in *Encyclopedia of Caves*, eds W. White, D. C. Culver, and T. Pipan (Waltham, MA: Academic Press), doi: 10.1016/B978-0-12-814124-3.00117-5

Wolkers-Rooijackers, J., Rebmann, K., Bosch, T., and Hazeleger, W. (2019). Fecal bacterial communities in insectivorous bats from the Netherlands and their role as a possible vector for foodborne diseases. *Acta Chiroptera* 20, 475–483. doi: 10.3161/15081109acc2018.20.2.017

Wurster, C. M., Munksgaard, N., Zwart, C., and Bird, M. (2015). The biogeochemistry of insectivorous cave guano: a case study from insular Southeast Asia. *Biogeochemistry* 124, 163–175. doi: 10.1007/s10533-015-0089-0

Yang, W., Zhang, Z., Zhang, Z., Chen, H., Liu, J., Ali, M., et al. (2013). Population structure of manganese-oxidizing bacteria in stratified soils and properties of manganese oxide aggregates under manganese–complex medium enrichment. *Public Library Sci. One* 8:e73778. doi: 10.1371/journal.pone.0073778

Zada, S., Sajjad, W., Rafiq, M., Ali, S., Hu, Z., Wang, H., et al. (2021). Cave microbes as a potential source of drugs development in the modern era. *Microb. Ecol.* Online ahead of print. doi: 10.1007/s00248-021-01889-3

Zhu, H. Z., Zhang, Z. F., Zhou, N., Jiang, C. Y., Wang, B. J., Cai, L., et al. (2019). Diversity, distribution and co-occurrence patterns of bacterial communities in a karst cave system. *Front. Microbiol.* 10:1726. doi: 10.3389/fmicb.2019.01726

Conflict of Interest: The authors declare that the research was conducted in the absence of any commercial or financial relationships that could be construed as a potential conflict of interest.

frontiers | Frontiers in Microbiology

ORIGINAL RESEARCH
published: 23 June 2022
doi: 10.3389/fmicb.2022.913452

Biospeleothems Formed by Fungal Activity During the Early Holocene in the "Salar de Uyuni"

Angélica Anglés[1,2,3]*, *Qitao He*[1,2], *Laura Sánchez García*[4], *Daniel Carrizo*[4], *Nuria Rodriguez*[4], *Ting Huang*[1,2], *Yan Shen*[1,2], *Ricardo Amils*[4] and *David C. Fernández-Remolar*[1,2,5]

[1] State Key Laboratory of Lunar and Planetary Sciences, Macau University of Science and Technology, Macau, China, [2] China National Space Administration (CNSA) Macau Center for Space Exploration and Science, Macau, China, [3] Blue Marble Space Institute of Science, Seattle, WA, United States, [4] Centro de Astrobiología Instituto Nacional de Tecnica Aeroespacial - Consejo Superior de Investigaciones Científicas (INTA-CSIC), Madrid, Spain, [5] Carl Sagan Center, The SETI Institute, Mountain View, CA, United States

The Chiquini and Galaxias caves contain speleothems that are templated by long fungal structures. They have been associated with the carbonate lacustrine deposits in the margins of the Coipasa and Uyuni Salar basins. During a wetter episode, such carbonates formed at the end of the last glaciation raising the lake level to more than 100 m in the Tauca events (15–12 ky). Such an event flooded the caves that eventually became a cryptic habitat in the lake. The caves show bizarre speleothems framed by large (>1 m) fungal buildings covering the older algal mineralized structures. Although the origin of the caves is not fully understood, the occurrence of two carbonatic units with very distinctive fabric suggests that they formed in two separated humid events. In this regard, the mineralized algal structures, showing the same features as the lacustrine carbonates, likely formed during the Tauca flooding events in the terminal Pleistocene that inundated older caves. The different caves were exposed to the atmosphere after a drop in the lake level that promoted alluvial erosion by <12–10 ky (Ticaña episode) under arid conditions. A last humid episode rising the lake surface 10 m above the Salar level, which was not enough to inundate the caves a second time, drove the formation of the biospeleothems by fungi biomineralization. The abundance and size of the preserved fungal structures suggest that they were sustained by a stable hydrological activity plus a constant organic supply. While nutrients could have been primarily sourced from the vegetal communities that occupied the exhumated lake margins, they might have also been released from the lacustrine carbonatic unit. The combination of hydrology and biological activities were likely determinants for a fast rock dissolution and mineralization ending in the construction of the fungal biospeleothems.

Keywords: karst, fungi, bioweathering, Salar de Uyuni, quaternary terraces, carbonates

OPEN ACCESS

Edited by:
Valme Jurado, Institute of Natural Resources and Agrobiology of Seville (CSIC), Spain

Reviewed by:
Juan Ramon Vidal Romani, University of A Coruña, Spain
Alsu Kuznetsova, University of Alberta, Canada

***Correspondence:**
Angélica Anglés
angelica.angles@bmsis.org

Specialty section:
This article was submitted to Terrestrial Microbiology, a section of the journal Frontiers in Microbiology

Received: *05 April 2022*
Accepted: *28 April 2022*
Published: *23 June 2022*

Citation:
Anglés A, He Q, Sánchez García L, Carrizo D, Rodriguez N, Huang T, Shen Y, Amils R and Fernández-Remolar DC (2022) Biospeleothems Formed by Fungal Activity During the Early Holocene in the "Salar de Uyuni". Front. Microbiol. 13:913452. doi: 10.3389/fmicb.2022.913452

INTRODUCTION

Along the margins of the Coipasa and Uyuni Salar basins (**Figure 1**), different caves occur in the lower part of a lacustrine carbonate unit, which is composed of biohermal and algal structures (Servant and Fontes, 1978). Such carbonate deposits formed through a transgressive episode during the terminal stages of the last glaciation under humid conditions by 15–12 ky

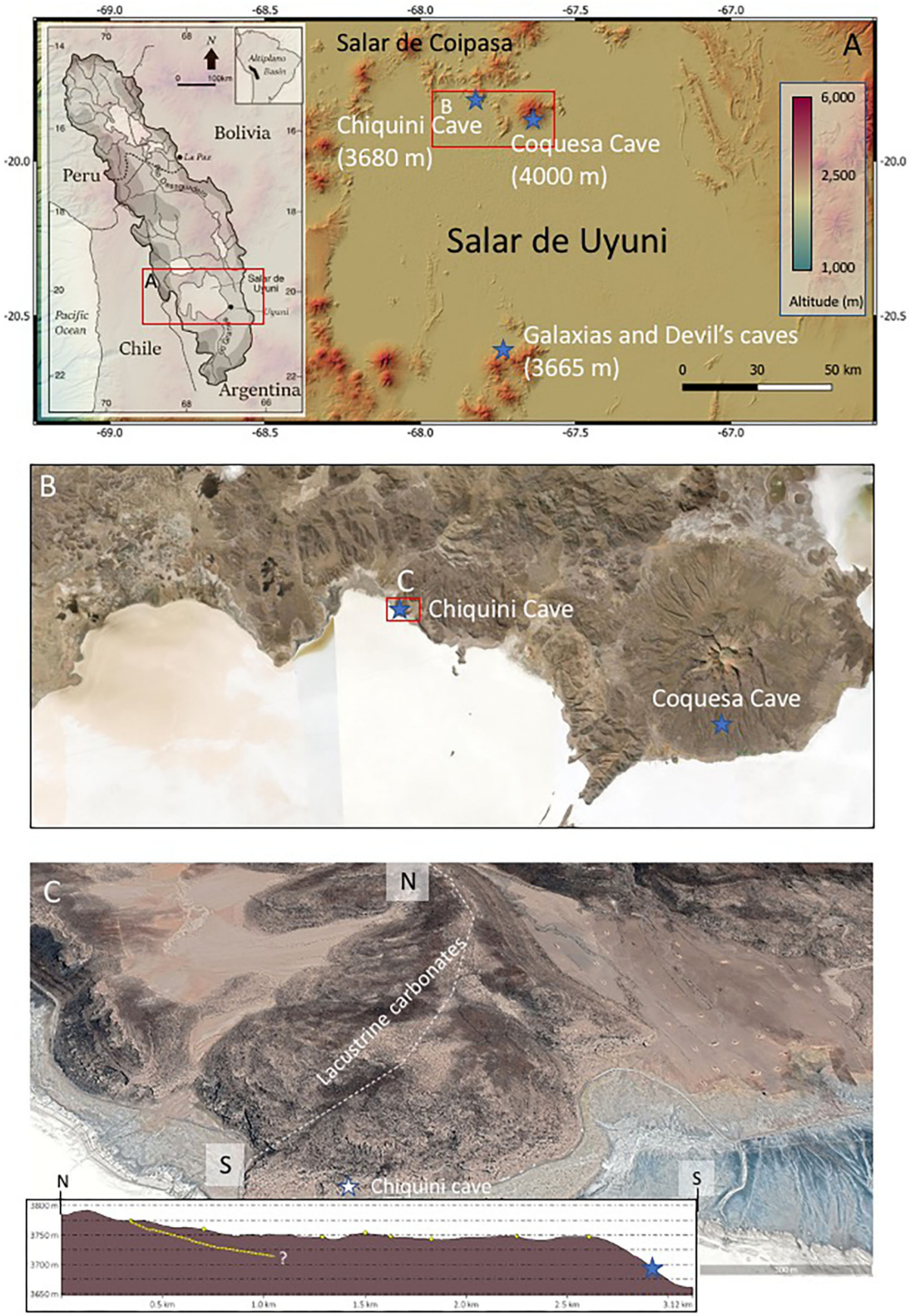

FIGURE 1 | Geographic distribution of the different caves in the Uyuni basin. **(A)** Digital Elevation Model showing the occurrence of the three different caves, including Chiquini, Coquesa, and Galaxias and Devil's. **(B)** Satellite image Situation of Chiquini and Coquesa caves in the North area of the Salar Uyuni. **(C)** Geomorphological settings of the Chiquini cave emplaced in the Pleistocene lacustrine carbonates forming a terrace on the volcanic deposits of Pleistocene age (Tibaldi et al., 2009). The dashed white line traces the direction of the topographic profile, while the yellow dashed line traces the boundary between the volcanic and lacustrine deposits inside the altitude profile.

(Sylvestre et al., 1995, 1999). As a result of this lacustrine transgression, the caves occurring below 3,690 m were completely flooded and partially infilled by mineralized biological structures of calcareous composition. In this regard, mineralized algal fabrics in the interior of the caves similar to the lacustrine biosedimentary fabrics likely record the transgressive episode that formed the carbonate shelf in the lake. Intriguingly, a very distinctive set of speleothems framed with mineralized fungi are also found covering the ceiling and floor of the caves, which are mainly formed by the older cryptic lacustrine carbonates. The occurrence of speleothems in the cave suggests that they were formed during a drop in the lake level under humid conditions that sustained an active weathering of the lacustrine carbonates deposited in the Late Pleistocene (Sylvestre et al., 1995, 1999).

The speleothems are mineralized by long filamentous structures of microbial fungal hyphae (**Figure 2**). Although it has been reported that fungi are a common component in the microbial communities in karstic systems and caves (Engel, 2011; Hershey et al., 2018), they are not found as the main mineralizing agent in the construction of the speleothems. However, the occurrence of the Uyuni speleothems framed by a dense network of fungal hyphae (**Figure 2**) has not been reported on such a large scale. When considering microbial mineralization, most studies concern prokaryotes. However, induced microbial biomineralization by eukaryotes is scarcely documented, especially when considering the fungal kingdom (Sterflinger, 2000; Burford et al., 2003; Gadd, 2008; Gadd and Raven, 2010). Fungi are everywhere on the surface of the Earth, wherever there is oxygen. They are also able to survive without oxygen, however, this is not their natural lifestyle (Bindschedler et al., 2016). The most preferred habitat for fungi is believed to be soil, but they are also very common in rock surfaces and caves (Sterflinger, 2000; Ritz and Young, 2004; Vanderwolf et al., 2013).

Fungi are chemo-organo-heterotrophic organisms, thus, depending on organic matter to survive and sustain their metabolism (Bindschedler et al., 2016). They obtain their carbon source either from associations with living partners or from available organic matter (Bindschedler et al., 2016). Fungi acquire their nutrients by absorption, by, first, pre-digesting their substrate using oxidative or hydrolytic enzymes secreted in the external environment, and then, transporting solubilized nutrients inside their cells. Therefore, their metabolic activity depends mainly on the available nutrients. Fungi also interact with inorganic minerals and metals and are, thus, involved in the biogeochemical cycling of compounds, such as Ca, Fe, K, and Mg (Bindschedler et al., 2016).

In this regard, it is known that fungi also colonize rock surfaces in arid environments, interacting with their mineral substrate, therefore, influencing their physical and chemical stability (Gorbushina, 2007; Parchert et al., 2012). Fungi are also known to be involved in both $CaCO_3$ bioweathering and biomineralization (Verrecchia and Dumont, 1996; Sterflinger, 2000; Burford et al., 2006; Kolo et al., 2007; Hou et al., 2013). Both bioweathering and biomineralization are strongly related since the products released from the $CaCO_3$ dissolution can further re-precipitate as $CaCO_3$ depending on factors, such as pH, temperature, carbonate alkalinity, and pCO_2 (Burford et al., 2006). Carbonate alkalinity is mainly controlled by the pH level, which in turn will define the carbonate species in the solution, therefore, to precipitate $CaCO_3$ two factors are of crucial importance: the carbonate alkalinity and the calcium concentration (Ca^{2+}) (Castanier et al., 1999; Dupraz et al., 2009). Fungal activity can influence both of those factors. Additionally, fungi can also influence those two factors through organomineralization (biologically influenced mineralization), as fungal cell walls can adsorb various cations, such as Ca^{2+} (Bindschedler et al., 2016). Numerous past studies on fungi organomineralization prove that this process might be more important than previously thought (Dupraz and Visscher, 2005; Dupraz et al., 2009; Bindschedler et al., 2014).

Consequently, there are various factors in relationship to fungal communities influencing the stability of $CaCO_3$. In addition, as fungi are provided by rigid and resistant filaments consisting of elongated cells arranged one after another, they have been observed to actively drill into mineral surfaces (Jongmans et al., 1997; Van Schöll et al., 2008; Moore et al., 2011), and take advantage for the structural Spatio-temporal and nutritional heterogeneities in the rock substrate.

In this article, we investigate the role of fungal communities in forming the speleothems that occur in the caves associated with the carbonates formed during the terminal Pleistocene and early Holocene in the Uyuni Salar. For such a purpose, we will conduct a multidisciplinary approach that linked the area's paleoclimatic evolution with microbial communities' development. The fungal structures are directly involved in the formation of the speleothem buildings but are also an active agent in rock weathering and ion mobilization. Thus, wet climatic conditions found in different episodes of the Pleistocene and the Holocene in the region would have favored weathering and mineralization. In this context, we explored how the climatic activity drove the biogeochemical pathways ending in the formation of the speleothems through the activity of the fungal communities in the Uyuni and Coipasa basins.

ENVIRONMENTAL AND GEOLOGICAL SETTINGS

Regional Settings

The Altiplano of Bolivia is a 200,000 km^2 internally drained basin, located between the western and eastern of the Andes Cordillera at an altitude of 4,000 m (**Figure 1A**). The western cordillera has a volcanic origin. Volcanoes, ignimbrites, and lava flow generally overlie the Cenozoic formations by more recent volcanic activity (Risacher and Fritz, 1991; Salisbury et al., 2015). The eastern cordillera contains Paleozoic sediments (shales and sandstones) and granitic plutons, which constitute the Altiplano basement (Risacher and Fritz, 1991). This basement is filled with continental sediments from the Cretaceous and Cenozoic ages. During the Pleistocene, the central and southern part of the Altiplano was persistently covered by large saline lakes, characterized by alternating episodes of expansion and desiccation, a phenomenon commonly explained by climatic fluctuations in the region (Rouchy et al., 1996; Fornari et al.,

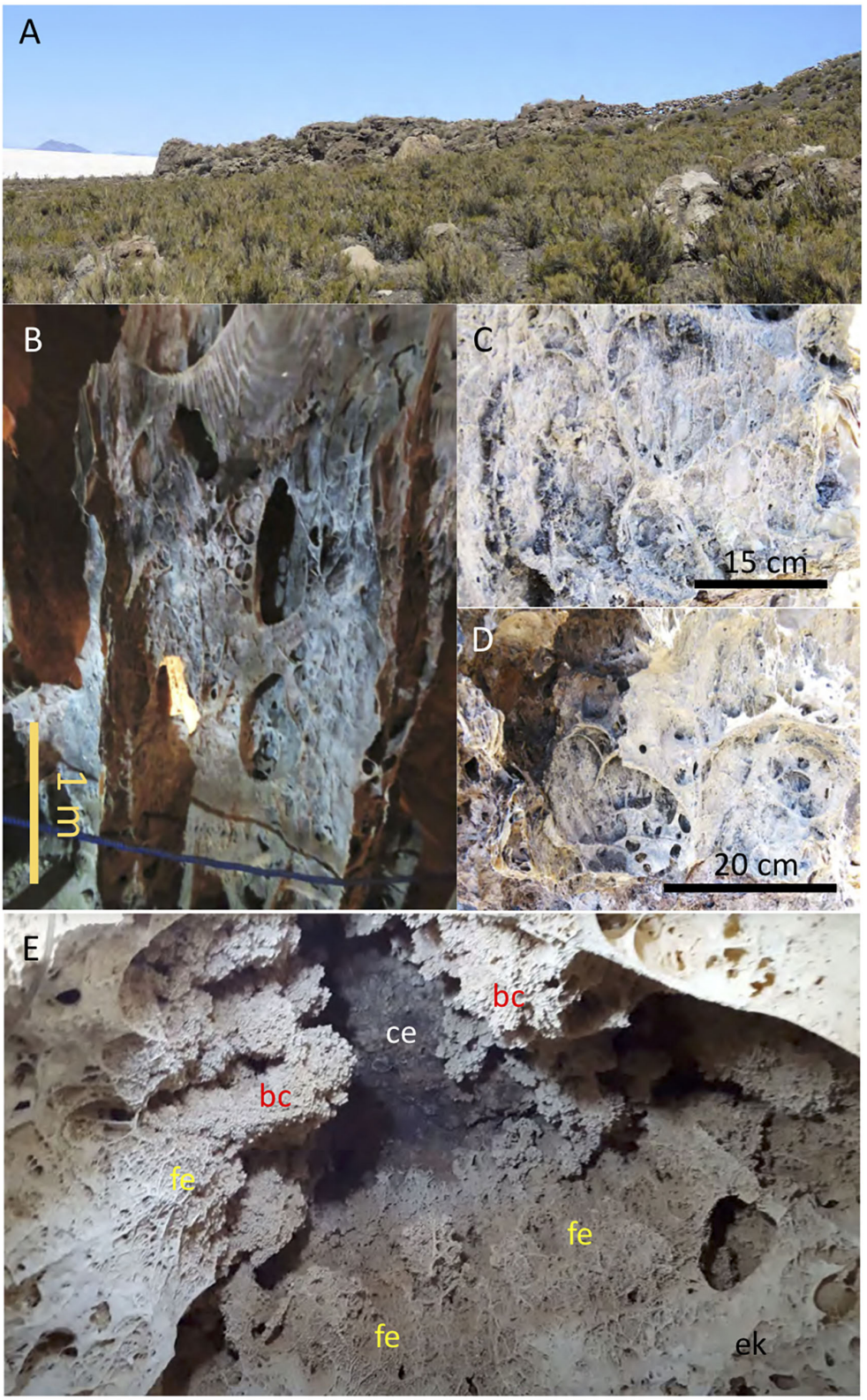

FIGURE 2 | Pictures showing the outcrops of carbonate deposits of lacustrine and cave environments. **(A)** Lacustrine terrace of late Pleistocene carbonates (Rouchy et al., 1996; Sylvestre et al., 1999) around the Chiquini cave. **(B)** Speleothem in Chiquini cave framed by long filaments **(C,D)** mineralized by Mg-rich carbonate. **(E)** Image pointing the Galaxias cave ceiling (ce) of volcanic composition that is covered by biohermal carbonates (bc), which are encased by long and thick mineralized filaments (fe) building the cave speleothems. In such material succession, the biohermal carbonates (bc) formed inside the cave by karstic processes are older than the biohermal structures (bc), which formed when the cave was fully flooded. The picture showing the Galaxias cave ceiling in E is a courtesy of Geoffrey SG.

2001). The depth and extent of these large paleolakes varied greatly depending on variations in the rainfall/evaporation rates (Hastenrath and Kutzbach, 1985; Servant et al., 1995; Sylvestre et al., 1995). Well-preserved outcrops are recorded from the last two of these lacustrine phases, the Minchin (30,000–20,000 yrs) and Tauca (>16,000–14,000 yrs) episodes (Sylvestre et al., 1999; Fornari et al., 2001). A development of carbonate accumulations took place during successive lacustrine highlands, discontinuously covering the terraces and slopes of the paleolake (Rouchy et al., 1996; Placzek et al., 2006). During lowstands, the level of the lake dropped, leaving behind salt deposits in the deepest part of the basin, which corresponds to the current Salar de Uyuni (Rouchy et al., 1996; Sylvestre et al., 1999; Fornari et al., 2001).

Geological and Geobiological Settings of Caves

The basement of the Uyuni and Coipasa basins is formed by a large synclinal structure (Corque syncline) composed of thick (>10 km) synorogenic deposits of Eocene to Oligocene age (Mcquarrie, 2002). The basins are limited by younger volcanic edifices and lava flows (**Figure 1B**) dating back to the late Cenozoic and the Early Quaternary (Tibaldi et al., 2009; Salisbury et al., 2015). Such materials were subsequently reworked by fluvioglacial activity that has been recorded as moraines, which are found covering the Tunupa hillsides above 4,100 msl (Clapperton et al., 1997). During the Pleistocene, the synclinal structure was flooded by different water bodies, which formed through different humid episodes (Sylvestre et al., 1999; Argollo and Mourguiart, 2000). The water level was high enough to join the Uyuni and Coipasa Salars in the gigantic paleolake, known as Tauca, dating back to 120 ky (Martin Léo et al., 2018). The paleolake reached a maximum level of ∼ 3,760 msl at 40 and 16 ky in the area of study (**Figures 1B,C**) during the Minchin and Tauca phases (Sylvestre et al., 1999; Chepstow-Lusty et al., 2005), respectively. The highstand paleolake episodes in the area hosted the formation of carbonate deposits, which mineralized very diverse structures of biological origin (Rouchy et al., 1996; Blard et al., 2011).

In the Uyuni Salar, caves are found associated with volcanic materials (**Figures 1A–C**). There is little scientific information about the cave's origin in the area. Thus, the information comes from the inspection of caves done in the Chiquini and Coquesa locations (**Figures 1B,C**) suggesting that are emplaced in volcanic materials. The Coquesa cave formed in breccias and conglomerates of the Tunupa volcano, which shelter several mummies of the Chullpa people. This cave shows no evidence of karstic structures as occurs at ∼4,000 m well above the different highstand episodes inundating the Uyuni and Coipasa basins (Sylvestre et al., 1999). On the contrary, the Chiquini cave, occurring at ∼3,680 m, is found below the carbonate unit (**Figures 1C**, **2A**), formed during the Tauca phase in the terminal Pleistocene (Sylvestre et al., 1999). In this case, the cave is filled with abundant speleothems framed by long buckles of hanging filamentous structures from the cave ceiling to the floor (**Figures 2B–D**). Chiquini cave measures up to 5 m high and more than 10-m width. The speleothems are, in the majority of cases, of high magnitude, as they can be up to 4-m high. Some of them reach the cave floor and seem to be associated with stalagmites. We believe the speleothem formation is associated with a humid episode that incremented the lake dimensions, suggesting that the speleothems were formed by water circulation.

Interestingly, the same structures are found in the Gruta de las Galaxias (Cavern of the Galaxies). Such a cave occurs 4 km west of the Aguaquisa village at ∼3,670 m (**Figure 2E**) flanked by alignments of Miocene volcanic edifices (Tibaldi et al., 2009), like Caltama and Qaral. The Cavern of the Galaxies also occurs below the carbonatic deposits of the Tauca phase. It hosts the same structures framed by networks of long filaments, which grow from a volcanic ceiling covered by carbonates showing a different fabric (**Figure 2E**). Such a fabric consists of short-branched stems that are also found in the thrombolytic structures of the Tauca lacustrine carbonates (Rouchy et al., 1996; Blard et al., 2011). The presence of two different carbonate materials in the interior of the caves suggests that they were formed under different environmental conditions. While the speleothem carbonates formed in a karstic system, the ceiling's thrombolytic carbonates were likely formed when the cave was completely flooded during a highstand episode in the area (Sylvestre et al., 1999).

METHODS

Sample Collection

A geological survey was performed to inspect the lacustrine carbonate terraces and caves in the Uyuni Salar (**Figures 1C**, **2A–D**, **Supplementary Figures 1**, **2**, **Supplementary Table 1**). We mostly looked for the different carbonate structures to distinguish the biospeleothems from the lacustrine materials in the interior of caves. Samples 134–1, 134–2, and 134–4 were collected from two different speleothems in the Chiquini cave to characterize the speleothem's geobiological content through the microstructure and elemental composition under the Scanning Electron Microscope and Electron Dispersive Spectroscopy (SEM-EDS). In addition, lipid analyses were conducted to determine the speleothem biological origin (**Supplementary Table 2**). Some additional samples like 129, from the lacustrine carbonates, and 134–3, obtained in the outcrops occurring at the cave entrance, were also collected to compare their structure, elemental, and molecular composition with the speleothem carbonates. It was done to recognize differences in the biological communities as the lacustrine carbonates formed under quite different environmental conditions than the speleothems, which should be accordingly observed in the molecular record of organic compounds and biomolecules. Samples were carefully collected using nitrile gloves, covered by aluminum foil, and introduced into a sterilized sampling bag to prevent contamination.

Mineral Identification by X-Ray Diffraction

The mineral identification of the carbonate samples 129, 134–1, 134–2, and 134–3 (**Supplementary Table 1**) was done through

the X-ray diffraction technique. For such a purpose, a fragment of the speleothem sample was powdered using an agate mortar. The mineral characterization was done by a Seifert 3003 T–T X-ray diffractometer (copper radiation source) scanning 2θ° diffraction angles from 0 to 70°. For mineral identification, we performed a semi-quantitative analysis using the RIR (Reference Intensity Ratio) method from the I/Ic data (intensity ratio of the highest intensity peak of the phase, compared to the most intense corundum peak). This value is tabulated for many of the phases in the database that we have. When the identified phase has no value for I/Ic, the value of 1 is automatically assigned. The calculation of the semi-quantitative analysis assumes that all the phases are identified, so that the software assumes that the sum is 100% ($\Sigma ci = 100\%$). The mineral identification was performed using the Diffract.Ev, a program under the PDF2 mineral database.

Scanning Electron Microscope and Electron Dispersive Spectroscopy

Microscopic and chemical evaluation of the Uyuni samples was performed by three types of Scanning Electron Microscopes, including: (1) a JEOL-5600, coupled to an Oxford INCA X-sight EDAX Energy Dispersive X-ray Microanalysis, (2) a JEOL IT500 coupled with an Oxford MAX170 microanalysis, and (3) a Scanning Electron Microscopy-Field Emission Gun (SEM-FEG) Philips XL30-FEG. SEM measurements and chemical analyses (EDS) were performed on uncoated and gold-coated sample pieces using a ZEISS EVO 10 (Carl Zeiss, Oberkochen, Germany). Before analysis, the sample was repeatedly cleaned with a rubber air dust blower to eliminate impurities. Electrically conductive carbon tabs and double sticks were pressed to conductive graphite stubs and were gold-coated using a Quorum, Q150T-S device to enhance electrical conductivity and prevent charging under electron beams. Various stubs with sample pieces were then placed inside the SEM chamber in high vacuum mode to analyze the sample microstructure with a secondary electron detector. The Philips XL30-FEG was used to perform SEM-EDS analysis to follow the microstructure and composition variation of samples showing a diverse structure like the 134–3, which is a heterogeneous material displaying a varying structure. Analytical conditions were variable set at 0.2 mA current and 15 kV accelerating voltage for the uncoated samples, while conditions for the gold-coated samples were 50 pA and 10 kV.

Transmission Electron Microscope

The TEM was used to reveal the internal microstructure of sample 134–1 corresponding with a speleothem fragment with laminated microstructure. For such a purpose, the sample was consolidated and fixed in 4% paraformaldehyde and 2% glutaraldehyde in 0.1-M phosphate buffer (pH 7.2) for 2 h at room temperature. The fixed samples were subsequently washed three times by the phosphate buffer and post-fixed with 1% of OsO4 in water for 60 min at room temperature in the dark. Later, they were washed three times by distillate water, and subsequently incubated with 2% aqueous uranyl acetate for 1 h at room temperature, washed again, and dehydrated in increasing concentrations of ethanol 30, 50, and 70% at 20 min each, 90% 2 × 20 min, and 100% 2 × 30 min at room temperature. Dehydration was terminated with a mixture of ethanol/propylene oxide (1:1) for 10 min and pure propylene oxide for 3 × 10 min. Infiltration of the resin was accomplished with propylene oxide/Epon (1:1) for 45 min and pure LR White resin (London Resin Company limited, England), overnight at room temperature. Polymerization of infiltrated samples was done at 60°C for 2 days. Ultrathin sections of the samples were done using an Ultracut of Leica that was stained with uranyl acetate and lead citrate by standard procedures.

Extraction and Analysis of Lipid Biomarkers

We performed the analysis of the total lipid extract (TLE) to identify the main biological groups that have been involved in the carbonate formation in the lacustrine and cave paleoenvironments. Lipids of four lyophilized and ground subsamples (50–80 g) of the Uyuni speleothems were extracted with ultrasound sonication (3 × 15 min) using 15 ml of a 3:1 (v/v) mixture of dichloromethane (DCM) and methanol (MeOH) to obtain ca. with 45 ml of TLE. Before the extraction, tetracosane-D_{50}, myristic acid-D_{27}, and 2-hexadecanol were added as internal standards.

The concentrated and desulfurized TLE (Sánchez-García et al., 2018) was hydrolyzed overnight with KOH (6% MeOH) at room temperature (Grimalt et al., 1992). Then, liquid-liquid extraction with *n*-hexane (3 x 30 ml) was performed to recover the neutral fraction first and the acid compounds afterward, after acidification with HCl (37%) (Sánchez-García et al., 2020). Further separation of the neutral fraction into non-polar (hydrocarbons) and polar (alkanols and sterols) was done according to a method described elsewhere (Carrizo et al., 2019). The acidic fraction was transesterified with BF_3 in MeOH to produce fatty acid methyl esters (FAME), and the polar fraction was derivatized with N,O -bis [tri- methylsilyl] trifluoroacetamide (BSTFA) to analyze the resulting trimethyl silylated alcohols (Sánchez-García et al., 2020).

All fractions were analyzed by gas chromatography-mass spectrometry (GC–MS) using a 6850 GC System coupled to a 5975C VL MSD Triple-Axis detector (Agilent Technologies, Santa Clara, CA, USA), which operated with electron ionization at 70 eV and scanning from m/z 50 to 650 (analytical details can be found in Sánchez-García et al., 2020). Compound identification was based on retention time and mass spectra comparison with reference materials and the NIST mass spectral database. Quantification was performed with the use of external calibration curves of *n*-alkanes (C_{10}-C_{40}), FAME (C_6-C_{24}), and *n*-alkanols (C_{14}, $C_{1,8}$, and C_{22}), all supplied by Sigma-Aldrich (Madrid, Spain). A procedural blank doped with the three internal standards were analyzed in parallel to the samples, to check for contamination and estimate the method recovery (74 ± 16%). No significant contamination of target analytes was recorded. Lipid concentration was measured as micrograms per gram of dry weight sample ($\mu g \cdot gdw^{-1}$).

RESULTS

Cave Inspection

In July 2019, we visited and sampled the Chiquini and Coquesa caves that are emplaced in the volcanic deposits

of the Pliocene age (Tibaldi et al., 2009) produced by the activity of the Tunupa volcano (**Figure 1A**). As discussed above, the Coquesa cave occurs at ∼4,000 msl showed no evidence of any speleothem material but was formed by brecciated deposits of volcanic composition. On the other hand, the Chiquini cave (**Figures 1A–C**) emplaced at ∼3,670 msl under a lacustrine carbonate terrace (**Figure 1A**) is occupied by a dense population of speleothems that are framed by large filaments (**Figures 2B–D**). The cave ceiling is covered by two different carbonate deposits (**Figure 2E**), which are distinguished by their distinctive fabrics. The first unit consists of carbonatic deposits with millimeter- to centimeter-long short-branched structures, which occur at the cave ceiling following a patchy distribution. They are encrusted and covered by the speleothems buildings that grow from the ceiling to the floor cave. They are composed of networks of long-branched filaments (>10 cm), whose filament density decreases, but their length increases from the ceiling to the cave bottom (**Figures 1B**, **2E**). As the building growth is controlled by the development of filamentous networks (**Figures 2B–D**), they usually have a flat morphology, whose size is limited by the ceiling height and the fungal network growth. As a result, they form flattened speleothems with an internal complex structure merging different corrugated and undulate surfaces (**Figures 2A–D**). The same distribution of carbonate materials is also observed in the Galaxias cave (Cueva de las Galaxias) found NW of the Colcha location at an altitude of 3,665 msl (**Figures 1A**, **2E**). In turn, the Galaxias cavern is more densely populated by filamentous buildings than the Chiquini cave, which show a larger volume and a more complex structure formed by corrugated laminae. Interestingly, the Chiquini and Galaxias caves do not host any hydrological activity associated with the speleothem formation, which agrees with the current arid climate.

Mineral Identification

The XRD analysis of different samples collected in the lacustrine carbonate deposits and the Chiquini cave has resulted in identifying different calcite type minerals characterized by the magnesium concentration (**Supplementary Figures 4A–C**, **Supplementary Table 1**). In this regard, the XRD analysis from the lacustrine carbonates with columnar fabrics in Coipasa (sample 129) results in low magnesium calcite (LMC), which diffraction diagram matches a composition of $Mg_{0.03}Ca_{0.97}CO_3$ in the PDF2 database (**Supplementary Figure 3A**). Samples 134-1 and 134-2, corresponding with the speleothem laminated carbonates (**Supplementary Figure 3B**, **Supplementary Table 1**), have provided a mineral composition that also fits well in an LMC crystal structure ($Mg_{0.06}Ca_{0.94}CO_3$). Furthermore, the XRD analysis shows that the carbonatic tuff (sample 134–3) is mostly composed of high magnesium calcite (HMC) ($Mg_{0.1}Ca_{0.9}CO_3$), which comes together with a secondary carbonate identified as kutnahorite [$Ca_{1.11}Mn_{0.89}(CO_3)_2$] (**Supplementary Figure 3C**).

SEM-EDS Analysis

The SEM-EDS analysis of samples 134–1 and 134–4 (**Supplementary Table 1**) has revealed the occurrence of three different mineral microstructures in the speleothem. They correspond with thin external sheets formed by needle-like crystal palisades (**Figures 3A–D**, **4A**), laminas with a non-crystalline massive microstructure containing discontinuous layers (**Figures 4A,B**), and spongy globules, whose microstructure is built by nanoscale spicules (**Figures 3–6**).

The external sheet palisades have a thickness of around 2 microns and are composed of 10-micron long and 5-micron thick crystal prisms forming fans, wherein its apex follows an orientation inward of the main structure (**Figures 3A–C**). The crystal needles can combine to build larger needle-like rays to form star-shaped microstructures (**Figures 3C,D**). The calcite crystals do not show evidence of secondary mineral alteration, such as recrystallization and corrosion. The sheet composed of needle palisades covers a thicker lamina that has no morphological features, but a massive appearance (**Figures 4A,B**). It is affected by microporosity filled by other mineral components, like ovoid, to undulated laminas built by a spicular mesh and aggregates of micron-sized and ovoid- to rod-like units (**Figures 4C,D**, **5A,B**). In this regard, the SEM-EDS microanalysis has revealed that the external sheet built with needle palisades and the internal massive lamina is primarily composed of C, O, Ca, and, to a minor extent, Mg (**Figures 6A,B**). In turn, the spongy undulated to ovoidal microstructures displays a high concentration of Mn and O, while the rod aggregates are mainly composed of Si and O, with minor amounts of Mn (**Figures 6C,D**).

We have also observed several sack-shaped oval microstructures averaging ∼50 microns in size (**Figures 7A–G**), which, in some cases, have a dentate operculum with circular morphology (**Figure 7A**). Although most specimens show a partial collapse of the entire structure (**Figures 7A,C,D**), the complete individuals have a rounded section. The microstructures are built by the amalgamation of circular to elliptical tiny platelets sizing between 1 and 5 mm, which show a composition rich in Si, O, and Mg (**Figures 7C,D**). In some cases, the platelets are covered by a thin layer of ∼2 microns devoid of any evidence of internal fabric and texture (**Figures 7E,F**). Interestingly, oval microstructures are found embedded inside the crystalline matrix, in which elongation axes are parallel to the needles forming fan bundles (**Figure 7G**).

Additionally, the SEM analysis of the speleothem sample revealed the presence of shells sizing up to 100 μm, with elliptical to round morphology, which showed internal transverse stripes with a varying length of 5 to 20 microns (**Figures 8A–D**). The EDS microanalysis of such microbial structures shows that it has a high concentration of silicon, oxygen, and magnesium (**Figure 8D**). The silica-bearing thecae show a very diverse distribution in the mineral substrate as they are found in mineral surfaces, pore spaces, narrow fissures, and cracks on the calcite crystals (**Figures 8A–D**).

Detailed observations of the sample 134–4 also show several types of filaments with morphologies were observed, which can be grouped into two basic categories: thick (>10 microns), straight to sinuous, and long filaments (**Figures 9A–F**), and thin (<1 micron), curved, and tiny filaments form unregular networks of entangled threads (**Figures 9A–D**). The larger and thicker

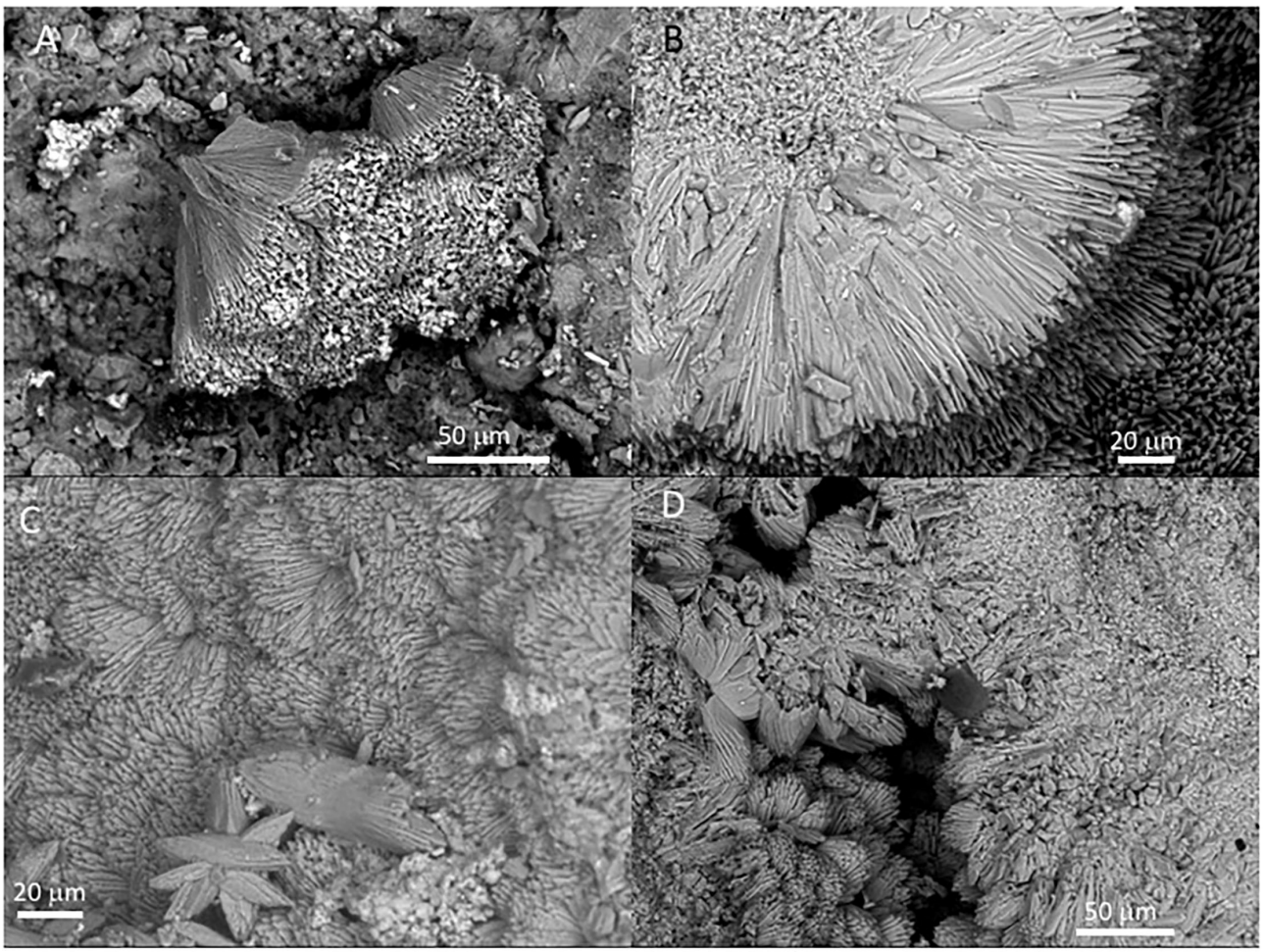

FIGURE 3 | Scanning Electron Microscope (SEM) of Mg-calcite crystals occurring at the outer sheet in the speleothem sample 134–4. **(A)** Fan-like intergrowth of Mg-calcite needles. **(B)** Detail of pristine primary mineralogy of calcite with needle-like crystals. **(C)** Star-shaped microstructures from the aggregation of calcite needles. **(D)** Coalescence of two external sheets with a needle-like microstructure.

filaments are found well-spread in the cave sample, where they appear partially embedded or covered by the mineral matrix (**Figures 9A,B**). The more prominent filaments vary in size and width and can be easily seen with the naked eye (**Figure 9A**). The sinuous and curved filaments form intricated networks inside the mineral substrate (**Figure 9B**). Some filaments have cylindrical to conical morphologies ending in an apical area attached to the mineral surface (**Figures 9D,E**). Such filaments have a distinctive surface pattern, showing longitudinal and subparallel or reticular texture (**Figures 9D,E**). While the filaments display diverse morphologies, their chemical composition is relatively invariable, showing a high content in C and Si (**Figure 9E**). The delicate and tiny filaments (**Figures 10A–D**) occur as 10 micron-sized dense clusters of entangled threads, which spread irregularly over the mineral substrate or different elements of microbial origin. The EDS microanalysis shows that the thread networks are mainly composed of C and Si in the same way as the large filaments.

The SEM analysis for sample 134–3, associated with the carbonate outcrops of the Chiquini cave entrance, exposed a quite different record of microstructures. As described before, 134–3 show two distinctive fabrics: a tuff-like and a thrombolitic structure (**Figures 11A–G**, **Supplementary Figures 2A–C**). The SEM imaging of the tuff level unveils the abundance of mineralized filaments (**Figures 11A–C**) with a branching growth, while the thrombolytic area shows a high population of micron-sized and rod-like microstructures (**Figures 11D,E**). Interestingly, the rod-like microelements are also found on the surface of >10-micron thick mineralized filaments (**Figure 11F**) in the 134–3 tuff fabric. The thrombolite fabric follows another internal arrangement in form of clumps of rod-like microstructures associated with void filaments (**Figure 11G**).

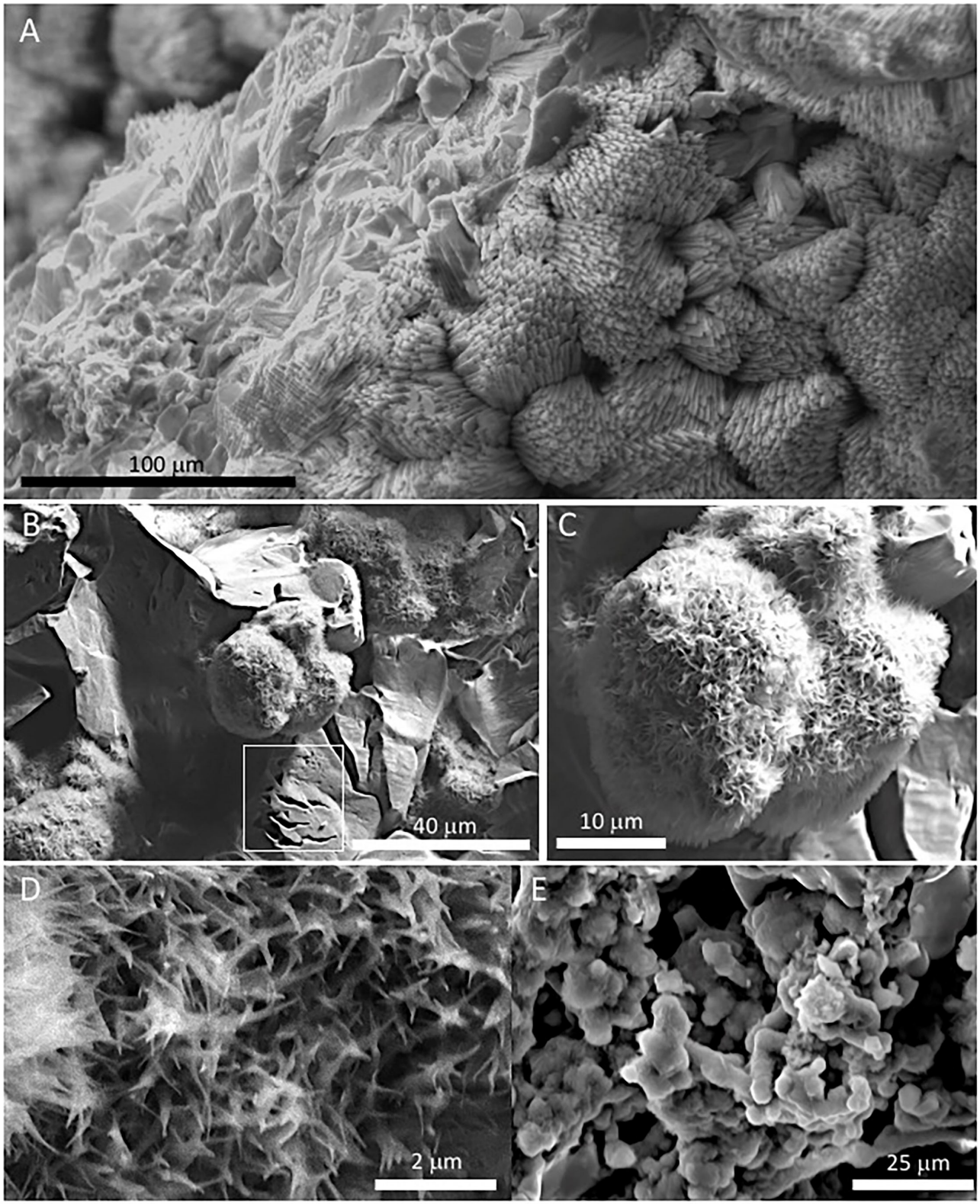

FIGURE 4 | SEM images of samples 134–1 show the massive inner lamina **(A)** occurring beneath the 10-micron thick needle-bearing sheet. It has microporosity filled by different mineral microstructures as ovoidal to laminar elements **(B,C)** that are formed by **(D)** a spicule-like mesh; and, additionally, by **(E)** aggregates of micron-sized ovoid- to rod-like units. The white square in **(B)** marks the presence of microborings having a diameter lower than 5 microns. The SEM image in **(A)** suggests that the massive microstructure of the inner lamina results from the tight packing of the same needle crystals found in the external sheet.

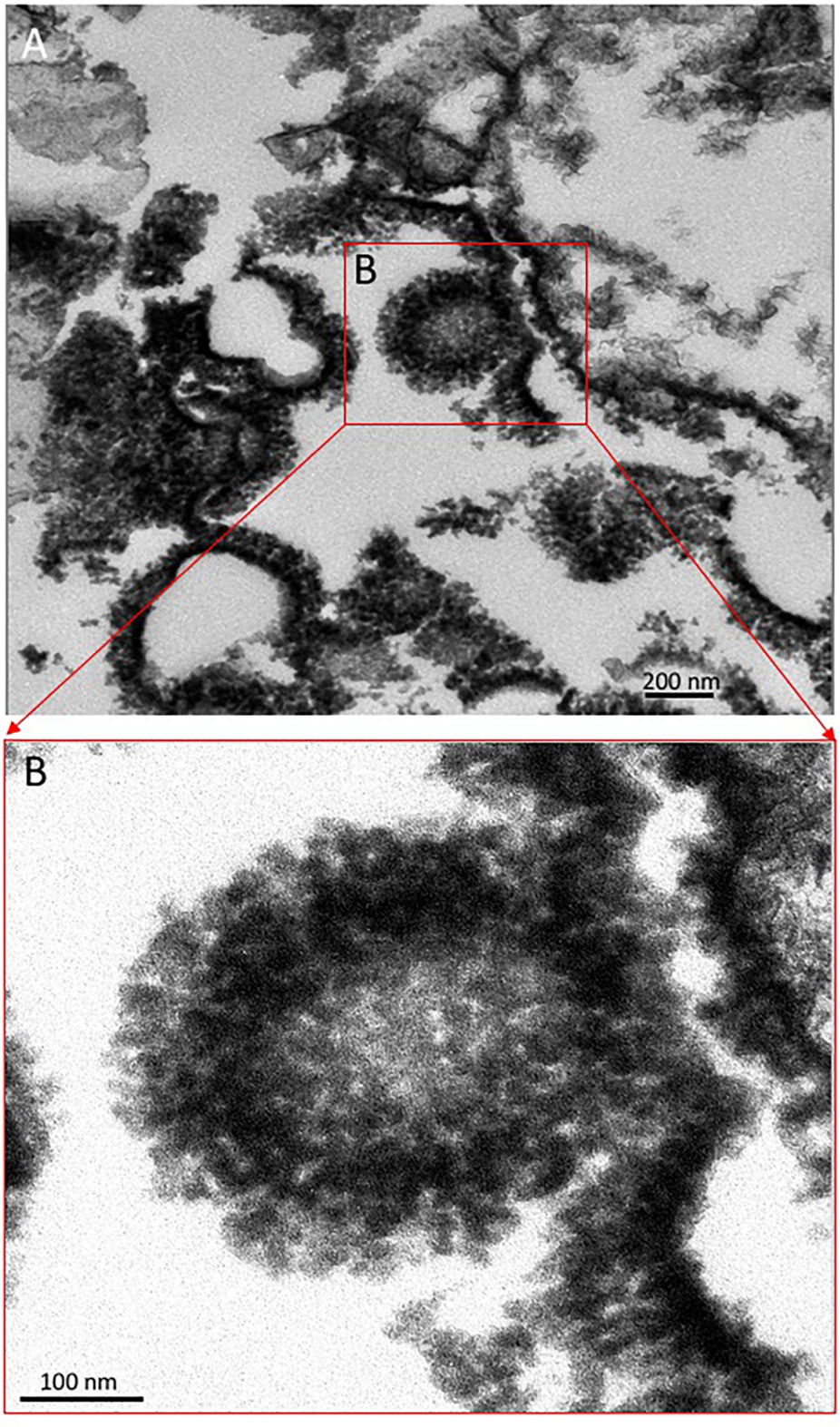

FIGURE 5 | Transmission Electron Microscope (TEM) image from sample 134–1 **(A)** showing the internal structure of the spicule-meshed elements displaying sheet to ovoidal morphologies that are internally voided. **(B)** Detail of an ovoidal element enrooted in a laminar mesh of spicule-like crystals.

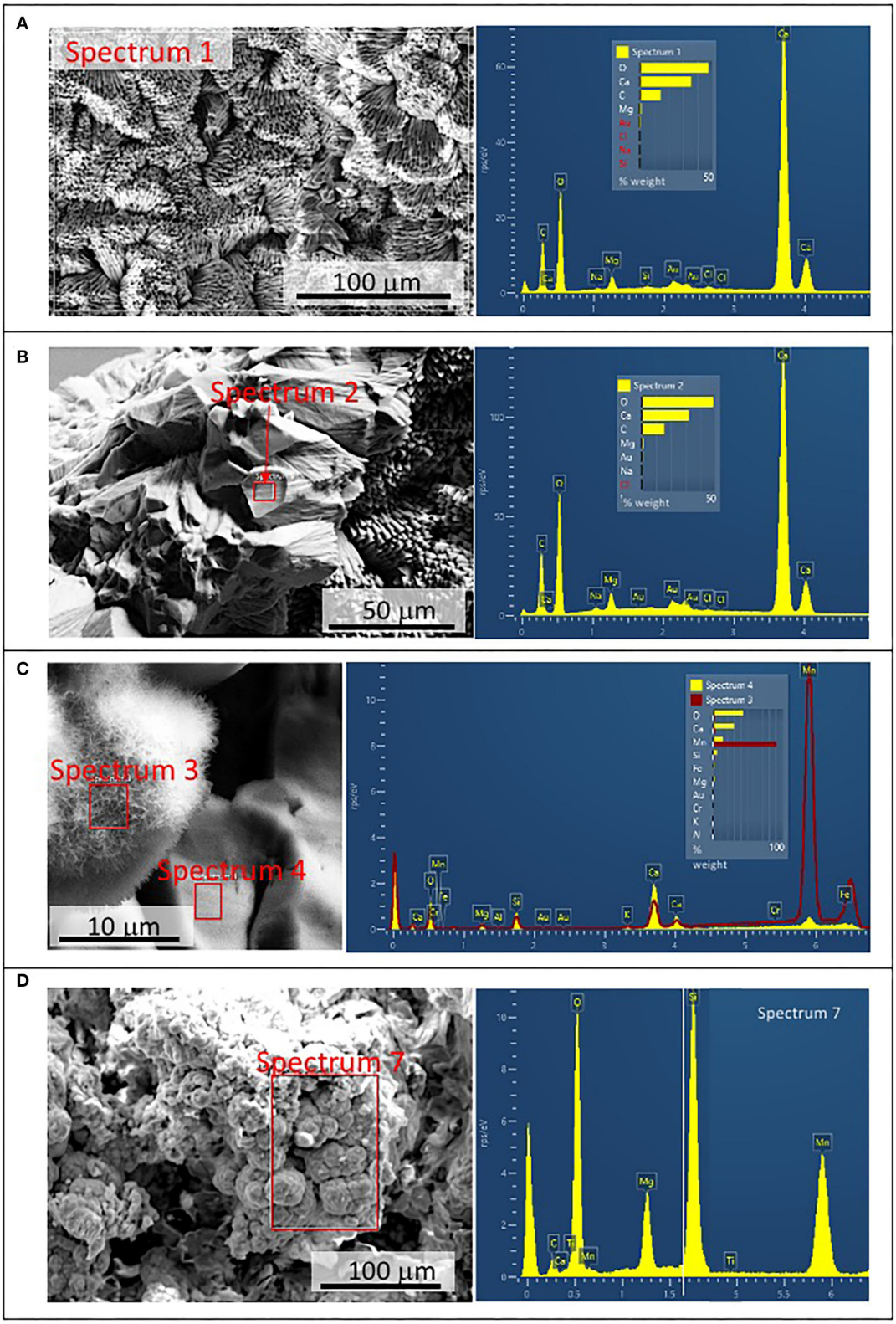

FIGURE 6 | Scanning Electron Microscope and Electron Dispersive Spectroscopy (SEM-EDS) microanalysis of different components found in samples 134–1. **(A)** Chemical composition of the external needle-bearing sheet showing C, O, Ca, and Mg as major elements. **(B)** Microanalysis from the internal layer with the same chemical composition as in the external sheet shown in **(A)**. **(C)** Chemical analysis from an ovoidal element with spicular mesh exhibiting a primary composition of O, Mn, and Fe (spectrum 3 in red), which is very different of the composition of the internal layer (spectrum 4 in yellow) dominated by C, O, Ca, and Mg. **(D)** Microanalysis of the silica-rich aggregates of micron-sized components revealing a high concentration in Si, O, and Mn.

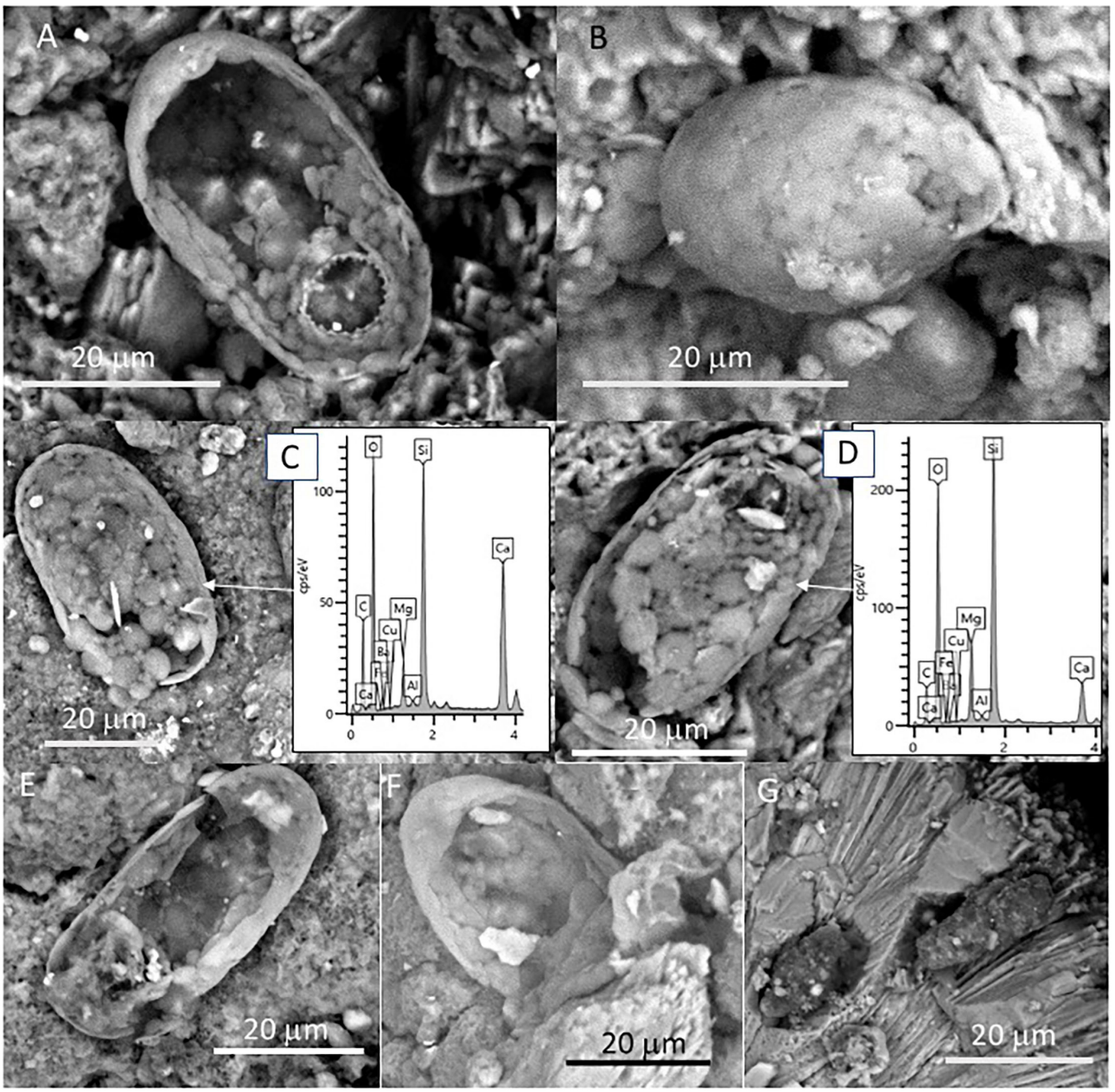

FIGURE 7 | SEM micrographs showing oval-shaped microstructures showing **(A–G)** different preservation stages in samples 134–4. The morphological and compositional features of the specimens suggest that they correspond with the remains of silica-biomineralized testate protozoa. **(A)** Specimen with a dentate operculum. **(B)** Well-preserved specimen revealing the test as the coalescence of different platelets known as idiosomes. SEM-EDS analyses of different specimens **(C,D)** show that the specimen test is composed mainly of Si, C, and O with minor amounts of Mg and Fe, where the Ca likely comes from the mineral matrix. Most of the specimens show varying disintegration degrees of the test **(E,F)** through the degradation of the organic cement releasing idiosomes and ending in the test collapse. Some elements embedded in the mineral matrix **(G)** could correspond with testate amoeba boring the mineral matrix, as they show similar morphological and compositional features.

Lipid Analysis

The analysis of the three lipidic fractions (non-polar, acidic, and polar) extracted from the samples collected in the cave and lacustrine deposits revealed the presence of diverse lipid families, including *normal* (i.e., straight and saturated), branched (i.e., with methyl groups), and unsaturated (i.e., with double bonds) chains (**Supplementary Table 2**). The non-polar fraction was mostly composed of *n*-alkanes from 12 to 36 carbons that showed a molecular distribution with a general maximum at C_{17} except for the sample 134-2 (max. at C_{18}), and secondary peaks at C_{25} (samples 134–1, 134–2, and 134–3) or C_{27} (sample 129) (see **Figure 12**). Sample 134–1, which is a finely laminated

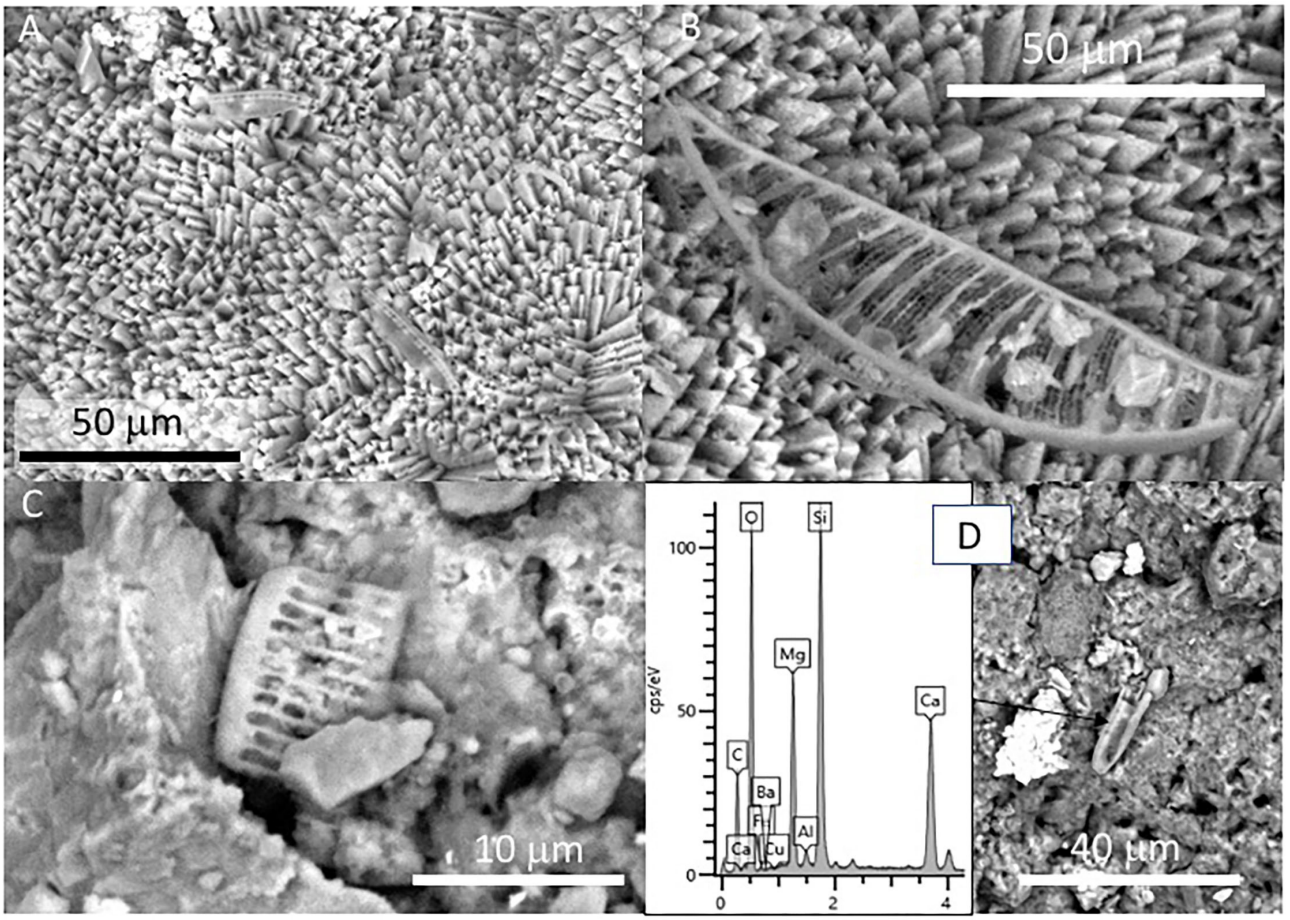

FIGURE 8 | SEM micrographs showing diatom frustules of sample 134–4 collected from a speleothem. **(A)** Two specimens of pennate diatoms located on the surface of the external sheet. **(B)** Detail of one of the pennate diatoms found in **(A)** showing a simple asymmetric valve. **(C)** Frustule fragment of diatom showing a more symmetric morphology included in the internal lamina of the speleothem sample. **(D)** Chemical microanalysis of a diatom frustule characterized by high Si-content together with O, while C, Mg, and Ca is received from the mineral matrix analysis.

fragment from a speleothem, showed the largest concentration of *n*-alkanes and a similar molecular profile to that of sample 134–3 (**Figures 12B,C**). Other compounds detected in the non-polar fraction were the isoprenoids pristane, phytane, and squalene, which were particularly abundant in sample 134–1 (**Figure 13A**, **Supplementary Table 2**).

The acidic fraction contained *n*-fatty acids ranging from 10 to 26 carbons (**Figure 13B**) in concentrations 1–2 orders of magnitude higher than the *n*-alkanes (**Supplementary Figure 4A**). They were particularly abundant in samples 134–1 and 134–2, where *n*-$C_{16:0}$ and *n*-$C_{18:0}$ were prevailing among the generally predominant even short chains (i.e., >20 carbons). In sample 129, only the *n*-fatty acids $C_{14:0}$, $C_{16:0}$, and $C_{18:0}$ were detected. Other compounds found in the acidic fraction were monounsaturated fatty acids of 16 and 18 carbons [$C_{16:1(\omega7)}$, $C_{18:1(\omega5)}$, $C_{18:1(\omega8)}$, and $C_{18:1(\omega9)}$], branched fatty acids of *iso*/*anteiso* (*i*/*a*) configurations (methyl groups at ultimate or penultimate positions, respectively) from 12 to 17 carbons (aC_{12}, iC_{14}, i/aC_{15}, iC_{16}, and iC_{17}), the 10-methyl hexadecanoic acid (10Me–$C_{16:0}$), and a few ketones (**Figure 13B**, **Supplementary Figures 4B,C**, **Supplementary Table 2**). Interestingly, only *n*-fatty acids were found in sample 129, whereas the branched fatty acids were only present in samples 134–1 and 134–2 (**Supplementary Figure 4B**).

The polar fraction was primarily composed of *n*-alkanols (**Figure 13C**) with chains from 12 to 24 carbons of even-over-odd preference. In contrast to the *n*-alkanes and *n*-fatty acids, the *n*-alkanols series show maximum peaks at compounds of larger chains (C_{22} and C_{24}) in all samples but 129, whose content of *n*-alkanol was generally low. Other compounds found in the polar fraction were sterols like stigmastanol, coprostanol, and cholesterol, and various derivatives (cholestenone or cholestanol) were also found in the polar fraction (**Figure 13D**, **Supplementary Table 2**). Most sterols occurred in samples 134–1 and 134–2, or those with fragments of finely laminated structure (**Figure 13D**,

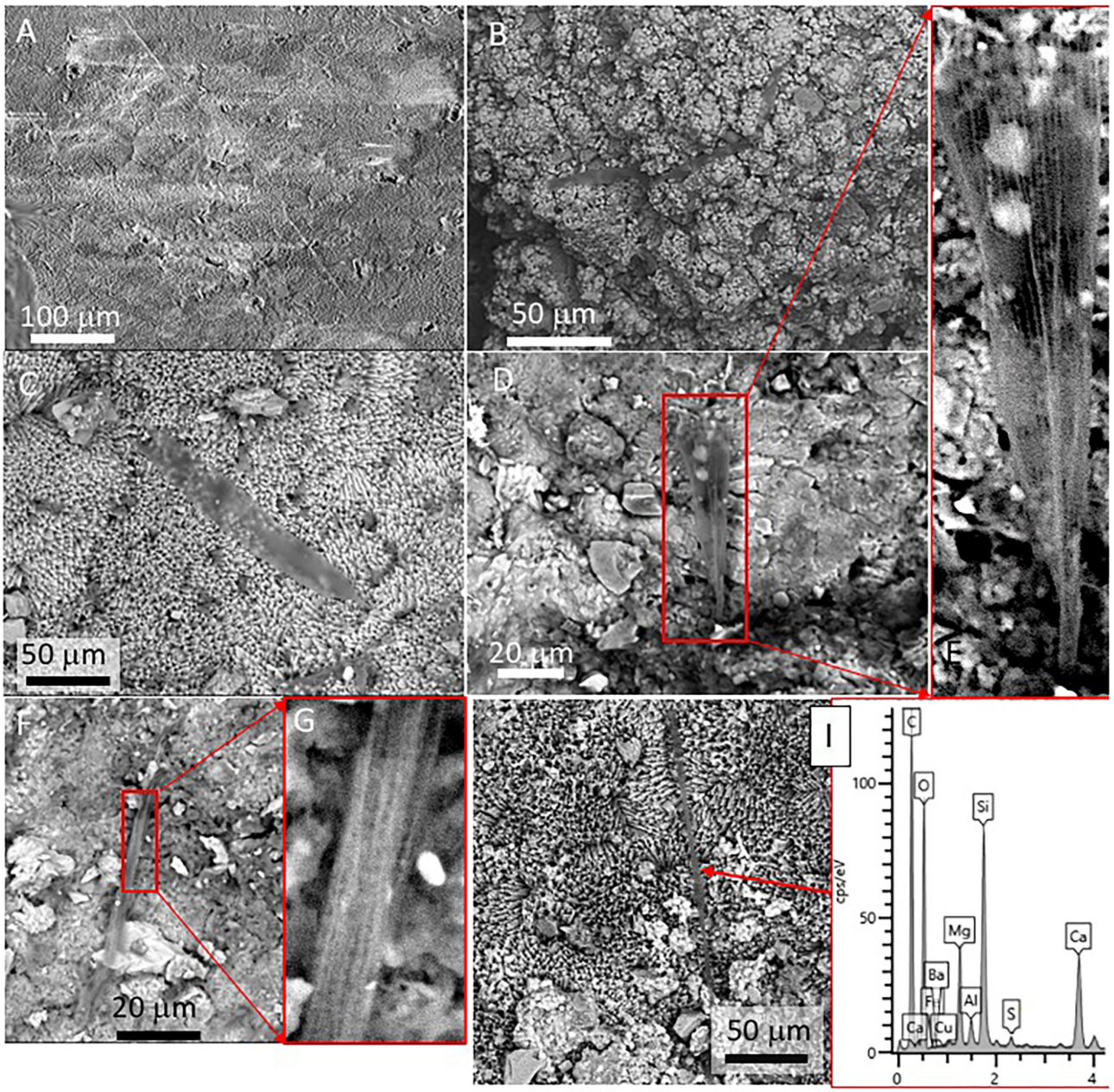

FIGURE 9 | SEM view of thick filaments (10 > microns) in samples 134–4. **(A)** 500-micron long filament, partially mineralized. **(B)** Network of large filaments with varying directions embedded in the mineral substrate. **(C)** Thirty-micron thick filamentous structure showing an apical area attached to the mineral substrate. **(D,E)** Thick filament also with an apical end bond to the mineral surface, which shows € a wall texture consisting of longitudinal and subparallel lines. **(F)** ∼5-micron thick straight filament with **(G)** reticulate texture. **(H)** SEM-EDS analysis of a straight filament revealing a high C and Si content with smaller amounts of S suggesting organic composition exposed to silicification. **(I)** Chemical microanalysis of a thick filament, characterized by high C, O and Si content, while Mg and Ca are received from the mineral matrix.

Supplementary Figures 1B,C, **Supplementary Table 1**). Finally, a series of alkenones from C_{18} to C_{27} were also found only in sample 134–3, the carbonatic tuff (**Figure 13D**).

Several lipid ratios were calculated (**Figure 13E**, **Supplementary Figure 4D**) to trace back biosources and environmental conditions. The average chain length (ACL) of *n*-alkanes informs about the dominance of prokaryotic (≤20) or eukaryotic (>20) sources (van Dongen et al., 2008), and here, it was found to range from 14 (134–3) to 18 (134–2) (**Figure 13E**). The carbon preference index (CPI) of the *n*-alkane is a proxy for the extent of biomass degradation, where living plants commonly have values of >5 (Rielley

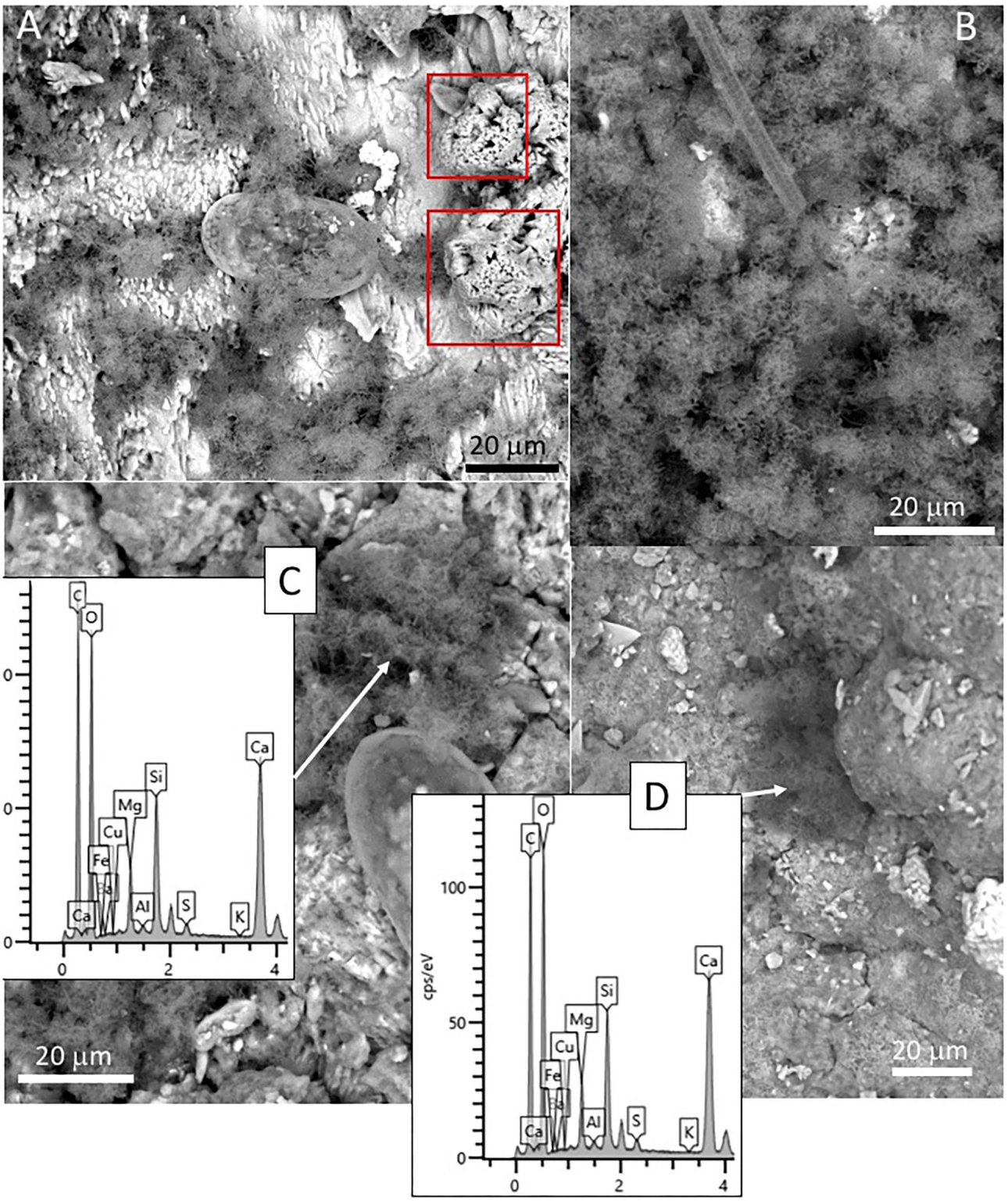

FIGURE 10 | Different images displaying unregular networks of entangled threads interpreted as extracellular polymeric substances (EPS) produced by microbial biofilms. **(A)** EPS embedding one testate amoeba, where red squares are tracing mineral sites with strong corrosion likely of microbial origin. **(B)** EPS densely covering the mineral surface associated with a large filament with reticulated texture. **(C,D)** SEM-EDS analysis of two different sites with EPS revealing a composition dominated by C, Si, and S. Other elements like Ca, Mg, Fe, Al, and Ba are likely sourced on the mineral matrix.

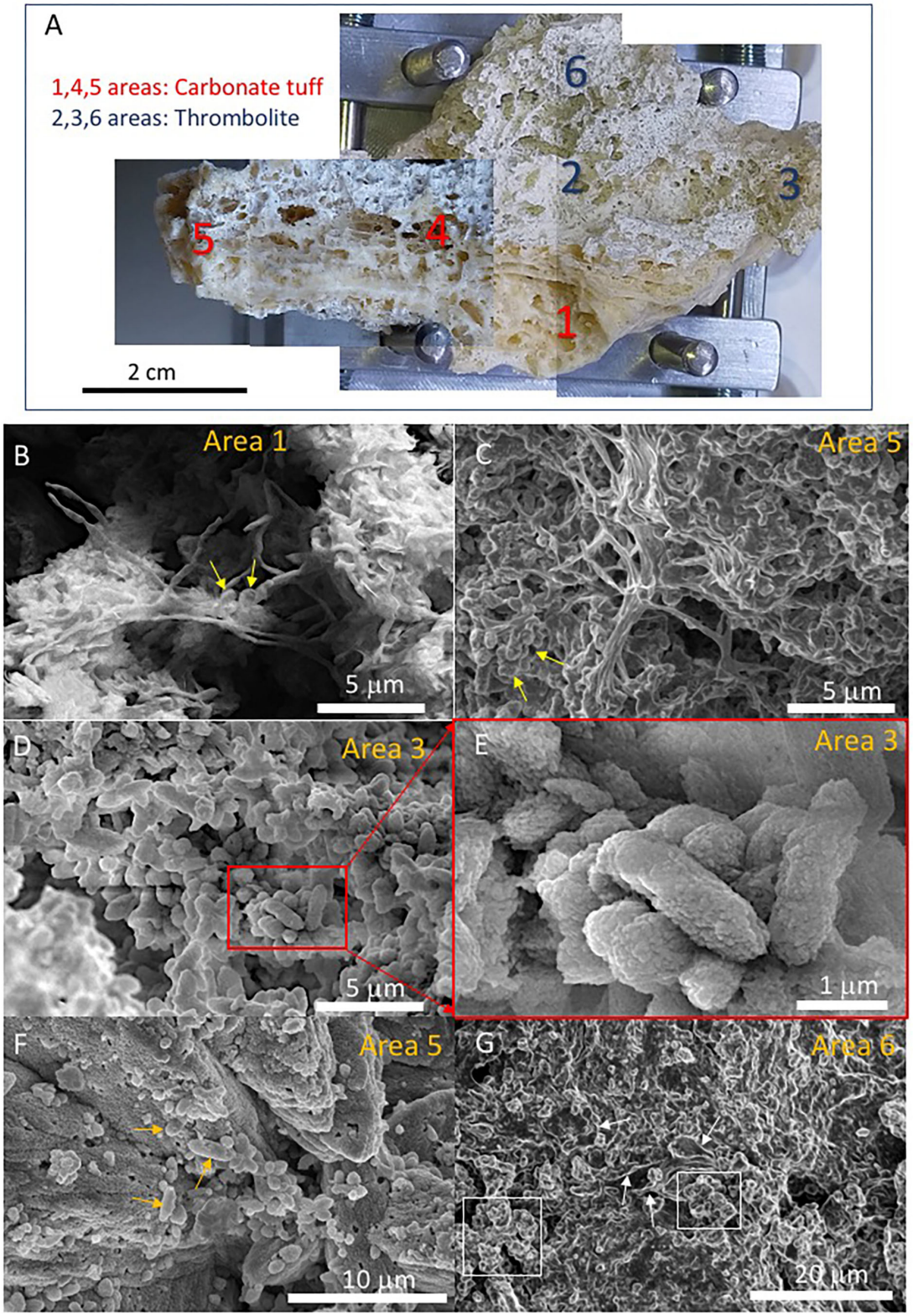

FIGURE 11 | Microscope images of samples 134–3 obtained using the SEM Philips XL30 powered with a Field Emission Gun scanning large samples up to 8 cm. **(A)** Mosaic of pictures captured from the SEM visible camera showing the different scanned areas. The sample reveals two main different sedimentary fabrics, including

(Continued)

FIGURE 11 | a tuff-like carbonatic material with large filamentous elements (scanned areas 1, 4, and 5) and microbially built deposits (scanned areas 2, 3, and 6). SEM images in areas 1 and 5 **(B,C)** likely displaying mineralized branching hyphae bearing sporangia. **(D)** Scanning image in area 3 revealing 2-micron size rod-like microstructures© corresponding with mineralized bacteria. **(F)** Large filaments associated with rod-like bacteria (yellow arrows) mineralized by Mg-calcite. **(E)** Image on area 6 showing clumps of rod-like microstructures (white squares) associated with void filamentous elements (white arrows) suggesting mineralization of cell wall followed by organic degradation. However, the captures a low intensity from the secondary electron signal that agrees with a composition dominated by carbon. **(G)** The thrombolite fabric follows another internal arrangement in form of clumps of rod-like microstructures associated with void filaments.

et al., 1991) and approaching 1 with increasing maturity. In the Uyuni samples, all values were higher than 1, especially in samples 134–3 (**Figure 13E**), which denotes an odd-over-even predominance of long-chain terrestrial compounds (Hedges and Prahl, 1993). The P_{aq} ratio traces the input of vegetal material from submerged/floating aquatic macrophytes vs. those of emergent and land plants (Ficken et al., 2000), and here, it was found to be between 0.44 (sample 129) and 0.61 (134–2 and 134–3). The terrigenous-over-aquatic ratio [defined as TAR $= (C_{27} + C_{29} + C_{31})/(C_{17} + C_{19} + C_{21})$; Bourbonniere and Meyers, 1996] was higher than one in all samples but 134–1 (**Figure 13E**). The ratio of pristane over phytane (Pr/Ph), two compounds largely derived from chlorophyll-a (Didyk et al., 1978), is commonly used to discriminate between oxic (>1) or anoxic (<1) conditions in a deposition environment (Peters et al., 2005), and here, it was observed to be higher than one in samples 134–1 and 134–3, and lower than one in samples 129 and 134–2 (**Supplementary Figure 4D**).

DISCUSSION

The structure and distribution of the speleothems that are framed with large filamentous structures are consistent with their formation during a wet and alteration episode that affected the lacustrine carbonates topping the volcanic deposits. As observed *in-situ* (**Figures 2B,E**), the cave ceilings are composed of volcanic deposits that are covered by a first carbonate unit showing a short-branched fabric found in the lacustrine thrombolitic carbonates of Pleistocene (**Figures 2B,E**, **Supplementary Figures**; Rouchy et al., 1996; Placzek et al., 2006). As it has been observed, such unit is followed by other two with distinctive filamentous structures that correspond to dense hyphae networks that have been mineralized by Mg-calcite as identified through XRD (**Supplementary Figure 3B**). The sequence of those carbonate units agrees with: (1) the flooding of a pre-existent cave emplaced in the volcanic host rock by a highstand lacustrine episode, followed by (2) a low-standing pulse, which finally (3) ended with the speleothem formation by a novel wet lacustrine episode not high enough for flooding the cave (**Figures 14A–D**). It resulted from the evolution of the Salar de Uyuni during the late Pliocene to the early Holocene. First, the saline basin experienced a highstand (>3,700 mls) episode in the Tauca event (>12 ky). Then, it was followed by a dramatic drop in the lake level during an arid phase in the Ticaña event (>10 ky) and ended by the Coipasa wet episode (10–8 ky). Interestingly, the cave has recorded carbonatic materials that formed under quite different paleoenvironmental conditions. During the Tauca highstand, the cave flooding sustained a cryptic habitat where likely the sunlight was a limiting factor for the photosynthetic microbial communities that might change to heterotrophic and/or chemosynthetic in the deeper areas of the caves. The environmental conditions changed drastically when the Coipasa episode took place, which favored the emplacement of a karst system through an active hydrological cycle.

The sedimentary context, fabric, and structure of the different samples are consistent with the paleoenvironmental conditions where they were formed (**Supplementary Figures 1**, **2**, **Supplementary Table 1**). The columnar fabric found in sample 129 collected from lacustrine carbonates of the Coipasa area (**Supplementary Figure 1A**, **Supplementary Table 1**) suggests that is the result of the microbial clot accretion resulting in the generation of a columnar thrombolite fabric in a lake with brackish to saline waters (Rouchy et al., 1996; Placzek et al., 2006). In turn, the laminar and leafy internal structures observed in samples 134–1, 134–2, and 134–3 concur with the precipitation of Mg- calcite (**Supplementary Figures 3B,C**, **Supplementary Table 1**) by different microbial and non-biological pathways, where fungi played an essential role in the ion mobilization and the speleothem formation. The XRD analysis suggests that the mineral precipitated occurred under varying saline solutions (Risacher and Fritz, 1991) leading to the production of Mg-calcite. Furthermore, the occurrence of kutnahorite $Ca_{1.1}(Mn^{2+}, Fe^{2+}, Mg)_{0.9}(CO_3)_2$ in samples 134–3 (**Supplementary Figure 3C**) concur with the carbonate precipitation under microbial reduction of iron and manganese in the ancient lacustrine and ground solutions enriched with carbonate and magnesium (Rincón-Tomás et al., 2016).

The SEM-EDAX analysis of the different samples has provided additional information about the forming paleoenvironmental conditions through their geochemical and biological composition. The SEM-EDS analysis of samples 134–1, 134–2, and 134–4 corresponding to the speleothems show that the mineral matrix has a fibrous radial habit (**Figures 3**, **4A**), which is composed of Ca, C and O, and secondary Mg (**Figure 6A**). It greatly agrees with the occurrence of the Mg-calcite composition identified by XRD. Furthermore, the mineral matrix comes together with other elements like Fe, Cu, Mn, and Si (**Figures 6C,D**) suggesting that they are sourced from the degradation of the volcanic host rock that is the Uyuni basin basement (Tibaldi et al., 2009; Salisbury et al., 2015). Such a set of elements are abundant in very distinctive microstructures like the spongy ovoids and undulate laminas bearing Mn, and the aggregates of rod-like units that are mineralized by Si (**Figures 4B–D**, **5A,B**). The Mn-enriched microstructures suggest that kutnahorite and Mn oxides locally formed through microbial reduction of Mn and Fe in the speleothems (Rincón-Tomás et al., 2016), while the silica-rich aggregates of rod-like

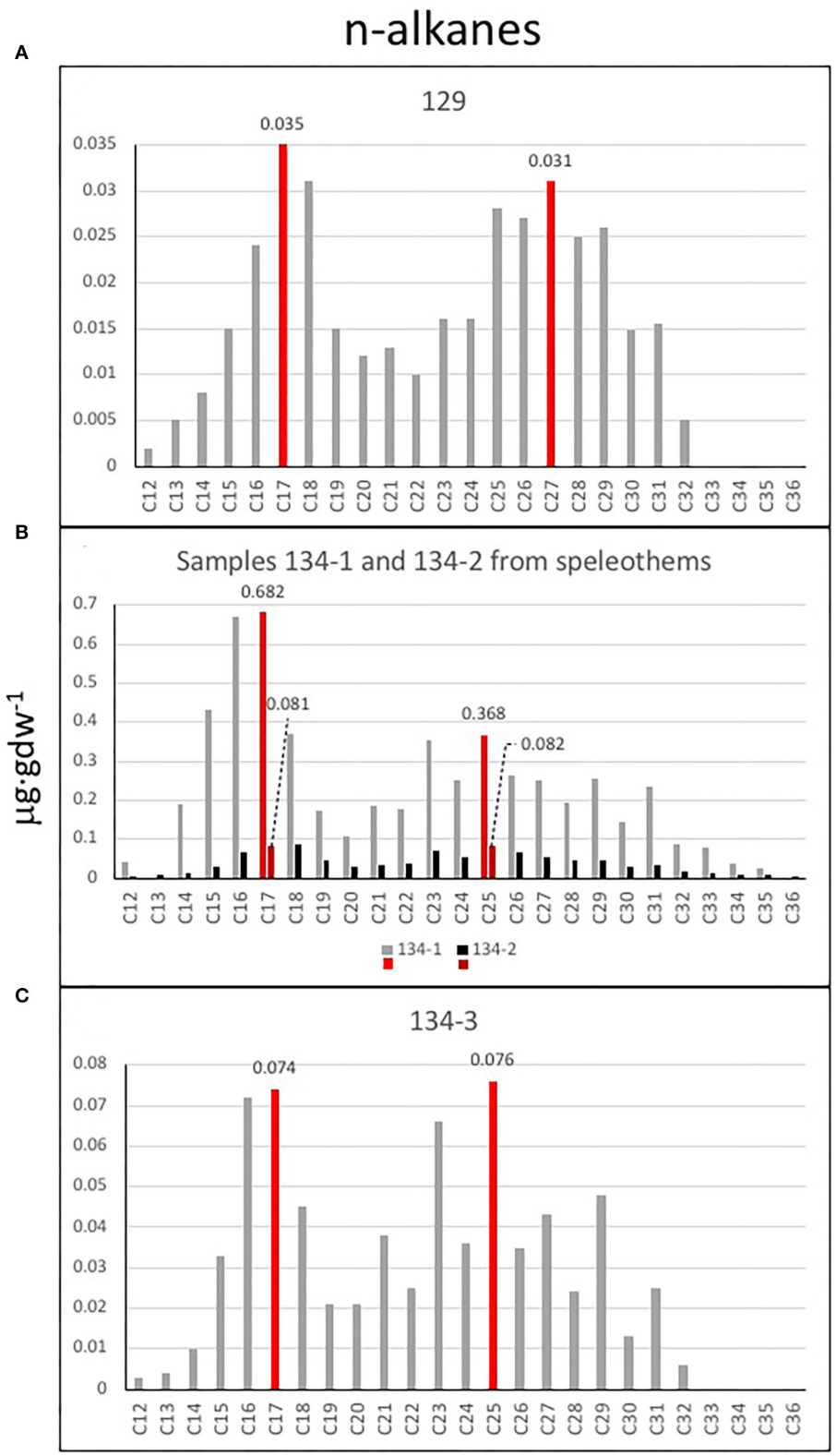

FIGURE 12 | Bar diagrams plotting the C_{12}-C_{36} *n*-alkane distribution in samples **(A)** 129, **(B)** 134–1 and 134–2, and **(C)** 134–3. In general, the diagram profiles reveal two different sources for *n*-alkanes. A dominance of microbial remnants (<C_{20}) with the major peaks indicating potential relevance of cyanobacteria (C_{15} and mostly C_{17}) among other microorganisms represented by *n*-alkanes C_{16} and C_{18}; and a second group of relative high peaks in C_{23} and C_{25} suggest a source in macrophytes and/or mosses, as well as higher plants (C_{27}, C_{29}, and C_{31}). Sample 134–1 **(B)** has the largest concentration of *n*-alkanes suggesting a higher microbial activity.

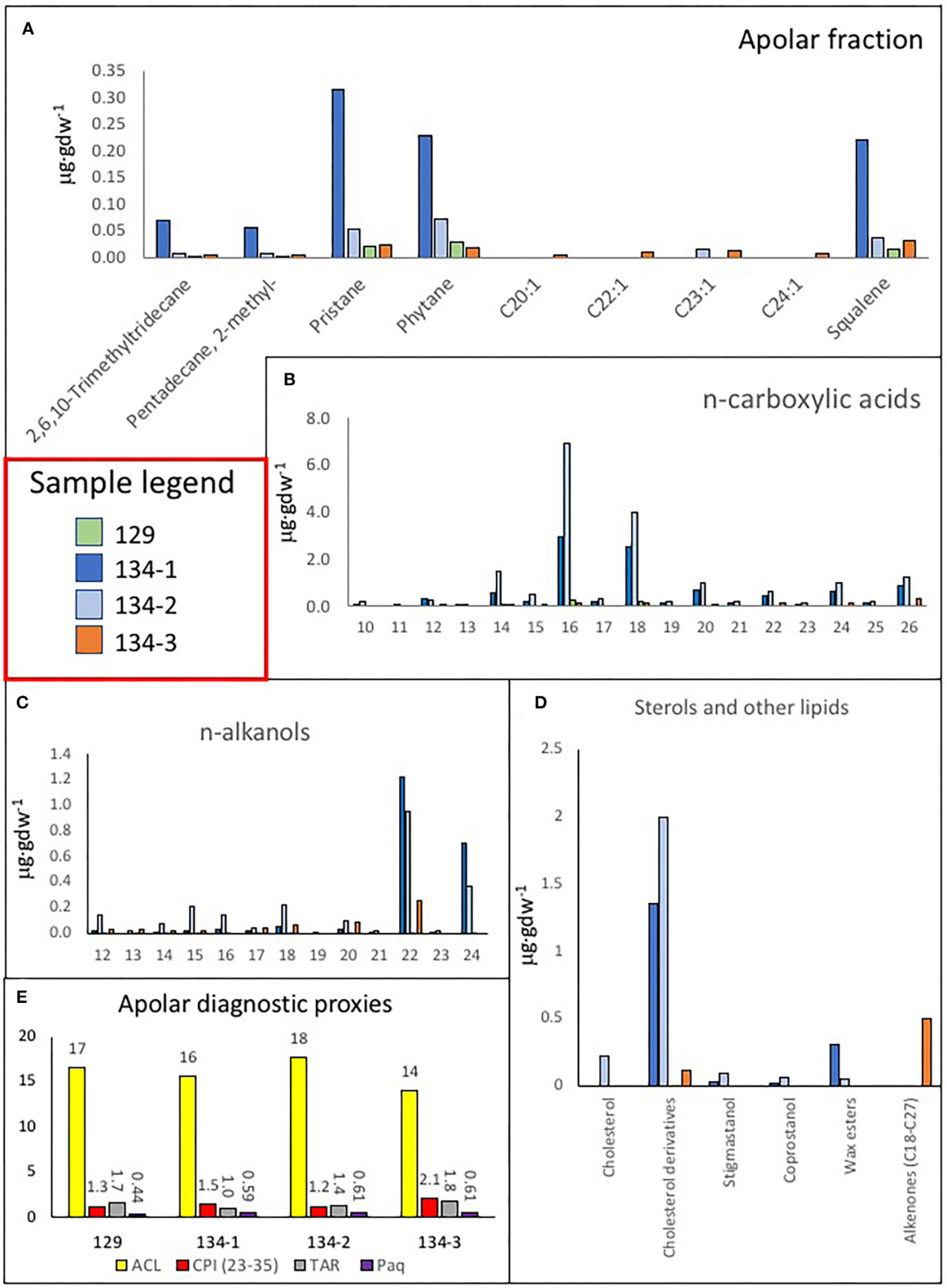

FIGURE 13 | Bar diagrams revealing the occurrence and distribution of different lipids. **(A)** Concentration of some lipids extracted in the apolar fraction like trimethyl-tridecane, methyl-pentadecane, pristane, phytane, squalene, eicosene ($C_{20:1}$), docosene ($C_{22:1}$), tricosene ($C_{23:1}$), and tetracosene ($C_{24:1}$). **(B)** Distribution

(Continued)

FIGURE 13 | of *n*-fatty acids from $C_{12:0}$ to $C_{26:0}$ revealing a similar distribution in all samples suggesting the predominance of microbial sources in all samples ($<C_{20:0}$, mostly $C_{16:0}$ and $C_{18:0}$) but 134–3, where the eukaryotic source ($C_{26:0}$) seems to be relatively higher; interestingly, sample 129 has only recorded microbial sources ($C_{14:0}$, $C_{16:0}$, and $C_{18:0}$). **(C)** Distribution of C_{12}-C_{24} alkanols in the four samples, where a dominance of mid-molecular weight alkanols (C_{22}-C_{24}) was found in all samples denoting a eukaryotic source like fungal, algal, or macrophyta, but sample 129 with a stronger microbial signal. **(D)** Bar diagram displaying the concentration of cholesterol, cholesterol derivatives (cholestenone and cholestanol), wax esters (lauryl stearate, myristyl stearate and cetyl stearate) (see **Supplementary Table 2**) and C_{18}-C_{27} alkenones in the four samples 129, 134–1, 134–2, and 134–3. **(E)** Apolar compound ratios like the average chain length (ACL), the carbon preference index (CPI), the terrigenous over aquatic ratio of hydrocarbons (TAR), and the P_{aq} proxy for submerged/floating aquatic macrophyte input vs. emergent and terrestrial plant estimated reveal the organic source in samples.

elements can result from the silicification of bacteria biofilm (Toporski et al., 2002; Moore et al., 2020) by circulating solutions within the speleothem.

The SEM-EDS technique has also identified small and delicate tests, with an orderly distribution pattern and geometry (**Figures 7A–F**). The tests have a flask-shaped form and on one of the sides, there is an opening or hexagonal apertural margin surrounded by indentations evenly distributed around the aperture and containing several teeth (**Figure 7A**). The SEM-EDS analysis shows that they are built by the coalescence of different units composed of silica (**Figures 7C,D**). Such a microstructure test fits well with the testate amoeba carapace, which is formed by platy units known as idiosomes with silica composition (Lahr et al., 2015). Amoeba is unicellular organisms that normally live protected by a test in both subaerial or subterranean environments (González López et al., 2013). In the subterranean environment, the tests are normally formed by amorphous silica and agglutinated idiosomes that resemble pollen grains contained inside the organism (González López et al., 2013).

The speleothems, formed by the precipitation of carbonates coming from the rock dissolution due to chemical weathering, should have created a suitable and organic-rich environment for the testate amoebae to thrive. The testate amoebae were found on the external surface of speleothems protected inside small depressions or inside speleothem micropores (**Figure 7G**). The tests appear mostly intact, although a few specimens were found with the tests partially collapsed by flattening or dismantled where the idiosomes are released (**Figures 7A,C,D**). The specimens appear as isolated individuals and the great homogeneity in the distribution of the testate amoebae indicates that the microsystem inside the cave was very similar for the time of their formation, as any changes in the humidity levels, availability of silica, or any transport process would undoubtedly affect the formation of the test and inhibiting the occurrence of such protozoans. There is extensive literature describing amoebae; however, they are normally referred to as naked amoebae (without tests). The observations made in several samples allowed us to elaborate on the origin of the testate amoebae in the Uyuni caves, however, it is obvious that more samples should be studied, both in the origin zones and in the number of speleothems.

Furthermore, the siliceous thecae co-occurring with the testate amoeba have the same morphological and compositional features as diatom frustules (**Figures 8A–D**). They have also been found in the ancient deposits of the Uyuni basin (Servant-Vildary, 1978). The appearance of such remains in the speleothem samples (134–1, 134–2, and 134–4) suggests that diatoms were a biological component of the Uyuni cave ecosystems. Interestingly, cave diatoms have been found associated with different karstic structures, including the speleothems (Kashima et al., 1987; Falasco et al., 2014), in the same way as they have in the speleothems of the Uyuni caves (**Figures 6A–D**). The distribution of the diatoms in the cave should correspond to the cave topology, which is the main constraint for the light availability in the cave interior (Falasco et al., 2014). The diatom frustules show different morphology and preservation degrees depending on the site where they are found. While the specimens occurring in the external sheet of the speleothem samples (e.g., 134–4) are intact and have an asymmetric morphology (**Figures 8A,B**), those observed in the internal lamina are symmetric and fragmented, have traces of dissolution, and are partially filled and covered by carbonatic material (**Figures 8C,D**, **Supplementary Figure 5**). Interestingly, the morphology and preservation degree of the diatom frustules in sample 134–4 from the carbonate tuff (**Supplementary Figure 5**, **Supplementary Table 1**) shows the same features (e.g., internal mineralization, dissolution traces) as those found in the internal lamina of the samples collected from the speleothems. Consequently, the microbial remains, including the diatoms that are found on the surface of the external mineral sheet (**Figures 3A–D**, **4A**, **8A,B**), are relatively younger than the mineral matrix that contains them.

The observation through the SEM of straight to slightly sinuous long (>1 mm) filamentous structures of samples 134–4 (**Figures 9A,B**) shows that they are partially or fully mineralized by Mg-calcite, suggesting that they have grown before or when the mineral precipitated. In this regard, the macrofilaments forming the speleothems show that their features are widely recognized in typical fungi hyphae as thick filaments and a high branching degree (**Figures 2B–E**, **Supplementary Figure 2**). As these are completely mineralized by the Mg-calcite, it can be inferred that the cave fungal community played an essential role in the speleothem formation. On the contrary, the entangling threads forming unregular networks (**Figures 10A–D**) resemble the extracellular polymeric substances (EPS) of microbial biofilms (Dohnalkova et al., 2011). The size and morphology of the EPS threads are consistent with a bacterial source as it is shown by Dohnalkova et al. (2011) and references therein.

Furthermore, the preservation degree and mineralization of filaments and EPS are also variable. In sample 134–1, they show a high content of organic carbon and incipient mineralization by silica (**Figures 9I**, **10C,D**). In turn, sample 134–3 show high mineralization by carbonate (**Figures 11A–E**) and, likely, silica (**Figure 11G**) with a varying concentration in C. Such disparate preservation can be a consequence of

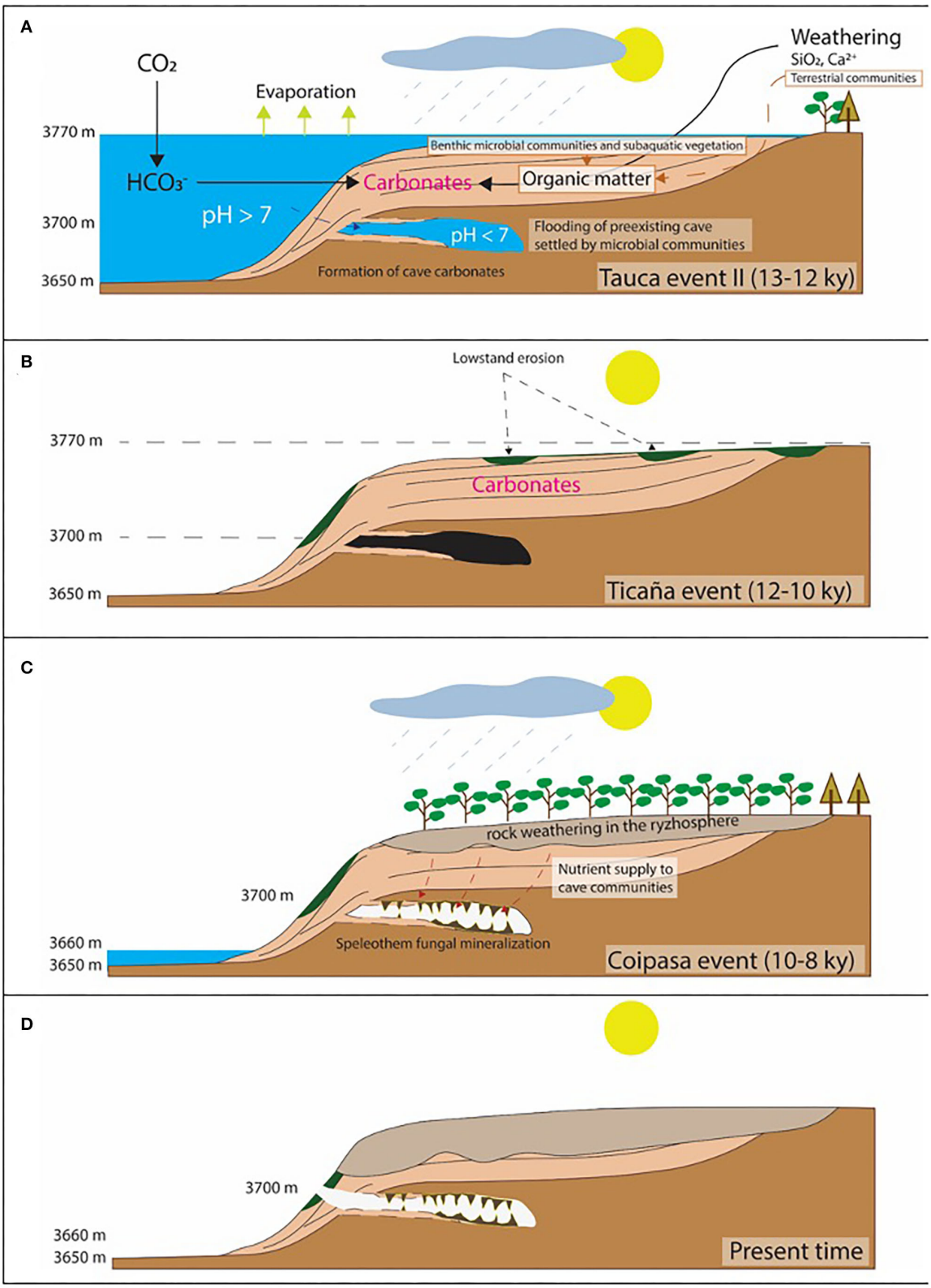

FIGURE 14 | Sketch describing the stages leading to the formation of the carbonate structures in the cave interior consisting of thrombolite-like and speleothems framed by fungal colonies. **(A)** Flooding of a cave initially emplaced in the volcanic deposits around Tunupa volcano. It was caused by a highstand episode reaching an

(Continued)

FIGURE 14 | altitude of 3,770 m corresponding with the wet Tauca event (13–13 ky), promoting the precipitation of lacustrine and cave carbonates with thrombolitic fabric mediated by microbes. **(B)** The lake level dramatically dropped during an aridic incursion (Ticaña event) associated with an erosive fluvial activity. **(C)** Subsequent wet episode (Coipasa event) leading to a highstand stage lower than the cave bottom greatly enhanced the weathering of the lacustrine carbonates and other exhumated deposits. The hydrological activity triggered the forest expansion in the lake margins, augmented substrate weathering, incremented the ecosystem productivity and the nutrient circulation from the surface to the cave interior. Such processes sustained the fungal community in the cave, which activity ended in the speleothem formation. **(D)** A last aridic event in the Holocene collapsed the Uyuni hydrological activity that formed the modern saline basin. Under these conditions, the cave community was obliterated, and the speleothem formation ended.

the different sample and microstructure ages; while in samples 134–1 and 134–4, the external sheet contains the elements with a higher preservation degree (**Figures 8A,B**), which have lower preservation and high mineralization in the internal lamina (**Figures 8C,D**, **Supplementary Figure 5**). This is also the case for the microbial remains in sample 134–3, where the diatoms appear fragmented and with clear evidence of corrosion (**Supplementary Figure 6**).

The molecular distribution of the *n*-alkane series revealed that the dominance of microbial remnants ($<C_{20}$) is likely related to cyanobacteria (peaks at C_{15} and mostly C_{17}) (Ladygina et al., 2006), among other microorganisms [ubiquitous *n*-C_{16} and *n*-C_{18}]; (Grimalt and Albaigés, 1987; **Figures 12A–C**). The prevailing microbial sources were reflected by homogeneously low values of ACL in the four samples (14–18) (**Figure 13E**, **Supplementary Figure 4D**). In particular, the signal of cyanobacteria (as *n*-C_{17}) was prevailing in all samples but 134–2, where other microorganisms (as *n*-C_{18}) appeared relatively more abundant (**Figure 12B**). Furthermore, the widespread presence of 2-methylpentadecane (**Figure 13A**) supported the relevant contribution of cyanobacteria in the samples (Brocks and Summons, 2014). Still, there was also a presence of eukaryotic signals related to diatoms and algae [possibly $C_{16:1(\omega7)}$ and $C_{18:1(\omega9)}$ fatty acids], mosses, and macrophytes (*n*-C_{23} and *n*-C_{25} alkanes; Ficken et al., 2000; Pancost et al., 2002), and higher plants (*n*-C_{27}, *n*-C_{29}, and *n*-C_{31} alkanes; Eglinton and Hamilton, 1967; Hedges and Prahl, 1993). As a result, three of the four samples (129, 134–2, and 134–3) showed TAR values slightly higher than 1 (**Figure 13D**), which revealed that the proportion of aqueous biomass (algae and cyanobacteria), as represented by the *n*-alkanes C_{17}, C_{19}, and C_{21}, was lower than that derived from higher plants (as the sum of C_{27}, C_{29}, and C_{31}), except for the sample 134–1 (i.e., TAR = 0.8).

Still, sample 134–1 showed together with the rest of the samples' CPI values higher than one that denoted an odd-over-even predominant character, slightly higher in 134–3 (**Figure 13E**, **Supplementary Figure 4D**). This may be interpreted in relation to the still fresh nature of the terrigenous long-chain *n*-alkanes, likely due to good preservation of the vegetal biomass after death (Carrizo et al., 2019). This was supported by the relative enrichment of *n*-fatty relative to *n*-alkanes observed in all samples (**Supplementary Figure 4A**). The particularly high ratio of n-fatty/n-alkanes in 134–2 (ratio of 19) implies a much lower defunctionalization of the organic matter over time (i.e., loss of functional groups) relative to the other samples. Furthermore, it cannot be discarded that some organics could be very recent as resulting from later microbial activity in the cave as observed through the SEM-EDS in sample 134–1 (**Figures 8A,B**, **9A–I**). This is consistent with a younger age for sample 134–2 collected from the fungal-framed speleothems.

Regarding aqueous sources, values of the P_{aq} index from 0.44 (sample 129) to 0.61 (samples 134–2 and 134–3) suggested organic matter inputs from a mix of emergent and submerged/floating macrophytes (Ficken et al., 2000), as well as mosses (Nott et al., 2000). The presence in the apolar fraction of other compounds like the isoprenoids pristane, phytane, and squalene (**Figure 13A**) was related mostly to photosynthetic sources. Pristane and phytane are largely derived from the degradation of phytol, a side chain of chlorophyll-a mostly used by phototropic organisms like cyanobacteria, algae, and land plants (Rontani and Volkman, 2003; Peters et al., 2005), while squalene is practically ubiquitous in all type of organisms, including animals (Grice et al., 1998; Brocks and Summons, 2014). Assuming a common origin in phytol of both pristane and phytane, we can learn about the deposition environment of the samples by calculating the ratio of one over the other (i.e., Pr/Ph; Peters et al., 2005). Here, values of the ratio from 0.7 to 1.4 (**Supplementary Figure 4D**) allowed us to differentiate anoxic environment for samples 134–1 and 134–3 (ratio >1) and an anoxic environment for samples 129 and 134–2 (ratio > 0.7) (Powell and Mckirdy, 1973). Changes in paleoenvironmental conditions may have driven periodic transitions from dry to lacustrine systems in the cave that explain the mix of depositional environments and aqueous/terrigenous fingerprints found in the samples. In general, anoxic conditions recorded in sample 129 are consistent with the formation of lacustrine thrombolites, where anaerobic microbial communities take part in the formation of the carbonatic biostructures (Feldmann and Mckenzie, 1998). In the same way, anoxic to oxic conditions, shown in samples 134–1 and 134–2, will likely result from changing environmental conditions in the speleothem formation, while aerobic conditions are consistent with the paleoenvironment where the carbonatic tuff (sample 124–3) was formed.

In the four samples, the similar dominance of short-chain *n*-fatty acids ($< C_{20:0}$, mostly $C_{16:0}$ and $C_{18:0}$) supported the mentioned dominance of microbial sources in the caves (**Figure 13B**). In particular, the detection of branched fatty acids, such as 10Me-$C_{16:0}$, *a*-$C_{12:0}$, *i*-$C_{14:0}$, *i*/*a*-$C_{15:0}$, *i*-$C_{16:0}$, and *i*-$C_{17:0}$, was related to *Actinomycetes* (*Actinobacteria* phylum), *Desulfobacter* (*Proteobacteria* phylum), and other sulfate-reducing bacteria (Taylor and Parkes, 1983; Parkes et al., 1993). Still, a certain eukaryotic signal was observed in sample 134–3 in form of a peak at $C_{26:0}$, most likely related to algae, mosses, or aquatic macrophytes (Ficken et al., 2000; Nott et al., 2000),

according to its P_{aq} value (0.61; **Supplementary Figure 4D**). In contrast, in samples 134–1 and 134–2, the eukaryotic signal in the acidic fraction was, instead, related to higher plants, according to the presence of oxodehydroabietic acid, a typical resin acid derived from coniferous plants (Rybicki et al., 2016; Marynowski et al., 2020). Furthermore, the presence of unsaturated fatty acids, such as $C_{16:1[\omega7]}$ and $C_{18:1[\omega9]}$ in samples 134–1, 134–2, and 134–3, might also indicate contributions from eukaryotic sources, such as aquatic diatoms, microalgae, and fungi, as well as cyanobacteria or other gram-negative bacteria (Ahlgren et al., 1992; Dijkman and Kromkamp, 2006; Coates et al., 2014), or type II methanotrophs [$C_{18:1(\omega8)}$] (Bowman et al., 1991; Brocks and Summons, 2014). The relatively higher concentration of unsaturated fatty acids in samples 134–1 and 134–2 (**Supplementary Figures 4B,C**, **Supplementary Table 2**) suggested a fresher nature of these samples agreeing with their highest *n*-fatty acids/*n*-alkanes values (**Supplementary Figure 4A**) since diagenesis and alteration over time tend to cause the loss of double bonds (Stefanova and Disnar, 2000).

In the polar fraction, the dominance of C_{22} and C_{24} among the *n*-alkanols series in samples 134–1, 134–2, and 134–3 (**Figure 13C**) supported the presence of biomass from eukaryotic sources. In particular, the relationship of *n*-C_{24} with higher plants is well-described (Peters et al., 2005; Burdige, 2007), and would agree with a potential source here in the forest communities associated with the soil formation above the speleothem. In contrast, the origin of *n*-C_{22} remains unknown, and we hypothesize that it could stem from fungi biomass. In sample 129, only compounds of microbial sources (*n*-C_{14}, *n*-C_{16}, and *n*-C_{18}) were found in the polar fraction (**Figure 13B**), which agrees with a composition related to thrombolite formations by cyanobacteria (Rouchy et al., 1996).

The recovery of several sterols, including stigmastanol and cholesterol derivatives (**Figure 13D**, **Supplementary Table 2**), confirmed the presence of eukaryotic biomass. Stigmastanol is a product derived from stigmasterol, a phytosterol produced by higher plants and micro-/macroalgae (Volkman, 1986, 2003). Cholesterol derivatives, such as cholestadienone and cholestadienol (Melendez et al., 2013), and coprostanol (**Figure 13D**, **Supplementary Table 2**), suggest the occurrence of organics produced by animals, protozoa, and red algae (Volkman et al., 1998). In particular, the detection of cholestadienone (cholesta-3,5-dien-7-one) and cholestadienol (3β-cholesta-4,6-dien-3-ol) are derivatives from cholesterol that denote a low extent of degradation (Melendez et al., 2013), while coprostanol has been reported as a fecal degradation product found in mammals and birds feces (Harrault et al., 2019; Gallant et al., 2021). Among the samples, cholestadienol and coprostanol mainly occurred in samples 134–1 and 134–2, where speleothem fragments were present, whereas cholestadienone was dominant in sample 134–3, the sample with tuff-like material (**Supplementary Figures 2A–C**, **Supplementary Table 1**). Finally, alkenones from C_{17} to C_{26} were also found in the polar fraction only of sample 134–3 (**Figure 13D**). While long-chained alkenones (C_{36}-C_{38}) are attributed to planktonic unicellular algae (Pagani, 2009), the origin of chains from C_{17} to C_{26} is uncertain.

CONCLUSION

The analysis of the different samples in the Salar de Uyuni provides unique information about the paleoenvironmental conditions where they were formed, by diverse microbial and non-biological pathways, where the fungal communities played a crucial role in the formation of the speleothems. Likely, nutrients were primarily provided by the vegetal communities in the lake margins, however, they may have also been released from the lacustrine carbonatic unit. The combination of biological activity and hydrology most likely triggered a quick rock dissolution and mineralization, which formed the speleothem fungal structures.

The size and abundance of the preserved fungal structures suggest a constant supply of organic matter and stable hydrological activity at the time of their formation. The high porosity and large size of cavities in the paleoterraces ensured a long-lasting and continuous fluid flow and supply of materials. All the elements necessary for the mineral formation were released during the alteration of the host rocks and supplied by percolating fluids. The biological control of element cycling is also an important factor, for instance, the silica detected in the carapace of the testate amoebae, or the diatom frustules indicates the role of the organisms in the Si cycle, where weathering and transportation of Si from the older lacustrine deposits and the soils moved through the speleothems.

The analysis of the lipids recorded in the samples has also provided some insights into the paleoenvironmental conditions accompanying the formation of the biospeleothems (samples 134–1, 134–2, and 134–4), the carbonatic tuff (sample 134–3), and the thrombolitic carbonates (sample 129). The organic compounds are mostly sourced in bacteria, but also with a high input from aquatic and terrestrial plant inputs, which were lately degraded by fungi. In this regard, the signal of cyanobacteria is dominant in all samples but 134–2, where other microorganisms could be more abundant. The occurrence of sterols like stigmastanol and cholesterol derivatives prove relevant to eukaryotic activity in the past. While stigmastanol is a stigmasterol derivative produced by higher plants and micro-/macroalgae, derivatives of cholesterol like cholestadienone and cholestadienol, and coprostanol evidence the molecular record of animals, protozoa, and red algae. The characterization of cholestadienone and cholestadienol denote a low extent of degradation of the original sterols, while coprostanol, is identified as a sterol from fecal degradation by mammals and birds in caves. In this regard, cholestadienol and coprostanol are found in the speleothem samples, which is consistent with the activity of animals in the cave. However, cholestadienone is prevailing in the carbonatic tuff suggesting a red algal origin.

Searching for biomarkers in caves allows us to understand the contribution of fungal communities to biokarst not only on Earth but also in Martian cave environments. Cave microbiology can answer questions about the limits of life and allow us to recognize

the geochemical signatures of life. Given that such signatures have survived geologic uplift, we should be able to detect them on other planetary surfaces, such as Mars, if they are present. In addition, due to the absence of liquid water on the surface of Mars, extant life will likely be restricted to the subsurface, making it crucial to understand the processes, which create and preserve signatures of microbial life in cave environments.

DATA AVAILABILITY STATEMENT

The original contributions presented in the study are included in the article/**Supplementary Material**, further inquiries can be directed to the corresponding author.

AUTHOR CONTRIBUTIONS

AA and DF-R wrote the manuscript with input from TH, QH, YS, RA, NR, DC, and LS. DC and LS conducted and provided the main information regarding the lipid content found in the samples. Furthermore, AA and NR prepared and analyzed the samples under the different SEM-EDS and TEM techniques. All authors contributed to the discussion and final confection of the manuscript.

FUNDING

This research has been supported by the National Key Research and Development Program of China (2021YFA0716100), project PID2019-104812GH-100CTM funded by the MICINN of Spain, and project FDCT-0005-2020-A1 funded by the Fundo de Desenvolvimento das Cientifico e da Tecnologia da RAE de Macau.

ACKNOWLEDGMENTS

The authors would like to thank the Transmission Electron Microscopy Service of the Centro de Biología Molecular personnel, especially Milagros Guerra, for this service. We are also grateful to Prof. Agata Dias and Pedro Costa of the Institute of Science and Environment in Macau and Maite Fernández Sampedro of the Center of Astrobiology in Spain for their mineral analysis using the XRD methodology. Furthermore, we also thank Geoffrey SG for providing some images that have been used to infer the speleothem formation.

SUPPLEMENTARY MATERIAL

The Supplementary Material for this article can be found online at: https://www.frontiersin.org/articles/10.3389/fmicb.2022.913452/full#supplementary-material

Supplementary Figure 1 | Pictures showing the analyzed samples like **(A)** 129 with columnar fabric collected in the Coipasa area corresponding to a thrombolitic carbonate, **(B)** 134–1 and **(C)** 134–2 laminated samples recovered from a large speleothem in the Chiquini cave. Black color in sample 134–1 is found in distinct sides of the speleothems and likely corresponds with Mn-bearing minerals as detected by SEM-EDS and XRD techniques.

Supplementary Figure 2 | Images displaying **(A)** sample 134–3 that has **(B)** thrombolitic and **(C)** filamentous tuff-like fabrics. **(D)** Corresponds with sample 134–4 collected from a speleothem showing a leafy fabric with internal microlaminar structure and the occurrence of filamentous networks with forked pattern (red squares) and large filaments (red arrow).

Supplementary Figure 3 | XRD analysis for samples **(A)** 129, **(B)** 134–1 and 134–2, and **(C)** 134–3 resulting in different Mg-calcite species with varying content in such a cation. In addition, a Mn-bearing carbonate like kutnahorite **(C)** has been found in sample 134–3.

Supplementary Figure 4 | Additional diagrams of different organic compounds revealing **(A)** a higher abundance of *n*-fatty acids over the *n*-alkanes, **(B)** the diversity of fatty acids in samples, **(C)** iso/anteiso, monounsaturated and branched fatty acids, and **(D)** the full set of apolar diagnostic ratios, including the average chain length (ACL), the carbon preference index (CPI), the terrigenous over aquatic ratio of hydrocarbons (TAR), terrestrial index from *n*-C29 over *n*-C27 alkane (C29/C17), P_{aq} proxy for submerged/floating aquatic macrophyte input vs. emergent and terrestrial plant, pristane vs. phytane (Pr/Ph), *n*-C17 alkane vs. pristane (C17/Pr), and *n*-C18 alkane vs. phytane (C18/Phy).

Supplementary Figure 5 | Fragmented valve of a diatom found in the internal lamina of sample 134–4 collected from a speleothem that is infilled by carbonate sediment.

Supplementary Figure 6 | Diatom frustule found in area 4 of sample 134–3 covered by mineralized filaments (yellow arrows) likely of fungal origin. The diatom valve is fragmented and reveals evidence of partial corrosion.

Supplementary Table 1 | Description of the samples collected in the Salar de Uyuni for this study.

Supplementary Table 2 | List of compounds found in the Uyuni samples.

REFERENCES

Ahlgren, G., Gustafsson, I.-B., and Boberg, M. (1992). Fatty acid content and chemical composition of freshwater microalgae. *J. Phycol.* 28, 37–50. doi: 10.1111/j.0022-3646.1992.00037.x

Argollo, J., and Mourguiart, P. (2000). Late quaternary climate history of the bolivian altiplano. *Quat. Int.* 72, 37–51. doi: 10.1016/S1040-6182(00)00019-7

Bindschedler, S., Cailleau, G., Braissant, O., Millière, L., Job, D., and Verrecchia, E. P. (2014). Unravelling the enigmatic origin of calcitic nanofibres in soils and caves: purely physicochemical or biogenic processes? *Biogeosciences* 11, 2809–2825. doi: 10.5194/bg-11-2809-2014

Bindschedler, S., Cailleau, G., and Verrecchia, E. (2016). Role of fungi in the biomineralization of calcite. *Minerals* 6, 41. doi: 10.3390/min6020041

Blard, P. H., Sylvestre, F., Tripati, A. K., Claude, C., Causse, C., Coudrain, A., et al. (2011). Lake highstands on the altiplano (tropical andes) contemporaneous with heinrich 1 and the younger dryas: new insights from 14C, U–Th dating and δ18O of carbonates. *Quat. Sci. Rev.* 30, 3973–3989. doi: 10.1016/j.quascirev.2011.11.001

Bourbonniere, R. A., and Meyers, P. A. (1996). Anthropogenic influences on hydrocarbon contents of sediments deposited in eastern Lake Ontario since 1800. *Environ. Geol.* 28, 22–28.

Bowman, J. P., Skerratt, J. H., Nichols, P. D., and Sly, L. I. (1991). Phospholipid fatty acid and lipopolysaccharide fatty acid signature lipids in methane-utilizing bacteria. *FEMS Microbiol. Lett.* 85, 15–21. doi: 10.1111/j.1574-6968.1991.tb04693.x

Brocks, J. J., and Summons, R. E. (2014). "10.3 - Sedimentary Hydrocarbons, Biomarkers for Early Life," in *Treatise on Geochemistry, 2nd Edin,* eds H. D. Holland, and K. K. Turekian (Oxford: Elsevier), 61–103. doi: 10.1016/B978-0-08-095975-7.00803-2

Burdige, D. J. (2007). Preservation of organic matter in marine sediments: controls, mechanisms, and an imbalance in sediment organic carbon budgets? *Chem. Rev.* 107, 467–485. doi: 10.1021/cr050347q

Burford, E. P., Fomina, M., and Gadd, G. M. (2003). Fungal involvement in bioweathering and biotransformation of rocks and minerals. *Min. Mag.* 67, 1127–1155. doi: 10.1180/0026461036760154

Burford, E. P., Hillier, S., and Gadd, G. M. (2006). Biomineralization of fungal hyphae with calcite (CaCO3) and calcium oxalate mono- and dihydrate in carboniferous limestone microcosms. *Geomicrobiol. J.* 23, 599–611. doi: 10.1080/01490450600964375

Carrizo, D., Sánchez-García, L., Menes, R. J., and García-Rodríguez, F. (2019). Discriminating sources and preservation of organic matter in surface sediments from five antarctic lakes in the fildes peninsula (King George Island) by lipid biomarkers and compound-specific isotopic analysis. *Sci. Total Environ.* 672, 657–668. doi: 10.1016/j.scitotenv.2019.03.459

Castanier, S., Le Métayer-Levrel, G., and Perthuisot, J.-P. (1999). Ca-carbonates precipitation and limestone genesis — the microbiogeologist point of view. *Sediment. Geol.* 126, 9–23. doi: 10.1016/S0037-0738(99)00028-7

Chepstow-Lusty, A., Bush, M. B., Frogley, M. R., Baker, P. A., Fritz, S. C., and Aronson, J. (2005). Vegetation and climate change on the bolivian altiplano between 108,000 and 18,000 yr ago. *Quat. Res.* 63, 90–98. doi: 10.1016/j.yqres.2004.09.008

Clapperton, C. M., Clayton, J. D., Benn, D. I., Marden, C. J., and Argollo, J. (1997). Late Quaternary glacier advances and palaeolake highstands in the bolivian altiplano. *Quat. Int.* 38–39, 49–59. doi: 10.1016/S1040-6182(96)00020-1

Coates, R. C., Podell, S., Korobeynikov, A., Lapidus, A., Pevzner, P., Sherman, D. H., et al. (2014). Characterization of cyanobacterial hydrocarbon composition and distribution of biosynthetic pathways. *PLoS ONE* 9, e85140. doi: 10.1371/journal.pone.0085140

Didyk, B. M., Simoneit, B. R. T., Brassell, S. C., and Eglinton, G. (1978). Organic geochemical indicators of paleo-environmental conditions of sedimentation. *Nature* 272, 216–222. doi: 10.1038/272216a0

Dijkman, N. A., and Kromkamp, J. C. (2006). Phospholipid-derived fatty acids as chemotaxonomic markers for phytoplankton: application for inferring phytoplankton composition. *Mar. Ecol. Prog. Ser.* 324, 113–125. doi: 10.3354/meps324113

Dohnalkova, A. C., Marshall Matthew, J., Arey Bruce, W., Williams Kenneth, H., Buck Edgar, C., and Fredrickson James, K. (2011). Imaging hydrated microbial extracellular polymers: comparative analysis by electron microscopy. *Appl. Environ. Microbiol.* 77, 1254–1262. doi: 10.1128/AEM.02001-10

Dupraz, C., Reid, R. P., Braissant, O., Decho, A. W., Norman, R. S., and Visscher, P. T. (2009). Processes of carbonate precipitation in modern microbial mats. *Earth-Science Reviews* 96, 141–162. doi: 10.1016/j.earscirev.2008.10.005

Dupraz, C., and Visscher, P. T. (2005). Microbial lithification in marine stromatolites and hypersaline mats. *Trends Microbiol.* 13, 429–438. doi: 10.1016/j.tim.2005.07.008

Eglinton, G., and Hamilton, R. G. (1967). Leaf epicuticular waxes. *Science* 156, 1322–1335.

Engel, A. S. (2011). "Karst ecosystems," in *Encyclopedia of Geobiology*, eds J. Reitner, and V. Thiel (Dordrecht: Springer), 521–531. doi: 10.1007/978-1-4020-9212-1_125

Falasco, E., Ector, L., Isaia, M., Wetzel, C. E., Hoffmann, L., and Bona, F. (2014). Diatom flora in subterranean ecosystems: a review. *Int. J. Speleol.* 43, 231–251. doi: 10.5038/1827-806X.43.3.1

Feldmann, M., and Mckenzie, J. A. (1998). Stromatolite-thrombolite associations in a modern environment, Lee Stocking Island, Bahamas. *Palaios* 13, 201–212. doi: 10.2307/3515490

Ficken, K. J., Li, B., Swain, D. L., and Eglinton, G. (2000). An n-alkane proxy for the sedimentary input of submerged/floating freshwater aquatic macrophytes. *Org. Geochem.* 31, 745–749. doi: 10.1016/S0146-6380(00)00081-4

Fornari, M., Risacher, F., and Féraud, G. (2001). Dating of paleolakes in the central Altiplano of Bolivia. *Palaeogeogr. Palaeoclimatol. Palaeoecol.* 172, 269–282. doi: 10.1016/S0031-0182(01)00301-7

Gadd, G. M. (2008). Bacterial and fungal geomicrobiology: a problem with communities? *Geobiology* 6, 278–284. doi: 10.1111/j.1472-4669.2007.00137.x

Gadd, G. M., and Raven, J. A. (2010). Geomicrobiology of eukaryotic microorganisms. *Geomicrobiol. J.* 27, 491–519. doi: 10.1080/01490451003703006

Gallant, L. R., Fenton, M. B., Grooms, C., Bogdanowicz, W., Stewart, R. S., Clare, E. L., et al. (2021). A 4,300-year history of dietary changes in a bat roost determined from a tropical guano deposit. *J. Geophys. Res. Biogeosci.* 126, e2020JG006026. doi: 10.1029/2020JG006026

González López, L., Vidal Romaní, J. R., López Galindo, M. J., Vaqueiro Rodríguez, M., and Sanjurjo Sánchez, J. (2013). First data on testate amoebae in speleothems of caves in igneous rocks. *Cadernos Lab. Xeolóx. Laxe* 37, 37–55. doi: 10.17979/cadlaxe.2013.37.0.3581

Gorbushina, A. A. (2007). Life on the rocks. *Environ. Microbiol.* 9, 1613–1631. doi: 10.1111/j.1462-2920.2007.01301.x

Grice, K., Schouten, S., Nissenbaum, A., Charrach, J., and Sinninghe Damst,é, J. S. (1998). Isotopically heavy carbon in the C21 to C25 regular isoprenoids in halite-rich deposits from the sdom formation, Dead Sea Basin, Israel. *Org. Geochem.* 28, 349–359. doi: 10.1016/S0146-6380(98)00006-0

Grimalt, J., and Albaigés, J. (1987). Sources and occurrence of C12 C22n-alkane distributions with even carbon-number preference in sedimentary environments. *Geochim. Cosmochim. Acta* 51, 1379–1384. doi: 10.1016/0016-7037(87)90322-X

Grimalt, J. O., De Wit, R., Teixidor, P., and Albaigés, J. (1992). Lipid biogeochemistry of Phormidium and microcoleus mats. *Org. Geochem.* 19, 509–530. doi: 10.1016/0146-6380(92)90015-P

Harrault, L., Milek, K., Jard,é, E., Jeanneau, L., Derrien, M., and Anderson, D. G. (2019). Faecal biomarkers can distinguish specific mammalian species in modern and past environments. *PLoS ONE* 14, e0211119. doi: 10.1371/journal.pone.0211119

Hastenrath, S., and Kutzbach, J. (1985). Late pleistocene climate and water budget of the South American Altiplano. *Quat. Res.* 24, 249–256. doi: 10.1016/0033-5894(85)90048-1

Hedges, J. I., and Prahl, F. G. (1993). "Early diagenesis: consequences for applications of molecular biomarkers," in *Organic Geochemistry, Principles and Applications*, eds M. H. Engel and S. A. Mecko (New York, NY: Plenum Press), 237–253.

Hershey, O. S., Kallmeyer, J., Wallace, A., Barton, M. D., and Barton, H. A. (2018). High microbial diversity despite extremely low biomass in a deep karst aquifer. *Front. Microbiol.* 9, 2823. doi: 10.3389/fmicb.2018.02823

Hou, W., Dou, C., Lian, B., and Dong, H. (2013). The interaction of fungus with calcite and the effects on aqueous geochemistry in karst systems. *Carbon. Evap.* 28, 413–418. doi: 10.1007/s13146-013-0136-7

Jongmans, A. G., Van Breemen, N., Lundström, U., Van Hees, P. A. W., Finlay, R. D., Srinivasan, M., et al. (1997). Rock-eating fungi. *Nature* 389, 682–683. doi: 10.1038/39493

Kashima, N., Irie, T., and Kinoshita, N. (1987). Diatom, contributors of coralloid speleothems, from togawa-sakaidani-do cave in miyazaki prefecture, central Kyushu, Japan. *Int. J. Speleol.* 16, 95–100. doi: 10.5038/1827-806X.16.3.3

Kolo, K., Keppens, E., Préat, A., and Claeys, P. (2007). Experimental observations on fungal diagenesis of carbonate substrates. *J. Geophys. Res. Biogeosci.* 112, G01S90. doi: 10.1029/2006JG000203

Ladygina, N., Dedyukhina, E. G., and Vainshtein, M. B. (2006). A review on microbial synthesis of hydrocarbons. *Proc. Biochem.* 41, 1001–1014. doi: 10.1016/j.procbio.2005.12.007

Lahr, D. J. G., Bosak, T., Lara, E., and Mitchell, E. D. (2015). The Phanerozoic diversification of silica-cycling testate amoebae and its possible links to changes in terrestrial ecosystems. *PeerJ* 3, e1234. doi: 10.7717/peerj.1234

Martin Léo, C. P., Blard, P.-H., Lavé, J., Condom, T., Prémaillon, M., Jomelli, V., et al. (2018). Lake Tauca highstand (heinrich stadial 1a) driven by a southward shift of the bolivian high. *Sci. Adv.* 4, eaar2514. doi: 10.1126/sciadv.aar2514

Marynowski, L., Rahmonov, O., Smolarek-Lach, J., Rybicki, M., and Simoneit, B. R. T. (2020). Origin and significance of saccharides during initial pedogenesis in a temperate climate region. *Geoderma* 361, 114064. doi: 10.1016/j.geoderma.2019.114064

Mcquarrie, N. (2002). The kinematic history of the central Andean fold-thrust belt, Bolivia: Implications for building a high plateau. *GSA Bull.* 114, 950–963. doi: 10.1130/0016-7606(2002)114<0950:TKHOTC>2.0.CO;2

Melendez, I., Grice, K., and Schwark, L. (2013). Exceptional preservation of *Palaeozoic steroids* in a diagenetic continuum. *Sci. Rep.* 3, 2768. doi: 10.1038/srep02768

Moore, D., Robson, G. D., and Trinci, A. P. J. (2011). *21st Century Guidebook to Fungi.* Cambridge: Cambridge University Press.

Moore, K. R., Pajusalu, M., Gong, J., Sojo, V., Matreux, T., Braun, D., et al. (2020). Biologically mediated silicification of marine cyanobacteria and implications for the *Proterozoic fossil* record. *Geology* 48, 862–866. doi: 10.1130/G47394.1

Nott, C. J., Xie, S., Avsejs, L. A., Maddy, D., Chambers, F. M., and Evershed, R. P. (2000). n-Alkane distributions in ombrotrophic mires as indicators of

vegetation change related to climatic variation. *Org. Geochem.* 31, 231–235. doi: 10.1016/S0146-6380(99)00153-9

Pagani, M. (2009). "Alkenones," in *Encyclopedia of Paleoclimatology and Ancient Environments*, ed V. Gornitz (Dordrecht: Springer Netherlands), 4–6. doi: 10.1007/978-1-4020-4411-3_3

Pancost, R. D., Baas, M., van Geel, B., and Sinninghe Damsté, J. S. (2002). Biomarkers as proxies for plant inputs to peats: An example from a sub-boreal ombrotrophic bog. *Org. Geochem.* 33, 675–690.

Parchert, K. J., Spilde, M. N., Porras-Alfaro, A., Nyberg, A. M., and Northup, D. E. (2012). Fungal communities associated with rock varnish in black canyon, New Mexico: casual inhabitants or essential partners? *Geomicrobiol. J.* 29, 752–766. doi: 10.1080/01490451.2011.619636

Parkes, R. J., Dowling, N. J. E., White, D. C., Herbert, R. A., and Gibson, G. R. (1993). Characterization of sulphate-reducing bacterial populations within marine and estuarine sediments with different rates of sulphate reduction. *FEMS Microbiol. Ecol.* 11, 235–250. doi: 10.1111/j.1574-6968.1993.tb05815.x

Peters, K. E., Walters, C. C., and Moldowan, J. M. (2005). *The Biomarker Guide—Part II—Biomarkers and Isotopes in Petroleum Exploration and Earth History*. New York, NY: Cambridge University Press.

Placzek, C., Quade, J., and Patchett, P. J. (2006). Geochronology and stratigraphy of late pleistocene lake cycles on the southern bolivian altiplano: implications for causes of tropical climate change. *GSA Bull.* 118, 515–532. doi: 10.1130/B25770.1

Powell, T. G., and Mckirdy, D. M. (1973). Relationship between ratio of pristane to phytane, crude oil composition and geological environment in Australia. *Nat. Phys. Sci.* 243, 37–39. doi: 10.1038/physci243037a0

Rielley, G., Collier, R. J., Jones, D. M., and Eglinton, G. (1991). The biogeochemistry of Ellesmere Lake, U.K.—I: source correlation of leaf wax inputs to the sedimentary lipid record. *Org. Geochem.* 17, 901–912. doi: 10.1016/0146-6380(91)90031-E

Rincón-Tomás, B., Khonsari, B., Mühlen, D., Wickbold, C., Schäfer, N., Hause-Reitner, D., et al. (2016). Manganese carbonates as possible biogenic relics in Archean settings. *Int. J. Astrobiol.* 15, 219–229. doi: 10.1017/S1473550416000264

Risacher, F., and Fritz, B. (1991). Quaternary geochemical evolution of the salars of Uyuni and Coipasa, Central Altiplano, Bolivia. *Chem. Geol.* 90, 211–231. doi: 10.1016/0009-2541(91)90101-V

Ritz, K., and Young, I. M. (2004). Interactions between soil structure and fungi. *Mycologist* 18, 52–59. doi: 10.1017/S0269915X04002010

Rontani, J.-F., and Volkman, J. K. (2003). Phytol degradation products as biogeochemical tracers in aquatic environments. *Org. Geochem.* 34, 1–35. doi: 10.1016/S0146-6380(02)00185-7

Rouchy, J. M., Servant, M., Fournier, M., and Causse, C. (1996). Extensive carbonate algal bioherms in upper pleistocene saline lakes of the central Altiplano of Bolivia. *Sedimentology* 43, 973–993. doi: 10.1111/j.1365-3091.1996.tb01514.x

Rybicki, M., Marynowski, L., Misz-Kennan, M., and Simoneit, B. R. T. (2016). Molecular tracers preserved in lower jurassic "blanowice brown coals" from southern poland at the onset of coalification: organic geochemical and petrological characteristics. *Org. Geochem.* 102, 77–92. doi: 10.1016/j.orggeochem.2016.09.012

Salisbury, M. J., Kent, A. J. R., Jiménez, N., and Jicha, B. R. (2015). Geochemistry and 40Ar/39Ar geochronology of lavas from Tunupa volcano, Bolivia: implications for plateau volcanism in the central Andean Plateau. *Lithosphere* 7, 95–107. doi: 10.1130/L399.1

Sánchez-García, L., Aeppli, C., Parro, V., Fernández-Remolar, D., García-Villadangos, M., Chong-Diaz, G., et al. (2018). Molecular biomarkers in the subsurface of the salar grande (Atacama, Chile) evaporitic deposits. *Biogeochemistry* 140, 31–52. doi: 10.1007/s10533-018-0477-3

Sánchez-García, L., Carrizo, D., Molina, A., Muñoz-Iglesias, V., Lezcano, M. Á., Fernández-Sampedro, M., et al. (2020). Fingerprinting molecular and isotopic biosignatures on different hydrothermal scenarios of Iceland, an acidic and sulfur-rich Mars analog. *Sci. Rep.* 10, 21196. doi: 10.1038/s41598-020-78240-2

Servant, M., and Fontes, J.-C. (1978). *Les lacs Quaternaires Des Hauts Plateaux Des Andes Boliviennes: Premières Interprétations Paléoclimatiques.* ORSTOM Sér géologie X, 9–23.

Servant, M., Fournier, M., Argollo, J., Servant-Vildary, S., Sylvestre, F., Wirmann, D., et al. (1995). La dernière transition glaciaire /interglaciaire des Andes tropicales sud (Bolivie d'après l'é tude des variations des niveaux lacustres et des fluctuations glaciaires. *Comp. Rendus Acad. Sci. Paris* 320, 729–736.

Servant-Vildary, S. (1978). Les diatomées des dépôts lacustres quaternaires de l'Altiplano bolivien. *ORSTOM Sér. Géol. X* 10, 25–35.

Stefanova, M., and Disnar, J. R. (2000). Composition and early diagenesis of fatty acids in lacustrine sediments, lake Aydat (France). *Org. Geochem.* 31, 41–55. doi: 10.1016/S0146-6380(99)00134-5

Sterflinger, K. (2000). Fungi as geologic agents. *Geomicrobiol. J.* 17, 97–124. doi: 10.1080/01490450050023791

Sylvestre, F., Servant, M., Servant-Vildary, S., Causse, C., Fournier, M., and Ybert, J.-P. (1999). Lake-Level chronology on the southern bolivian altiplano (18°-23°S) during late-glacial time and the early holocene. *Quat. Res.* 51, 54–66. doi: 10.1006/qres.1998.2017

Sylvestre, F., Servant-Vildary, S., Fournier, M., and Servant, M. (1995). Lake levels in the southern bolivian altiplano (19°-21°S.) during the late glacial based on diatom studies. *Int. J. Salt Lake Res.* 4, 281–300. doi: 10.1007/BF01999113

Taylor, J., and Parkes, R. J. (1983). The cellular fatty acids of the sulphate-reducing bacteria, *Desulfobacter* sp., *Desulfobulbus* sp. and *Desulfovibrio desulfuricans*. *Microbiology* 129, 3303–3309. doi: 10.1099/00221287-129-11-3303

Tibaldi, A., Corazzato, C., and Rovida, A. (2009). Miocene–quaternary structural evolution of the Uyuni–Atacama region, Andes of Chile and Bolivia. *Tectonophysics* 471, 114–135. doi: 10.1016/j.tecto.2008.09.011

Toporski, J. K. W., Steele, A., Westall, F., Thomas-Keprta, K. L., and Mckay, D. S. (2002). The simulated silicification of bacteria—new clues to the modes and timing of bacterial preservation and implications for the search for extraterrestrial microfossils. *Astrobiology* 2, 1–26. doi: 10.1089/153110702753621312

van Dongen, B. E., Semiletov, I.,Weijers, J. W. H., and Gustafsson, Ö. (2008). Contrasting lipid biomarker composition of terrestrial organic matter exported from across the eurasian arctic by the five great russian arctic rivers. *Global Biogeochem. Cy.* 22, GB1011. doi: 10.1029/2007GB002974

Van Schöll, L., Kuyper, T. W., Smits, M. M., Landeweert, R., Hoffland, E., and Breemen, N. V. (2008). Rock-eating mycorrhizas: their role in plant nutrition and biogeochemical cycles. *Plant Soil* 303, 35–47. doi: 10.1007/s11104-007-9513-0

Vanderwolf, K. J., Malloch, D., Mcalpine, D. F., and Forbes, G. J. (2013). A world review of fungi, yeasts, and slime molds in caves. *Int. J. Speleol.* 42, 77–96. doi: 10.5038/1827-806X.42.1.9

Verrecchia, E. P., and Dumont, J.-L. (1996). A biogeochemical model for chalk alteration by fungi in semiarid environments. *Biogeochemistry* 35, 447–470. doi: 10.1007/BF02183036

Volkman, J. K. (1986). A review of sterol markers for marine and terrigenous organic matter. *Org. Geochem.* 9, 83–99. doi: 10.1016/0146-6380(86)90089-6

Volkman, J. K. (2003). Sterols in microorganisms. *Appl. Microbiol. Biotechnol.* 60, 495–506. doi: 10.1007/s00253-002-1172-8

Volkman, J. K., Barrett, S. M., Blackburn, S. I., Mansour, M. P., Sikes, E. L., and Gelin, F. (1998). Microalgal biomarkers: a review of recent research developments. *Org. Geochem.* 29, 1163–1179. doi: 10.1016/S0146-6380(98)00062-X

Conflict of Interest: The authors declare that the research was conducted in the absence of any commercial or financial relationships that could be construed as a potential conflict of interest.

frontiers | Frontiers in Microbiology

ORIGINAL RESEARCH
published: 29 June 2022
doi: 10.3389/fmicb.2022.909494

The Characterization of Microbiome and Interactions on Weathered Rocks in a Subsurface Karst Cave, Central China

Yiheng Wang[1,2†], Xiaoyu Cheng[1,2†], Hongmei Wang[1,2], Jianping Zhou[2], Xiaoyan Liu[2] and Olli H. Tuovinen[3]*

[1] State Key Laboratory of Biogeology and Environmental Geology, China University of Geosciences, Wuhan, China, [2] School of Environmental Studies, China University of Geosciences, Wuhan, China, [3] Department of Microbiology, The Ohio State University, Columbus, OH, United States

OPEN ACCESS

Edited by:
Cesareo Saiz-Jimenez, Institute of Natural Resources and Agrobiology of Seville (CSIC), Spain

Reviewed by:
Ariel Kushmaro, Ben-Gurion University of the Negev, Israel
Taha Menasria, University of Tébessa, Algeria

***Correspondence:**
Hongmei Wang
wanghmei04@163.com;
hmwang@cug.edu.cn

† These authors have contributed equally to this work

Specialty section:
This article was submitted to Extreme Microbiology, a section of the journal Frontiers in Microbiology

Received: *31 March 2022*
Accepted: *19 May 2022*
Published: *29 June 2022*

Citation:
Wang Y, Cheng X, Wang H, Zhou J, Liu X and Tuovinen OH (2022) The Characterization of Microbiome and Interactions on Weathered Rocks in a Subsurface Karst Cave, Central China. Front. Microbiol. 13:909494. doi: 10.3389/fmicb.2022.909494

Karst caves are a natural oligotrophic subsurface biosphere widely distributed in southern China. Despite the progress in bacterial and fungal diversity, the knowledge about interactions between bacteria, fungi, and minerals is still limited in caves. Hence, for the first time, we investigated the interaction between bacteria and fungi living on weathered rocks in the Heshang Cave *via* high-throughput sequencing of 16S rRNA and ITS1 genes, and co-occurrence analysis. The mineral compositions of weathered rocks were analyzed by X-ray diffraction. Bacterial communities were dominated by *Actinobacteria* (33.68%), followed by *Alphaproteobacteria* (8.78%), and *Planctomycetia* (8.73%). In contrast, fungal communities were dominated by *Sordariomycetes* (21.08%) and *Dothideomycetes* (14.06%). Mineral substrata, particularly phosphorus-bearing minerals, significantly impacted bacterial (hydroxyapatite) and fungal (fluorapatite) communities as indicated by the redundancy analysis. In comparison with fungi, the development of bacterial communities was more controlled by the environmental selection indicated by the overwhelming contribution of deterministic processes. Co-occurrence network analysis showed that all nodes were positively linked, indicating ubiquitous cooperation within bacterial groups and fungal groups, as well as between bacteria and fungi under oligotrophic conditions in the subsurface biosphere. In total, 19 bacterial ASVs and 34 fungal OTUs were identified as keystone taxa, suggesting the fundamental role of fungi in maintaining the microbial ecosystem on weathered rocks. *Ascomycota* was most dominant in keystone taxa, accounting for 26.42%, followed by *Actinobacteria* in bacteria (24.53%). Collectively, our results confirmed the highly diverse bacterial and fungal communities on weathered rocks, and their close cooperation to sustain the subsurface ecosystem. Phosphorus-bearing minerals were of significance in shaping epipetreous bacterial and fungal communities. These observations provide new knowledge about microbial interactions between bacteria, fungi, and minerals in the subterranean biosphere.

Keywords: subsurface biosphere, karst caves, phosphate-bearing minerals, microbial interaction, community assembly, co-occurrence network

INTRODUCTION

Karst caves are thought to be barren with few microorganisms and a weak reflection of the microbiology of surface soils due to oligotrophic conditions (Hess, 1900; Høeg, 1946; Caumartin, 1963; Palmer, 1991). Autotrophic microorganisms in caves usually obtain energy by chemosynthesis using inorganic energy sources (reduced Fe, Mn, and S compounds), organic and inorganic nutrients in host rocks, cave sediments, groundwater, and atmosphere (Jones and Macalady, 2016; Tomczyk-Żak and Zielenkiewicz, 2016; Hershey and Barton, 2018). The occurrence of various metabolic pathways is concurrent in cave microbiota (Kováč, 2018). In consideration of the oligotrophic conditions in caves, the microbial diversity encountered is surprisingly higher than expected as indicated by the application of molecular technology (routinely 10^6 cells/g; Hershey and Barton, 2018).

Surfaces of various materials have been demonstrated to serve as important niches for microbial communities in diverse ecosystems, such as the surface of the painted murals, heritage buildings, petroglyph panels, and rock surfaces (Ma et al., 2015; Brewer and Fierer, 2018; Zhang et al., 2018; Irit et al., 2019; Ren et al., 2019; He et al., 2021). Rock surfaces are subjected to weathering by physical, chemical, and biological processes, thus offering special niches for microorganisms (Cañveras et al., 2001; Lian et al., 2008). Abundant radiation-resistant bacteria on the surface of limestone outcrops were detected, which were associated with lichens and grew under neutral to alkaline pH conditions (Brewer and Fierer, 2018). Usually, bacterial communities living on outcrop carbonate rocks exposed to sunlight and rainfall were dominated by *Actinobacteria*, *Proteobacteria*, *Chloroflexi*, *Bacteroidetes*, and *Acidobacteria*, whereas fungal communities consisted of *Eurotiomycetes*, *Lecanoromycetes*, *Dothideomycetes*, and *Leotiomycetes* (Choe et al., 2018). Microbial communities inhabiting the surfaces of carbonate rocks in permanently dark caves (Man et al., 2015; Yun et al., 2016; Zhu et al., 2021) are far less studied than those associated with outcrop rocks. Rock surfaces in subsurface caves are directly exposed to air, aerosol, and water vapor (high humidity), as well as a variety of physicochemical and biological dissolution–precipitation and oxidation–reduction reactions, leading with time to weathering and the formation of various secondary minerals (Aloisi et al., 2006; Gallagher et al., 2012). Rock walls act as surface biofilms for exchanges between the bedrock and the atmosphere. Microorganisms can use many minerals as sources of nutrients, carbon, and energy (Tomczyk-Żak et al., 2013). Nevertheless, the current knowledge is ambiguous on microbial communities in relation to mineral substrates and secondary minerals formed during rock weathering in subsurface caves.

Studies have shown that microbial communities in caves are affected by a variety of physical and chemical parameters. Studies in the Heshang Cave, a karst dolomite cave, have shown that pH and TOC are important drivers of the variations in bacterial communities among sediments, overlying soils, dripping water, and weathered rocks (Yun et al., 2016; Cheng et al., 2021). The underlying factors resulting in differences in bacterial and fungal communities living on rocks in caves are poorly understood. The physical properties and chemical compositions of minerals can profoundly impact the composition of microbial communities. Mineral phases in rocks serve as nutrients, substrates, and habitats for microbial communities (Shi L. et al., 2016). Some microbes use conductive mineral particles as conduits of interspecies electron transfer and cooperative catabolism (Kato et al., 2012). *Actinobacteria* are prevalent in Ca carbonate environments, and *alpha-*, *beta-*, and *gamma-Proteobacteria* are typically associated with complex minerals in cave environments (Barton et al., 2007).

Metabolic activities of microorganisms have important effects on the dissolution and formation of minerals. Moderately halophilic bacteria in liquid media cause the precipitation of calcite, Mg-calcite, and struvite (Arias et al., 2019). Carbonate biomineralization can be enhanced by ureolytic bacteria (Dhami et al., 2013; Arias et al., 2019). *Paracoccus versutus* XT0.6 isolated from the Xikuangshan antimony mine could dissolve stibnite and oxidize released Sb(III) to Sb(V), subsequently resulting in the formation of secondary Sb(V)-bearing minerals (Loni et al., 2020).

Highly diverse bacterial communities were detected from the weathered rocks in caves with the dominance of *Proteobacteria*, *Actinomycetes*, and *Firmicutes* (Yun et al., 2016; Zhu et al., 2019, 2021; Ma et al., 2021). In contrast, the diversity of fungi is relatively low due to the limited input of organic matter by photosynthesis in caves (Lee et al., 2012; Man et al., 2015). It was estimated that the content of organic matter in caves is three orders of magnitude less than that on the surface (Lavoie et al., 2010). Sunlight penetrates into the cave *via* the cave entrance to a limited distance and thus divides the cave into three zones: the photic zone with relatively strong light, the twilight zone with weak light, and the totally dark aphotic zone (Yun et al., 2016; Zhao et al., 2018). Due to the different light intensities, physical and chemical conditions vary in the three zones, resulting in different geochemical gradients and biological distribution patterns (Bonacci et al., 2009). In the photic zone, algae and green plants are visible on the rock surface and ground. Light is sufficient to support photosynthesis, thereby supporting CO_2 fixation and primary production (Kozlova and Mazina, 2020). The availability of organic matter in the twilight and aphotic zones is extremely limited as it mainly depends on the input of exogenous organic matter *via* airflow, bat feces, and external organic matter excreted by burrowing animals such as cave rats (Pape and OConnor, 2014; Pfendler et al., 2019). Due to the differences in light, mineral components, and organic matter from different light zones, we hypothesize that (1) microbial communities living on the rocks vary with the zones, and mineral substrates significantly contribute to the variation; (2) bacterial and fungal communities interact intensively to sustain the microbial ecosystem on the rock; and (3) different ecological processes would contribute to the community assembly of bacteria and fungi, respectively.

To test these hypotheses, we collected weathered rock samples from different light zones in the Heshang Cave and subjected them to high-throughput sequencing of bacterial 16S rRNA and fungal ITS1 genes to investigate microbial communities. Variations in microbial communities and the driving forces

responsible for these changes would be elucidated *via* the redundancy analysis. Interactions between bacterial and fungal communities were studied *via* co-occurrence network analysis to decipher how microbes interact with other microorganisms and sustain the ecosystem. Ecological processes and their contributions to the bacterial and fungal community assembly will be conducted to help understand how the specific microbial communities are established in caves. Our results will provide new insights into the interactions between bacteria and fungi living on carbonate rocks and the ecological processes responsible for microbial communities within subsurface caves.

MATERIALS AND METHODS

Site Description and Sample Collection

The Heshang Cave, a dolomite karst cave, is 250 m long, 20–30 m wide, and 15–20 m high. It is located on the steep south bank of the Qingjiang River, northwest Hubei province, central China, with an elevation of 194 m above sea level (**Supplementary Figure 1**). An intermittent stream develops inside the cave during the rainy season, and dripping water is frequently observed from the ceiling of the cave all year round. The humidity is above 90% till saturated (Hu et al., 2008).

Weathered rock samples from the cave walls were collected along the cave from the entrance to the end on October 25, 2015. In total, nine sites were selected for sampling, with triplicates at each site (**Supplementary Figure 1D**), and the samples were designated as R1 to R9 accordingly. Green microbial mats were present on the surface of the cave walls close to the cave entrance (**Supplementary Figure 2**). At each sampling site, weathered rock samples were carefully scraped off with a sterilized scalpel and stored in 50 mL centrifuge tubes. The samples were placed on ice and transported to the Geomicrobiology Laboratory of China University of Geosciences (Wuhan) within 24 h and stored at −80 °C upon arrival until analysis. The wind speed and relative humidity were measured *in situ* with a handheld weather station (XYZ06E, Dalian Hede Technologies Corporation, China; **Supplementary Figures 3A,B**). The wind speed and relative humidity at each sampling site were continuously monitored for over 10 min. Values at 3, 6, and 9 min were read, and the mean values were used.

Mineralogical Analysis

The weathered rock samples were freeze-dried (ALPHA 1-2 LD, Christ, Germany) and fully ground into powder. Mineral phases were analyzed by X-ray powder diffraction (XRD, Shimadzu XRF-1800) at a scanning speed of 0.05 s per step, with a step scan of 0.02° ($10° \leq 2\theta \leq 90°$) *via* a Cu target Kα radiation source (Ni filter, 40 kV, 40 mA). The phase composition and content of minerals in the samples were qualitatively and semi-quantitatively analyzed by Jade7 and X-powder software.

DNA Extraction and Sequencing

Genomic DNA was extracted using a FastDNA^{TM} SPIN Kit for soil DNA extraction (MP Biomedicals) in accordance with the instructions. The concentration and quality of extracted DNA were detected by using a micro-nucleic acid protein detector (Nanodrop 2000, Thermo Fisher). The primer set of 520F (5'-AYTGGGYDTAAAGNG-3') and 802R (5'-TACNVGGGTATCTAATCC-3') targeting the bacterial 16S rRNA V4 region (Claesson et al., 2009, 2010) and the primer set of ITS5F (5'-GGAAGTAAAAGTCGTAACAAGG-3') and ITS1R (5'-GCTGCGTTCTTCATCGATGC-3') targeting the fungal internal transcribed spacer (ITS1) region (Chang et al., 2001) were used for bacterial and fungal sequencing, respectively. All the sequences were conducted using an Illumina MiSeq PE250 platform (Shanghai Personal Biotechnology Co., Shanghai, China). All data are accessible *via* BioProject IDs of PRJNA337918 and PRJNA821722 for bacteria and fungi, respectively, on the NCBI.

Data Processing and Statistical Analysis

FLASH (v1.2.7)[1] was used for quality checking the original readings with Q30 and sequence assembly. Chimeras were removed by a DADA2 plugin in QIIME2 (2019.7, Quantitative Insight into Microbial Ecology). A table of bacterial amplicon sequence variants was constructed from the clean sequences with a 100% similarity, and the representative sequence of each ASV was obtained. Fungal OTUs were identified with a 97% similarity using Vsearch (2.15.1) software. All samples were resampled to the same sequencing depth. Bacterial annotation was carried out against the SILVA database,[2] and fungal annotation was based on the UNITE database[3] (Nilsson et al., 2019).

The microbial diversity index was calculated by a diversity plugin of QIIME2. The one-way analysis of variance (ANOVA) and Pearson correlation analysis were carried out using SPSS (v10.0). The heatmap analysis was performed using the OmicShare tools, a free online platform for data analysis.[4] The vegan package of R software was used for NMDS analysis and output of rarefaction curves (Dixon, 2003), and the box diagram and stacked bar chart were visualized by the ggplot2 package of R software (Wickham et al., 2016). The Venn diagram was drawn using the plotrix package (Lemon et al., 2021). The redundancy analysis (RDA) of bacterial communities and physicochemical parameters was conducted by Canoco5 software. Indicator groups in the different light zones were obtained online with the interactive web pages[5] by using the least discriminant analysis effect size (LEfSe) method, in which the linear discriminant analysis (LDA) threshold was set to 3.0. To reduce the network complexity, bacterial ASVs and fungal OTUs detected in at least three samples were selected. The relative abundance of retained bacterial ASVs accounted for > 36.6%, and the numbers of ASVs accounted for 6.6% of the total. The relative abundance of retained fungal OTUs accounted for > 94.4%, and the numbers of OTUs accounted for 15.2% of the total. The Gephi software (v.0.9.2) was used to visualize the co-occurrence network of bacteria and fungi. The ecological

[1]http://ccb.jhu.edu/software/FLASH/

[2]http://greengenes.secondgenome.com/

[3]https://unite.ut.ee/

[4]https://www.omicshare.com/tools

[5]http://huttenhower.sph.harvard.edu/galaxy/

roles of each node were determined based on within-module connectivity (*Zi*) and among-module connectivity (*Pi*; Guimera and Amaral, 2005). Highly associative "hubs" in the microbiome can be identified from the network and are considered keystone taxa (Banerjee et al., 2018). Node topologies were classified as module hubs (highly connected nodes within modules, $Zi \geq 2.5$ and $Pi \leq 0.62$), network hubs (highly connected nodes within the entire network, $Zi \geq 2.5$ and $Pi > 0.62$), connectors (nodes that connect modules, $Zi < 2.5$ and $Pi \geq 0.62$), and peripherals (nodes connected in modules with few outside connections, $Zi < 2.5$ and $Pi < 0.62$; Deng et al., 2012; Shi S. et al., 2016). The assessment of ecological processes was performed with a mature workflow from the published literature (Stegen et al., 2012, 2013). The nearest taxon index (NTI), mean nearest taxon distance (MNTD), weighted β-mean nearest taxon distance (βMNTD), and weighted β-nearest taxon index (βNTI) were utilized to measure the phylogenic turnover using the theory of null model analyses across samples using the picante package (Kembel et al., 2010). Ecological processes were divided into deterministic processes with a $|\beta NTI| > 2$ and stochastic processes with a $|\beta NTI| < 2$. If βNTI values are above 2, variable selection is the crucial assembly process in the microbial community; otherwise, homogeneous selection dominates ($\beta NTI < -2$). To further specify the stochastic processes, the Raup–Crick matrix (RC_{bray}) based on the Bray–Curtis matrix of microbial community was calculated using the vegan package. Dispersal limitation acting with the drift, undominated processes, and homogenizing dispersal were, respectively, dominant in bacterial communities under the conditions of RC_{bray} values > 0.95, $|RC_{bray}| < 0.95$, and $RC_{bray} < -0.95$ (Stegen et al., 2012, 2013).

RESULTS

Mineralogy, Wind Speed, and Relative Humidity in Heshang Cave

Minerals of the weathered rocks in the photic zone were dolomite, calcite, Mg-calcite, quartz, and amorphous materials (**Supplementary Table 1**). More minerals were detected in samples collected in the twilight zone, with the dominance of dolomite and quartz and a minor proportion of amorphous materials (**Supplementary Table 1**). Phosphate minerals (hydroxyapatite and fluorapatite), gypsum, and illite were also observed in twilight zone samples. Samples in the aphotic zone harbored eight minerals with Mg-calcite (18.6%) and phosphate minerals as the most abundant.

The average wind speed decreased from the cave entrance inward to the cave throughout the year. It was relatively stable (< 0.3 m/s) in the aphotic zone (**Supplementary Figure 3A** and **Supplementary Table 2**). The average relative humidity increased from inward to the cave and stabilized in the aphotic zone (>80%; **Supplementary Figure 3B** and **Supplementary Table 3**).

Bacterial and Fungal Communities on the Weathered Rocks

A total of 6,885 bacterial ASVs and 5,320 fungal OTUs were obtained in this study, and 511 bacterial ASVs and 1,269 fungal OTUs were found in samples from photic, twilight, and aphotic zones as indicated by the Venn diagram (**Supplementary Figure 4**). The rarefaction curves of bacterial communities were leveled off across all sampling sites, whereas those of fungal communities at the R5 sampling site were rather steeper (**Supplementary Figure 5**).

No significant differences were observed in the alpha diversity of bacterial communities among different zones. The Shannon indices varied between 7.56 and 8.12, and ACE values ranged between 4.18 and 10.60 (**Figures 1A,B** and **Supplementary Table 4**). The alpha diversity of fungi showed significant differences in the Shannon indices but not in ACE values between the three zones (**Figures 1C,D** and **Supplementary Table 4**).

The NMDS analysis showed poor interpretation of bacterial communities between the three light zones (stress > 0.2; **Figure 1E**), but clearly separated the fungal communities between the photic zone and the aphotic zone, while those in the twilight zone were scattered around (**Figure 1F**).

Taxonomically, 26 phyla and 55 classes of bacteria were detected with the dominance of *Actinobacteria* (relative abundance 33.68%). The most abundant class in all samples was *Actinobacteria*, followed by *Alphaproteobacteria* and *Planctomycetia*. The class of *Cyanobacteria* (4.31%) was only detected in the photic zone, which matched well with the presence of light (**Figure 2A**). At the genus level, *Rubrobacter* (4.61%), *Gemmatimonas* (2.25%), and *Solirubrobacter* (1.61%) ranked the top three in relative abundance in the photic zone. *Rubrobacter* (2.87%), *Gaiella* (1.92%), and *Thermoleophilum* (1.49%) were the three most abundant genera in the twilight zone, whereas *Gaiella* (3.00%), *Rubrobacter* (2.50%), and *Gemmatimonas* (2.41%) were the top three genera in the aphotic zone (**Figure 2B**). LEfSe identified *Cyanobacteria* (4.31%), *Gemmatimonas* (2.25%), *Nitrolancea* (0.94%), *Brevundimonas* (0.63%), and *Zavarzinella* (0.58%) as indicator groups in the photic zones with an LDA score of 3 (**Figure 2E**). Indicator groups in the twilight zone included *Aquisphaera* (0.83%), *Gimesia* (0.1%), and *Streptomyces* (0.58%), whereas *Conexibacter* (1.90%), *Actinomadura* (0.32%), *Aciditerrimonas* (0.35%), *Planctopirus* (0.16%), and *Chthonomonas* (0.19%) were indicator groups of the aphotic zone (**Figure 2E**).

Totally, 6 phyla and 21 classes of fungi were detected in all samples. *Sordariomycetes* was most abundant in photic (18.54%) and twilight zones (28.08%), followed by *Dothideomycetes* (13.74%) and *Eurotiomycetes* (7.43%) in the photic zone, *Dothideomycetes* (7.64%) and *Mortierellomycetes* (3.06%) in the twilight zone. The top three classes in the aphotic zone were *Dothideomycetes* (23.49%), *Sordariomycetes* (14.84%), and *Eurotiomycetes* (5.05%; **Figure 2C**). Among the top 15 genera, *Parengyodontium* ranked first in relative abundance among all samples. In the photic zone, *Neodevriesia* (6.23%) and *Penicillium* (5.64%) were the second and third abundant genera, whereas those in the twilight zone were *Mortierella* (3.06%), *Cladosporium* (1.15%), and in the aphotic zone, *Penicillium* (4.46%) and *Simplicillium* (0.97%) ranked second and third most abundant genera. To be noted, unidentified fungal genera in the aphotic zone accounted for a relatively high proportion (80.9%; **Figure 2D**). *Lecanoromycetes* (0.37%), *Hypocreales fam incertae sedis* (4.14%), *Bionectriaceae* (2.11%), and *Cladosporiaceae*

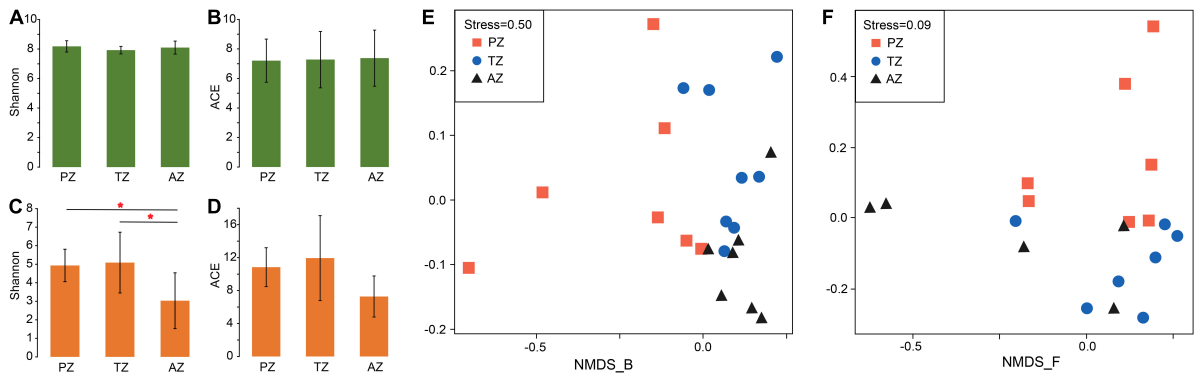

FIGURE 1 | Alpha-diversity indices and non-metric multidimensional scaling (NMDS) analysis of bacterial **(A,B,E)** and fungal **(C,D,F)** communities of weathered rocks in the Heshang Cave, Hubei province, China. PZ: photic zone; TZ: twilight zone; AZ: aphotic zone. The mark with * indicates significant differences between the two groups ($P < 0.05$).

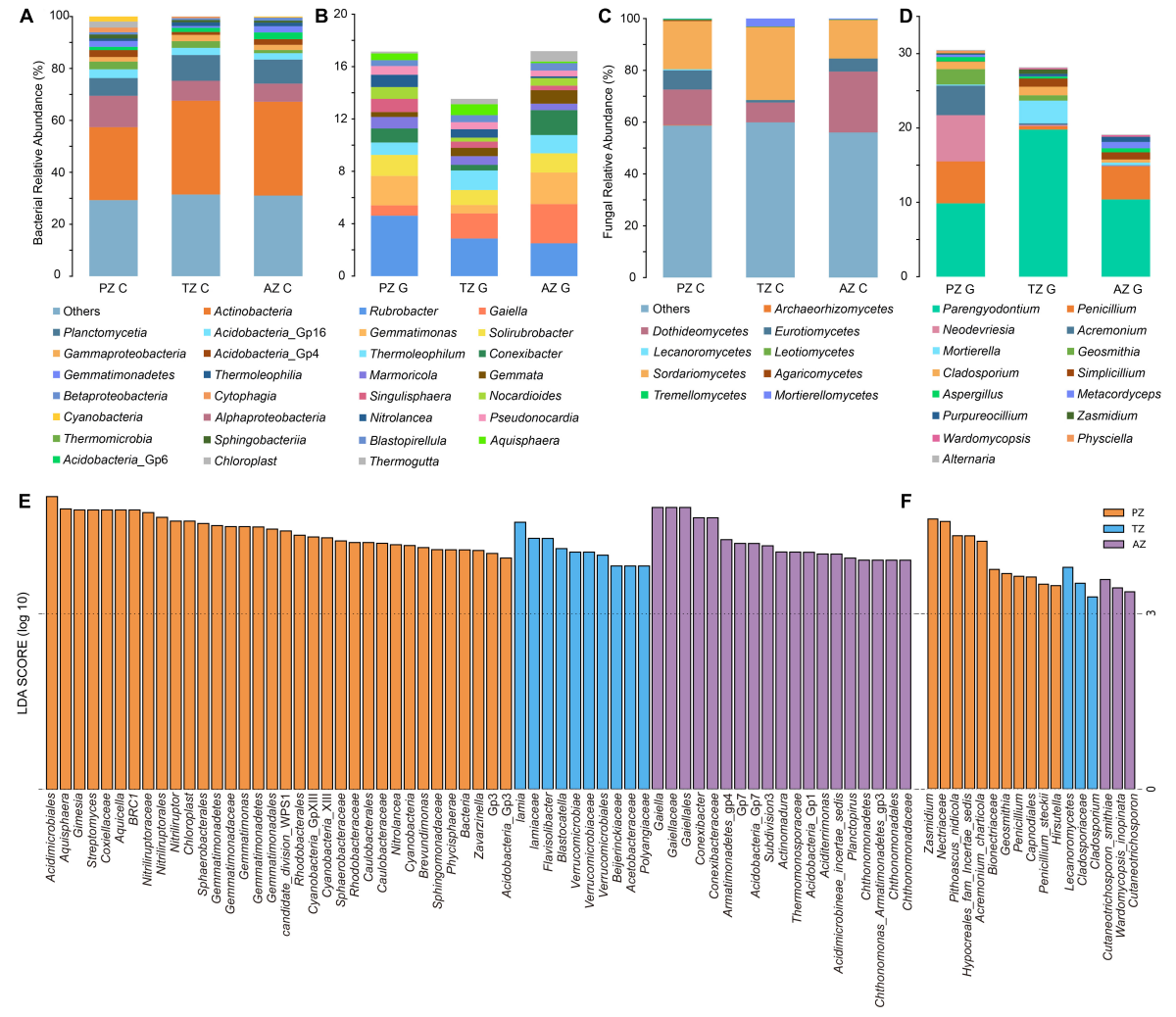

FIGURE 2 | Bacterial **(A,B)** and fungal community **(C,D)** compositions of the top 15 classes **(A,C)** and genera **(B,D)** of weathered rocks in the Heshang Cave. Linear discriminant analysis (LDA) effect size taxonomic histogram with LDA = 4 of bacterial **(E)** and LDA = 3 of fungal **(F)** communities of the weathered rocks in the Heshang Cave, Hubei province, China. PZ: photic zone, TZ: twilight zone, AZ: aphotic zone. C and G after the sampling zone abbreviation indicate classes and genera of microbial taxonomy in the corresponding sampling location.

(0.99%) were indicator groups in the photic zone, and those in the twilight zone were mainly *Nectriaceae* (0.15%) and *Zasmidium* (0.59%). The main indicator groups in the aphotic zone were *Cutaneotrichosporon* (0.05%) and *Wardomycopsis inopinata* (0.21%; **Figure 2F**).

The Correlation Between Microbial Communities and Mineral Substrate

RDA was conducted to investigate the relationship between mineral phases and microbial communities living on the weathered rock. All minerals such as quartz, carbonate minerals (including dolomite, calcite, Mg-calcite, and aragonite), gypsum, illite, phosphate minerals (including white apatite, hydroxyapatite, and fluorapatite), and amorphous materials were included to elucidate their impact on bacterial and fungal communities. The results showed that hydroxyapatite and fluorapatite significantly affected bacterial and fungal communities with an explanation of 22.9% ($P = 0.018$) and 31.2% ($P = 0.006$), respectively (**Figures 3A,B**).

Microbial Community Assembly on the Weathered Rocks

The median of the βNTI matrix was below −2, indicating that the deterministic process controlled the assembly of bacterial communities (**Figure 4A**). Bacterial community assembly was overwhelmingly dominated by the homogeneous selection, with a contribution from 71.43 to 92.86% (**Figure 4C**). By contrast, the median of the βNTI matrix of fungal communities was between −2 and 2, indicating the dominance of the stochastic process in fungal community assembly (**Figure 4B**). Thus, ecological processes responsible for fungal community assembly were more complex than those for bacterial communities. Variable selection contributed 42.86 and 47.62% in the photic and twilight zones, respectively, but decreased to 10% in the aphotic zone, which was dominated by homogeneous selection (40%; **Figure 4C**). The contribution of dispersal limitation decreased inward to the cave from 23.81% in the photic zone, 19.05% in the twilight zone, to no contribution in the aphotic zone (**Figure 4C**).

Interactions Between Bacterial and Fungal Communities Living on Weather Rocks

In total, 924 nodes and 7,425 links were observed in the co-occurrence network of bacteria and fungi with good modularity (0.788). Among the links, 800 connected fungal and bacterial nodes, 2,776 connected bacterial nodes, and 3,849 connected fungal nodes, respectively (**Figure 5A**). All nodes were positively linked. The average path length, diameter, and clustering coefficient were 5.634, 14, and 0.618, respectively.

Totally 28 modules were observed in the fungal–bacterial interaction network, and nine of the modules had a node relative abundance of over 4%, which were subject to further analysis (**Figure 5B**). Module 14 had the most nodes, accounting for 20.56% of the total nodes in the network. Nodes in modules 6, 18, and 22 mainly originated from PZ and TZ, whereas those in module 7 were mainly from AZ (**Figure 5C**). Nodes in modules 13 and 14 were evenly contributed by the three zones. Fungi dominated in modules 6, 13, 14, 18, and 22 (**Figure 5D**), and nodes in these modules were mainly affiliated with *Ascomycetes*. By contrast, bacteria dominated in modules 7, 9, 11, and 17 (**Figure 5D**), with the dominance of *Actinobacteria*. *Actinobacteria* and *Ascomycota* accounted for 19.59 and 16.99% of the total nodes, respectively.

Microbial keystone taxa were highly connected taxa that individually or in a guild exerted a considerable influence on the microbiome structure and functioning (Banerjee et al., 2018). Overall, 53 keystone taxa were identified (**Figure 5E**), five of them were module hubs (0.54% of all nodes), and the rest were connectors (5.19% of the total nodes). The module hubs and connectors accounted for 35.85, and 64.15% of all keystone taxa, respectively. Among 53 keystone taxa, 34 were affiliated with fungi and 19 were from bacteria. *Ascomycota* was the most dominant in keystone taxa, accounting for 26.42%, of which the

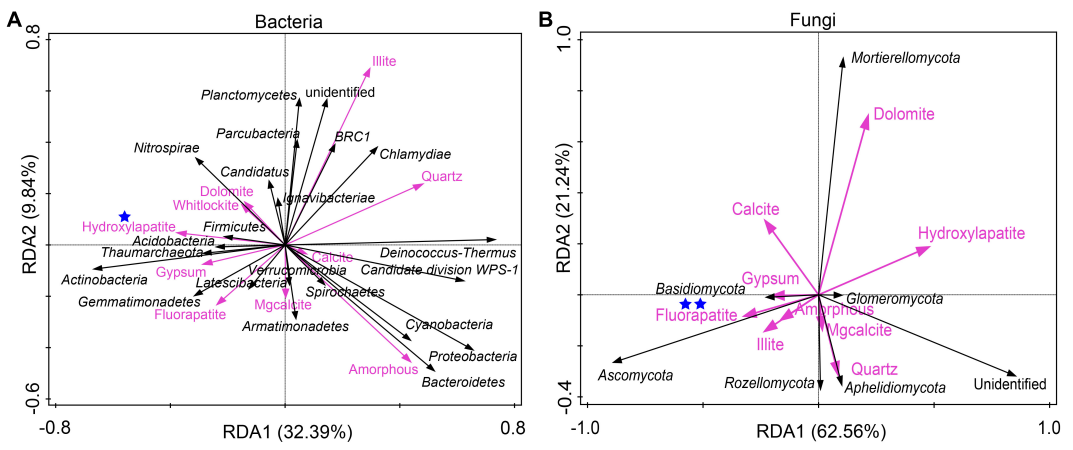

FIGURE 3 | Redundancy analysis of mineral compositions and bacterial communities **(A)** and fungal communities **(B)** of the weathered rocks in the Heshang Cave, China. Mineral phases significantly impacting microbial communities were marked with one (with $P < 0.05$) or two blue stars ($P < 0.01$), respectively.

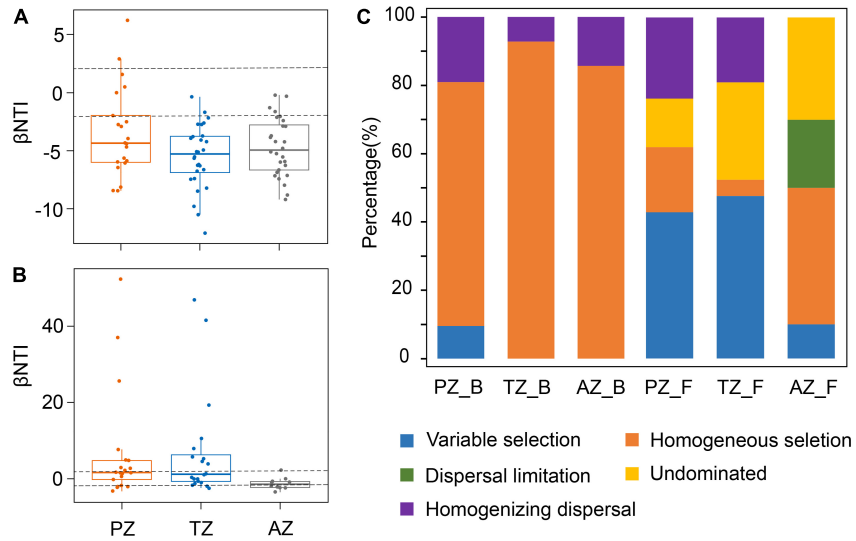

FIGURE 4 | Phylogenetic and null model analyses show the assembly processes of bacterial **(A)** and fungal communities **(B)** in the photic zone (PZ), twilight zone (TZ), and aphotic zone (AZ) tested by βNTI values. The contribution of each ecological process to microbial community assembly in different zones in the Heshang Cave **(C)**. PZ_B, TZ_B, and AZ_B indicate the ecological processes responsible for bacterial community assembly in the photic zone, twilight zone, and aphotic zone, respectively, whereas those PZ_F, TZ_F, and AZ_F denote fungal community assembly.

most dominant class is *Sordariomycetes*, accounting for 15.09%, followed by *Actinobacteria* (24.53%). Module 13 harbored most keystone taxa, accounting for 22.64% of the total keystone taxa, followed by those in modules 6 (18.87%), 18 (13.21%), and 14 (13.21%).

DISCUSSION

Variation of Microbial Communities on Weathered Rocks Along the Cave Passage

Proteobacteria and *Actinomycetes* were previously reported to dominate bacterial communities living on the weathered rocks (Tomczyk-Żak and Zielenkiewicz, 2016), which matched well with our observation of the dominance of *Actinomycetes* (37.66%) and *Proteobacteria* (12.68%) in the Heshang Cave. *Actinomycetes* can interact with a variety of mineral phases (Abdulla, 2009; Cuezva et al., 2012) and metals (Manimaran and Kannabiran, 2017) and are capable of degrading various organic compounds (Ningthoujam et al., 2012), which enables them to survive in extreme environments like caves. *Proteobacteria* (12.68%) ranked the second most abundant linage in the Heshang Cave, indicating highly diverse metabolic capabilities and important roles in the global carbon (Huügler et al., 2005; Kang et al., 2019; Schada von Borzyskowski et al., 2019), nitrogen (Shapleigh, 2011; De Mandal et al., 2017; Delmont et al., 2017), and sulfur cycles (Campbell et al., 2006; Marshall and Morris, 2013). The relative abundance of *Planctomycetes* (8.92%) in the Heshang Cave was relatively higher than that previously reported for other caves (<5%; Ortiz et al., 2013; Ma et al., 2015; Wu et al., 2015; Gulecal-Pektas, 2016), suggesting the uniqueness of bacterial communities in our study. The dominance of *Ascomycetes* (40%) in the Heshang Cave was consistent with previous reports on fungal communities in many other caves (Ogórek et al., 2013; Vaughan et al., 2015). Some of the fungal top 15 fungal genera observed in our study were also common in other caves, such as *Acremonium*, *Aspergillus*, *Cladosporium*, and *Penicillium* (Popović et al., 2015; Zhang et al., 2017; Zhang and Cai, 2019). *Parengyodontium* (13.66%) was the most abundant genus, which was frequently observed in other caves (Leplat et al., 2017, 2019). *Parengyodontium album* had often been the most abundant detected species when salt efflorescence was present (Ponizovskaya et al., 2019; Trovão et al., 2019). The high abundance of *Penicillium* (3.42%) may be related to bat activity (Karkun et al., 2012). The species *Penicillium janczewskii* is characterized by habitation in dry substrates depleted in organic matter, which is partially consistent with its presence in the cave (Mazina et al., 2020). *Neodevriesia* (2.37%) was reported as a dominant group on mural paintings in North Thai temples (Suphaphimol et al., 2022).

Alpha diversities and bacterial community compositions on the rocks did not show significant differences as indicated by Shannon and ACE indices and NMDS analysis in the sampling zones (the photic zone, twilight zone, and aphotic zone), suggesting a fundamental role of the rock substrate (carbonate especially), rather than sunlight in the shaping of bacterial communities. In contrast, the alpha diversity of fungal communities in the aphotic zone was significantly lower than that in the other two zones, which may be related to the isolation of the aphotic zone from light and plants. Fungal communities are known to be tightly associated with plant communities (Tedersoo et al., 2014; Purahong et al., 2018; Adamczyk et al., 2019), and almost 20% of total fungal species are symbiotic with lichens (Kirk et al., 2001; Honegger, 2009). Our results also found high

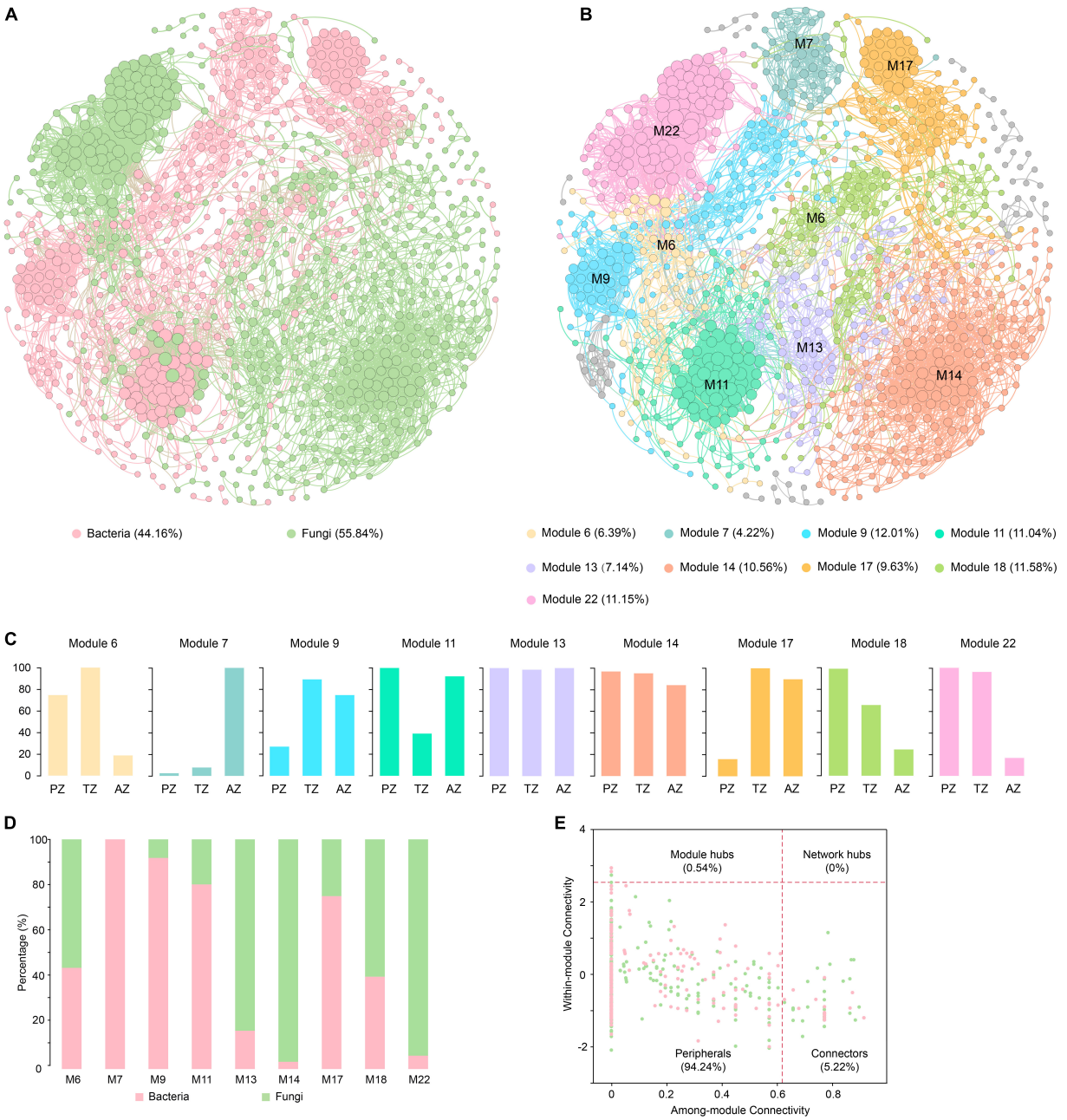

FIGURE 5 | Co-occurrence networks of bacterial and fungal communities of weathered rocks in the Heshang Cave colored by bacteria and fungi **(A)** and by modules **(B)**. The proportion of ASVs/OTUs based on sampling zonation in each module **(C)**. The proportion of bacterial ASVs and fungal OTUs in each module **(D)**. The within-module connectivity (*Zi*)–among-module connectivity (*Pi*) plot shows distribution of ASVs/OTUs according to their module-based topological roles in the co-occurrence networks of bacterial and fungal communities **(E)**. Each dot represents an ASV in the dataset of bacteria (pink) or an OTU of fungi (green). PZ: photic zone, TZ: twilight zone, AZ: aphotic zone.

fungal diversity at the entrance of the Heshang Cave, where lichens were observed on the rock surface. The decrease in fungal diversity inward to the cave may result from the impediment in the transfer of fungal spores due to the slow wind speed inside the cave (**Supplementary Figure 3A**). In fact, our observation of the significant positive correlations between the relative abundances of fungal classes such as *Wallemiomycetes*, *Agaricomycetes*, *Tremellomycetes*, *Lecanoromycetes*, *Exobasidiomycetes*, and the wind speed (**Supplementary Figure 3C**) also supported the decrease in the fungal diversity inward to the cave.

Despite small differences in bacterial communities, indicator groups were distinct in three light zones. The indicator groups in the photic zone were *Cyanobacteria*, *Gemmatimonas*, *Nitrolancea*, *Brevundimonas*, and *Zavarzinella*, which are closely

related to light-dependent metabolism. Many cyanobacterial species can survive on soil and other terrestrial habitats and play important roles in the carbon and nitrogen cycles (Wegener et al., 2010; Forchhammer and Selim, 2020). Some species in *Gemmatimonas* such as *Gemmatimonas aurantiaca* can accumulate polyphosphate (Zhang et al., 2003), and other species like *Gemmatimonas phototrophica* are able to use light as an energy source (Zeng et al., 2015). *Nitrolancea* spp. are obligately aerobic, which are chemolithoautotrophic nitrite-oxidizers (Sorokin et al., 2014). *Flavisolibacter* are aerobic chemoheterotrophs in the phylum *Bacteroidetes* (Lee J. J. et al., 2016). The main indicator groups in the twilight zone were *Aquisphaera*, *Gimesia*, and *Streptomyces*. *Aquisphaera* and *Gimesia* belong to the phylum *Planctomycetes*. *Aquisphaera* forms large visible cell aggregates during growth, which may affect the survival of other microorganisms (Bondoso et al., 2011). Isolates of *Gimesia chilikensis* are salt- and alkali-tolerant (Kumar et al., 2020). Many *Streptomyces* species produce multiple antibiotics or other secondary metabolites, which act synergistically or contingently against biological competition (Challis and Hopwood, 2003). *Conexibacter*, *Actinomadura*, *Aciditerrimonas*, *Planctopirus*, and *Chthonomonas* were the indicator groups in the aphotic zone. They can survive in extreme environments, which is consistent with the lack of organic matter in the depths of the cave. *Conexibacter*, *Actinomadura*, and *Aciditerrimonas* all belong to class *Actinobacteria* and have been frequently isolated from extreme environments. For example, *Conexibacter stalactiti* was isolated from samples of stalactites collected from a lava cave (Lee, 2017), and *Actinomadura namibiensis* was isolated from desert sandy soil in Namibia (Wink et al., 2003). *Chthonomonas calidirosea* was thermophilic and isolated from geothermal soil (Lee K. C. et al., 2016; Compton et al., 2020). Microbes in the aphotic zone can also be involved in iron reduction. For example, *Aciditerrimonas ferrireducens* is capable of reducing ferric iron aerobically or anaerobically (Itoh et al., 2011; Hu et al., 2014).

The indicator groups of fungi also varied in the zones. In the photic zone, *Lecanoromycetes*, *Hypocreales*, *Bionectriaceae*, and *Cladosporiaceae* were identified as indicator groups. *Lecanoromycetes* is the largest class of lichenized fungi and includes most of the lichen-forming fungal species (> 13,500 species; Miadlikowska et al., 2006; Hofstetter et al., 2007). The majority of lichenized fungi in *Lecanoromycetes* are obligate mutualists, which can obtain organic nutrients from photosynthetic symbiotes and N compounds fixed by cyanobacteria (Gueidan et al., 2015; Jüriado et al., 2017). The *Bionectriaceae* is a family in the order *Hypocreales*, which tends to grow on plant materials (Khodosovtsev et al., 2012), and some species are related to algae (Khodosovtsev et al., 2012), bryophytes (Döbbeler et al., 2015), or other fungi. *Cladosporiaceae* is also associated with plants (Alghuthaymi, 2017) and is dominant in highly saline environments (Yang and Sun, 2020). The indicator groups in the twilight zone were *Nectriaceae* and *Zasmidium*. Numerous members in the family *Nectriaceae* (*Hypocreales*) are plant and human pathogens, and several species belonging to this family are used extensively in industrial and commercial applications for biodegradation and as biocontrol agents (Lombard et al., 2014, 2015). *Zasmidium cellare* has been reported in the Mammoth Cave, Kentucky (Barr, 1968), and is a strain known for living in dark and ethanol-rich environments (Cailhol et al., 2020). The indicator groups in the aphotic zone included *Cutaneotrichosporon* and *Wardomycopsis inopinata*. *Cutaneotrichosporon oleaginosus* is an oleaginous yeast with fast growth and also grows as filamentous fungus in the soil and leaf litter (Bracharz et al., 2017). Information on the function of *Wardomycopsis inopinata* in the environment is not available.

The Impact of Mineral Substrate on Microbial Communities and Ecological Processes in Community Assembly

RDA indicated that bacterial communities were significantly affected by hydroxyapatite, mainly due to phosphate-solubilizing bacteria *Streptomyces* and *Pseudomonas*. An isolate of *Pseudomonas fluorescens* from the Heshang Cave has been demonstrated to solubilize fluorapatite, making phosphate bioavailable for microorganisms (Zhou et al., 2017). Fungal communities were positively impacted by fluorapatite, attributed to phosphorus-solubilizing soilborne fungi *Aspergillus niger* and *Penicillium* spp. (Reyes et al., 2007; Farhat et al., 2009; Li et al., 2016). The mechanism of phosphorus-solubilizing microorganisms is generally attributed to organic acid metabolites produced by bacteria and fungi (Kavanagh, 2005; Jones and Oburger, 2011). Phosphate is a common minor element in many silicate, sulfide, and carbonate minerals. Under phosphate-limited conditions in soil environments, microorganisms colonizing minerals may acquire bioavailable phosphate as it solubilizes from the mineral phase (Rogers and Bennett, 2004). Our observation of the significant impact of phosphate-bearing minerals on bacterial and fungal communities on the weathered rocks substantiates the development of microbial communities nutritionally dependent on the mineral-phase substrate.

Ecological processes responsible for the development of microbial communities were also investigated in the Heshang Cave. The assembly of bacterial communities is mainly a deterministic process, with the dominance of homogeneous selection across different sampling zones, indicating a spatial homogeneity in environmental conditions and the convergence in bacterial communities (Dini-Andreote et al., 2015). This conclusion is also consistent with the result of the NMDS (**Figure 1E**). In contrast, different ecological processes contributed to fungal assembly in sampling zones. Variable selection dominated the assembly of fungal communities in both the photic and twilight zones, indicating the strong environmental selection of fungal communities partially due to sunlight. Many fungal groups were associated with algae, cyanobacteria, and plant debris, all of which were highly dependent on sunlight. Homogeneous selection only dominated the fungal assembly in the aphotic zone, indicating that a homogeneous environmental condition resulted in the convergence in fungal communities. The occurrence of dispersal limitation in the aphotic zone indicates a weakening selection, which may have resulted from slow wind speed and

high relative humidity toward the end of the cave entrance (**Supplementary Tables 3,4**). Slow airflow is known to decrease airborne transmission of fungal spores (Quintero et al., 2010), and fungal survival increases with relative humidity (Oliveira et al., 2005; Hameed et al., 2012). The relative abundances of fungal classes *Wallemiomycetes*, *Agaricomycetes*, *Tremellomycetes*, *Lecanoromycetes*, and *Exobasidiomycetes* showed significant positive correlations with the wind speed (**Supplementary Figure 3C**), and similar phenomena in air have also been reported (Begerow and Kemler, 2018; Els et al., 2019).

Interaction Between Bacteria and Fungi Living on Weathered Rocks

The co-occurrence network of bacteria and fungi showed good modularity and positive links between nodes, indicating that the bacterial and fungal communities formed a close organization through cooperation among different species. Their interactions increased the complexity of the community structure and the stability of the ecosystem (Chen et al., 2018).

In total, 53 keystone taxa were identified, which usually interact with many other groups, thus promoting the exchange and flow of energy, information, metabolites, and nutrients among different species and maintaining the balance of microbial communities (Berry and Widder, 2014; Ma et al., 2016). There are many unknown functions of the keystone taxa in this study, but some clues can be garnered from the previous investigations. The fungal keystone taxa mainly belonged to classes of *Sordariomycetes*, *Dothideomycetes*, and *Eurotiomycetes*. Members of *Sordariomycetes* are ubiquitous in natural environments (Zhang and Wang, 2015). They participate in the decomposition of organic matter and nutrient cycling as saprotrophs in almost all ecosystems, and they include endophytes and pathogens of plants (Arnold and Lutzoni, 2007), arthropods (Samuels and Blackwell, 2001), and mammals (O'Donnell et al., 2010), and even as mycoparasites attacking other fungi (Broberg et al., 2021). *Sordariomycetes* also contain species known to produce secondary metabolites such as potent mycotoxins (Zhang and Wang, 2015). *Dothideomycetes* is the largest class of *Ascomycetes*, which includes numerous rock-inhabiting fungi, adapted well to nutrient-poor and dry habitats on rock surfaces (Ruibal et al., 2009; Haridas et al., 2020). *Eurotiomycetes* can degrade a wide variety of organic substrates and can tolerate high salinity, complete darkness, and oligotrophic conditions (Greiner et al., 2014; Zhang and Wang, 2015), which favor their survival in caves.

Nocardioidaceae, *Planctomycetaceae*, and *Rubrobacteraceae* were keystone taxa of bacterial classes in the network. *Nocardioidaceae* uses a wide range of carbon and nitrogen sources, including unusual organic compounds and toxic environmental pollutants, and has versatile metabolic pathways (Evtushenko et al., 2015). Like many other actinomycetes, *Nocardioidaceae* can survive under extreme conditions such as desiccation, low and high temperatures, UV damage, and toxic compounds (Kirby et al., 2006; Brodie et al., 2007; Griffin, 2007; Polymenakou et al., 2008). Members of the *Nocardioidaceae* are symbiotic with plants and may exist as reciprocal endophytes. They can also occur in association with lichens (Li et al., 2007) and fungi (Lauer et al., 2007). *Marmoricola* is a genus of *Nocardioidaceae*, which are found in different environments, such as marble, beach sediments, and agricultural soil (Lee, 2007; Freed et al., 2019). Some species are alkali-tolerant or display alkaliphilic properties (Evtushenko, 2015). The family *Planctomycetaceae* is distributed in both soil and water (Wiegand et al., 2018) and shows strong tolerance to seawater, acid peat bog, hot springs, and low temperature (Kulichevskaya et al., 2007, 2008; Fuerst and Sagulenko, 2011). It can use a special mechanism to absorb and digest complex polysaccharides, which may help it compete for nutrients in natural habitats (Boedeker et al., 2017; Schubert et al., 2020). The family *Rubrobacteraceae* is usually represented by its thermophilic and radiation-resistant types (Albuquerque et al., 2014). The genus *Rubrobacter* of *Rubrobacteraceae* is involved in chlorophyll biosynthesis (Gupta and Khadka, 2016). These keystone bacteria and fungi impact microbial community composition and symbiotic or parasitic relationships on rock walls. Some of their secondary metabolites have antibiotic or toxin properties that can promote or inhibit effector species and modulate interactions in microbial communities.

The co-occurrence network analysis provides us with a new way to find potential symbiotic or parasitic associations between bacteria and fungi. Bacteria can be endosymbiotic with fungi (termed endohyphal bacteria), which are phylogenetically and ecologically widespread. Endohyphal bacteria recently have been documented in diverse *Ascomycota*, including members of multiple classes (*Pezizomycetes*, *Eurotiomycetes*, *Dothideomycetes*, and *Sordariomycetes*; Hoffman and Arnold, 2010; Shaffer et al., 2016, 2017). Our network analysis found that many unannotated groups within *Eurotiomycetes*, *Dothideomycetes*, and *Sordariomycetes* serve as keystone taxa in the network, which are also tightly connected with bacteria. For example, *Betaproteobacteria* has a connection with unidentified fungi, and related studies have demonstrated that some genera of *Betaproteobacteria* can parasitize as endosymbionts in fungal hyphae (Hoffman and Arnold, 2010). *Xanthomonadaceae* has been found to subsist in fungal hyphae (Hoffman and Arnold, 2010), as also notices for unidentified fungi in our network. The observation of the connection between *Caldiline* and unidentified fungi in our study is consistent with a previous report of a negative correlation between *Caldiline* and an unclassified fungus of *Pezizomycotina* (Fouts et al., 2012). *Gammaproteobacteria* in the network are linked to many OTUs in *Dothideomycetes*, *Sordariomycetes*, and unidentified fungi. Arendt et al. (2016) demonstrated that some species of *Gammaproteobacteria* can be successfully introduced into *Dothideomycetes* and *Sordariomycetes*, thus substantiating their symbiotic relationships.

It should be emphasized that co-occurrence networks visualize the correlations between microbial groups, including real ecological interactions (such as reciprocity), and also include non-random processes (such as niche overlap). They do not, therefore, necessarily reflect direct interactions between the groups. Future experiments will assess whether the identified key species directly affect other members of the microbiome or indirectly affect the performance and fitness of the host, thus affecting other community members.

CONCLUSION

We studied the ecological processes responsible for the community assembly, endeavoring to provide new insights into microbial interactions and establishment of microbial communities under extreme conditions in the subsurface cave biosphere.

1. Microbial indicator groups varied with different light zones, indicating functional changes in response to the light variation in karst caves. Phosphate minerals such as hydroxyapatite and fluorapatite significantly influenced bacterial and fungal communities living on weathered rock surfaces.
2. The co-occurrence network analysis showed that bacteria and fungi on rock surfaces were mainly positively linked, indicating extensive, close cooperations among microbial groups across different domains connected under stark environmental conditions to maintain the microbial ecosystem. The co-occurrence network may also provide us with a new robust way to decipher symbiosis and parasitism between bacterial and fungal groups.
3. Homogeneous selection dominated bacterial community assembly throughout the cave, resulting in the convergence of bacterial communities. Variable selection contributed most to the fungal community assembly in the photic and twilight zones, whereas homogeneous selection with dispersal limitation contributed more to fungal assembly in the dark zone.

DATA AVAILABILITY STATEMENT

The datasets presented in this study can be found in online repositories. The names of the repository/repositories and accession number(s) can be found below: https://www.ncbi.nlm.nih.gov/bioproject/337918, http://www.ncbi.nlm.nih.gov/bioproject/821722.

AUTHOR CONTRIBUTIONS

YW, JZ, and XL completed the sample collection. JZ finished DNA extraction. YW and XC completed data analysis, visualization, and original draft preparation. HW designed this experiment, supervised data analysis, acquired funding, and wrote and edited this manuscript. OT participated in data discussion and manuscript drafting. All authors contributed to the article and approved the submitted version.

FUNDING

This work was supported by the National Natural Science Foundation of China (91951208 and 41130207).

SUPPLEMENTARY MATERIAL

The Supplementary Material for this article can be found online at: https://www.frontiersin.org/articles/10.3389/fmicb.2022.909494/full#supplementary-material

REFERENCES

Abdulla, H. (2009). Bioweathering and biotransformation of granitic rock minerals by actinomycetes. *Microb. Ecol.* 58, 753–761. doi: 10.1007/s00248-009-9549-1

Adamczyk, M., Hagedorn, F., Wipf, S., Donhauser, J., Vittoz, P., Rixen, C., et al. (2019). The soil microbiome of Gloria Mountain summits in the Swiss Alps. *Front. Microbiol.* 10:1080. doi: 10.3389/fmicb.2019.01080

Albuquerque, L., Johnson, M. M., Schumann, P., Rainey, F. A., and da Costa, M. S. (2014). Description of two new thermophilic species of the genus *Rubrobacter*, *Rubrobacter calidifluminis* sp. nov. and *Rubrobacter naiadicus* sp. nov., and emended description of the genus *Rubrobacter* and the species *Rubrobacter bracarensis*. *Syst. Appl. Microbiol.* 37, 235–243. doi: 10.1016/j.syapm.2014.03.001

Alghuthaymi, M. A. (2017). Nanotools for molecular identification two novels *Cladosporium cladosporioides* species (*Cladosporiaceae*) collected from tomato phyloplane. *J. Yeast Fungal Res.* 8, 11–18. doi: 10.5897/JYFR2017.0178

Aloisi, G., Gloter, A., Kruger, M., Wallmann, K., Guyot, F., and Zuddas, P. (2006). Nucleation of calcium carbonate on bacterial nanoglobules. *Geology* 34, 1017–1020. doi: 10.1130/G22986A.1

Arendt, K. R., Hockett, K. L., Araldi-Brondolo, S. J., Baltrus D. A., and Arnold, A. E. (2016). Isolation of endohyphal bacteria from foliar ascomycota and *in vitro* establishment of their symbiotic associations. *Appl. Environ. Microbiol.* 82, 2943–2949. doi: 10.1128/AEM.00452-16

Arias, D., Cisternas, L. A., Miranda, C., and Rivas, M. (2019). Bioprospecting of ureolytic bacteria from Laguna Salada for biomineralization applications. *Front. Bioeng. Biotechnol.* 6:209. doi: 10.3389/fbioe.2018.00209

Arnold, A. E., and Lutzoni, F. (2007). Diversity and host range of foliar fungal endophytes: are tropical leaves biodiversity hotspots? *Ecology* 88, 541–549. doi: 10.1890/05-1459

Banerjee, S., Schlaeppi, K., and van der Heijden, M. G. (2018). Keystone taxa as drivers of microbiome structure and functioning. *Nat. Rev. Microbiol.* 16, 567–576. doi: 10.1038/s41579-018-0024-1

Barr, T. C. Jr. (1968). Ecological studies in the Mammoth Cave system of Kentucky. *Int. J. Speleol.* 3, 147–204. doi: 10.5038/1827-806x.3.1.10

Barton, H. A., Taylor, N. M., Kreate, M. P., Springer, A. C., Oehrle, S. A., and Bertog, J. L. (2007). The impact of host rock geochemistry on bacterial community structure in oligotrophic cave environments. *Int. J. Speleol.* 36, 93–104. doi: 10.5038/1827-806x.36.2.5

Begerow, D., and Kemler, M. (2018). Phylogeny, biogeography and host specificity of smut fungi. *Biosyst. Ecol. Ser.* 34, 311–329.

Berry, D., and Widder, S. (2014). Deciphering microbial interactions and detecting keystone species with co-occurrence networks. *Front. Microbiol.* 5:219. doi: 10.3389/fmicb.2014.00219

Boedeker, C., Schüler, M., Reintjes, G., Jeske, O., van Teeseling, M. C., Jogler, M., et al. (2017). Determining the bacterial cell biology of Planctomycetes. *Nat. Commun.* 8:14853. doi: 10.1038/ncomms14853

Bonacci, O., Pipan, T., and Culver, D. C. (2009). A framework for karst ecohydrology. *Environ. Geol.* 56, 891–900. doi: 10.1007/s00254-008-1189-0

Bondoso, J., Albuquerque, L., Nobre, M. F., Lobo-da-Cunha, A., da Costa, M. S., and Lage, O. M. (2011). *Aquisphaera giovannonii* gen. nov., sp. nov., a planctomycete isolated from a freshwater aquarium. *Int. J. Syst. Evol. Microbiol.* 61, 2844–2850. doi: 10.1099/ijs.0.027474-0

Bracharz, F., Beukhout, T., Mehlmer, N., and Brück, T. (2017). Opportunities and challenges in the development of *Cutaneotrichosporon oleaginosus* ATCC 20509 as a new cell factory for custom tailored microbial oils. *Microb. Cell Fact.* 16:178. doi: 10.1186/s12934-017-0791-9

Brewer, T. E., and Fierer, N. (2018). Tales from the tomb: the microbial ecology of exposed rock surfaces. *Environ. Microbiol.* 20, 958–970. doi: 10.1111/1462-2920.14024

Broberg, M., Dubey, M., Iqbal, M., Gudmundssson, M., Ihrmark, K., Schroers, H. J., et al. (2021). Comparative genomics highlights the importance of drug efflux transporters during evolution of mycoparasitism in *Clonostachys* subgenus *Bionectria* (Fungi, Ascomycota, Hypocreales). *Evol. Appl.* 14, 476–497. doi: 10.1111/eva.13134

Brodie, E. L., DeSantis, T. Z., Parker, J. P. M., Zubietta, I. X., Piceno, Y. M., and Andersen, G. L. (2007). Urban aerosols harbor diverse and dynamic bacterial populations. *Proc. Natl. Acad. Sci. U. S. A.* 104, 299–304. doi: 10.1073/pnas.0608255104

Cailhol, D., Ciadamidaro, L., Dupuy, D., Allegra, S., Girardot, F., and Pfendler, S. (2020). Fungal and bacterial outbreak in the wine vinification area in the Saint-Marcel show cave. *Sci. Total Environ.* 733:138756. doi: 10.1016/j.scitotenv.2020.138756

Campbell, B. J., Engel, A. S., Porter, M. L., and Takai, K. (2006). The versatile ε-*proteobacteria*: key players in sulphidic habitats. *Nat. Rev. Microbiol.* 4, 458–468. doi: 10.1038/nrmicro1414

Cañveras, C., Sanchez-Moral, S., Sloer, V., and Saiz-Jimenez, C. (2001). Microorganisms and microbially induced fabrics in cave walls. *Geomicrobiol. J.* 18, 223–240. doi: 10.1080/01490450152467769

Caumartin, V. (1963). Review of the microbiology of underground environments. *Bull. Natl. Speleol. Soc.* 25, 1–14.

Challis, G. L., and Hopwood, D. A. (2003). Synergy and contingency as driving forces for the evolution of multiple secondary metabolite production by *Streptomyces* species. *Proc. Natl. Acad. Sci. U. S.A.* 100(Suppl. 2), 14555–14561. doi: 10.1073/pnas.1934677100

Chang, H. C., Leaw, S. N., Huang, A. H., Wu, T. L., and Chang, T. C. (2001). Rapid identification of yeasts in positive blood cultures by a multiplex PCR method. *J. Clin. Microbiol.* 39, 3466–3471. doi: 10.1128/jcm.39.10.3466-3471.2001

Chen, S., Qi, G., Luo, T., Zhang, H., Jiang, Q., Wang, R., et al. (2018). Continuous-cropping tobacco caused variance of chemical properties and structure of bacterial network in soils. *Land. Degrad. Dev.* 29, 4106–4120. doi: 10.1002/ldr.3167

Cheng, X., Yun, Y., Wang, H., Ma, L., Tian, W., Man, B., et al. (2021). Contrasting bacterial communities and their assembly processes in karst soils under different land use. *Sci. Total Environ.* 751:142263. doi: 10.1016/j.scitotenv.2020.142263

Choe, Y. H., Kim, M., Woo, J., Lee, M. J., Lee, J. I., Lee, E. J., et al. (2018). Comparing rock-inhabiting microbial communities in different rock types from a high arctic polar desert. *FEMS Microbiol. Ecol.* 94:fiy070. doi: 10.1093/femsec/fiy070

Claesson, M. J., O'Sullivan, O., Wang, Q., Nikkilä, J., Marchesi, J. R., Smidt, H., et al. (2009). Comparative analysis of pyrosequencing and a phylogenetic microarray for exploring microbial community structures in the human distal intestine. *PLoS One* 4:e6669. doi: 10.1371/journal.pone.0006669

Claesson, M. J., Wang, Q., O'Sullivan, O., Greene-Diniz, R., Cole, J. R., Ross, R. P., et al. (2010). Comparison of two next-generation sequencing technologies for resolving highly complex microbiota composition using tandem variable 16S rRNA gene regions. *Nucleic Acids Res.* 38:e200. doi: 10.1093/nar/gkq873

Compton, B. J., Lagutin, K., Dyer, B. S., Ryan, J., MacKenzie, A., Stott, M. B., et al. (2020). Isolation and synthesis of glycophospholipids from the extremophile *Chthonomonas calidirosea*. *Asian J. Org. Chem.* 9, 1802–1814. doi: 10.1002/ajoc.202000357

Cuezva, S., Fernandez-Cortes, A., Porca, E., Pašić, L., Jurado, V., Hernandez-Marine, M., et al. (2012). The biogeochemical role of *Actinobacteria* in Altamira Cave, Spain. *FEMS Microbiol. Ecol.* 81, 281–290. doi: 10.1111/j.1574-6941.2012.01391.x

De Mandal, S., Chatterjee, R., and Kumar, N. S. (2017). Dominant bacterial phyla in caves and their predicted functional roles in C and N cycle. *BMC Microbiol.* 17:90. doi: 10.1186/s12866-017-1002-x

Delmont, T. O., Quince, C., Shaiber, A., Esen, ÖC., Lee, S. T., Lücker, S., et al. (2017). Nitrogen-fixing populations of *Planctomycetes* and *Proteobacteria* are abundant in the surface ocean. *bioRxiv Preprint.* doi: 10.1101/129791

Deng, Y., Jiang, Y. H., Yang, Y., He, Z., Luo, F., and Zhou, J. (2012). Molecular ecological network analyses. *BMC Bioinform.* 13:13. doi: 10.1186/1471-2105-13-113

Dhami, N. K., Reddy, M. S., and Mukherjee, A. (2013). Biomineralization of calcium carbonates and their engineered applications: a review. *Front. Microbiol.* 4:314. doi: 10.3389/fmicb.2013.00314

Dini-Andreote, F., Stegen, J. C., Van Elsas, J. D., and Salles, J. F. (2015). Disentangling mechanisms that mediate the balance between stochastic and deterministic processes in microbial succession. *Proc. Natl. Acad. Sci. U. S. A.* 112, E1326–E1332. doi: 10.1073/pnas.1414261112

Dixon, P. (2003). VEGAN, a package of R functions for community ecology. *J. Veg. Sci.* 14, 927–930. doi: 10.1111/j.1654-1103.2003.tb02228.x

Döbbeler, P., Davison, P. G., and Buck, W. R. (2015). Two new hypocrealean ascomycetes on bryophytes from North America. *Nova Hedwigia* 100, 383–390. doi: 10.1127/nova_hedwigia/2015/0244

Els, N., Larose, C., Baumann-Stanzer, K., Tignat-Perrier, R., Keuschnig, C., Vogel, T. M., et al. (2019). Microbial composition in seasonal time series of free tropospheric air and precipitation reveals community separation. *Aerobiologia* 35, 671–701. doi: 10.1007/s10453-019-09606-x

Evtushenko, L. I. (2015). "Marmoricola," in *Bergey's Manual of Systematics of Archaea and Bacteria*, ed. W. B. Whitman (Hoboken, NJ: John Wiley & Sons), 1–27. doi: 10.1002/9781118960608.gbm00158

Evtushenko, L. I., Krausova, V. I., and Yoon, J. H. (2015). "Nocardioidaceae," in *Bergey's Manual of Systematics of Archaea and Bacteria*, ed. W. B. Whitman (Hoboken: John Wiley & Sons), 1–81. doi: 10.1002/9781118960608.fbm00042

Farhat, M. B., Farhat, A., Bejar, W., Kammoun, R., Bouchaala, K., Fourati, A., et al. (2009). Characterization of the mineral phosphate solubilizing activity of *Serratia marcescens* CTM 50650 isolated from the phosphate mine of Gafsa. *Arch. Microbiol.* 191, 815–824. doi: 10.1007/s00203-009-0513-8

Forchhammer, K., and Selim, K. A. (2020). Carbon/nitrogen homeostasis control in cyanobacteria. *FEMS Microbiol. Rev.* 44, 33–53. doi: 10.1093/femsre/fuz025

Fouts, D. E., Szpakowski, S., Purushe, J., Torralba, M., Waterman, R. C., MacNeil, M. D., et al. (2012). Next generation sequencing to define prokaryotic and fungal diversity in the bovine rumen. *PLoS One* 7:e48289. doi: 10.1371/journal.pone.0048289

Freed, S. Jr., Ramaley, R. F., and Kyndt, J. A. (2019). Whole-genome sequence of the novel *Rubrobacter taiwanensis* strain Yellowstone, isolated from Yellowstone National Park. *Microbiol. Resour. Announce.* 8:e00287-e19. doi: 10.1128/mra.00287-19

Fuerst, J. A., and Sagulenko, E. (2011). Beyond the bacterium: planctomycetes challenge our concepts of microbial structure and function. *Nat. Rev. Microbiol.* 9, 403–413. doi: 10.1038/nrmicro2578

Gallagher, K. L., Kading, T. J., Braissant, O., Dupraz, C., and Visscher, P. T. (2012). Inside the alkalinity engine: the role of electron donors in the organomineralization potential of sulfate-reducing bacteria. *Geobiology* 10, 518–530. doi: 10.1111/j.1472-4669.2012.00342.x

Greiner, K., Peršoh, D., Weig, A., and Rambold, G. (2014). *Phialosimplex salinarum*, a new species of *Eurotiomycetes* from a hypersaline habitat. *IMA Fungus* 5, 161–172. doi: 10.5598/imafungus.2014.05.02.01

Griffin, D. W. (2007). Atmospheric movement of microorganisms in clouds of desert dust and implications for human health. *Clin. Microbiol. Rev.* 20, 459–477. doi: 10.1128/CMR.00039-06

Gueidan, C., Hill, D. J., Miadlikowska, J., and Lutzoni, F. (2015). "Pezizomycotina: Lecanoromycetes," in *Systematics and Evolution*, eds D. J. McLaughlin and J. W. Spatafora (Heidelberg: Springer), 89–120.

Guimera, R., and Amaral, L. A. N. (2005). Cartography of complex networks: modules and universal roles. *J. Stat. Mech. Theory Exp.* 2005, P02001-1–P02001-13. doi: 10.1088/1742-5468/2005/02/p02001

Gulecal-Pektas, Y. (2016). Bacterial diversity and composition in Oylat Cave (Turkey) with combined Sanger/pyrosequencing approach. *Pol. J. Microbiol.* 65, 69–75. doi: 10.5604/17331331.1197277

Gupta, R. S., and Khadka, B. (2016). Evidence for the presence of key chlorophyll-biosynthesis-related proteins in the genus *Rubrobacter* (Phylum Actinobacteria) and its implications for the evolution and origin of photosynthesis. *Photosyn. Res.* 127, 201–218. doi: 10.1007/s11120-015-0177-y

Hameed, A. A., Khoder, M., Ibrahim, Y., Saeed, Y., Osman, M., and Ghanem, S. (2012). Study on some factors affecting survivability of airborne fungi. *Sci. Total Environ.* 414, 696–700. doi: 10.1016/j.scitotenv.2011.10.042

Haridas, S., Albert, R., Binder, M., Bloem, J., LaButti, K., Salamov, A., et al. (2020). 101 *Dothideomycetes* genomes: a test case for predicting lifestyles and

emergence of pathogens. *Stud. Mycol.* 96, 141–153. doi: 10.1016/j.simyco.2020.01.003

He, D., Wu, F., Ma, W., Zhang, Y., Gu, J. D., Duan, Y., et al. (2021). Insights into the bacterial and fungal communities and microbiome that causes a microbe outbreak on ancient wall paintings in the Maijishan Grottoes. *Int. Biodeterior. Biodegrad.* 163:105250. doi: 10.1016/j.ibiod.2021.105250

Hershey, O. S., and Barton, H. A. (2018). "The microbial diversity of caves," in *Cave Ecology*, eds O. T. Moldovan, Ľ. Kováč, and S. Halse (Heidelberg: Springer), 69–90.

Hess, W. H. (1900). The origin of nitrates in cavern earths. *J. Geol.* 8, 129–134. doi: 10.1086/620781

Høeg, O. (1946). Cyanophyceae and bacteria in calcareous sediments in the interior of limestone caves in Nord-Rana, Norway. *Nytt Mag. Naturvidensk.* 85, 99–104.

Hoffman, M. T., and Arnold, A. E. (2010). Diverse bacteria inhabit living hyphae of phylogenetically diverse fungal endophytes. *Appl. Environ. Microbiol.* 76, 4063–4075. doi: 10.1128/aem.02928-09

Hofstetter, V., Miadlikowska, J., Kauff, F., and Lutzoni, F. (2007). Phylogenetic comparison of protein-coding versus ribosomal RNA-coding sequence data: a case study of the Lecanoromycetes (Ascomycota). *Mol. Phylogenet. Evol.* 44, 412–426. doi: 10.1016/j.ympev.2006.10.016

Honegger, R. (2009). "Lichen-forming fungi and their photobionts," in *Plant Relationships*, 2nd Edn, ed. H. B. Deising (Heidelberg: Springer), 307–333.

Hu, C., Henderson, G. M., Huang, J., Chen, Z., and Johnson, K. R. (2008). Report of a three-year monitoring programme at Heshang Cave, Central China. *Int. J. Speleol.* 37, 143–151. doi: 10.5038/1827-806x.37.3.1

Hu, L., Cao, L., and Zhang, R. (2014). Bacterial and fungal taxon changes in soil microbial community composition induced by short-term biochar amendment in red oxidized loam soil. *World J. Microbiol. Biotechnol.* 30, 1085–1092. doi: 10.1007/s11274-013-1528-5

Huügler, M., Wirsen, C. O., Fuchs, G., Taylor, C. D., and Sievert, S. M. (2005). Evidence for autotrophic CO2 fixation via the reductive tricarboxylic acid cycle by members of the ε subdivision of *Proteobacteria*. *J. Bacteriol.* 187, 3020–3027. doi: 10.1128/jb.187.9.3020-3027.2005

Irit, N., Hana, B., Yifat, B., Esti, K. W., and Ariel, K. (2019). Insights into bacterial communities associated with petroglyph sites from the Negev Desert, Israel. *J. Arid Environ.* 166, 79–82. doi: 10.1016/j.jaridenv.2019.04.010

Itoh, T., Yamanoi, K., Kudo, T., Ohkuma, M., and Takashina, T. (2011). *Aciditerrimonas ferrireducens* gen. nov., sp. nov., an iron-reducing thermoacidophilic actinobacterium isolated from a solfataric field. *Int. J. Syst. Evol. Microbiol.* 61, 1281–1285. doi: 10.1099/ijs.0.023044-0

Jones, D. L., and Oburger, E. (2011). "Solubilization of phosphorus by soil microorganisms," in *Phosphorus in Action*, eds E. K. Bünemann, A. Oberson, and E. Frossard (Heidelberg: Springer), 169–198.

Jones, D. S., and Macalady, J. L. (2016). "The snotty and the stringy: energy for subsurface life in caves," in *Their World: A Diversity of Microbial Environments*, ed. C. J. Hurst (Heidelberg: Springer), 203–224.

Jüriado, I., Kaasalainen, U., and Rikkinen, J. (2017). Specialist taxa restricted to threatened habitats contribute significantly to the regional diversity of *Peltigera* (Lecanoromycetes, Ascomycota) in Estonia. *Fungal Ecol.* 30, 76–87. doi: 10.1016/j.funeco.2017.08.004

Kang, C. S., Dunfield, P. F., and Semrau, J. D. (2019). The origin of aerobic methanotrophy within the *Proteobacteria*. *FEMS Microbiol. Lett.* 366:fnz096. doi: 10.1093/femsle/fnz096

Karkun, A., Tiwari, K., and Jadhav, S. (2012). Fungal diversity of Mandeepkhol cave in Chhattisgarh. *India Adv. Biores* 3, 119–123.

Kato, S., Hashimoto, K., and Watanabe, K. (2012). Microbial interspecies electron transfer via electric currents through conductive minerals. *Proc. Natl. Acad. Sci. U. S. A.* 109, 10042–10046. doi: 10.1073/pnas.1117592109

Kavanagh, K. (2005). "Fungal fermentation systems and products," in *Fungi: Biology and Applications*, ed. K. Kavanagh (Hoboken, NJ: John Wiley & Sons), 125–146.

Kembel, S. W., Cowan, P. D., Helmus, M. R., Cornwell, W. K., Morlon, H., Ackerly, D. D., et al. (2010). Picante: R tools for integrating phylogenies and ecology. *Bioinformatics* 26, 1463–1464. doi: 10.1093/bioinformatics/btq166

Khodosovtsev, A., Vondrák, J., Naumovich, A., Kocourková, J., Vondráková, O., and Motiejnait, J. (2012). Three new *Pronectria* species in terricolous and saxicolous microlichen communities (Bionectriaceae, Ascomycota). *Nova Hedwigia* 95, 211–220. doi: 10.1127/0029-5035/2012/0026

Kirby, B. M., Le Roes, M., and Meyers, P. R. (2006). *Kribbella karoonensis* sp. nov. and *Kribbella swartbergensis* sp. nov., isolated from soil from the Western Cape, South Africa. *Int. J. Syst. Evol. Microbiol.* 56, 1097–1101. doi: 10.1099/ijs.0.63951-0

Kirk, P. M., Cannon, P. F., David, J., and Stalpers, J. A. (2001). *Ainsworth and Bisby's Dictionary of the Fungi*. Wallingford: CABI publishing.

Kováč, Ľ. (2018). "Caves as oligotrophic ecosystems," in *Cave Ecology*, eds O. T. Moldovan, Ľ. Kováč, and S. Halse (Cham: Springer), 297–307.

Kozlova, E. V., and Mazina, S. E. (2020). Biodiversity of Fungi in the photic and aphotic zones of Montenegro caves. *Aerobiologia* 36, 589–604. doi: 10.1007/s10453-020-09654-8

Kulichevskaya, I. S., Ivanova, A. O., Baulina, O. I., Bodelier, P. L., Damste, J. S. S., and Dedysh, S. N. (2008). *Singulisphaera acidiphila* gen. nov., sp. nov., a non-filamentous, Isosphaera-like planctomycete from acidic northern wetlands. *Int. J. Syst. Evol. Microbiol.* 58, 1186–1193. doi: 10.1099/ijs.0.65593-0

Kulichevskaya, I. S., Ivanova, A. O., Belova, S. E., Baulina, O. I., Bodelier, P. L., Rijpstra, W. I. C., et al. (2007). *Schlesneria paludicola* gen. nov., sp. nov., the first acidophilic member of the order *Planctomycetales*, from Sphagnum-dominated boreal wetlands. *Int. J. Syst. Evol. Microbiol.* 57, 2680–2687. doi: 10.1099/ijs.0.65157-0

Kumar, D., Gaurav, K., Sreya, P., Shabbir, A., Uppada, J., and Ch, S. (2020). Gimesia chilikensis sp. nov., a haloalkali-tolerant planctomycete isolated from Chilika lagoon and emended description of the genus *Gimesia*. *Int. J. Syst. Evol. Microbiol.* 70, 3647–3655. doi: 10.1099/ijsem.0.004211

Lauer, A., Simon, M. A., Banning, J. L., André, E., Duncan, K., and Harris, R. N. (2007). Common cutaneous bacteria from the eastern red-backed salamander can inhibit pathogenic fungi. *Copeia* 2007, 630–640.

Lavoie, K. H., Northup, D. E., and Barton, H. A. (2010). "Microbe-mineral interactions: cave geomicrobiology," in *Geomicrobiology*, eds S. K. Jain, A. A. Khan, and M. K. Rai (New York, NY: CRC Press), 1–46.

Lee, J. J., Kang, M. S., Kim, G. S., Lee, C. S., Lim, S., Lee, J., et al. (2016). *Flavisolibacter tropicus* sp. nov., isolated from tropical soil. *Int. J. Syst. Evol. Microbiol.* 66, 3413–3419. doi: 10.1099/ijsem.0.001207

Lee, K. C., Stott, M. B., Dunfield, P. F., Huttenhower, C., McDonald, I. R., and Morgan, X. C. (2016). The *Chthonomonas calidirosea* genome is highly conserved across geographic locations and distinct chemical and microbial environments in New Zealand's Taupō Volcanic Zone. *Appl. Environ. Microbiol.* 82, 3572–3581. doi: 10.1128/aem.00139-16

Lee, N. M., Meisinger, D. B., Aubrecht, R., Kovacik, L., Saiz-Jimenez, C., Baskar, S., et al. (2012). "Caves and karst environments," in *Life at Extremes: Environments, Organisms and Strategies for Survival*, ed. E. M. Bell (Oxfordshire: CAB International), 320–344.

Lee, S. D. (2007). *Marmoricola aequoreus* sp. nov., a novel actinobacterium isolated from marine sediment. *Int. J. Syst. Evol. Microbiol.* 57, 1391–1395. doi: 10.1099/ijs.0.64696-0

Lee, S. D. (2017). *Conexibacter stalactiti* sp. nov., isolated from stalactites in a lava cave and emended description of the genus *Conexibacter*. *Int. J. Syst. Evol. Microbiol.* 67, 3214–3218. doi: 10.1099/ijsem.0.002083

Lemon, J., Bolker, B., Oom, S., Klein, E., Rowlingson, B., Wickham, H., et al. (2021). *Package 'plotrix'*. Vienna: R Development Core Team.

Leplat, J., Francois, A., and Bousta, F. (2017). White fungal covering on the wall paintings of the Saint-Savin-sur-Gartempe Abbey church crypt: a case study. *Int. Biodeterior. Biodegrad.* 122, 29–37. doi: 10.1016/j.ibiod.2017.04.007

Leplat, J., François, A., Touron, S., Galant, P., and Bousta, F. (2019). Aerobiological behavior of Paleolithic decorated caves: a comparative study of five caves in the Gard department (France). *Aerobiologia* 35, 105–124. doi: 10.1007/s10453-018-9546-2

Li, B., Xie, C. H., and Yokota, A. (2007). *Nocardioides exalbidus* sp. nov., a novel actinomycete isolated from lichen in Izu-Oshima Island, Japan. *Actinomycetologica* 21, 22–26. doi: 10.3209/saj.saj210103

Li, Z., Bai, T., Dai, L., Wang, F., Tao, J., Meng, S., et al. (2016). A study of organic acid production in contrasts between two phosphate solubilizing fungi:

Penicillium oxalicum and *Aspergillus niger*. *Sci. Rep.* 6:25313. doi: 10.1038/srep25313

Lian, B., Chen, Y., Zhu, L., and Yang, R. (2008). Progress in the study of the weathering of carbonate rock by microbes. *Earth Sci. Front.* 15, 90–99.

Lombard, L., Van Der Merwe, A., Groenewald, J. Z., and Crous, P. W. (2014). Lineages in *Nectriaceae*: re-evaluating the generic status of *Ilyonectria* and allied genera. *Phytopathol. Mediterr.* 53, 515–532. doi: 10.14601/Phytopathol_Mediterr-14976

Lombard, L., Van der Merwe, N., Groenewald, J., and Crous, P. W. (2015). Generic concepts in *Nectriaceae*. *Stud. Mycol.* 80, 189–245. doi: 10.1016/j.simyco.2014.12.002

Loni, P. C., Wu, M., Wang, W., Wang, H., Ma, L., Liu, C., et al. (2020). Mechanism of microbial dissolution and oxidation of antimony in stibnite under ambient conditions. *J. Hazard. Mater.* 385:121561. doi: 10.1016/j.jhazmat.2019.121561

Ma, B., Wang, H., Dsouza, M., Lou, J., He, Y., Dai, Z., et al. (2016). Geographic patterns of co-occurrence network topological features for soil microbiota at continental scale in eastern China. *ISME J.* 10, 1891–1901. doi: 10.1038/ismej.2015.261

Ma, L., Huang, X., Wang, H., Yun, Y., Cheng, X., Liu, D., et al. (2021). Microbial interactions drive distinct taxonomic and potential metabolic responses to habitats in karst cave ecosystem. *Microbiol. Spectr.* 9:e011521. doi: 10.1128/spectrum.01152-21.

Ma, Y., Zhang, H., Du, Y., Tian, T., Xiang, T., Liu, X., et al. (2015). The community distribution of bacteria and fungi on ancient wall paintings of the Mogao Grottoes. *Sci. Rep.* 5:7752. doi: 10.1038/srep07752

Man, B., Wang, H., Xiang, X., Wang, R., Yun, Y., and Gong, L. (2015). Phylogenetic diversity of culturable fungi in the Heshang Cave, central China. *Front. Microbiol.* 6:1158. doi: 10.3389/fmicb.2015.01158

Manimaran, M., and Kannabiran, K. (2017). Actinomycetes-mediated biogenic synthesis of metal and metal oxide nanoparticles: progress and challenges. *Lett. Appl. Microbiol.* 64, 401–408. doi: 10.1111/lam.12730

Marshall, K. T., and Morris, R. M. (2013). Isolation of an aerobic sulfur oxidizer from the SUP05/Arctic96BD-19 clade. *ISME J.* 7, 452–455. doi: 10.1038/ismej.2012.78

Mazina, S., Kozlova, E., Popkova, A., Kochetkov, S., Mannapova, R., and Yakushev, A. (2020). A first assessment of the microbiota of Taurida Cave. *Ecol. Montenegrina* 37, 1–10. doi: 10.37828/em.2020.37.1

Miadlikowska, J., Kauff, F., Hofstetter, V., Fraker, E., Grube, M., Hafellner, J., et al. (2006). New insights into classification and evolution of the Lecanoromycetes (Pezizomycotina, Ascomycota) from phylogenetic analyses of three ribosomal RNA-and two protein-coding genes. *Mycologia* 98, 1088–1103. doi: 10.1080/15572536.2006.11832636

Nilsson, R. H., Larsson, K. H., Taylor, A. F. S., Bengtsson-Palme, J., Jeppesen, T. S., Schigel, D., et al. (2019). The UNITE database for molecular identification of fungi: handling dark taxa and parallel taxonomic classifications. *Nucleic Acids Res.* 47, D259–D264. doi: 10.1093/nar/gky1022

Ningthoujam, D. S., Sanasam, S., and Mutum, A. (2012). Characterization of p-nitrophenol degrading actinomycetes from Hundung limestone deposits in Manipur, India. *Afr. J. Biotechnol.* 11, 10210–10220. doi: 10.5897/ajb11.4123

O'Donnell, K., Sutton, D. A., Rinaldi, M. G., Sarver, B. A., Balajee, S. A., Schroers, H. J., et al. (2010). Internet-accessible DNA sequence database for identifying fusaria from human and animal infections. *J. Clin. Microbiol.* 48, 3708–3718. doi: 10.1128/jcm.00989-10

Ogórek, R., Lejman, A., and Matkowski, K. (2013). Fungi isolated from Niedźwiedzia cave in Kletno (lower Silesia, Poland). *Int. J. Speleol.* 42, 161–166. doi: 10.5038/1827-806x.42.2.9

Oliveira, M., Ribeiro, H., and Abreu, I. (2005). Annual variation of fungal spores in atmosphere of Porto: 2003. *Ann. Agric. Environ. Med.* 12, 309–315.

Ortiz, M., Neilson, J. W., Nelson, W. M., Legatzki, A., Byrne, A., Yu, Y., et al. (2013). Profiling bacterial diversity and taxonomic composition on speleothem surfaces in Kartchner Caverns, AZ. *Microb. Ecol.* 65, 371–383. doi: 10.1007/s00248-012-0143-6

Palmer, A. N. (1991). Origin and morphology of limestone caves. *Geol. Soc. Am. Bull.* 103, 1–21.

Pape, R., and OConnor, B. (2014). Diversity and ecology of the macro-invertebrate fauna (Nemata and Arthropoda) of Kartchner Caverns, Cochise County, Arizona, United States of America. *Check List* 10:761. doi: 10.15560/10.4.761

Pfendler, S., Karimi, B., Alaoui-Sosse, L., Bousta, F., Alaoui-Sossé, B., Abdel-Daim, M. M., et al. (2019). Assessment of fungi proliferation and diversity in cultural heritage: reactions to UV-C treatment. *Sci. Total Environ.* 647, 905–913. doi: 10.1016/j.scitotenv.2018.08.089

Polymenakou, P. N., Mandalakis, M., Stephanou, E. G., and Tselepides, A. (2008). Particle size distribution of airborne microorganisms and pathogens during an intense African dust event in the eastern Mediterranean. *Environ. Health Perspect.* 116, 292–296. doi: 10.1289/ehp.10684

Ponizovskaya, V. B., Rebrikova, N. L., Kachalkin, A. V., Antropova, A. B., Bilanenko, E. N., and Mokeeva, V. L. (2019). Micromycetes as colonizers of mineral building materials in historic monuments and museums. *Fungal Biol.* 123, 290–306. doi: 10.1016/j.funbio.2019.01.002

Popović, S., Subakov Simić, G., Stupar, M., Unković, N., Predojević, D., Jovanović, J., et al. (2015). Cyanobacteria, algae and microfungi present in biofilm from Božana Cave (Serbia). *Int. J. Speleol.* 44:4. doi: 10.5038/1827-806x.44.2.4

Purahong, W., Wubet, T., Krüger, D., and Buscot, F. (2018). Molecular evidence strongly supports deadwood-inhabiting fungi exhibiting unexpected tree species preferences in temperate forests. *ISME J.* 12, 289–295. doi: 10.1038/ismej.2017.177

Quintero, E., Rivera-Mariani, F., and Bolaños-Rosero, B. (2010). Analysis of environmental factors and their effects on fungal spores in the atmosphere of a tropical urban area (San Juan, Puerto Rico). *Aerobiologia* 26, 113–124. doi: 10.1007/s10453-009-9148-0

Ren, G., Yan, Y., Nie, Y., Lu, A., Wu, X., Li, Y., et al. (2019). Natural extracellular electron transfer between semiconducting minerals and electroactive bacterial communities occurred on the rock varnish. *Front. Microbiol.* 10:293. doi: 10.3389/fmicb.2019.00293

Reyes, I., Valery, A., and Valduz, Z. (2007). "Phosphate-solubilizing microorganisms isolated from rhizospheric and bulk soils of colonizer plants at an abandoned rock phosphate mine," in *First International Meeting on Microbial Phosphate Solubilization*, eds E. Velázquez and C. Rodríguez-Barrueco (Dordrecht: Springer), 69–75.

Rogers, J. R., and Bennett, P. C. (2004). Mineral stimulation of subsurface microorganisms: release of limiting nutrients from silicates. *Chem. Geol.* 203, 91–108. doi: 10.1016/j.chemgeo.2003.09.001

Ruibal, C., Gueidan, C., Selbmann, L., Gorbushina, A., Crous, P., Groenewald, J., et al. (2009). Phylogeny of rock-inhabiting fungi related to *Dothideomycetes*. *Stud. Mycol.* 64, 123–133. doi: 10.3114/sim.2009.64.06

Samuels, G. J., and Blackwell, M. (2001). "Pyrenomycetes—fungi with perithecia," in *Systematics and Evolution*, eds D. J. McLaughlin, E. G. McLaughlin, and P. A. Lemke (Heidelberg: Springer), 221–255.

Schada von Borzyskowski, L. S., Severi, F., Krüger, K., Hermann, L., Gilardet, A., Sippel, F., et al. (2019). Marine *Proteobacteria* metabolize glycolate via the β-hydroxyaspartate cycle. *Nature* 575, 500–504. doi: 10.1038/s41586-019-1748-4

Schubert, T., Kallscheuer, N., Wiegand, S., Boedeker, C., Peeters, S. H., Jogler, M., et al. (2020). *Calycomorphotria hydatis* gen. nov., sp. nov., a novel species in the family *Planctomycetaceae* with conspicuous subcellular structures. *Antonie van Leeuwenhoek* 113, 1877–1887. doi: 10.1007/s10482-020-01419-0

Shaffer, J. P., Sarmiento, C., Zalamea, P. C., Gallery, R. E., Davis, A. S., Baltrus, D. A., et al. (2016). Diversity, specificity, and phylogenetic relationships of endohyphal bacteria in fungi that inhabit tropical seeds and leaves. *Front. Ecol. Evol.* 4:116. doi: 10.3389/fevo.2016.00116

Shaffer, J. P., U'ren, J. M., Gallery, R. E., Baltrus, D. A., and Arnold, A. E. (2017). An endohyphal bacterium (*Chitinophaga*, *Bacteroidetes*) alters carbon source use by *Fusarium keratoplasticum* (*F. solani* species complex, Nectriaceae). *Front. Microbiol.* 8:350. doi: 10.3389/fmicb.2017.00350

Shapleigh, J. P. (2011). Oxygen control of nitrogen oxide respiration, focusing on α-*proteobacteria*. *Biochem. Soc. Trans.* 39, 179–183. doi: 10.1042/bst0390179

Shi, L., Dong, H., Reguera, G., Beyenal, H., Lu, A., Liu, J., et al. (2016). Extracellular electron transfer mechanisms between microorganisms and minerals. *Nat. Rev. Microbiol.* 14, 651–662. doi: 10.1038/nrmicro.2016.93

Shi, S., Nuccio, E. E., Shi, Z. J., He, Z., Zhou, J., and Firestone, M. K. (2016). The interconnected rhizosphere: high network complexity dominates rhizosphere assemblages. *Ecol. Lett.* 19, 926–936. doi: 10.1111/ele.12630

Sorokin, D. Y., Vejmelkova, D., Lücker, S., Streshinskaya, G. M., Rijpstra, W. I. C., Damste, J. S. S., et al. (2014). *Nitrolancea hollandica* gen. nov., sp. nov., a chemolithoautotrophic nitrite-oxidizing bacterium isolated from a bioreactor

belonging to the phylum Chloroflexi. *Int. J. Syst. Evol. Microbiol.* 64, 1859–1865. doi: 10.1099/ijs.0.062232-0

Stegen, J. C., Lin, X., Fredrickson, J. K., Chen, X., Kennedy, D. W., Murray, C. J., et al. (2013). Quantifying community assembly processes and identifying features that impose them. *ISME J.* 7, 2069–2079. doi: 10.1038/ismej.2013.93

Stegen, J. C., Lin, X., Konopka, A. E., and Fredrickson, J. K. (2012). Stochastic and deterministic assembly processes in subsurface microbial communities. *ISME J.* 6, 1653–1664. doi: 10.1038/ismej.2012.22

Suphaphimol, N., Suwannarach, N., Purahong, W., Jaikang, C., Pengpat, K., Semakul, N., et al. (2022). Identification of microorganisms dwelling on the 19th century Lanna mural paintings from Northern Thailand using culture-dependent and-independent approaches. *Biology* 11:228. doi: 10.3390/biology11020228

Tedersoo, L., Bahram, M., Põlme, S., Kõljalg, U., Yorou, N. S., Wijesundera, R., et al. (2014). Global diversity and geography of soil fungi. *Science* 346:1256688. doi: 10.1126/science.1256688

Tomczyk-Żak, K., Kaczanowski, S., Drewniak, Ł., Dmoch, Ł., Sklodowska, A., and Zielenkiewicz, U. (2013). Bacteria diversity and arsenic mobilization in rock biofilm from an ancient gold and arsenic mine. *Sci. Total Environ.* 461, 330–340. doi: 10.1016/j.scitotenv.2013.04.087

Tomczyk-Żak, K., and Zielenkiewicz, U. (2016). Microbial diversity in caves. *Geomicrobiol. J.* 33, 20–38. doi: 10.1080/01490451.2014.1003341

Trovão, J., Portugal, A., Soares, F., Paiva, D. S., Mesquita, N., Coelho, C., et al. (2019). Fungal diversity and distribution across distinct biodeterioration phenomena in limestone walls of the old cathedral of Coimbra, UNESCO World Heritage Site. *Int. Biodeterior. Biodegrad.* 142, 91–102. doi: 10.1016/j.ibiod.2019.05.008

Vaughan, M. J., Nelson, W., Soderlund, C., Maier, R. M., and Pryor, B. M. (2015). Assessing fungal community structure from mineral surfaces in Kartchner Caverns using multiplexed 454 pyrosequencing. *Microb. Ecol.* 70, 175–187. doi: 10.1007/s00248-014-0560-9

Wegener, K. M., Singh, A. K., Jacobs, J. M., Elvitigala, T., Welsh, E. A., Keren, N., et al. (2010). Global proteomics reveal an atypical strategy for carbon/nitrogen assimilation by a cyanobacterium under diverse environmental perturbations. *Mol. Cell. Proteomics* 9, 2678–2689. doi: 10.1074/mcp.m110.000109

Wickham, H., Chang, W., and Wickham, M. H. (2016). *Package 'ggplot2'. Create Elegant Data Visualisations Using the Grammar of Graphics*. Available online at: https://cran.r-project.org/web/packages/ggplot2/index.html [accessed on May 3, 2022].

Wiegand, S., Jogler, M., and Jogler, C. (2018). On the maverick Planctomycetes. *FEMS Microbiol. Rev.* 42, 739–760. doi: 10.1093/femsre/fuy029

Wink, J., Kroppenstedt, R. M., Seibert, G., and Stackebrandt, E. (2003). *Actinomadura namibiensis* sp. nov. *Int. J. Syst. Evol. Microbiol.* 53, 721–724. doi: 10.1099/ijs.0.02286-0

Wu, Y., Tan, L., Liu, W., Wang, B., Wang, J., Cai, Y., et al. (2015). Profiling bacterial diversity in a limestone cave of the western Loess Plateau of China. *Front. Microbiol.* 6:244. doi: 10.3389/fmicb.2015.00244

Yang, C., and Sun, J. (2020). Soil salinity drives the distribution patterns and ecological functions of fungi in saline-alkali land in the Yellow River Delta, China. *Front. Microbiol.* 11:594284. doi: 10.3389/fmicb.2020.594284

Yun, Y., Wang, H., Man, B., Xiang, X., Zhou, J., Qiu, X., et al. (2016). The relationship between pH and bacterial communities in a single karst ecosystem and its implication for soil acidification. *Front. Microbiol.* 7:1955. doi: 10.3389/fmicb.2016.01955

Zeng, Y., Selyanin, V., Lukeš, M., Dean, J., Kaftan, D., Feng, F., et al. (2015). Characterization of the microaerophilic, bacteriochlorophyll a-containing bacterium *Gemmatimonas phototrophica* sp. nov., and emended descriptions of the genus *Gemmatimonas* and *Gemmatimonas aurantiaca*. *Int. J. Syst. Evol. Microbiol.* 65, 2410–2419. doi: 10.1099/ijs.0.000272

Zhang, H., Sekiguchi, Y., Hanada, S., Hugenholtz, P., Kim, H., Kamagata, Y., et al. (2003). *Gemmatimonas aurantiaca* gen. nov., sp. nov., a Gram-negative, aerobic, polyphosphate-accumulating micro-organism, the first cultured representative of the new bacterial phylum *Gemmatimonadetes* phyl. nov. *Int. J. Syst. Evol. Microbiol.* 53, 1155–1163. doi: 10.1099/ijs.0.02520-0

Zhang, N., and Wang, Z. (2015). "3 Pezizomycotina: Sordariomycetes and Leotiomycetes," in *Systematics and Evolution*, eds D. McLaughlin and J. Spatafora (Heidelberg: Springer), 57–88.

Zhang, X., Ge, Q., Zhu, Z., Deng, Y., and Gu, J. D. (2018). Microbiological community of the Royal Palace in Angkor Thom and Beng Mealea of Cambodia by Illumina sequencing based on 16S rRNA gene. *Int. Biodeterior. Biodegrad.* 134, 127–135. doi: 10.1016/j.ibiod.2018.06.018

Zhang, Z., Liu, F., Zhou, X., Liu, X., Liu, S., and Cai, L. (2017). Culturable mycobiota from karst caves in China, with descriptions of 20 new species. *Persoonia* 39, 1–31. doi: 10.3767/persoonia.2017.39.01

Zhang, Z. F., and Cai, L. (2019). Substrate and spatial variables are major determinants of fungal community in karst caves in Southwest China. *J. Biogeogr.* 46, 1504–1518. doi: 10.1111/jbi.13594

Zhao, R., Wang, H., Cheng, X., Yun, Y., and Qiu, X. (2018). Upland soil cluster γ dominates the methanotroph communities in the karst Heshang Cave. *FEMS Microbiol. Ecol.* 94:fiy192. doi: 10.1093/femsec/fiy192

Zhou, J., Wang, H., Cravotta, I. I. I. C. A., Dong, Q., and Xiang, X. (2017). Dissolution of fluorapatite by *Pseudomonas* fluorescens P35 resulting in fluorine release. *Geomicrobiol. J.* 34, 421–433. doi: 10.1080/01490451.2016.1204376

Zhu, H. Z., Zhang, Z. F., Zhou, N., Jiang, C. Y., Wang, B. J., Cai, L., et al. (2019). Diversity, distribution and co-occurrence patterns of bacterial communities in a karst cave system. *Front. Microbiol.* 10:1726. doi: 10.3389/fmicb.2019.01726

Zhu, H. Z., Zhang, Z. F., Zhou, N., Jiang, C. Y., Wang, B. J., Cai, L., et al. (2021). Bacteria and metabolic potential in karst caves revealed by intensive bacterial cultivation and genome assembly. *Appl. Environ. Microbiol.* 87:e02440-20. doi: 10.1128/AEM.02440-20

Conflict of Interest: The authors declare that the research was conducted in the absence of any commercial or financial relationships that could be construed as a potential conflict of interest.

Publisher's Note: All claims expressed in this article are solely those of the authors and do not necessarily represent those of their affiliated organizations, or those of the publisher, the editors and the reviewers. Any product that may be evaluated in this article, or claim that may be made by its manufacturer, is not guaranteed or endorsed by the publisher.

frontiers | Frontiers in Microbiology

ORIGINAL RESEARCH
published: 01 July 2022
doi: 10.3389/fmicb.2022.933388

Biomineralization in Cave Bacteria—Popcorn and Soda Straw Crystal Formations, Morphologies, and Potential Metabolic Pathways

Keegan Koning[1‡], Richenda McFarlane[2‡], Jessica T. Gosse[2‡], Sara Lawrence[1], Lynnea Carr[1], Derrick Horne[3], Nancy Van Wagoner[4], Christopher N. Boddy[2] and Naowarat Cheeptham[1†]*

[1] Department of Biology, Faculty of Science, Thompson Rivers University, Kamloops, BC, Canada, [2] Department of Chemistry and Biomolecular Sciences, University of Ottawa, Ottawa, ON, Canada, [3] The University of British Columbia Bioimaging Facility, Biological Sciences Building, Vancouver, BC, Canada, [4] Department of Physical Sciences, Faculty of Science, Thompson Rivers University, Kamloops, BC, Canada

Caves are extreme, often oligotrophic, environments that house diverse groups of microorganisms. Many of these microbes can perform microbiologically induced carbonate precipitation (MICP) to form crystalline secondary cave deposits known as speleothems. The urease family is a group of enzymes involved in MICP that catalyze the breakdown of urea, which is a source of energy, into ammonia and carbonate. Carbonate anions are effluxed to the extracellular surface of the bacterium where it then binds to environmental calcium to form calcium carbonate which then continues to grow in crystal form. Here, we studied bacterial communities from speleothems collected from the Iron Curtain Cave (ICC) in Chilliwack, B.C., Canada, to characterize these organisms and determine whether urease-positive (U+) bacteria were present in the cave and their potential impact on speleothem formation. The ICC is a carbonate cave located on the northside of Chipmunk Ridge, presenting a unique environment with high iron content sediment and limestone structures throughout. With six pools of water throughout the cave, the environment is highly humid, with temperatures ranging between 4 and 12°C depending on the time of year. Ninety-nine bacterial strains were isolated from popcorn (PCS) and soda straw (SSS) speleothems. These isolates were screened for urease enzymatic activity, with 11 candidates found to be urease-positive. After incubation, species-specific crystal morphologies were observed. Popcorn speleothem provided more bacterial diversity overall when compared to soda straw speleothem when examined under a culture-based method. Nearly twice as many U+ isolates were isolated from popcorn speleothems compared to soda straw speleothems. The U+ candidates were identified to the genus level by 16S rRNA analysis, and two isolates underwent whole-genome sequencing. Two novel species were identified as *Sphingobacterium* sp. PCS056 and *Pseudarthrobacter* sp. SSS035. Both isolates demonstrated the most crystal production as well as the most morphologically dissimilar crystal shapes in broth culture and were found to produce

OPEN ACCESS

Edited by:
Cesareo Saiz-Jimenez, Institute of Natural Resources and Agrobiology of Seville (CSIC), Spain

Reviewed by:
Ilenia M. D'Angeli, University of Padua, Italy
Fernando Gazquez, University of Almería, Spain

***Correspondence:**
Naowarat Cheeptham
ncheeptham@tru.ca

†Present address:
Naowarat Cheeptham, Department of Microbiology and Immunology, University of British Columbia, Vancouver, BC, Canada

‡*These authors have contributed equally to this work*

Specialty section:
This article was submitted to Terrestrial Microbiology, a section of the journal Frontiers in Microbiology

Received: *30 April 2022*
Accepted: *25 May 2022*
Published: *01 July 2022*

Citation:
Koning K, McFarlane R, Gosse JT, Lawrence S, Carr L, Horne D, Van Wagoner N, Boddy CN and Cheeptham N (2022) Biomineralization in Cave Bacteria—Popcorn and Soda Straw Crystal Formations, Morphologies, and Potential Metabolic Pathways. Front. Microbiol. 13:933388. doi: 10.3389/fmicb.2022.933388

crystals as previously observed in both agar and broth media. The results from this study are consistent with the involvement of urease-positive bacteria isolated from the ICC in the formation of cave speleothems. 16S rRNA sequencing revealed a diverse set of microbes inhabiting the speleothems that have urease activity. Whole-genome sequencing of the two chosen isolates confirmed the presence of urease pathways, while revealing differences in urease pathway structure and number. This research contributes to understanding microbial-associated cave formation and degradation, with applications to cave conservation, microbiota composition, and their role in shaping the cave environment.

Keywords: cave microorganisms, cave microbiology, geomicrobiology, MICP, urease, biomineralization, speleothems, cave formation

INTRODUCTION

Caves are generally defined as areas of subterranean space which occur naturally in the environment and which are accessible by living organisms. Caves can be characterized by many variables; however, typically, they are classified by the type of rock and the formation process of the caves (Northup and Lavoie, 2001). Limestone caves are formed via acid dissolution, when groundwater flows through the soil and rock (vadose) layers, where it interacts with carbon dioxide (CO_2) gas and produces carbonic acid (H_2CO_3), which slowly dissolves the carbonate rock. In sulfuric acid dissolution, hydrogen sulfide (H_2S) gas rises from rock fissures (narrow openings of rocks, commonly found in tectonically active areas) and reacts with atmospheric oxygen to form sulfuric acid (H_2SO_4) that dissolves the carbonate rock to form caves (Palmer, 1991; Northup and Lavoie, 2001). Furthermore, decomposition of organic matter by microorganisms can be a source of sulfuric acid dissolution (Beolchini et al., 2017).

Of particular interest are limestone caves, which can be found throughout British Columbia, Canada (Pike et al., 2010). The Iron Curtain Cave (ICC) is a restricted-access cave located in the Chilliwack River Valley (CRV), British Columbia, Canada. The cave is hosted by the Chilliwack Group which includes Pennsylvanian Permian basic volcanic rocks, Jurassic pelite, sandstone, and limestone karst (Saunders et al., 1987). The ICC is decorated by several speleothems, including popcorn, soda straw, stalactites, stalagmites, and bacon strips, with a large curtain of iron-containing minerals which gave the cave its name. Cave temperature ranges between 4 and 12°C annually (Ghosh et al., 2017) with relative humidity at greater than 90% (Carlyle-Moses, personal correspondence 2018).

Though chemical mechanisms of cave formation and cave architecture have been well researched, more recent studies have been focused on the biological mechanisms of cave formation. Engel et al. (2004) demonstrated that microbial mats, containing species of the class Epsilonproteobacteria, could oxidize hydrogen sulfide (H_2S) into H_2SO_4, thus increasing the dissolution of limestone, while Barton et al. (2007) demonstrated that bacteria of the genus *Massilia* from a New Mexico cave system could utilize aqueous carbohydrates originating from surface water, to produce acids as a metabolic byproduct, dissolving carbonate bedrock in the caves.

Speleothems are distinct secondary cave mineral deposits/structures (Northup and Lavoie, 2001; Mason et al., 2016) that take many macroscopic and microscopic forms and are often composed of calcium carbonate polymorphs (Palmer, 1991; Baskar et al., 2014; Dhami et al., 2018). Speleothems are known to form by two mechanisms: abiotic (chemical) formation where water saturated with calcium interacts with dissolved organic carbon forming calcareous crystal structures (Dreybrodt, 1999; Banks et al., 2010; Szymczak and Ladd, 2011) and/or biotic formation by microorganisms that actively extrude carbonate extracellularly which then interacts with calcium saturated water to form calcareous crystal structures (Northup and Lavoie, 2001; Banks et al., 2010). As of 2001, there are 38 official speleothem types recognized by specialists at the forefront of speleology (Northup and Lavoie, 2001). Soda straw speleothems (SSS) precipitate from drip water points with water flowing down the center of the straw. At the tip of the straw, carbon dioxide (CO_2) degasses which can allow calcium carbonate precipitation (Paul et al., 2013). Popcorn speleothem (PCS) form on cave walls, stalagmites, and stalactites by the evaporation of water and when airflow is present (Warren et al., 1990). In this study, PCS and SSS speleothems were sampled to study their bacterial profile and its ability to biologically form crystal structures that contribute to cave formation and degradation. From this, 11 such isolates demonstrated various degrees of crystal production, with varying morphologies.

Microbially induced carbonate precipitation (MICP) is a form of biomineralization and is a natural process of carbonate precipitation, occurring worldwide and mediated primarily by bacteria. MICP occurs through three primary pathways: biologically induced mineralization (BIM), biologically mediated mineralization (BMM), or biologically controlled mineralization (BCM) (Castanier et al., 1999; Banks et al., 2010; Castro-Alonso et al., 2019; Seifan and Berenjian, 2019). Caves are often defined as oligotrophic and highly mineralized environments and can be further characterized as being devoid or nearly devoid of natural light (Cheeptham et al., 2013; Seifan and Berenjian, 2019). Due to these environmental pressures, bacteria utilize alternative pathways for energy production, and the ability for MICP to

occur depends on four variables: (1) The pH of the environment, (2) the abundance of nucleation sites, (3) the concentration of calcium ions, and (4) dissolved inorganic carbon (Chou et al., 2011; Seifan and Berenjian, 2019).

MICP is a well-documented metabolic process which contributes to the formation of secondary cave deposits known as speleothems (Castanier et al., 1999; Stocks-Fischer et al., 1999; Northup and Lavoie, 2001; Engel et al., 2004; Banks et al., 2010; Cheeptham et al., 2013). One common metabolic pathway that leads to MICP is the ureolysis pathway, where bacteria catalyze urea found in the environment, mediated by urease enzymes, producing carbonate as a byproduct. In this instance, the carbonate is secreted extracellularly, where it interacts with calcium ions that have adsorbed to the cell by the following chemical pathways (Northup and Lavoie, 2001; Ferris et al., 2003; Banks et al., 2010; Chou et al., 2011; Castro-Alonso et al., 2019):

$$CO(NH_2)_2 + H_2 \rightarrow NH_2COOH + NH_3$$

$$NH_2COOH + H_2O \rightarrow NH_3 + H_2CO_3$$

$$H_2CO_3 \leftrightarrow HCO_3^- + H^+$$

$$2NH_3 + 2H_2O \rightarrow 2NH_4^+ + 2OH$$

$$HCO_3^- + H^+ + 2NH_4^+ + 2OH \rightarrow (CO_3)^{2-} + 2NH_4^+ + 2H_2O$$

$$Ca^{2+} + Cell\ Surface \rightarrow Cell\ Surface - Ca^{2+}$$

$$Cell\ Surface - Ca^{2+} + (CO_3)^{2-} \rightarrow Cell - CaCO_3$$

When carbonate and calcium concentrations are at their saturation points, calcium carbonate crystals can form. The two most thermodynamically stable crystal structures common to MICP are aragonite and calcite (Stocks-Fischer et al., 1999; Hammes and Verstraete, 2002; Banks et al., 2010; Seifan and Berenjian, 2019) with vaterite acting as a metastable phase transient intermediate which favors the more stable aragonite and calcite (Christy, 2017). Bacteria that perform MICP then become self-fossilized and act as nucleation sites for further calcium carbonate crystal growth, which in turn aids in the process of speleothem formation (Palmer, 1991; Northup and Lavoie, 2001; Türkgenci and Dogruöz Güngör, 2011; Seifan and Berenjian, 2019; Lyu et al., 2021).

Urease enzymes are broadly distributed throughout the bacterial domain, always occurring as multimeric proteins with nickel incorporated into the enzyme structure (Mobley et al., 1995; Konieczna et al., 2013). Most bacteria have three different polypeptides making up the urease enzyme, with different protein structures present in different organisms (Konieczna et al., 2013). In many bacterial species, the alpha, beta, and gamma subunits encoded by genes *ureA, ureB,* and *ureC* form a trimer of trimers (Benini et al., 1999). In addition, three accessory proteins, UreD, UreF, and UreG, are urease molecular chaperones that are dependent on GTP binding and hydrolysis by UreG (Soriano and Hausinger, 1999), while a fourth accessory protein, UreE, coordinates nickel in the active site of the enzyme (Colpas and Hausinger, 2000; Soriano et al., 2000; Mulrooney et al., 2005).

This study aimed to determine whether cave bacteria isolated from popcorn and soda straw speleothems were involved in MICP and to simulate crystal production and speleothem formation in the lab setting. This evidence demonstrates that these isolated cave bacteria are mainly involved in and contribute to the growth of cave speleothems. In addition, based on analysis of the genome to determine urease enzyme copies present, we sought to connect the ureolytic pathway to microbially induced carbonate precipitation for these cave bacteria and determine which strains have a more prominent role in shaping the cave environment.

MATERIALS AND METHODS

Sample Collection

Samples were collected from two distinct areas of the ICC as shown in **Supplementary Figure 1**. PCS and SSS samples were collected into 50 mL conical tubes. PCS samples were scraped into the tubes using a sterilized scoopula, while SSS was collected by gently breaking off a speleothem into the tube with sterilized forceps. Temperature readings were taken at each sample site ranging from 8.8 to 9.4°C. Examples of the speleothems collected within the cave can be found in **Supplementary Figure 2**.

Bacterial Isolation

Fresh PCS and SSS samples were weighed to a wet weight of 1 g. Each speleothem was then transferred to a sterilized mortar and pestle and ground to a paste. The paste was transformed into a slurry by adding 2 mL of distilled H_2O. The slurry was transferred to a 2.5-mL microfuge tube. Microfuge tubes were closed and hand-shaken for 2 min. Microfuge tubes were then placed in a rotating incubator at 9°C set to 100 revolutions per minute (RPM) for 1 h. Samples were removed from the rotating incubator and left to stand for 5 min. A series of serial dilutions ($\log_{10}$) were performed with sequential dilutions ranging from 10^0 through to 10^{-4}. For each dilution, 100 μL of the sample was pipetted and spread onto 22-mL agar plates (in triplicate) of the following media types: nutrient agar (NA), ten times diluted nutrient agar (d_{10}NA), and Reasoner's 2-A agar (R2A). Plates were then left to dry before incubation at 9°C until distinguishable colonies had formed.

Bioprecipitation and Urease Activity

B4 precipitation medium (Boquet et al., 1973) was used with specific modifications which included substituting the source of calcium from the original calcium acetate [$Ca(C_2H_3O_2)_2$] to one of the following: calcium nitrate ($CaNO_3$), calcium citrate [$Ca_3(C_6H_5O_7)_2$], and calcium chloride ($CaCl_2$) all at 0.25% w/v. The modification of the calcium salt component

of the B4 medium aimed to test calcium water solubility and the availability of aqueous calcium ions to interact with precipitated carbonate on the extracellular surface of the bacterial isolates, that is, to determine whether one calcium salt increased the rate of biocrystallization, over another. Each isolated bacterium was then inoculated onto the modified B4 agar medium in 33 mm thick agar plates, to prevent premature drying due to lengthy incubation period. A container of diH_2O water was placed in the incubator to increase humidity. Modified B4 plates were inoculated, streaking one isolated colony from each of the pure culture plates (NA, R2A, d_{10}NA). Plates were inverted and incubated at 9°C until crystals formed.

To determine urease activity, solid agar slants were prepared and poured following the manufacturer's instructions [BBLTM Urea Agar Base Concentrate 10× (BD, Franklin Lakes, New Jersey, United States]. Urea base concentrate was filtered through a 0.22 μm polyethersulfone (PES) filter to a final volume of 5.0 mL using an Omnispense pump (Thermo Fisher, Waltham, United States). Inoculated slants were incubated at 9°C until bacterial growth was observed. Isolates demonstrating urease activity were then inoculated onto 114 mm plates containing modified B4 media. Plates were inverted and incubated at 9°C. Daily observation occurred for the first 30 days and then weekly for a further 9 weeks until crystals were detected.

To determine crystal formation in an aqueous environment, 40.0 mL of MICP broth [0.25% $Ca(C_2H_3O_2)_2$, 0.5% dextrose, 0.0–0.4% urea and/or yeast extract w/v, pH 8.0] was made for each U+ candidate with the introduction of urea (1 M) as a nitrogen source over a concentration-dependent manner, substituting yeast extract. U+ candidates were grown in liquid B4 precipitation medium until reached log phase (∼1.0 A600 nm) and inoculated. Incubation conditions remained the same. After 12 weeks of incubation, the broth cultures were slowly poured off, laid flat, and placed on the viewing platform of a stereomicroscope (Kyowa Optical Sdz-Pl Zoom Microscope, Tokyo, Japan). Crystals were imaged at 40× using an iPhone 11 Pro (Apple Inc. Cupertino, United States).

Petrographic and Scanning Electron Microscopy

Photomicrographs of closed 90-mL agar plates were taken using a Leica DMV6 digital microscope fitted with a Leica PlanApo FOV 12.55 mid-magnification objective that has a maximum field of view of 12.55 mm, magnification range from 46× to 675×, and working distance up to 33 mm (Leica, Germany).

Popcorn and soda straw speleothem samples were sent to the BioImaging Facility at the University of British Columbia, Vancouver, Canada for Scanning Electron Microscopy (SEM). Samples were freeze-dried and osmium-fumed in their storage tubes for approximately 1 h, and then transferred to polypropylene petri dishes with a saturated filter paper (4% w/v OSO_4 aqueous solution) and 16% v/v formaldehyde (∼ 0.5 mL not touching the sample) for another 2 h. The samples were inverted after 1 h and further osmium-fumed over 48 h. Then, samples were mounted using a bulk sample holder and coated with 12 nm of gold using a Cressington 208 HR sputter coater (Cressington, Watford, United Kingdom). Samples were then imaged at various accelerating voltages, modes, and working distances on a Hitachi S4700 FESEM (Hitachi, Tokyo, Japan).

Genetic Identification and Whole-Genome Sequencing

16s rRNA identification was performed by heating a single colony of each urease-positive isolate in 10 μL of nuclease-free water at 95°C for 10 min and using 2 μL of the resulting lysate for PCR amplification. An amplicon of approximately 570 bp was amplified using 1.25 U *Taq* DNA Polymerase (New England Biolabs), 0.5 mM dNTPs, 0.16 mM bovine serum albumin, 0.5 μM forward primer 5′-GTG CCA GCM GCN GCG G, and 0.5 μM reverse primer 5′-GGG TTN CGN TCG TTG. Cycling conditions were 95°C for 2 min, 25 cycles of 95°C for 1 min, 68°C for 45 s, and 68°C for 45 s, with final elongation at 68°C for 5 min. The resulting PCR product was Sanger-sequenced at Génome Québec (Montréal, Quebec, Canada). The sequencing results were trimmed, and genus-level identification was performed using NCBI Blast (Altschul et al., 1990), with one isolate identified to species level.

Two isolates with strong urease activity and observed carbonate-precipitation ability were selected for whole-genome sequencing (WGS). WGS was performed by Integrated Microbiome Technologies (Halifax, Nova Scotia, Canada) on the PacBio Sequel II instrument. Genome analyses were performed in the Galaxy platform (Afgan et al., 2018). Genomes were assembled using Flye Version 2.6 (Lin et al., 2016) and annotated using PATRIC Version 3.6.12 (Brettin et al., 2015). Quast Version 5.0.2 (Mikheenko et al., 2018) was used to analyze the quality of the assembled genome. PubMLST (accessed March 20, 2022) was then used to confirm genus-level identifications of the two isolates (Jolley et al., 2018).

Chemical Analysis of Speleothems by Inductively Coupled Plasma Mass Spectrometry

Both PCS and SSS were ground into a slurry to determine their relative pH. Speleothem samples were ground using a sterile mortar and pestle into a fine powder (for SSS) and a wet slurry (for PCS). To the ground, SSS was added 6 mL of diH_2O to form a slurry of similar consistency to PCS. Speleothem pH was determined using a FieldScout SoilStik pH meter (Spectrum Technologies, United States). SSS and PCS were also ground into fine powder and shipped to ALS Global Laboratories to perform inductively coupled plasma mass spectrometry (ICP-MS) total elemental analysis of sixteen elements, including biologically relevant elements such as magnesium and calcium.

RESULTS

Isolation, Bioprecipitation, and Urease Activity

A total of 99 isolates were grown successfully in the lab setting. A total of four SSS isolates and seven PCS isolates exhibited urease activity of varying degrees while incubating at 9°C. The 11 total urease-positive isolates, henceforth known as U+ candidates, represent 8.2% of culturable sample size. **Table 1** summarizes urease-positive candidates by showing how quickly the urea media changed color to intense pink, an indicator of increasing alkalinity. Isolates which had marginal urease activity were denoted as "+" (color change occurred 3–5 days post-inoculation), isolates with sufficient urease activity were denoted as "++" (color change occurred 2–3 days post-inoculation), and samples with generous urease activity were denoted as "+++" (color change occurred 0–1 days post-inoculation).

After 62 days from incubation, agar plates inoculated with U+ candidates demonstrated crystal formation on three of the four modified B4 media types. U+ candidates from both PCS and SSS grew on all media types; however, no growth was detected on B4 agar plates supplemented with calcium acetate for SSS U+ candidates only. Both PCS and SSS U+ candidates demonstrated crystal formations with varying morphologies. For the aqueous B4 experiment, broth cultures revealed crystal formations on the inside face of test tubes of three PCS and one SSS U+ candidates, respectively. For both the agar plate and aqueous B4 assays, U+ candidates, similar crystal morphologies, were seen, as demonstrated in **Figure 1**. SSS035 and PCS056 were chosen for whole-genome sequencing (WGS) based on their increased urease activity.

TABLE 1 | Isolate designation, preliminary identification using 16S rRNA analysis, and urease activity.

Isolate Designation	Preliminary characterization	Activity
SSS006	*Sporosarcina* sp.	++
SSS031	*Arthrobacter* sp.	+++
SSS032	*Arthrobacter* sp.	+++
SSS035	*Pseudarthrobacter* sp.	+++
PCS003	*Sphingobacterium anheuense*	++
PCS018	*Sphingobacterium* sp.	+
PCS039	*Streptomyces* sp.	++
PCS042	–	+++
PCS049	*Streptomyces* sp.	+++
PCS054	*Variovorax* sp.	++
PCS056	*Sphingobacterium* sp.	+++

Isolates which had marginal urease activity were denoted as "+" (color change occurred 3–5 days post-inoculation), isolates with sufficient urease activity were denoted as "++" (color change occurred 2–3 days post-inoculation), and samples with generous urease activity were denoted as "+++" (color change occurred 0–1 days post-inoculation).

Scanning Electron and Petrographic Microscopy

A total of six micrographs were produced for both PCS and SSS by the Bioimaging Facility at the University of British Columbia (**Figure 2**). A total of eighty-two photomicrographs of SSS and PCS were taken with the petrographic microscope with an array of crystal structures, including rhombic and complex, as shown in **Figure 3**.

Whole-Genome Sequencing and Phylogenetic Analysis

Pseudarthrobacter sp. SSS035 and *Sphingobacterium* sp. PCS056 underwent WGS by PacBio Sequel II. The resulting reads were assembled using Flye and annotated using PATRIC. *Pseudarthrobacter* sp. SSS035 was assembled into three contigs with lengths of 4,611,850, 272,440, and 149,359 nucleotides. Average coverage of each contig was over 400×, with the average coverage of the three contigs being 537×. The total genome size was determined to be 5.03 Mbp and consisted of 64.86% GC content. PubMLST determined this isolate has an 82% match to *Pseudarthrobacter sulfonivorans,* indicating that this is likely a previously uncharacterized species of *Pseudarthrobacter.* Phylogenetic analysis of the most similar organisms by genome (**Figure 4**) associated the strain with *Arthrobacter* and *Pseudarthrobacter* species using NCBI Taxonomy tool (Schoch et al., 2020) was found in a diverse set of environments ranging from high humane activity areas such as coal mine and agricultural soil to wetlands on Tibetan Plateau lakes and

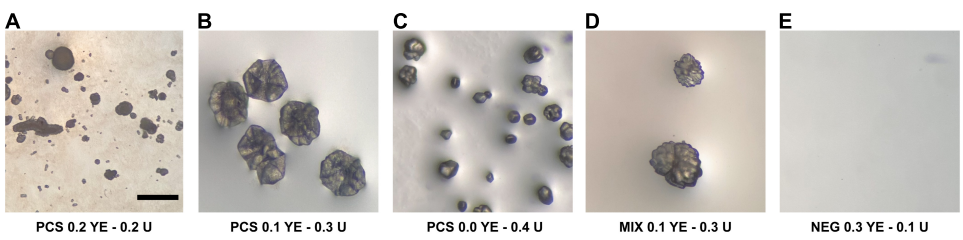

FIGURE 1 | Crystal-like formations observed in modified liquid B4 media inoculated with isolates from the soda straw and popcorn speleothems observed by a stereomicroscope. **(A)** PCS056 (*Sphingobacterium* sp.) supplemented with 0.2% w/w yeast extract (YE) and 0.2% w/w urea (U). **(B)** PCS056 supplemented with 0.1% w/w YE and 0.3% w/w U. **(C)** PCS-56 supplemented with 0.0% w/w YE and 0.4% w/w U. **(D)** Mixed culture of SSS006 (*Sporosarcina* sp.) and SSS035 (*Pseudarthrobacter* sp.) supplemented with 0.1% w/w YE and 0.3% w/w U. **(E)** Negative control supplemented with 0.3% YE and 0.1% U. All micrographs under 40× magnification.

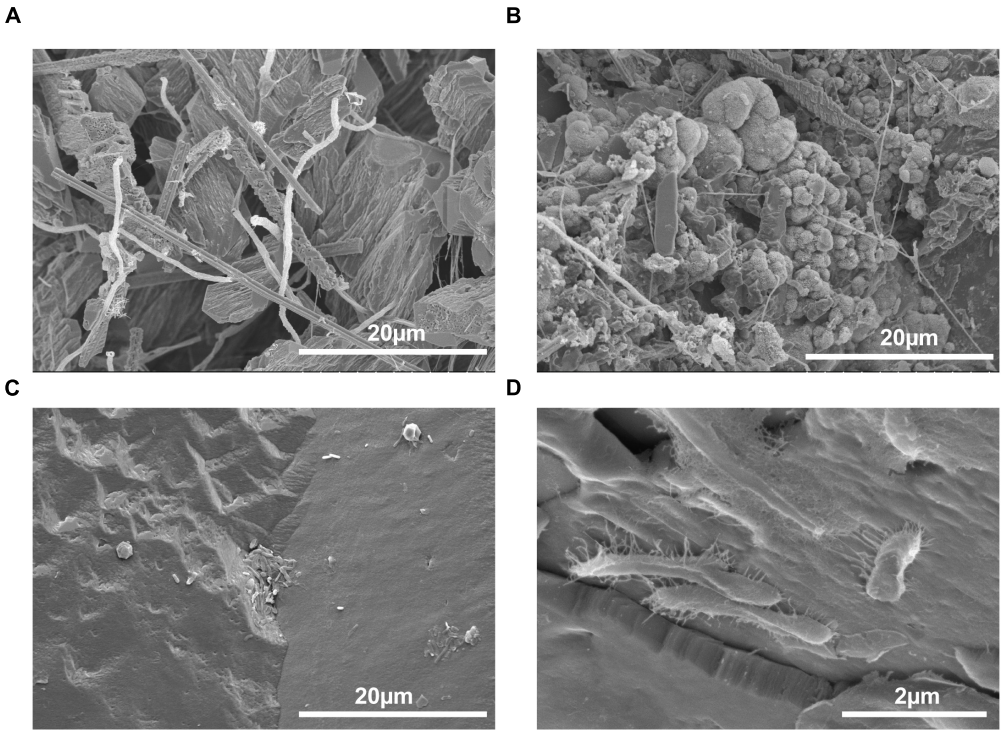

FIGURE 2 | Scanning electron micrographs of speleothems with an abundance and variety of microorganisms present. **(A)** Inside of a popcorn speleothem sample (1000×), **(B)** outside of a popcorn speleothem sample (2500×), **(C)** internal base of a soda straw speleothem (2500×), and **(D)** exterior surface of a soda straw speleothem (1500×).

tsunami-affected areas (Zhang et al., 2016; Park et al., 2019; Shen et al., 2021).

Sphingobacterium sp. PCS056 reads were assembled into a single contig with a length of 5,195,665 nucleotides with 36.78% GC content. Average coverage for this genome was 329×, and the genome was able to be circularized during assembly. PubMLST determined this isolate has an 80% match to *Sphingobacterium faecium*, also indicating the likelihood of a previously uncharacterized species. Phylogenetic analysis based on genome similarity (**Figure 5**) placed our isolate with other species of *Sphingobacterium* isolated from animal sources and agricultural soil such as pig pens and cow's milk (Almeida et al., 2014; Ghosh et al., 2014), being very distinct from soil sources observed for the previous isolate described and cave bacteria in general.

Genome annotation determined the presence of urease genes in each isolate (**Figure 6**). *Sphingobacterium* sp. PCS056 encodes the genes for alpha, beta, and gamma urease subunits, as well as the urease accessory proteins UreD, UreE, UreF, and UreG. Two gene clusters were observed, with similar genetic elements, but slightly different gene sizes. Upon further inspection, *Pseudarthrobacter* sp. SSS035 also has a full urease pathway encoding the same genes, running in the reverse sense. All gene clusters are 5 kb in size and are shown as a continuous pathway in *Pseudarthrobacter* sp. SSS035 as opposed to the ones observed in *Sphingobacterium* sp. PCS056, where an uncharacterized gene sequence is located in between *ureC* and *ureE*.

Chemical Analysis of Speleothems

Both PCS and SSS were pH-analyzed in triplicate. PCS was found to be slightly acidic with a mean pH of 6.67, while SSS was found to be alkaline with a mean pH of 9.25.

A total of fifteen biologically relevant elements were analyzed by ICP-MS and conducted by ALS Global commercial laboratory. **Table 2** summarizes the chemical profile of the samples. Of note, the largest elemental concentration among both SSS and PCS is calcium with concentrations of 411,000 mg/kg and 427,000 mg/kg, respectively. Further, nickel, which is responsible for binding urea and water in the active site of urease (Benini et al., 1999), was also present in both samples in concentrations of 1.88 mg/kg for SSS and 1.36 mg/mg for PCS.

DISCUSSION AND CONCLUSION

MICP is a general phenomenon demonstrated by bacteria among other microorganisms and is found in many habitats throughout the world. Though MICP as a process has been studied for over 20 years, research has focused on the ability for bacteria to precipitate calcium carbonate for use in biocements (Chou et al., 2011; Chu et al., 2012; Chaparro-Acuña et al., 2018; Seifan and Berenjian, 2019). However, research on bacterial-mediated MICP and how it plays an important role in shaping natural environments has focused mainly on terranean and subterranean soil studies. Research on MICP and how it contributes to cave

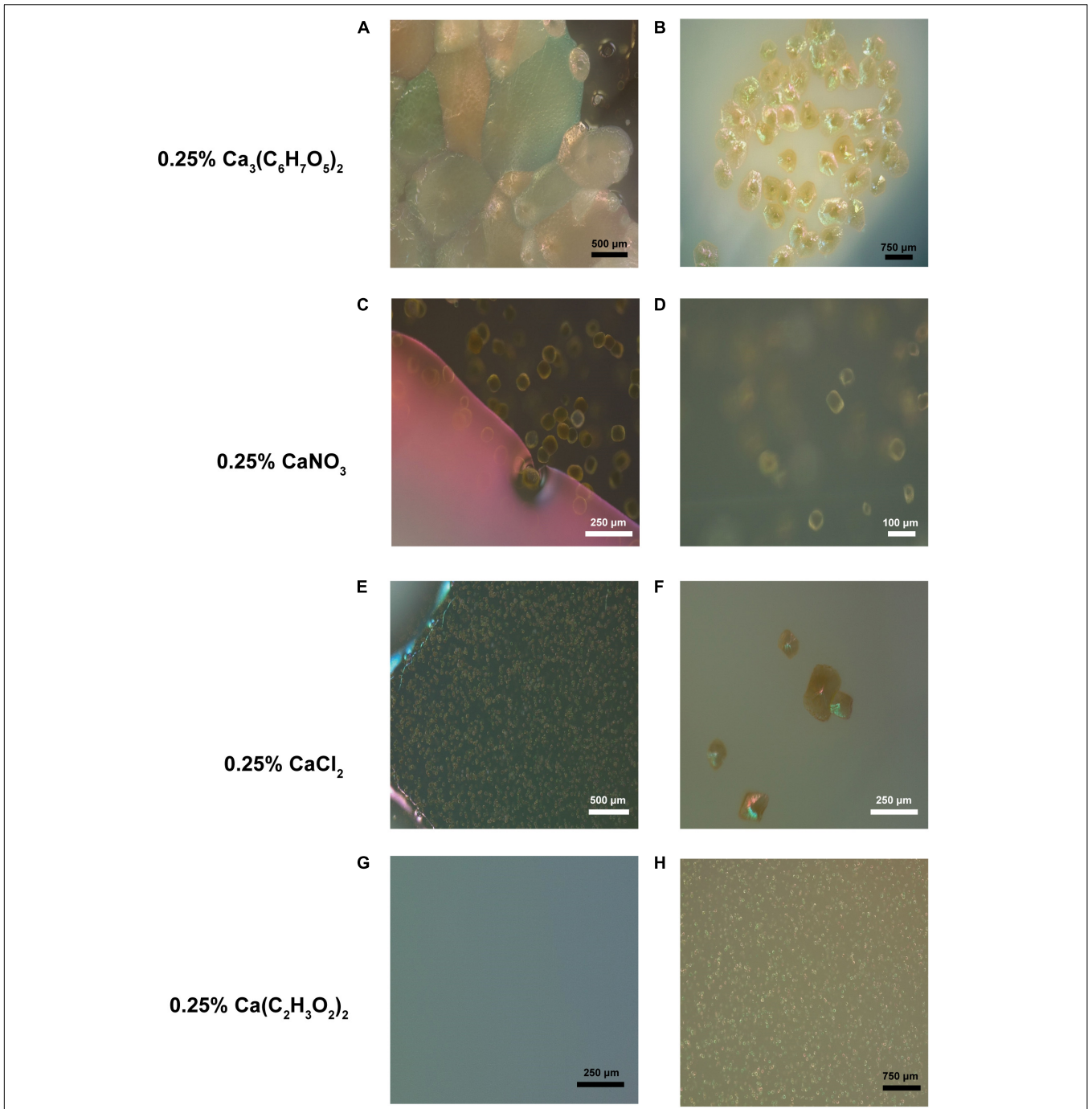

FIGURE 3 | Crystal-like formations observed in various B4 media inoculated with isolates from the soda straw and popcorn speleothems observed by a petrographic microscope. **(A)** Formations observed adjacent a bacterial colony in the media of a B4 calcium citrate medium plate (131×). **(B)** Formations observed on the surface of a bacterial colony on calcium citrate B4 medium (69×). **(C)** Formations observed adjacent a bacterial colony in the media of a B4 calcium nitrate medium plate (343×). **(D)** Magnified formation on same colony as C (452×). **(E)** Crystals observed in calcium chloride B4 medium (151×). **(F)** Formations observed on calcium chloride B4 medium (306×). **(G)** Uninoculated B4 acetate media plate as a negative control (222×). **(H)** Crystals observed in calcium acetate B4 medium (91×).

formations is still not well known. Identifying whether MICP-capable bacteria play a role in the formation of cave speleothems and whether they contribute to the vastly different macroscopic morphologies exhibited by speleothems will help improve our understanding of bacterial-mediated MICP in subterranean environments. With vastly different speleothem morphologies, it is wondered whether bacteria act as nucleation sites for crystal growth, thus producing different crystal growth patterns. Further,

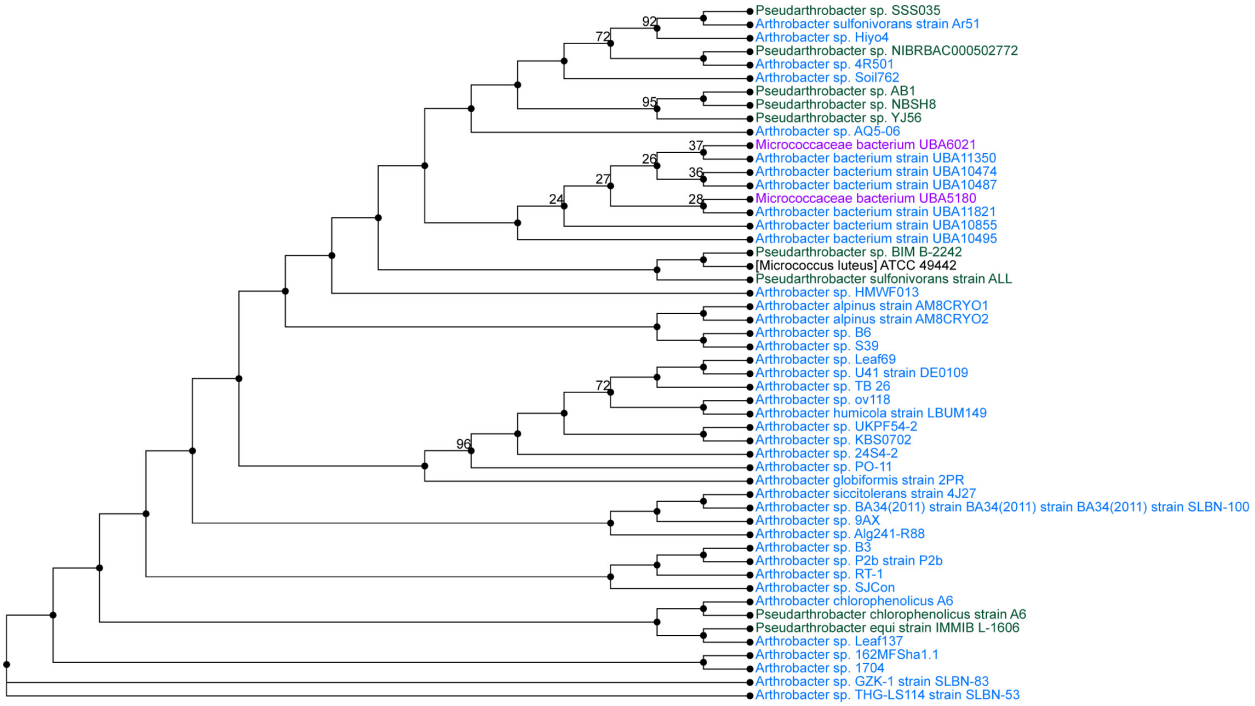

FIGURE 4 | Phylogenetic tree from maximum likelihood analysis of bacterial whole-genome sequence. The numbers in branch points denote confidence levels of the relationship of sequences determined by bootstrap statistical analysis. *Pseudarthrobacter sp.* SSS035 is grouped with *A. sulfonivorans* strain Ar51 with maximum confidence level of 92.

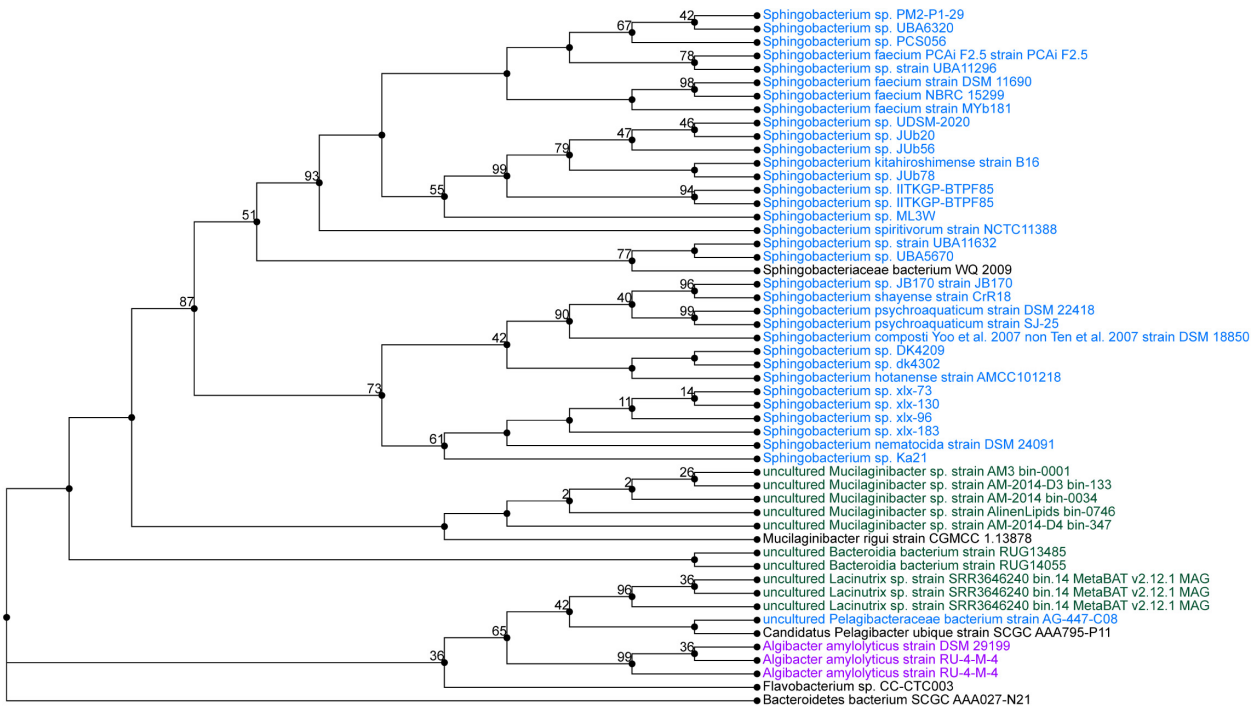

FIGURE 5 | Phylogenetic tree from maximum likelihood analysis of bacterial whole-genome sequence. The numbers in branch points denote confidence levels of the relationship of sequences determined by bootstrap statistical analysis. *Sphingobacterium PCS056* was aligned with other representatives of the genus *Sphingobacterium*, with a confidence level of 67.

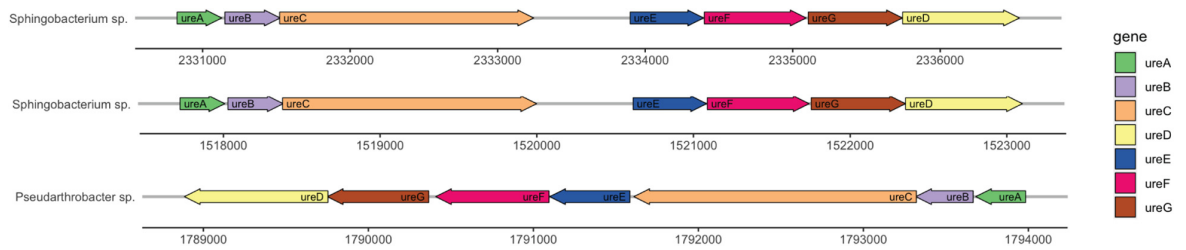

FIGURE 6 | Urease gene clusters of cave bacterial isolates show similar genetic features. *Sphingobacterium* sp. PCS056 encodes two copies of the urease pathway genes (*ureABCDEFG*), with similar orientation and gene sizes, and a hypothetical gene in between *ureC* and *ureD*, represented as a gap. *Pseudarthrobacter* sp. SSS035 also presents a continuous cluster in a reverse orientation.

TABLE 2 | ICP-MS chemical analyses of PCS and SSS extracted from the ICC reported as concentration (mg/kg).

Element	Popcorn	Soda straw
Aluminum (Al)	604.00	76.00
Barium (Ba)	12.70	16.30
Cadmium (Cd)	1.12	0.43
Calcium (Ca)	427000.00	411000.00
Chromium (Cr)	1.77	< 0.50
Cobalt (Co)	< 0.10	<0.10
Copper (Cu)	3.63	0.56
Iron (Fe)	308.00	184.00
Lead (Pb)	< 0.50	<0.50
Magnesium (Mg)	309.00	1060.00
Molybdenum (Mo)	0.13	0.18
Nickel (Ni)	1.36	1.88
Potassium (K)	< 100	<100
Sodium (Na)	< 50	64.00
Strontium (Sr)	23.80	63.20
Zinc (Zn)	3.10	2.20

with most speleothems being made of crystallized minerals, understanding how cave bacteria can survive and proliferate in such oligotrophic environments may well speak to their need to employ alternative metabolic pathways for energy, including those associated with MICP.

Here, we studied the MICP potential of cave bacteria isolated from the ICC in Chilliwack, Canada. Through a combination of biochemical, MICP-specific assays and genomics, we identified that MICP may be a common process found across different genera as demonstrated by bacteria isolated from PCS and SSS. MICP has been observed worldwide in a vast array of environments and microbial niches (Castanier et al., 1999; Stocks-Fischer et al., 1999; Chou et al., 2011; Seifan and Berenjian, 2019). Moreover, bacteria capable of MICP have participated in the formation of secondary cave deposits (Castanier et al., 1999; Stocks-Fischer et al., 1999; Northup and Lavoie, 2001; Engel et al., 2004; Banks et al., 2010). A previous study identified $CaCO_3$ production in several genera of bacteria isolated from an Indian cave and further demonstrated their ability to precipitate on artificial B4 medium (Baskar et al., 2016). Furthermore, two genera isolated in the study by Baskar et al. (2016), *Arthrobacter* spp. and *Streptomyces* spp., were also identified in our study and were isolated from soda straw speleothems. Our results are consistent with MICP being a phenomenon demonstrated by bacteria found within caves and associated with speleothems (**Figure 2**) and is a process mediated by biochemical pathways found in a broad range of genera (Weiner and Dove, 2003; Zhu and Dittrich, 2016; Chaparro-Acuña et al., 2018; Castro-Alonso et al., 2019; Chaurasia et al., 2019; Seifan and Berenjian, 2019; Zhang et al., 2019; Ortega-Villamagua et al., 2020).

The bacterial isolates studied through WGS showed complete urease pathways, with some key differences in cluster structure and correlated species. Analysis of whole genome determined the closest correlated organisms to *Pseudarthrobacter* sp. SSS035 and *Sphingobacterium* sp. PCS056 (**Figures 3**, **4**). *Pseudarthrobacter* sp. SSS035 was found to be related to other organisms commonly found in non-acidic soils and belonging to the same genus or the associated *Arthrobacter* genus with a high level of correlation confidence. Being known for their versatility in adapting to several conditions including desiccation, starvation, and the ability to use a wide range of carbon sources (Jones and Keddie, 2006), *Pseudarthrobacter* presence would be expected in a challenging cave environment. In our analysis, *Sphingobacterium* sp. PCS056 was related to other organisms from the same genus that are present in habitats with heavy human influence such as pig pens. Although the preferred habitat of the genus is not well characterized, the presence of several enzymes such as DNAse, oxidase, catalase, and urease, as well as antibiotic resistance genes (Steinberg and Burd, 2015), is indicative of adaptation to high evolutionary pressure conditions.

Pseudarthrobacter sp. SSS035 encodes a single and complete urease pathway, whereas *Sphingobacterium* sp. PCS056 shows two urease pathways encoded in the genome, with an unknown gene in the middle of the sequence (**Figure 6**). Gene duplications are common in prokaryotic organisms and can confer a variety of advantages. Duplications in genes related to transcription, defense mechanisms, and metabolism as we see in the urease pathway duplication can help the microbe adapt to a changing environment (Argyris and Pomerantz, 2004). Given that the cave environment is highly delicate and subject to small changes in nutrient availability, this could provide selective pressure to keep the duplicated pathway. Organisms that are better able to survive their environment due to gene duplication

may experience convergent evolution toward the beneficial trait (Bratlie et al., 2010).

Fisher et al. (2017) found that in environmental bacteria, higher habitat pH correlated with higher copy numbers of *ureC*. The same trend occurs with the two isolates studied here, where duplication occurs in the isolate exposed to higher pH. However, we do see duplication of the entire pathway rather than just in *ureC*, in a similar manner to several *Helicobacter* species, where the urease is associated with host iron-rich diets and presents reduced activity (Carter et al., 2009, 2011; Fong et al., 2013). Considering the cave high levels of iron, hence its name, this duplication, and the altered configuration with a hypothetical gene between *ureC* and *ureD* could arise from the presence of an alternative iron-dependent urease(s) in addition or in replacement of nickel-dependent enzymes due to limited nickel levels in comparison with iron (**Table 2**).

The urease pathway occurring in the reverse direction in *Pseudarthrobacter* sp. SSS035 could be due to a variety of reasons, including differences in operon regulation or convergent evolution with the urease genes arising in the two microbes based on two separate events. One study proposes that inversion of whole operons occurs more often in genes associated with antibiotic resistance and virulence and increases evolvability of the microbe to better adapt to its environment and lifestyle (Merrikh and Merrikh, 2018). The pathogenicity of *Pseudarthrobacter sulfonivorans*, the closest related bacteria to *Pseudarthrobacter* sp. SSS035, is undetermined, but there are members of the genus that are known to be pathogenic, supporting the possibility of another pathogenic microbe in this genus.

In addition, we studied the chemical composition of the PCS and SSS speleothems to determine differences in available nutrients and in the immediate microenvironment that bacteria inhabited. Recent studies by Dhami et al. (2018) have analyzed the chemical composition of groundwater and analyzed six speleothems from Margaret River caves to elucidate what minerals and free aqueous species are available to cave-dwelling bacteria. Interestingly, a similar trend was observed between the three caves sampled in the study and our observations at the ICC with respect to calcium, iron, and magnesium, despite the geographic distance between Margaret Rivers in Australia and ICC in Canada. Likewise, similar trends in trace elements demonstrate that a similar chemical environment would be available to cave-dwelling bacteria.

Dhami et al. (2018) also performed metagenomic sequencing and reported an amplicon library where all five phyla and two genera specific (*Pseudarthrobacter* sp. and *Sporosarcina* sp.) U+ candidates from the ICC were found in the Australian caves, further cementing the idea that the microenvironment (i.e., available dissolved minerals and drip water on speleothem surfaces) may be an important selective pressure, favoring these genera. To corroborate these findings, the results from a study by Ortiz et al. (2012) on the bacterial diversity in the Kartchner Cave in Arizona, United States, demonstrated that bacteria belonging to all five phyla found at the ICC were also present in the Kartchner Cave. These studies suggest that these organisms might utilize alternative metabolic pathways to inhabit and persist in such oligotrophic environments under different environmental variables all over the world, consolidating the importance of urease in our isolates for cave survival.

While bacterial abundance may allow us to understand the community composition, we must not forget the role the pH plays in both the geological and biological worlds. We have a good understanding of how caves form, and the role that pH plays; however, we do not have a great understanding of the role pH plays in the microenvironment that cave bacteria inhabit. In this study, PCS was determined to be slightly acidic pH, while SSS was alkaline. With these findings, PCS likely undergo passive influx of calcium ions and SSS undergo active extrusion of calcium ions for calcium carbonate precipitation as demonstrated in a study conducted by Hammes and Verstraete (2002) whereby researchers outlined mechanisms by which bacteria participate in active and passive calcium carbonate precipitation thereby demonstrating a clear mechanistic approach.

Lastly, it is imperative to understand the role that solid mineral surfaces of speleothems and their aqueous environments play in the physical geological formation of crystals. Calcium carbonate crystal formations exist as either calcite, aragonite, or vaterite. Here, we employed petrographic microscopy to discern what crystal shapes were formed from MICP of U+ candidates, and whether the crystal shapes differed between the solid and liquid MICP assays. A wide array of crystal morphologies was found upon imaging U+ candidates from both liquid and solid MICP assays, as demonstrated in **Figures 1**, **3**. Regarding crystal morphology, even though we understand that the conditions between *in vitro* experiments vs. cave environments differ greatly, discrepancies in the observed shapes of crystal made by different single isolates vs. mixed cultures were observed. Hence, we are convinced that the makeup of bacteria may influence the diversity in crystal morphology and may be related to the macroscopic shape of the speleothems themselves, suggesting that crystal budding from urease-positive candidates may influence a larger exponentiation of the crystal growth, aided along by either evaporation pattern and/or dripping of the groundwater saturated with mineral contents, to form the macroscopic speleothems that we see today.

Since speleothem formation is very complex and time-consuming process, lots of metabolic pathways and steps involved in cave speleothem formation remain unknown. From our lab-based crystal formations found in U+ candidate MICP assays, we now have many more questions about it than we started off. For example, we wonder whether the growth of speleothems and their structures are first nucleated at the extracellular surface of cave bacteria that precipitate calcium carbonate. How about the pH role and impact in an overall crystal formation relating to the bacterial cell membrane and subsequent cascading of proton gradients, and its effects in the microenvironment? These questions warrant us to look further into how bacterial diversity and activity influence or are influenced by the cave speleothem dynamics.

Prospects include determining the nucleation role of cave bacteria in speleothem growth by performing carbonatogenic

yield experiments to better understand growth kinetics of U+ candidates, and their quantitative contribution to overall speleothem formation. Moreover, determining the quantity of nucleation sites on these candidates is imperative but requires careful assessment of the number of urease enzyme copies found in their genomes and the available surface area to act as nucleation sites. Determining surface area nucleation sites requires further imaging with SEM when bacteria are in their ureolytic metabolic state. Lastly, to confirm the crystal structure being produced by U+ candidates is indeed the calcite form of calcium carbonate, X-ray diffraction microscopy must be employed.

DATA AVAILABILITY STATEMENT

The datasets presented in this study can be found in online repositories. The names of the repository/repositories and accession number(s) can be found in the article/ **Supplementary Material**.

AUTHOR CONTRIBUTIONS

NC, SL, and RM obtained funding. NC, KK, and RM conceived the study and designed the experiment. KK, RM, LC, and SL conducted the experiments. KK, RM, JG, and NC designed the MS workflow. KK, RM, SL, and JG were instrumental in collecting the MS data sets. KK, RM, and JG drafted the manuscript. NV and DH assisted with microscopy. NC, NV, KK, RM, SL, and JG read and edited the manuscript. CB was JG's Ph.D. supervisor. All authors contributed to the article and approved the submitted version.

FUNDING

This study was funded by TRU Undergraduate Research Experience Award Program, UREAP (RM), Society of Applied Microbiology (S*f*AM), Summer Student Placement Scholarship (NC and SL), and TRU Internal Research Grant #102646.

ACKNOWLEDGMENTS

We respectfully acknowledge that this research was conducted—in part—on the traditional and unceded territory of the Secwepemc People located in Tk'emlúìps te Secwepemc and the traditional and unceded Algonquin territory. We would like to thank Thompson Rivers University's Department of Biological Sciences and Faculty of Science for in-kind support. We would like to thank Rob Wall and Doug Storozynski of the Chilliwack River Valley Cavers, who are the caretakers of the Iron Curtain Cave. We would like to thank all the undergraduate and graduate volunteers who, throughout the entirety of this process, provided their time and experience with the success of this study in mind.

SUPPLEMENTARY MATERIAL

The Supplementary Material for this article can be found online at: https://www.frontiersin.org/articles/10.3389/fmicb.2022.933388/full#supplementary-material

Supplementary Figure 1 | Map of the Iron Curtain Cave demonstrating the location of the two speleothem collection sites. **(A)** PCS sampling and **(B)** SSS sampling. Locations are approximate.

Supplementary Figure 2 | Examples of speleothems present in ICC collected for this study. **(A)** Popcorn speleothem. **(B)** Soda straw speleothem.

REFERENCES

Afgan, E., Baker, D., Batut, B., Van Den Beek, M., Bouvier, D., Ech, M., et al. (2018). The Galaxy platform for accessible, reproducible and collaborative biomedical analyses: 2018 update. *Nucleic Acids Res.* 46, W537–W544. doi: 10.1093/nar/gky379

Almeida, M., Hébert, A., Abraham, A.-L., Rasmussen, S., Monnet, C., Pons, N., et al. (2014). Construction of a dairy microbial genome catalog opens new perspectives for the metagenomic analysis of dairy fermented products. *BMC Genom.* 15:1101. doi: 10.1186/1471-2164-15-1101

Altschul, S. F., Gish, W., Miller, W., Myers, E. W., and Lipman, D. J. (1990). Basic local alignment search tool. *J. Mol. Biol.* 215, 403–410. doi: 10.1016/S0022-2836(05)80360-2

Argyris, E. G., and Pomerantz, R. J. (2004). HIV-1 Vif versus APOBEC3G: newly appreciated warriors in the ancient battle between virus and host. *Trends Microbiol.* 12, 145–148. doi: 10.1016/j.tim.2004.02.004

Banks, E. D., Taylor, N. M., Gulley, J., Lubbers, B. R., Giarrizzo, J. G., Bullen, H. A., et al. (2010). Bacterial calcium carbonate precipitation in cave environments: a function of calcium homeostasis. *Geomicrobiol. J.* 27, 444–454. doi: 10.1080/01490450903485136

Barton, H., Taylor, N., Kreate, M., Springer, A., Oehrle, S., and Bertog, J. (2007). The impact of host rock geochemistry on bacterial community structure in oligotrophic cave environments. *Int. J. Speleol.* 36, 93–104. doi: 10.5038/1827-806X.36.2.5

Baskar, S., Baskar, R., and Routh, J. (2014). Speleothems from Sahastradhara Caves in Siwalik Himalaya, India: possible Biogenic Inputs. *Geomicrobiol. J.* 31, 664–681. doi: 10.1080/01490451.2013.871087

Baskar, S., Routh, J., Baskar, R., Kumar, A., Miettinen, H., and Itävaara, M. (2016). Evidences for microbial precipitation of calcite in speleothems from Krem Syndai in Jaintia Hills, Meghalaya, India. *Geomicrobiol. J.* 33, 906–933. doi: 10.1080/01490451.2015.1127447

Benini, S., Rypniewski, W. R., Wilson, K. S., Miletti, S., Ciurli, S., and Mangani, S. (1999). A new proposal for urease mechanism based on the crystal structures of the native and inhibited enzyme from Bacillus pasteurii: why urea hydrolysis costs two nickels. *Structure* 7, 205–216. doi: 10.1016/S0969-2126(99)80026-4

Beolchini, F., Fonti, V., Özdemiroğlu, S., Akcil, A., and Dell'Anno, A. (2017). Sulphur-oxidising bacteria isolated from deep caves improve the removal of arsenic from contaminated harbour sediments. *Chem. Ecol.* 33, 103–113. doi: 10.1080/02757540.2017.1281252

Boquet, E., Boronat, A., and Ramos-Cormenzana, A. (1973). Production of calcite (calcium carbonate) crystals by soil bacteria is a general phenomenon. *Nature* 246, 527–528.

Bratlie, M. S., Johansen, J., Sherman, B. T., Huang, D. W., Lempicki, R. A., and Drabløs, F. (2010). Gene duplications in prokaryotes can be associated with environmental adaptation. *BMC Genom.* 11:588. doi: 10.1186/1471-2164-11-588

Brettin, T., Davis, J. J., Disz, T., Edwards, R. A., Gerdes, S., Olsen, G. J., et al. (2015). RASTtk: a modular and extensible implementation of the RAST algorithm for

building custom annotation pipelines and annotating batches of genomes. *Sci. Rep.* 5:8365. doi: 10.1038/srep08365

Carter, E. L., Flugga, N., Boer, J. L., Mulrooney, S. B., and Hausinger, R. P. (2009). Interplay of metal ions and urease. *Metallomics* 1, 207–21. doi: 10.1039/b903311d

Carter, E. L., Tronrud, D. E., Taber, S. R., Karplus, P. A., and Hausinger, R. P. (2011). Iron-containing urease in a pathogenic bacterium. *PNAS* 108, 13095–13099. doi: 10.1073/pnas.1106915108

Castanier, S., Le Métayer-Levrel, G., and Perthuisot, J. P. (1999). Ca-carbonates precipitation and limestone genesis - the microbiogeologist point of view. *Sediment. Geol.* 126, 9–23. doi: 10.1016/S0037-0738(99)00028-7

Castro-Alonso, M. J., Montañez-Hernandez, L. E., Sanchez-Muñoz, M. A., Macias Franco, M. R., Narayanasamy, R., and Balagurusamy, N. (2019). Microbially induced calcium carbonate precipitation (MICP) and its potential in bioconcrete: microbiological and molecular concepts. *Front. Mater.* 6:126. doi: 10.3389/fmats.2019.00126

Chaparro-Acuña, S. P., Becerra-Jiménez, M. L., Martínez-Zambrano, J. J., and Rojas-Sarmiento, H. A. (2018). Soil bacteria that precipitate calcium carbonate: mechanism and applications of the process. *Acta Agron.* 67, 277–289. doi: 10.15446/acag.v67n2.66109

Chaurasia, L., Bisht, V., Singh, L. P., and Gupta, S. (2019). A novel approach of biomineralization for improving micro and macro-properties of concrete. *Constr. Build. Mater.* 195, 340–351. doi: 10.1016/j.conbuildmat.2018.11.031

Cheeptham, N., Northup, D. E., de Lurdes, N. E. D., Whitefield, P., Saiz-Jimenez, C., Riquelme Gabriel, C., et al. (2013). "Advances and Challenges in Studying Cave Microbial Diversity," in *Cave Microbiomes: A Novel Resource for Drug Discovery*, ed. N. Cheeptham (New York, NY: Springer), doi: 10.1007/978-1-4614-5206-5

Chou, C.-W., Seagren, E. A., Aydilek, A. H., and Lai, M. (2011). Biocalcification of sand through ureolysis. *J. Geotech. Geoenviron. Eng.* 137, 1179–1189. doi: 10.1061/(ASCE)GT.1943-5606.0000532

Christy, A. G. (2017). A review of the structures of vaterite: the impossible, the possible, and the likely. *Cryst. Growth Des.* 17, 3567–3578. doi: 10.1021/acs.cgd.7b00481

Chu, J., Stabnikov, V., and Ivanov, V. (2012). Microbially induced calcium carbonate precipitation on surface or in the bulk of soil. *Geomicrobiol. J.* 29, 544–549. doi: 10.1080/01490451.2011.592929

Colpas, G. J., and Hausinger, R. P. (2000). In vivo and in vitro kinetics of metal transfer by the Klebsiella aerogenes urease nickel metallochaperone. *UreE. J. Biol. Chem.* 275, 10731–10737. doi: 10.1074/jbc.275.15.10731

Dhami, N. K., Mukherjee, A., and Watkin, E. L. J. (2018). Microbial diversity and mineralogical-mechanical properties of calcitic cave speleothems in natural and in vitro biomineralization conditions. *Front. Microbiol.* 9:40. doi: 10.3389/fmicb.2018.00040

Dreybrodt, W. (1999). Chemical kinetics, speleothem growth and climate. *Boreas* 28, 347–356. doi: 10.1111/j.1502-3885.1999.tb00224.x

Engel, A. S., Stern, L. A., and Bennett, P. C. (2004). Microbial contributions to cave formation: new insights into sulfuric acid speleogenesis. *Geology* 32, 369–372. doi: 10.1130/G20288.1

Ferris, F. G., Phoenix, V., Fujita, Y., and Smith, R. W. (2003). Kinetics of calcite precipitation induced by ureolytic bacteria at 10 to 20°C in artificial groundwater. *Geochim. Cosmochim. Acta* 67, 1701–1710. doi: 10.1016/S0016-7037(00)00503-9

Fisher, K. A., Yarwood, S. A., and James, B. R. (2017). Soil urease activity and bacterial ureC gene copy numbers: effect of pH. *Geoderma* 285, 1–8. doi: 10.1016/j.geoderma.2016.09.012

Fong, Y. H., Wong, H. C., Yuen, M. H., Lau, P. H., Chen, Y. W., and Wong, K. B. (2013). Structure of UreG/UreF/UreH complex reveals how urease accessory proteins facilitate maturation of Helicobacter pylori urease. *PLoS Biol.* 11:e1001678. doi: 10.1371/journal.pbio.1001678

Ghosh, S., LaPara, T. M., and Sadowsky, M. J. (2014). Draft genome sequence of Sphingobacterium sp. Strain PM2-P1-29, a tetracycline-degrading TetX-expressing aerobic bacterium isolated from agricultural soil. *Genome Announc.* 2, e00963–14. doi: 10.1128/genomeA.00963-14

Ghosh, S., Paine, E., Wall, R., Kam, G., Lauriente, T., Sa-ngarmangkang, P.-C., et al. (2017). In situ cultured bacterial diversity from Iron Curtain Cave, Chilliwack, British Columbia, Canada. *Diversity* 9, 36. doi: 10.3390/d9030036

Hammes, F., and Verstraete, W. (2002). Key roles of pH and calcium metabolism in microbial carbonate precipitation. *Rev. Environ. Sci. BioTechnol.* 1, 3–7. doi: 10.1023/A:1015135629155

Jolley, K. A., Bray, J. E., and Maiden, M. C. J. (2018). Open-access bacterial population genomics: BIGSdb software, the PubMLST.org website and their applications. *Wellcome Open Res.* 3:124. doi: 10.12688/wellcomeopenres.14826.1

Jones, D., and Keddie, R. (2006). "The Genus Arthrobacter," in *The Prokaryotes*, eds E. F. DeLong, S. Lory, E. Stackebrandt, and F. Thompson (New York: Springer), 945–960. doi: 10.1007/0-387-30743-5_36

Konieczna, I., Zarnowiec, P., Kwinkowski, M., Kolesinska, B., Fraczyk, J., Kaminski, Z., et al. (2013). Bacterial Urease and its Role in Long-Lasting Human Diseases. *Curr. Protein Pept. Sci.* 13, 789–806. doi: 10.2174/138920312804871094

Lin, Y., Yuan, J., Kolmogorov, M., Shen, M. W., Chaisson, M., and Pevzner, P. A. (2016). Assembly of long error-prone reads using de Bruijn graphs. *Proc. Natl. Acad. Sci. U. S. A.* 113, E8396–E8405. doi: 10.1073/pnas.1604560113

Lyu, J., Li, F., Zhang, C., Gower, L., Wasman, S., Sun, J., et al. (2021). From the inside out: elemental compositions and mineral phases provide insights into bacterial calcification. *Chem. Geol.* 559:119974. doi: 10.1016/j.chemgeo.2020.119974

Mason, C., Randhawa, A., Watson, K., Friedman, C. R., and Cheeptham, N. (2016). Using scanning electron microscopy to study microbial communities in speleothem samples collected from Iron Curtain Cave. *J. Exp. Microbiol. Immunol.* 2, 1–7.

Merrikh, C. N., and Merrikh, H. (2018). Gene inversion potentiates bacterial evolvability and virulence. *Nat. Commun.* 9:4662. doi: 10.1038/s41467-018-07110-3

Mikheenko, A., Prjibelski, A., Saveliev, V., Antipov, D., and Gurevich, A. (2018). Versatile genome assembly evaluation with QUAST-LG. *Bioinformatics* 34, i142–i150. doi: 10.1093/bioinformatics/bty266

Mobley, H. L. T., Island, M. D., and Hausinger, R. P. (1995). Molecular biology of microbial ureases. *Microbiol. Rev.* 59, 451–480. doi: 10.1128/mmbr.59.3.451-480.1995

Mulrooney, S. B., Ward, S. K., and Hausinger, R. P. (2005). Purification and properties of the Klebsiella aerogenes UreE metal-binding domain, a functional metallochaperone of urease. *J. Bacteriol.* 187, 3581–3585. doi: 10.1128/JB.187.10.3581-3585.2005

Northup, D. E., and Lavoie, K. H. (2001). Geomicrobiology of caves: a review. *Geomicrobiol. J.* 18, 199–222. doi: 10.1080/01490450152467750

Ortega-Villamagua, E., Gudiño-Gomezjurado, M., and Palma-Cando, A. (2020). Microbiologically Induced Carbonate Precipitation in the Restoration and Conservation of Cultural Heritage Materials. *Molecules* 25:5499. doi: 10.3390/molecules25235499

Ortiz, M., Neilson, J. W., Nelson, W. M., Legatzki, A., Byrne, A., Yu, Y., et al. (2012). Profiling bacterial diversity and taxonomic composition on speleothem surfaces in Kartchner Caverns. *AZ. Microb. Ecol.* 65, 371–383. doi: 10.1007/s00248-012-0143-6

Palmer, A. N. (1991). Origin and morphology of limestone caves. *Geol. Soc. Am. Bull.* 103, 1–21. doi: 10.1130/0016-76061991103<0001:OAMOLC<2.3.CO;2

Park, M., Park, Y., Kim, M., Kang, G., Kim, M., Jo, Y., et al. (2019). Complete genome sequence of Pseudarthrobacter sp. NIBRBAC000502771 isolated from shooting range soil in Republic of Korea. *Korean J. Microbiol.* 55, 419–421. doi: 10.7845/kjm.2019.9094

Paul, B., Drysdale, R., Green, H., Woodhead, J., Hellstrom, J., and Eberhard, R. (2013). A model for the formation of layered soda-straw stalactites. *Int. J. Speleol.* 42, 155–160. doi: 10.5038/1827-806X.42.2.8

Pike, R. G., Redding, T. E., Moore, R. D., Winkler, R. D., and Bladon, K. D. (eds) (2010). *Compendium of Forest Hydrology and Geomorphology in British Columbia, LMH 66, Volume 2 of 2*. New York: Crown Publishing Group.

Saunders, I. R., Clague, J. J., and Roberts, M. C. (1987). Deglaciation of Chilliwack River valley, British Columbia. *Can. J. Earth Sci.* 24, 915–923. doi: 10.1139/e87-089

Schoch, C. L., Ciufo, S., Domrachev, M., Hotton, C. L., Kannan, S., Khovanskaya, R., et al. (2020). NCBI Taxonomy: a comprehensive update on curation, resources and tools. *Database* 2020:baaa062. doi: 10.1093/database/baaa062

Seifan, M., and Berenjian, A. (2019). Microbially induced calcium carbonate precipitation: a widespread phenomenon in the biological world. *Appl. Microbiol. Biotechnol.* 103, 4693–4708. doi: 10.1007/s00253-019-09861-5

Shen, L., Liu, Y., Allen, M. A., Xu, B., Wang, N., Williams, T. J., et al. (2021). Linking genomic and physiological characteristics of psychrophilic Arthrobacter to metagenomic data to explain global environmental distribution. *Microbiome* 9:136. doi: 10.1186/s40168-021-01084-z

Soriano, A., and Hausinger, R. P. (1999). GTP-dependent activation of urease apoprotein in complex with the UreD, UreF, and UreG accessory proteins. *Proc. Natl. Acad. Sci. U. S. A.* 96, 11140–11144. doi: 10.1073/pnas.96.20.11140

Soriano, A., Colpas, G. J., and Hausinger, R. P. (2000). UreE stimulation of GTP-dependent urease activation in the UreD-UreF-UreG-urease apoprotein complex. *Biochemistry* 39, 12435–12440. doi: 10.1021/bi001296o

Steinberg, J. P., and Burd, E. M. (2015). "Other Gram-Negative and Gram-Variable Bacilli," in *Douglas, and Bennett's Principles and Practice of Infectious Diseases (Eighth Edition)*, eds J. E. Bennett, R. Dolin, and M. J. Blaser (Philadelphia: Saunders), doi: 10.1016/B978-1-4557-4801-3.00238-1

Stocks-Fischer, S., Galinat, J. K., and Bang, S. S. (1999). Microbiological precipitation of CaCO3. *Soil Biol. Biochem.* 31, 1563–1571. doi: 10.1016/S0038-0717(99)00082-6

Szymczak, P., and Ladd, A. J. C. (2011). The initial stages of cave formation: beyond the one-dimensional paradigm. *Earth Planet. Sci. Lett.* 301, 424–432. doi: 10.1016/j.epsl.2010.10.026

Türkgenci, M. D., and Dogruöz Güngör, N. (2021). Profiling of bacteria capable of precipitating CaCO3 on the speleothem surfaces in Dupnisa Cave, Kirklareli, *Turkey. Geomicrobiol. J.* 38, 816–827. doi: 10.1080/01490451.2021.1964110

Warren, J. K., Havholm, K. G., Rosen, M. R., and Parsley, M. J. (1990). Evolution of gypsum karst in the Kirschberg Evaporite Member near Fredericksburg. *Texas. J. Sediment. Petrol.* 60, 721–734. doi: 10.1306/212F925A-2B24-11D7-8648000102C1865D

Weiner, S., and Dove, P. M. (2003). An Overview of Biomineralization Processes and the Problem of the Vital Effect. *Rev. Mineral. Geochem.* 54, 1–29. doi: 10.2113/0540001

Zhang, H., Sun, H., Yang, R., Li, S., Zhou, M., Gao, T., et al. (2016). Complete genome sequence of a psychotrophic Pseudarthrobacter sulfonivorans strain Ar51 (CGMCC 4.7316), a novel crude oil and multi benzene compounds degradation strain. *J. Biotechnol.* 231, 81–82. doi: 10.1016/j.jbiotec.2016.04.010

Zhang, J., Zhao, C., Zhou, A., Yang, C., Zhao, L., and Li, Z. (2019). Aragonite formation induced by open cultures of microbial consortia to heal cracks in concrete: insights into healing mechanisms and crystal polymorphs. *Constr. Build. Mater.* 224, 815–822. doi: 10.1016/j.conbuildmat.2019.07.129

Zhu, T., and Dittrich, M. (2016). Carbonate precipitation through microbial activities in natural environment, and their potential in biotechnology: a review. *Front. Bioeng. Biotechnol.* 4:4. doi: 10.3389/fbioe.2016.00004

Conflict of Interest: The authors declare that the research was conducted in the absence of any commercial or financial relationships that could be construed as a potential conflict of interest.

frontiers | Frontiers in Microbiology

ORIGINAL RESEARCH
published: 14 July 2022
doi: 10.3389/fmicb.2022.926558

Cultivable Skin Mycobiota of Healthy and Diseased Blind Cave Salamander (*Proteus anguinus*)

*Polona Zalar[1], Ana Gubenšek[1], Cene Gostincar[1], Rok Kostanjšek[2], Lilijana Bizjak-Mali[2] and Nina Gunde-Cimerman[1]**

[1] Chair of Molecular Genetics and Biology of Microorganisms, Department of Biology, Biotechnical Faculty, University of Ljubljana, Ljubljana, Slovenia, [2] Chair of Zoology, Department of Biology, Biotechnical Faculty, University of Ljubljana, Ljubljana, Slovenia

Proteus anguinus is a neotenic cave salamander, endemic to the Dinaric Karst and a symbol of world natural heritage. It is classified as "vulnerable" by the International Union for Conservation of Nature (IUCN) and is one of the EU priority species in need of strict protection. Due to inaccessibility of their natural underground habitat, scientific studies of the olm have been conducted mainly in captivity, where the amphibians are particularly susceptible to opportunistic microbial infections. In this report, we focused on the diversity of cultivable commensal fungi isolated from the skin of asymptomatic and symptomatic animals obtained from nature (20 specimens) and captivity (22 specimens), as well as from underground water of two karstic caves by direct water filtration and by exposure of keratin-based microbial baits and subsequent isolation from them. In total 244 fungal isolates were recovered from the animals and additional 153 isolates were obtained from water samples. Together, these isolates represented 87 genera and 166 species. Symptomatic animals were colonized by a variety of fungal species, most of them represented by a single isolate, including genera known for their involvement in chromomycosis, phaeohyphomycosis and zygomycosis in amphibians: *Acremonium*, *Aspergillus*, *Cladosporium*, *Exophiala*, *Fusarium*, *Mucor*, *Ochroconis*, *Phialophora* and *Penicillium*. One symptomatic specimen sampled from nature was infected by the oomycete *Saprolegnia parasitica*, the known causative agent of saprolegniosis. This is the first comprehensive report on cultivable skin mycobiome of this unique amphibian in nature and in captivity, with an emphasis on potentially pathogenic fungi and oomycetes.

Keywords: ***Proteus anguinus*, olm, fungi, opportunistic pathogens, *Saprolegnia***

OPEN ACCESS

Edited by:
Cesareo Saiz-Jimenez, Institute of Natural Resources and Agrobiology of Seville (CSIC), Spain

Reviewed by:
Pedro Martin-Sanchez, University of Oslo, Norway
Alena Nováková, Institute of Microbiology, Academy of Sciences of the Czech Republic (ASCR), Czechia

****Correspondence:***
Nina Gunde-Cimerman
nina.gunde-cimerman@bf.uni-lj.si

Specialty section:
This article was submitted to Terrestrial Microbiology, a section of the journal Frontiers in Microbiology

Received: *22 April 2022*
Accepted: *24 June 2022*
Published: *14 July 2022*

Citation:
Zalar P, Gubenšek A, Gostincar C, Kostanjšek R, Bizjak-Mali L and Gunde-Cimerman N (2022) Cultivable Skin Mycobiota of Healthy and Diseased Blind Cave Salamander (Proteus anguinus). Front. Microbiol. 13:926558. doi: 10.3389/fmicb.2022.926558

INTRODUCTION

Cave salamander *Proteus anguinus*, also known as the olm, is a symbol of world natural heritage, a flagship species of the subterranean environment and a Slovenian national symbol. Olm is the longest-living amphibian, the largest troglobiotic tetrapod in the World and the only European troglobiotic vertebrate. Original description dates in Laurenti (1768). Since the discovery of pigmented form (Sket and Arntzen, 1994), two subspecies are known: the originally described and more spread non-pigmented variant *P. anguinus anguinus* (Paa), and the black olm or *P. anguinus parkelj* (Pap). Olm belongs to the family Proteidae, an ancient group of aquatic salamanders with

only two genera, the European *Proteus* (with one currently recognized species) and the North American genus *Necturus* (with five currently recognized species). While *Necturus* lives in surface water, *Proteus* is endemic to the subterranean waters of the Dinaric Karst of souterneast Europe, with most known localities in Slovenia (Sket, 1997; Gorički et al., 2017). Its major troglobiotic adaptations include depigmented skin, degenerated eyes and elongated body parts, high tolerance to anoxia, slow metabolism, and unusual resistance to starvation. Since olms are also neotenic, they retain certain larval characteristics through their life, including external gills, gill slits and skin morphology (Bulog et al., 2000; Voituron et al., 2011; McGaugh et al., 2020; Kostanjšek et al., 2021a).

The olm is one of the EU priority species in need of strict protection (Vörös et al., 2017), listed in the EU Habitats Directive and Bern and Ramsar Conventions, and is classified as "vulnerable" by the International Union for Conservation of Nature "(IUCN Red)" (Arntzen et al., 2009) and EDGE lists (Safi et al., 2013).[1] In Slovenia it is protected by national legislation since 1922.

As an endemic and neotenic species with a narrow ecological niche, olm is highly susceptible to infections (Heard et al., 2013), especially to pathogens with a high mortality potential for urodelans (Price et al., 2016; Spitzen-van der Sluijs et al., 2016) and amphibians in general. According to the Global Amphibian Assessment (GAA), more than 40% of amphibian species are in decline, while an additional 32% are threatened (Latney and Klaphake, 2013). The main microbial threats to amphibian diversity are the fungal disease chytridiomycosis, caused by the fungi *Batrachochytrium dendrobatidis* and *B. salamandrivorans* (Scheele et al., 2019), and ranaviruses (Price et al., 2016; Spitzen-van der Sluijs et al., 2016). Both chytrids infect many amphibian species across Europe, including countries neighboring Slovenia (Fisher and Garner, 2020). During the first monitoring study performed in Slovenia between 2015 and 2019, we collected swab samples from 173 live amphibians of 22 species, from 53 natural sites across Slovenia and from 41 captive amphibians. Sampling also included 70 olm individuals from five wild populations in Slovenia and 18 captive specimens. All samples were analyzed by real-time quantitative polymerase chain reaction (qPCR) for the presence of *B. salamandrivorans* (Blooi et al., 2013) and ranaviruses (Leung et al., 2017). We identified a single infection with *B. dendrobatidis* on an edible frog (*Pelophylax* kl. *esculentus*) from a natural habitat and no infections with *B. salamandrivorans* or ranaviruses of other amphibians sampled, including the olm (Kostanjšek et al., 2021b).

Other important fungal infections that contribute to global amphibian declines (Latney and Klaphake, 2013) include chromomycosis, phaeohyphomycosis, zygomycosis, and saprolegniosis, the latter caused by water molds (Oomycota, Stramenopiles). Due to the unique physiology and ecology of amphibians, water is one of the main vectors for transmission of these pathogens (Robert et al., 2011). Although it is known that stressed animals in captivity can become infected *via* traumatized gills or skin and through contact with contaminated water (Seyedmousavi et al., 2013), only three reports on fungal infections of olms in captivity have been published so far (Kogej, 1999; Bizjak-Mali et al., 2018; Lukač et al., 2019; Li et al., 2020), and no data exist on fungal infections of the olm in its natural underground habitats.

The focus of this study was isolation and identification of cultivable fungi from the skin of olm specimens inhabiting underground water of five karstic caves, representing different Slovenian natural populations of olm (Sket, 1997; Gorički et al., 2017) and from three vivaria where they were kept in captivity. Commensal fungi were isolated both from the skin of healthy animals and from animals with visible symptoms of disease, as well as from microbial baits exposed in water of three selected karstic caves, and by water filtration from two locations. Results of this study provide the first comprehensive insight into cultivable skin mycobiota of the olm and into its exposure and susceptibility to fungi populating underground karstic water environment, with emphasis on potential pathogens.

MATERIALS AND METHODS

Sampling Sites

Animals of *Proteus anguinus* have been sampled in five different karstic caves in Slovenia: Planinska jama and Črna jama, both part of Postojna–Planina cave system in southwestern Slovenia, Vir pri Stični, Kompoljska jama and Jelševnik in southeastern Slovenia (**Figure 1**), as well as three different sites (vivaria) where olm was kept in captivity. Water from Vivarium 1 originated from the Postojna–Planina cave system, water in Vivarium 2 was dechlorinated tap water, while water in Vivarium 3 originated from the vicinity of Kranj SW Slovenia. Additional water samples were taken in Krška jama, where no olms were found. In total 42 skin swab samples were collected from 42 animals (20 in the wild, 22 in captivity) over the period of 3 years (2017–2019). Nine of the swabs were taken from symptomatic animals, one of them was from the natural habitat and the other eight from captivity. Sampling sites and olm specimens are presented in **Figure 1** and in **Supplementary Table 1**.

Sampling of Animals and Environment

Animals

Animals were collected under permit 35601-27/2021-8 issued by the Ministry of the Environment and Spatial Planning of the Republic of Slovenia and Slovenian Agency for the Environment. Skin of asymptomatic olm specimens was sampled for the presence and identification of commensal fungi. The specimens were handled with fresh sterile gloves and were rinsed with 100 ml of sterile water prior to sampling to ensure that the skin sample primarily included skin-associated fungi. Sampling was non-destructive using sterile swabs (4N6 FLOQSwabs®, COPAN) with plastic shafts following the standard procedures established for amphibians (Boyle et al., 2004; McKenzie and Peterson, 2012). Immediately after sampling the swabs were placed into sterile transport Amies liquid at 4°C and processed within 24 h after sampling. Animals were released immediately after sampling at the site where they were captured. Symptomatic specimens were

[1] http://www.edgeofexistence.org/species/olm/

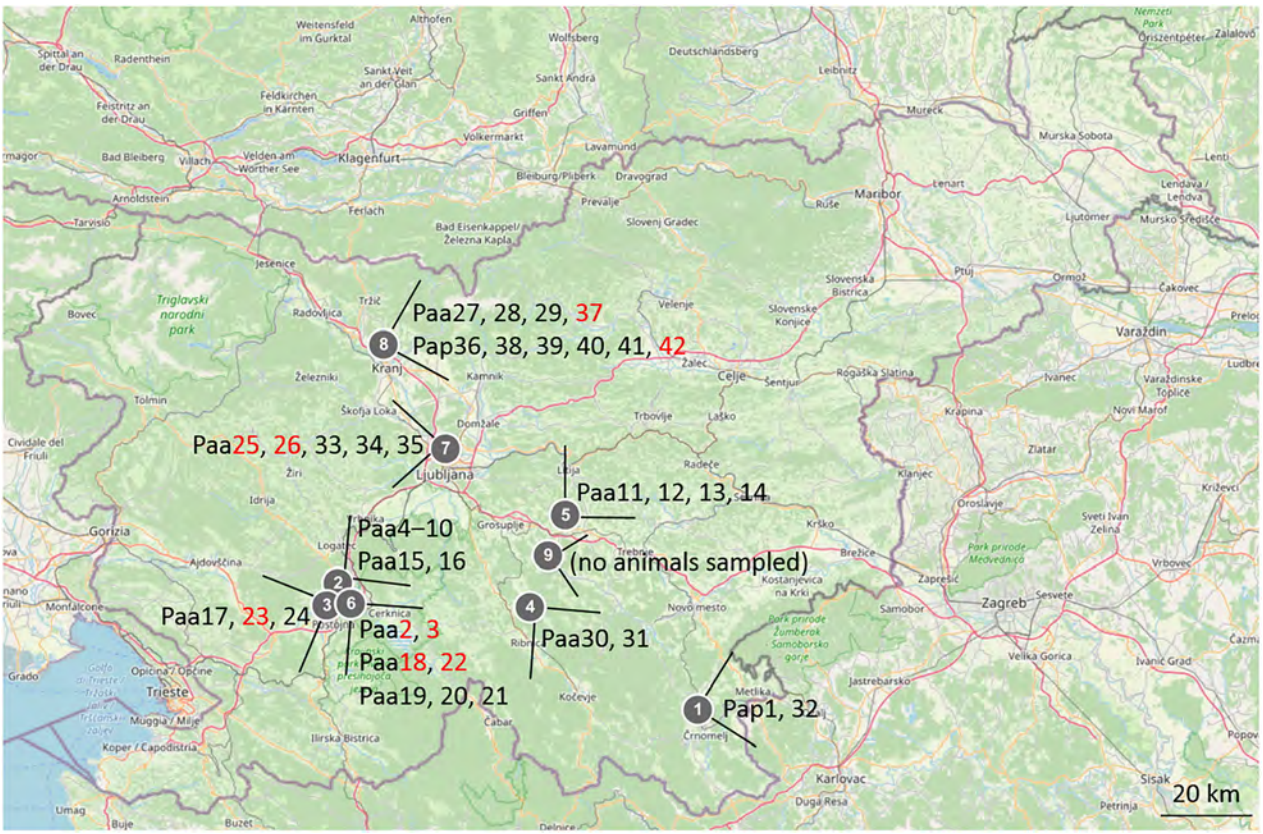

FIGURE 1 | Map of Slovenia with marked sampling locations and sampled olm specimens. 1-Jelševnik, 2-Planinska jama, 3-Èrna jama, 4-Kompoljska jama, 5-Vir pri Stièni, 6-Vivarium 1, 7-Vivarium 2, 8-Vivarium 3, 9-Krška jama. The labels of animals (Paa, *Poteus anguinus anguinus*; Pap, *Proteus anguinus parkelj*) are written next to locations, in black for asymptomatic, and in red for symptomatic animals.

swab-sampled only in regions with visible signs of disease. In order to control a potential disease, spread and to get more information about the pathology, they were then euthanized by prolonged immersion in 1.0% tricaine methanesulfonate solution (MS222, Sigma Chemical) buffered with 0.2% sodium bicarbonate (pH 7) and were submitted for necropsy. The carcass of these specimens and the isolated organs were fixed in 10% buffered formalin, rinsed in tap water, and then stored in 70% ethanol. Gross pathological changes were observed and documented using the MZFLIII dissecting stereomicroscope (Leica) equipped with the DFC 425C digital camera (Leica) and LAS software (V4.0) (Leica).

Environment

At selected sampling sites in caves (Jelševnik, Krška jama, Planinska jama), keratin baits (moulten snake skin, chicken feathers), and dialysis tubes filled with water agar, all separately sterilized by autoclaving in 50 ml Falcon tubes and covered with nylon fabric, were placed into perforated plastic containers, and exposed to the cave water by fixation with ropes (**Figure 2**). Baits were retrieved after 1, 3, 6, 12 and 15 months and checked for the presence of fungi. Water was collected in sterile containers at the point of animal capture, and in aliquots of 100 mL filtered through 0.45 μm membrane filters (Millipore) using a vacuum.

Isolation and Characterization of Fungi and Oomycetes

Animals

Fungi and oomycetes were isolated from the skin swabs of asymptomatic and symptomatic olms from nature and captivity, sampled as described above. Tubes with swabs and transport liquid were vigorously shaken in order to release the material from the swabs; 30–50 μl of transport liquid was pipetted on the surface of DRBC with chloramphenicol (50 mg/L), SabG, and TGhL with a mixture of penicillin/streptomycin (penicillin-G: 200 mg/L, streptomycin: 400 mg/L). In addition, the same amount of Amies, Copan transport liquid, was placed into a Petri dish with cooked hemp seeds (100°C, 20 min) and sterile distilled water was added up to 20 ml.

Environment

Fungi and oomycetes were also isolated from microbial baits incubated in water and from cave water samples. Baits were cut in approx. 1 × 1 cm^2 pieces and placed onto the surface of all above listed culture media. After environmental water filtration, filters were placed onto the following culture media: Dichloran Rose Bengal Chloramphenicol agar (DRBC; Biolife), Sabouraud's

FIGURE 2 | Baits placed in Falcon tubes, closed with nylon textile, protected by perforate plastic container, firmly fixed into cave water by ropes.

dextrose agar (SabD; Biolife), malt extract agar (MEA), tryptone gelatine hydrolyzate lactose agar (TGhL; Longcore et al., 1999).

All culture media were inoculated in duplicates; one set was incubated at 15°C (close to the temperature of cave environment, appropriate for *B. salamandrivorans*) and the other at 20°C (appropriate for *B. dendrobatidis*) until visible growth. Fungi were isolated in pure cultures and deposited in the Ex Culture Collection of the Infrastructural Centre Mycosmo, MRIC UL, Slovenia,[2] at the Department of Biology, Biotechnical Faculty, University of Ljubljana. All isolated fungi were identified to the genus or species level by their morphology and by sequencing the molecular taxonomic markers as described below. Microscopic characters were observed with Nomarski interference contrast optics on Olympus BX-51 microscope, and micrographs were recorded with DP72 camera (Olympus).

Molecular Identification of Isolates

Genomic DNA of yeast isolates was extracted using the PrepMan Ultra reagent (Applied Biosystems) according to the manufacturer instructions. DNA of filamentous fungi was extracted after mechanical lysis in CTAB buffer according to the protocol described by Gerrits van den Ende and de Hoog (1999). DNA regions/genes used for identification were internal transcribed spacers 1 and 2 including the 5.8S rDNA (ITS), partial large ribosomal subunit rDNA including its D1/D2 domains (LSU) for the majority of isolates, partial sequences of genes encoding for actin (*act*) for genus *Cladosporium*, translation elongation factor one alpha (EF-1α) for genera *Trichoderma* and *Fusarium*, and β-tubulin (*benA*) for genera *Aspergillus* and *Penicillium*. These were PCR amplified and Sanger sequenced with the following primer sets: ITS1/ITS4 and NL1/NL4 (White et al., 1990), ACT-512F/ACT-738R (Carbone and Kohn, 1999), EF1-983F/EF1-2218R (Rehner and Buckley, 2005), Ben2f (Hubka and Kolarik, 2012)/Bt2b (Glass and Donaldson, 1995). After sequencing the sequences of the most similar type strains and other taxonomically important reference strains were retrieved from the non-redundant GenBank nucleotide database with the blast algorithm (Altschul et al., 1990) and aligned with sequences of olm isolates, followed by phylogenetic analyses with maximum likelihood method as implemented in Mega7, version 7 (Kumar et al., 2016). All DNA sequences from the representative strains from this study were deposited in the GenBank database: ON261225–ON261330, ON312944–ON312998 (ITS rDNA), ON777803–ON777808 (actin), ON777793–ON777802 (beta tubulin), ON804224–ON804232 (translation elongation factor 1-alpha).

Statistical Methods

To identify potential connections between environmental variables and microbial diversity, machine learning methods were

[2]http://www.ex-genebank.com/

used to analyze the data. All analyses have been performed in the environment R and Microsoft Excel, 2016.

Hierarchical clustering was employed to determine the similarity among samples, using function "hclust()" from the package "stats" v3.6.1, which is part of the base R.

Correlation of occurrence of fungal species was obtained by the function "cor()" from the package "stats" v3.6.1. Graphical images were produced with the function "pheatmap()" from the package "pheatmap" v1.0.12 (Kolde, 2019). Species cooccurrence was investigated with the package "cooccur" v1.3 (Griffith et al., 2016) in R. R package "randomForest" (Liaw and Wiener, 2002) was used for the construction of decision trees as a means to identify fungal taxa (based on their presence/absence) with good predictive power of different environmental variables (e.g., animal health or captivity). We have calculated 10001 trees at each condition studied. Visualization of taxonomic units was made by software package ggplot2 (Wickham, 2016).

RESULTS

Sampling of Healthy and Symptomatic Animals

Over a 2-year period, a total of 42 animals were sampled in five karstic caves and at three locations where animals are held in long-term captivity (**Figure 1**). Thirty-three swab samples (78.6%) were from healthy, asymptomatic animals, out of which 19 were from the natural subterranean environment (57.6%) and 14 were from captivity (42.4%). Nine symptomatic animals are briefly described in **Table 1**. Eight were from captivity and one from the natural environment of the Postojna-Planina cave system (from Črna jama cave).

Fungal Diversity From Asymptomatic Animals

Total number of fungal isolates from all animals was 244. These isolates represent 73 different genera and 115 species. The complete list of isolated fungi from all animals is presented in **Supplementary Table 2**, and the list of fungal species isolated from at least two animals in **Table 2**. The highest diversity of fungi was determined for 14 asymptomatic captive animals. Fungi that were isolated exclusively from these animals belong to 39 different genera and 60 different species. On average, 9.5 strains and 7.4 different species were isolated per animal (3 to 22 strains and 1 to 18 different species per animal). The majority of species were represented by only one or two isolates. Species that were represented with at least 3 and up to 7 isolates were: *Acremonium* sp. (nov.), *Apiotrichum laibachii*, *Ap. porosum*, *Candida saitoana*, *C. sake*, *Cyphellophora olivacea*, *Dipodascus geotrichum*, *Exophiala castellanii*, *Penicillium roseopurpureum*, *P. roseopurpureum*, *Pseudogymnoascus* spp., *Samsoniella hepiali*, and unidentified isolates belonging to *Rutstroemiaceae*.

On 19 asymptomatic animals sampled in the wild, fungal diversity was much lower (**Supplementary Table 2**). In 6 animals, no fungal strains were obtained at all, while on the remaining 13 animals, 12 different species from 11 genera were found. On average, 1.3 isolates were obtained per animal (1 to 6 strains, 1 to 4 different species per animal). Again, the frequency of most species was 1 to 2 strains per animal (**Supplementary Table 2**). Only two species were represented by six (*Cystofilobasidium* aff. *macerans*) and five strains (*Tausonia pullulans*), respectively. With the exception of one species (*Bjerkandera adusta)*, there was no overlap in the diversity of fungi from asymptomatic animals in nature and captivity. Examples of culture media with swab samples from asymptomatic animals from wild and captivity, incubated for 14 days at 20°C, are presented on **Figure 3**.

Fungal Diversity From Symptomatic Animals

Fungi were isolated also from animals (**Figure 4A**) with very different symptoms. Summarized symptoms of animals are presented in **Table 1**.

Based on the most common pathologies, the symptomatic animals were assigned to three groups: (i) edema, (ii) visible fungal overgrowth, and (iii) lethargy.

(i) Edema is the most prominent morphologic pathology in olms. They occasionally grow to extent of impaired movement and disfigurement of symptomatic specimens. The first animal in this group (specimen Paa2) developed an extensive edema throughout the body cavity after being held in captivity for over 10 years. After removal of 22 ml of fluid from the body cavity, the edema recurred after 3 months. The recurrence of edema was accompanied by bleeding into the body cavity and lethargy of the animal. Autopsy of the euthanized specimen revealed yellow nodular formations on the kidneys and

TABLE 1 | Symptoms of visibly diseased (symptomatic) animals.

Animal	Captivity (C)/Nature (N) and location	Symptoms
Paa2	C (Vivarium 1)	Extensive and recurring edema of body cavity, yellow nodular formations on kidneys and mottled lesions on internal organs
Paa3	C (Vivarium 1)	Lethargic, underweight
Paa18	C (Vivarium 1)	Moldy overgrowth on the detached limb
Paa22*	C (Vivarium 1)	Visible mycelium on the limb
Paa23	N (Črna jama, Planina-Postojna cave system)	Extensive edema of body cavity, yellow nodular formations on internal organs
Paa25*	C (Vivarium 2)	Lethargic, visible mycelia on the head and limbs
Paa26	C (Vivarium 2)	Visible moldy overgrowth on the body surface
Paa37	C (Vivarium 3)	Edemas in pectoral and pelvis region
Paa42	C (Vivarium 3)	Lethargic

**Animals originated from the Planina-Postojna cave system. They showed symptoms after 1 month in captivity.*

TABLE 2 | List of fungal species isolated from at least two sampled olm specimens: asymptomatic animals (A), symptomatic animals (S), natural cave environment (N), captivity (C), number of olm specimens from which fungal strains were isolated (P).

Taxon name	A	S	N	C	P	Olm specimen
Acremonium sp. (nov.)*	+	+		+	6	Paa20, Paa21, **Paa26**, Paa29, Pap36, Pap39
*Apiotrichum laibachii***,Y	+			+	3	Paa33, Paa35, Paa41
*Aspergillus creber**	+	+	+	+	2	Paa20, **Paa22**
*Aspergillus jensenii**	+	+		+	2	Paa28, **Paa42**
*Bjerkandera adusta***	+		+	+	2	Paa15, Paa41
*Candida vartiovaarae**,Y	+	+		+	2	**Paa26**, Paa35
*Cladosporium allicinum**		+	+	+	2	**Paa2**, **Paa23**
*Cladosporium neolangeronii**	+	+	+	+	3	Paa15, Paa20, Paa29
*Cladosporium pseudocladosporioides**	+	+	+	+	3	Paa2, Paa7, Paa41
*Cyphellophora olivacea**	+			+	2	Paa20, Paa21
Cystofilobasidium sp. (nov.)**,Y	+		+		3	Paa30, Paa31, Paa32
*Debaryomyces hansenii**,Y	+	+	+	+	4	Paa32, Pap38, Pap39, Paa40
*Dipodascus geotrichum**,Y	+			+	2	Paa35, Paa41
*Exophiala castellanii**,BY	+			+	2	Paa20, Paa21
*Lecanicillium coprophilum**	+	+		+	4	Paa29, Pap36, **Paa37**, Pap39
*Mucor circinelloides****	+			+	2	Paa33, Paa35
*Mucor racemosus****	+			+	2	Paa33, Paa35
*Parengyodontium album**	+	+	+	+	2	Paa11, Paa27
*Penicillium atrosanguineum**	+			+	2	Pap38, Pap39
*Penicillium brevicompactum**	+	+	+	+	2	**Paa2**, Paa32
*Penicillium chrysogenum**	+	+	+	+	5	**Paa2**, Paa20, **Paa18**, Paa27, Paa28, Paa29
*Penicillium citreonigrum**	+			+	2	Pap38, Pap39
*Penicillium roseopurpureum**	+			+	3	Paa20, Pap38, Pap39
Pseudogymnoascus sp.*	+			+	4	Paa20, Paa21, Paa27, Paa28
*Pyrenochaetopsis leptospora**	+	+	+		2	Pap1, **Paa23**
*Samsoniella hepiali**	+			+	2	Pap36, Paa41
*Saprolegnia parasitica*****		+	+		2	**Paa22**, **Paa25**
*Trichoderma simmonsii**	+	+	+	+	2	**Paa3**, Paa4
*Trichoderma viride**	+			+	2	Paa33, Paa35

*+Isolation of fungal species from a particular source. *****Affiliation to the main fungal phyla, *Ascomycota, **Basidiomycota, ***Mucoromycota, ****Chytridiomycota, ***** Oomycota; Y: yeast; BY: – black yeast; Paa, Poteus anguinus anguinus; Pap, Proteus anguinus parkelj. Labels of symptomatic animals are written in bold and underlined.*

white mottled lesions on the internal organs. Two fungal genera were isolated: melanized filamentous *Cladosporium allicinum, Cl. pseudocladosporioides,* and filamentous *Penicillium brevicompactum,* and *P. chrysogenum* (**Table 2**). Similar pathology was observed in specimen Paa23 captured in the natural environment of the Postojna-Planina cave system. Again, the pronounced edema extended over the entire body cavity (**Figure 4B**) and autopsy revealed yellow nodular formations on the liver and kidneys. The specimen was colonized by 15 different genera comprising 15 species (data shown in **Table 2** and in **Supplementary Table 2**). Among them three melanized species (*Cladosporium allicinum*, *Cadophora melinii*, and *Phialocephala glacialis*) are recognized as potential causative agents of phaeohyphomycosis. Other isolated species were *Cystobasidium minutum*, *Juxtiphoma eupyrena*, *Plectosphaerella plurivora*, *Pyrenochaetopsis leptospora*, *Sistotrema brinkmannii, Talaromyces kabodanensis, Truncatella angustata*, and *Xylodon flaviporus*, potentially new species of genera *Paracremonium* and *Paraphoma*, and yet unidentified species belonging to Pleosporales and Helotiales. The edemas of a third specimen in this group (specimen Paa37) were localized in the pectoral and pelvic regions. Specimen developed symptoms after being kept

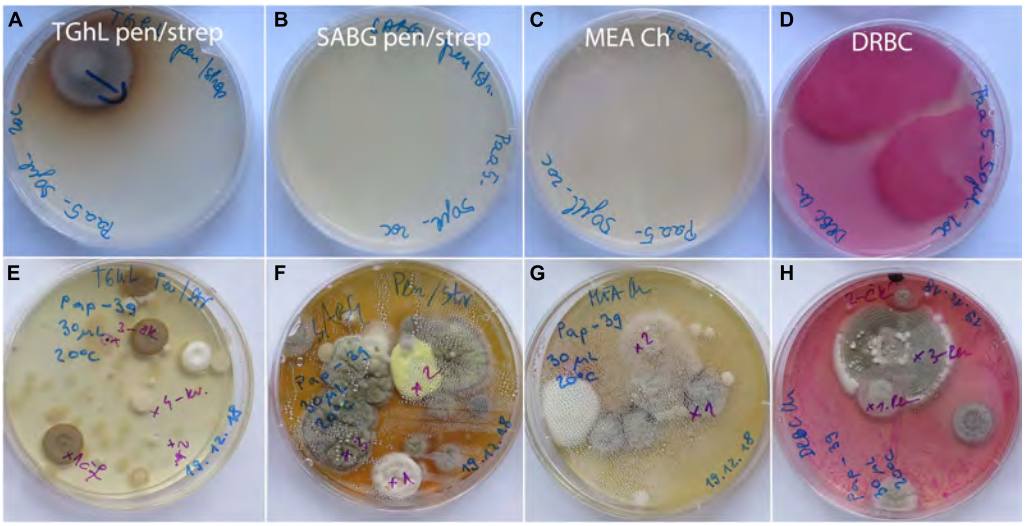

FIGURE 3 | Primary isolation plates after 14 days of incubation at 20°C with skin surface swab samples of asymptomatic *Proteus anguinus*. **(A–D)** Paa5 from wild; **(E–H)** Pap39 from captivity (Vivarium 2).

FIGURE 4 | Healthy asymptomatic olm, *Proteus anguinus* from captivity **(A)**. Specimen Paa23 with extensive edema throughout body cavity **(B)**. Dense, boot-resembling *Sporolegnia* overgrowth on hind limb of symptomatic animal Paa22 **(C)**.

in captivity for several years and only a single fungal species was isolated from the animal: *Lecanicillium coprophilum.*

(ii) The group of symptomatic animals with visible fungal overgrowth includes four specimens. The first specimen, Paa18, was a 2-year-old juvenile bred in Postojna cave aquaria. The specimen lost its hind limb after a fight with its sibling. Direct microscopy revealed coenocytic hyphae and sporangia typical for *Cunninghamella*, which was not isolated in pure culture. Isolated fungi from hyphal overgrowth of the injured limb included three fungal species: *Penicillium chrysogenum, Sydowia polyspora* and *Trichoderma citrinum*. Second individual with visible fungal infection (Paa22) developed symptoms after being held in captivity for 1 month. Besides dense, fungal cotton-like overgrowth on the hind limb, resembling a boot (**Figure 4C**),

the specimen exhibited impaired swimming ability. The limb of the specimen was primarily colonized by several strains of the opportunistic pathogenic oomycete *Saprolegnia parasitica*, and additionally by *Aspergillus creber, A. sydowii, Chalara holubovae, Gnomoniopsis* sp. (nov.), *Peniophora pithya* and *Rutstroemia conformata*. None of the latter three fungal species were isolated from the specimen Paa23 with prominent edema (see above), which was caught at the same locality. Specimen Paa25, held in captivity for 1 month, was infected as well with *Saprolegnia parasitica,* with distinctive hyphal overgrowth on its head and limbs. The last specimen (Paa26) developed moldy overgrowth all over its body after being held in captivity for several years. Fungi isolated from the overgrowth were *Acremonium* sp. (nov.) and *Candida vartiovaarae*.

(iii) The third group of symptomatic animals included two lethargic specimens without other visible pathologies. The first specimen (Paa3) was kept in captivity for over 10 years. It gradually became lethargic and ceased to feed resulting in weight loss. No fungal isolates were obtained from the skin surface of this animal. Second animal with lethargy as the most distinctive symptom (Paa42) has been brought to the cave laboratory, which serves as an asylum for olms washed out of their cave habitat, and only *Aspergillus jensenii* was isolated from this specimen.

Isolates exclusively from symptomatic animals belong to 24 genera and 27 species, most of them with only 1 or 2 isolates: *Acremonium* sp. (nov.) (**Figure 5**), *Aspergillus sydowii, Cadophora ramosa, Chalara holubovae, Cladosporium halotolerans, Cl. pulvericola, Colpoma* sp. (nov.), *Cystobasidium minutum, Gnomoniopsis* sp. (nov.), *Juxtiphoma eupyrena, Paracremonium* sp. (nov.), *Paracremonium variiforme, Paraphoma* sp. (nov.), *Penicillium crustosum, P. expansum, Peniophora pithya, Phialocephala glacialis, Rutstroemia conformata, Sistotrema brinkmannii, Sydowia polyspora, Talaromyces kabodanensis, Trichoderma citrinum, Truncatella angustata, Xylodon flaviporus*, and unidentified isolates belonging to *Phanerochaete,* Pleosporales, and Helotiales. *Plectosphaerella plurivora* was represented by three isolates from an olm specimen (Paa23), and one additional isolate from environmental water (**Supplementary Table 2**). The only exception with a higher abundance was the oomycete *Saprolegnia parasitica* with seven isolates from two animals (**Table 2**), sampled at two different localities, with approximately 3 weeks between the samplings.

The overlap between symptomatic animals in captivity and in nature consisted of one species only: *Cladosporium allicinum.* There were only eight fungal species retrieved from symptomatic or asymptomatic, and/or in nature or in captivity: *A. creber*, *Cl. neolangeronii*, *Cl. pseudocladosporioides*, *Debaryomyces hansenii*, *Parengyodontium album*, *P. brevicompactum*, *P. chrysogenum,* and *T. simmonsii* (**Table 2**).

Fungal Diversity From Water and Baits

Water was sampled in two locations (Jelševnik, Planinska jama), while baits were placed in water at four locations (Jelševnik, Krška jama, Planinska jama, Kompoljska jama).

In total 129 strains were isolated exclusively from water and baits and were not retrieved from swab samples of animals. They were represented by 22 genera and 52 species. The dominant genera were *Mucor* with six different species and a total of 43 isolates, primarily due to 34 isolates of *Mucor laxorrhizus*, and *Trichoderma* with 12 species and 43 isolates. The diversity of fungi obtained by baiting with keratin, hemp seeds and water agar in dialysis tubes was much higher than obtained by water filtration, mostly due to the overgrowth of fast spreading fungi, like *Trichoderma*, *Fusarium,* and *Mucor* in the latter case (**Supplementary Table 3**). Some fungi observed on the baits by direct microscopy could not be isolated into pure culture (**Figure 6**). For example, a chytrid fungus (**Figures 6B,C**) was

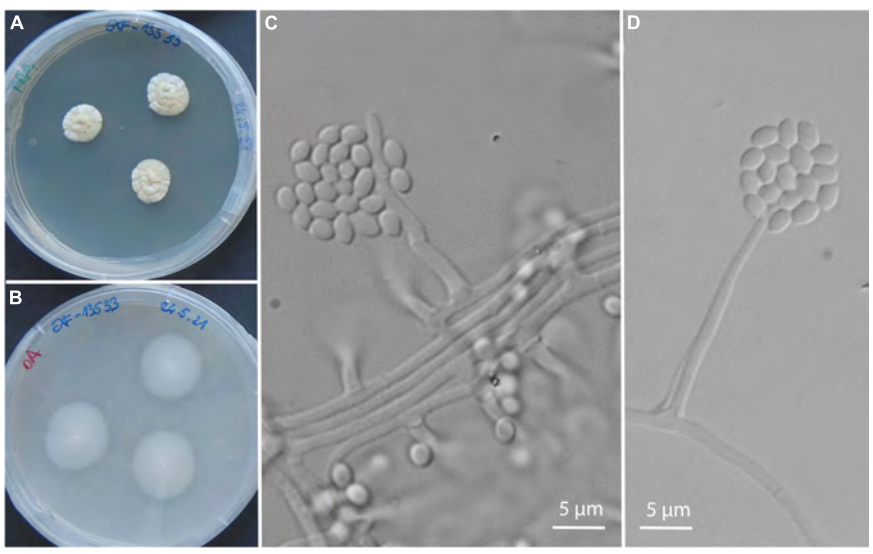

FIGURE 5 | A new species of the genus *Acremonium* isolated from olms in captivity: from several asymptomatic and from a single symptomatic animal. Culture of EXF-13533 on PDA **(A)**, on OA **(B)**; micromorphology of the strain EXF-14260 on PDA **(C,D)**.

only grown on feathers, and mycelia of unidentified, presumably oomycete, from molten snake skin bait (**Figures 6E,F**).

Statistical Evaluation of Results

Since most isolated fungi appeared only in individual samples, statistical analyses were performed based on the presence/absence data of individual genera and not individual species.

Statistically significant differences in the presence of fungal genera were observed between different types of samples (ANOVA $p < 0.01$), and the significant difference was confirmed with a *post-hoc* estimated marginal means pairwise comparison between animal swabs and microbial baits ($p < 0.01$) and also between water and baits ($p < 0.05$).

Among animal isolates we observed a statistically significant co-occurrence of the genera *Penicillium* and *Debaryomyces* (**Supplementary Figure 1**). When considering all samples

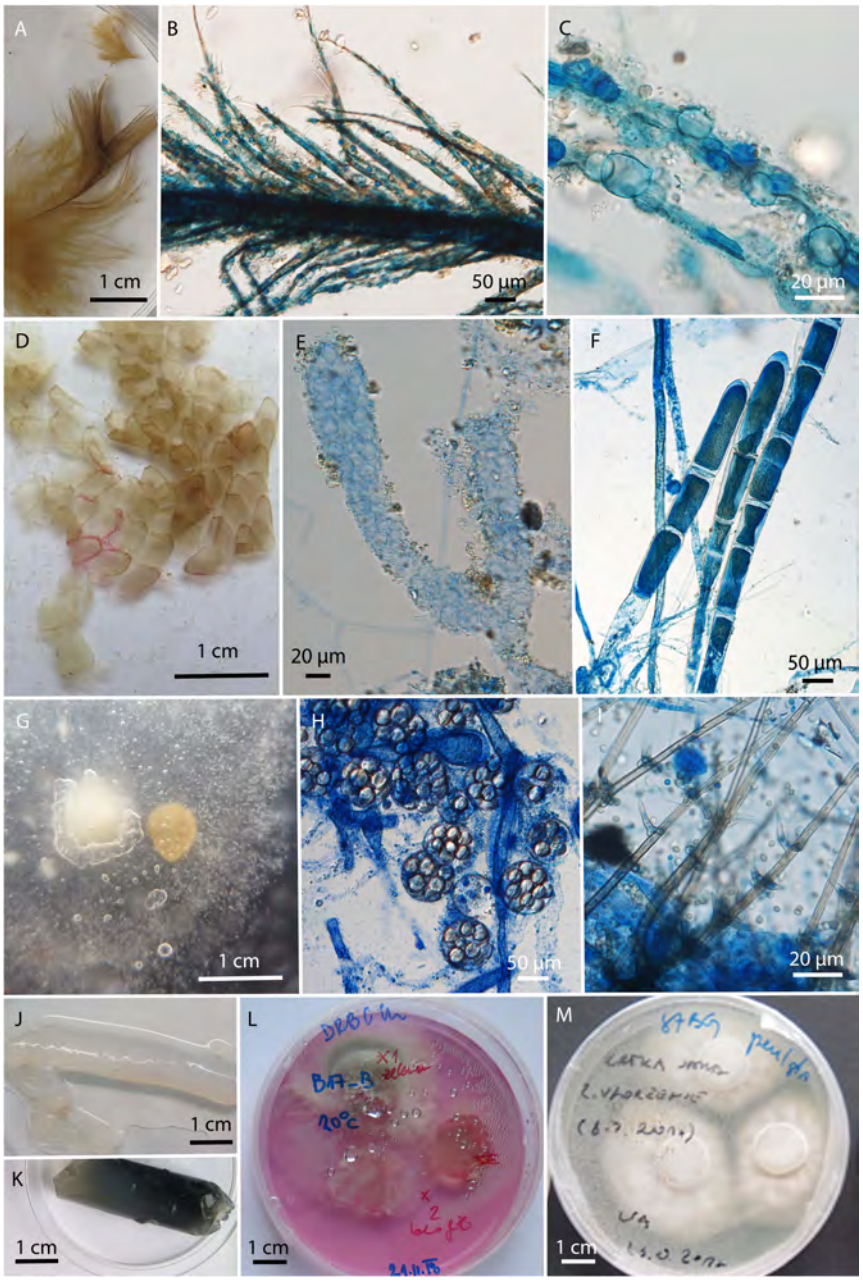

FIGURE 6 | Microbiological baits after incubation in the environmental water. **(A–C)** Bird feathers colonized by unknown chytrid; **(D)** molten snake skin; **(E–F)** unknown filamentous organism growing on molten snake skin; **(G)** canopy seeds after incubation, overgrown with **(H)** *Saprolegnia* () and **(I)** *Chloridium aseptatum*; **(J,K)** dialysis tubes filled with water agar; **(L,M)** cut pieces of agar after incubation on isolation culture media.

(animals, baits, and water) the genus *Trichoderma* co-occurred with *Clonostachys*, *Fusarium*, *Mortierella,* and *Mucor*, while *Penicillium* additionally co-occurred with *Pseudogymnoascus*.

Differences in the presence of fungal genera between animals in captivity and nature and differences between symptomatic and healthy animals were not statistically significant (ANOVA $p > 0.05$).

Also, in hierarchical clustering analysis, the samples from symptomatic or captive samples failed to cluster together (**Figure 7**).

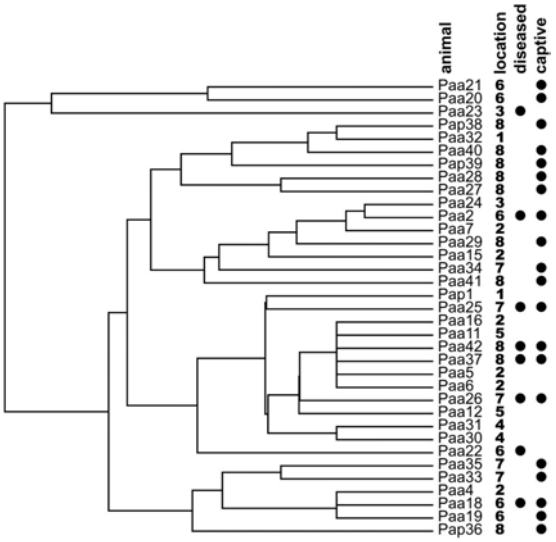

FIGURE 7 | Hierarchical clustering analysis of the olm specimens based on the presence/absence of cultivable fungal genera on the skin of the sampled animals. Locations of specimen samplings are given next to the names of specimen (1: Vivarium 1; 2: crna jama; 3: Vivarium 3; 4: Jelševnik; 5: Planinska jama; 6: Vivarium 2; 7: Vir pri Sticni; and 8: Kompoljska jama). Symptomatic diseased animals and animals held in captivity prior to sampling are marked with black circles.

DISCUSSION

Olm's Opportunistic Fungal Pathogens

The olm is an endemic cave amphibian with a number of extraordinary and unique characteristics. Understanding the interactions of the olm with its environment, including interactions with microbes, is essential for its successful protection. The main goal of this study was to identify potential fungal pathogens of olms and to contribute to a little-known topic for amphibians in general. There are few reports of fungal diseases in wild and captive amphibians, and the causal relationships with clinical signs of infection are often vague, as confirmed with symptoms observed in olms. Symptoms of fungal infection in amphibians include weight loss, ulcers, or multiple granulomas in the skin, skeletal muscles, meninges, and bone marrow (Cicmanec et al., 1973; Taylor et al., 2001). In addition, swelling and lesions of internal organs may occur with visible hyphae and sclerotic bodies in the spleen, liver, kidney, heart, and lungs. Death usually occurs 1–6 months after the first signs of infection. These symptoms were not observed in olms. Zygomycosis, primarily due to infections with *Mucor* spp. (Frank, 1976; Fowler, 1986; Speare et al., 1994; Taylor et al., 1999; Perpinan et al., 2010) and *Rhizopus* spp. (Taylor et al., 1999), can occur in a systemic form (Speare et al., 1994) or as external dermatitis (Taylor et al., 1999). Clinical signs include lethargy and multifocal hyperemic nodules with visible fungal growth, that is in general progressive and leads to death within 2 weeks (Taylor et al., 1999). Although lethargy was an observed symptom in two olms, both in long term captivity, no zygomycosis was determined and only three fungal species were isolated: human opportunistic pathogen *A. jensenii* (Zen Siqueira et al., 2016), plant pathogenic psychrotolerant *P. expansum* (Al Riachy et al., 2021) and soil and plant litter associated saprophytic *Trichoderma simmonsii* (Chaverri et al., 2015). Similar symptoms can occur in cutaneous and disseminated systemic chromomycosis, and phaeohyphomycosis (Seyedmousavi et al., 2013), caused by different pigmented ascomycetous species of the genera *Cladosporium*, *Exophiala*, *Fonsecaea*, *Ochroconis*, *Phialophora*, *Rhinocladiella* and *Scolecobasidium* (Juopperi et al., 2002; Seyedmousavi et al., 2013), which have been isolated from various wild and captive anurans (Dhaliwal and Griffiths, 1963; Elkan and Philpot, 1973; Rush et al., 1974; Beneke, 1978; Miller et al., 1992; Seyedmousavi et al., 2013). Although some of the above listed fungi were isolated from symptomatic olms, they did not cause chromomycosis, and phaeohyphomycosis. If information on fungal diseases of toads and frogs are few, information on fungal diseases of salamanders are even scarcer. In addition to reports of *B. salamandrivorans* infections, only Nickerson et al. (2011) have reported fungal infections in a giant aquatic ozark hellbender salamander (*Cryptobranchus alleganiensis bishopi*). Intact skin was infected with fungal species of the genera *Aureobasidium*, *Cladosporium*, and *Penicillium*, while injured skin sites were colonized with species of the genera *Acremonium*, *Aspergillus*, *Cladosporium*, *Curvularia*, *Exophiala*, *Fusarium*, *Penicillium*, *Sporothrix,* and streptomycetes. With the exception of three reports of saprolegniosis and *Exophiala* infection of olms in captivity, there were so far no data in the literature about fungal infections in cave salamanders (Kogej, 1999; Bizjak-Mali et al., 2018; Lukač et al., 2019).

Out of nine symptomatic olms sampled in this study, only one was from the wild. The time in captivity ranged from only 1 month and up to more than 10 years. The symptomatic olms from captivity were divided into three groups. First, two lethargic specimens described above. Extensive edema was the prevailing symptom in the second group, that included two animals in long- term captivity and the only symptomatic animal from the wild. Although isolates comprised many different fungal species, only the human opportunistic pathogen *C. allicinum* (Sandoval-Denis et al., 2016) was isolated from two of them. From the third specimen only *Lecanicillium coprophilum* was recovered. Species in *Lecanicillium* are known pathogens of arthropods, nematodes, and other fungi (Su et al., 2019). The third group included specimens with visible fungal growth. In the first case (lethargic specimens), diverse fungi, probably representing

secondary infectious agents, were isolated from a traumatic injury. The second specimen, which had been in captivity for several years, was moldy all over its body. The dominant isolate likely represents a new species of the genus *Acremonium* which is most similar to *Acremonium sclerotigenum* group according to ITS rDNA sequences (92% similarity). However, the same *Acremonium* species was also detected on skin of asymptomatic animals exclusively in captivity, at two different locations. Other two olm specimens kept in captivity for only 1 month, developed cotton-like overgrowth which was identified as *Saprolegnia parasitica* in one case and as *Cunninghamella* in the other case. Oomycete water molds *Saprolegnia ferax*, *S. parasitica* or *Aphanomyces* spp. are known to cause saprolegniasis in amphibians (Densmore and Green, 2007). Species of *Saprolegnia* are primary skin or oral pathogens in larval amphibians and causative agents of secondary superficial infections in aquatic anurans and urodelans (Kiesecker et al., 2001; Densmore and Green, 2007). These oomycetes can also have a significant impact on amphibian fecundity as well as on egg mortality (Blaustein et al., 1994). Clinical signs include external appearance of mycelium with cotton-like texture, visible hyphae and zoospores in lesions, erythematous or ulcerated skin on tail, hind limbs, gills, and oral mucosa, but rarely with deep tissues lesions (Densmore and Green, 2007). Additional symptoms may include weight loss, lethargy, vomiting, and respiratory distress (Frye and Gillespie, 1989). Previously, there were two reports of infection with *Saprolegnia* spp. on the limbs, gills and even disseminated in other body parts of captive olm specimens (Kogej, 1999; Lukač et al., 2019). It should be noted that the olm has a thin larval skin that is particularly susceptible to infection (Lindinger, 1984). The epidermis of the olm consists of a stratified squamous epithelium covered with mucus, while keratinized skin is present only on the feet (Lindinger, 1984; Bulog, 1994).

Mycoflora of Asymptomatic Olm Specimens

Since olm has an important ecological role as top predator of underground water systems, its presence reflects the stability of food chains in karst underground water, a unique ecosystem with the highest underground biodiversity in the World. In this light, the health of natural populations of olms may reflect disturbances in their environment such as pollution of water sources that could represent a serious threat to endemic biodiversity and a risk to human health. A study of bacterial diversity of olm skin and their groundwater environment revealed that the identified bacterial taxa were a strongly filtered subset of the environmental microbial community. It was hypothesized that this microbiome protects against invading microbes by competitive exclusion, and thus could serve as an indicator of health status (Kostanjšek et al., 2019). In this light we investigated the diversity of cultivable fungi obtained by swab sampling of asymptomatic specimens both in the wild and in captivity. In accordance, asymptomatic olms from nature resulted in isolation of sporadic colonies, displaying the lowest diversity of fungi in general and few opportunistic species. Although only a small number of fungal isolates were obtained, these isolates differed from specimen to specimen. Among them, the identified genera *Bjerkandera*, *Cystofilobasidium*, *Exophiala, Fusarium, Penicillium, Pseudogymnoascus, Stereum*, *Tausonia,* and *Trametes*, were previously reported from cave environments around the globe (Vanderfolf et al., 2013; Novak-Babič et al., 2016, 2017).

In comparison, the total number of isolates and diversity of fungi isolated from asymptomatic captive animals was considerably higher. Among the fungal genera previously reported from cave environments were *Aspergillus, Barnettozyma, Candida, Cladosporium, Debaryomyces, Exophiala, Mortierella, Mucor, Naganishia*, *Penicillium, Phoma, Pseudogymnoascus, Sporobolomyces*, and *Trichoderma* (Grishkan et al., 2004; Vanderfolf et al., 2013; Novak-Babič et al., 2016, 2017). In addition to these, representatives of 23 fungal genera were isolated that, to the best of our knowledge, had not previously been reported from underground water habitats. Their presence may be related to the human presence and water quality (e.g., *Candida*) or to the materials used in vivaria, e.g., wood related to basidiomycetous genera *Bjerkandera, Byssomerulius, Clitocybe, Peniophora*, and *Phanerochaete* (Boddy et al., 2008; Kirk et al., 2008). Interestingly, the number of yeasts on captive animals was considerably higher than those reported from cave waters, among them *Apiotrichum laibachii*, *A. porosum, A. akiyoshidainum, Barnettozyma californica, Candida friedrichii*, *C. glaebosa, C. saitoana, C. sake*, *C. vartiovaarae, Cutaneotrichosporon cutaneum, Cu. dermatis*, *Cyphellophora olivacea*, *Debaryomyces vindobonensis*, *Dipodascus geotrichum*, *Exophiala alcalophila*, *E. castellanii*, *Naganishia* sp., *Rhodosporidiobolus fluvialis,* and *Sporobolomyces ruberrimus.*

Subterranean Water Environment as Vector for Amphibian Opportunistic Pathogenic Fungi

Water is crucial for the amphibian life cycle and is one of the main vectors for pathogen transmission. *Batrachochytrium dendrobatidis* and *B. salamandrivorans*, species of *Saprolegnia*, *Cladosporium*, *Mucor*, *Fusarium* and melanized fungi, such as species of genera *Exophiala*, *Rhinocladiella*, *Phialophora* and *Aureobasidium melanogenum* are present in various aquatic environments worldwide (Kiesecker et al., 2001; Göttlich et al., 2002; de Hoog et al., 2011; Defra, 2011; Novak-Babič et al., 2016). In addition to water, amphibians can also become infected through the soil or dead plant matter after stress or traumatic injury of the skin, by ingestion, or by inhalation of fungal spores that can be transported into caves by numerous organisms, including invertebrates, bats, rodents, other animals and humans, as well as by air circulation (Whitaker and Jaw, 2021). In the northern hemisphere, where most cave mycological studies have been conducted, caves are generally characterized by a lack of organic substrates and stable temperatures. This environment favors communities of oligotrophic, psychrotolerant fungi (Vanderfolf et al., 2013). Fungi isolated from asymptomatic animals in the wild reflect this ecology. In this study, Basidiomycota isolates, often associated with nutrient rich substrates such as wood and dung, represented only 8.6% (6 strains of 70) and 1.2% (3 strains of 155) of isolates from animals in nature and captivity, respectively, and only 2.6% (4 strains of 152) of isolates from cave water. Amongst the genera and species

most frequently reported in studies on cave mycology (Vanderfolf et al., 2013), we identified the genera *Aspergillus* (3 isolates), *Chaetomium* (1), *Cladosporium* (5), *Fusarium* (11), *Mortierella* (6), *Mucor* (50), *Penicillium* (3), *Trichoderma* (51), and species *Penicillium brevicompactum* (1) and *Trichoderma viride* (2), from both undergound waters and asymptomatic animals. Since the most commonly reported cave fungal taxa were likely influenced by the cultivation media and conditions, rather than biological patterns in cave mycology, we tried to diminish this bias by using four different media and two incubation temperatures (15 and 20°C). This approach resulted in isolation of many rare and unusual taxa, with very low abundance and with 15 taxa that are most probably new for science. As we did not see any pattern of the diversity of commensal fungi isolated from asymptomatic animals from the wild or from captivity, we can conclude that olm in nature is considerably resistant to fungi, with many different species of fungi isolated as single isolates from asymptomatic animals.

CONCLUSION

The European blind cave salamander *Proteus anguinus* is a charismatic endemic amphibian that lives in the subterranean waters of the Dinaric Karst. Despite its exceptional conservation importance, not much is known about its ecology and interactions with the groundwater microbiome. The cutaneous microbiota of amphibians is an important driver of metabolic capabilities and immunity, and thus a key factor in their well-being and survival. In this study, we identified a high diversity of fungi to which olm's skin is exposed in nature and in captivity, reflecting the environmental status of the groundwater. In addition, this study provided the first insight into the presence of opportunistic fungi that threaten proteus in its natural habitat and could represent a health threat not only to proteus, but also to other endangered neotenic salamanders and amphibians inhabiting surface karstic waters. These results provide an initial step toward a comprehensive evaluation and mitigation of fungal threats to this unique amphibian species, which is an important component of its much-needed conservation plan.

DATA AVAILABILITY STATEMENT

The datasets presented in this study can be found in online repositories. The names of the repository/repositories and accession number(s) can be found in the article/ **Supplementary Material**.

ETHICS STATEMENT

Animals were collected under permit 35601-27/2021-8 issued by Ministry of the Environment and Spatial Planning of the Republic of Slovenia and Slovenian Agency for the Environment.

AUTHOR CONTRIBUTIONS

NG-C: conceptualization. PZ, CG, RK, and LB-M: methodology. PZ, AG, RK, and LB-M: investigation. NG-C and RK: resources. PZ and AG: data curation. NG-C, RK, and PZ: writing – original draft preparation. PZ and NG-C: writing – review and editing. RK and PZ: visualization. NG-C and RK: funding acquisition. All authors have read and agreed to the published version of the manuscript.

FUNDING

This research was funded by Slovenian Research Agency, "Emerging microbial threats to endemic troglobiotic amphibian *Proteus anguinus*" (grant number: J1-8141); research programs "Molecular Biology of Microorganisms" (grant number: P1-0198), and "Integrative zoology and speleobiology" (P1-0184).

ACKNOWLEDGMENTS

We acknowledge the financial support from the Slovenian Research Agency: research project J1-8141, Infrastructural Centers "Mycosmo" and "Microscopy of Biological Samples" located at Biotechnical Faculty, University of Ljubljana, a part of MRIC UL network. We also like to thank Mojca Matul and Barbara Kastelic Bokal for their excellent technical assistance, and Domin Dalessi for the foto material.

SUPPLEMENTARY MATERIAL

The Supplementary Material for this article can be found online at: https://www.frontiersin.org/articles/10.3389/fmicb.2022.926558/full#supplementary-material

REFERENCES

Al Riachy, R., Strub, C., Durand, N., Guibert, B., Guichard, H., Constancias, F., et al. (2021). Microbiome status of cider-apples, from orchard to processing, with a special focus on *Penicillium expansum*. Occurrence and patulin contamination. *J. Fungi* 7, 244. doi: 10.3390/jof7040244

Altschul, S. F., Gish, W., Miller, W., Myers, E. W., and Lipman, D. J. (1990). Basic local alignment search tool. *J. Mol. Biol.* 215, 403–410. doi: 10.1016/S0022-2836(05)80360-2

Arntzen, J. W., Denoël, M., Miaud, C., Andreone, F., Vogrin, M., Edgar, P., et al. (2009). *Proteus anguinus*. . *IUCN Red List Threat. Species* 2009:e.T18377A8173419.

Beneke, E. S. (1978). *Dermatiaceous Fungi in Laboratory-Housed Frogs*, 356. Washington, DC: Pan American Health Organisation Scientific Publication, 101–108.

Bizjak-Mali, L., Zalar, P., Turk, M., Novak Babic, M., Kostanjšek, R., and Gunde-Cimerman, N. (2018). Opportunistic fungal pathogens isolated from a captive individual of the European blind cave salamander *Proteus anguinus*. *Dis. Aquat. Organ.* 129, 15–30. doi: 10.3354/dao03229

Blaustein, A. R., Hoffman, P. D., Hokit, D. G., Kiesecker, J. M., Walls, S. C., and Hays, J. B. (1994). UV repair and resistance to solar UV-B in amphibian eggs: a link to population declines? *PNAS* 91, 1791–1795. doi: 10.1073/pnas.91.5.1791

Blooi, M., Pasmans, F., Longcore, J. E., Spitzen-van der Sluijs, A., Vercammen, F., and Martel, A. (2013). Duplex real-time PCR for rapid simultaneous detection of *Batrachochytrium dendrobatidis* and *Batrachochytrium salamandrivorans* in amphibian samples. *J. Clin. Microbiol.* 51, 4173–4177. doi: 10.1128/JCM.02313-13

Boddy, L., Frankland, J. C., and West, P. (2008). *Ecology of Saprotrophic Basidiomycetes*. Cambridge, MA: Academic Press, 226.

Boyle, D. G., Boyle, D. B., Olsen, V., Morgan, J. A. T., and Hyatt, A. D. (2004). Rapid quantitative detection of chytridiomycosis (*Batrachochytrium dendrobatidis*) in amphibian samples using real-time Taqman PCR assay. *Dis. Aquat. Organ.* 60, 141–8. doi: 10.3354/dao060141

Bulog, B. (1994). Dve desetletji funkcionalno-morfoloških raziskav pri mocerilu (*Proteus anguinus*, Amphibia, Caudata). *Acta Carsol.* 23, 248–263.

Bulog, B., Bizjak Mali, L., Kos, M., Mihajl, K., Prelovšek, P.-M., and Aljancic, G. (2000). Biology and functional morphology of *Proteus anguinus* (Amphibia, Caudata). *Acta. Biol. Slov.* 43, 85–102.

Carbone, I., and Kohn, L. M. (1999). A method for designing primer sets for speciation studies in filamentous ascomycetes. *Mycologia* 91, 553–556. doi: 10.1080/00275514.1999.12061051

Chaverri, P., Branco-Rocha, F., Jaklitsch, W., Gazis, R., Degenkolb, T., and Samuels, G. J. (2015). Systematics of the *Trichoderma harzianum* species complex and the re-identification of commercial biocontrol strains. *Mycologia* 107, 558–590. doi: 10.3852/14-147

Cicmanec, J. L., Ringler, D. H., and Beneke, E. S. (1973). Spontaneous occurrence and experimental transmission of the fungus, *Fonsecaea pedrosoi*, in the marine toad, *Bufo marinus*. *Lab. Anim. Sci.* 23, 43–47.

de Hoog, G. S., Vicente, V. A., Najafzadeh, M. J., Harrak, M. J., Badali, H., and Seyedmousavi, S. (2011). Waterborne *Exophiala* species causing disease in cold-blooded animals. *Persoonia* 27, 46–72. doi: 10.3767/003158511X614258

Defra. (2011). *Review of Fungi in Drinking Water and the Implications for Human Health*. London: Defra.

Densmore, C. L., and Green, D. E. (2007). Diseases of amphibians. *Ilar. J.* 48, 235–254. doi: 10.1093/ilar.48.3.235

Dhaliwal, S. S., and Griffiths, D. A. (1963). Fungal disease in Malayan toads – an acute lethal inflammatory reaction. *Nature* 197, 467–569. doi: 10.1038/197467a0

Elkan, E., and Philpot, C. M. (1973). Mycotic infections in frogs due to a *Phialophora* like fungus. *Sabouraudia* 11, 99–105. doi: 10.1080/00362177385190201

Fisher, M. C., and Garner, T. W. J. (2020). Chytrid fungi and global amphibian declines. *Nat. Rev. Microbiol.* 18, 332–343. doi: 10.1038/s41579-020-0335-x

Fowler, M. E. (1986). "Amphibians," in *Zoo and Wild Animal Medicine*, ed. M. E. Fowler (Philadelphia, PA: W.B. Saunders Company), 99–184.

Frank, W. (1976). "Mycotic infections in amphibians and reptiles," in *Wildlife Diseases*, ed. L. A. Page (Boston, MA: Springer), 73–88. doi: 10.1007/978-1-4757-1656-6_10

Frye, F. L., and Gillespie, D. S. (1989). *Saprolegniasis in a Zoo Collection of Aquatic Amphibians*. Orlando, FL: International Colloquium on the Pathology of Reptiles and Amphibians, 43.

Gerrits van den Ende, B., and de Hoog, S. (1999). Variability and molecular diagnostics of the neurotropic species *Cladophialophora bantiana*. *Stud. Mycol.* 43, 151–162.

Glass, N. L., and Donaldson, G. C. (1995). Development of primer sets designed for use with the PCR to amplify conserved genes from filamentous Ascomycetes. *Appl. Environ. Microbiol.* 61, 1323–1330. doi: 10.1128/aem.61.4.1323-1330.1995

Gorički, S., Stanković, D., Snoj, A., Kuntner, M., Jeffery, W. R., Trontelj, P., et al. (2017). Environmental DNA in subterranean biology: range extension and taxonomic implications for Proteus. *Sci. Rep.* 7:45054. doi: 10.1038/srep45054

Göttlich, E., van der Lubbe, W., Lange, B., Fiedler, S., Melchert, I., Reifenrath, M., et al. (2002). Fungal flora in groundwater-derived public drinking water. *Int. J. Hyg. Environ. Health* 205, 269–279. doi: 10.1078/1438-4639-00158

Griffith, D. M., Veech, J. A., and Marsh, C. J. (2016). cooccur: probabilistic species co-occurrence analysis in R. *J. Stat. Softw.* 69, 1–17. doi: 10.18637/jss.v069.c02

Grishkan, I., Nevo, E., and Wasser, S. P. (2004). Micromycetes from the saline arubotaim cave: Mount Sedom, the dead sea southwestern shore, Israel. *J. Arid. Environ.* 57, 431–443. doi: 10.1016/S0140-1963(03)00119-8

Heard, M. J., Smith, K. F., Ripp, K. J., Berger, M., Chen, J., Dittmeier, J., et al. (2013). The threat of disease increases as species move toward extinction. *Conserv. Biol.* 27, 1378–1388. doi: 10.1111/cobi.12143

Hubka, V., and Kolarik, M. (2012). β-tubulin paralogue tubC is frequently misidentified as the benA gene in *Aspergillus* section Nigri taxonomy: primer specificity testing and taxonomic consequences. *Persoonia* 29, 1–10. doi: 10.3767/003158512X658123

Juopperi, T., Karli, K., De Voe, R., and Grindem, C. B. (2002). Granulomatous dermatitis in a spadefoot toad (*Scaphiopus holbrooki*). *Vet. Clin. Pathol.* 31, 137–139. doi: 10.1111/j.1939-165X.2002.tb00294.x

Kiesecker, J. M., Blaustein, A. R., and Miller, C. L. (2001). Transfer of a pathogen from fish to Amphibians. *Conserv. Biol.* 15, 1064–1070. doi: 10.1046/j.1523-1739.2001.0150041064.x

Kirk, P. M., Cannon, P. F., Minter, D. W., and Stalpers, J. A. (2008). *Dictionary of the Fungi*, 10th Edn. Wallingford: CABI.

Kogej, T. (1999). *Infection of Proteus anguinus with the fungi of the genus Saprolegnia: graduation thesis*. Ljubljana: University of Ljubljana.

Kolde, R. (2019). *pheatmap: Pretty Heatmaps. R package version 1.0.12*. Available online at: https://CRAN.R-project.org/package=pheatmap

Kostanjšek, R., Diderichsen, B., Recknagel, H., Gunde-Cimerman, N., Gostincar, C., Fan, G., et al. (2021a). Toward the massive genome of *Proteus anguinus*—illuminating longevity, regeneration, convergent evolution, and metabolic disorders. *Ann. N. Y. Acad. Sci.* 1507, 5–11. doi: 10.1111/nyas.14686

Kostanjšek, R., Prodan, Y., Stres, B., and Trontelj, P. (2019). Composition of the cutaneous bacterial community of a cave amphibian, *Proteus anguinus*. *FEMS Microbiol. Ecol.* 95, 1–7. doi: 10.1093/femsec/fiz007

Kostanjšek, R., Turk, M., Vek, M., Gutiérrez-Aguirre, I., and Gunde-Cimerman, N. (2021b). First screening for *Batrachochytrium dendrobatidis*, *B. salamandrivorans* and *Ranavirus* infections in wild and captive amphibians in Slovenia. *Salamandra* 57, 162–166.

Kumar, S., Stecher, G., and Tamura, K. (2016). MEGA7: molecular evolutionary genetics analysis version 7.0 for bigger datasets. *Mol. Biol. Evol.* 33, 1870–1874. doi: 10.1093/molbev/msw054

Latney, L. V., and Klaphake, E. (2013). Selected emerging diseases of amphibia. *Vet. Clin. North. Am. Exot. Anim. Pract.* 16, 283–301. doi: 10.1016/j.cvex.2013.01.005

Laurenti, J. N. (1768). *Specimen Medicum Exhibens Synopsis Reptilium Emendatam*. Viennae: BiblioLife. doi: 10.5962/bhl.title.5108

Leung, W. T. M., Thomas-Walters, L., Garner, T. W. J., Balloux, F., Durrant, C., and Price, S. J. (2017). A quantitative-PCR based method to estimate *Ranavirus* viral load following normalisation by reference to an ultraconserved vertebrate target. *J. Virol. Methods* 249, 147–155. doi: 10.1016/j.jviromet.2017.08.016

Li, Z., Verbrugghe, E., Konstanjšek, R., Lukaè, M., Pasmans, F., Cizelj, I., et al. (2020). Dampened virulence and limited proliferation of *Batrachochytrium salamandrivorans* during subclinical infection of the troglobiont olm (*Proteus anguinus*). *Sci. Rep.* 10:16480. doi: 10.1038/s41598-020-73800-y

Liaw, A., and Wiener, M. (2002). Classification and regression by randomforest. *R News* 2, 18–22.

Lindinger, M. I. (1984). Fine structure of the abdominal epidermis of the adult mudpuppy, *Necturus maculosus* (Rafinesque). *Cell. Tissue Res.* 238, 395–405. doi: 10.1007/BF00217313

Longcore, J. E., Pessier, A. P., and Nichols, D. K. (1999). *Batrachochytrium dendrobatidis* gen. et sp. nov., a chytrid pathogenic toamphibians. *Mycologia* 91, 219–227. doi: 10.1080/00275514.1999.12061011

Lukač, M., Cizelj, I., and Mutschmann, F. (2019). "Health research and ex situ keeping of *Proteus anguinus*," in *Proteus*, eds K. Šariè, D. Jelić, P. Konrad, and B. Jalžić (Zagreb: Udruga Hyla), 219–232.

McGaugh, S. E., Kowalko, J. E., Duboue, E., Lewis, P., Franz-Odendaal, T. A., Rohner, N., et al. (2020). Dark world rises: the emergence of cavefish as a model for the study of evolution, development, behavior, and disease. *J. Exp. Zool. B. Mol. Dev. Evol.* 334, 397–404. doi: 10.1002/jez.b.22978

McKenzie, V. J., and Peterson, A. C. (2012). Pathogen pollution and the emergence of a deadly amphibian pathogen. *Mol. Ecol.* 21, 5151–5154. doi: 10.1111/mec.12013

Miller, E. A., Montali, R. J., Ramsay, E. C., and Rideout, B. A. (1992). Disseminated chromoblastomycosis in a colony of ornate-horned frogs (*Ceratophrys ornata*). *J. Zoo Wildl. Med.* 23, 433–438.

Nickerson, C. A., Ott, C. M., Castro, S. L., Garcia, V. M., Molina, T. C., Briggler, J. T., et al. (2011). Evaluation of microorganisms cultured from injured and repressed tissue regeneration sites in endangered giant aquatic Ozark hellbender salamanders. *PLoS One* 6:e28906. doi: 10.1371/journal.pone.0028906

Novak-Babič, M., Gunde-Cimerman, N., Vargha, M., Tischner, Z., Magyar, D., Veríssimo, C., et al. (2017). Fungal contaminants in drinking water regulation? A tale of ecology, exposure, purification and clinical relevance. *Int. J. Environ. Res. Public Health* 14, 636. doi: 10.3390/ijerph14060636

Novak-Babič, M., Zalar, P., Ženko, B., Džeroski, S., and Gunde-Cimerman, N. (2016). Yeasts and yeast-like fungi in tap water and groundwater, and their transmission to household appliances. *Fungal Ecol.* 20, 30–39. doi: 10.1016/j.funeco.2015.10.001

Perpinan, D., Trupkiewicz, J. G., Armbrust, A. L., Geiser, D. M., Armstrong, S., Garner, M. M., et al. (2010). Dermatitis In captive wyoming toads (*Bufo baxteri*) associated with *Fusarium* spp. *J. Wildl. Dis.* 46, 1185–1195. doi: 10.7589/0090-3558-46.4.1185

Price, S. J., Garner, T. W. J., Cunningham, A. A., Langton, T. E. S., and Nichols, R. A. (2016). Reconstructing the emergence of a lethal infectious disease of wildlife supports a key role for spread through translocations by humans. *Proc. Biol. Sci.* 283:20160952. doi: 10.1098/rspb.2016.0952

R and Microsoft Excel (2016). *R: A Language and Environment for Statistical Computing*. Vienna: R Foundation for Statistical Computing.

Rehner, S. A., and Buckley, E. (2005). A *Beauveria* phylogeny inferred from nuclear ITS and EF1-α sequences: evidence for cryptic diversification and links to *Cordyceps* Teleomorphs. *Mycologia* 97, 84–98. doi: 10.3852/mycologia.97.1.84

Robert, J., George, E., De Jesús Andino, F., and Chen, G. (2011). Waterborne infectivity of the Ranavirus frog virus 3 in *Xenopus laevis*. *Virology* 417, 410–417. doi: 10.1016/j.virol.2011.06.026

Rush, H. G., Anver, M. R., and Beneke, E. S. (1974). Systemic chromomycosis in *Rana pipiens*. *Lab. Anim. Sci.* 24, 646–655.

Safi, K., Armour-Marshall, K., Baillie, J. E. M., and Isaac, N. J. B. (2013). Global patterns of evolutionary distinct and globally endangered amphibians and mammals. *PLoS One* 8:e63582. doi: 10.1371/journal.pone.0063582

Sandoval-Denis, M., Gené, J., Sutton, D. A., Wiederhold, N. P., Cano-Lira, J. F., and Guarro, J. (2016). New species of *Cladosporium* associated with human and animal infections. *Persoonia* 36, 281–298. doi: 10.3767/003158516X691951

Scheele, B. C., Pasmans, F., Skerratt, L. F., Berger, L., Martel, A., Beukema, W., et al. (2019). Amphibian fungal panzootic causes catastrophic and ongoing loss of biodiversity. *Science* 363, 1459–1463. doi: 10.1126/science.aav0379

Seyedmousavi, S., Guillot, J., and de Hoog, G. S. (2013). Phaeohyphomycoses, emerging opportunistic diseases in animals. *Clin. Microbiol. Rev.* 26, 19–35. doi: 10.1128/CMR.00065-12

Sket, B. (1997). Distribution of Proteus (Amphibia: Urodela: Proteidae) and its possible explanation. *J. Biogeogr.* 24, 263–280. doi: 10.1046/j.1365-2699.1997.00103.x

Sket, B., and Arntzen, J. W. (1994). A black, non-troglomorphic amphibian from the karst of Slovenia: *Proteus anguinus* parkelj n. ssp. (Urodela: Proteidae). *Bijdr. Dierkd.* 64, 33–53. doi: 10.1163/26660644-06401002

Speare, R., Thomas, A. D., O'Shea, P., and Shipton, W. A. (1994). *Mucor Amphibiorum* in the Toad, *Bufo Marinus*, in Australia. *J. Wildl. Dis.* 30, 399–407. doi: 10.7589/0090-3558-30.3.399

Spitzen-van der Sluijs, A., Martel, A., Asselberghs, J., Bales, E. K., Beukema, W., Bletz, M. C., et al. (2016). Expanding distribution of lethal amphibian fungus *Batrachochytrium salamandrivorans* in Europe. *Emerg. Infect. Dis.* 22, 1286–1288. doi: 10.3201/eid2207.160109

Su, L., Zhu, H., Guo, Y., Du, X., Guo, J., Zhang, L., et al. (2019). *Lecanicillium coprophilum* (Cordycipitaceae, Hypocreales), a new species of fungus from the feces of *Marmota monax* in China. *Phytotaxa* 387, 58–62. doi: 10.11646/phytotaxa.387.1.4

Taylor, S. K., Green, D. E., Wright, K. M., and Whitaker, B. R. (2001). ""Bacterial diseases"," in *Amphibian Medicine and Captive Husbandry*, eds K. M. Wright and B. R. Whitaker (Malabar, FL: Krieger Publishing Company), 159–179.

Taylor, S. K., Williams, E. S., and Mills, K. W. (1999). Effects of Malathion on disease susceptibility In woodhouse's toads. *J. Wildl. Dis.* 35, 536–541. doi: 10.7589/0090-3558-35.3.536

Vanderfolf, K. J., Malloch, D., McAlpine, D. F., and Forbes, G. J. (2013). A world review of fungi, yeasts, and slime molds in caves. *IJS* 42, 77–96. doi: 10.5038/1827-806X.42.1.9

Voituron, Y., de Fraipont, M., Issartel, J., Guillaume, O., and Clobert, J. (2011). Extreme lifespan of the human fish (*Proteus anguinus*): a challenge for ageing mechanisms. *Biol. Lett.* 7, 105–107. doi: 10.1098/rsbl.2010.0539

Vörös, J., Marton, O., Schmidt, B. R., Gal, J. T., and Jelić, D. (2017). Surveying Europe's only cave-dwelling chordate species (*Proteus anguinus*) using environmental DNA. *PLoS One* 12:e0170945. doi: 10.1371/journal.pone.0170945

Whitaker B., and Jaw, T.J. (2021). Infectious diseases of amphibians. *MSD Veterinary Manual*. https://www.msdvetmanual.com/exotic-and-laboratory-animals/amphibians/overview-of-amphibians

White, T. J., Bruns, T., Lee, S., and Taylor, J. (1990). "Amplification and direct sequencing of fungal ribosomal RNA genes for phylogenetics," in *PCR Protocols-A Guide to Methods and Applications*, eds M. A. Innis, D. H. Gelfand, J. J. Sininsky, and T. J. White (San Diego, CA: Academic Press), 282–287. doi: 10.1016/B978-0-12-372180-8.50042-1

Wickham, H. (2016). *ggplot2*. Cham: Springer International Publishing. doi: 10.1007/978-3-319-24277-4

Zen Siqueira, J. P., Sutton, D. A., García, D., Gené, J., Thomson, P., Wiederhold, N., et al. (2016). Species diversity of *Aspergillus* section Versicolores in clinical samples and antifungal susceptibility. *Fungal Biol.* 120, 1458–1467. doi: 10.1016/j.funbio.2016.02.006

Conflict of Interest: The authors declare that the research was conducted in the absence of any commercial or financial relationships that could be construed as a potential conflict of interest.

Publisher's Note: All claims expressed in this article are solely those of the authors and do not necessarily represent those of their affiliated organizations, or those of the publisher, the editors and the reviewers. Any product that may be evaluated in this article, or claim that may be made by its manufacturer, is not guaranteed or endorsed by the publisher.

frontiers | Frontiers in Microbiology

ORIGINAL RESEARCH
published: 21 July 2022
doi: 10.3389/fmicb.2022.934708

Islands Within Islands: Bacterial Phylogenetic Structure and Consortia in Hawaiian Lava Caves and Fumaroles

Rebecca D. Prescott[1,2], Tatyana Zamkovaya[3], Stuart P. Donachie[2], Diana E. Northup[4], Joseph J. Medley[4], Natalia Monsalve[5], Jimmy H. Saw[5], Alan W. Decho[1], Patrick S. G. Chain[6] and Penelope J. Boston[7]*

[1] Department of Environmental Health Sciences, Arnold School of Public Health, University of South Carolina, Columbia, SC, United States, [2] School of Life Sciences, University of Hawai'i at Mānoa, Honolulu, HI, United States, [3] Department of Microbiology and Cell Science, University of Florida, Gainesville, FL, United States, [4] Department of Biology, University of New Mexico, Albuquerque, NM, United States, [5] Department of Biological Sciences, The George Washington University, Washington, DC, United States, [6] Biosciences Division, Los Alamos National Laboratory, Los Alamos, NM, United States, [7] National Aeronautics and Space Administration (NASA) Ames Research Center, Moffett Field, CA, United States

OPEN ACCESS

Edited by:
Paola Di Donato,
University of Naples Parthenope, Italy

Reviewed by:
Errol Duncan Cason,
University of the Free State, South Africa
John R. Spear,
Colorado School of Mines, United States

***Correspondence:**
Rebecca D. Prescott
rebeccap@hawaii.edu

Specialty section:
This article was submitted to Extreme Microbiology, a section of the journal Frontiers in Microbiology

Received: 03 May 2022
Accepted: 16 June 2022
Published: 21 July 2022

Citation:
Prescott RD, Zamkovaya T, Donachie SP, Northup DE, Medley JJ, Monsalve N, Saw JH, Decho AW, Chain PSG and Boston PJ (2022) Islands Within Islands: Bacterial Phylogenetic Structure and Consortia in Hawaiian Lava Caves and Fumaroles. Front. Microbiol. 13:934708. doi: 10.3389/fmicb.2022.934708

Lava caves, tubes, and fumaroles in Hawai'i present a range of volcanic, oligotrophic environments from different lava flows and host unexpectedly high levels of bacterial diversity. These features provide an opportunity to study the ecological drivers that structure bacterial community diversity and assemblies in volcanic ecosystems and compare the older, more stable environments of lava tubes, to the more variable and extreme conditions of younger, geothermally active caves and fumaroles. Using 16S rRNA amplicon-based sequencing methods, we investigated the phylogenetic distinctness and diversity and identified microbial interactions and consortia through co-occurrence networks in 70 samples from lava tubes, geothermal lava caves, and fumaroles on the island of Hawai'i. Our data illustrate that lava caves and geothermal sites harbor unique microbial communities, with very little overlap between caves or sites. We also found that older lava tubes (500–800 yrs old) hosted greater phylogenetic diversity (Faith's PD) than sites that were either geothermally active or younger (<400 yrs old). Geothermally active sites had a greater number of interactions and complexity than lava tubes. Average phylogenetic distinctness, a measure of the phylogenetic relatedness of a community, was higher than would be expected if communities were structured at random. This suggests that bacterial communities of Hawaiian volcanic environments are phylogenetically over-dispersed and that competitive exclusion is the main driver in structuring these communities. This was supported by network analyses that found that taxa (Class level) co-occurred with more distantly related organisms than close relatives, particularly in geothermal sites. Network "hubs" (taxa of potentially higher ecological importance) were not the most abundant taxa in either geothermal sites or lava tubes and were identified as unknown families or genera of the phyla, Chloroflexi and Acidobacteria.

These results highlight the need for further study on the ecological role of microbes in caves through targeted culturing methods, metagenomics, and long-read sequence technologies.

Keywords: lava caves, fumaroles, taxonomic distinctness, networks, cave microbiology, microbial consortia, volcanic environments

INTRODUCTION

Volcanic features in Hawai'i, such as lava caves and fumaroles, are often oligotrophic, yet they host unexpectedly high microbial diversity (Northup and Lavoie, 2015; Riquelme et al., 2015; Wall et al., 2015). Lava caves and tubes form when the surface of flowing molten lava cools, crust over, and the molten lava beneath continues to flow, leaving tube-like structures or pockets behind that to form caves. Temperature and humidity within caves vary less than over the surface terrain above, and sunlight penetrates over cave and tube entrances, or through "skylights" where the cave ceiling collapses. In such environments, several studies have documented high microbial diversity from around the world, including Iceland, the Azores, the Canary Islands, and Hawai'i (Gabriel and Northup, 2013; Northup and Lavoie, 2015) with high levels of endemism (Snider, 2010).

Fumaroles and geothermally active lava caves are more dynamic, extreme environments that are formed when steam and volcanic gases exit cracks in basalt deposits, creating vents (Ellis et al., 2008; Costello et al., 2009; Wall et al., 2015). Fumaroles are far less studied than lava caves, even though they are one of the most common geothermal features on Earth (Bizzoco and Kelley, 2019). Wall et al. (2015) studied samples from deposits in contact with steam in fumaroles on the island of Hawai'i and concluded that Hawaiian fumaroles are biodiversity hotspots, with exceptionally high diversity. Lava caves above deeper situated magma can also have characteristics similar to fumaroles, with higher temperatures, deposits on cave walls that arise through pH reductions caused by volcanic gasses, and high humidity from magmatic heating of air and groundwater. These geothermally active sites represent a unique type, or early stage in the development of volcanic ecosystems, often occurring on younger basalts that are less oxidized and weathered. They also often harbor a wide variety of chemolithotrophic microbes and other extremophiles (Wall et al., 2015). Therefore, lava tubes and geothermal sites present a spectrum of environmental conditions and community stability in volcanic ecosystems and provide excellent systems which help identify and study drivers of bacterial community diversity and structure.

Volcanic environments are also systems in which the formation and persistence of robust and adaptable microbial consortia may be critical for community survival in extreme conditions, including those characterized by low nutrient availabilities or extreme temperatures. Microbial consortia are defined here as consistent subgroups of bacteria in a community that occur and function together, and which may possess emerging, synergistic activities that cannot be attributed to any one species in the group (Bosse et al., 2015; Vishwakarma et al., 2020). In volcanic ecosystems, microbial neighbors may be highly interdependent, particularly in relationships with chemolithotrophs which can utilize reduced compounds in basalts as energy sources (Gomez-Alvarez et al., 2007; Northup and Lavoie, 2015). These may be "hub" organisms, the community members that have ecologically important roles and which can be identified through network analysis (Toju et al., 2018; Zamkovaya et al., 2020). Hub organisms might also include bacteria that are capable of photoautotrophy in very low light levels, such as cave-dwelling Cyanobacteria like *Gloeobacter kilaueensis* (Saw et al., 2013).

Previous studies have concluded that subsurface microbial consortia establish small-scale, site-specific microbial–mineral interactions over time, such as when bacteria acclimate and adapt to specific mineral chemistry, nutrient, and atmospheric conditions over microscopic scales (Miller et al., 2014; Barton, 2015). Experimental studies of biofilm-mineral interactions related to caves or basalts have also been completed, but our understanding of these interactions remains limited (Edwards et al., 2005; Cockell et al., 2020). Jones and Bennett (2014) found that in experiments using pure and mixed cultures of *Thiothrix unzii*, the competitive exclusion between species, as well as other factors, were related to biomass density and diversity on mineral and rock surfaces. This would create a pattern of high diversity at very small spatial scales that are dependent on the type of minerals in the basalt and other micro-scale environmental variables that are difficult to observe and record in the field.

Large-scale ecological factors may also influence bacterial diversity in lava caves and fumaroles, including the age and degree of basalt weathering, and stochastic and deterministic processes that shape microbial communities over time. For example, in a study of Hawaiian volcanic deposits, increasing deposit age was generally accompanied by increasing concentrations of organic matter and microbial biomass (King, 2007). Northup and Lavoie (2015) also noted that lava caves provide an opportunity to study microbial successional patterns as microbes invade fresh lava tubes and diversify over time, with additional microbial introductions through water and sediments that enter the caves, animal entry, aerosols, and penetrating plant roots. However, such patterns and their potential underlying drivers, including mineral composition-driven selection (i.e., habitat filtering by the environment) or competitive exclusion due to low nutrient availability have not been investigated in lava tubes or fumaroles. However, stochastic and deterministic patterns that drive community structure can be investigated through the study of the phylogenetic structure or "breadth," which determines the phylogenetic signature, or taxonomic distinctness, of a community, and how well a given sample represents the larger, regional pool of the given taxa (see Clarke

and Warwick's taxonomic distinctness; Clarke and Warwick, 1998, 2001).

In this study, 70 samples were collected from lava tubes and geothermal sites (including fumaroles and geothermal caves) on the island of Hawai'i between 2006 and 2009 and 2017 and 2019. Data were used to investigate the drivers of phylogenetic distinctness and diversity in these features and their microbial consortia, which may, in turn, contribute to the high bacterial diversity observed in lava caves and fumaroles. We hypothesized that older lava tubes would have higher phylogenetic diversity, likely due to the greater stability of environmental conditions in lava tubes and greater bio-weathering of the rock, thus making nutrients more readily available. We also hypothesized that lava tubes would provide for greater complexity in co-occurrence networks due to the development of unique microbial consortia at very small spatial scales due to the mineralogical variability at those small scales, which could create complex interactions over time.

Using massively parallel sequencing of a fragment of the 16S rRNA gene from microbial communities of lava tubes and geothermal sites, this study investigated the following: (1) the effect of age of the surface lava flow, and other environmental and study variables, on bacterial phylogenetic diversity, (2) if bacterial phylogenetic structure occurs by chance, or if over-dispersion or habitat filtering is evident, and (3) co-occurrence patterns of bacteria through network analysis to determine hubs and phylogenetic diversity within bacterial consortia at small spatial scales. Understanding the phylogenetic distinctness, diversity patterns, and microbial consortia in natural, volcanic environments will address questions in a variety of fields, including the structure of possible microbial communities on an early Earth and Mars in astrobiology studies, potential use of microbial consortia in biotechnology and bioremediation, and improving our understanding of microbial communities in volcanic or desert soils for enhanced agricultural production.

MATERIALS AND METHODS

Sampling Sites

In total, 70 samples were collected over multiple years from lava caves and fumaroles across the island of Hawai'i. Samples collected from Kaūmana cave did not require a permit because they were microbiological in nature, and we did not collect rock or damage surfaces. All other samples, except for geothermal caves within Kīlauea Caldera (see below), were collected from caves or vents on private lands, and permission was granted for the collection. Samples varied in terms of date of collection, type of material, DNA extraction method, estimated age of the basalt, the temperature at the time of collection, elevation, and average annual rainfall received at the surface (**Supplementary Table 1**). Lava flow age provides an approximate age of a cave or fumarole, and for each site, the approximate age was determined from a US Geological Survey (USGS) National Geologic database (https://ngmdb.usgs.gov/ngmdb/ngmdb_home.html) and in communication with the Hawaiian Volcano Observatory (HVO). Annual rainfall amounts were collected from the Rainfall Atlas of Hawai'i (http://rainfall.geography.hawaii.edu; Frazier et al., 2016). Estimates of the elevation were determined during sample collection or from Google Earth using GPS coordinates of each site.

Lava caves in the 1922 lava flow in Kīlauea Caldera, Hawai'i, were sampled between 2006 and 2009 under permit #HAVO-2009-SCI-0029 issued to Stuart P. Donachie by the Hawai'i Volcanoes National Park (National Parks Service, Department of the Interior) and were the only samples collected in this study that required a permit. Based on the time of the last lava flow, the caves are thought to be ∼100 years old. Cores of epilithic biofilms were collected from each cave wall directly into sterile cryovials. Conditions differed among the caves, with temperatures ranging from ambient at the surface to almost 46°C, and relative humidity from ambient to 102%. Cave floor temperatures ranged from 20 to over 60°C. For example, in Big Ell cave, the mean air temperature recorded by a Hobo data-logger (Bourne, Massachusetts) for the 4 months in the summer of 2006 was 26°C, with a range from 17.9 to 45.9°C (data not shown). Water in the cave mostly occurred in the form of dripping condensation that exceeded meteoric rainfall on the surface by about six times. Heated groundwater in Big Ell drove relative humidity in the same period to a mean of 95.2% (range, 52.25–102.25%).

Samples were collected from Pahoa and Kaumana caves in 2017; both are lava tubes on the windward side of the island of Hawai'i. Pahoa cave is located in flows that dated to 300–750 years of age, and the cave is considered to be older than 500 years (pers. comm., HVO, USGS). Kaumana cave is much younger, at ∼130 years, and formed in lava flows from Mauna Loa in 1881. Samples from Pahoa and Kaumana were collected by scraping a 1 cm^2 area of the cave wall with a sterile spatula into a cryovial. These samples were stored on ice until arrival the same day at the University of Hawai'i at Mānoa, whereupon they were transferred to a −80°C freezer until DNA was extracted, as described below.

Samples were collected from the Kipuka Kanohina Cave System on the southeast side of the island of Hawai'i in December 2017, January 2018, and January 2019, with the permission of the landowners. Sites sampled included the Kula Kai Caverns, Tapa, and Maelstrom segments, all of which were ∼800 years old. Here, small pieces of rock with epilithic biofilms, spheroids, coralloids, moonmilk, or mineral crusts were chipped from the cave wall with a flame-sterilized chisel. A sterile scopula also scraped ooze from cave walls. Separate samples were placed directly into sterile 50 ml polypropylene tubes and immediately covered with a sterile sucrose lysis buffer and sealed with parafilm after recapping. Samples were stored in a refrigerator until transported to the Northup lab at the University of New Mexico, where they were stored in a −80°C freezer until DNA extraction, as described below.

Samples were taken from several centimeter thick biofilms in the vicinity of steam vents in the East Rift Zone located near the town of Pahoa, Hawai'i, in August 2019. These fumaroles occur on two lava flows, with one dating to ∼65 years ago and another to ∼400 years ago (pers. comm, HVO, USGS). Therefore, these samples were assigned a wide age range (64–400 years). Samples were collected directly into sterile 15 or

50 ml polypropylene tubes, which were sealed with parafilm immediately after recapping, and stored on ice during transport the same day to a nearby −20°C freezer. Frozen samples were wrapped with ThermoSafe U-tek cold packs at −23°C and shipped to the University of Hawai'i at Mānoa or the George Washington University. Samples were then immediately placed in a −80°C freezer until DNA extraction.

DNA Extraction

The DNA extraction method varied depending on the sample type (**Supplementary Table 1**). Extractions of DNA from samples taken from the Pahoa, Kaumana, Big Ell, Big Mouth, Ahu Too caves, and some steam vent samples were extracted using the Qiagen DNeasy PowerSoil DNA Kit (Germantown, MD) according to the instructions of the manufacturer and included a bead-beating step of 1.5 min in a Mini-Beadbeater-24 (BioSpec Products, Inc., Bartlesville, OK). Samples from the Kipuka Kanohina cave system were also extracted with the Qiagen DNeasy PowerSoil DNA Kit with a BioSpec Products Mini-Beadbeater-8 for 1.5 min at medium intensity and 50 μl of powdered skimmed milk (Difco) incorporated into the extraction protocol before bead-beating in order to increase the DNA yield (Takada-Hoshino and Matsumoto, 2004). DNA extracted according to these methods was shipped to Los Alamos National Laboratory (LANL) for 16S rRNA amplicon sequencing on an Illumina MiSeq.

DNA from samples collected along the East Rift Zone steam vents (referred to here as Pahoa Steam Vents) was extracted using the ZymoBIOMICS DNA Kit according to the manufacturer's instructions (Zymo Research, Orange CA, USA). The extracted DNA was sequenced at the Advanced Studies in Genomics, Proteomics and Bioinformatics (ASGPB) core DNA sequencing facility at the University of Hawai'i at Mānoa using the Illumina MiSeq platform. Both LANL and ASGPB sequencing facilities used the same protocols, kits, and primers for sequencing (refer to the section below).

16S rRNA Gene Amplicon Sequencing

Degenerate primers 341F (5′CCTACGGGAGGCAGCAG 3′) and 806R (GGACTACHVHHHTWTCTAAT-3′) were used to amplify the V3–V4 region of 16S rRNA genes in all samples. The first round of PCR amplified the V4 region from 10 ng of DNA using the KAPA HiFi HotStart Ready Mix and denaturation at 95°C for 3 min. This was followed by 20 cycles of 95°C for 30 s, 55°C for 30 s, 72°C for 30 s, an extension step of 72°C for 5 min, and a final hold at 4°C. The second round of PCR used Nextera XT v2 indices (Illumina Inc., San Diego, CA, USA), with denaturation at 95°C for 3 min, 8 cycles of 95°C for 30 s, 55°C for 30 s, and 72°C for 30 s, followed by an extension of 72°C for 5 min, and a final hod at 4°C. Amplicons were cleaned using AMPure XP beads (Beckman Coulter Inc., Brea, CA, USA).

Unique barcodes allowed multiple amplicons to be pooled for sequencing. The concentration of the pooled amplicons was determined in the Qubit dsDNA HS Assay (ThermoFisher Scientific, Waltham, MA, USA). The average size of the library was determined by the Agilent High Sensitivity DNA Kit (Agilent Technologies, Inc., Santa Clara, CA, USA). Accurate library quantification was determined with the Library Quantification Kit, Illumina/Universal Kit (KAPA Biosystems, Cape Town, South Africa). The amplicon pool was sequenced on an Illumina MiSeq at either Los Alamos National Laboratory (LANL) or in the ASGPB core facility at the University of Hawai'i at Manoa. Both sequencing facilities generated paired-end 301 bp reads, with the expectation that each sample would provide 50,000–100,000 reads. Sequences were submitted to Dyrad and are publicly available at https://doi.org/10.5061/dryad.z612jm6f0.

Analyses

Raw sequence data were imported to the EDGE Bioinformatics platform (Li et al., 2017), utilizing QIIME 2 (vQIIME 2.4.1; Bolyen et al., 2019). Raw sequences were demultiplexed and denoised using the DADA2 pipeline (Callahan et al., 2016; command qiime dada2 denoise-paired). The 5′ ends of both forward and reverse sequences were trimmed by 20 base pairs (bp) to remove PCR primers. The 3′ end of the reverse read was truncated at 200 bp. Representative sequences for each amplicon sequence variant (ASV) were used for taxonomic classification (command q2-feature-classifier; Bokulich et al., 2018). A phylogenetic tree was generated using MAFFT alignment (Katoh et al., 2002) and FastTree (Price et al., 2009), using the command qiime phylogeny align-to-tree-mafft-fasttree, followed by alpha and beta diversity analyses (command qiime diversity core-metrics-phylogenetic). Taxonomic classification of ASVs was completed using an in-house subset of the SILVA database (v132; Yilmaz et al., 2014) for the V3–V4 region only, based on the primer set 341F and 806R. The data were then split into two sets for most analyses: lava tubes (n = 38), and geothermal sites (n = 32), the latter of which included geothermally active caves and fumaroles. Bar graphs of community composition at the class level (L3) were created in numbers (version 11.2 7032.0.145), with the proportion of each class-level taxon in each site calculated from raw abundance tables generated in EDGE-QIIME2.

Multivariate Analyses

For multivariate statistical analyses and exploration of data, abundance tables and distance matrices generated in the EDGE-QIIME2 platform were imported into PRIMER-e (v7.0). Principal Coordinates Analysis (PCoA) was completed using distance matrices of weighted Unifrac distances (Lozupone et al., 2005). All 70 samples were run together, based on rarefied data (minimum # sequences/per sample = 5,471), with the exploration of differences in DNA extraction methods, evaluated sequencing, and environmental variables (**Supplementary Table 1**). PCoA plots based on rarefied data were also generated from the two individual datasets of lava tubes (n = 38; minimum number of sequences/per sample = 5,471) and geothermal sites (n = 32; minimum number of sequences/per sample = 14,364).

Community Structure and Phylogenetic Distinctness Analysis

Average taxonomic distinctness (Delta+; referred to as *phylogenetic* distinctness here because the data are based

on a phylogenetic tree) summarizes features of the overall hierarchical structure of an ecological community based on a phylogenetic tree generated from that community's genetic information. This is calculated using a phylogenetic tree of all sequences (16S rRNA amplicon sequences in this study) from all samples and determination of the patristic distances between each pair of ASVs (*i* and *j*). Phylogenetic distinctness equals the average phylogenetic distance between species in a community. The variance of phylogenetic distinctness (Lambda+) equals the variance of the phylogenetic distances $\{\omega_{ij}\}$ between each pair of sequences, about their mean value (Delta+). These measurements are not dependent on sampling size or effort, unlike Faith's phylogenetic diversity, which increases with the increasing number of taxa, and therefore requires the use of rarefied sequencing data.

Average phylogenetic distinctness also provides a framework that tests departures from expectations through permutation tests, completed here through TAXDTEST in PRIMER-e (v7.0). A sample randomly drawn from the entire list of organisms in the tree can be taken to test if the observed subset of organisms in an actual sample represents the phylogenetic biodiversity expressed in the full phylogenetic inventory. Such information could help support or reject hypotheses about microbial interactions and the importance of syntropy in microbial consortia utilization of nutrients in the rock, and of other limited resources in caves.

To determine the average and variance of phylogenetic distinctness, a pairwise distance matrix of the rooted phylogenetic tree of all representative ASVs detected across all 70 samples (9,965 ASVs) was calculated in Geneious Prime (v2021.2.1), using the patristic distance calculation. Patristic distance is equivalent to cophenetic distance and is defined as the sum of the branch lengths between two pairs of ASVs (tips of the branches). The branch length is given in average nucleotide substitutions and is calculated back to their most recent common ancestor.

The patristic distance matrix generated in Geneious was then imported into PRIMER-e for calculations of average phylogenetic distinctness per sample (avgTD or Delta+) and variation around the mean of phylogenetic distinctness (varTD or lambda+; Clarke and Warwick, 1998, 1999, 2001). Delta+ is a univariate biodiversity index, which in this case, calculates the average patristic distance between all pairs of ASVs in a sample, and the distance is defined as the path length through a phylogenetic tree connecting these species. Using permutation tests, we then compared the actual Delta+ and Lambda+ of each sample to the null model of the phylogenetic community structure of each sample, which was random (i.e., no evidence of habitat filtering or over-dispersion). TAXDTEST routine completes permutation tests by selecting random subsets of ASVs from the phylogenetic tree distance matrix at various sample sizes, thereby testing for a departure from the null model of all ASVs in the phylogeny which has an equal probability of being included in any random sample draw (without replacement) and evaluates the phylogenetic relatedness and breadth of the community (Clarke and Warwick, 1998). This process generated a 95% probability funnel that illustrates the Delta+ and Lambda+ across the range of ASVs of our samples (**Figure 5**) and illustrates whether ASVs in a sample present a higher or lower than expected phylogenetic relatedness. If a sample falls near the mean predicted Delta+ or Lambda+ inside the 95% probability funnel, the null hypothesis cannot be rejected, and communities appear to be assembled in a random manner. If it falls either above (over-dispersion) or below (phylogenetic clustering) the mean, the null model is rejected, and communities do not appear to be assembled in a random manner.

Network Construction

To evaluate bacterial co-occurrence patterns in microbial communities from the geothermal sites and lava tubes sampled here, including the overall connectivity and structure of the dominant species of these systems, network models and metrics were evaluated (refer to Zamkovaya et al., 2020 for detailed methods). By mathematically modeling a microbial community as a network, wherein nodes are different species and edges represent their relationships (Wuchty et al., 2006; Ma'ayan, 2011), we can depict species interactions and study the interactions among and structure of the community and environment. Network metrics, such as hub score, betweenness centrality, closeness centrality, and degree centrality (Huang, 2004; Blüthgen et al., 2008; Ma'ayan, 2011), can be used to quantitatively assess these communities and may help identify important taxa in each environment, thereby providing important clues about how specific taxa or gene products may contribute to the function of an ecosystem (Gehlenborg et al., 2010).

To generate networks, each abundance table, taxonomy table, and rooted phylogenetic tree generated by EDGE-QIIME2 was imported into R with its corresponding sample metadata information using the QIIME2R (v0.99.35) and phyloseq (v1.30.0) packages and the qzatophyloseq() function. For each environment, using the get_back_res_meeting_min_occ() function from the mdmnets (v0.1.0) package (Zamkovaya et al., 2020), the ASV phyloseq object was first filtered to include taxa present across the majority (15 and 12.5% for lava tubes and geothermal sites, respectively) of samples and then normalized, transformed, and converted into an inverse covariance adjacency matrix, using the Meinshausen–Buhlmann (MB) neighborhood selection (method = "mb" parameter) algorithm [SpiecEASI (v.1.0.7) package; Kurtz et al., 2015]; this estimated the conditional dependence of each pair of ASVs and the stability approach to regularization selection (StARS) variability (i.e., minimum λ) threshold set to default (0.05; Liu et al., 2010), to calculate the most optimal, sparse, and direct co-occurrence relationship among ASVs. Each adjacency matrix was then converted into an igraph object and visualized as a network using the adj2igraph() and plot_network() functions from SpiecEasi. For both lava cave and geothermal sites, networks for all classification levels (phylum, class, family, order, genus) were constructed using the get_net_plots_all_ranks() function, and hub networks for all classification levels were created using the get_hub_plots_all_ranks() function from the mdmnets package. Network attributes (number of nodes, number of edges,

and network density) were calculated using the igraph package and theV(), E(), and edge_density() functions.

For each dataset (geothermal vs. lava tubes), subnetworks (sub-communities of the initial igraph object of the adjacency matrix) were extracted and calculated using the Louvain hierarchical multi-level modularity optimization algorithm cluster_louvain() function from the igraph package, which detects community structure in larger networks (Blondel et al., 2008). This scalable, greedy optimization method identifies communities from large networks by identifying modules (i.e., subnetworks) in the larger network through a measure of modularity. This is a scale value ranging from −0.5 to 1, which is based on the relative density of edges (actual number of edges/possible number of edges) inside each module in the larger network compared to the density of edges outside each module. The Louvain method first assigns each node in the larger network to its own local community, and in a greedy, hierarchical approach, reassigns and groups each node to the community to which it contributes the most value in its modularity measure. It then repeats and restarts these calculations until no nodes can be reassigned and end only when there is a single node left, or when the modularity of a community cannot be increased further. The modules identified in the lava tube and geothermal environments were then visualized as subnetworks using the get_net_plots_all_ranks() function and modified R scripts. The community number and overall community size of each node were saved and added to the other list of features (node number, classification, degree centrality score, betweenness centrality score, and hub score).

Using only ASVs that occurred in subnetworks, ASVs were clustered into operational taxonomic units (OTUs) at 98.6% sequence similarity using open-reference OTU picking in QIIME2 to reduce the likelihood of building a phylogenetic tree of subnetwork members that would contain sub-strains. OTU-clustered ASVs were then aligned in QIIME2 using MAFFT (Katoh et al., 2002) and FastTree (Price et al., 2009; command qiime phylogeny align-to-tree-mafft-fasttree) to build a phylogenetic tree. Newick tree (.tre) files generated in QIIME2 were imported into the Interactive Tree of Life v6.4.3 (ITOL: https://itol.embl.de; Letunic and Bork, 2021) to generate tree images. The subnetwork of a given ASV was added to the tree images as metadata in ITOL.

Shared ASV Comparison

The number of ASVs shared among lava tubes and geothermal samples was calculated and visualized using the UpSetR (v1.4.0) package, and the upset() function on the transformed ASV abundance table. Upset plots are an improved alternative to Venn diagrams, particularly when dealing with more than 3 or 4 groups, that visualize set intersections in a matrix layout. All upset plots were created in R, using ggplot2 (v3.3.2) and UpSetR packages, and with custom color palettes for each environment in the RColorBrewer (v1.1.2) package.

RESULTS

Community Composition and Environmental Variables

High-throughput sequencing of 16S rRNA gene fragments from samples of lava caves and geothermal sites on the island of Hawai'i produced 10,715,694 raw sequences, with a mean length of 300.46 bp (base pairs). After demultiplexing, the minimum number of sequences in each sample was 5,541, and the maximum number was 346,293, with a median sequence count per sample of 26,622. For geothermal sites only ($n = 32$), the minimum number of sequences in a sample was 14,365, with a median sequence count of 176,380, and a maximum of 346,293. A total of 4,296 ASVs was identified in unrarefied data. In the lava tube dataset, the minimum number of sequences in each sample was 5,541, with a maximum of 42,281, and a median of 16,651. The total number of ASVs from the lava tubes was 6,036 (unrarefied).

Rarefaction curves suggest that the sequencing depth was adequate to capture most of the diversity in most samples (**Supplementary Figure 1**). A total of 9,965 ASVs (i.e., taxa) were identified in unrarefied data for all 70 samples; these were used in co-occurrence network construction and phylogenetic distinctness analyses. Beta diversity analyses were completed using rarefied ASV tables. Environmental variables explored through multivariate analyses to detect ecological patterns included sample type (i.e., biofilm, ooze, mineral crust, etc.), average annual rainfall at surface, cave/site, temperature, cave age, elevation, year of collection, DNA extraction method, and sequencing lab (**Supplementary Table 1**). The PCoA of weighted Unifrac distances, a beta-diversity measure that incorporates phylogenetic diversity, abundance, and composition of samples, found that samples did not group consistently with the environmental variable rainfall at the surface, elevation, or cave/site, but instead clustered as geothermal sites and lava tubes (**Figure 1**). This was further supported by a Kruskal–Wallis analysis of the alpha-diversity measure, a phylogenetic diversity (Faith's PD; Faith, 1992; Kruskal-Wallis: $H = 17.3$; $p = 0.0002$; pairwise test results in **Supplementary Table 2**). Geothermal caves, which are the remains of inflation bubbles in lava flows near Kīlauea Caldera, were not statistically different from fumaroles in terms of Faith's PD (Kruska–Wallis pairwise test: $H = 0.183$; $q = 0.668$; **Supplementary Table 2**). Based on the outcomes of these analyses, some further analyses were applied separately to lava tubes and all geothermal sites. The PCoA also found no relationship or clustering of samples associated with the "DNA extraction method" or "sequencing facility," suggesting the methods and facilities used produced comparable results (**Supplementary Figures 2**, **3**). Samples collected from geothermal caves in Kīlauea Caldera were the only sites that were collected twice (in 2006 and 2019), and these samples clustered together as geothermal sites in PCoA analysis, but no other samples clustered together as a factor of date of collection (**Supplementary Figure 4**).

Additional multivariate analysis of the weighted Unifrac distances using PCoA of all 70 samples and separate analyses

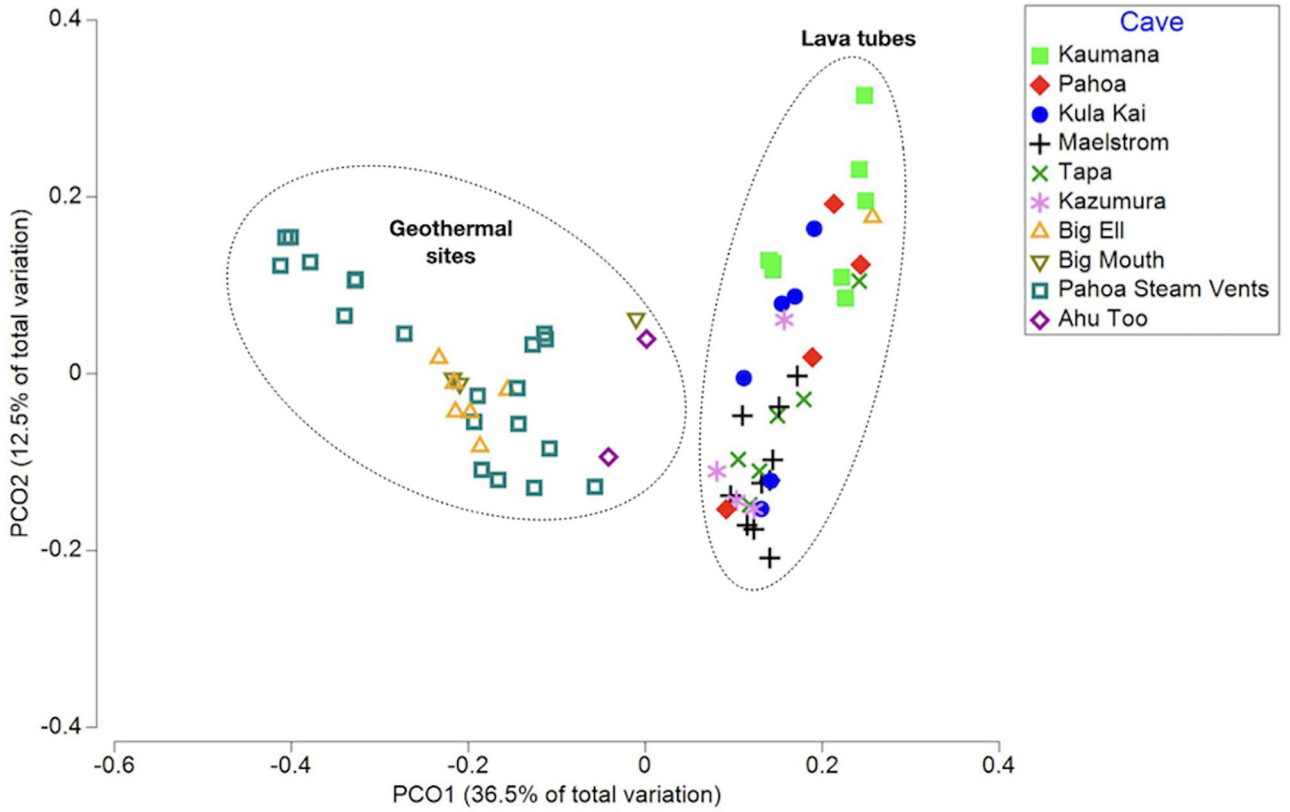

FIGURE 1 | A principal coordinates analysis (PCoA) of the weighted Unifrac distance measured between samples, capturing 49% of the variation in multivariate space. Samples are displayed as the cave or site they were collected from. This illustrates that samples from geothermal sites and lava caves are two distinct populations in terms of phylogenetic community composition and abundance.

of geothermal sites, suggests that the temperature of the cave or site may be the driver of community composition and abundance, with sites above 45°C grouping together. However, this was not further supported by a pairwise Kruskal–Wallis analysis of Faith's PD. Similarly, within lava tubes, microbially-mediated mineral deposits (i.e., mineral crusts, coralloids, etc.) were grouped together in PCoA analysis, but such groupings were not found in comparisons of all 70 samples, and there were no statistically significant differences found among pairwise Kruskal–Wallis tests to support these differences, likely due to the small sizes of various sample types.

Phylogenetic diversity was higher in sites from older lava flows than younger flows, with site age estimated from the time of the most recent lava flows on the surface (**Figure 2**). Faith's PD was higher in samples from sites that were between 500 and 820 years old when compared to sites up to 400 years old (Kruskal–Wallis: $H = 24.1$; $p = 0.00007$; pairwise test results in **Supplementary Table 3**). Although most of the geologically younger sites are from geothermal locations, Kaumana cave is ∼130 years and is a lava tube that is not geothermally active, suggesting that the age of basalt is related to diversity. Kaumana cave hosted less diversity relative to other lava tubes, but the difference was not statistically different (Kruskal–Wallis: $H = 8.3$; $p = 0.141$).

Diversity in geothermal sites at the taxonomic level of the class was dominated by sequences identified as Oxyphotobacteria (40.2% ± 25.3), followed by Chloroflexi, class Ktedonobacteria (10.6% ± 15.9), and the Deinococcus-Thermus, class Deinococci (5.4% ± 9.4; **Figure 3A**). Geothermal sites hosted 103 taxonomic classes, with only five of those classes comprising >5% of the average relative abundance of ASVs. Eighty-seven classes were <1% of the average relative abundance. **Figure 3B** illustrates the overlap of ASVs among all geothermal sites, with 2,518 ASVs occurring only in Pahoa steam vents, while just one ASV (998bd9a9277837ead97ae349a5ec4df7; Class Oxyphotobacteria, *Chlorogloeopsis* sp.) was detected in all sites. Geothermal caves in Kīlauea Caldera had 826 unique ASVs in Big Ell cave alone, 394 in Big Mouth, and 184 in Ahu Too. No ASV occurred in all three of these caves.

In total, 151 taxonomic classes were represented in lava tube samples, with three classes on average comprising >10% of the relative abundance, including Actinobacteria (16.0% ± 24.4), Gammaproteobacteria (15.4% ± 11.0), and Nitriliruptoria (13.7% ± 23.3; **Figure 4A**). Alphaproteobacteria were also

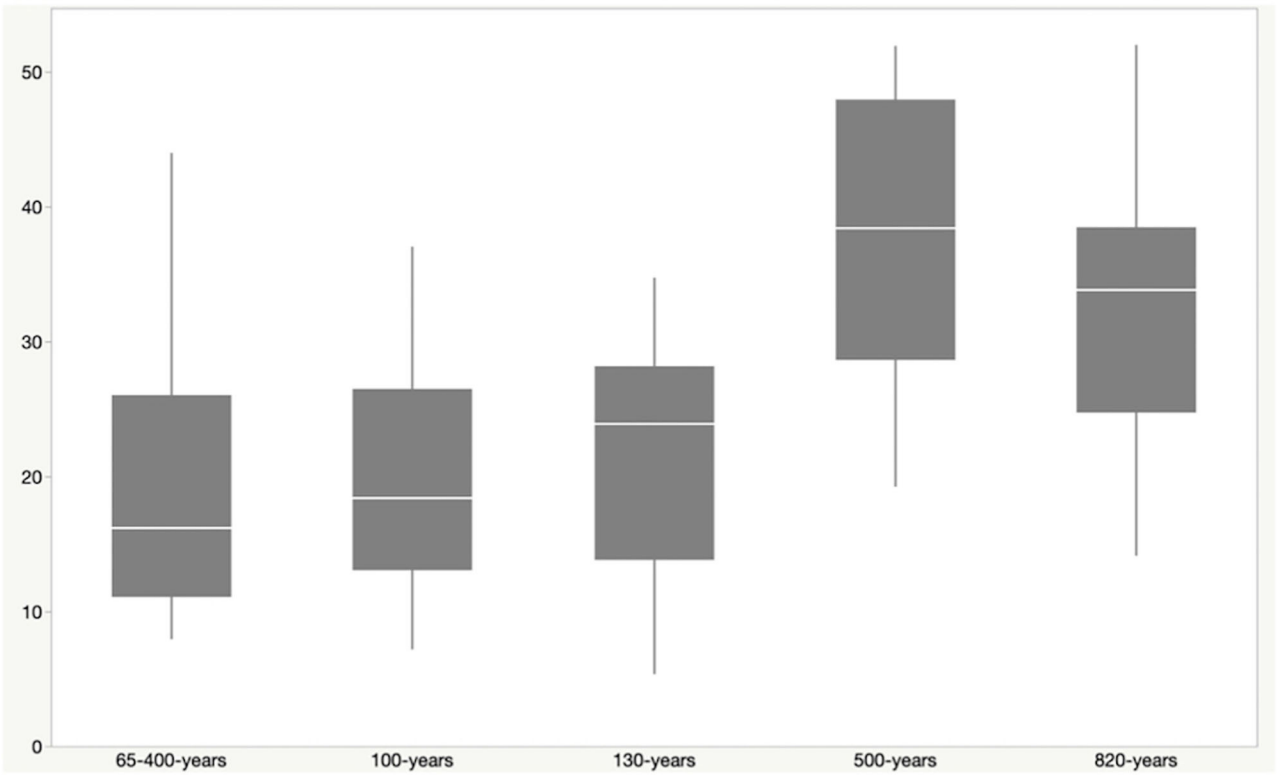

FIGURE 2 | Faith's Phylogenetic Diversity (PD) vs. estimated site age. The approximate age of a particular site was defined by the latest flow recorded for the location. Steam vents (sites P & S) are features in two possible flow events and were thus given the range of 65–400 years, representing the earliest and latest potential time periods for those flows. Phylogenetic diversity increases with the increasing age of the lava flow at that site. PD was higher among sites that were 500–820 year old, when compared to younger sites. This includes Kaumana cave, a lava tube, which is only ∼130 years old.

common, with a relative abundance of 9.3% (±5.3). Variation across samples was high, and no one class was dominated in all lava tubes. Only six classes were represented by mean relative abundances >5%. Conversely, 137 classes were each represented by <1% of the mean relative abundance of ASVs.

An Upset plot of lava tube samples illustrates that all lava tubes had hundreds, and occasionally thousands of unique ASVs, while only seven ASVs occurred in all lava tubes (**Figure 4B**). Maelstrom, a part of the Kipuka Kanohina cave system, hosted the most unique ASVs (1,277), followed by Kāumana cave (1,022). Kula Kai and Maelstrom caves, part of the same larger cave system, shared the most ASVs (284).

Phylogenetic Distinctness and Community Structure

Phylogenetic community structure in all 70 samples was investigated through average phylogenetic distinctness (Delta+ and Lambda +; Clarke and Warwick, 1998), which provides a framework to test departures from expectations from a null model through permutation tests using the TAXDTEST (PRIMER-e v7.0). This algorithm tests the null hypothesis with which the community composition and structure are randomly assembled. **Figure 5** illustrates that within lava tubes and geothermal sites, most samples had higher than expected average phylogenetic distinctness (Delta+; **Figure 5A**). The variance of phylogenetic distinctness was below what would be expected by chance (Lambda+; **Figure 5B**). This suggests that the breadth of phylogenetic diversity is higher in lava caves and geothermal sites than if community assemblages were structured randomly, with greater phylogenetic distances between ASVs than if communities were assembled randomly (i.e., over-dispersed). This pattern is often driven by competitive exclusion in oligotrophic environments (Begon et al., 1998; Barton, 2015), Five samples had lower than expected Delta+ and higher than expected Lambda+ values, suggesting habitat filtering may structure the communities in those samples, with ASVs having less phylogenetic distance than would be expected if communities were assembled randomly. Four of these samples were biofilm or microbial mats from different locations, along with a single blue-green mineral sample collected from the Maelstrom cave.

Network Analyses

Network analyses were completed to identify community interactions and microbial co-occurrence at the class level. Networks were analyzed separately for geothermal sites and

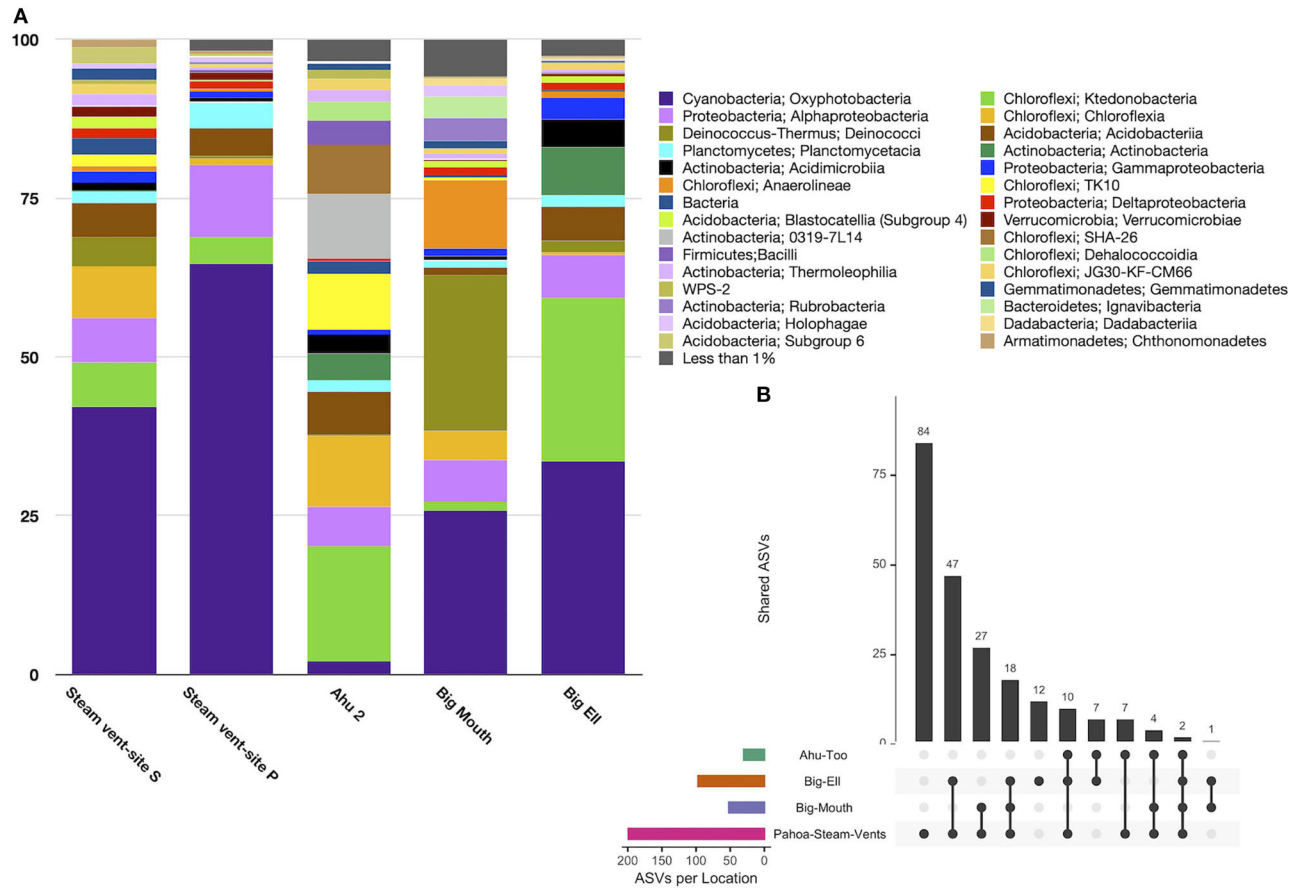

FIGURE 3 | (A) Relative abundance by the site of class-level taxa with >1% abundance in geothermally active sites. Geothermal caves are dominated by Cyanobacteria (Oxyphotobacteria; 40.2% ± 25.3) and Chloroflexi including classes Ktedonobacteria (10.6% ± 15.9) and Chloroflexia (5.8 ± 9.8). Steam vent sites hosted the highest abundance of Oxyphotobacteria. Ktedonobacteria was higher in geothermal caves. Deinococci were most abundant in Kīlauea Caldera's Big Mouth cave. **(B)** Upset plot illustrating overlapping ASVs among geothermal sites. Steam vents hosted many unique ASVs (2,518), followed by Big Ell cave. This shows that geothermal sites are largely unique environments, with few overlapping ASVs; the highest number of overlapping ASVs was in Big Ell and Pahoa Steam vents, which may in part be due to the larger number of samples from these locations. Only one ASV occurred in all sites (Class Oxyphotobacteria, *Chlorogloeopsis* sp.).

lava tubes due to a lack of overlapping among ASVs in both environments (refer to **Figures 6**, **9**). **Table 1** provides the overall network statistics for each environment. Geothermal sites had a greater number of edges (connections) than lava tubes, even though there were more nodes (ASVs) included in the lava tube network. Network density, or the ratio of edges to nodes, was, therefore, higher in geothermal sites (**Table 1**; network density = 3.078). The average degree of centrality (the average number of edges for a given node) was also higher in the geothermal network (**Table 1**).

Among the geothermal sites, a network was constructed using a filter threshold of ≥12.5% taxa from all geothermal samples. **Figure 6** illustrates the network constructed with hubs identified, while **Figure 7** provides neighbor interaction bar graphs, illustrating which classes had the greatest number of co-occurrence relationships (edges) in geothermal sites. There are 218 nodes in the geothermal network, with each node representing a single ASV identified at the class level and sized by the node's hub score. Hub scores are scaled from 0 to 1 and cannot be directly compared between networks but provide information on which nodes have the greatest number of connections and betweenness centrality, and therefore, the removal of those hubs causes the collapse of parts of a network.

There are 671 edges (positive interactions) in the geothermal network. The average number of connections to any one ASV was 6.16 (degree centrality; **Table 1**). The classes with the greatest number of co-occurrence interactions were Oxyphotobacteria, Alphaproteobacteria, and Ktedonobacteria (**Figure 7**). Consistently, taxa had more connections with other ASVs that were distantly related to taxa, rather than interactions with ASVs within the same phyla or class. Oxyphotobacteria had the most interactions with Alphaproteobacteria, while Alphaproteobacteria had the greatest number of interactions with Acidobacteriia, a class of Acidobacteria (**Figure 7**). Ktedonobacteria, the other taxa with a relatively high abundance

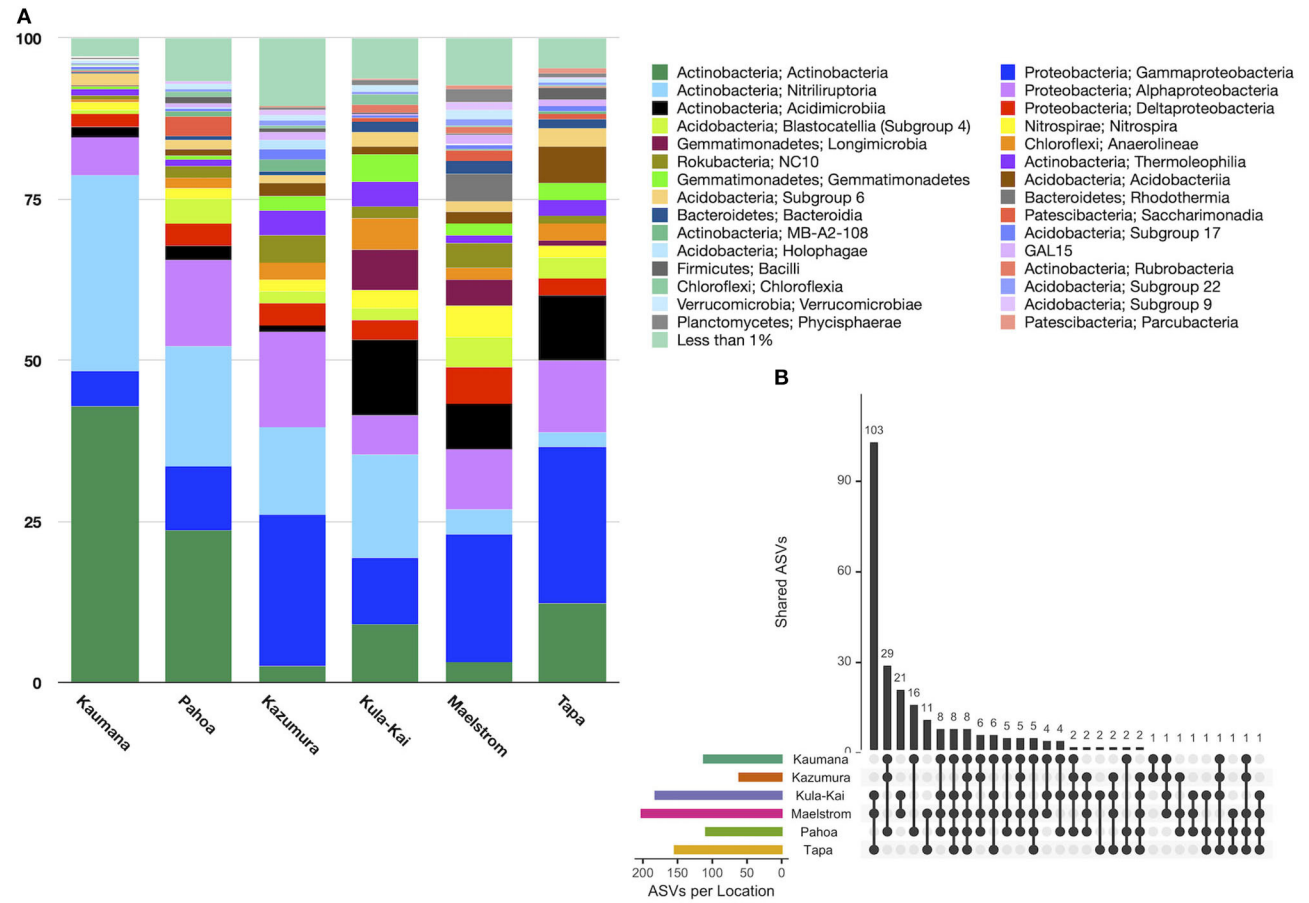

FIGURE 4 | (A) Relative abundance by the site of class-level taxa with >1% abundance in lava tubes. Dominant taxa in these features were Actinobacteria (16.0% ± 24.4), Gammaproteobacteria (15.4% ± 11.0), Nitriliruptoria (13.7% ± 23.3), and Alphaproteobacteria (9.8% ± 10.7). Longimicrobia and Acidimicrobiia ASVs were considerably more abundant in the Kipuka Kanohina cave system in the south of the island of Hawai'i. **(B)** Upset plot of lava tube sites shows that individual lava tubes are moderately unique, with Maelstrom cave hosting 1,277 unique ASVs, followed by Kaumana cave (1,022 unique ASVs). Only seven ASVs occurred in all lava tubes.

in many geothermal samples, had the greatest number of interactions with Alphaproteobacteria as well (**Figure 7**).

The ASV with the highest hub score was affiliated with the class Acidobacteriia (hub score = 1; **Supplementary Table 4**), while another Acidobacteriia (Subgroup 2) affiliated sequence had the second-highest hub score (0.961). These ASVs may be derived from organisms with potentially important ecological roles. An ASV identified as a Chloroflexi (class JG30-KF-CM66) had the third-highest hub score in the overall network (0.884). There were 100 ASVs with above average hub scores (**Supplementary Table 4**). Of those, 18% of ASVs affiliated with members of the Chloroflexi, mostly Ktedonobacteria, and 16% affiliated with Alphaproteobacteria, mostly Rhizobiales. Sequences affiliated with Oxyphotobacteria were the most abundant in geothermal samples, but only six ASVs (6%) were identified with above-average hub scores. Acidobacteriia-affiliated ASVs comprised 17% of the ASVs with above-average hub scores. Most of the Acidobacteriia ASVs affiliated with the Solibacteraceae (Subgroup 3), including three that were most closely identified with a *Bryobacter* sp.

Seven subnetworks (consortia) were identified and constructed from geothermal sites. **Table 2** provides information on all seven consortia, the dominant phyla, and the taxonomic identification of the ASV with the highest hub score (refer to **Supplementary Figure 5** for images of all geothermal subnetworks and **Supplementary Table 5** for subnetwork statistics and hub scores). A phylogenetic tree of all ASVs in geothermal subnetworks is illustrated in **Supplementary Figure 6**, highlighting the taxonomy of ASVs that occurred in more than one consortium, and ASVs that had the highest hub score within each of the seven subnetworks.

In general, geothermal subnetworks comprised ASVs that were affiliated with a wide range of phyla and classes, but Chloroflexi and Proteobacteria-affiliated ASVs were the most abundant except in consortia 7 which was dominated by Acidobacteria-affiliated ASVs (**Table 2**). Although there was a wide range of phyla and classes in consortia, there were often ASVs that were identified as the same family or genus in multiple consortia (**Supplementary Figure 6**; i.e., multiple branches of Gemmataceae, *Bryobacter* sp., etc.). In all but

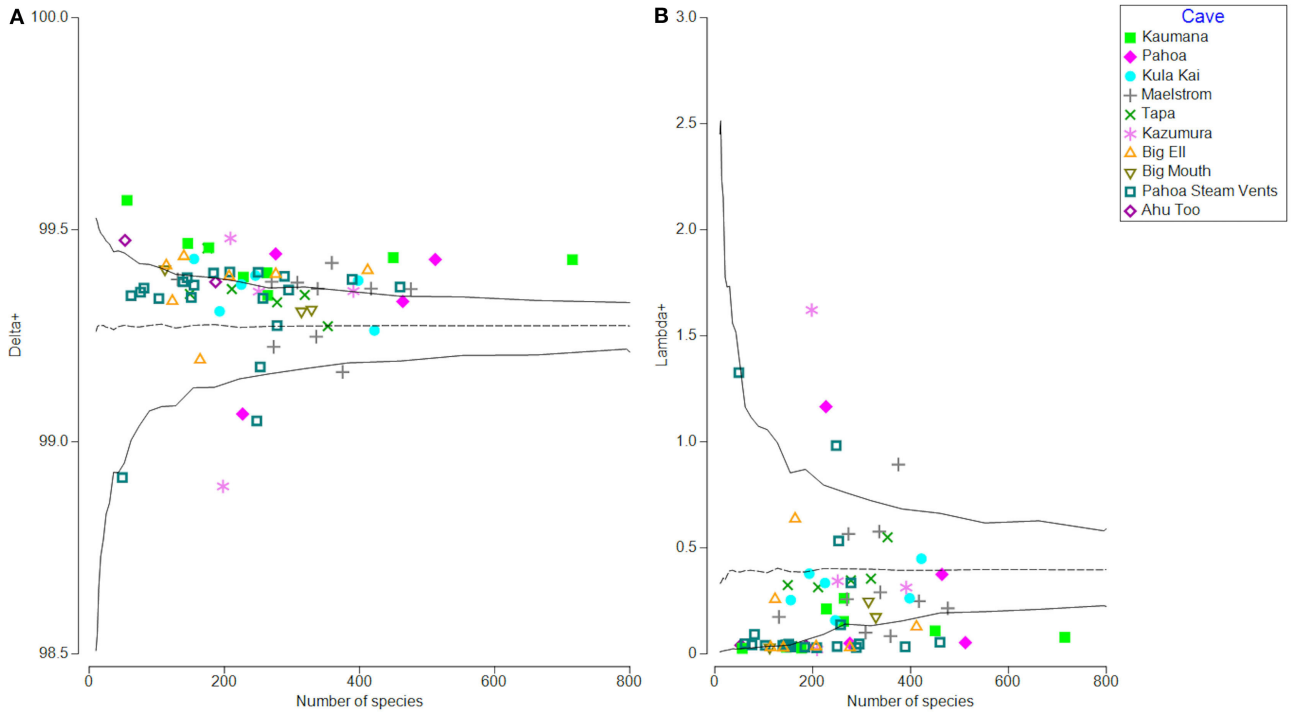

FIGURE 5 | Phylogenetic distinctness (Delta+) on the left **(A)** and variation of phylogenetic distinctness (Lambda+) on the right **(B)** for all samples based on patristic distances between identified taxa (ASVs). Samples are labeled by location. Most samples are either within expected values of Delta+ (null = randomly distributed) or higher than expected, meaning samples are phylogenetically over-dispersed, possibly due to competitive exclusion **(A)**. Variation in phylogenetic distinctness (Lambda+) is within expected values or lower than expected. Most samples had lower than expected variation in distances between branches on the phylogenetic tree, when compared to the null model of random assemblage, and represent that more distinctly related organisms are assembled into the community **(B)**.

one geothermal subnetwork, ASVs identified as the deep-branching phylum Chloroflexi had above-average hub scores, and in one consortium, a Chloroflexi-affiliated ASV had the highest hub scores (**Table 2**). This suggests they have high levels of interactions and may occupy an important ecological niche. Among the Chloroflexi, many were classified as yet-uncultured classes, such as JG30-KF-CM66, Anaerolineae, and Ktedonobacteria, with Consortia 2 and 3 containing the most Chloroflexi-affiliated sequences (**Table 2**). ASVs classified as Ktedonobacteria (order B10-SB3A) and JG30-KF-CM66 had the top two hub scores in that subnetwork (**Supplementary Table 5**).

Oxyphotobacteria were the most abundant taxa in geothermal samples, and 13 nodes in Consortium 4 comprised Oxyphotobacteria-affiliated ASVs. These co-occur with 18 Alphaproteobacteria-affiliated nodes, the other most abundant taxa identified in consortium 4 (**Supplementary Table 5**). Overall, 19 ASVs categorized as Oxyphotobacteria appeared in all subnetworks, but 68% of those occurred in one subnetwork, consortium 4 (**Supplementary Figure 5** and **Supplementary Table 5**).

Proteobacteria-affiliated ASVs were the most abundant across all geothermal subnetworks, representing 46 branches in the sub-network phylogenetic tree (**Supplementary Figure 6**). Proteobacteria were also among the top hub scores in consortia 4–6. A Proteobacteria ASV, affiliated with the genus *Pedomicrobium* sp., was detected across five different consortia, the most of any ASV, but it did not have high hub scores (**Supplementary Figure 6**). Members of this genus are known for biofilm formation and manganese or iron oxidation (Larsen et al., 1999).

Networks constructed for the lava tube samples used a threshold cutoff of 15% sample prevalence, and comprised 251 nodes and 521 edges, with an average degree centrality of 4.02 (**Figure 8**; **Table 1**), lower than geothermal sites, suggesting a less interactive environment overall. In addition, unlike geothermal sites, ASVs from lava tubes tended to have a greater number of interactions with ASVs in the same phylum or class (**Figure 9**). For example, Gammaproteobacteria and Alphaproteobacteria had the highest counts of neighbor interactions in both Proteobacteria classes (**Figure 9**). Gammaproteobacteria interacted with other Gammaproteobacteria, and also had a high number of interactions with Alphaproteobacteria and Acidomicrobiia. Alphaproteobacteria formed the most interactions with Gammaproteobacteria, followed by Deltaproteobacteria.

An ASV associated with the class Bacteroidia (*Microscillaceae* sp.) had the highest hub score in the overall lava tube network (hub score = 1), followed by an Acidobacteria (class Subgroup 9; hub score = 0.77), and a Rokubacteria (*Candidatus Methylomirabilis* sp.; hub score = 0.766;

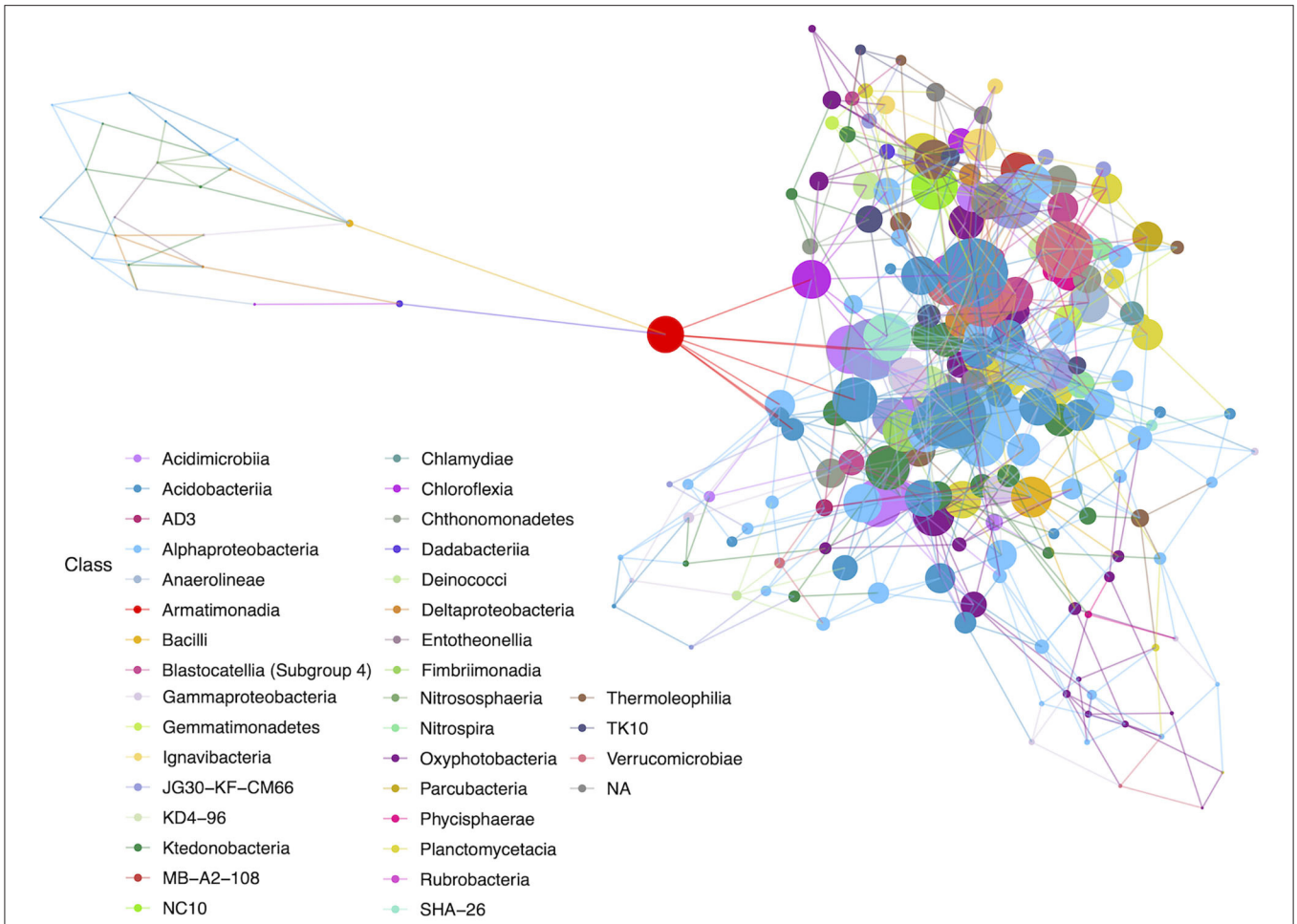

FIGURE 6 | Hub network for geothermal sites, illustrating a high level of complexity within the network. There are 100 nodes that have an above-average hub score (represented by larger circles in the network). Hubs are taxa that most likely have important ecological roles, such as keystone species, and help maintain the overall network structure.

TABLE 1 | Network statistics comparing geothermal sites to lava tubes.

Environment	# Nodes	# Edges	Avg. degree centrality	Avg. betweenness	Avg. closeness	# of edges/# of nodes
Geothermal sites	218	671	6.16	309.56	0.0012	3.078
Lava tubes	259	521	4.02	576.80	0.0006	2.012

Geothermal sites had a greater number of edges, a higher average degree of centrality, and a higher average hub score. The average betweenness centrality also was higher in lava tubes and suggests that interactions are greater in geothermal sites than in lava tubes. # Nodes, total number of ASVs in the network; # Edges, total number of connections (edges) between nodes; Avg. degree centrality, average number of edges in a network that connects to one node; Avg. betweenness, betweenness centrality measures the extent to which a node lies on paths between other nodes and can be used to identify which ASVs interact most with other members of the community network; Avg. closeness, average closeness centrality which measures how far a node is to all other nodes and can be used to find the most central taxa of a given community network; # edges/# nodes provides network density.

Supplementary Table 6). There were 69 ASVs with an above-average hub score, and 46.4% of those were affiliated with Proteobacteria. Nineteen of the ASVs with above-average hub scores were identified as Gammaproteobacteria (27.5%), seven were Alphaproteobacteria (10.1%), and six were Deltaproteobacteria (8.7%; **Supplementary Table 6**). This illustrates that in lava tubes, the phylum Proteobacteria dominates in terms of the number of interactions. Acidobacteria also had a large percentage of the above-average hub scores (20.2% of ASVs). Although Actinobacteria are commonly cultured from caves and had the highest relative abundance among lava tube samples, only one ASV identified as an

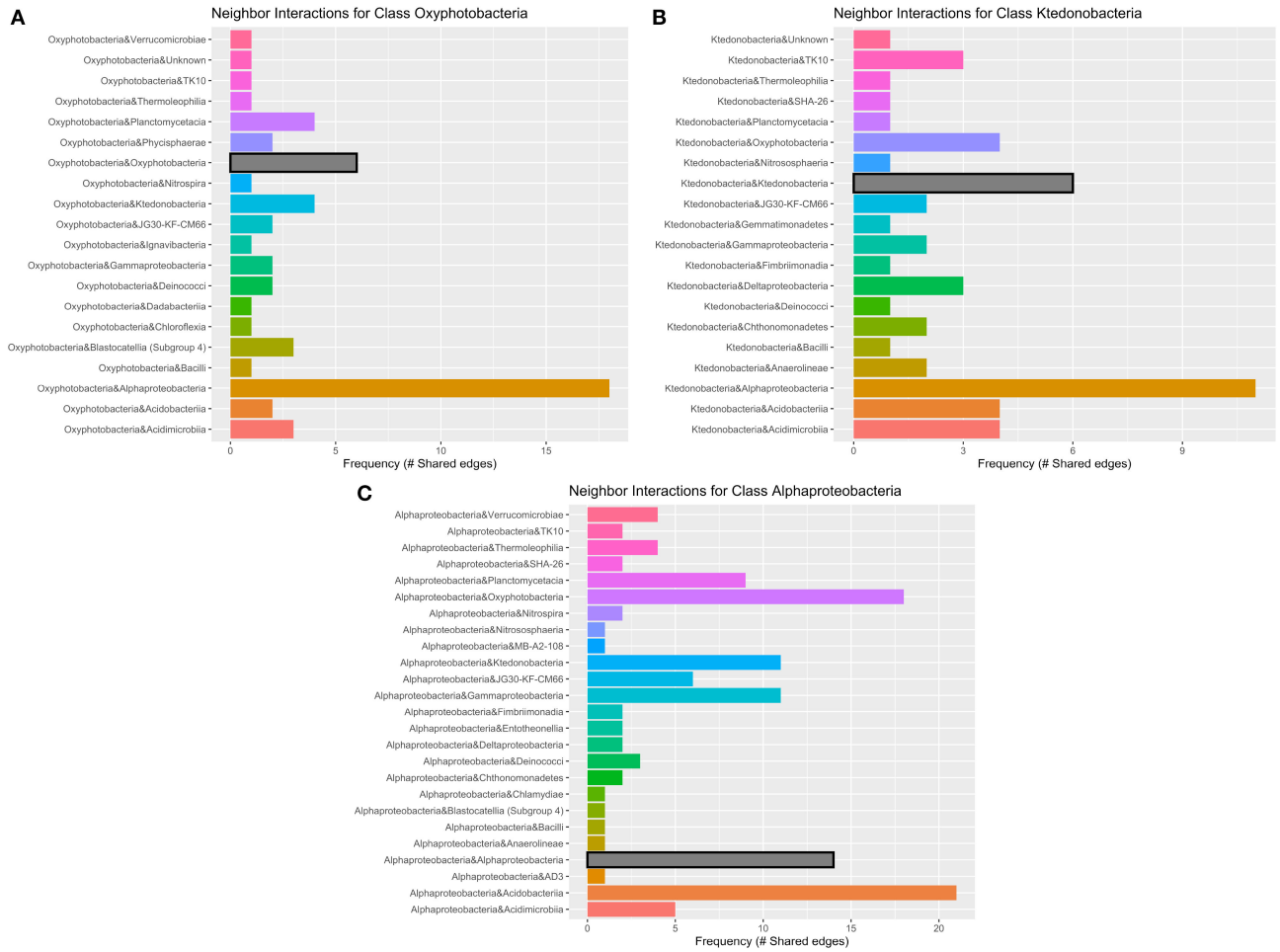

FIGURE 7 | Geothermal neighbor interaction frequency plots at the class level of the three classes with the greatest number of interactions (edges) within the geothermal network: **(A)** Oxyphotobacteria, **(B)** Alphaproteobacteria, and **(C)** Ktedonobacteria. Oxyphotobacteria have the largest number of interactions or co-occurrence with Alphaproteobacteria. However, Alphaproteobacteria have the most interactions with Acidobacteriia, followed by Oxyproteobacteria and then other Alphaproteobacteria. Ktedonobacteria, a common Chloroflexi group in geothermal sites, also has the greatest number of interactions with Alphaproteobacteria, followed by interactions with other Ktedonobacteria.

TABLE 2 | Subnetwork statistics and information for geothermal sites.

Subnetwork no.	Nodes	Edges	Edge density	Network density	Most abundant phyla	Highest hub score
Consortia 1	29	63	0.155	2.172	Proteobacteria (24.1%)	Phycisphaerae
Consortia 2	45	118	0.119	2.622	Chloroflexi (24.4%)	Thermoleophilia
Consortia 3	17	29	0.213	1.706	Chloroflexi (41.2%)	Ktedonobacteria
Consortia 4	53	116	0.0842	2.189	Proteobacteria (34.0%)	*Hyphomicrobium* sp.
Consortia 5	21	41	0.195	1.952	Proteobacteria (38.1%)	Xanthobacteraceae
Consortia 6	14	26	0.286	1.857	Proteobacteria (50%)	Elsterales
Consortia 7	39	95	0.128	2.435	Acidobacteria (28.2%)	Acidobacteriales

Edge density is defined as the number of actual edges/maximum possible edges. Network density is defined as the number of edges/number of nodes and expresses the level of modularity of a subnetwork. The most abundant taxa occurring in each subnetwork, as well as the nodes (ASVs) with the top two highest hub scores are provided.

Actinobacteria (class MB-A2-108) was found to have a higher-than-average hub score in the overall lava tube network (hub score = 0.646, which was the 7th highest hub score; **Supplementary Table 6**).

Eight subnetworks were constructed from the lava tube data set (**Table 3**; **Supplementary Figure 7** and **Supplementary Table 6**). A phylogenetic tree was constructed using only the ASVs within lava tube subnetworks, with Proteobacteria having the most ASVs identified in more than one consortium (**Supplementary Figure 8**). Within the Proteobacteria, five ASVs identified as Gammaproteobacteria occurred in more than one subnetwork. However, there was no ASV that occurred repeatedly in most subnetworks in lava tubes, unlike geothermal sites (**Supplementary Figure 6**; i.e., *Pedomicrobium* sp.). The majority of ASVs with top hub scores in subnetworks were affiliated with Proteobacteria, Acidobacteria, Actinobacteria, Gemmatimonadetes, and the phyla, GAL15 (**Table 3**). Candidate phylum, GAL15 has been recovered from subsurface soil communities previously (Brewer et al., 2019), and in the carbonate cave, Fort Stanton Cave (Kimble et al., 2018). Within Acidobacteria, ASVs associated with Blastocatellia (Subgroup 4) were common in lava tube consortia and had top hub scores in four of the subnetworks (**Table 3**; **Supplementary Figure 7** and **Supplementary Table 6**), and therefore may be species of ecological importance.

DISCUSSION

Lava Tubes and Geothermal Sites Harbor Unique Microbial Communities

Lava tubes, geothermal caves, and fumaroles on the island of Hawai'i contain unique microbial ecosystems with little overlap between caves or sites. Samples described here were collected over multiple visits spanning a decade, but no significant association was detected between diversity patterns and time of collection. In all samples, most ASVs were not able to be assigned with high confidence to a named genus or species, but were microbial "dark matter," those unidentified at the lower taxonomic levels of family or genus (Zamkovaya et al., 2020). This suggests that caves and fumaroles are under-explored diverse ecosystems. Moreover, the bacterial communities defined here are likely to be structured by competitive exclusion arising from low nutrient availability, creating a phylogenetic pattern with a broader range of taxa than would be expected by chance in most samples (over-dispersion). This may explain the relatively high diversity observed in Hawaiian lava caves and fumaroles, and potentially other locations around the world (Northup and Lavoie, 2015; Riquelme et al., 2015; Wall et al., 2015).

Consortia in lava caves and geothermal sites may be unique groups of microorganisms that reflect the small-scale spatial variations in mineral composition of basalts and other micro-environmental variables. However, network analysis, including the identification of subnetworks, suggests that there are several closely related ASVs that occur in multiple consortia. This is observed in **Supplementary Figures 6**, **8**, which show the phylogenetic relationships of ASVs identified in only subnetworks, and which subnetworks each ASV. Although there is a considerable diversity at higher taxonomic levels, within several classes, ASVs identified as the same order, family, or genus are found repeatedly (i.e., *Bryobacter* sp., in geothermal sites and Gemmatimonadaceae in lava caves). These may be the same organism or have the same functional role within consortia, but this information is unknown and cannot be defined using methods that target 16S rRNA fragments. Sequencing technology that generates longer sequences (i.e., MinION or PacBio), culture-based methods that target specific taxonomic groups, and metagenomic sequencing could help determine the identity of these organisms within consortia in Hawaiian volcanic environments, as well as what their ecological roles are likely in these communities.

Phylogenetic Diversity Is Greater in Lava Tubes and Older Caves

Geothermally active sites in Hawai'i, including lava caves in Kīlauea Caldera and fumaroles, host different bacterial communities than lava tubes. In general, phylogenetic diversity in geothermal sites, defined here by Faith's PD, was statistically lower than in lava tubes and was dominated by ASVs that were affiliated with Cyanobacteria and Chloroflexi. Lava tube bacterial communities were dominated by Actinobacteria and Proteobacteria-affiliated ASVs. However, Kaumana cave, a lava tube that is only ∼130 years old had lower phylogenetic diversity than other lava tubes, similar to geothermal caves and fumaroles that occurred in younger lava flows. We posit that this reflects the age of the basalt, consistent with previous studies that also concluded diversity was lower in younger basalts (King, 2007). Our data illustrate that caves aged 500–800 years old host greater phylogenetic diversity than sites that are 65–400 years old. Microbial communities in geothermal sites and lava tubes can likely be placed on a spectrum of diversity over time, with those in geothermal sites representative of early stages of microbial colonization on basalts and in areas of volcanic activity. As these communities age and/or cool, Proteobacteria and Actinobacteria may become prevalent.

Hawaiian Volcanic Features Are Phylogenetically Over-Dispersed

Geothermal sites and lava tubes have distinct phylogenetic signatures of over-dispersion, a phylogenetic community structure that has not been commonly documented in microbial communities (Lozupone and Knight, 2008). In many ecosystems, phylogenetic over-dispersion occurs when competitive exclusion is a driving factor in structuring communities (Webb, 2000; Lozupone and Knight, 2008). Competitive exclusion is more common in oligotrophic environments, such as caves and fumaroles, where there is strong competition for limited resources. In few studies using null models to determine a phylogenetic signature of microbial communities, and the possible underlying stochastic and deterministic processes, habitat filtering (phylogenetic clustering) was observed most often (Horner-Devine and Bohannan, 2006; Aguirre De Cárcer, 2019). Phylogenetic clustering occurs when closely

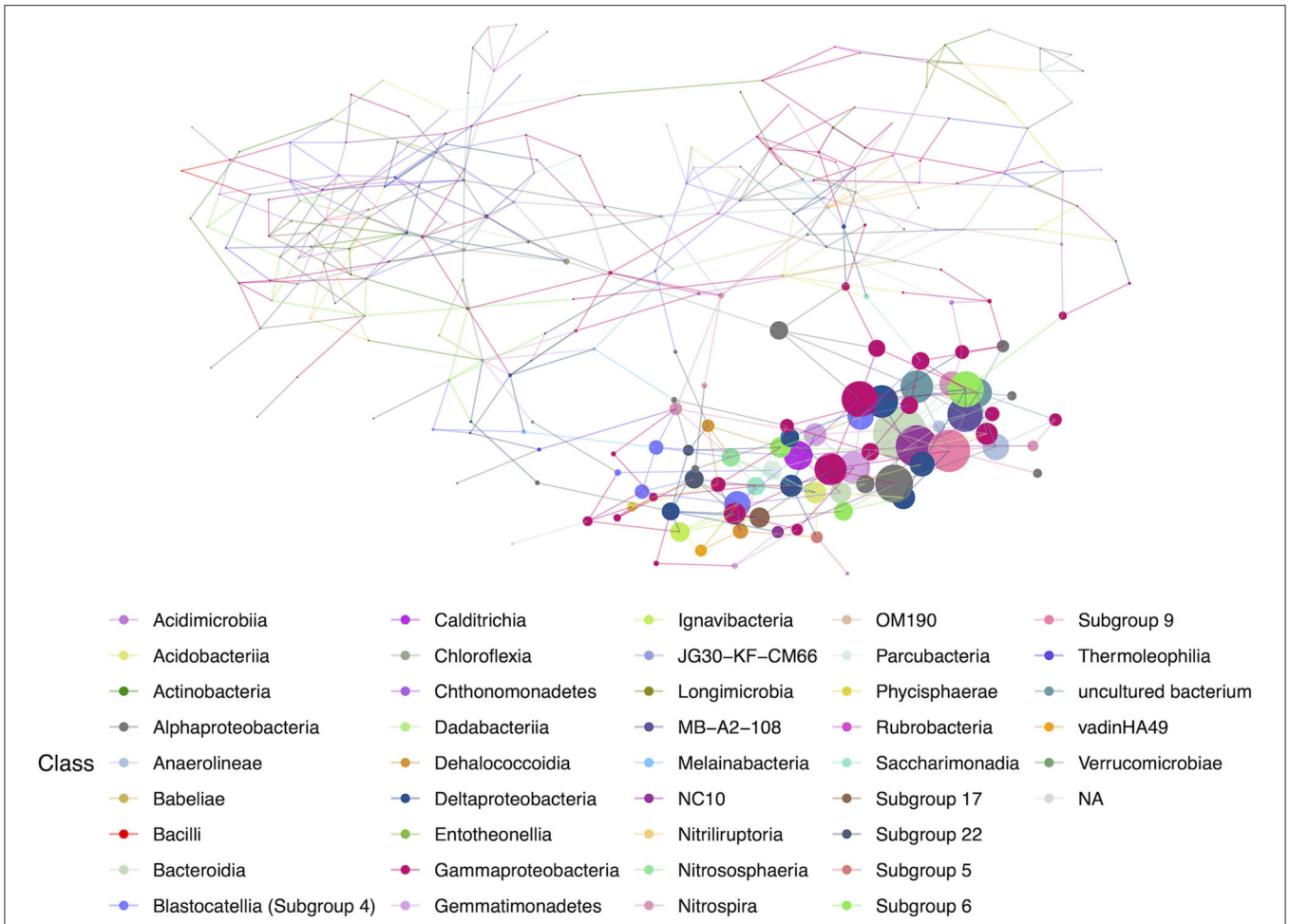

FIGURE 8 | Hub network for lava tubes, suggesting lower complexity than the geothermal network. There are 69 ASVs with an above-average hub score, represented by larger circles on the network graph. Hubs are taxa that most likely have important ecological roles, such as keystone species, and help maintain the overall network structure.

TABLE 3 | Subnetwork statistics and information for lava tubes.

Subnetwork no.	Nodes	Edges	Edge density	Network density	Most abundant phyla	Highest hub score
Consortia 1	28	40	0.106	1.429	Actinobacteria (32.1%)	Pyrinomonadaceae
Consortia 2	64	120	0.0596	1.875	Proteobacteria (34.9%)	Hyphomicrobiaceae
Consortia 3	34	57	0.102	1.677	Proteobacteria (41.2%)	Betaproteobacteriales
Consortia 4	13	20	0.256	1.538	Actinobacteria (30.8%) and Proteobacteria (30.8%)	Nitriliruptoraceae
Consortia 5	54	110	0.077	2.037	Proteobacteria (44.4%)	Blastocatellia (Subgroup 4)
Consortia 6	16	19	0.158	1.188	Proteobacteria (56.3%)	Acidimicrobiia (order IMCC26256)
Consortia 7	23	35	0.138	1.522	Proteobacteria (62.5%)	Gemmatimonadaceae
Consortia 8	26	46	0.142	1.769	Proteobacteria (50%)	GAL15

Edge density is defined as the number of actual edges/maximum possible edges. Network density is defined as the number of edges/number of nodes and expresses the level of modularity of a subnetwork. The most abundant taxa occurring in each subnetwork, as well as the nodes (ASVs) with the top highest hub score are provided.

related bacterial species share a trait, or suite of traits, that allow them to persist in a given habitat. However, our data do not support habitat filtering as the major factor structuring microbial community assemblies in lava caves and fumaroles, but instead, support high diversity driven by competitive exclusion.

In networks constructed from geothermal samples, phylogenetically similar species do not co-occur together,

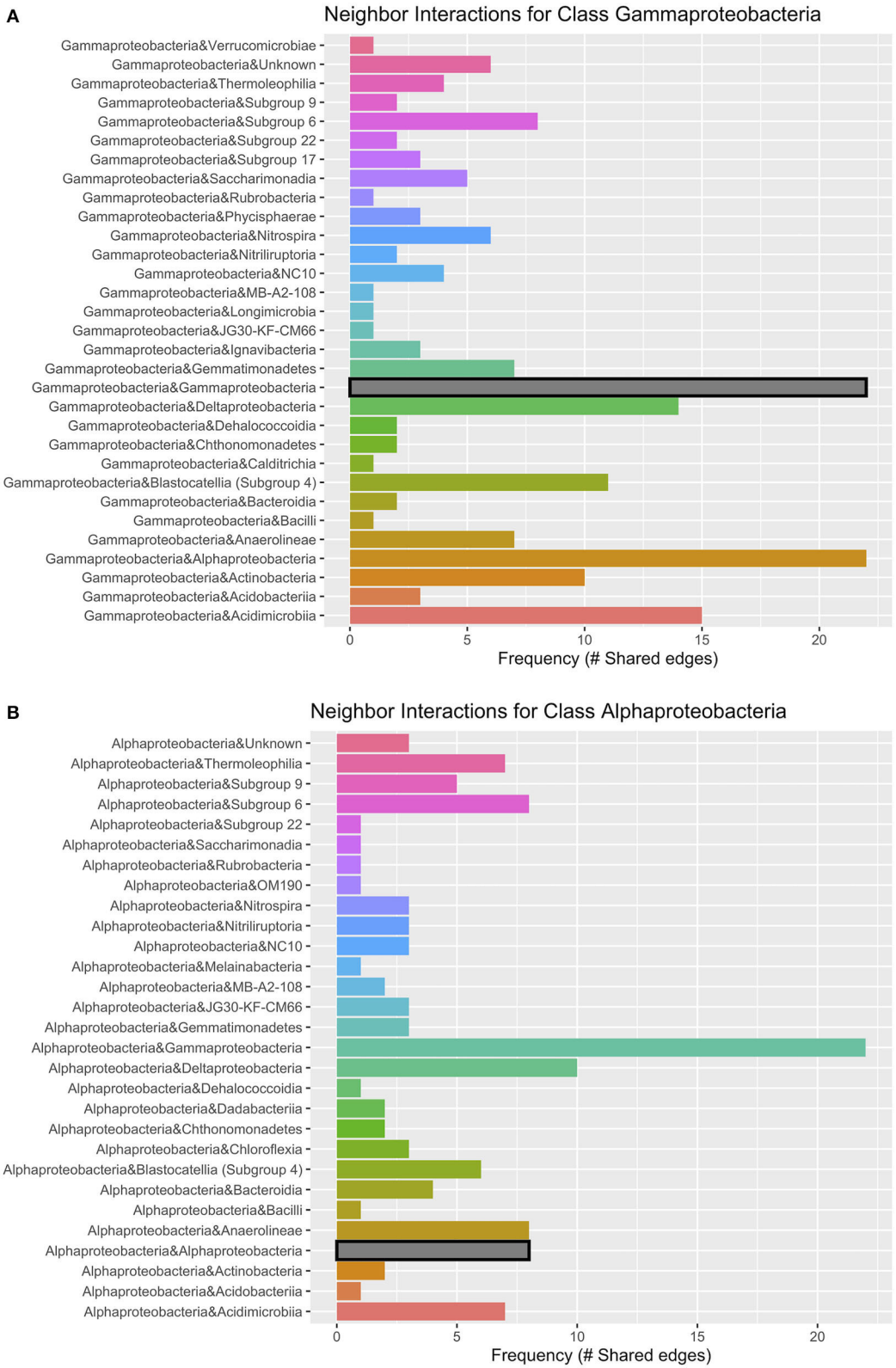

FIGURE 9 | Lava tube neighbor interaction frequency plots at the class level of the two classes with the greatest number of interactions (edges) within the network: **(A)** Gammaproteobacteria and **(B)** Alphaproteobacteria. Gammaproteobacteria have the highest frequencies of neighbor interactions with other Gammaproteobacteria, as well as Alphaproteobacteria. Gammaproteobacteria also interact or co-occur with Acidimicrobiia (phylum Actinobacteria), and Deltaproteobacteria. Alphaproteobacteria co-occur with Gammaproteobacteria at the greatest frequency and have much fewer interactions with other Alphaproteobacteria. Deltaproteobacteria and Chloroflexi class Anaerolineae also had a high frequency of interactions with Alphaproteobacteria within lava tubes.

and instead, more distantly related species co-occur, which also suggests that community assemblages are being driven by competitive interactions between closely related species that eliminate or reduce closely related species in the samples. The exception was Gammaproteobacteria within lava tubes, which have a higher frequency of interactions with other Gammaproteobacteria and Alphaproteobacteria. In lava tube networks, Proteobacteria interacted more with other Proteobacteria, unlike in geothermal sites. However, only five samples out of 70 had a phylogenetically clustered signature, but those five samples were not from any one location or sample type, and we could not determine a specific environmental reason that would explain the difference in pattern.

The Complexity of Bacterial Networks Is Higher in Geothermal Sites

Network analyses concluded that the overall complexity of interactions among bacteria is higher in geothermal environments than in lava caves. Bendia et al. (2021) reported a similar pattern of greater complexity in microbial communities along a thermal gradient. This observation may reflect the more extreme nature of the environment and lower diversity overall, a situation in which more synergistic metabolic interactions may be required for survival, with fewer individual strains or species able to fulfill the required ecological roles (greater number of hubs). Geothermal subnetworks were also more complex (higher number of nodes and edges) than those in lava tubes. These findings did not support our hypothesis that complexity would increase over time in volcanic environments as niche-specific consortia develop in the more stable environments of lava tubes.

Higher overall diversity occurred in lava tube samples, but the complexity of interactions was less in lava tubes. Moreover, the most abundant ASVs in these communities were not hubs in the overall networks or the subnetworks. This is important for subsequent investigations of the cave and fumarole environments, which should use culturing methods combined with sequencing technologies to target these taxa with potentially important ecological roles in these unique environments.

Chloroflexi may play important ecological roles in communities both in lava tubes and geothermal sites, given they occurred in almost every subnetwork (consortium), and frequently with high hub scores. Some cultivated Chloroflexi are aerobic thermophiles, while others are anoxygenic photoautotrophs, for example, green non-sulfur bacteria that utilize low levels of light for photosynthesis. Such conditions are found in cave entrances in the "twilight zone" and at "skylights." Therefore, ASVs identified as Chloroflexi may provide a carbon source through photoautotrophy in low light conditions. However, most of the Chloroflexi ASVs identified as hubs belong to groups with no cultured individuals and may have very different ecological roles in these understudied environments. Chloroflexi are also common in networks from lava tubes, where many of the samples would not have had any light. Further studies of these environments with a focus on Chloroflexi are needed to define their ecological roles in volcanic environments.

The most abundant groups, such as Oxyphotobacteria and Actinobacteria were not common in many consortia, and if they were present, they did not often have high hub scores. Therefore, the most abundant species may not have the most important ecological roles in these ecosystems, helping to create the overall stability of the community. Acidobacteria, another understudied group, commonly had the highest hub scores and is a group that requires further study to understand their ecological roles in caves and fumaroles. Cultivated members of Acidobacteria are considered aerobic oligotrophic bacteria due to their high abundances in low organic carbon environments (Kielak et al., 2016a) and were one of the five most numerous phyla in the Azorean lava caves (Riquelme et al., 2015). Others have been identified as acidophiles (Jones et al., 2009; Kielak et al., 2016a), which may suggest a possible reason these organisms were identified as "hubs." Bacteria are capable of creating a low pH environment through the release of organic acids or by thriving in those low pH environments may be able to breakdown basalts and access nutrients in the rock through solubilization (Kielak et al., 2016b). However, Acidobacteria is likely a diverse group that requires further study to understand their important ecological roles as "hubs" in caves and fumaroles.

Broader Context and Further Studies

Microbial communities associated with lava caves and fumaroles, representing a spectrum of environmental conditions commonly seen in volcanic environments, are of interest to a variety of fields and research beyond fundamental microbial ecology. In particular, Hawaiian lava tubes are of interest to astrobiology studies and upcoming missions to Mars (Boston et al., 2001; Northup et al., 2011; Bauermeister et al., 2014; Tarnas et al., 2021). Volcanic systems in Hawai'i are geologically like those on ancient Mars, which had active volcanoes and fumaroles (Farmer, 1996; Thollot et al., 2012; Hynek et al., 2018; Sauro et al., 2020). High-resolution satellite images from various orbital spacecraft show that Martian volcanoes were built from countless individual flows, many of which were created through channels and lava tubes, signaling a style of volcanism analogous to Hawaiian eruptions (Sauro et al., 2020). With these geological similarities, Hawaiian volcanic environments can provide some insight into the possibility of life on Mars in its ancient past and how microbial communities could survive today on Mars in lava caves, or if introduced from Earth (forward contamination).

The study of cave and fumarole microbial communities is also important to questions in biotechnology, sustainable resource management, and bioremediation (Brune and Bayer, 2012; Zhang et al., 2016; Kapoore et al., 2022). Bioleaching organisms are commonly used in mining, and previous research has discovered that the recovery of target metals is often greater with co-cultures of chemolithotrophic organisms (Mathew and Krishnaswamy, 2017). Within the field of study focused on rare earth elements and biomining, the use and discovery of microbial consortia for higher rates of recovery of those elements are critical for more environmentally friendly mining methods (Fathollahzadeh et al., 2018). This also applies to space exploration and the potential to mine other planetary bodies and nearby asteroids (Cockell et al., 2020).

Understanding chemolithotrophic and acidophilic microbial consortia may also have importance in soil health and agriculture production, particularly in the desert or volcanic soils (Kielak et al., 2016b; Woo and Pepe, 2018). Chemolithothrophs and other organisms that bioweather basalts, are important in the breakdown of lava flows into soils, releasing nutrients into the biogeochemical cycle. Understanding these processes has become more important as we are faced with climate change and growing food concerns in areas with less water and low-nutrient soils than in previous decades. In addition, fungi play a very important role in bio-weathering in soils and rocks (Finlay et al., 2009), with one study suggesting that fungi may be responsible for ∼40–50% of the breakdown of rock through bio-weathering (Li et al., 2016). Therefore, studies of cave systems and roles of microbes should include fungal communities, along with additional studies of rock–microbe interactions using geological methods (i.e., Wavelength-Dispersive X-Ray Spectroscopy, Ramen Spectroscopy, etc.). Additional studies that examine fungal–bacterial interactions in lava caves and geothermal sites are also needed to better define underlying mechanistic interactions in the bio-weathering process.

DATA AVAILABILITY STATEMENT

The datasets presented in this study can be found at Dryad: https://doi.org/10.5061/dryad.z612jm6f0, and with accession #PRJNA806456 in NCBI database.

AUTHOR CONTRIBUTIONS

RP completed most analyses and writing for this manuscript, the collection of samples in 2017, and DNA extractions. TZ completed network analyses and contributed largely to the interpretation and writing of the manuscript. SD and JS collected samples in 2006–2009 and 2019. DN and JM collected samples in 2017 and 2019. NM contributed to the analysis of samples through DNA extraction and molecular methods. JS, AD, and PC contributed funding for the project. RP, DN, and PB largely contributed to the ideas in this manuscript. All authors contributed to the editing and writing of the manuscript.

FUNDING

This research was supported by the NASA Exobiology grant (80NSSC18K1064) and startup and University Facilitating Funds from George Washington University. This research was supported by funding from the NASA Exobiology Program (grant No. 80NSSC18K1064), startup and University Facilitating Funds from George Washington University and the University of Hawai'i at Mānoa; NSF Postdoctoral Research Fellowship in Biology (grant No. 1711856), and U.S. Department of Energy, Office of Science, Biological and Environmental Research Division (award number LANLF59T). This is contribution #167 from the School of Life Sciences at the University of Hawai'i at Mānoa.

ACKNOWLEDGMENTS

The authors would like to thank Christy Handel and Jennifer Saito at the University of Hawai'i at Mānoa and Karen Davenport and Cheryl Gleasner at Los Alamos National Laboratory for assistance with sample preparation and sequencing. We also thank Asa Aue for local guidance and Native Hawaiian cultural information into these caves to avoid burial grounds or sights of significant cultural value. We thank Harry Shick for access and guidance into Kazumura cave. We acknowledge that samples collected and used in this study are from Hawai'i, the Native Lands of the Hawaiian people. Additional research and education from these samples have supported the ongoing culture-based science education programs in Hawai'i.

SUPPLEMENTARY MATERIAL

The Supplementary Material for this article can be found online at: https://www.frontiersin.org/articles/10.3389/fmicb.2022.934708/full#supplementary-material

REFERENCES

Aguirre De Cárcer, D. (2019). A conceptual framework for the phylogenetically constrained assembly of microbial communities. *Microbiome* 7, 1–11. doi: 10.1186/s40168-019-0754-y

Barton, H. (2015). "Starving artists: bacterial oligotrophic heterotrophy in caves," in *Microbial Life of Cave Systems*, ed A. S. Engel (Berlin: De Gruyter), 79–104.

Bauermeister, A., Rettberg, P., and Flemming, H. C. (2014). Growth of the acidophilic iron-sulfur bacterium Acidithiobacillus ferrooxidans under Mars-like geochemical conditions. *Planet. Space Sci.* 98, 205–215. doi: 10.1016/j.pss.2013.09.009

Begon, M., Harper, J. L., and Townsend, C. R. (1998). *Ecology: Individuals, Populations, and Communities, 3rd Edn*. Cambridge, MA: Blackwell Scientific Publications.

Bendia, A. G., Lemos, L. N., Mendes, L. W., Signori, C. N., Bohannan, B. J. M., and Pellizari, V. H. (2021). Metabolic potential and survival strategies of microbial communities across extreme temperature gradients on Deception Island volcano, Antarctica. *Environ. Microbiol.* 23, 4054–4073. doi: 10.1111/1462-2920.15649

Bizzoco, R., and Kelley, S. T. (2019). "Geothermal steam vents of Hawai'i," in *Astrobiology Exploring Life on Earth and Beyond, Model Ecosystems in Extreme Environments*, eds J. Seckbach and P. Rampelotto (Hoboken, NJ: John Wiley & Sons Inc.), 23–40.

Blondel, V. D., Guillaume, J.-L., Lambiotte, R., and Lefebvre, E. (2008). Fast unfolding of communities in large networks. *J. Stat. Mech. Theory Exp.* 2008, P10008. doi: 10.1088/1742-5468/2008/10/P10008

Blüthgen, N., Fründ, J., Vazquez, D. P., and Menzel, F. (2008). What do interaction network metrics tell us about specialization and biological traits? *Ecology* 89, 3387–3399. doi: 10.1890/07-2121.1

Bokulich, N. A., Kaehler, B. D., Rideout, J. R., Dillon, M., Bolyen, E., Knight, R., et al. (2018). Optimizing taxonomic classification of marker-gene amplicon sequences with QIIME 2's q2-feature-classifier plugin. *Microbiome* 6, 1–17. doi: 10.1186/s40168-018-0470-z

Bolyen, E., Rideout, J. R., Dillon, M. R., Bokulich, N. A., Abnet, C. C., Al-Ghalith, G. A., et al. (2019). Reproducible, interactive, scalable and extensible microbiome data science using QIIME 2. *Nat. Biotechnol.* 37, 852–857. doi: 10.1038/s41587-019-0209-9

Bosse, M., Heuwieser, A., Heinzel, A., Nancucheo, I., Melo Barbosa Dall'Agnol, H., Lukas, A., et al. (2015). Interaction networks for identifying coupled molecular processes in microbial communities. *BioData Min*. 8, 1–17. doi: 10.1186/s13040-015-0054-4

Boston, P. J., Spilde, M. N., Northup, D. E., Melim, L. A., Soroka, D. S., Kleina, L., et al. (2001). Cave biosignature suites: microbes, minerals and Mars. *Astrobiology* 1, 25–55. doi: 10.1089/153110701750137413

Brewer, T. E., Aronson, E. L., Arogyaswamy, K., Billings, S. A., Botthoff, J. K., Campbell, A. N., et al. (2019). Ecological and genomic attributes of novel bacterial taxa that thrive in subsurface soil horizons. *MBio* 10, e01318-19. doi: 10.1128/mBio.01318-19

Brune, K. D., and Bayer, T. S. (2012). Engineering microbial consortia to enhance biomining and bioremediation. *Front. Microbiol*. 3, 203. doi: 10.3389/fmicb.2012.00203

Callahan, B. J., McMurdie, P., Rosen, M. J., Han, A., Johnson, A., and Holmes, S. P. (2016). DADA2: high resolution sample inference from Illumina amplicon data. *Nat. Methods* 13, 4–5. doi: 10.1038/nmeth.3869

Clarke, K. R., and Warwick, R. M. (1998). A Taxonomic Distinctness index and its statistical properties. *J. Appl. Ecol*. 35, 523–531. doi: 10.1046/j.1365-2664.1998.3540523.x

Clarke, K. R., and Warwick, R. M. (1999). The taxonomic distinctness measure of biodiversity: weighting of step lengths between hierarchical levels. *Mar. Ecol. Prog. Ser*. 184, 21–29. doi: 10.3354/meps184021

Clarke, K. R., and Warwick, R. M. (2001). A further biodiversity index applicable to species lists: variation in taxonomic distinctness. *Mar. Ecol. Prog. Ser*. 216, 265–278. doi: 10.3354/meps216265

Cockell, C. S., Santomartino, R., Finster, K., Waajen, A. C., Eades, L. J., Moeller, R., et al. (2020). Space station biomining experiment demonstrates rare earth element extraction in microgravity and Mars gravity. *Nat. Commun*. 11, 5523. doi: 10.1038/s41467-020-19276-w

Costello, E. K., Halloy, S. R. P., Reed, S. C., Sowell, P., and Schmidt, S. K. (2009). Fumarole-supported islands of biodiversity within a hyperarid, high-elevation landscape on Socompa volcano, Puna de Atacama, Andes. *Appl. Environ. Microbiol*. 75, 735–747. doi: 10.1128/AEM.01469-08

Edwards, K. J., Bach, W., and McCollom, T. M. (2005). Geomicrobiology in oceanography: microbe-mineral interactions at and below the seafloor. *Trends Microbiol*. 13, 449–456. doi: 10.1016/j.tim.2005.07.005

Ellis, D. G., Bizzoco, R. W., and Kelley, S. T. (2008). Halophilic Archaea determined from geothermal steam vent aerosols. *Environ. Microbiol*. 10, 1582–1590. doi: 10.1111/j.1462-2920.2008.01574.x

Faith, D. P. (1992). Conservation evaluation and phylogenetic diversity. *Biol. Conserv*. 61, 1–10 doi: 10.1016/0006-3207(92)91201-3

Farmer, J. D. (1996). Hydrothermal systems on Mars: an assessment of present evidence. *CIBA Found. Symp*. 202, 273–299. doi: 10.1002/9780470514986.ch15

Fathollahzadeh, H., Hackett, M. J., Khaleque, H. N., Eksteen, J. J., Kaksonen, A. H., and Watkin, E. L. J. (2018). Better together: potential of co-culture microorganisms to enhance bioleaching of rare earth elements from monazite. *Bioresour. Technol. Reports* 3, 109–118. doi: 10.1016/j.biteb.2018.07.003

Finlay, R., Wallander, H., Smits, M., Holmstrom, S., van Hees, P., Lian, B., et al. (2009). The role of fungi in biogenic weathering in boreal forest soils. *Fungal Biol. Rev*. 23, 101–106. doi: 10.1016/j.fbr.2010.03.002

Frazier, A. G., Giambelluca, T. W., Diaz, H. F., and Needham, H. L. (2016). Comparison of geostatistical approaches to spatially interpolate month-year rainfall for the Hawaiian Islands. *Int. J. Climatol*. 36, 1459–1470. doi: 10.1002/joc.4437

Gabriel, C. R., and Northup, D. E. (2013). "Microbial ecology: caves as an extreme habitat," in *Cave Microbiomes: A Novel Resource for Drug Discovery*, ed N. Cheeptham, New York, NY: Springer 85–108.

Gehlenborg, N., O'Donoghue, S. I., Baliga, N. S., Goesmann, A., Hibbs, M. A., Kitano, H., et al. (2010). Visualization of omics data for systems biology. *Nat Methods* 7, S56–S68. doi: 10.1038/nmeth.1436

Gomez-Alvarez, V., King, G. M., and Nüsslein, K. (2007). Comparative bacterial diversity in recent Hawaiian volcanic deposits of different ages. *FEMS Microbiol. Ecol*. 60, 60–73. doi: 10.1111/j.1574-6941.2006.00253.x

Horner-Devine, M. C., and Bohannan, B. J. M. (2006). Phylogenetic clustering and overdispersion in bacterial communities. *Ecology* 87, 100–108. doi: 10.1890/0012-9658(2006)87[100:PCAOIB]2.0.CO;2

Huang, S. (2004). Back to the biology in systems biology: what can we learn from biomolecular networks? *Brief. Funct. Genom*. 2, 279–297. doi: 10.1093/bfgp/2.4.279

Hynek, B. M., Rogers, K. L., Antunovich, M., Avard, G., and Alvarado, G. E. (2018). Lack of microbial diversity in an extreme Mars analog setting: Poás Volcano, Costa Rica. *Astrobiology* 18, 923–933. doi: 10.1089/ast.2017.1719

Jones, A. A., and Bennett, P. C. (2014). Mineral microniches control the diversity of subsurface microbial populations. *Geomicrobiol. J*. 31, 246–261. doi: 10.1080/01490451.2013.809174

Jones, R. T., Robeson, M. S., Lauber, C. L., Hamady, M., Knight, R., and Fierer, N. (2009). A comprehensive survey of soil acidobacterial diversity using pyrosequencing and clone library analyses. *ISME J*. 3, 442–453. doi: 10.1038/ismej.2008.127

Kapoore, R. V., Padmaperuma, G., Maneein, S., and Vaidyanathan, S. (2022). Co-culturing microbial consortia: approaches for applications in biomanufacturing and bioprocessing. *Crit. Rev. Biotechnol*. 42, 46–72. doi: 10.1080/07388551.2021.1921691

Katoh, K., Misawa, K., Kuma, K. I., and Miyata, T. (2002). MAFFT: a novel method for rapid multiple sequence alignment based on fast Fourier transform. *Nucleic Acids Res*. 30, 3059–3066. doi: 10.1093/nar/gkf436

Kielak, A. M., Barreto, C. C., Kowalchuk, G. A., van Veen, J. A., and Kuramae, E. E. (2016a). The ecology of acidobacteria: moving beyond genes and genomes. *Front. Microbiol*. 7, 744. doi: 10.3389/fmicb.2016.00744

Kielak, A. M., Cipriano, M. A. P., and Kuramae, E. E. (2016b). Acidobacteria strains from subdivision 1 act as plant growth-promoting bacteria. *Arch. Microbiol*. 198, 987–993. doi: 10.1007/s00203-016-1260-2

Kimble, J. C., Winter, A. S., Spilde, M. N., Sinsabaugh, R. L., and Northup, D. E. (2018). A potential central role of Thaumarchaeota in N-Cycling in a semi-arid environment, Fort Stanton Cave, Snowy River passage, New Mexico, USA. *FEMS Microb. Ecol*. 94, fiy173. doi: 10.1093/femsec/fiy173

King, G. M. (2007). Chemolithotrophic bacteria: distributions, functions and significance in volcanic environments. *Microbes Environ*. 22, 309–319. doi: 10.1264/jsme2.22.309

Kurtz, Z. D., Müller, C. L., Miraldi, E. R., Littman, D. R., Blaser, M. J., and Bonneau, R. A. (2015). Sparse and compositionally robust inference of microbial ecological networks. *PLoS Comput. Biol*. 11, e1004226. doi: 10.1371/journal.pcbi.1004226

Larsen, E., Sly, L., and McEwan, A. (1999). Manganese(II) adsorption and oxidation by whole cells and a membrane fraction of *Pedomicrobium* sp. ACM 3067. *Arch. Microbiol*. 171, 257–264. doi: 10.1007/s002030050708

Letunic, I., and Bork, P. (2021). Interactive tree of life (iTOL) v5: an online tool for phylogenetic tree display and annotation. *Nucleic Acids Res*. 49, W293–W296. doi: 10.1093/nar/gkab301

Li, P. E., Lo, C. C., Anderson, J. J., Davenport, K. W., Bishop-Lilly, K. A., Xu, Y., et al. (2017). Enabling the democratization of the genomics revolution with a fully integrated web-based bioinformatics platform. *Nucleic Acids Res*. 45, 67–80. doi: 10.1093/nar/gkw1027

Li, Z., Liu, L., Chen, J., and Teng, H. H. (2016). Cellular dissolution at hypha- and spore-mineral interfaces revealing unrecognized mechanisms and scales of fungal weathering. *Geology* 44, 319–322. doi: 10.1130/G37561.1

Liu, B., Lin, H., Yu, G., Zhang, S., and Zhao, C. (2010). Stability approach to regularization selection (StARS) for high dimensional graphical models. *Adv. Neural Inf. Process. Syst*. 34, 325–330.

Lozupone, C., Knight, R., Lladser, M. E., Knights, D., Stombaugh, J., and Knight, R. (2005). UniFrac: a new phylogenetic method for comparing microbial communities. *Appl. Environ. Microbiol*. 71, 8228–8235. doi: 10.1128/AEM.71.12.8228-8235.2005

Lozupone, C. A., and Knight, R. (2008). Species divergence and the measurement of microbial diversity. *FEMS Microbiol. Rev*. 32, 557–578. doi: 10.1111/j.1574-6976.2008.00111.x

Ma'ayan, A. (2011). Introduction to network analysis in systems biology. *Sci. Signal*. 4, 1–7. doi: 10.1126/scisignal.2001965

Mathew, R., and Krishnaswamy, V. G. (2017). Remediation of mixed heavy metals using acidotolerant bacterial co-cultures. *Int. J. Agric. Environ. Sci*. 4, 43–52. doi: 10.14445/23942568/IJAES-V4I4P108

Miller, A. Z., Pereira, M. F. C., Calaforra, J. M., Forti, P., Dionísio, A., and Saiz-Jimenez, C. (2014). Siliceous speleothems and associated microbe-mineral

interactions from Ana Heva lava tube in Easter Island (Chile). *Geomicrobiol. J.* 31, 236–245. doi: 10.1080/01490451.2013.827762

Northup, D. E., and Lavoie, K. H. (2015). "Microbial diversity and ecology of lava caves," in *Microbial Life of Cave Systems*, ed. A. S. Engel (Berlin: De Gruyter), 161–192.

Northup, D. E., Melim, L. A., Spilde, M. N. N., Hathaway, J. J. M. J. M., Garcia, M. G., Moya, M., et al. (2011). Lava cave microbial communities within mats and secondary mineral deposits: implications for life detection on other planets. *Astrobiology* 11, 601–618. doi: 10.1089/ast.2010.0562

Price, M. N., Dehal, P. S., and Arkin, A. P. (2009). Fasttree: computing large minimum evolution trees with profiles instead of a distance matrix. *Mol. Biol. Evol.* 26, 1641–1650. doi: 10.1093/molbev/msp077

Riquelme, C., Rigal, F., Hathaway, J. J. M., Northup, D. E., Spilde, M. N., Borges, P. A. V., et al. (2015). Cave microbial community composition in oceanic islands: disentangling the effect of different colored mats in diversity patterns of Azorean lava caves. *FEMS Microb. Ecol.* 91, fiv141. doi: 10.1093/femsec/fiv141

Sauro, F., Pozzobon, R., Massironi, M., De Berardinis, P., Santagata, T., and De Waele, J. (2020). Lava tubes on Earth, Moon and Mars: a review on their size and morphology revealed by comparative planetology. *Earth Sci Rev.* 209, 103288. doi: 10.1016/j.earscirev.2020.103288

Saw, J. H. W., Schatzm, M., Brown, M. V., Kunkel, D. D., Foster, J. S., Shick, H., et al. (2013). Cultivation and complete genome sequencing of *Gloeobacter kilaueensis* sp. nov., from a lava cave in Kīlauea Caldera, Hawai'i. *PLoS ONE* 8, e76376. doi: 10.1371/journal.pone.0076376

Snider, J. (2010). *Comparison of microbial communities on roots, ceilings and floors of two lava tube caves in New Mexico* (MSci Thesis). University of New Mexico. Available online at: http://repository.unm.edu/handle/1928/11135

Takada-Hoshino, Y., and Matsumoto, N. (2004). An improved DNA extraction method using skim milk from soils that strongly adsorb DNA. *Microbes Environ.* 19, 13–19. doi: 10.1264/jsme2.19.13

Tarnas, J. D., Mustard, J. F., Sherwood Lollar, B., Stamenković, V., Cannon, K. M., Lorand, J. P., et al. (2021). Earth-like habitable environments in the subsurface of Mars. *Astrobiology* 21, 741–756. doi: 10.1089/ast.2020.2386

Thollot, P., Mangold, N., Ansan, V., Le Mouélic, S., Milliken, R. E., Bishop, J. L., et al. (2012). Most Mars minerals in a nutshell: various alteration phases formed in a single environment in Noctis Labyrinthus. *J. Geophys. Res. E Planets* 117, 1–28. doi: 10.1029/2011JE004028

Toju, H., Tanabe, A. S., and Sato, H. (2018). Network hubs in root-associated fungal metacommunities. *Microbiome* 6, 1–16. doi: 10.1186/s40168-018-0497-1

Vishwakarma, K., Kumar, N., Shandilya, C., Mohapatra, S., Bhayana, S., and Varma, A. (2020). Revisiting plant-microbe interactions and microbial consortia application for enhancing sustainable agriculture: a review. *Front. Microbiol.* 11, 560406. doi: 10.3389/fmicb.2020.560406

Wall, K., Cornell, J., Bizzoco, R. W., and Kelley, S. T. (2015). Biodiversity hot spot on a hot spot: novel extremophile diversity in Hawaiian fumaroles. *Microbiol. Open* 4, 267–281. doi: 10.1002/mbo3.236

Webb, C. O. (2000). Exploring the phylogenetic structure of ecological communities: an example for rain forest trees. *Am. Nat.* 156, 145–155. doi: 10.1086/303378

Woo, S. L., and Pepe, O. (2018). Microbial consortia: promising probiotics as plant biostimulants for sustainable agriculture. *Front. Plant Sci.* 9, 1801. doi: 10.3389/fpls.2018.01801

Wuchty, S., Ravasz, E., and Barabási, A. L. (2006). *The Architecture of Biological Networks*. Boston, MA: Springer.

Yilmaz, P., Parfrey, L. W., Yarza, P., Gerken, J., Pruesse, E., Quast, C., et al. (2014). The SILVA and "all-species Living Tree Project (LTP)" taxonomic frameworks. *Nucleic Acids Res.* 42, 643–648. doi: 10.1093/nar/gkt1209

Zamkovaya, T., Foster, J. S., de Crécy-Lagard, V., and Conesa, A. (2020). A network approach to elucidate and prioritize microbial dark matter in microbial communities. *ISME J.* 15, 228–244. doi: 10.1038/s41396-020-00777-x

Zhang, Y., Deng, C. P., Shen, B., Yang, J., shui, Wang, E. T., and Yuan, H. L. (2016). Syntrophic interactions within a butane-oxidizing bacterial consortium isolated from Puguang Gas Field in China. *Microb. Ecol.* 72, 538–548. doi: 10.1007/s00248-016-0799-4

Conflict of Interest: The authors declare that the research was conducted in the absence of any commercial or financial relationships that could be construed as a potential conflict of interest.

Publisher's Note: All claims expressed in this article are solely those of the authors and do not necessarily represent those of their affiliated organizations, or those of the publisher, the editors and the reviewers. Any product that may be evaluated in this article, or claim that may be made by its manufacturer, is not guaranteed or endorsed by the publisher.

frontiers | Frontiers in Microbiology

TYPE Original Research
PUBLISHED 28 July 2022
DOI 10.3389/fmicb.2022.933398

OPEN ACCESS

EDITED BY
Diana Eleanor Northup,
University of New Mexico,
United States

REVIEWED BY
Prashant Kumar Singh,
Pachhunga University College, India
Slađana Popović,
University of Belgrade, Serbia

*CORRESPONDENCE
Marika Pellegrini
marika.pellegrini@univaq.it
Anna Maria D'Alessandro
annamaria.dalessandro@univaq.it

SPECIALTY SECTION
This article was submitted to Extreme Microbiology, a section of the journal Frontiers in Microbiology

RECEIVED 30 April 2022
ACCEPTED 27 June 2022
PUBLISHED 28 July 2022

CITATION
Djebaili R, Mignini A, Vaccarelli I, Pellegrini M, Spera DM, Del Gallo M and D'Alessandro AM (2022) Polyhydroxybutyrate-producing cyanobacteria from lampenflora: The case study of the "Stiffe" caves in Italy.
Front. Microbiol. 13:933398.
doi: 10.3389/fmicb.2022.933398

Polyhydroxybutyrate-producing cyanobacteria from lampenflora: The case study of the "Stiffe" caves in Italy

Rihab Djebaili[1], Amedeo Mignini[1], Ilaria Vaccarelli[1], Marika Pellegrini[1]*, Daniela M. Spera[2], Maddalena Del Gallo[1] and Anna Maria D'Alessandro[1]*

[1]Department of Life, Health and Environmental Sciences, University of L'Aquila, L'Aquila, Italy, [2]Quality Engineering S.r.l., Pescara, Italy

This study aimed to estimate the green formation lampenflora of "Stiffe" caves in order to evaluate their suitability as an isolation source of cyanobacteria useful for the production of polyhydroxyalkanoates (PHAs). The cave system was chosen as the sampling site due to its touristic use and the presence of high-impact illuminations. The biofilms and the mats of the illuminated walls were sampled. Samples were investigated by 16S rRNA gene analysis and culturable cyanobacteria isolation. The isolated strains were then screened for the production of PHAs under typical culturing and nutritional starvation. Cultures were checked for PHA accumulation, poly-β-hydroxybutyrate (PHB) presence (infrared spectroscopy), and pigment production. The 16S rRNA gene metabarcoding. Highlighted a considerable extent of the pressure exerted by anthropogenic activities. However, the isolation yielded eleven cyanobacteria isolates with good PHA (mainly PHB)-producing abilities and interesting pigment production rates (chlorophyll a and carotenoids). Under normal conditions ($BG11_0$), the accumulation abilities ranged from 266 to 1,152 ng mg dry biomass^{-1}. The optimization of bioprocesses through nutritional starvation resulted in a 2.5-fold increase. Fourier transform infrared (FTIR) studies established the occurrence of PHB within PHAs extracted by cyanobacteria isolates. The comparison of results with standard strains underlined good production rates. For C2 and C8 strains, PHA accumulation rates under starvation were higher than *Azospirillum brasilense* and similar to *Synechocystis* cf. *salina* 192. This study broadened the knowledge of the microbial communities of mats and biofilms on the lightened walls of the caves. These findings suggested that these structures, which are common in tourist caves, could be used to isolate valuable strains before remediation measures are adopted.

KEYWORDS

microbial communities of caves, deep biosphere, biopolymers, polyhydroxyalkanoates, 16S rRNA gene metabarcoding

Introduction

Due to the involvement of the underground environments in various biological processes and the great scenarios present within them, many caves across the world have been converted into scientific laboratories and tourist attractions. These caves undergo several environmental transformations due to paths' construction, visitors' presence, and artificial lighting installation. These changes modify the caves' physicochemical conditions (Cigna, 2019; Piano et al., 2021), with significant alterations to biotic and abiotic components (Lim et al., 2018; Šebela et al., 2019; Nicolosi et al., 2021; Piano et al., 2021). Visitors' presence changes the local microclimate and introduces fungal spores and bacteria into the cave environment (Mammola et al., 2017; Novas et al., 2017; Zhelyazkova et al., 2020). Humidity, temperature, CO_2 levels, and electrical lighting enhance the growth of specific photosynthetic communities known as lampenflora in cave entrances and the speleothem (Piano et al., 2015; Nikolić et al., 2020). Generally, microbial communities in cave entrances constitute biofilms (Albertano, 2012), where there is also the presence of cyanobacteria and microalgae (Poulíčková and Hasler, 2007; Czerwik-Marcinkowska, 2013; Lamprinou et al., 2014). Lampenflora typically causes biodeterioration of colonized surfaces (Figueroa et al., 2017; Muñoz-Fernández et al., 2021), and a variety of approaches (i.e., physical, mechanical, and chemical) are utilized to limit photosynthesis and propagation (Mulec and Kosi, 2009; Cigna, 2016; Figueroa et al., 2017). These strategies to devise the existence of lampenflora have been studied for many years. Few studies, however, have investigated the traits that microbes develop in these harsh conditions and whether they can act as a source of interesting molecules.

In this study, we have focused our attention on the cyanobacteria of lampenflora. Cyanobacteria are an ancient lineage of slow-growing ubiquitous photosynthetic prokaryotes found in a wide range of terrestrial and aquatic lightened environments (Abed and Garcia-Pichel, 2001; Abed et al., 2009; Lemes-da-Silva et al., 2011; Panou and Gkelis, 2022). Cyanobacteria are the most important primary producers on Earth, including extreme environments (Gan and Bryant, 2015). They are well adapted to extreme environments due to their ability to withstand high osmotic pressure, low temperatures, arid conditions, and UV radiations (Sechrest and Brooks, 2002; Satyanarayana et al., 2005; Chrismas et al., 2015; Rasouli-Dogaheh et al., 2022). Many authors have described their presence in caves as most close to entrances lit by direct or indirect sunlight or by artificial light in those open to tourists (Pentecost, 1992; Giordano et al., 2000; Asencio and Aboal, 2011; Czerwik-Marcinkowska and Mrozińska, 2011; Albertano, 2012; Czerwik-Marcinkowska, 2013; Pfendler et al., 2018; Puente-Sánchez et al., 2018; Behrendt et al., 2020; Havlena et al., 2021; Panou and Gkelis, 2022).

Numerous new bioactive compounds and polymers have been identified in cyanobacteria belonging to different environments (Abarzua et al., 1999; Shimizu, 2003; Dahms et al., 2006) produced, in particular, in response to environmental changes and biotic and abiotic stresses, providing protection and promoting survival (Singh and Mallick, 2017). Among polymers, cyanobacteria produce polyhydroxyalkanoates (PHAs) (Balaji et al., 2013; Koch et al., 2020). PHAs are lipoid materials accumulated by a wide variety of microorganisms in the presence of abundant carbon sources, which can have various uses, including the production of bioplastics (Anderson and Dawes, 1990; Abed et al., 2009). The most common PHA in prokaryotic cells is poly-β-hydroxybutyrate (PHB), an abundant energy and carbon source storage material (Balaji et al., 2013). Several heterotrophic bacteria, such as *Cupriavidus necator* and *Escherichia coli*, can produce PHB by fermentation (Liebergesell et al., 1994; Kichise et al., 1999; Abed et al., 2009; Wang et al., 2013; Ansari and Fatma, 2016; Utharn et al., 2021). However, these production processes use organic carbon sources mainly derived from crops (Koch et al., 2020). Cyanobacteria are a promising alternative for PHB production (Balaji et al., 2013). Cyanobacteria have minimal nutrient requirements for growth and accumulate PHAs through oxygenated photosynthesis (Singh and Mallick, 2017). Under nutrient-limited conditions, such as nitrogen starvation, cells enter a quiescent state known as chlorosis (Koch et al., 2020). Cyanobacteria degrade their photosynthetic apparatus during chlorosis. Beyond this degradation, the accumulation of large amounts of glycogen for carbon and energy storage occurs. At the end of the process, the cells begin to degrade glycogen and convert it into PHB (Koch et al., 2019).

Given the anthropogenic pressure present in the "Stiffe" touristic cave (L'Aquila, Italy), we hypothesized that cyanobacterial strains within artificial lightened walls' biofilms and mats might serve as good producers of PHB. To examine the bacterial and archaeal communities' composition of green formations of lighted walls, we investigated a global sample with 16S rRNA gene metabarcoding. To investigate the suitability of these formations as an isolation source of industrially valuable microbial strains, we carried out samplings from five sites inside this cave, and we performed an isolation of cyanobacteria. Strains were studied for the PHA and pigment production abilities under normal and nutritional starvation conditions. PHAs recovered were further characterized by infrared spectroscopy.

Materials and methods

"Stiffe" caves site

The sampling was carried out in the Stiffe caves (42°15′20.62″ North; 13°32′32.51″ East; 695 m Altitude). It consists of complex hydrologically active karst paths, with a vertical cave development of + 186 m from the entrance. The Stiffe caves are about 130 km from Rome. At present, the Stiffe caves receive around 45,000 tourists a year and have been open to the public since the 1990s. The accessible touristic pathway includes artificial tunnels and footbridges. Currently, the total length of the show path represents 1 km from the total known layout, which is approximately 2.3 km. The external light covers the first 20 m and gradually gives way to artificial lighting systems that have been installed both along the tourist way and around inaccessible tourist areas illuminating different morphologies and concretions. In the beginning of the 1990s, the lighting system of the Stiffe caves was designed following a technical study counting the environmental impact to prevent the green formations near the light sources. Illuminated areas were not directly visible on the tourist path, with the initially lighting color consisting of a warm and bright light like the natural one. The underground stream was lit directly with warmer light. According to earlier technical reports, wood's lights illuminated some concretions. Subsequently, the mismanagement of lighting systems led to the proliferation of many photosynthetic communities on illuminated limestone walls, including vascular plants throughout the tourist way. The lamps inside the cave are of different types and colors, and so far, no steps have been taken to set low-impact lighting.

Collection of the samples

The sampling was performed in May 2021 in a period of cave closure. According to the measures adopted to contain the COVID-19 spread, touristic visits were interrupted from March to July 2020 and from November to June 2021. Except for ordinary and extraordinary maintenance work, the whole internal lighting stayed off during the cave closures. Before sampling, portable probes were used to record temperature, relative humidity (TACKLIFE HM03), and light intensity (URCERI portable lux meter). A handheld thermal camera (FLIR One Android USB-C) was used to acquire the thermic photos of each site, measuring the temperature lamp and the temperature variations. Samples from photosynthetic biofilms were then collected from five different sites near lighting systems along the tourist walkway. They were swabbed from the surface with a sterile knife, collected in sterility, and stored in refrigerated containers. The samples for the isolation of cyanobacteria were processed as soon as they were brought to the laboratory. For the DNA isolation, three samples from each site were collected and then directly pooled together in the same tube (Sample C6). According to the manufacturer's instructions, this global sample was stabilized with a solution of RNAlater (Ambion, Austin, TX, United States) and stored at −80°C until processed. Sample site characteristics are shown in **Table 1**, while sampling site localization and photos are depicted in **Figure 1**. On average, in sampling sites, there was a temperature of 13.7°C and a relative humidity of 73.8%. All samples grew on limestone walls subjected to any water scrolling or dripping. On average, the light intensity of the light source was 186.15 lux, while the samples received a 13.65 lux exposure (except for sample C5).

16S rRNA gene metabarcoding

To assess the overall lampenflora bacterial and archaeal communities, three replicates were taken from the C6 global sample and subjected to DNA extraction. Briefly, 500 mg was processed by NucleoSpin®Soil kit (Macherey-Nagel, Germany). To determine DNA content and purity, extracted samples were subjected to spectrophotometric and fluorometric examination utilizing a NanoDrop spectrophotometer (Thermo Scientific™) and a Qubit fluorometer (Thermo Scientific™). Using paired-end 16S rRNA gene community sequencing on the MiSeq Illumina platform, a specific 16S rRNA gene technique was performed to amplify bacteria and archaea (Bio-Fab Research, Italy). Using the analytical approach previously reported (Vaccarelli et al., 2021), we focused on the V3 and V4 regions of 16S rRNA gene (Mizrahi-Man et al., 2013; Choi et al., 2020). After filtering, the reads were examined for quality and counted. The DADA2 plugin in QIIME2 (qiime2-2020.2 version) was utilized for amplicon sequence variant (ASV) assembly (Bolyen et al., 2019). The V3-V4 specific region was extracted from the 16S file retrieved from the SILVA 132 database[1] and utilized for classifier training by the fit-classifier-naive-Bayes plugin. For the taxonomic assignment, a 97% similitude was used.

Cyanobacteria isolation

For cyanobacterial isolation, several dilutions up to 10^{-4} were prepared from each sample and plated on BG11 (H_3BO_3 0.003, $CaCl_2$ $2H_2O$ 0.036, $C_6H_8O_7$ 0.006, Co $(NO_3)_2$ $6H_2O$ 0.00005, $CuSO_4$ $5H_2O$ 0.00008, EDTA 0.001, $C_6H_8FeNO_7$ 0.006, MgSO4 $7H_2O$ 0.075, $MnCl_2$ 4H2O 0.002, K_2HPO_4 $3H_2O$ 0.04, Na_2CO_3 H_2O 0.04, Na_2MoO_4 $2H_2O$ 0.0004, $NaNO_3$ 1.5, $ZnSO_4$ $7H_2O$ 0.0002, H_2O 1,000 ml, and pH 8.5 ± 2) (Allen and Stanier, 1968). Enrichment cultures for all the samples were also prepared in liquid BG11 (1:10 ratio). Liquid and

1 https://www.arb-silva.de/ (accessed on October 2021).

10.3389/fmicb.2022.933398

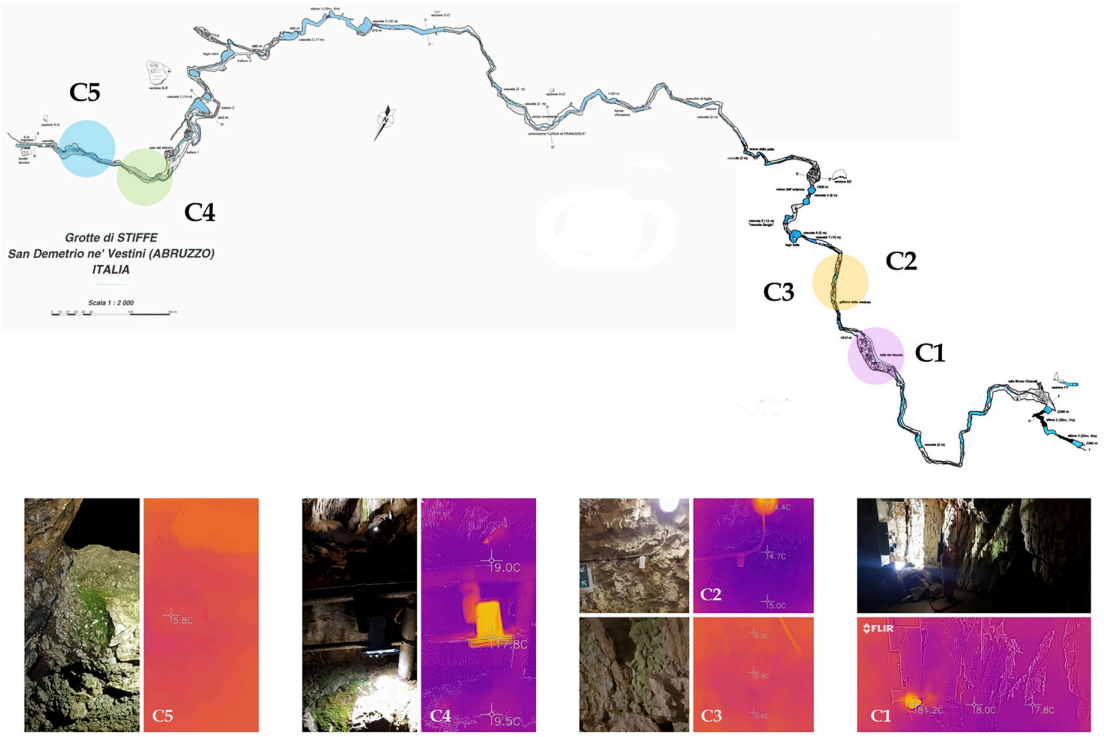

FIGURE 1
Cave survey of the "Stiffe" caves. Sampling areas are highlighted in the plan view and pictures on the bottom show the thermic camera and normal photos for each site.

TABLE 1 Cyanobacterial isolates and environmental variables measured at the different sampling sites of "Stiffe" caves.

Strain ID	Sampling site	Site temperature (°C)	RH (%)	LS (Lux)	
				Light system	Sample
C1	C1 – A parietal biofilm adheres to the concrete in the innermost part of the cave.	15.0	67.6	280.0	10.0
C2					
C3	C2 – On the concrete along the walls of the last man-made tunnel.	15.1	67.6	220.0	20.0
C4					
C5	C3 – A parietal biofilm.	13.0	75.1	120.0	10.0
C6					
C7	C4 – Mosses from the photosynthetic formation.	12.6	80.2	124.6	14.6
C8					
C9					
C10	C5 – No functioning light site.	12.9	78.5	–	–
C11					

solid cultures were incubated for 1 week at 28°C and a 12-h photoperiod lightening of 150–200 μmol (photon) m^{-2} s^{-1}. After incubation, enrichment cultures were plated on solid BG11 following the same procedure. Biomass clumps developed on plates were subcultured several times until individual colonies appeared pure. Putative cyanobacteria colonies were examined with optical microscopy (LEICA DME) to provide preliminary identification based on the morphotype. Each compliant isolate received an identification code (ID). In total, we obtained eleven isolates (C1–C11). The isolated strains were cultured on a liquid BG11 medium in flasks (500 ml) and small bioreactors (a 500-ml glass bottle equipped with GLS 45

screw cap with three-port lids and filled with 250 ml of BG11). After uniformity and purity checks, isolates were stored at the Environmental Microbiology culture collection (LMUNIVAQ) in BG11 agar slants and glycerolates (50% v/v, -80°C storage).

Polyhydroxyalkanoate production

The different cyanobacterial strains were cultured on a $BG11_0$ liquid medium for 5 days under optimal growth conditions (28°C, 120 rpm, and constant illumination of 40–50 μmol of photons $m^{-2}s^{-1}$). Exponentially growing cells (OD 0.4–0.8) were harvested by centrifugation (4,000 *g* for 10 min). The starvation was induced by suspending the pellet in a modified BG11 medium (devoid of basic nutrients) until reaching an OD of 0.4 (for nitrogen starvation, BG11 without $NaNO_3$; for phosphorus deprivation, BG11 supplemented with KCl instead of K_2HPO_4; and for sulfur deprivation, BG11 supplemented with MgCl instead of $MgSO_4$) and incubated under the same conditions until the late log phase of growth for approximately 20 days. After incubation, the calcium acetate (10 mM) was added to the cultures as an organic carbon source and incubated under the same growth conditions for another 10 days. Cultures are then extracted and quantitated for PHB production (Koch et al., 2019, 2020; Utharn et al., 2021). To compare the PHA production rates recorded for isolates, we quantified the PHAs produced by *Synechocystis* cf. *salina* 192 (CCALA 192), *Azospirillum brasilense* Cd (ATCC 29729), and *Halomonas eurihalina* (DMSZ 5710), bacteria known for their PHA-producing abilities.

Polyhydroxyalkanoate extraction and quantification

The cells' dry pellets, obtained by centrifugation of 10 ml from each liquid culture, were screened for the production of PHAs. The biomass was placed in a thermostatic bath at 100°C for 1 min; after cooling, the samples were placed in the freezer (−20°C) for 2 h and dried at 90°C until constant weight. According to the method of Zilliges and Damrow (2017), PHB extraction was realized by the PHB hydrolysis into its monomer (R)-3-hydroxybutyric acid (R-3-HB). Briefly, 300 μl of NaOH (0.5 N) was introduced into glass tubes containing 5 mg of each dry sample and incubated in an ultrasonic bath at 85°C for 1 h. After a rapid cooling on ice, the samples were neutralized with the addition of 100 μl of HCl (1 N) and vortexed for a few seconds. Later, centrifugation was performed for 1 min/4,500 *g* to remove the cell debris, and the supernatant of each sample was transferred to 1.5 ml tubes. The PHA concentration was determined by an enzymatic test using the Beta-Hydroxybutyrate Assay Kit (Sigma Aldrich).

Polyhydroxyalkanoate characterization by attenuated total reflectance-fourier transform infrared

The PHA extracted functional groups were characterized by attenuated total reflectance-Fourier transform infrared (ATR-FTIR) spectroscopy (Bruker Vertex 70 V), using a spectral range of 4,000–400 cm^{-1}. The powders of the PHA extracted samples were placed against the ATR crystal, the system was vacuumed (up to ∼ 2 hPA), and the spectra were scanned using a resolution of 4 cm^{-1} and 64 scans. Acquired spectra were processed and studied using the SpectraGryph version 1.2.15 software. The spectra of PHAs extracted from "Stiffe" isolates were merged. The spectrum obtained was compared to the *Synechocystis* cf. and the PHB standard ones (Sigma-Aldrich, St. Louis, MI, United States).

Determination of photosynthetic pigment contents

Chlorophyll a and carotenoid contents in each strain were determined according to the protocol published by Zavrel and collaborators (Zavřel et al., 2015). Briefly, a volume of 1 ml of cyanobacterial culture suspension in the stationary phase was centrifuged at 15,000 *g* for 7 min to recover the pellet. Then, 1 ml of methanol previously cooled at + 4°C was introduced into each tube. The samples are then vortexed, covered with aluminum foil, and incubated at + 4°C for 20 min to extract the cells' pigments. Centrifugation at 15,000 *g* for 7 min was performed (visually checking the bluish/purple coloration of the pellet). Then, the absorbance of each sample was measured at 470, 665, and 720 nm.

Statistical analysis

All experimental data are the mean of three replicates ± standard deviation. Statistical significance between groups was evaluated by one-way analysis of variance (ANOVA) followed by Fisher's LSD *post hoc* test, comparing mean values at a 5% level of significance ($p < 0.05$). Differences between the two groups were investigated by Student's *t*-test. All statistical calculations were performed using the XLSTAT 2016 software (Addinsoft, Paris, France).

Results

16S rRNA gene metabarcoding

The 16S rRNA gene metabarcoding generated a total number of 30,200 ASVs. Results were first used to calculate

the alpha-diversity metrics. The indexes showed 1,721 taxa, with the same value as the calculated Chao-1 index (1,721). Both Simpson 1-D (0.9959) and Shannon H' (6.657) indexes underlined high diversity. ASVs were then filtered to retain values over > 0.5% and studied at the different taxonomic levels. The sample was mainly constituted by bacteria at the domain level, accounting for 98.6% of the total abundances, while archaea accounted for the left 1.4%. **Figure 2** and **Supplementary Tables 1**, **2** of **Supplementary Material** show the abundance of the main taxonomic levels. At phylum level (**Figure 2A** and **Supplementary Table 1**), the SAR324_clade (Marine_group_B) constituted 32.6%, followed by Bacteroidota (11.0%), Actinobacteriota (9.4%), Campylobacterota (7.5%), Fusobacteriota (6.9%), Cyanobacteria (4.3%), Patescibacteria (3.3%), Proteobacteria (3.3%), and Planctomycetota (2.3%). At genus level (**Figure 2B** and **Supplementary Table 2**), the ASVs were mainly composed of uncultured taxa (22.5%) mainly associated with Proteobacteria phylum (Gammaproteobacteria), followed by *Crossiella* (9.9%), and unknown taxa (8.6%) mainly associated with Proteobacteria phylum (Gammaproteobacteria, Enterobacterales, and Pasteurellaceae), *MND1* (6.5%), *Vicinamibacteracea* (5.9%), and *Nitrospira* (3.5%). Among the ASVs with abundances less than 2%, an important result obtained was the presence of *Cyanobium*_PCC-6307 (0.8%).

Strains' isolation and identification

Strains' isolation and purification on BG11 agar medium were used to obtain eleven strains with different morphologies. Two strains were isolated from each site, except for sample site 4, which yielded three strains. The isolation source of each strain is reported in **Table 1**. **Supplementary Figure 1** represents the photos obtained with the microscopic observations of the strains. Based on these observations, the strains were putatively associated with *Synechocystis* (strains C2, C3, C8, and C9) and *Synechococcus* (strains C1, C4, C5, C6, C7, C10, and C11).

Polyhydroxyalkanoate production, optimization, and quantification

The eleven isolates were initially checked for their ability to produce PHAs in $BG11_0$. Extractions and quantifications of 30 days bioreactions showed that all the tested strains could produce PHAs, with different accumulation rates according to the strain type. To establish the PHA production rates, we cultivated standard strains with renewed PHAs accumulation abilities, namely, *Synechocystis* cf., *A. brasilense*, and *H. eurihalina*. The PHA results obtained for "Stiffe" isolates and *Synechocystis* cf. grown in $BG11_0$ and for *A. brasilense* and *H. eurihalina* grown in NFCC and HM, respectively, are reported in **Figure 3**. The PHA quantities of the cyanobacterial isolates ranged from 266 to 1,152 ng mg dry biomass^{-1}. The highest results among the isolates were recorded for strain C3, with amounts significantly lower than *A. brasilense* standard strain ($p < 0.05$). The lowest results among the isolates were recorded for C5 and C6 strains, with amounts significantly lower than *Synechocystis* cf. but still higher than *H. eurihalina* ($p < 0.05$). The other isolates, C1, C2, C4, and C7–C11, produced PHA amounts higher than *Synechocystis* cf., with an average production rate of 617 ng mg dry biomass^{-1}. To evaluate the possibility of enhancing PHB production by cyanobacterial strains, isolates and *Synechocystis* cf. bioreactions were optimized by subjecting strains to nitrogen, phosphate, and sulfur starving and acetate addition after 20 days. As shown in **Figure 4**, all the strains reached a maximum PHA production after 30 days of culturing and after 10 days of adding acetate. After 30 days, some isolates recorded a drastic decrease in the PHAs, while some kept the PHs level almost stationary. For all the strains, on the 30th day, an average fold change of 2.5 was recorded. For each cyanobacterium, PHA amounts recorded in BG11 modified for starvation cultures showed significant increases than $BG11_0$ (Student's *t*-test, $p < 0.01$). The best increases were recorded for CCALA192 (fold change of 9.3), followed by strain C8 (fold change of 4.2). The lowest increases were registered for strain C3 (fold change of 0.2). As depicted in **Figure 5**, starving and acetate addition allowed CCALA192 to accumulate a quantity of PHAs higher than those recorded for standard strains. Among the isolates, a similar situation was recorded for strain C2 and strain C8, which accumulated PHA amounts higher than those of *A. brasilense* ($p < 0.05$). The other cyanobacterial isolates recorded PHA amounts lower than *A. brasilense* but higher than *H. eurihalina* ($p < 0.05$).

Polyhydroxyalkanoate characterization by attenuated total reflectance-fourier transform infrared

The PHAs extracted from cyanobacterial isolates were characterized by ATR-FTIR. The spectra obtained for each isolate are shown in **Figure 6A**. The spectra comparison identified overlapping peaks among isolates and, for this reason, we processed data by creating an average spectrum for C1–C11 isolates. The average spectrum was first compared to that obtained for *Synechocystis* cf. (**Figure 6B**). The evaluation is performed to underline completely overlapping spectra, suggesting a similar production ability of PHAs and similar compounds within extracts. The C1–C11 average spectrum was also compared to the one acquired for the PHB standard. As presented in **Figure 7**, the comparison identified within the C1–C11 average spectrum the peaks at 2,997, 2,976, 2,934, 1,723, and 1,690 (transmittance over 5%). These peaks were also observed within the standard polymer spectrum. Due to the presence of other compounds within PHA extracts, the other signals at 1,282

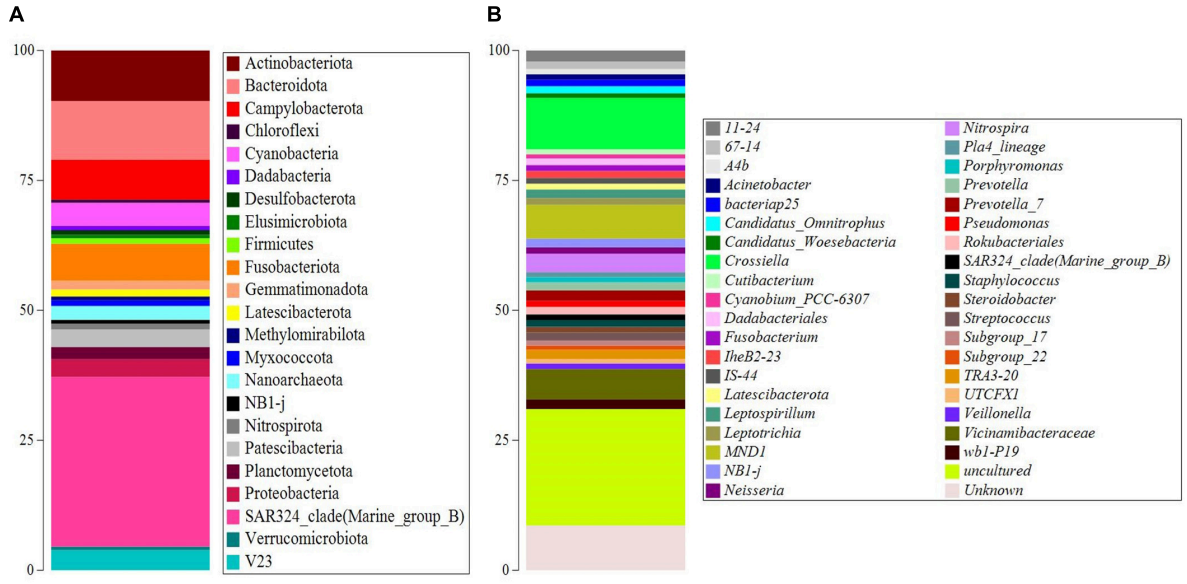

FIGURE 2
Taxonomy barplots of the main ASVs (abundances > 0.5%) at phylum **(A)** and genus level **(B)**.

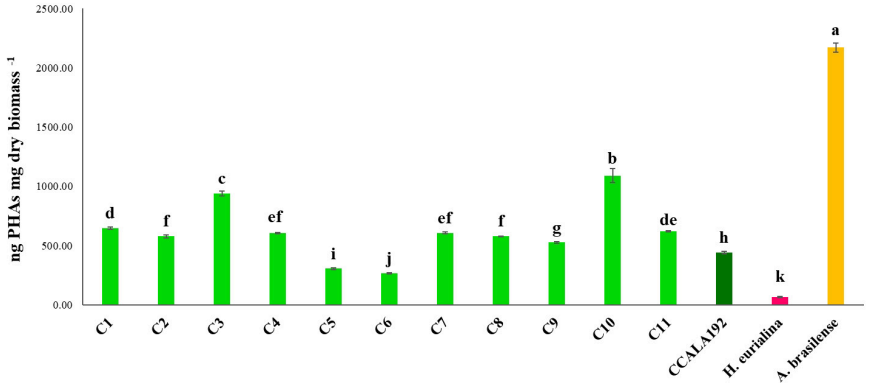

FIGURE 3
Polyhydroxyalkanoates contents recorded for "Stiffe" caves' cyanobacteria and *Synechocystis* cf. *salina*, grown in $BG11_0$, and for *A. brasilense* and *H. eurihalina*, cultured on NFCC and MH, respectively. Uppercase letters refer to the comparison among $BG11_0$ growths and *A. brasilense* and *H. eurihalina*. Lowercase letters refer to the comparison among BG11 starving growths and *A. brasilense* and *H. eurihalina*. For both conditions, results followed by the same case letters are not significantly different according to Fisher's LSD *post hoc* test ($p > 0.05$) (LSD value, 40.3).

and 1,058 were masked. However, the signals recorded suggested the presence of PHB polymer within the extracts.

Determination of photosynthetic contents

The biomass obtained from cyanobacterial bioreactions under normal and starving conditions was investigated for the photosynthetic pigments' contents. Table 2 shows the contents of chlorophyll a of cyanobacteria from "Stiffe" cave and *Synechocystis* cf. *salina* cultivated in $BG11_0$ and BG11 modified for starvation. In $BG11_0$, chlorophyll a was 2.3–269.6 μg g fresh weight biomass^{-1}. Starving led to a significant decrease in the chlorophyll a production, with a range of 0.3–4.2 μg chlorophyll a g fresh weight biomass^{-1}. As reported in Table 3, an opposite behavior was recorded for carotenoids, which were low in $BG11_0$ (0.06–5.50 μg carotenoids g fresh weight biomass^{-1}) and high in BG11 modified for starvation (up to 114.74 μg carotenoids g fresh weight biomass^{-1}). In both conditions, the best production rate was recorded for strain C9.

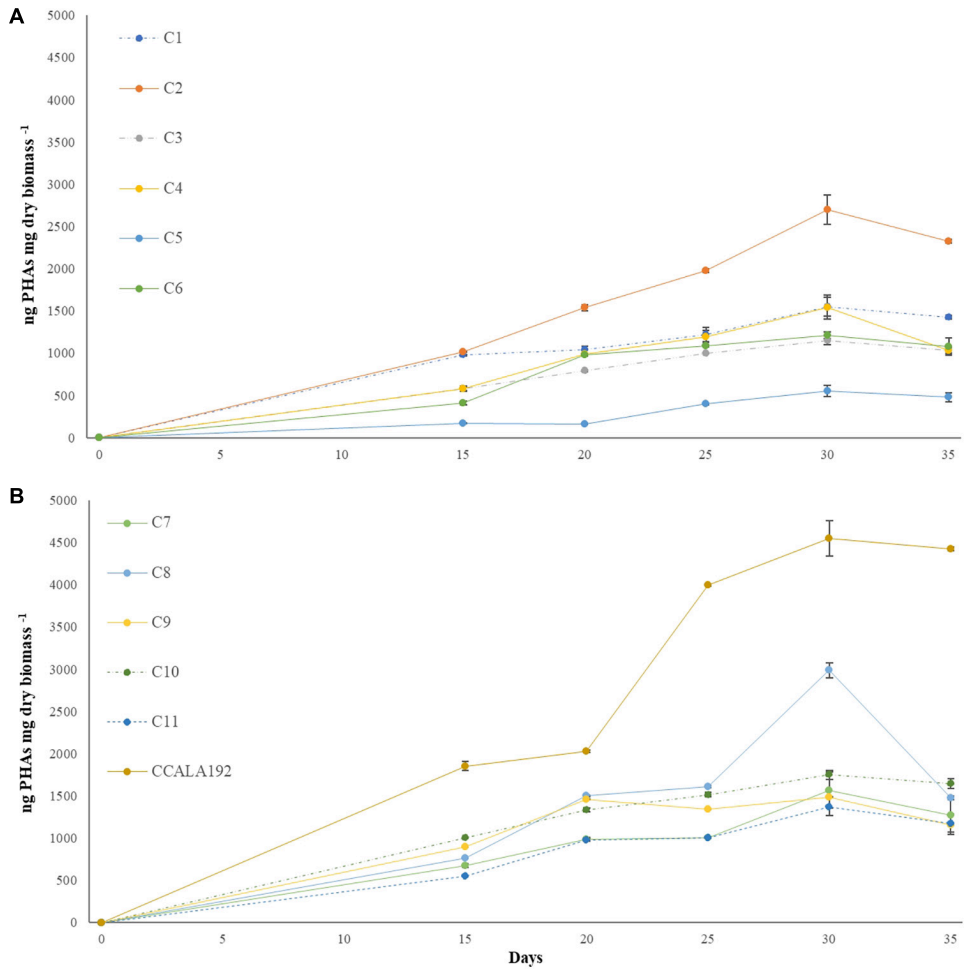

FIGURE 4
Polyhydroxyalkanoates production curves recorded for "Stiffe" caves' cyanobacteria and *Synechocystis* cf. *salina*, grown in BG11 modified for starvation. **(A)** C1-C6 curves; **(B)** C7-C11 and CCALA192 curves.

Discussion

The search for novel biomolecules is based on the selection of microorganisms that express new chemistry due to various extreme environmental conditions (Panou and Gkelis, 2022). Caves are energy-poor ecosystems characterized by high humidity, low natural light, spatial confinement, climatic stability, and low biodiversity (Lamprinou et al., 2012; Culver and Pipan, 2019). For this reason, these ecosystems are very sensitive to anthropogenic pressures (Mammola et al., 2019), which can promote the development of microflora with peculiar characteristics. Some caves are used as tourist attractions or as *in situ* scientific laboratories. The anthropogenic pressure generated by these activities leads to a change in microbial communities, which are extremely sensitive to environmental changes. Among the factors that most induce changes in microbial communities is electric lighting. Introducing light in caves favors the development of biofilms and mats of photosynthetic microorganisms on the surface of walls and speleothems. These communities have been studied to devise strategies and light sources that can limit their formation. However, few studies have investigated the characteristics that microorganisms develop in these extreme environments. This study focused on cyanobacterial lampenflora and its ability to produce polymers and pigments.

The 16S rRNA gene metabarcoding of the lampenflora bacterial and archaeal community confirmed the presence of cyanobacteria within the community. The most abundant genus was *Cyanobium*, a genus already described in Sybil's Cave (Naples, Italy), colonizing high light intensity sites (Cennamo et al., 2012). This genus was also described in Saint Cave (Licodia Eubea, Catania, Italy) by Di Carlo et al. (2016) who found it colonizing pigmented biofilm sited in several mural areas of Saints Cave (Palermo, Italy) (Di Carlo et al., 2016), and Palla et al. (2012) described its presence in a pigmented biofilm covering the "*Antro delle Sepolture*" surfaces.

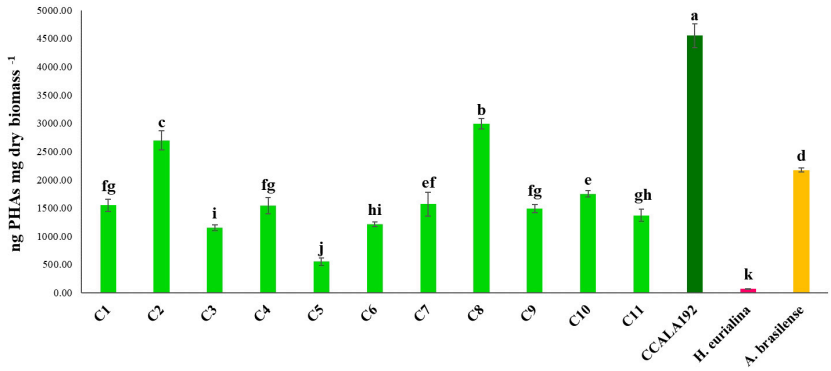

FIGURE 5
Polyhydroxyalkanoates contents recorded for "Stiffe" caves' cyanobacteria and *Synechocystis* cf. *salina*, grown in BG11 modified for starvation, and for *A. brasilense* and *H. eurihalina*, cultured on NFCC and MH, respectively. Uppercase letters refer to the comparison among $BG11_0$ growths and *A. brasilense* and *H. eurihalina*. Lowercase letters refer to the comparison among BG11 starving growths and *A. brasilense* and *H. eurihalina*. For both conditions, results followed by the same case letters are not significantly different according to Fisher's LSD *post hoc* test ($p > 0.05$) (LSD value, 192.1).

Metabarcoding also highlighted the presence of SAR324 clade (Marine_group_B). The presence of this marine taxon within the cave ecosystem is quite unusual and highly likely induced by anthropogenic pressure to which the cave has been subjected (Zhelyazkova et al., 2020). The SAR324 clade was described for the first time in the Sargasso Sea (Wright et al., 1997). The distribution of this taxon is relevant in deep waters and oceans (DeLong et al., 2006; Brown and Donachie, 2007; Ghiglione et al., 2012; Dick et al., 2013; Boeuf et al., 2021; Flood et al., 2021) and is a major component of low-oxygen environments, under dysoxic and suboxic conditions (Boeuf et al., 2021). The SAR324 reports underline a high flexible metabolism and a chemoautotrophic regime (Boeuf et al., 2021). Metagenome data support a flexible lifestyle, with carbon monoxide and methane oxidation, methylotrophy, adhesion, and motility genes (Yilmaz et al., 2016). The anthropogenic pressure underlined is also in line with the findings of Manenti et al. (2018) who reported considerable alterations to the stream that runs through the cave, including dam construction and stream bed modifications. During their survey, they also found signs of water contamination in the form of widespread periphyton covering on the stream's bottom (Manenti et al., 2018). The other representative ASVs belonged to the *Crossiella* genus, a dominant member of the microbial communities of speleothems (Riquelme et al., 2015; Jurado et al., 2020; Miller et al., 2020). The other ASVs belonged to unknown and uncultured taxa mainly associated with Gammaproteobacteria, another common phylum of environments of caves. The Pasteurellaceae family, which mainly constituted the unknown community, is usually described as part of the bat guano bacterial community (Newman et al., 2018).

The isolates tested are good producers of PHAs, especially under starvation. The best PHA producers were strains C2 and C8. The PHA production ability is relevant in the new biopolymers search, which falls among the goals of the 2030 Agenda for Sustainable Development. The non-biodegradable plastics are threatening the environment by accumulating petrochemical derivatives in soil and water (Jambeck et al., 2015; Gomes Gradíssimo et al., 2020). The PHAs have physicochemical characteristics in comparable with petrochemical plastics (Philip et al., 2007; Abed et al., 2009; Geyer et al., 2017), are easily handled with widespread industrial techniques (Wu et al., 2001), and are entirely mineralized into water and carbon dioxide by the action of natural microorganisms (Williams et al., 1999). These characteristics make PHAs a valuable alternative to non-biodegradable plastics, which is of industrial interest for several applications.

The chemical characterization of PHA extracts suggested the presence of PHB within biomass extracts. Bioplastics have been widely studied and applied for their shorter degradation time when exposed to a biologically active environment during the last decades. Among biopolymers, PHB has been investigated for food packaging purposes. Dimensional and mechanical tests showed that PHB could be a good substitute for polypropylene (PP) to produce food packaging. Compared to PP, PHB has a different resistance to dynamic compression, and the deformation value is 50% lower than PP, defining a more rigid and less flexible material. PHB resists higher temperatures than PP while recording lower performances at low-temperature conditions (Bucci et al., 2005). However, the limitations of some studies address the cost and performance of blending PHB with certain polyethers, polyesters, polyvinylacrylates, and polysaccharides in ways that improve mechanical properties without affecting the biodegradability advantage. A wide range of properties emerged from the blending, such as crystallinity, glass transition, and melting temperatures, also posing the

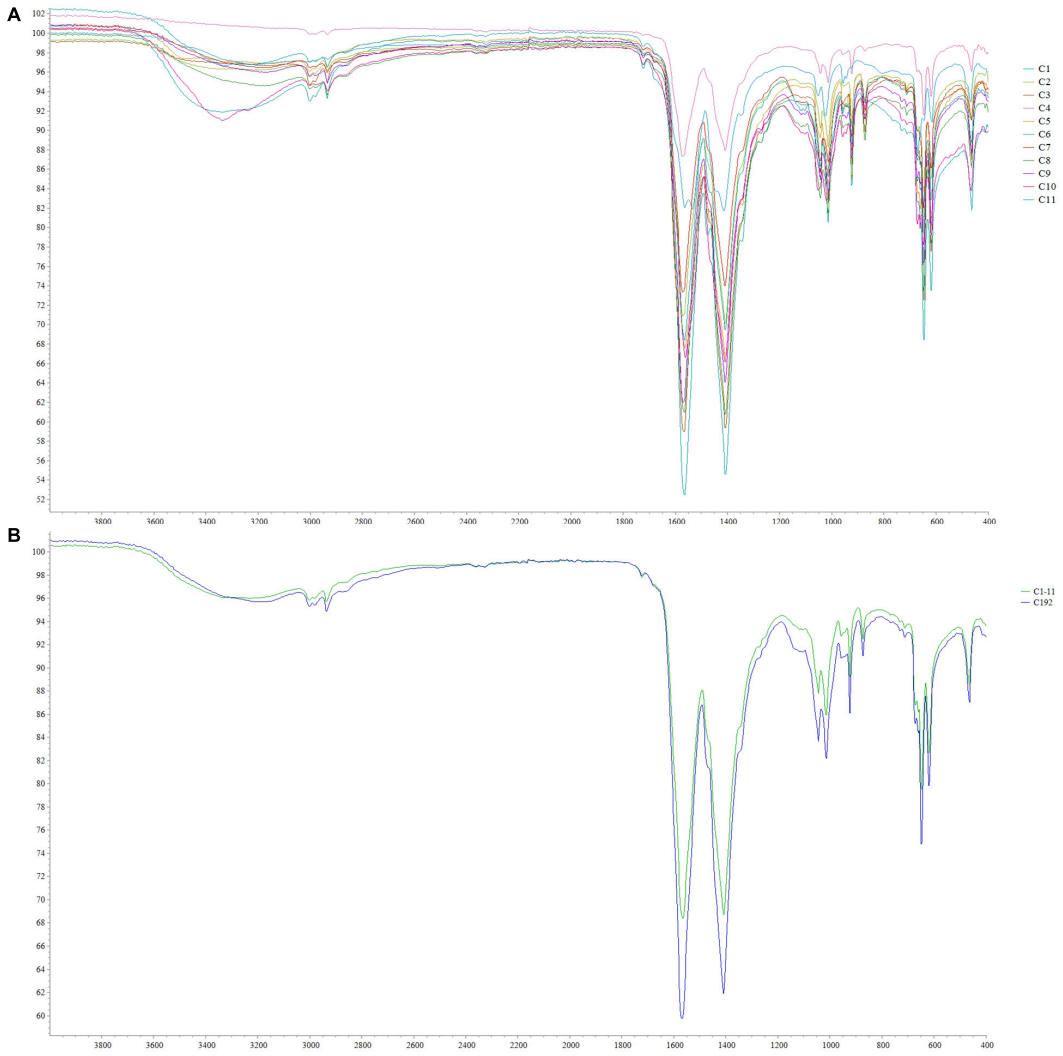

FIGURE 6
ATR-FTIR spectra obtained from C1–C11 isolates **(A)** and comparison between the average spectrum obtained for C1–C11 isolates with that obtained for *Synechocystis* cf. *salina* (C192) **(B)**.

hypotheses on the possible "driving force" that such a blend takes (Avella et al., 2000). PHB has also been investigated in the medical field for long-range repair in peripheral nerves and cartilage tissue engineering.

Autologous nerve grafting remains the treatment of choice for peripheral nerve injury repair. However, progress is being made concerning the use of PHB to fill long nerve gaps (up to 4 cm) in a model of peroneal nerve injury (Young et al., 2002). The tests were performed on rabbits, and regeneration was evaluated for 63 days. By day 42, the area of immune-stained regenerating fibers in the PHB group was more significant than in the nerve autograft group, suggesting their adaptability for this type of repair. PHB had no cytotoxicity on mice and the production of a cartilage-like tissue for 24 weeks after implantation was observed (Ye et al., 2009).

Due to their reduced productivity compared to heterotrophic bacteria, PHB production by cyanobacteria is feasible if paired with the production of other metabolites. The presence of valuable by-products within industrial productions is of interest for cost reduction. Our findings underlined that the isolates could also be a good source of chlorophyll a and carotenoids, under normal and starving conditions, respectively. Pigments, especially chlorophylls and carotenoids, are considered key bioactive chemicals (Hosikian et al., 2010). In biotechnology, pigments can be used as a natural dye (Timberlake and Henry, 1986) and in cosmetic and pharmaceutical products (da Silva Ferreira and Sant'Anna, 2017). Chlorophyll a has interesting antioxidant and anti-inflammatory properties (Subramoniam et al., 2012; da Silva Ferreira and Sant'Anna, 2017). Carotenoids are the

10.3389/fmicb.2022.933398

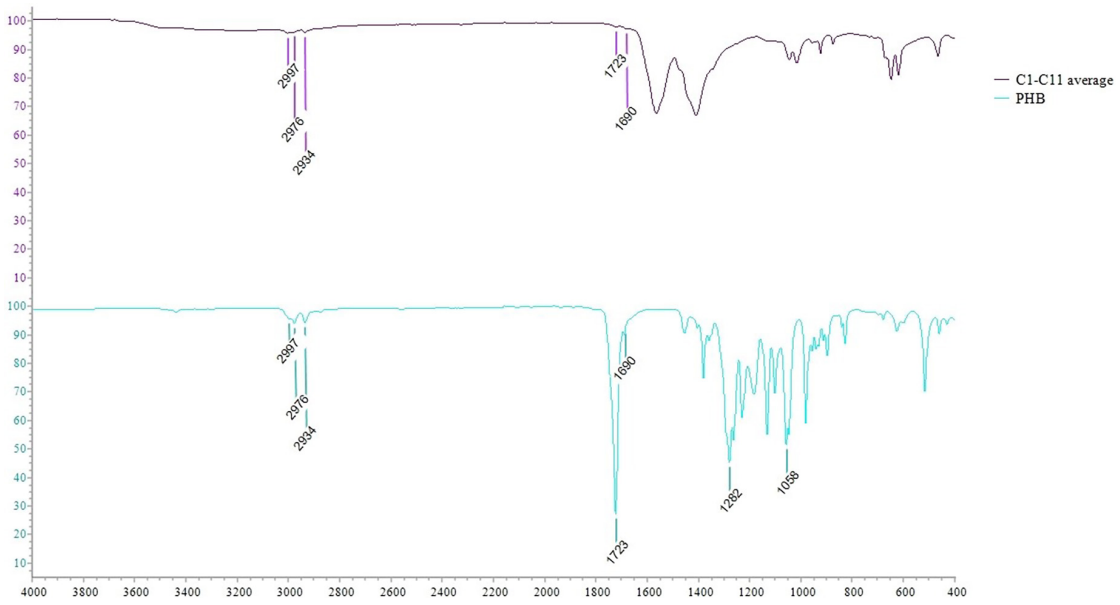

FIGURE 7
ATR-FTIR spectra comparison between the average spectrum obtained for C1–C11 isolates with that obtained for PHB pure standard.

TABLE 2 Chlorophyll *a* contents recorded for "Stiffe" caves' cyanobacteria and *Synechocystis* cf. *salina*, grown in $BG11_0$ and BG11 modified for starvation.

	Chlorophyll *a* (μg g fresh weight biomass $^{-1}$)		
Strain	**BG11**	**BG11 m**	***t*-Student *P*-value**
C1	24.87 ± 0.93de	4.18 ± 0.28a	*
C2	25.14 ± 1.87de	0.29 ± 0.01gh	**
C3	8.48 ± 0.39fg	0.73 ± 0.02f	*
C4	2.74 ± 0.17g	0.26 ± 0.04gh	**
C5	2.28 ± 0.19g	0.08 ± 0.01hi	***
C6	8.97 ± 0.21fg	1.08 ± 0.11e	*
C7	162.28 ± 12.10b	2.51 ± 0.05c	**
C8	34.96 ± 2.82d	0.69 ± 0.11f	**
C9	269.64 ± 22.37a	1.63 ± 0.09d	**
C10	108.82 ± 6.61c	1.65 ± 0.12d	**
C11	16.41 ± 1.63ef	0.38 ± 0.04g	**
CCALA192	113.79 ± 6.47c	3.25 ± 0.39b	**
LSD	12.22	0.24	

For each column, results followed by the same case letter are not significantly different according to Fisher's LSD *post hoc* test ($p > 0.05$). For each strain, the *p* levels in the right column refer to statistical differences between chlorophylls of BG11 growth and under starving according to Student's *t*-test (* $p < 0.001$; ** $p < 0.01$; *** $p < 0.05$).

most diverse group of pigments found in living organisms (Hirschberg and Chamovitz, 1994). It is estimated that around 600 pigments are classified as carotenoids (Guedes et al., 2011). They absorb light during the photosynthesis process and maintain thylakoid membranes and provide a photoprotection as well as the elimination of reactive oxygen species (ROS) (Lawlor, 1995; Schagerl and Müller, 2006; Pagels et al., 2021). Microalgae carotenoids have a great interest in the industry, food, cosmetics, and pharmaceutical applications due to their bioactive properties as an antioxidant, anti-inflammatory, and antitumor (Guedes et al., 2011; Raposo et al., 2015; Cezare-Gomes et al., 2019; Pagels et al., 2020). Several carotenoids are used in agriculture for soil remediation as antioxidants, fertilizers, and biopesticides, to improve soil quality and crop protection. At present, they are used to increase provitamin A availability contributing

TABLE 3 Carotenoids contents recorded for "Stiffe" caves' cyanobacteria and *Synechocystis* cf. *salina*, grown in $BG11_0$ and BG11 modified for starvation.

	Carotenoids (µg g fresh weight biomass $^{-1}$)		
	BG11	**BG11 m**	***t*-Student *P*-value**
C1	5.50 ± 0.62a	14.93 ± 0.43fg	*
C2	1.99 ± 0.06cd	16.72 ± 1.22f	**
C3	0.39 ± 0.06gh	4.85 ± 0.17ij	*
C4	0.06 ± 0.00hi	8.87 ± 0.73hi	*
C5	0.55 ± 0.09g	0.98 ± 0.03j	**
C6	1.43 ± 0.04ef	10.54 ± 0.38gh	*
C7	2.09 ± 0.24c	60.35 ± 4.45b	**
C8	0.17 ± 0.00hi	23.20 ± 1.68e	**
C9	1.54 ± 0.13e	114.74 ± 9.56a	**
C10	1.73 ± 0.15de	49.41 ± 2.91c	**
C11	1.13 ± 0.06f	12.65 ± 1.20fgh	**
CCALA192	4.88 ± 0.23b	43.25 ± 2.81d	**
LSD	0.33	5.17	

For each column, results followed by the same case letter are not significantly different according to Fisher's LSD *post hoc* test ($p > 0.05$). For each strain, the *p* levels in the right column refer to statistical differences between carotenoids of BG11 growth and under starving according to Student's *t*-test (*$p < 0.001$; **$p < 0.01$).

to biofortified crop development (Sakamoto et al., 2017; Gonçalves, 2021).

Conclusion

"Stiffe" caves' greenish mats and biofilms 16S rRNA gene metabarcoding underlined anthropogenic pressure-driven bacterial and archaeal communities' alterations. However, the lightning sources promoted the proliferation of culturable cyanobacterial strains with good PHB accumulation abilities (266 to 1,152 ng mg dry biomass^{-1}). The optimization of bioprocesses by nutrient starving improved PHA accumulation, with an average fold change of 2.5. The FTIR analyses suggested the PHB presence within PHAs extracted by cyanobacteria isolates. The comparison of cyanobacterial bioprocesses with those of *A. brasilense* and *H. eurihalina* showed that even if the optimal bioprocess last 30 days, cyanobacteria can produce PHA amounts employing a lower amount of nutrients and producing bioproducts with interesting biological properties. The isolation of these cyanobacteria that produces these large quantities of PHB could be linked to the critical environmental conditions of the lack of light for an extended period of closure linked to the COVID-19. PHB accumulation in cyanobacteria allows coping with unfavorable environmental conditions. Reasonably, during the switch-off, the PHB-producing cyanobacteria with high resilience and adaptability were selected by adverse environmental conditions.

Further studies on cyanobacterial bioprocesses and characterizations of PHB should be carried out to understand the biotechnological potential at the industrial level. The optimal bioreaction parameters should be studied to maximize the PHB production and pigments (e.g., temperature, effects of different lights, and light intensity). The molecular identification of the isolates and the study of the PHA production pathway gene expression will also clarify the biotechnological potential of the selected isolates. However, the findings broadened the knowledge of the microbial communities of mats and biofilms on the lightened walls of the "Stiffe" caves. The results showed that these formations could be possible sources of biomolecules and biopolymers, underlying the importance of exploring their potentialities before taking device strategies.

Data availability statement

The datasets generated and analyzed during this study are available from the corresponding author on reasonable request. The nucleotide sequences of the partial 16S rRNA gene segments determined in this study have been deposited in the NCBI database repository, BioProject: PRJNA833652 (http://www.ncbi.nlm.nih.gov/bioproject/833652).

Author contributions

IV, RD, and MP performed the samplings. RD and AM carried out the experiments and analyses. MP and DS coordinated the research activities. MP, RD, and AM handled the data and performed the results interpretation. RD, IV, and DS wrote the original draft of the manuscript. AD'A, MP, and MD performed the manuscript revision. MP handled manuscript processing and correspondence. MP, DS, AD'A,

and MD conceptualized the experiments. AD'A, DS, and MD coordinated the project. All authors contributed to the article and approved the submitted version.

Funding

This research was funded by the Hygienic Biopolymers Recovered from Algae – HYBRA. 04/2021 – CUP F/190097/01-02/X44, decree number 3540 of 12 November 2020.

Acknowledgments

We thank Quality Engineering for financial support and Lorenzo Arrizza for SEM-EDS and FTIR analysis, and the Group "Grotte di Stiffe" for sampling support.

Conflict of interest

DS was employed by Quality Engineering S.r.l.

The remaining authors declare that the research was conducted in the absence of any commercial or financial relationships that could be construed as a potential conflict of interest.

Publisher's note

All claims expressed in this article are solely those of the authors and do not necessarily represent those of their affiliated organizations, or those of the publisher, the editors and the reviewers. Any product that may be evaluated in this article, or claim that may be made by its manufacturer, is not guaranteed or endorsed by the publisher.

Supplementary material

The Supplementary Material for this article can be found online at: https://www.frontiersin.org/articles/10.3389/fmicb.2022.933398/full#supplementary-material

References

Abarzua, S., Jakubowski, S., Eckert, S., and Fuchs, P. (1999). Biotechnological investigation for the prevention of marine biofouling ii. blue-green algae as potential producers of biogenic agents for the growth inhibition of microfouling organisms. *Bot. Mar.* 42, 459–465. doi: 10.1515/BOT.1999.053

Abed, R. M. M., Dobretsov, S., and Sudesh, K. (2009). Applications of cyanobacteria in biotechnology. *J. Appl. Microbiol.* 106, 1–12. doi: 10.1111/j.1365-2672.2008.03918.x

Abed, R. M. M., and Garcia-Pichel, F. (2001). Long-term compositional changes after transplant in a microbial mat cyanobacterial community revealed using a polyphasic approach. *Environ. Microbiol.* 3, 53–62. doi: 10.1046/j.1462-2920.2001.00159.x

Albertano, P. (2012). "Cyanobacterial biofilms in monuments and caves," in *BT - Ecology of Cyanobacteria II: Their Diversity in Space and Time*, ed. B. A. Whitton (Dordrecht: Springer), 317–343. doi: 10.1007/978-94-007-3855-3_11

Allen, M. M., and Stanier, R. Y. (1968). Growth and division of some unicellular blue-green algae. *J. Gen. Microbiol.* 51, 199–202. doi: 10.1099/00221287-51-2-199/CITE/REFWORKS

Anderson, A. J., and Dawes, E. A. (1990). Occurrence, metabolism, metabolic role, and industrial uses of bacterial polyhydroxyalkanoates. *Microbiol. Rev.* 54, 450–472. doi: 10.1128/mr.54.4.450-472.1990

Ansari, S., and Fatma, T. (2016). Cyanobacterial polyhydroxybutyrate (PHB): screening, optimization and characterization. *PLoS One* 11:e0158168. doi: 10.1371/journal.pone.0158168

Asencio, A., and Aboal, M. (2011). In situ nitrogen fixation by cyanobacteria at the andragulla cave, Spain. *J. Cave Karst Stud.* 73, 50–54. doi: 10.4311/jcks2009lsc0129

Avella, M., Martuscelli, E., and Raimo, M. (2000). Review properties of blends and composites based on poly(3-hydroxy)butyrate (PHB) and poly(3-hydroxybutyrate-hydroxyvalerate) (PHBV) copolymers. *J. Mater. Sci.* 35, 523–545. doi: 10.1023/A:1004740522751

Balaji, S., Gopi, K., and Muthuvelan, B. (2013). A review on production of poly β hydroxybutyrates from cyanobacteria for the production of bio plastics. *Algal Res.* 2, 278–285. doi: 10.1016/j.algal.2013.03.002

Behrendt, L., Trampe, E. L., Nord, N. B., Nguyen, J., Kühl, M., Lonco, D., et al. (2020). Life in the dark: far-red absorbing cyanobacteria extend photic zones deep into terrestrial caves. *Environ. Microbiol.* 22, 952–963. doi: 10.1111/1462-2920.14774

Boeuf, D., Eppley, J. M., Mende, D. R., Malmstrom, R. R., Woyke, T., and DeLong, E. F. (2021). Metapangenomics reveals depth-dependent shifts in metabolic potential for the ubiquitous marine bacterial SAR324 lineage. *Microbiome* 9:172. doi: 10.1186/s40168-021-01119-5

Bolyen, E., Rideout, J. R., Dillon, M. R., Bokulich, N. A., Abnet, C. C., Al-Ghalith, G. A., et al. (2019). Reproducible, interactive, scalable and extensible microbiome data science using QIIME 2. *Nat. Biotechnol.* 37, 852–857. doi: 10.1038/s41587-019-0209-9

Brown, M., and Donachie, S. (2007). Evidence for tropical endemicity in the deltaproteobacteria marine group B/SAR324 bacterioplankton clade. *Aquat. Microb. Ecol.* 46, 107–115. doi: 10.3354/ame046107

Bucci, D. Z., Tavares, L. B. B., and Sell, I. (2005). PHB packaging for the storage of food products. *Polym. Test.* 24, 564–571. doi: 10.1016/j.polymertesting.2005.02.008

Cennamo, P., Marzano, C., Ciniglia, C., Pinto, G., Cappelletti, P., Caputo, P., et al. (2012). A survey of the algal flora of anthropogenic caves of Campi Flegrei (Naples, Italy) archeological district. *J. Cave Karst Stud.* 74, 243–250. doi: 10.4311/2011JCKS0194

Cezare-Gomes, E. A., Mejia-da-Silva, L., del, C., Pérez-Mora, L. S., Matsudo, M. C., Ferreira-Camargo, L. S., et al. (2019). Potential of microalgae carotenoids for industrial application. *Appl. Biochem. Biotechnol.* 188, 602–634. doi: 10.1007/s12010-018-02945-4

Chrismas, N. A. M., Anesio, A. M., and Sánchez-Baracaldo, P. (2015). Multiple adaptations to polar and alpine environments within cyanobacteria: a phylogenomic and Bayesian approach. *Front. Microbiol.* 6:1070. doi: 10.3389/fmicb.2015.01070

Choi, K., Choi, J., Lee, P. A., Roy, N., Khan, R., Lee, H. J., et al. (2020). Alteration of bacterial wilt resistance in tomato plant by microbiota transplant. *Front. Plant Sci.* 11:1186. doi: 10.3389/fpls.2020.01186

Cigna, A. A. (2016). Tourism and show caves. *Z. Geomorphol. Suppl. Issues* 60, 217–233. doi: 10.1127/zfg_suppl/2016/00305

Cigna, A. A. (2019). "Show caves," in *Encyclopedia of Caves*, eds W. B. White, D. C. Culver, and T. Pipan (Amsterdam: Elsevier), 909–921. doi: 10.1016/B978-0-12-814124-3.00108-4

Culver, D. C., and Pipan, T. (2019). *The Biology of Caves and Other Subterranean Habitats*. Oxford: Oxford University Press, doi: 10.1093/oso/9780198820765.001.0001

Czerwik-Marcinkowska, J. (2013). Observations on aerophytic cyanobacteria and algae from ten caves in the Ojców National Park. *Acta Agrobot.* 66, 39–52. doi: 10.5586/aa.2013.005

Czerwik-Marcinkowska, J., and Mrozińska, T. (2011). Algae and cyanobacteria in caves of the Polish Jura. *Pol. Bot. J.* 56, 203–243.

da Silva Ferreira, V., and Sant'Anna, C. (2017). Impact of culture conditions on the chlorophyll content of microalgae for biotechnological applications. *World J. Microbiol. Biotechnol.* 33:20. doi: 10.1007/s11274-016-2181-6

Dahms, H.-U., Ying, X., and Pfeiffer, C. (2006). Antifouling potential of cyanobacteria: a mini-review. *Biofouling* 22, 317–327. doi: 10.1080/08927010600967261

DeLong, E. F., Preston, C. M., Mincer, T., Rich, V., Hallam, S. J., Frigaard, N.-U., et al. (2006). Community genomics among stratified microbial assemblages in the ocean's interior. *Science* 311, 496–503. doi: 10.1126/science.1120250

Di Carlo, E., Chisesi, R., Barresi, G., Barbaro, S., Lombardo, G., Rotolo, V., et al. (2016). Fungi and bacteria in indoor cultural heritage environments: microbial-related risks for artworks and human health. *Environ. Ecol. Res.* 4, 257–264. doi: 10.13189/eer.2016.040504

Dick, G. J., Anantharaman, K., Baker, B. J., Li, M., Reed, D. C., and Sheik, C. S. (2013). The microbiology of deep-sea hydrothermal vent plumes: ecological and biogeographic linkages to seafloor and water column habitats. *Front. Microbiol.* 4:124. doi: 10.3389/fmicb.2013.00124

Figueroa, F. L., Álvarez-Gómez, F., del Rosal, Y., Celis-Plá, P. S. M., González, G., Hernández, M., et al. (2017). In situ photosynthetic yields of cave photoautotrophic biofilms using two different Pulse amplitude modulated fluorometers. *Algal Res.* 22, 104–115. doi: 10.1016/j.algal.2016.12.012

Flood, B. E., Louw, D. C., van der Plas, A. K., and Bailey, J. V. (2021). Giant sulfur bacteria (Beggiatoaceae) from sediments underlying the Benguela upwelling system host diverse microbiomes. *PLoS One* 16:e0258124. doi: 10.1371/journal.pone.0258124

Gan, F., and Bryant, D. A. (2015). Adaptive and acclimative responses of cyanobacteria to far-red light. *Environ. Microbiol.* 17, 3450–3465. doi: 10.1111/1462-2920.12992

Geyer, R., Jambeck, J. R., and Law, K. L. (2017). Production, use, and fate of all plastics ever made. *Sci. Adv.* 3:e1700782. doi: 10.1126/sciadv.1700782

Giordano, M., Mobili, F., Pezzoni, V., Hein, M. K., and Davis, J. S. (2000). photosynthesis in the caves of frasassi (Italy). *Phycologia* 39, 384–389. doi: 10.2216/i0031-8884-39-5-384.1

Ghiglione, J.-F., Galand, P. E., Pommier, T., Pedrós-Alió, C., Maas, E. W., Bakker, K., et al. (2012). Pole-to-pole biogeography of surface and deep marine bacterial communities. *Proc. Natl. Acad. Sci.* 109, 17633–17638. doi: 10.1073/pnas.1208160109

Gomes Gradíssimo, D., Pereira Xavier, L., and Valadares Santos, A. (2020). Cyanobacterial polyhydroxyalkanoates: a sustainable alternative in circular economy. *Molecules* 25:4331. doi: 10.3390/molecules25184331

Gonçalves, A. L. (2021). The use of microalgae and cyanobacteria in the improvement of agricultural practices: a review on their biofertilising, biostimulating and biopesticide roles. *Appl. Sci.* 11:871. doi: 10.3390/app11020871

Guedes, A. C., Amaro, H. M., and Malcata, F. X. (2011). Microalgae as sources of carotenoids. *Mar. Drugs* 9, 625–644. doi: 10.3390/md9040625

Havlena, Z., Kieft, T. L., Veni, G., Horrocks, R. D., and Jones, D. S. (2021). Lighting effects on the development and diversity of photosynthetic biofilm communities in carlsbad cavern, New Mexico. *Appl. Environ. Microbiol.* 87, e02695–e02720. doi: 10.1128/AEM.02695-20

Hirschberg, J., and Chamovitz, D. (1994). "Carotenoids in cyanobacteria," in *The Molecular Biology of Cyanobacteria*, ed. D. A. Bryant (Dordrecht: Springer), 559–579. doi: 10.1007/978-94-011-0227-8_18

Hosikian, A., Lim, S., Halim, R., and Danquah, M. K. (2010). Chlorophyll extraction from microalgae: a review on the process engineering aspects. *Int. J. Chem. Eng.* 2010, 1–11. doi: 10.1155/2010/391632

Jambeck, J. R., Geyer, R., Wilcox, C., Siegler, T. R., Perryman, M., Andrady, A., et al. (2015). Marine pollution. plastic waste inputs from land into the ocean. *Science* 347, 768–771. doi: 10.1126/science.1260352

Jurado, V., Gonzalez-Pimentel, J. L., Miller, A. Z., Hermosin, B., D'Angeli, I. M., Tognini, P., et al. (2020). Microbial communities in vermiculation deposits from an alpine cave. *Front. Earth Sci.* 8:586248. doi: 10.3389/feart.2020.586248

Kichise, T., Fukui, T., Yoshida, Y., and Doi, Y. (1999). Biosynthesis of polyhydroxyalkanoates (PHA) by recombinant Ralstonia eutropha and effects of PHA synthase activity on in vivo PHA biosynthesis. *Int. J. Biol. Macromol.* 25, 69–77. doi: 10.1016/S0141-8130(99)00017-3

Koch, M., Bruckmoser, J., Scholl, J., Hauf, W., Rieger, B., and Forchhammer, K. (2020). Maximizing PHB content in Synechocystis sp. PCC 6803: a new metabolic engineering strategy based on the regulator PirC. *Microb. Cell Factories* 19:231. doi: 10.1186/s12934-020-01491-1

Koch, M., Doello, S., Gutekunst, K., and Forchhammer, K. (2019). PHB is Produced from Glycogen Turn-over during Nitrogen Starvation in *Synechocystis* sp. PCC 6803. *Int. J. Mol. Sci.* 20:1942. doi: 10.3390/ijms20081942

Lamprinou, V., Danielidis, D., Economou-Amilli, A., and Pantazidou, A. (2012). Distribution survey of cyanobacteria in three greek caves of peloponnese. *Int. J. Speleol.* 41, 267–272. doi: 10.5038/1827-806X.41.2.12

Lamprinou, V., Danielidis, D., Pantazidou, A., Oikonomou, A., and Economou-Amilli, A. (2014). The show cave of Diros vs. wild caves of Peloponnese, Greece - distribution patterns of Cyanobacteria. *Int. J. Speleol.* 43, 335–342. doi: 10.5038/1827-806X.43.3.10

Lawlor, D. W. (1995). Photosynthesis, productivity and environment. *J. Exp. Bot.* 46, 1449–1461. doi: 10.1093/jxb/46.special_issue.1449

Lemes-da-Silva, N., Branco, L., and Necchi, O. Jr. (2011). Corticolous cyanobacteria from tropical forest remnants in northwestern São Paulo State, Brazil. *Braz. J. Bot.* 35, 169–179. doi: 10.1590/S0100-84042012000200006

Liebergesell, M., Sonomoto, K., Madkour, M., Mayer, F., and Steinbuchel, A. (1994). Purification and characterization of the poly(Hydroxyalkanoic Acid) synthase from *Chromatium* vinosum and localization of the enzyme at the surface of poly(Hydroxyalkanoic Acid) granules. *Eur. J. Biochem.* 226, 71–80. doi: 10.1111/j.1432-1033.1994.tb20027.x

Lim, T., Cappelle, J., Hoem, T., and Furey, N. (2018). Insectivorous bat reproduction and human cave visitation in cambodia: a perfect conservation storm? *PLoS One* 13:e0196554. doi: 10.1371/journal.pone.0196554

Mammola, S., Cardoso, P., Culver, D. C., Deharveng, L., Ferreira, R. L., Fišer, C., et al. (2019). Scientists' warning on the conservation of subterranean ecosystems. *BioScience* 69, 641–650. doi: 10.1093/biosci/biz064

Mammola, S., di Piazza, S., Ziotti, M., Badino, G., and Marco, I. (2017). Human-induced alterations of the mycobiota in an alpine show cave (Italy, SW-Alps). *Acta Carsol.* 46, 11–123. doi: 10.3986/ac.v46i1.2531

Manenti, R., Barzaghi, B., Lana, E., Stocchino, G. A., Manconi, R., and Lunghi, E. (2018). The stenoendemic cave-dwelling planarians (Platyhelminthes, Tricladida) of the italian alps and apennines: conservation issues. *J. Nat. Conserv.* 45, 90–97. doi: 10.1016/j.jnc.2018.08.001

Miller, A. Z., García-Sánchez, A. M., Coutinho, M. L., Costa Pereira, M. F., Gázquez, F., Calaforra, J. M., et al. (2020). Colored Microbial Coatings in Show Caves from the Galapagos Islands (Ecuador): First Microbiological Approach. *Coatings* 10:1134. doi: 10.3390/coatings10111134

Mizrahi-Man, O., Davenport, E. R., and Gilad, Y. (2013). Taxonomic Classification of bacterial 16S rRNA genes using short sequencing reads: evaluation of effective study designs. *PLoS One* 8:e53608. doi: 10.1371/journal.pone.0053608

Mulec, J., and Kosi, G. (2009). Lampenflora algae and methods of growth control. *J. Cave Karst Stud.* 71, 109–115.

Muñoz-Fernández, J., del Rosal, Y., Álvarez-Gómez, F., Hernández-Mariné, M., Guzmán-Sepúlveda, R., Korbee, N., et al. (2021). Selection of LED lighting systems for the reduction of the biodeterioration of speleothems induced by photosynthetic biofilms in the Nerja Cave (Malaga, Spain). *J. Photochem. Photobiol. B Biol.* 217:112155. doi: 10.1016/j.jphotobiol.2021.112155

Newman, M. M., Kloepper, L. N., Duncan, M., McInroy, J. A., and Kloepper, J. W. (2018). Variation in bat guano bacterial community composition with depth. *Front. Microbiol.* 9:914. doi: 10.3389/fmicb.2018.00914

Nicolosi, G., Mammola, S., Costanzo, S., Sabella, G., Cirrincione, R., Signorello, G., et al. (2021). Microhabitat selection of a Sicilian subterranean woodlouse and its implications for cave management. *Int. J. Speleol.* 50, 53–63. doi: 10.5038/1827-806X.50.1.2370

Nikolić, N., Zarubica, N., Gavrilović, B., Predojević, D., Trbojević, I., Subakov Simić, G., et al. (2020). Lampenflora and the entrance biofilm in two show caves: comparison of microbial community, environmental, and biofilm parameters. *J. Cave Karst Stud.* 82, 69–81. doi: 10.4311/2018EX0124

Novas, N., Gázquez, J. A., MacLennan, J., García, R. M., Fernández-Ros, M., and Manzano-Agugliaro, F. (2017). A real-time underground environment monitoring system for sustainable tourism of caves. *J. Clean. Prod.* 142, 2707–2721. doi: 10.1016/j.jclepro.2016.11.005

Pagels, F., Salvaterra, D., Amaro, H. M., and Guedes, A. C. (2020). "Pigments from microalgae," in *Handbook of Microalgae-Based Processes and Products*, eds

E. Jacob-Lopes, M. M. Maroneze, M. I. Queiroz, and L. Q. Zepka (Amsterdam: Elsevier), 465–492. doi: 10.1016/B978-0-12-818536-0.00018-X

Pagels, F., Vasconcelos, V., and Guedes, A. C. (2021). Carotenoids from cyanobacteria: biotechnological potential and optimization strategies. *Biomolecules* 11:735. doi: 10.3390/biom11050735

Palla, F., Billeci, N., Mancuso, F. P., Sineo, L., and Caruso, G. (2012). "Un Cimitero rupestre di epoca tardoantica in sicilia: studio interdisciplinare dell'ambiente e dei reperti archeologici," in *Acta - VII Congresso Nazionale Società Italiana di Archeometria (AIAr), UNIMORE Modena 22-24 febbraio 2012*, (Bologna: Patron Editore).

Panou, M., and Gkelis, S. (2022). Unravelling unknown cyanobacteria diversity linked with HCN production. *Mol. Phylogenet. Evol.* 166:107322. doi: 10.1016/j.ympev.2021.107322

Pentecost, A. (1992). A note on the colonization of limestone rocks by cyanobacteria. *Arch. Hydrobiol.* 124, 167–172. doi: 10.1127/archiv-hydrobiol/124/1992/167

Pfendler, S., Karimi, B., Maron, P.-A., Ciadamidaro, L., Valot, B., Bousta, F., et al. (2018). Biofilm biodiversity in French and Swiss show caves using the metabarcoding approach: First data. *Sci. Total Environ.* 615, 1207–1217. doi: 10.1016/j.scitotenv.2017.10.054

Philip, S., Keshavarz, T., and Roy, I. (2007). Polyhydroxyalkanoates: biodegradable polymers with a range of applications. *J. Chem. Technol. Biotechnol.* 82, 233–247. doi: 10.1002/jctb.1667

Piano, E., Bona, F., Falasco, E., la Morgia, V., Badino, G., and Isaia, M. (2015). Environmental drivers of phototrophic biofilms in an alpine show cave (SW-Italian Alps). *Sci. Total Environ.* 536, 1007–1018. doi: 10.1016/j.scitotenv.2015.05.089

Piano, E., Nicolosi, G., and Isaia, M. (2021). Modulating lighting regime favours a sustainable use of show caves: a case study in NW-Italy. *J. Nat. Conserv.* 64:126075. doi: 10.1016/j.jnc.2021.126075

Poulíčková, A., and Hasler, P. (2007). Aerophytic diatoms from caves in central Moravia (Czech Republic). *Preslia* 79, 185–204.

Puente-Sánchez, F., Arce-Rodríguez, A., Oggerin, M., García-Villadangos, M., Moreno-Paz, M., Blanco, Y., et al. (2018). Viable cyanobacteria in the deep continental subsurface. *Proc. Natl. Acad. Sci.U.S.A.* 115, 10702–10707. doi: 10.1073/pnas.1808176115

Raposo, M., de Morais, A., and de Morais, R. (2015). Carotenoids from marine microalgae: a valuable natural source for the prevention of chronic diseases. *Mar. Drugs* 13, 5128–5155. doi: 10.3390/md13085128

Rasouli-Dogaheh, S., Komárek, J., Chatchawan, T., and Hauer, T. (2022). Thainema gen. nov. (Leptolyngbyaceae, Synechococcales): a new genus of simple trichal cyanobacteria isolated from a solar saltern environment in Thailand. *PLoS One* 17:e0261682. doi: 10.1371/journal.pone.0261682

Riquelme, C., Rigal, F., Hathaway, J. J. M., Northup, D. E., Spilde, M. N., Borges, P. A. V., et al. (2015). Cave microbial community composition in oceanic islands: disentangling the effect of different colored mats in diversity patterns of Azorean lava caves. *FEMS Microbiol. Ecol.* 91:fiv141. doi: 10.1093/femsec/fiv141

Sakamoto, Y., Mori, K., Matsuo, Y., Mukojima, N., Watanabe, W., Sobaru, N., et al. (2017). Breeding of a new potato variety 'Nagasaki Kogane' with high eating quality, high carotenoid content, and resistance to diseases and pests. *Breed. Sci.* 67, 320–326. doi: 10.1270/jsbbs.16168

Satyanarayana, T., Raghukumar, C., and Shivaji, S. (2005). Extremophilic microbes: Diversity and perspectives. *Curr. Sci.* 89, 78–90.

Schagerl, M., and Müller, B. (2006). Acclimation of chlorophyll a and carotenoid levels to different irradiances in four freshwater cyanobacteria. *J. Plant Physiol.* 163, 709–716. doi: 10.1016/j.jplph.2005.09.015

Šebela, S., Baker, G., and Luke, B. (2019). Cave temperature and management implications in lehman caves, great basin national park, USA. *Geoheritage* 11, 1163–1175. doi: 10.1007/s12371-019-00367-0

Sechrest, W. W., and Brooks, T. M. (2002). "Biodiversity – Threats ," in *eLS*, (Hoboken, NJ: Wiley), doi: 10.1038/npg.els.0003257

Shimizu, Y. (2003). Microalgal metabolites. *Curr. Opin. Microbiol.* 6, 236–243. doi: 10.1016/S1369-5274(03)00064-X

Singh, A. K., and Mallick, N. (2017). Advances in cyanobacterial polyhydroxyalkanoates production. *FEMS Microbiol. Lett.* 364:fnx189. doi: 10.1093/femsle/fnx189

Subramoniam, A., Asha, V. V., Nair, S. A., Sasidharan, S. P., Sureshkumar, P. K., Rajendran, K. N., et al. (2012). Chlorophyll revisited: anti-inflammatory activities of chlorophyll a and inhibition of expression of TNF-α gene by the same. *Inflammation* 35, 959–966. doi: 10.1007/s10753-011-9399-0

Timberlake, C. F., and Henry, B. S. (1986). Plant pigments as natural food colours. *Endeavour* 10, 31–36. doi: 10.1016/0160-9327(86)90048-7

Utharn, S., Yodsang, P., Incharoensakdi, A., and Jantaro, S. (2021). Cyanobacterium Synechocystis sp. PCC 6803 lacking adc1 gene produces higher polyhydroxybutyrate accumulation under modified nutrients of acetate supplementation and nitrogen-phosphorus starvation. *Biotechnol. Rep.* 31:e00661. doi: 10.1016/j.btre.2021.e00661

Vaccarelli, I., Matteucci, F., Pellegrini, M., Bellatreccia, F., and del Gallo, M. (2021). Exploring microbial biosignatures in mn-deposits of deep biosphere: a preliminary cross-disciplinary approach to investigate geomicrobiological interactions in a cave in central Italy. *Front. Earth Sci.* 9:590257. doi: 10.3389/feart.2021.590257

Wang, B., Pugh, S., Nielsen, D. R., Zhang, W., and Meldrum, D. R. (2013). Engineering cyanobacteria for photosynthetic production of 3-hydroxybutyrate directly from CO2. *Metab. Eng.* 16, 68–77. doi: 10.1016/j.ymben.2013.01.001

Williams, S. F., Martin, D. P., Horowitz, D. M., and Peoples, O. P. (1999). PHA applications: addressing the price performance issue. *Int. J. Biol. Macromol.* 25, 111–121. doi: 10.1016/S0141-8130(99)00022-7

Wright, T. D., Vergin, K. L., Boyd, P. W., and Giovannoni, S. J. (1997). A novel delta-subdivision proteobacterial lineage from the lower ocean surface layer. *Appl. Environ. Microbiol.* 63, 1441–1448. doi: 10.1128/aem.63.4.1441-1448.1997

Wu, G. F., Wu, Q. Y., and Shen, Z. Y. (2001). Accumulation of poly-β-hydroxybutyrate in cyanobacterium *Synechocystis* sp. PCC6803. *Bioresour. Technol.* 76, 85–90. doi: 10.1016/S0960-8524(00)00099-7

Ye, C., Hu, P., Ma, M.-X., Xiang, Y., Liu, R.-G., and Shang, X.-W. (2009). PHB/PHBHHx scaffolds and human adipose-derived stem cells for cartilage tissue engineering. *Biomaterials* 30, 4401–4406. doi: 10.1016/j.biomaterials.2009.05.001

Yilmaz, P., Yarza, P., Rapp, J. Z., and Glöckner, F. O. (2016). Expanding the world of marine bacterial and archaeal clades. *Front. Microbiol.* 6:1524. doi: 10.3389/fmicb.2015.01524

Young, R. C., Terenghi, G., and Wiberg, M. (2002). Poly-3-hydroxybutyrate (PHB): a resorbable conduit for long-gap repair in peripheral nerves. *Br. J. Plast. Surg.* 55, 235–240. doi: 10.1054/bjps.2002.3798

Zavřel, T., Sinetova, M. A., and Červený, J. (2015). Measurement of chlorophyll a and carotenoids concentration in cyanobacteria. *Bio. Protoc.* 5:e1467. doi: 10.21769/BioProtoc.1467

Zhelyazkova, V., Hubancheva, A., Radoslavov, G., Toshkova, N., and Puechmaille, S. (2020). Did you wash your caving suit? Cavers' role in the potential spread of Pseudogymnoascus destructans, the causative agent of White-Nose Disease. *Int. J. Speleol.* 49, 149–159. doi: 10.5038/1827-806X.49.2.2326

Zilliges, Y., and Damrow, R. (2017). Quantitative determination of poly-β-hydroxybutyrate in *Synechocystis* sp. PCC 6803. *Bio-Protocol.* 7:e2402. doi: 10.21769/BioProtoc.2402

frontiers | Frontiers in Microbiology

TYPE Original Research
PUBLISHED 23 September 2022
DOI 10.3389/fmicb.2022.930302

OPEN ACCESS

EDITED BY
Diana Eleanor Northup,
University of New Mexico, United States

REVIEWED BY
Jennifer J. Marshall Hathaway,
University of New Mexico, United States
Ana Z. Miller,
Spanish National Research Council (CSIC), Spain

*CORRESPONDENCE
Daniele Ghezzi
daniele.ghezzi3@unibo.it
Martina Cappelletti
martina.cappelletti2@unibo.it

†These authors share senior authorship

SPECIALTY SECTION
This article was submitted to Terrestrial Microbiology, a section of the journal Frontiers in Microbiology

RECEIVED 27 April 2022
ACCEPTED 25 August 2022
PUBLISHED 23 September 2022

CITATION
Ghezzi D, Foschi L, Firrincieli A, Hong P-Y, Vergara F, De Waele J, Sauro F and Cappelletti M (2022) Insights into the microbial life in silica-rich subterranean environments: microbial communities and ecological interactions in an orthoquartzite cave (Imawarì Yeuta, Auyan Tepui, Venezuela).
Front. Microbiol. 13:930302.
doi: 10.3389/fmicb.2022.930302

Insights into the microbial life in silica-rich subterranean environments: microbial communities and ecological interactions in an orthoquartzite cave (Imawarì Yeuta, Auyan Tepui, Venezuela)

Daniele Ghezzi[1,2]*, Lisa Foschi[1], Andrea Firrincieli[1], Pei-Ying Hong[3], Freddy Vergara[4,5], Jo De Waele[5,6], Francesco Sauro[4,5,6†] and Martina Cappelletti[1*†]

[1]Department of Pharmacy and Biotechnology, University of Bologna, Bologna, Italy, [2]Laboratory of NanoBiotechnology, IRCCS Istituto Ortopedico Rizzoli, Bologna, Italy, [3]Division of Biological and Environmental Science and Engineering, King Abdullah University of Science and Technology (KAUST), Thuwal, Saudi Arabia, [4]Teraphosa Exploring Team, Puerto Ordaz, Venezuela, [5]La Venta Geographic Explorations Association, Treviso, Italy, [6]Department of Biological Geological and Environmental Sciences, University of Bologna, Bologna, Italy

Microbial communities inhabiting caves in quartz-rich rocks are still underexplored, despite their possible role in the silica cycle. The world's longest orthoquartzite cave, Imawarì Yeuta, represents a perfect arena for the investigation of the interactions between microorganisms and silica in non-thermal environments due to the presence of extraordinary amounts of amorphous silica speleothems of different kinds. In this work, the microbial diversity of Imawarì Yeuta was dissected by analyzing nineteen samples collected from different locations representative of different silica amorphization phases and types of samples. Specifically, we investigated the major ecological patterns in cave biodiversity, specific taxa enrichment, and the main ecological clusters through co-occurrence network analysis. Water content greatly contributed to the microbial communities' composition and structures in the cave leading to the sample clustering into three groups DRY, WET, and WATER. Each of these groups was enriched in members of *Actinobacteriota*, *Acidobacteriota*, and *Gammaproteobacteria*, respectively. Alpha diversity analysis showed the highest value of diversity and richness for the WET samples, while the DRY group had the lowest. This was accompanied by the presence of correlation patterns including either orders belonging to various phyla from WET samples or orders belonging to the *Actinobacteriota* and *Firmicutes* phyla from DRY group samples. The phylogenetic analysis of the dominant species in WET and DRY samples showed that *Acidobacteriota* and *Actinobacteriota* strains were affiliated with uncultured bacteria retrieved from various oligotrophic and silica/quartz-rich environments, not only associated with subterranean sites. Our results suggest that the water content greatly contributes to shaping

the microbial diversity within a subterranean quartzite environment. Further, the phylogenetic affiliation between Imawarì Yeuta dominant microbes and reference strains retrieved from both surface and subsurface silica- and/or CO_2/CO-rich environments, underlines the selective pressure applied by quartz as rock substrate. Oligotrophy probably in association with the geochemistry of silica/quartz low pH buffering activity and alternative energy sources led to the colonization of specific silica-associated microorganisms. This study provides clues for a better comprehension of the poorly known microbial life in subsurface and surface quartz-dominated environments.

KEYWORDS

cave microbiology, *Actinobacteriota*, *Acidobacteriota*, oligotrophic environment, silica speleothems, co-occurrence network, subterranean microbiome

Introduction

Bacteria and archaea are numerically the most dominant and ubiquitous organisms of the Earth's surface and subsurface (Merino et al., 2019). They can thrive in a wide variety of environmental conditions, overpowering barriers that are not compatible with life of higher organisms, including low and high temperatures, pH, radiation, pressure, salinity, absence of light, and nutrient limitation. In this context, dark and oligotrophic caves host abundant and complex microbial communities, whose structures are regulated by mechanisms that are distinct from those at the Earth's surface. The subsurface is estimated to house 50%–87% of the Earth's microorganisms (Kallmeyer et al., 2012; Magnabosco et al., 2018), most of which are still unknown or understudied. This aspect makes caves unique ecosystems suitable to study the evolution of microbial life and the survival mechanisms in the absence of primary productivity associated with sunlight and photosynthesis (Barton and Northup, 2007; Northup et al., 2011).

In caves, microbes take advantage of the interaction with the rock substrate to acquire essential elements for growth. Despite the nutrient-limited conditions, caves contain surprisingly diverse microbial communities with compositions that are influenced by a series of geochemical parameters including the host rock composition and other environmental factors such as temperature, organic carbon availability, and humidity (Barton et al., 2007). Nevertheless, cave microbiome studies have focused on limited amounts of samples that rarely allow detailed ecological correlation analyses. Furthermore, most of these studies focused on microbial diversity in carbonate caves (Brannen-Donnelly and Engel, 2015; Wu et al., 2015; Alonso et al., 2018; D'Angeli et al., 2019; Paun et al., 2019; Zhu et al., 2019). On the other hand, very little is known about the environmental variables influencing the microbial community composition and therefore the interactions between microbes and silica in quartz-dominated caves carved in orthoquartzites or metaquartzites (Barton et al., 2014; Sauro et al., 2018).

The importance of studying microbial interactions with silica resides in the fact that silicon is the seventh most abundant element in the universe and the second most abundant element on Earth, after oxygen. It can be found in the form of silicates, aluminosilicates, and crystalline and amorphous silicon dioxide (e.g., quartz and amorphous silica, respectively). The knowledge of the processes involved in the silica amorphization (transformation of crystalline silica into amorphous silica), dissolution, and precipitation is of great interest for the comprehension of the formation of ancient natural quartz-rich environments (Riquelme et al., 2015; Wray and Sauro, 2017; Sauro et al., 2018; Miller et al., 2022). Microbes are known to be involved in silica mineral dissolution and precipitation although in non-hydrothermal environments, the molecular and biochemical mechanisms are still unclear (Miller et al., 2014; Sauro et al., 2018). These processes leave traces of microbial features or metabolic activity in the rock record that are considered biosignatures valuable for astrobiology as potential analogs of silica-rich rocks detected on Mars (Cady and Farmer, 1996; Rice et al., 2010; Northup et al., 2011; Ruff and Farmer, 2016).

Quartzite caves in Venezuelan tepuis (i.e., orthoquartzite table mountains), represent an excellent natural laboratory to investigate microbe-mineral interactions in dark, low-temperature Si-rich environments. In particular, Imawarì Yeuta cave is composed of 98% of silica in the form of α-quartz and minor amounts of amorphous silica, i.e., opal-A, opal-G (Sauro et al., 2018; Ghezzi et al., 2021b). The cave was discovered in the Auyan Tepui in 2013 and is considered one of the most ancient caves in the world (Sauro et al., 2013). It hosts an extraordinary amount and variety of amorphous silica speleothems whose origin seems to be associated with biological activity. In fact, the absence of extreme chemical (pH) and/or physical (temperature, pressure) variations that would allow abiotic speleothem formation suggests possible biological mediation (Aubrecht et al., 2012; Sauro et al., 2018). Thus, the interaction between microbes and the orthoquartzite rocky substrates seems to contribute to this

impressive speleothem formation process. In this regard, our previous works described the shifting of the composition/structure of microbial communities associated with some speleothems characterized by distinct silica amorphization phases (Sauro et al., 2018; Ghezzi et al., 2021b). Imawarì Yeuta provides a unique window to further investigate the microbial ecology of quartz/silica-rich environments under aphotic and non-thermal conditions. In addition to the absence of light, the isolation of the deepest Imawarì Yeuta cave zones from the exterior atmosphere determines a general low nutrient availability and low organic carbon sources, associable to highly selective oligotrophic conditions (Mecchia et al., 2014; Sauro et al., 2018).

In this work, the microbial diversity in Imawarì Yeuta cave is described by performing Illumina sequencing of 16S rRNA hypervariable regions on several samples collected from different cave niches. Statistical and correlation analyses were performed to investigate the environmental parameters driving the microbial community structure and composition in this silica-dominated cave. Phylogenetic analyses of computationally reconstructed near-full-length 16S rRNA genes further provided deeper inferences to the affiliation of the poorly classified microbes that dominate representative niches within the cave.

Materials and methods

Sample collection

Samples have been collected in Imawarì Yeuta cave system during two field campaigns in March 2014 and March 2016. The cave system opens with seven different entrances at about 1,830 m a.s.l. in the northern-east sector of the Auyan Tepui massif (Sauro et al., 2013). Previous studies have shown that the cave is carved within Precambrian orthoquartzites of the Mataui Formation (Sauro, 2014) with an estimated speleogenetic age of over 30–40 million years (Mecchia et al., 2019). Cave conduits have been mapped for 23,079 m of length with 7 entrances, with an average depth of 80–100 m from the surface. Nineteen samples were collected from biofilms on water ponds, quartzite host rocks, sediments, and speleothems visible on the pavement, walls, and ceiling in different sites within the cave (Figure 1; Supplementary Table S1). The sampling strategy aimed to collect the most representative samples of different geochemical environments (niches) along the same cave system. However, each sample was kept to a minimum volume equivalent of 0.8 ml to a maximum of 30 ml in order to limit the damage to the very delicate cave deposits and environments. After scraping/collection with sterilized tools, all samples were stored in Eppendorf tubes and those designed for the molecular analysis were filled with LifeGuard RNA solution. The transport from the site to the lab was carried out in a portable fridge, then samples were stored at −80°C until analysis which happened within a few months after the expeditions.

Geochemical and environmental analyses

Given the different nature of the samples (waters, sediments, mineral aggregates, rocks), the overall environmental and geochemical characterization was performed using different approaches. The water content of all samples was determined by measuring the water loss after drying them at 80°C to a constant weight. Temperature (T) and acidity (pH) of water samples were measured by handheld field instruments (HI991301 from Hanna Instruments, Italy) after calibration on site. Accuracy was 0.1°C and 0.01, respectively. In WATER and WET samples, pH was measured on site also with pH stripes with the range 2–9 and 0.5 pH unit increments (Macherey Nagel 92118), while T was measured through a portable probe thermometer (Hanna Instruments, Italy). For sediments, rocks, and mineral aggregates, pH was measured by resuspending the samples in distilled water and using pH stripes as previously described (Barton et al., 2014). Dissolved silica concentration (DSi) in waters was measured by using a field colorimetric test kit (Aquaquant 14410 Silicon – Merck) that allows the determination of silica in the concentration range 0.01–0.25 mg L^{-1} with an error <20%. The water samples presenting concentrations higher than 0.25 mg L^{-1} were diluted with distilled water and then analyzed. Results were expressed following the convention of representing dissolved silica as the oxide SiO_2. To determine dissolved elements through inductively coupled plasma-mass spectrometry (ICP-MS) analyses in the laboratory, double water samples were collected in streams and ponds at Imawarì Yeuta in March 2013: a 250 ml bottle of untreated and unfiltered water, and a 100 ml bottle of 0.45 micron-filtered and 1 ml 65% HNO_3 acid-preserved water. ICP-MS was applied (method EPA 6020 A) for determination of multi-elemental sub µg L^{-1} concentrations (Al, Sb, As, Ba, Cd, Ca, Fe, Mg, Pb, K, Na, Zn) for which the recovery of the Laboratory Control Sample (LCS) resulted between 85% and 115%, as expected by the method lines. Anion Chromatography (method EPA 9056 A) was used to determine chloride, fluoride, nitrate, and sulfate in the solution. NH_4^+ concentration was measured on the untreated sample with the method APAT CNR IRSA 4030 A2 MAN 292003. Analyses were carried out as described in Mecchia et al. (2014).

X-Ray Fluorescence (XRF) analysis was carried out for samples that had enough solid material (15 g) to conduct the analysis (7 samples out of 19). Bulk chemical analyses were conducted by a wave dispersive X-ray fluorescence spectrometer (WD-XRF) operating at the BIGEA department, University of Bologna (Italy). Ultra-fine powdered samples were mounted on rounded boric acid casts (~5 cm diameter, ~0.5 cm height), which were prepared according to the matrix correction method (Sauro et al., 2018). Thirty-five international reference materials were used for calibrating the raw results, allowing an accuracy better than 5% for elements >10 ppm, and between 10% and 15% for elements <10 ppm. Bulk XRD analysis was performed on all sediments, rocks, and mineral aggregate samples to identify the

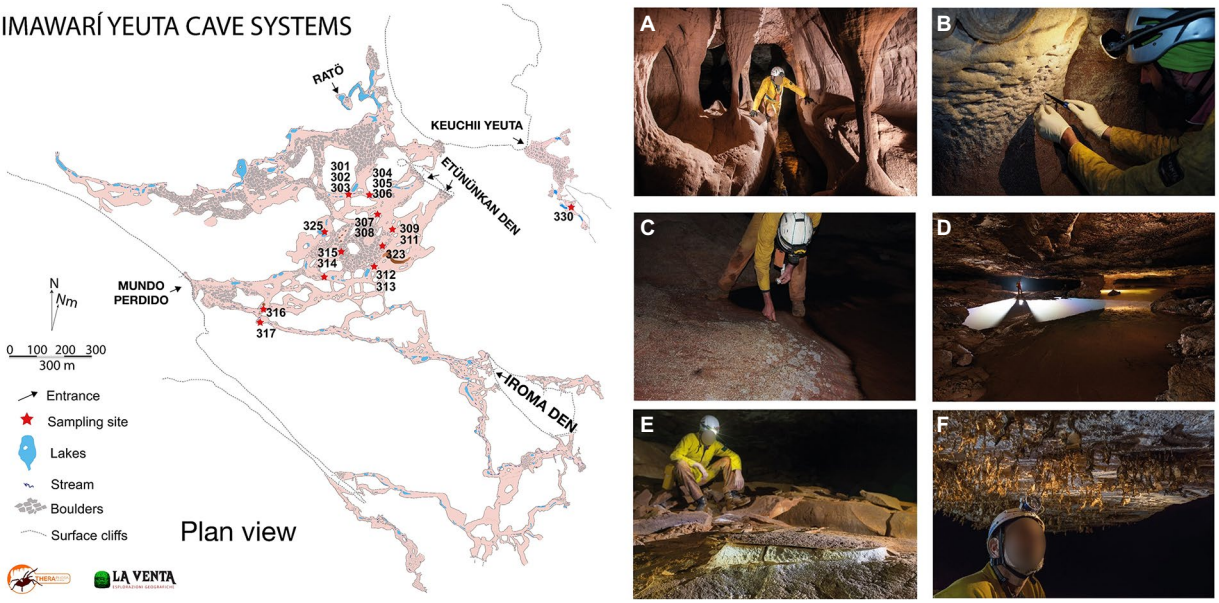

FIGURE 1
Map of Imawarì Yeuta cave and collection sites and examples of different geochemical, morphological, and hydrological environments in the cave. **(A)** Orthoquartzite columns and eroded walls are typical of hydrologically active branches of the cave, as those where sample Ay317 has been collected (photo La Venta-Alessio Romeo). **(B)** Cave walls undergoing quartz amorphization are usually covered by a wet paste of Opal-A, as in the sample location of Ay301 and Ay302 (photo La Venta-Francesco Lo Mastro). **(C)** Polished cave floors on a side of a stream are covered by whitish patches of biological material, as for Ay305 (photo La Venta-Francesco Lo Mastro). **(D)** Ponds of water covered by iridescent patinas and floating biological material, as for samples Ay303 and Ay314 (photo La Venta-Robbie Shone). **(E)** Deposits of powdery dry sulfates on the cave floors as for Ay308 and Ay315 (photo La Venta-Riccardo de Luca). **(F)** Fragile molds of silica resembling spider webs hanging from cave roofs, as for sample Ay323 (photo La Venta-Riccardo de Luca).

major mineral phase. Mineral phases were investigated by a Philips PW3710 X-Ray diffractometer (current: 20 mA, voltage: 40 kV, range 2θ: 5°–80°, step size: 0.02° 2θ, time per step: 2 s) as described by De Waele et al. (2017). Acquisition and processing of data was carried out using the Philips High Score software package. Major minerals are indicated in Supplementary Table S1, whereas for samples missing XRF analysis, prevalent chemical elements have been indicated based on mineral formulas. EDS analysis has been further used to confirm the prevalent composition of each sample as described by Sauro et al. (2018).

DNA extraction, V4-V5 16S rRNA gene amplification, and sequencing

Nineteen cave samples were extracted for their total DNA using the PowerSoil DNA Isolation Kit (Qiagen) with slight modifications implementing pretreatments with proteinase K and lysozyme at 37°C, followed by an additional lysis step using a solution of sodium dodecyl sulfate (SDS; Cappelletti et al., 2016). To provide amplicon for Illumina MiSeq analysis, the total DNA was amplified for the V4-V5 hypervariable region of 16S rRNA gene with universal forward 515F (5′-Illumina overhang-GTGYCAGCMGCCGCGGTA-3′) and reverse 907R (5′-Illumina overhang-CCGTCAATTCMTTTRAGTTT-3′) primers (IDT DNA Technologies). The PCR reaction mixture contained 10 ng of total DNA, 1x Takara Ex Taq buffer with $MgCl_2$ (10x, Takara Bio Inc., Tokyo, Japan), dNTP mix 200 µM, primers 500 nM, and Takara Ex Taq Polymerase 0.5 U and water (Lichrosolv®; Merck, Darmstadt, Germany) up to a total volume of 50 µl (Ghezzi et al., 2021a). Amplification reactions were carried out under the following thermocycling conditions: 95°C for 3 min, 30 cycles of 95°C for 30 s, 55°C for 30 s, 72°C for 30 s, with a final extension at 72°C for 5 min. PCR amplicons were confirmed by electrophoresis with a 1% (w/v) agarose gel and then purified by AMPure XP beads (Beckman Coulter) prior to the index PCR. Nextera XT Index was incorporated into each of the individual samples during PCR. The thermal cycling program included a first denaturation step at 95°C for 3 min, followed by 8 cycles of denaturation at 95°C for 30 s, annealing at 55°C for 30 s, elongation at 72°C for 30 s, with a final extension at 72°C for 5 min. Purified amplicons were submitted to KAUST Genomic Core Lab[1] for unidirectional sequencing reads on an Illumina MiSeq platform.

Statistical and co-occurrence network analyses

The sequence analysis of 16S rRNA gene amplicons was performed in QIIME2 using the DADA2 package. Trimmed

1 https://corelabs.kaust.edu.sa/

sequences were dereplicated, denoised, and merged, and chimeras were removed. The resulting 16S rRNA gene Amplicon Sequence Variants (ASVs) were taxonomically classified *via* the SILVA ACT: Alignment, Classification and Tree Service[2] online server (Pruesse et al., 2012). Alpha diversity estimates were generated by using the Shannon, Simpson's, Chao1, and Evenness indexes with statistical significance determined by ANOVA in Calypso (Zakrzewski et al., 2017). The correlation of environmental parameters with the microbial community composition of samples was determined with Redundancy Analysis (RDA) in Calypso (Zakrzewski et al., 2017). *p*-Value was provided for the significance of the grouping. Microbial taxa associated with specific environmental conditions were identified by a Linear Discriminant Analysis Effect Size (LefSe) approach and plotted as a cladogram. This comparison used an all-against-all approach with cut-off values of 0.05 for the Kruskal-Wallis alpha and 2.0 for the Linear Discriminant Analysis (LDA). Additional insights regarding the significant enrichment of the microbial taxa identified in LefSe were visualized in box plots through rank test analysis by Kruskal-Wallis test.

A correlation network, i.e., co-occurrence network, was established to identify clusters of strongly associated microbial taxa. The nodes indicate the orders, while the edges, which are connecting the nodes, represent correlations between orders. In this analysis, we included the microbial orders with a relative abundance >1% in at least five of the 19 samples under study. The R package NetCoMi (Peschel et al., 2021) was used to build a co-occurrence network based on SparCC estimated correlation values (Friedman and Alm, 2012). Edges were retained in the final network if the Benjamini–Hochberg adjusted *p*–values were below a given threshold, FDR < 0.05.

Near-full-length 16S rRNA gene amplification, sequencing, and analysis through EMIRGE

Universal primer pair 9F-1406R was used to amplify the near-full-length 16S rRNA from the total DNA extracted from Ay311 and Ay323 (for the DRY group), Ay312 and Ay313 (for the WET group). The PCR reaction mixture contained 10 ng of total DNA, 1x Takara Ex Taq buffer with $MgCl_2$ (10x; Takara Bio Inc., Tokyo, Japan), primers 300 nM, BSA (Roche Life Science, Basel, Switzerland) 1 mg mL^{-1}, dNTP mix 200 µM, Takara Ex Taq Polymerase 0.5 U, and water (Lichrosolv®; Merck, Darmstadt, Germany) up to a total volume of 50 µl. After shearing PCR amplicons using restriction endonucleases, libraries were prepared using NEB Next Ultra II FS DNA Library Prep Kit (New England Biolabs; Ghezzi et al., 2021b). Paired-end Illumina sequencing was performed at the Core Facility Molecular Biology of the Medical University of Graz (Austria). Raw reads were trimmed, and quality filtered using an in-house Galaxy set-up (Klymiuk et al., 2016), which included the algorithm Expectation Maximization Iterative Reconstruction of Genes from the Environment (EMIRGE), to carry out the reconstruction of (near) full-length 16S rRNA genes (approximately 1,400 bp long) from Illumina metagenomic sequences (Miller et al., 2011, 2013; Ghezzi et al., 2021b). We utilized the script EMIRGE_amplicon.py that allows the reconstruction of complete 16S rRNA genes from PCR amplicon sequencing data (Miller et al., 2013). Specifically, EMIRGE was run for 120 iterations with default parameters designed to merge reconstructed 16S rRNA genes if candidate consensus sequences shared ≥97% sequence identity in any given iteration (Miller et al., 2011, 2013). Reconstructed near-full-length 16S rRNA sequences were clustered into Operational Taxonomic Units (OTUs) at 97% identity to remove similar sequences. Chimeras were identified and removed with Uchime2 v11 (Edgar et al., 2011).

Phylogenetic analysis of the EMIRGE reconstructed near-full-length 16S rRNA genes

Phylogenetic trees were constructed using the OTU sequences deriving from EMIRGE assembly or the ASVs obtained with DADA2. For each ASV/OTU sequence included in the trees, the most closely related sequences retrieved from the GenBank database (Best BLAST Hits) were included in the phylogenetic analyses. All the sequences (ASV/OTUs and reference sequences) were aligned with ClustalW and used to construct phylogenetic trees based on neighbor-joining clustering method using MEGAX with bootstrap values of 1,000 (Kumar et al., 2018).

Results

Environmental and geochemical analyses of the cave samples

All the analyzed samples were collected from cave zones showing stable temperatures ranging between 13°C and 15°C. The samples were subjected to several analyses to obtain the geochemical parameters reported in Supplementary Table S1. Based on XRD mineralogical composition, SiO_2 dominated in 16 out of 19 samples, whereas three samples (Ay307, Ay308, and Ay315) were also composed of sulfates like gypsum and alunite (Supplementary Table S1). In addition, the XRF analysis of those samples providing enough material for this analytical method, showed that samples of quartzite, amorphous silica, and speleothems from cave walls, floor, and ceiling contained very low amounts of iron. This element was more abundant in the WATER samples Ay314 and Ay316. The latter also revealed the highest amount of aluminum detected among all samples. Barium was present in various cave samples independently from the cave niche.

2 http://www.arb-silva.de/aligner

10.3389/fmicb.2022.930302

Sequencing results, clustering, and diversity indexes

A total of 5,244,569 raw reads were generated through Illumina sequencing and corresponded to 5,794 ASVs, with a minimum of 74 ASVs (Ay315) and a maximum of 869 ASVs per sample (Ay317; Supplementary Table S1).

The relationship between the microbial communities' composition and the available cave samples' characteristics was analyzed using redundancy analysis (RDA; Figure 2). Water content, pH value, cave niche/location, major mineral composition, and sample color (indicated in Supplementary Table S1) were used as grouping parameters. As a result, RDA analysis distinguished three groups of samples corresponding to the three water content conditions ($p = 0.001$), whereas the effects of the other environmental and geochemical parameters were not significant (Supplementary Table S2). Based on the water content, the three groups were named WATER (water content >89%), WET (water content between 4% and 20%), and DRY (water content <1%). Regarding the cave collection sites, the WATER group included only samples collected from stagnant water ponds (with patinas and mats floating on the water surface). Conversely, both the WET and DRY groups included different sample types (orthoquartzite, sediments, and speleothems) deriving from different cave locations, i.e., the walls, the ceiling, and the floor. However, all the samples within the WET group shared the proximity of their collection site to small water flows (for those samples collected from the floor) or percolating water (for those samples collected from the cave wall).

In terms of alpha diversity indices, the microbial communities of WET samples were significantly more diverse and richer as compared to those inhabiting WATER and DRY samples (Shannon: $p = 0.04$; Figure 3). These two groups showed similar diversity value, while DRY samples had the lowest Chao1 index ($p = 0.0069$).

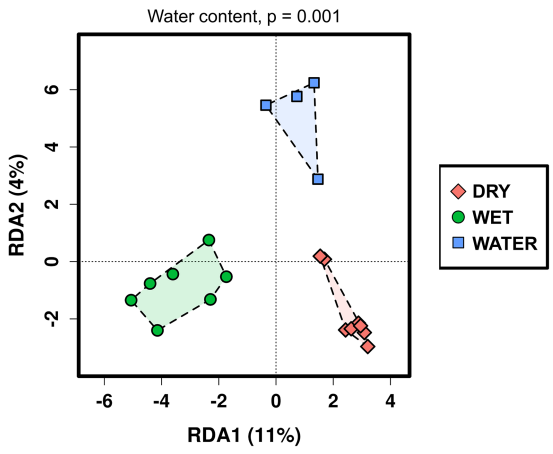

FIGURE 2
Redundancy analysis (RDA) of the Imawarì Yeuta microbial communities based on the water content of the cave samples. The value of $p = 0.001$ resulting from RDA analysis considering the water content as grouping parameter is indicated above the graph. The p-values of the other environmental parameters that were considered in the RDA analysis but did not result significant, are reported in Supplementary Table S2.

Microbial community composition

Bacteria dominated the microbial communities of all nineteen samples, while *Archaea* accounted for <1% in all samples except for the Ay312 and Ay330 belonging to the WET group, in which *Crenarchaeota* covered 2.3% and 1.5%, respectively. Rank tests analysis at phylum level showed significant differences in the relative abundance of *Acidobacteriota* ($p = 0.0041$), *Actinobacteriota* ($p = 0.012$), and *Proteobacteria* ($p = 0.039$; Figure 4), which characterized each of the three sample groups, i.e., WET, DRY, and WATER, respectively. In addition to *Acidobacteriota*, WET group was also significantly enriched with *Crenarchaeota* ($p = 0.0017$), RCP-254 ($p = 0.015$), *Verrucomicrobiota* ($p = 0.0038$), GAL15 ($p = 0.0038$), *Elusimicrobiota* ($p = 0.0088$), *Dependentiae* ($p = 0.027$), *Gemmatimonadota* ($p = 0.006$), and *Myxococcota* ($p = 0.0084$). In addition to *Actinobacteriota* and *Proteobacteria*, DRY and WATER were characterized by *Firmicutes* ($p = 0.014$) and *Armatimonadota* ($p = 0.025$; Figure 4), respectively.

At lower taxonomy levels, WATER was characterized by members of *Gammaproteobacteria* of *Pseudomonadaceae* family, and *Pseudomonas* genus ($p < 0.0001$), as well as members of *Yersiniaceae* family ($p = 0.031$) (Figures 5C–E). On the other hand DRY and WET groups were generally dominated by members of unclassified genera and/or families belonging to *Acidobacteriota* and *Alphaproteobacteria* in the WET samples and belonging to *Actinobacteriota* in the DRY samples (Figures 5A,B; Supplementary Figure S1). In particular, within these groups, WET group was mainly characterized by members of the class *Acidobacteriae* (*Acidobacteriota*, $p = 0.0049$), Subgroup 2 order (*Acidobacteriae*, $p = 0.0011$), unclassified *Acidobacteriota* ($p < 0.001$), *Beijerinckiaceae* family (*Alphaproteobacteria*, $p = 0.001$) and the archaeal *Nitrosotaleceae* family (*Nitrosotaleales*, $p = 0.001$) (Figures 5C,D). Microbial members enriched in DRY group belonged to *Acidimicrobiia* class (*Actinobacteriota*, $p = 0.0049$) of *Corynebacteriales* order (*Actinobacteria*, $p = 0.005$), *Mycobacteriaceae* family, and *Mycobacterium* genus ($p = 0.024$; Figures 5C–E).

Dissecting community structure *via* co-occurrence network analysis

To capture the relationships and interactions between microbial taxa present in Imawarì Yeuta samples, a co-occurrence network was built (Figure 6A). This analysis considered microbial diversity at the order level (Supplementary Table S3) since at lower taxonomic levels, i.e., family and genus, the data became too sparse to compute meaningful co-occurrence patterns. The

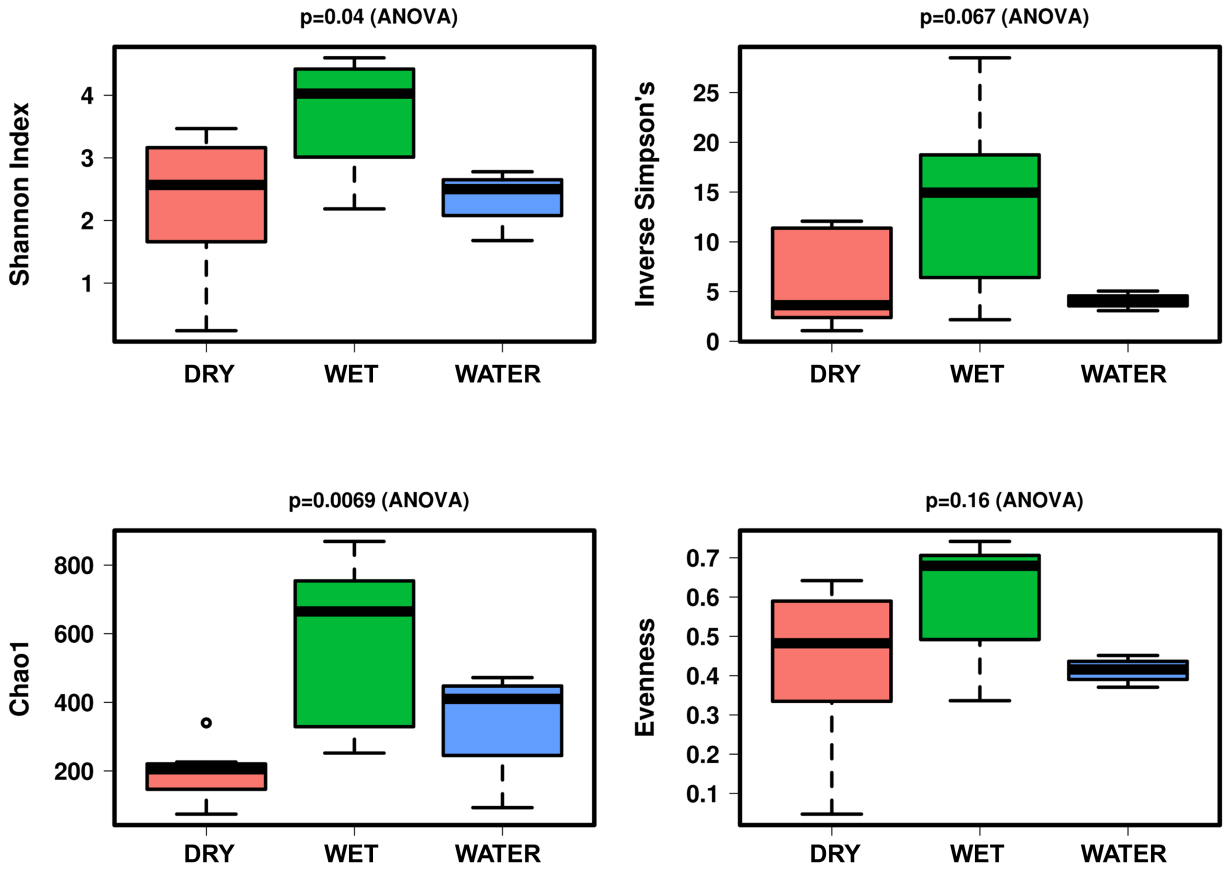

FIGURE 3
Boxplot of alpha diversity indices (Shannon, Simpson, Evenness, and Chao1) of the Imawari Yeuta samples grouped based on water content. The *p*-value indicating the statistical significance of the analysis (calculated by one-way ANOVA) is indicated above each boxplot.

resulting network showed that distinct co-occurrence relationships existed between members of the WET and DRY communities although a large proportion of taxa did not cluster together (modularity index of 0.34). WATER communities did not show any topologically distinct cluster.

In the resulting network, most of the co-occurrences were included in three clusters, i.e., Cluster1 (C1), C3, and C4, which comprised orders that characterized either the WET or DRY samples (Figure 6A). Specifically, cluster C4 included orders that were dominant (Subgroup 2 and *Solibacteriales*) and significantly enriched (*Rhizobiales*, *Nitrosotaleales*, and *Ktedonobacterales* with LDA > 3) in the only WET samples (Figure 6B). Clusters C1 and C3 included most of the orders that were enriched in DRY samples. C3 clustered members of the orders *Corynebacteriales*, *Frankiales*, *Solirubrobacterales,* and other three uncharacterized/unclassified orders of *Acidimicrobiia* and *Actinobacteria* classes (Figure 6B). Cluster C1 comprised members of the orders *Propionibacteriales*, *Peptostreptococcales*, and *Lachnospirales*. Therefore, co-occurrences in C1 and C3 indicated relationships between orders from DRY samples belonging to *Actinobacteriota* and *Firmicutes* phyla. Conversely, C4 included orders from WET samples that belonged to various phyla; those having the highest LDA score were *Acidobacteriota*, *Proteobacteria (Alphaproteobacteria)*, *Chloroflexi*, and *Crenarchaeota* (Figure 6B).

Phylogenetic analyses of the microbial members dominating each sample group

We further analyzed the phylogenetic relationship of the members belonging to the phyla characterizing each of the sample group WET (*Acidobacteriota*), DRY (*Actinobacteriota*), and WATER (*Proteobacteria,* specifically *Gammaproteobacteria*), with reference sequences from the NCBI database (Supplementary Figures S2–S4; Supplementary Table S4). In WATER samples, the ASVs belonging to *Gammaproteobacteria* showed high similarity (>99%) with reference sequences of isolated and cultured strains which are characterized at genus level (Supplementary Figure S2). Among these, the ASVs belonging to *Burkholderiales* were mainly affiliated to the genera *Delftia*, *Janthinobacterium*, *Nitrosospira*, and *Nitrosovibrio* and share high similarity with clones and sequences retrieved from volcanic deposits, lava caves, marine and lake environments, FACE soils, and other caves (Supplementary Table S4). Among these, the

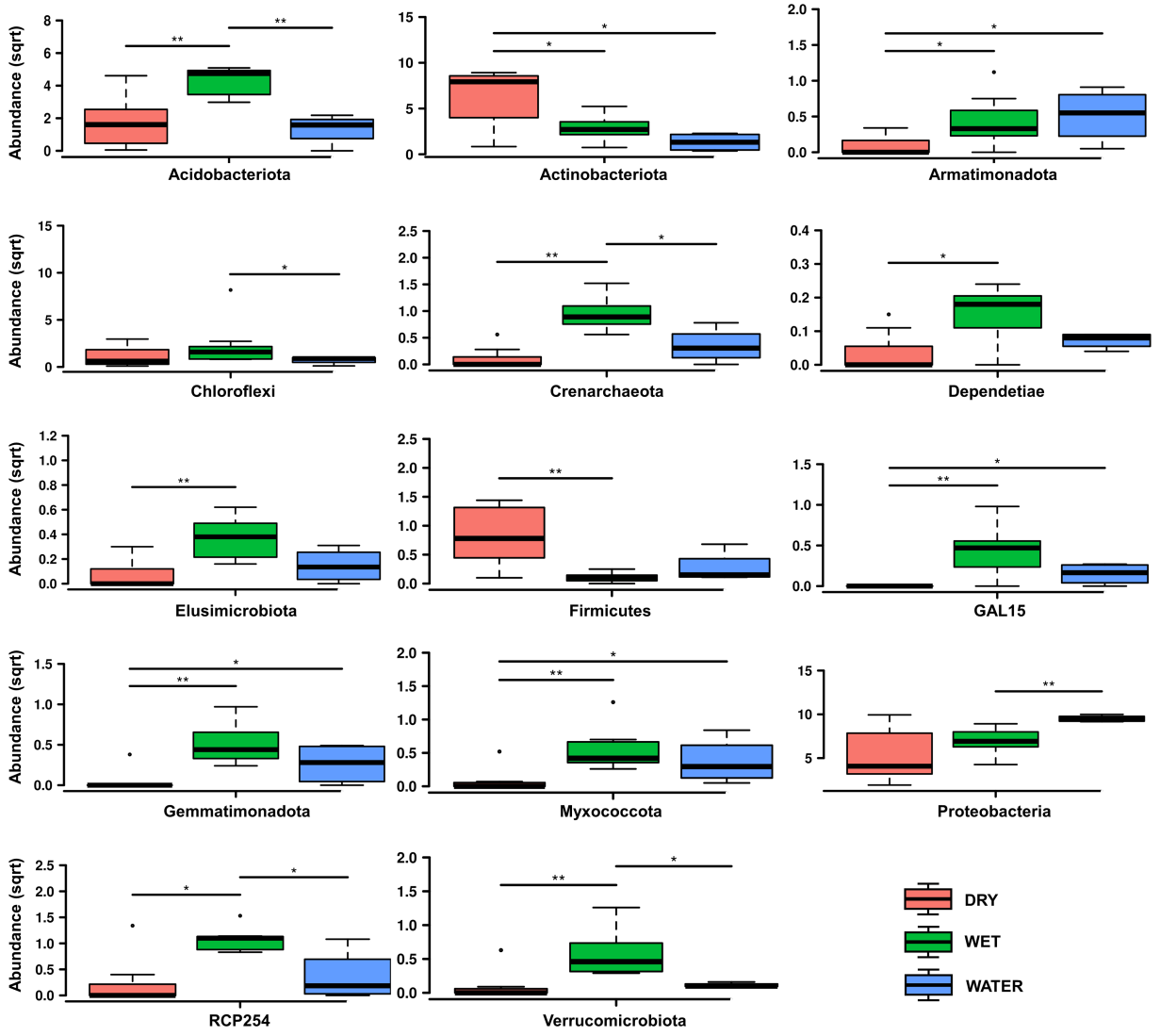

FIGURE 4
Rank test of significantly enriched microbial phyla in DRY, WET, and WATER sample groups. Abundance in the y axes stands for Relative abundance. The statistical significance is indicated by * and ** that stand for $p<0.05$ and $p<0.01$, respectively. (sqrt) stands for square root transformation.

Janthinobacterium-affiliated ASV4662 shared 100% of similarity with clones retrieved from the quartzite Roraima Sur Cave (Venezuela) and the stripe karst (marble within quartz-dominated schists) Raspberry Rising Cave (Glacier National Park, Canada) (Supplementary Table S4). Other ASVs abundant in Imawarì Yeuta water samples were highly affiliated (>99%) with *Pseudomonas*, *Stenotrophomonas*, and *Acinetobacter* genera, and to different genera of the *Enterobacterales* order, including *Erwinia*, *Serratia*, and *Enterobacter*, retrieved from acidic environments, forest soils, and tropical marine locations. The *Serratia*-affiliated ASV513 and the *Pseudomonas*-affiliated ASV1934 shared 100% of similarity with sequences retrieved from a Hungarian karst cave and Lascaux Cave (France), respectively (Supplementary Table S4).

Different to WATER samples, the ASVs belonging to the dominant taxa in the DRY and WET groups, i.e., *Actinobacteriota* and *Acidobacteriota*, generally showed low similarity (<98%) with sequences from strains that are taxonomically characterized at family and genus levels (Supplementary Table S4). The only exceptions were the ASV304 and ASV322 belonging to *Mycobacterium* genus. In the light of the novelty of the microorganisms characterizing the WET and DRY samples, we decided to deeply analyze the dominant taxa of these sample groups. Therefore, we reconstructed and studied the near-full-length sequences (OTUs) of the 16S rRNA gene of the dominant groups of WET and DRY samples, i.e., *Acidobacteriota* and *Actinobacteriota*, by carrying out EMIRGE analysis. We performed this analysis on two representative samples from each group, i.e.,

10.3389/fmicb.2022.930302

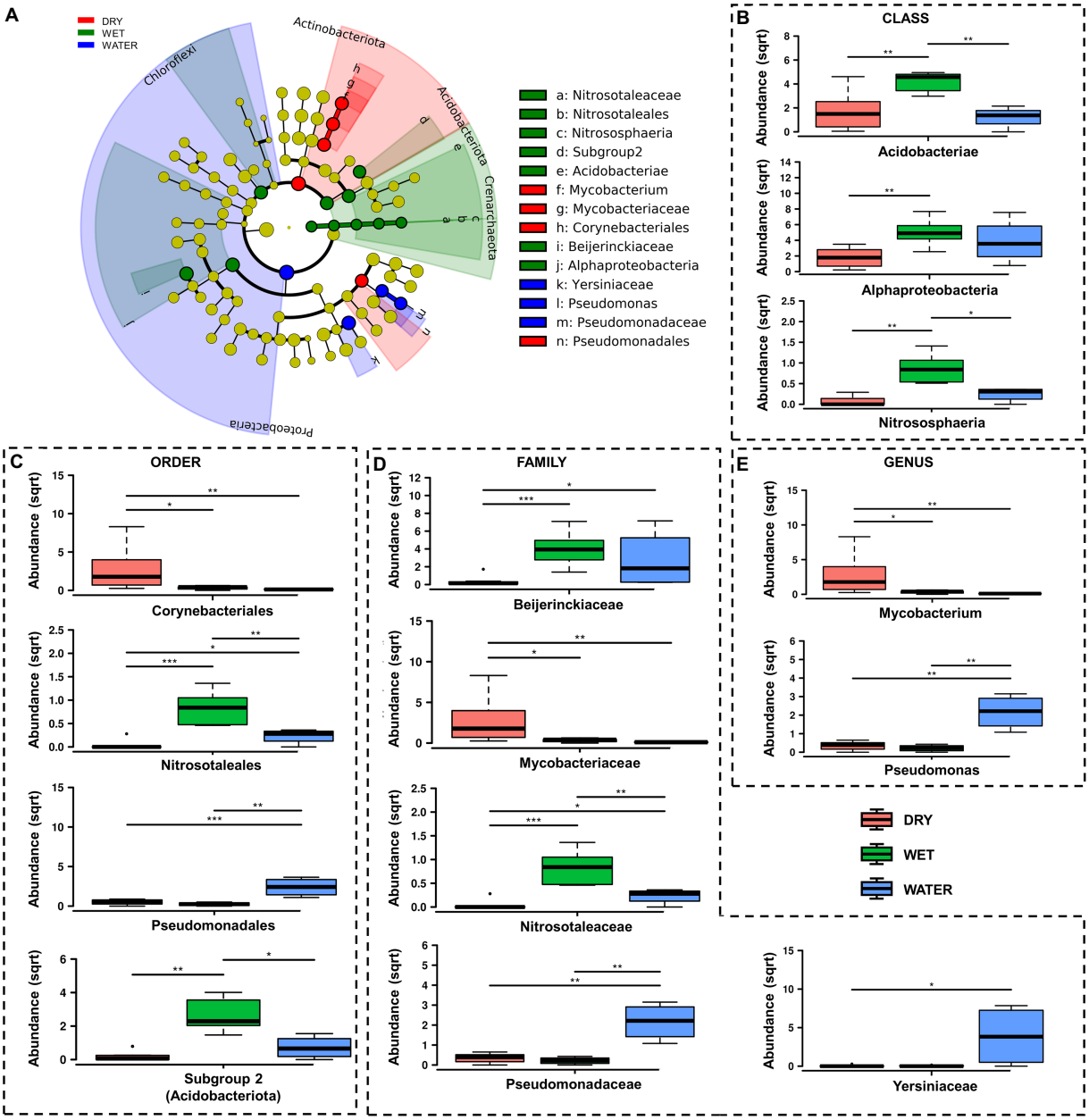

FIGURE 5
LefSe analysis of microbial communities from Imawarì Yeuta samples. **(A)** LefSe cladogram showing the microbial taxa (represented by the dots) with significant differences in the three groups. Red, green, and blue shades group different taxa, with the species classification at the level of phylum, class, order, family, and genus shown from the inside to the outside. The red, green, and blue nodes in the phylogenetic tree represent microbial taxa that play an important role in the DRY, WET, and WATER groups, respectively. Yellow nodes represent taxa with no significant difference. **(B–E)** Rank test results for classes, orders, families, and genera identified in LefSe analysis. Abundance in the y-axes stands for relative abundance. (sqrt) stands for square root transformation. The statistical significance is indicated by *, **, and *** that stand for $p<0.05$, $p<0.01$, and $p<0.001$, respectively.

Ay311 and Ay323 for the DRY group, Ay312 and Ay313 for the WET group. The OTUs were further used to construct phylogenetic trees together with the reference sequences from the NCBI database (Supplementary Figures S3, S4). As a result, the most abundant OTUs affiliated to *Acidobacteriota* from WET samples formed two distinct clades, one including members belonging to the Subgroup 2 order and the other including members of the *Acidobacteriales* order. They shared their highest nucleotide similarity (97%) with reference sequences of uncultured strains retrieved from quarzitic soils and samples collected within different cave systems including lava tubes and the quartzite Roraima Sur Cave (Supplementary Figure S3). The most abundant *Actinobacteriota*-related OTUs in DRY samples included many members affiliated to *Mycobacterium* genus, although the sequence identity with reference strains was below 98%, suggesting a certain degree of taxonomy separation from the

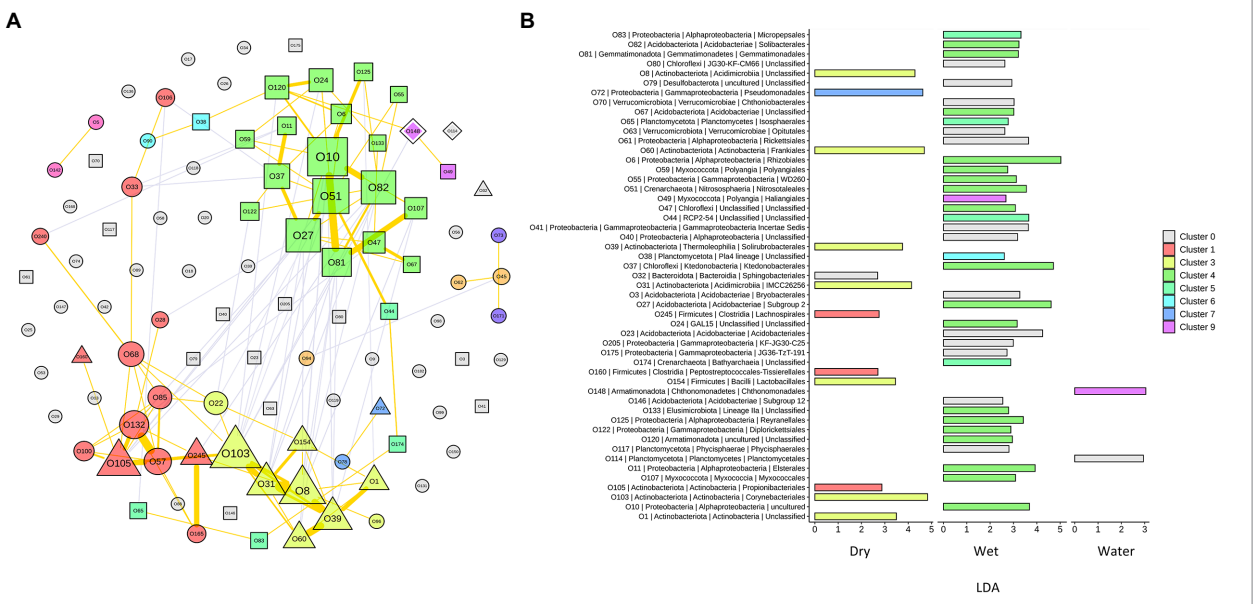

FIGURE 6
Network analysis of the microbial communities from Imawarì Yeuta cave. **(A)** Co-occurrence network of the most abundant orders (with relative abundance >1% in at least 5 samples) in the communities. Node codes ("O" followed by a number) correspond to the order/taxonomy shown in panel B, node color indicates the order assignment to each network cluster. Node size scales according to the node's centrality. Node shapes correspond to the orders significantly enriched in DRY (triangle), WET (square), and WATER (diamond) groups. The circle shape indicates order that is not significantly enriched in any of the three sample groups. The yellow lines indicate positive interactions, and grey lines indicate negative interactions. The thickness of the lines is proportional to the correlation strength. **(B)** LDA scores of the orders included in the network analysis. The color shown in the legend indicates the cluster membership. C0 (in grey) indicates those orders that do not belong to any cluster.

database sequences (at species or even genus level; Yarza et al., 2014). Among the closest uncultured reference sequences, we identified the highest nucleotide similarities with many actinobacterial clones retrieved from other cave environments including Roraima Sur Cave, Lower Kane Cave (Wyoming, USA), and lava tube walls, even though the percentage identity was generally low (94%–97%; Supplementary Figure S4). In line with this, our OTUs formed clades in the tree that were distinct from both cultured and uncultured references, except for OTU1 that clustered with clone sequences retrieved from Roraima Sur Cave (98%–99% of nucleotide sequence identity). The taxonomy affiliation of this OTU and its branch was not definable as the closest reference strains only shared 93%–94% of nucleotide identity and belonged to different genera including *Goodfellowiella*, *Pseudonocardia*, *Rhodococcus*, and *Streptoalloteichus*. In addition to the similarity with sequences from cave environments, many DRY and WET OTUs shared high similarities with uncultured bacteria retrieved from other oligotrophic and silica-rich environments that however were not subterranean such as FACE soils, ferralsol, and bamboo forest soils (Supplementary Figures S3, S4).

Discussion

This work reports the microbiome of a quartzite cave by describing the composition and structure of microbial communities inhabiting the different niches of Imawarì Yeuta. Quartzite caves in tepuis represent peculiar environments for microbial growth as, in addition to the absence of light, the orthoquartzite rock has a low buffering capacity. The deep zones of this cave are also characterized by organic carbon limitation. Possible sources of nutrients derive from the water leakage or condensation of water moisture from the surroundings (Sauro et al., 2018). These infiltration/interstitial waters are transparent and show extremely low conductivity values (close to distilled water) with contents of organic acids and dissolved carbon always below the detection limits (Mecchia et al., 2014). In this work, we found that, among the environmental parameters analyzed, only water content/presence significantly influenced the microbial communities' structure and composition within Imawarì Yeuta (Figure 2). In a previous study, Barton et al. (2014), suggested the major impact of pH on the microbial communities present in three rocky samples from the quartzite Roraima Sur Cave (RSC). These samples were collected at different distances from the cave entrance and were characterized by acidic pH values ranging between 4.9 and 5.6. In our work, we did not find the pH value to significantly correlate with the microbiome of Imawarì Yeuta (Supplementary Table S2), although the pH values of the samples we analyzed were similar to those from Roraima Sur Cave. Moreover, no significant correlation was found between the microbial community structure and the other parameters we could analyze, including the presence of specific minerals and the cave location (floor, wall, ceiling). Conversely, previous studies

reported a significant correlation between the microbial composition and the cave niche (defined as air, rock, sediment, or water) or the mineral substrate present in limestone and dolomite caves (Alonso et al., 2018; Dhami et al., 2018; Zhu et al., 2019). These correlations were mostly associated with the different nutrient levels related to the analyzed cave niches and their different origins (i.e., rocks were related to autochthonous origin from the cave, while sediments were allochthonous and brought into caves from the outside). The absence of significant correlation between the diversity of the microbial communities and the cave niche/location we report here, might be due to the fact that, differently from the previous cave studies, all the niches we analyzed in Imawarì Yeuta are under the same nutritional (oligotrophic) conditions. Some indications on the poor nutrient conditions of tepuis' caves are reported in works by Barton et al. (2014) and Mecchia et al. (2014). On the other hand, our results are in line with other studies that showed the water content to be the main driving force of the microbial communities' composition in various environments such as agricultural and grassland soils, surface litter, and deserts (Stres et al., 2008; Manzoni et al., 2012; Li et al., 2021). However, some environmental parameters could not be included in our RDA analysis, such as the minor elements and the silica amorphization stage, as they were available only for a few samples. Our previous studies suggested a relation between the silica amorphization phase and the microbial diversity in Imawarì Yeuta (Sauro et al., 2018; Ghezzi et al., 2021b). The lack of knowledge on the silica amorphization stage of most of the samples did not allow the evaluation of this environmental factor in the correlation analysis, although this could greatly influence microbial communities' structures and compositions. In this regard, based on full 16S rRNA gene similarity analysis, the silica amorphization stage seemed to have a strong impact on *Ktedonobacterales* members (Ghezzi et al., 2021b). Indeed, these strains were more phylogenetically related when we compared samples with similar silica amorphization stages rather than samples collected from proximal locations (Ghezzi et al., 2021b).

Based on the correlation with the water content, the samples of Imawarì Yeuta were divided in the three groups DRY, WET, and WATER (Figure 2). The samples with intermediate water content levels (WET) presented higher richness and diversity as compared to WATER and DRY samples (Figure 3). This can be related to previous findings that reported an increase of microbial richness depending on the moisture in soil microcosms and the promotion of rare bacterial species in the presence of intermediate water content (Xu et al., 2017; Bickel and Or, 2020). The higher diversity and richness shown by the WET samples from Imawarì Yeuta might be due in part to the microelements provided by the water that enters this cave mostly by dripping through cracks from the overlying rocks. The water in this cave has been reported to be extremely deficient in both organic carbon and inorganic dissolved chemicals (Mecchia et al., 2014). However, this low amount of nutrients, including oxygen and other gases, can greatly impact microbial diversity in oligotrophic and aphotic environments (Zhou et al., 2002; Stres et al., 2008; Hershey et al., 2018; Ghezzi et al., 2021b). Unclassified genera, families, and orders belonging to several phyla (e.g., *Elusimicrobiota*, *Gemmatimonadota*, *Dependetiae*) were significantly enriched in WET samples. Specifically, this group was dominated by members of Subgroup 2 and *Solibacterales* of *Acidobacteriota* phylum, and members of *Beijerinckiaceae* family of *Alphaproteobacteria* class (Figures 5C,D). Similarly, previous studies demonstrated that the rewetting of arid soils favored the increase of the microbial diversity together with the establishment of *Acidobacteriota* and the decrease of *Actinobacteriota* (Barnard et al., 2015; Schimel, 2018; She et al., 2018). In line with this, we found members of *Actinobacteriota* to be enriched in DRY samples that also showed the lowest values of microbial diversity and richness (Figures 3, 4–5). *Actinobacteriota*- and *Firmicutes*-affiliated microbial taxa associated with the DRY samples, such as the actinobacterial members of *Corynebacteriales* order and *Pseudonocardiaceae* family, have been previously found to dominate low-diverse microbial communities and typically inhabit arid soils due to their resistance to adverse environmental conditions including nutrient shortage, acidic pH, and scarce availability of water (Mohammadipanah and Wink, 2016; Rego et al., 2019).

The dominant taxa of the DRY and WET groups also showed a correlation at order level in the co-occurrence network analysis (Figure 6A). This indicates ecological interactions occurring among the microbial taxa as well as their associations to the possible differences in physicochemical and nutritional variables present in the DRY and WET groups. The network analysis grouped the orders characterizing the DRY samples that only belonged to *Actinobacteriota* and *Firmicutes*, in the two clusters C1 and C3 (Figure 6B). A separate single cluster (C4) exclusively included orders characterizing the WET samples; these orders belonged to various phyla. This indicates that in WET samples ecological interactions occur among microbial strains that are more heterogeneous from a taxonomy point of view (as compared to the DRY samples), in turn suggesting that the dominant microbial taxa contribute to different functions in each sample group or cave niche (Mandakovic et al., 2018; Ma et al., 2021). Furthermore, as the network clustering was generated based on positive correlations, the inclusion in one single cluster (C4) of almost all the dominant orders characterizing WET samples indicates that these taxa mostly rely on cooperative relationships rather than on competitive ones. Microbial cooperation is a possible strategy to survive and persist under poor nutrients and adverse conditions. Promotion effects among microbes were previously detected through network analysis of microbial communities from other oligotrophic caves (Ma et al., 2021). On the other hand, orders dominant in WATER samples did not generate any topologically distinct clusters. This might be due to the reduced number of samples and/or to the higher heterogeneity of the WATER samples as compared to WET and DRY in terms of microbial community composition.

Generally, we found *Pseudomonas* and, more generally, *Gammaproteobacteria* to be enriched in Imawarì Yeuta WATER samples (Figure 5E; Supplementary Figure S1). This finds

analogies with other caves that were described hosting high abundance of *Pseudomonadales* and former *Betaproteobacteria* in cave waters (Shabarova and Pernthaler, 2010; Shabarova et al., 2013; Brannen-Donnelly and Engel, 2015; Zhu et al., 2019). In particular, Zhu et al. (2019) assessed that the moisture level in karst caves promotes the establishment of *Proteobacteria* species and represents the most important factor affecting the microbial community composition.

All the dominant microbial taxa we identified in this study to be significantly enriched in WET, DRY, and WATER samples have been described to include genera/species involved in biomineralization processes and/or rock weathering. In particular, several *Acidobacteriota* members of the WET-characterizing Subgroup 2 order have been associated with mineral-rich acidic and quartz-based sandy soils. They have been described to be involved in mineral weathering and to be capable of slowing down their metabolism to persist under starving conditions on quartzite substrates (Jones et al., 2009; Ward et al., 2009; Nishiyama et al., 2012; Wakelin et al., 2012). Members of *Alphaproteobacteria* of Imawarì Yeuta WET samples, mostly belonging to the nitrogen-fixing *Rhizobiales*, were significantly abundant in sediment or rock samples from other karst caves (Zhu et al., 2019). Furthermore, metabolically active *Rhizobiales* have also been found underneath desertic quartzitic rocks suggesting their contribution in providing primary reactions to sustain the development of other microbial groups (Van Goethem et al., 2017). Ammonia-oxidizers of the family *Nitrosotaleaceae* (*Crenarchaeota*) were also significantly enriched in WET samples. Although they are low in abundance, they might contribute to the nitrogen cycle in Imawarì Yeuta as suggested in other caves (Mihajlovski et al., 2019). Cave-dwelling *Actinobacteriota* belonging to DRY-abundant *Corynebacteriales* and, at lower extent, *Solirubrobacterales* and *Pseudonocardiales* orders were described to be involved in both biomineralization and rock weathering in volcanic and limestone cave rocks (Cuezva et al., 2012; Cockell et al., 2013) and were found to be associated with the most advanced stages of silica-amorphization and formation of coralloid speleothems in Imawarì Yeuta (Ghezzi et al., 2021b). RNA-based cave studies suggested *Actinobacteriota* to be among the most abundant metabolically active microbial group in caves and to be capable to exploit complex metabolic pathways to switch their metabolism according to the settings of the environment they live in (Gonzalez-Pimentel et al., 2018; Paun et al., 2019). Biomineralization activities were also observed in cave samples enriched in *Gammaproteobacteria* including WATER-characterizing *Pseudomonas*, *Serratia*, and *Janthinobacterium* genera (Rusznyák et al., 2012; Carmichael et al., 2013). In particular, iron biomineralization processes associated to these genera have been observed in ferromanganese deposits from carbonate caves (Rusznyák et al., 2012). Interestingly, noticeable iron amounts were detected in Imawarì Yeuta cave waters.

The most abundant ASVs belonging to WATER samples revealed sequence identity >99% with strains that are classified up to genus level (in the GenBank database) and/or that have been isolated from different environments (Supplementary Table S4). On the other hand, both the ASVs and OTUs characterizing the DRY and WET samples shared relatively low similarities with sequences in the database, and the Best BLAST Hits corresponded to unclassified sequences retrieved from other caves such as the quartzite Roraima Sur Cave, lava tubes, the limestone Lascaux Cave and Raspberry Rising Cave and oligotrophic/extreme locations, like Antarctic environments and deserts (Supplementary Table S4; Supplementary Figures S3, S4). The high novelty of microbial strains retrieved from the WET and DRY samples is probably due to the fact that the microbiology of silica-rich rocks/minerals and speleothems associated with quartzite cave environments is still mostly unknown. Conversely, microbes from Imawarì Yeuta WATER share similarities with strains retrieved from other fresh and river waters, acidic environments, and cave samples (Supplementary Table S2). This is probably due to the fact that, in Imawarì Yeuta, the surface environments above the cave have more influence, even if still limited compared to other ecosystems, on waters infiltrating in the cave rather than on the silica rocks/minerals. Furthermore, quartzite rocks/minerals in Imawarì Yeuta cave probably impose unique selective pressures leading to a specific microbial communities' evolution and selection (i.e. microbial endemism).

Additional environmental sources of microbial strains taxonomically affiliated with those from Imawarì Yeuta are FACE soil, ferralsol, and bamboo forest soil (Supplementary Table S4). FACE (Free-Air CO_2 and O_3 Enrichment) soil shares the high partial pressure of CO_2 in the atmosphere with caves (Dunbar et al., 2012; Houillon et al., 2017), while ferralsol and bamboo forest soil are well known to contain/present high amounts of silica and quartz (Collin et al., 2012; Jordanova, 2017). In parallel with this, on one hand, the use of atmospheric gases, like CO_2 and CO, has been recently described as one of the main microbial strategies to thrive under low organic carbon conditions (Ji et al., 2017; Ortiz et al., 2021; Ghezzi et al., 2021b), on the other hand, quartzite rocks have very low pH buffering capacities (Barton et al., 2014). In line with the latter, WET-derived archaeal ASVs shared 100% of 16S rRNA sequence similarity with clones retrieved not only from silica-rich forest sandy soil and rice paddy soil (Okuda and Takahashi, 1962; Chen et al., 2015) but also from acid mine drainage and gold mines that are characterized by acidic pH values (Kuang et al., 2013; Supplementary Table S4). Taken together, our results indicate that, within the Imawarì Yeuta cave, water content/presence greatly influences the microbial ecology, while when comparative and phylogenetic analyses are performed, oligotrophic conditions, high CO_2/CO partial pressures, and silica richness (in relation with the low pH) promote the dominance of specific microbial species.

In conclusion, this work provides a first global characterization of the biodiversity present in the quartzite Imawarì Yeuta cave, offering insights into some of the major environmental factors shaping the microbial communities thriving in oligotrophic quartzite caves. The water availability was found to greatly contribute to the microbial community

structure and composition within Imawarì Yeuta, probably in association with the role of water in energy and nutrient supply. Accordingly, microbial taxa established specific co-occurrence patterns within clusters partially linked to water content. Conducting a thorough phylogenetic analysis of the dominant microbial members distinctive of the Imawarì Yeuta environment, we found their affiliation with microbial members retrieved from environments characterized by silica dominance in the rock substrate and/or CO_2/CO atmospheric enrichment, suggesting these two being the main factors underlying the microbial diversity in association with the geochemistry of silica/quartz, the low pH value and possible alternative survival strategies. Future functional studies will investigate the genetic and metabolic aspects that contribute to the microbial interaction with the silica substrate and the microbial development in this unique oligotrophic quartzite cave.

Data availability statement

The data presented in the study are deposited in the NCBI repository (https://www.ncbi.nlm.nih.gov/), accession number PRJNA796549.

Author contributions

DG and MC designed the work, interpreted the data, and wrote the manuscript. FS, JW, and FV collected the samples. DG extracted the DNA from the cave samples. PH performed and financed the Illumina MiSeq run (V4-V5 region of the 16S rRNA gene amplicon) and conducted the initial quality check and filtering of the sequencing data. FS performed the geochemical analyses, made the cave map figure, and helped with the writing and interpretation of the manuscript results. DG, AF, and LF performed the bioinformatic analyses (both the 16S rRNA V4-V5 region and the near-full-length 16S rRNA gene sequencing data). AF made the network analysis and the corresponding figure, and helped in the network analysis text writing and interpretation. MC and FS supervised the work and contributed to funding acquisition. All authors contributed to the article and approved the submitted version.

Funding

We acknowledge the Rector Francesco Ubertini, the Vice-Rector for Research A. Rotolo, and the Governing Academic Bodies of the University of Bologna (UNIBO) for the financial support of the research project and the PhD scholarship for DG. The research activities were also partly supported by RFO UNIBO grants. Funding for EMIRGE analysis was provided by Europlanet 2020 17-EPN3-026 grant. Europlanet 2020 RI has received funding from the European Union's Horizon 2020 research and innovation program under grant agreement No 654208.

Acknowledgments

We thank Leonardo Piccini for his contribution in the sample collection, Hosam Zowawi for supporting contacts with KAUST and for further advancement of the research project in the last years, and Laura Negretti for technical assistance in SEM and FESEM analyses. We also thank Cristina Carbone (Dip. DISTAV, University of Genova) for her help with the investigations on mineral phases and EDS, and Andrea Columbu for the XRF analyses. Our gratitude goes to Christine Moissl-Eichinger, Kaisa Koskinen Mora, Alexander Mahnert, Slave Trajanoski, and Lisa Wink at the Medical University of Graz (Austria) for their help with sample preparation for Illumina sequencing and data analysis of EMIRGE data. We acknowledge the agencies and associations involved in granting the permit for the speleological expeditions and sample collection: Instituto National de Parques and the patronage of the Government of Bolivar State from Venezuela, the Embassy of the Bolivarian Republic of Venezuela in Italy. This article has been developed in the framework of the Rolex Award of Enterprise supporting Francesco Sauro in research and exploration on the tepui highlands of South America. We are grateful to UNIBO student Andrea Gozzi for his support with the experimental work.

Conflict of interest

The authors declare that the research was conducted in the absence of any commercial or financial relationships that could be construed as a potential conflict of interest.

Publisher's note

Supplementary material

The Supplementary material for this article can be found online at: https://www.frontiersin.org/articles/10.3389/fmicb.2022.930302/full#supplementary-material

References

Alonso, L., Creuzé-des-Châtelliers, C., Trabac, T., Dubost, A., Moënne-Loccoz, Y., and Pommier, T. (2018). Rock substrate rather than black stain alterations drives microbial community structure in the passage of Lascaux cave. *Microbiome* 6, 216–215. doi: 10.1186/s40168-018-0599-9

Aubrecht, R., Barrio-Amorós, C. L., Breure, A. S. H., Brewer-Carías, C., Derka, T., Fuentes-Ramos, O. A., et al. (2012). *Venezuelan Tepuis: Their Caves and Biota. Acta Geologica Slovaca Monograph*. Comenius University, Bratislava 168 pp.

Barnard, R. L., Osborne, C. A., and Firestone, M. K. (2015). Changing precipitation pattern alters soil microbial community response to wet-up under a Mediterranean-type climate. *ISME J.* 9, 946–957. doi: 10.1038/ismej.2014.192

Barton, H. A., Giarrizzo, J. G., Suarez, P., Robertson, C. E., Broering, M. J., Banks, E. D., et al. (2014). Microbial diversity in a Venezuelan orthoquartzite cave is dominated by the *Chloroflexi* (class Ktedonobacterales) and *Thaumarchaeota* group I.1c. *Front. Microbiol.* 5:615. doi: 10.3389/fmicb.2014.00615

Barton, H. A., and Northup, D. E. (2007). Geomicrobiology in cave environments: past, current and future perspectives. *J. Cave Karst Studies* 69, 163–178.

Barton, H. A., Taylor, N. M., Kreate, M. P., Springer, A. C., Oehrle, S. A., and Bertog, J. L. (2007). The impact of host rock geochemistry on bacterial community structure in oligotrophic cave environments. *Int. J. Speleol.* 36, 93–104. doi: 10.5038/1827-806X.36.2.5

Bickel, S., and Or, D. (2020). Soil bacterial diversity mediated by microscale aqueous-phase processes across biomes. *Nat. Commun.* 11:116. doi: 10.1038/s41467-019-13966-w

Brannen-Donnelly, K., and Engel, A. S. (2015). Bacterial diversity differences along an epigenic cave stream reveal evidence of community dynamics, succession, and stability. *Front. Microbiol.* 6:729. doi: 10.3389/fmicb.2015.00729

Cady, S. L., and Farmer, J. D. (1996). Fossilization processes in siliceous thermal springs: trends in preservation along thermal gradients. *Ciba Found. Symp.* 202, 150–173. doi: 10.1002/9780470514986.ch9

Cappelletti, M., Ghezzi, D., Zannoni, D., Capaccioni, B., and Fedi, S. (2016). Diversity of methane-oxidizing bacteria in soils from "hot lands of Medolla" (Italy) featured by anomalous high-temperatures and biogenic CO_2 emission. *Microbes Environ.* 31, 369–377. doi: 10.1264/jsme2.ME16087

Carmichael, M. J., Carmichael, S. K., Santelli, C. M., Strom, A., and Bräuer, S. L. (2013). Mn(II)-oxidizing bacteria are abundant and environmentally relevant members of ferromanganese deposits in caves of the upper Tennessee River basin. *Geomicrobiol J.* 30, 779–800. doi: 10.1080/01490451.2013.769651

Chen, C. R., Hou, E. Q., Condron, L. M., Bacon, G., Esfandbod, M., Olley, J., et al. (2015). Soil phosphorus fractionation and nutrient dynamics along the Cooloola coastal dune chronosequence, southern Queensland, Australia. *Geoderma* 257–258, 4–13. doi: 10.1016/j.geoderma.2015.04.027

Cockell, C. S., Kelly, L. C., and Marteinsson, V. (2013). Actinobacteria-an ancient phylum active in volcanic rock weathering. *Geomicrobiol J.* 30, 706–720. doi: 10.1080/01490451.2012.758196

Collin, B., Doelsch, E., Keller, C., Panfili, F., and Meunier, J. D. (2012). Distribution and variability of silicon, copper and zinc in different bamboo species. *Plant Soil* 351, 377–387. doi: 10.1007/s11104-011-0974-9

Cuezva, S., Fernandez-Cortes, A., Porca, E., Pašić, L., Jurado, V., Hernandez-Marine, M., et al. (2012). The biogeochemical role of Actinobacteria in Altamira cave, Spain. *FEMS Microbiol. Ecol.* 81, 281–290. doi: 10.1111/j.1574-6941.2012.01391.x

D'Angeli, I. M., Ghezzi, D., Leuko, S., Firrincieli, A., Parise, M., Fiorucci, A., et al. (2019). Geomicrobiology of a seawater-influenced active sulfuric acid cave. *PLoS One* 14:e0220706. doi: 10.1371/journal.pone.0220706

De Waele, J., Carbone, C., Sanna, L., Vattano, M., Galli, E., Sauro, F., et al. (2017). Secondary minerals from salt caves in the Atacama Desert (Chile): a hyperarid and hypersaline environment with potential analogies to the Martian subsurface. *Int. J. Speleol.* 46, 51–66. doi: 10.5038/1827-806X.46.1.2094

Dhami, N. K., Mukherjee, A., and Watkin, E. L. J. (2018). Microbial diversity and mineralogical-mechanical properties of Calcitic cave Speleothems in natural and in vitro biomineralization conditions. *Front. Microbiol.* 9:40. doi: 10.3389/fmicb.2018.00040

Dunbar, J., Eichorst, S. A., Gallegos-Graves, L. V., Silva, S., Xie, G., Hengartner, N. W., et al. (2012). Common bacterial responses in six ecosystems exposed to 10 years of elevated atmospheric carbon dioxide. *Environ. Microbiol.* 14, 1145–1158. doi: 10.1111/j.1462-2920.2011.02695.x

Edgar, R. C., Haas, B. J., Clemente, J. C., Quince, C., and Knight, R. (2011). UCHIME improves sensitivity and speed of chimera detection. *Bioinformatics* 27, 2194–2200. doi: 10.1093/bioinformatics/btr381

Friedman, J., and Alm, E. J. (2012). Inferring correlation networks from genomic survey data. *PLoS Comput. Biol.* 8:e1002687. doi: 10.1371/journal.pcbi.1002687

Ghezzi, D., Filippini, M., Cappelletti, M., Firrincieli, A., Zannoni, D., Gargini, A., et al. (2021a). Molecular characterization of microbial communities in a peat-rich aquifer system contaminated with chlorinated aliphatic compounds. *Environ. Sci. Pollut. Res. Int.* 28, 23017–23035. doi: 10.1007/s11356-020-12236-3

Ghezzi, D., Sauro, F., Columbu, A., Carbone, C., Hong, P. Y., Vergara, F., et al. (2021b). Transition from unclassified Ktedonobacterales to Actinobacteria during amorphous silica precipitation in a quartzite cave environment. *Sci. Rep.* 11:3921. doi: 10.1038/s41598-021-83416-5

Gonzalez-Pimentel, J. L., Miller, A. Z., Jurado, V., Laiz, L., Pereira, M. F. C., and Saiz-Jimenez, C. (2018). Yellow coloured mats from lava tubes of La Palma (Canary Islands, Spain) are dominated by metabolically active Actinobacteria. *Sci. Rep.* 8:1944. doi: 10.1038/s41598-018-20393-2

Hershey, O. S., Kallmeyer, J., Wallace, A., Barton, M. D., and Barton, H. A. (2018). High microbial diversity despite extremely low biomass in a deep karst aquifer. *Front. Microbiol.* 9:2823. doi: 10.3389/fmicb.2018.02823

Houillon, N., Lastennet, R., Denis, A., Malaurent, P., Minvielle, S., and Peyraube, N. (2017). Assessing cave internal aerology in understanding carbon dioxide (CO_2) dynamics: implications on calcite mass variation on the wall of Lascaux cave (France). *Environ. Earth Sci.* 76:170. doi: 10.1007/s12665-017-6498-8

Ji, M., Greening, C., Vanwonterghem, I., Carere, C. R., Bay, S. K., Steen, J. A., et al. (2017). Atmospheric trace gases support primary production in Antarctic desert surface soil. *Nature* 552, 400–403. doi: 10.1038/nature25014

Jones, R. T., Robeson, M. S., Lauber, C. L., Hamady, M., Knight, R., and Fierer, N. (2009). A comprehensive survey of soil acidobacterial diversity using pyrosequencing and clone library analyses. *ISME J.* 3, 442–453. doi: 10.1038/ismej.2008.127

Jordanova, N. (2017). "Magnetism of soils with limitations to root growth: Vertisols, Solonetz, Solonchaks, and Leptosols," in *Soil Magnetism, Applications in Pedology, Environmental Science and Agriculture*. 221–285.

Kallmeyer, J., Pockalny, R., Adhikari, R. R., Smith, D. C., and D'Hondt, S. (2012). Global distribution of microbial abundance and biomass in subseafloor sediment. *PNAS* 109, 16213–16216. doi: 10.1073/pnas.1203849109

Klymiuk, I., Bambach, I., Patra, V., Trajanoski, S., and Wolf, P. (2016). 16S based microbiome analysis from healthy subjects' skin swabs stored for different storage periods reveal phylum to genus level changes. *Front. Microbiol.* 7:2012. doi: 10.3389/fmicb.2016.02012

Kuang, J. L., Huang, L. N., Chen, L. X., Hua, Z. S., Li, S. J., Hu, M., et al. (2013). Contemporary environmental variation determines microbial diversity patterns in acid mine drainage. *ISME J.* 7, 1038–1050. doi: 10.1038/ismej.2012.139

Kumar, S., Stecher, G., Li, M., Knyaz, C., and Tamura, K. (2018). MEGA X: molecular evolutionary genetics analysis across computing platforms. *Mol. Biol. Evol.* 35, 1547–1549. doi: 10.1093/molbev/msy096

Li, W., Jiang, L., Zhang, Y., Teng, D., Wang, H., Wang, J., et al. (2021). Structure and driving factors of the soil microbial community associated with *Alhagi sparsifolia* in an arid desert. *PLoS One* 16:e0254065. doi: 10.1371/journal.pone.0254065

Ma, L., Huang, X., Wang, H., Yun, Y., Cheng, X., Liu, D., et al. (2021). Microbial interactions drive distinct taxonomic and potential metabolic responses to habitats in karst cave ecosystem. *Microbiol. Spectr.* 9:e011521. doi: 10.1128/spectrum.01152-21

Magnabosco, C., Lin, L. H., Dong, H., Bomberg, M., Ghiorse, W., Stan-Lotter, H., et al. (2018). The biomass and biodiversity of the continental subsurface. *Nat. Geosci.* 11, 707–717. doi: 10.1038/s41561-018-0221-6

Mandakovic, D., Rojas, C., Maldonado, J., Latorre, M., Travisany, D., Delage, E., et al. (2018). Structure and co-occurrence patterns in microbial communities under acute environmental stress reveal ecological factors fostering resilience. *Sci. Rep.* 8:5875. doi: 10.1038/s41598-018-23931-0

Manzoni, S., Schimel, J. P., and Porporato, A. (2012). Responses of soil microbial communities to water stress: results from a meta-analysis. *Ecology* 93, 930–938. doi: 10.1890/11-0026.1

Mecchia, M., Sauro, F., Piccini, L., Columbu, A., and De Waele, J. (2019). A hybrid model to evaluate subsurface chemical weathering and fracture karstification in quartz sandstone. *J. Hydrol.* 572, 745–760. doi: 10.1016/j.jhydrol.2019.02.026

Mecchia, M., Sauro, F., Piccini, L., de Waele, J., Sanna, L., Tisato, N., et al. (2014). Geochemistry of surface and subsurface waters in quartz sandstones: significance for the geomorphic evolution of tepui table mountains (gran Sabana, Venezuela). *J. Hydrol.* 511, 117–138. doi: 10.1016/j.jhydrol.2014.01.029

Merino, N., Aronson, H. S., Bojanova, D. P., Feyhl-Buska, J., Wong, M. L., Zhang, S., et al. (2019). Living at the extremes: extremophiles and the limits of life in a planetary context. *Front. Microbiol.* 10:780. doi: 10.3389/fmicb.2019.00780

Mihajlovski, A., Lepinay, C., Mirval, A. L., Touron, S., Bousta, F., and Di Martino, P. (2019). Characterization of the archaeal and fungal diversity associated with gypsum efflorescences on the walls of the decorated Sorcerer's prehistoric cave. *Ann. Microbiol.* 69, 1071–1078. doi: 10.1007/s13213-019-01506-2

Miller, C. S., Baker, B. J., Thomas, B. C., Singer, S. W., and Banfield, J. F. (2011). EMIRGE: reconstruction of full-length ribosomal genes from microbial community short read sequencing data. *Genome Biol.* 12:R44. doi: 10.1186/gb-2011-12-5-r44

Miller, C. S., Handley, K. M., Wrighton, K. C., Frischkorn, K. R., Thomas, B. C., and Banfield, J. F. (2013). Short-read assembly of full-length 16S amplicons reveals bacterial diversity in subsurface sediments. *PLoS One* 8:e56018. doi: 10.1371/journal.pone.0056018

Miller, A. Z., Jiménez-Morillo, N. T., Coutinho, M. L., Gazquez, F., Palma, V., Sauro, F., et al. (2022). Organic geochemistry and mineralogy suggest anthropogenic impact in speleothem chemistry from volcanic show caves of the Galapagos. *iScience*. 25:104556. doi: 10.1016/j.isci.2022.104556

Miller, A. Z., Pereira, M. F. C., Calaforra, J. M., Forti, P., Dionísio, A., and Saiz-Jimenez, C. (2014). Siliceous speleothems and associated microbe-mineral interactions from Ana Heva lava tube in Easter Island (Chile). *Geomicrobiol J.* 31, 236–245. doi: 10.1080/01490451.2013.827762

Mohammadipanah, F., and Wink, J. (2016). Actinobacteria from arid and desert habitats: diversity and biological activity. *Front. Microbiol.* 6:1541. doi: 10.3389/fmicb.2015.01541

Nishiyama, M., Sugita, R., Otsuka, O., and Senoo, K. (2012). Community structure of bacteria on different types of mineral particles in a sandy soil. *Soil Sci. Plant Nutr.* 58, 562–567. doi: 10.1080/00380768.2012.729226

Northup, D. E., Melim, L. A., Spilde, M. N., Hathaway, J. J. M., Garcia, M. G., Moya, M., et al. (2011). Lava cave microbial communities within mats and secondary mineral deposits: implications for life detection on other planets. *Astrobiology* 11, 601–618. doi: 10.1089/ast.2010.0562

Okuda, A., and Takahashi, E. (1962). Studies on the physiological role of silicon in crop plants (part 6). Effect of silicon on iron uptake by rice plant and oxidation power of root. *J. Sci. Soil Manure.* 33, 59–64.

Ortiz, M., Leung, P. M., Shelley, G., Jirapanjawat, T., Nauer, P. A., van Goethem, M. W., et al. (2021). Multiple energy sources and metabolic strategies sustain microbial diversity in Antarctic desert soils. *Proc. Natl. Acad. Sci.* 118:e2025322118. doi: 10.1073/pnas.2025322118

Paun, V. I., Icaza, G., Lavin, P., Marin, C., Tudorache, A., Perşoiu, A., et al. (2019). Total and potentially active bacterial communities entrapped in a late glacial through Holocene ice core from Scărişoara ice cave. *Romania. Front Microbiol.* 10:1193. doi: 10.3389/fmicb.2019.01193

Peschel, S., Müller, C. L., von Mutius, E., Boulesteix, A., and Depner, M. (2021). NetCoMi: network construction and comparison for microbiome data in R. *Brief. Bioinform.* 22:bbaa290. doi: 10.1093/bib/bbaa290

Pruesse, E., Peplies, J., and Glöckner, F. O. (2012). SINA: accurate high-throughput multiple sequence alignment of ribosomal RNA genes. *Bioinformatics* 28, 1823–1829. doi: 10.1093/bioinformatics/bts252

Rego, A., Raio, F., Martins, T. P., Ribeiro, H., Sousa, A. G. G., Séneca, J., et al. (2019). Actinobacteria and cyanobacteria diversity in terrestrial Antarctic microenvironments evaluated by culture-dependent and independent methods. *Front. Microbiol.* 10:1018. doi: 10.3389/fmicb.2019.01018

Rice, M. S., Bell, J. F., Cloutis, E. A., Wang, A., Ruff, S. W., Craig, M. A., et al. (2010). Silica-rich deposits and hydrated minerals at Gusev crater, Mars: Vis-NIR spectral characterization and regional mapping. *Icarus* 205, 375–395. doi: 10.1016/j.icarus

Riquelme, C., Marshall Hathaway, J. J., Dapkevicius, M. d. L. N., Miller, A. Z., Kooser, A., Northup, D. E., et al. (2015). Actinobacterial diversity in volcanic caves and associated geomicrobiological interactions. *Front. Microbiol.* 6:1342. doi: 10.3389/fmicb.2015.01342

Ruff, S. W., and Farmer, J. D. (2016). Silica deposits on Mars with features resembling hot spring biosignatures at El Tatio in Chile. *Nat. Commun.* 7, 1–10. doi: 10.1038/ncomms13554

Rusznyák, A., Akob, D. M., Nietzsche, S., Eusterhues, K., Totsche, K. U., Neu, T. R., et al. (2012). Calcite biomineralization by bacterial isolates from the recently discovered pristine karstic Herrenberg cave. *Appl. Environ. Microbiol.* 78, 1157–1167. doi: 10.1128/AEM.06568-11

Sauro, F. (2014). Structural and lithological guidance on speleogenesis in quartz–sandstone: evidence of the arenisation process. *Geomorphology* 226, 106–123. doi: 10.1016/j.geomorph.2014.07.033

Sauro, F., Cappelletti, M., Ghezzi, D., Columbu, A., Hong, P. Y., Zowawi, H. M., et al. (2018). Microbial diversity and biosignatures of amorphous silica deposits in orthoquartzite caves. *Sci. Rep.* 8, 17569–17514. doi: 10.1038/s41598-018-35532-y

Sauro, F., De Vivo, A., Vergara, F., and De Waele, J. (2013). "Imawarì Yeuta: a new giant cave system in the quartz sandstones of the Auyan Tepui, Bolivar State, Venezuela," in *Proceedings of the 16th International Congress of Speleology*. *Vol. 2*. Eds. M. Filippi and P. Bosak, 142–146.

Schimel, J. P. (2018). Life in dry soils: effects of drought on soil microbial communities and processes. *Annu. Rev. Ecol. Evol. Syst.* 49, 409–432. doi: 10.1146/annurev-ecolsys-110617-062614

Shabarova, T., and Pernthaler, J. (2010). Karst pools in subsurface environments: collectors of microbial diversity or temporary residence between habitat types. *Environ. Microbiol.* 12, 1061–1074. doi: 10.1111/j.1462-2920.2009.02151.x

Shabarova, T., Widmer, F., and Pernthaler, J. (2013). Mass effects meet species sorting: transformations of microbial assemblages in epiphreatic subsurface karst water pools. *Environ. Microbiol.* 15, 2476–2488. doi: 10.1111/1462-2920.12124

She, W., Bai, Y., Zhang, Y., Qin, S., Feng, W., Sun, Y., et al. (2018). Resource availability drives responses of soil microbial communities to short-term precipitation and nitrogen addition in a desert Shrubland. *Front. Microbiol.* 9:186. doi: 10.3389/fmicb.2018.00186

Stres, B., Danevcic, T., Pal, L., Mrkonjic Fuka, M., Resman, L., Leskovec, S., et al. (2008). Influence of temperature and soil water content on bacterial, archaeal and denitrifying microbial communities in drained fen grassland soil microcosms. *FEMS Microbiol. Ecol.* 66, 110–122. doi: 10.1111/j.1574-6941.2008.00555.x

Van Goethem, M. W., Makhalanyane, T. P., Cowan, D. A., and Valverde, A. (2017). Cyanobacteria and Alphaproteobacteria may facilitate cooperative interactions in niche communities. *Front. Microbiol.* 8:2099. doi: 10.3389/fmicb.2017.02099

Wakelin, S. A., Anand, R. R., Reith, F., Gregg, A. L., Noble, R. R. P., Goldfarb, K. C., et al. (2012). Bacterial communities associated with a mineral weathering profile at a sulphidic mine tailings dump in arid Western Australia. *FEMS Microbiol. Ecol.* 79, 298–311. doi: 10.1111/j.1574-6941.2011.01215.x

Ward, N. L., Challacombe, J. F., Janssen, P. H., Henrissat, B., Coutinho, P. M., Wu, M., et al. (2009). Three genomes from the phylum Acidobacteria provide insight into the lifestyles of these microorganisms in soils. *Appl. Environ. Microbiol.* 75, 2046–2056. doi: 10.1128/AEM.02294-08

Wray, R. A. L., and Sauro, F. (2017). An updated global review of solutional weathering processes and forms in quartz sandstones and quartzites. *Earth Sci. Rev.* 171, 520–557. doi: 10.1016/j.earscirev.2017.06.008

Wu, Y., Tan, L., Liu, W., Wang, B., Wang, J., Cai, Y., et al. (2015). Profiling bacterial diversity in a limestone cave of the western loess plateau of China. *Front. Microbiol.* 6:244. doi: 10.3389/fmicb.2015.00244

Xu, X., Liu, X., Li, Y., Ran, Y., Liu, Y., Zhang, Q., et al. (2017). Legacy effects of simulated short-term climate change on ammonia oxidisers, denitrifiers, and nitrous oxide emissions in an acid soil. *Environ. Sci. Pollut. Res. Int.* 24, 11639–11649. doi: 10.1007/s11356-017-8799-6

Yarza, P., Yilmaz, P., Pruesse, E., Glöckner, F. O., Ludwig, W., Schleifer, K. H., et al. (2014). Uniting the classification of cultured and uncultured bacteria and archaea using 16S rRNA gene sequences. *Nat. Rev. Microbiol.* 12, 635–645. doi: 10.1038/nrmicro3330

Zakrzewski, M., Proietti, C., Ellis, J. J., Hasan, S., Brion, M. J., Berger, B., et al. (2017). Calypso: a user-friendly web-server for mining and visualizing microbiome-environment interactions. *Bioinformatics* 33, 782–783. doi: 10.1093/bioinformatics/btw725

Zhou, J., Xia, B., Treves, D. S., Wu, L. Y., Marsh, T. L., O'Neill, R. V., et al. (2002). Spatial and resource factors influencing high microbial diversity in soil. *Appl. Environ. Microbiol.* 68, 326–334. doi: 10.1128/AEM.68.1.326-334.2002

Zhu, H. Z., Zhang, Z. F., Zhou, N., Jiang, C. Y., Wang, B. J., Cai, L., et al. (2019). Diversity, distribution and co-occurrence patterns of bacterial communities in a karst cave system. *Front. Microbiol.* 10:1726. doi: 10.3389/fmicb.2019.01726

frontiers | Frontiers in Microbiology

TYPE Review
PUBLISHED 28 September 2022
DOI 10.3389/fmicb.2022.950005

OPEN ACCESS

EDITED BY
Valme Jurado,
Institute of Natural Resources and Agrobiology of Seville (CSIC), Spain

REVIEWED BY
Yang Liu,
Shenzhen University,
China
Cecilia Susana Demergasso Semenzato,
Catholic University of the North, Chile

*CORRESPONDENCE
Shuang-Jiang Liu
liusj@im.ac.cn

SPECIALTY SECTION
This article was submitted to Terrestrial Microbiology, a section of the journal Frontiers in Microbiology

RECEIVED 22 May 2022
ACCEPTED 14 September 2022
PUBLISHED 28 September 2022

CITATION
Zhu H-Z, Jiang C-Y and Liu S-J (2022) Microbial roles in cave biogeochemical cycling.
Front. Microbiol. 13:950005.
doi: 10.3389/fmicb.2022.950005

Microbial roles in cave biogeochemical cycling

Hai-Zhen Zhu[1], Cheng-Ying Jiang[1,2] and Shuang-Jiang Liu[1,2,3]*

[1]State Key Laboratory of Microbial Resources and Environmental Microbiology Research Center, Institute of Microbiology, Chinese Academy of Sciences, Beijing, China, [2]College of Life Sciences, University of Chinese Academy of Sciences, Beijing, China, [3]State Key Laboratory of Microbial Technology, Shandong University, Qingdao, China

Among fundamental research questions in subterranean biology, the role of subterranean microbiomes playing in key elements cycling is a top-priority one. Karst caves are widely distributed subsurface ecosystems, and cave microbes get more and more attention as they could drive cave evolution and biogeochemical cycling. Research have demonstrated the existence of diverse microbes and their participance in biogeochemical cycling of elements in cave environments. However, there are still gaps in how these microbes sustain in caves with limited nutrients and interact with cave environment. Cultivation of novel cave bacteria with certain functions is still a challenging assignment. This review summarized the role of microbes in cave evolution and mineral deposition, and intended to inspire further exploration of microbial performances on C/N/S biogeocycles.

KEYWORDS

cave microbiome, biogeochemical cycling, cave evolution, mineral deposition, methane oxidation

Introduction

Caves are dark, underground hollow spaces with relatively constant temperature, high humidity, and limited nutrients. Many caves are associated with karst topography, which is formed by the dissolution of soluble bedrock, such as limestone, dolomite and gypsum, in areas where groundwaters are undersaturated with respect to the minerals in the host rock. Karst landforms spread widely, accounting for approximately 20% of the earth's dry ice-free surface (Ford and Williams, 2007). As a typical feature of subsurface landscape, karst caves develop globally, with over 50,000 distributed in the United States (Barton and Jurado, 2007). China also has a large contiguous karst terrain, and the Yunnan–Guizhou plateau in the southwest developed most karst caves, among which the longest cave exceeds 138 km (Zhang and Zhu, 2012). Many caves are relatively shallow and form near the water table in karst terranes, although some caves develop by deep-seated hypogenic process at substantial depths and by process other than dissolution such as lava flows.

Caves are oligotrophic ecosystems with less than 2 mg of total organic carbon per liter, yet host flourishing microbial groups (Figure 1A), with an average number of 10^6 microbial cells per gram of cave rock (Barton and Jurado, 2007). The study revealed a high diversity within *Bacteria* domain and *Proteobacteria* and *Actinobacteria* were abundant in

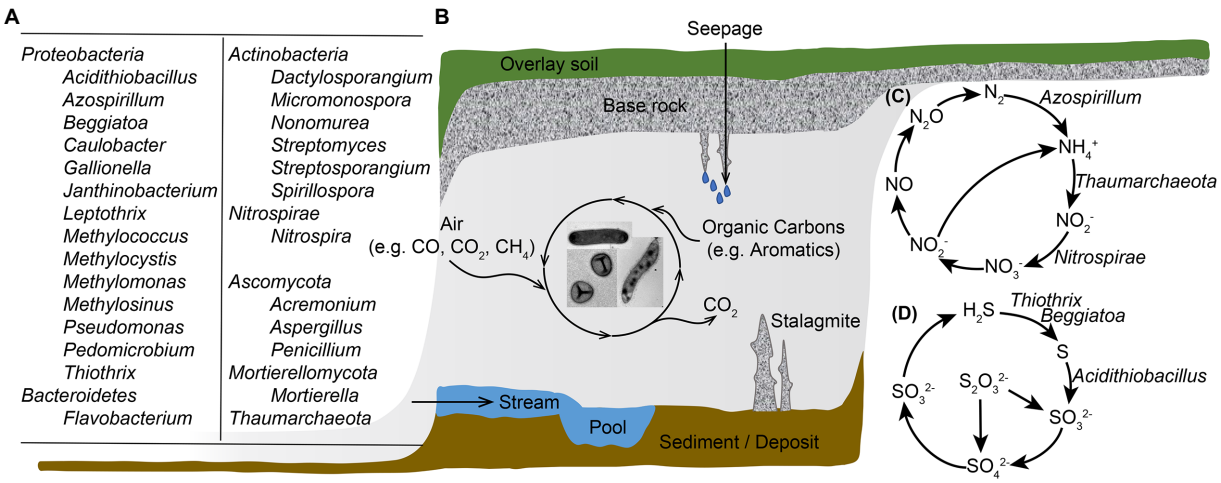

FIGURE 1
Illustration of microbial diversity and geobiochemical cycling of elements in a karst cave ecosystem. **(A)** Major cave microbial groups that are abundant and/or actively participate in biogeochemical cyclings; **(B)** Cave landscape and microbial carbon metabolisms; **(C)** Microbe-involved nitrogen transformation processes in caves; **(D)** Microbe-associated sulfur metabolisms in cave ecosystems. Microbes involved in goebiocycling processes in panels **(C,D)** are showed, except those genes were documented in cave samples yet no major microbial taxa responsible for the process was identified.

oligotrophic cave samples of air, rock, sediment and water. *Chloroflexi*, *Planctomycetes*, *Bacteroidetes*, *Firmicutes*, *Acidobacteria*, *Nitrospirae*, *Gemmatimonadetes*, and *Verrucomicrobia* also accounted for large proportions of the total microbial community in caves (Wu et al., 2015; Zhu et al., 2019). In some organic cave samples such as biofilms in sulfur cave, bat guanos, spiders' webs and earthworm castings, *Mycobacterium* was prevalently detected (Modra et al., 2017; Sarbu et al., 2018; Hubelova et al., 2021; Pavlik et al., 2021). Over 500 genera of fungi, such as *Penicillium*, *Aspergillus* and *Mortierella* have been reported in caves (Vanderwolf et al., 2013), and new fungal species were identified from cave air, rock, sediment and water samples (Zhang et al., 2017, 2021). These microbial communities contain novel diversity, and promote important biogeochemical processes. With no sunlight, microorganisms in cave environment cannot perform photosynthesis, and are intensively involved in the biogeochemical cycles of carbon, nitrogen, sulfur, and metals such as Fe and Mn to offset the lack of exogenous nutrients and energy.

Early studies of the participance of microbes in cave biogeochemical cyclings were carried out using traditional culturing techniques, and bacteria isolates participate in limestone calcification were obtained from cave deposits and pool waters (Danielli and Edington, 1983; Cunningham et al., 1995). Special attention was paid to cave *Actinobacteria*, as *Actinobacteria* members isolated from moonmilk deposits were proved to produce various novel antibiotic compounds (Axenovgibanov et al., 2016; Adam et al., 2018). The emerging new techniques greatly facilitated the investigations of cave microbial community structure and functional potential. By adopting metagenomic sequencing, chemolithotrophic microbial communities driven by nitrification and sulfur oxidation were identified from cave biofilms (Jones et al., 2012; Tetu et al., 2013). Based on both culture-dependent and culture-independent techniques, these studies expanded our knowledge of subsurface microbial diversity, provided a better understanding of the energy and nutrient dynamics of cave ecosystems.

Cave systems are geographically and geochemically complicated, and they might be formed from hydraulic (epigenic or hypogenic) or lava movements. Physical and chemical compositions of caves affect the microbial diversity and involvement in cave evolution. Readers who are interested in specificities of each cave system may refer to literatures (Palmer, 2011; Brannen-Donnelly and Engel, 2015; Martin-Pozas et al., 2020). In this review, we focus on discussion of the role of microbiomes in cave evolution and mineral deposition, and present case studies for microbial performance in cave nitrogen and sulfur cyclings. In addition, two emerging research topics related to cave carbon cycling, atmospheric methane oxidation and antibiotics production are explored.

Microbiomes drive cave evolution

Dissolution and deposition of carbonate minerals

There are two major mechanisms for the formation of karstic caves. Classical epigenic cave systems form as water flows through the soil and produces karst networks by seepages, absorbing CO_2 and forming a dilute carbonate solution. In epigenic caves, exchanges occur with subaerial processes (such as water movement and mixture), enhancing dissolution capacity in the

direction of flow (Sendra et al., 2014). In contrast, hypogenic cave systems form as water recharges the soluble bedrocks from below. The formation of hypogenic caves is fueled by hydrostatic pressure or other energy sources rather than recharge from the overlying or adjacent surface (Ford, 2006). Due to the deep origin of rising water, hypogenic cave systems are not directly influenced by seepages. Among explanations for hypogenic cave formation, sulfuric acid speleogenesis (the formation process of a cave) is a major one, resulting in some of the largest cave systems including Carlsbad Caverns and Lechuguilla Cave in New Mexico. Hydrogen sulfide leaked upward along with fractures from hydrocarbon deposits, and form sulfuric acid upon reaching oxygenated meteoric groundwater (Jagnow et al., 2000). Microbial communities dominated by sulfur-oxidizing acidophilic bacteria *Acidithiobacillus* formed dense biofilms in these caves, accelerating mineral dissolution and cave enlargement (Jones et al., 2014). Geobiochemical differences occur between epigenic and hypogenic cave systems, because caves formed from the two mechanisms would have different environmental conditions. For example, hypogenic caves such as sulfuric acid speleogenetic caves are sulfur-rich with relatively low pH, as a result, these caves support microbial communities that are acidophilic and actively involved in sulfur transformation. On the other hand, epigenic caves are pH neutral or slightly alkaline, and the microbial communities would be more diverse. Studies concerning snottites from sulfuric caves revealed very low biodiversity with Chao1 index ranged from 1 to 10 (Hose et al., 2000; Vlasceanu et al., 2000; Macalady et al., 2007), while more than ten thousand OTUs were detected from epigenic cave samples with Chao 1 index reached more than 1,000 (Zhu et al., 2019). Lava caves are also important subterrain environment, although karstic caves accounted for a larger proportion (Jones and Macalady, 2016). Lava caves formed from the heat volcanic flows and are mainly composed of basalt (Gabriel and Northup, 2013). These substantial differences from karstic caves granted lava caves unique microbial communities, which are mainly affected by geographical location and the availability of organic carbon, nitrogen and copper in the lava rock (Hathaway et al., 2014).

Multiple studies have suggested direct or indirect microbial involvement in the formation of carbonate minerals. Microbial calcite precipitation in calcium-rich environments was assumed to be the result of a detoxification process, through which growing cells actively export the excess calcium ions to maintain cellular metal homeostasis (Banks et al., 2010). Microbial biofilms also served as the initial crystal nucleation sites that contributed to the formation of secondary carbonate deposits within caves (Tisato et al., 2015). Cañaveras et al. (2006) proposed a model of moonmilk formation based on extensive observations in Altamira Cave (Spain) that microbial filaments provided a template for the precipitation of calcite fiber crystals in the early stages of moonmilk deposition. Moreover, the growth of microbes can increase the environmental pH, which would in turn increase the saturation index of carbonate and drive precipitation. For example, nitrogen metabolic pathways including ammonification of amino acids, dissimilatory reduction of nitrate and degradation of urea or uric acid induced formation of carbonate and bicarbonate ions, as the metabolic end product ammonia increased local pH (Castanier et al., 2000). Maciejewska et al. (2017) proved that *Streptomyces* promoted calcification in moonmilk through ammonification and, less importantly, ureolysis.

Biologically induced carbonate deposition was initially attributed mainly to fungi, studies reported that nano-fibers presented in the crystalline structure of moonmilk were related to biomineralized fungal hyphae (Bindschedler et al., 2010, 2014). However, recent studies indicated that bacteria played a major role in the induction of cave carbonate precipitation (Cañaveras et al., 2006; Portillo et al., 2009). γ-*Proteobacteria* and *Actinobacteria* were the major groups detected in white colonizations that were able to raise pH through metabolism in Altamira Cave (Portillo and Gonzalez, 2011); isolates belonging to α-*Proteobacteria*, β-*Proteobacteria*, γ-*Proteobacteria*, *Firmicutes* and *Actinobacteria* from cave speleothem were also confirmed to perform calcification (Banks et al., 2010). The presence of Archaea was identified in moonmilk deposits, yet their role in the formation of moonmilk remains to be discovered (Gonzalez et al., 2006; Reitschuler et al., 2016).

Deposition of iron and manganese oxides

Fe and Mn oxides were found in karst caves as sedimentary fills, walls, ceiling and floor coatings/crusts, and sometimes as their own speleothems (Hill and Forti, 1997; Palmer, 2007). The importance of biological Fe oxidation in caves has long been recognized (Caumartin, 1963). Early studies on the bacterial role in Fe and Mn deposits most relied on microscopy: Peck first reported the presence of Fe-precipitating *Leptothrix* and *Gallionella* species in enrichment cultures inoculated with mud from cave pools and sumps (Peck, 1986). Later, more and more studies hinted the participance of microorganisms in cave Fe oxidation. For instance, freshly Fe oxide precipitates in Pautler Cave showed consistency with biomineralization structures of the microbial genera *Gallionella* and *Leptothrix* (Frierdich et al., 2011), and the iron mats in Borra caves appeared to be related to a community of mostly *Leptothrix*-like iron-oxidizing bacteria (Baskar et al., 2008, 2012). Abiotic Fe oxidation is rapid and prevalent at circumneutral pH yet is inhibited at low pH and microoxic/anoxic environments, where biological Fe oxidation more often occurs (Jones and Northup, 2021). The formation of Fe oxides and the identification of Fe-oxidizing bacteria do not necessarily indicate biological Fe oxidation.

Although Fe oxide minerals generate *via* both biological and abiotic processes, the presence of secondary Mn oxides is usually related to Mn-oxidizing microbes, because abiotic Mn oxidation is kinetically inhibited even at anoxic conditions (Luther, 2010; Johnson et al., 2013). Microbes could increase the rate of Mn oxidation by five orders of magnitude (Emerson, 2000;

Tebo et al., 2005). Microbes related to Mn oxide production have long been reported from cave systems, and bacterial species belonging to *Proteobacteria*, *Firmicutes*, *Actinobacteria* and *Bacteroidetes* were reported to oxidize Mn (Carmichael and Bräuer, 2015). For example, Mn-oxidizing *Pseudomonas*, *Leptothrix*, *Flavobacterium* and *Janthinobacterium* species were isolated from cave ferromanganese deposits (Carmichael et al., 2013a); the well-known Mn-oxidizing *Pedomicrobium* and *Caulobacter* species were also observed in cave stromatolites (Lozano and Rossi, 2012). Most of the Mn oxidizers described to date are heterotrophic, they are supposed to oxidize Mn indirectly through producing superoxide during growth (Learman et al., 2011). However, Mn oxidation has long been regarded to be a potential energy-yielding reaction, and chemolithoautotrophic Mn oxidation was recently documented by Yu and Leadbetter (2020). A co-culture of two microbial species was obtained and the co-culture possibly coupled extracellular manganese oxidation to aerobic energy conservation and autotrophic carbon fixation (Yu and Leadbetter, 2020). Mn oxidation is largely influenced by exogenous carbon input, dilute sewage into the cave lead to massive bloom of a microbiome-driven and Mn-oxidizing biofilm (Carmichael et al., 2013b). Although bacteria attracted more attention in cave biogeochemical cycling, Mn-oxidizing fungi are also identified in caves. *Acremonium nepalense* was found responsible for black Mn oxides on clayey sediments of Lascaux Cave (Saiz-Jimenez et al., 2012); Mn-oxidizing members belonging to *Ascomycota* were obtained in southern Appalachian cave systems, and the results suggested that anthropogenic carbon sources stimulated fungi-driven Mn oxidation (Carmichael et al., 2015).

The role of microbes in cave N cycle

Due to the dark and oligotrophic conditions, cave microorganisms use various metabolic pathways to retrieve nutrients and energy. In the world's largest contiguous karst system, the Nullarbor Plain, extensive caves have been discovered (Webb and James, 2006). These caves are isolated from photosynthetically derived carbon, and no organic carbon was detected from filtered water flooding deeper portions of the caves (James and Rogers, 1994). However, dense biofilms with high biomass are widespread in Nullarbor caves, forming "mantles" of biological material associated with "snowfields" of microcrystals (Contos et al., 2001). Chemical analysis of water samples from Nullarbor caves showed relatively high levels of nitrite and remarkable sulfate and nitrate, indicating the existence of chemoautotrophic bacterial communities (Holmes et al., 2001). Holmes et al. (2001) also performed the first microbial community assessment of these slime biofilms, and revealed high proportion of clones belonging to *Nitrospira*, of which all characterized members carry the potential to oxidize nitrite into nitrate. These results suggested that nitrite oxidation could be essential to the trophic structure of Nullarbor cave communities. About 10 years later, Tetu et al. (2013) performed metagenomic and 16S rRNA amplicon sequencing of slime biofilms from one of the Nullarbor caves, providing in-deep knowledge of nitrogen transformations of these special communities. Their investigation indicated that *Thaumarchaeota* were abundant in the community, and *Thaumarchaeota* predominantly contributed to ammonia oxidation. Based on these studies, it was assumed that slime biofilms in Nullarbor caves had chemolithotrophic communities driven by nitrification. Except for caves with special biofilms like those in Nullarbor plain, sediment samples and ferromanganese deposits from other karstic caves also supported that *Thaumarchaeota* played an essential role in ammonia oxidation (Zhao et al., 2017; Kimble et al., 2018).

Studies with functional gene analysis of various cave samples documented other key N cycle pathways in addition to ammonia oxidation. For example, Kimble et al. (2018) found genes associated with nitrification, dissimilatory and assimilatory nitrate reduction, and denitrification in cave ferromanganese deposits with low fixed N; while Jones et al. detected nitrogen assimilation genes in cave biofilms where fixed N was available (Jones et al., 2012). In our previous work, a collection of cave bacterial genomes was established based on large-scale isolation and cultivation (Zhu et al., 2021). Except for many cave isolates carry genetic potential to perform denitrification and dissimilatory nitrate reduction, we also noticed that 11 genomes in the dataset showed the potential to fix nitrogen into biologically available ammonia. A novel nitrogen-fixing species *Azospirillum cavernae* was also identified from our cultured cave bacterial collections. These microbe-involved nitrogen transformation processes are summarized in Figure 1C.

The role of microbes in cave S cycle

The biogeochemical cycle of sulfur instead of those of carbon and nitrogen was assumed being the center stage in sulfuric acid speleogenetic (SAS) caves (Hedrich and Schippers, 2021). Italy has about 25% of identified SAS cave systems worldwide, among which Frasassi cave system is the best documented and still active one (Galdenzi and Menichetti, 1995; D'Angeli et al., 2019). Extremely acidic (pH 0–1) microbial biofilms, which are known as "snottites," hang on the walls and ceilings of these hydrogen sulfide-rich caves (Hose et al., 2000). Studies based on 16S rRNA cataloging showed that the Frasassi snottites were among the lowest diversities of natural microbial communities ever known, and were constituted mainly of bacteria related to *Acidithiobacillus* species, sometimes with other less abundant bacteria and archaea (Macalady et al., 2007). Jone et al. investigated the metabolic potential and ecological role of snottite *Acidithiobacillus* using metagenomics sequencing, and revealed that the population was autotrophic, and oxidizing sulfur *via* the sulfide-quinone reductase and *sox* pathways, indicating *Acidithiobacillus* was the snottite architect and main primary producer (Jones et al., 2012).

Moreover, *Acidithiobacillus thiooxidans* obtained from the Frasassi cave snottites was also reported to carry a high potential to remove arsenic from contaminated sediments (Beolchini et al., 2017).

Microbial activity is also crucial for cave sulfide oxidation below the water table; the springs and discharge streams in SAS caves are colonized by thick, filamentous microbial mats (Engel et al., 2004b). Sulfide can be oxidized completely to sulfate with sufficient electron acceptors such as oxygen or nitrate; however, incomplete sulfide oxidization to sulfur would occur if low oxygen and nitrate are available. Due to intracellular or extracellular elemental sulfur globules formed by the partial oxidation of dissolved sulfide, biofilms in cave water have a milky appearance (Jones and Northup, 2021). Based on fluorescence *in situ* hybridization (FISH) and 16S rRNA gene libraries, ε-*Proteobacteria* and γ-*Proteobacteria* are crucial biofilm-forming members, and their distribution is primarily influenced by water flow (shear stress) and sulfide to oxygen ratios (Engel et al., 2003, 2004a). In rock-attached streamers, filamentous ε-*Proteobacteria* dominated at high while *Thiothrix* belonging to γ-*Proteobacteria* dominated at low sulfide to oxygen ratios; and in sediment–water interface, *Beggiatoa* belonging to γ-*Proteobacteria* was the dominant group regardless of sulfide to oxygen ratio (Macalady et al., 2008). Stream biofilms from Frasassi cave system were abundant in filamentous γ-*Proteobacteria*, among which *Beggiatoa*-like and/or *Thiothrix*-like cells contain large amount of sulfur inclusions (Macalady et al., 2006). Hamilton et al. (2015) retrieved *Sulfurovum*-like ε-*Proteobacteria* genomes through metagenomic sequencing of SAS cave biofilms, and indicated that this group is genetically equipped to catalyze sulfur precipitation while employing a lithoautotrophic lifestyle. Genes for the transformation of other sulfur-containing compounds were also reported in caves (Zhu et al., 2021), and these processes are summarized in Figure 1D.

Featuring cave bioprocesses with C cycle

Due to limited nutrients, cave microbes have been reported to utilize diverse carbon and energy sources (Figure 1B). Our previous work noticed that genomes of cave bacterial isolates encode the genes for carbon monoxide oxidation (Zhu et al., 2021), a process that can either provide supplementary energy source without contributing biomass or couple with carbon dioxide fixation for biosynthesis under aerobic conditions (King and Weber, 2007). Carbon dioxide fixation is also active in cave microbial communities, there are six known carbon dioxide fixation pathways and the genes for all these pathways were detected in the metagenome of Kartchner cave surface (Ortiz et al., 2014). Aromatic hydrocarbons can be trapped by stalagmites or carried into caves through dripping water; consequently, bacteria that are able to degrade these compounds were detected in caves (Perrette et al., 2008; Marques et al., 2019). Microorganisms that are capable to use one-carbon compounds were obtained from Movile cave, and these microbes were proposed to be one of the main primary producers of the community (Wischer et al., 2015). In addition to traditional methanotrophs, the uncultured atmospheric methane-oxidizing bacteria were believed to be abundant in cave environment, which will be discussed detailly in the following part.

Atmospheric methane oxidizers

As a potent greenhouse gas, the concentration of atmospheric methane is increasing (Nisbet et al., 2016; Prather and Holmes, 2017). Estimation showed that human activities and natural sources produce about 680 Tg year^{-1} of methane to the atmosphere, while reactions with hydroxyl and chlorine radicals in the troposphere and stratosphere remove about 600 Tg year^{-1} of methane (Kirschke et al., 2013). Methanotrophic microorganisms in forests, grasslands, paddy and other unsaturated soils play an essential role in mediating carbon cycle, and are believed to filter 30 Tg year^{-1} of methane (Kirschke et al., 2013). However, there is still gap in the overall methane budget balances. Recent studies suggested that caves and related karst terrains may be an essential yet overlooked sink for atmospheric methane.

Fernandez-Cortes et al. (2015) first monitored the concentration of methane and carbon dioxide in seven caves located in Spain, and the results proved that subterranean environments acted as sinks for atmospheric methane on seasonal and daily scales. They also detected methane-oxidizing bacteria in some cave sediments where methane concentrations were near to the atmospheric background, yet no such microbes were detected in sample sites with minimal methane concentrations. Thus, Fernandez-Cortes et al. assumed that cave methane oxidation was mainly induced by oxidative capacity from high density of ions, and was not significantly intervened by methanotrophic bacteria. However, through controlled laboratory experiment, Nguyễn-Thuỳ et al. (2017) showed that the radiolysis hypothesis is kinetically constrained and is unlikely to lead to rapid methane loss. Instead, by performing a set of mesocosm experiments with rock samples from two Vietnamese caves, they revealed that the depleted concentrations of methane in caves were most likely associated with microbial activity rather than radiolysis. Following these pioneering works, more and more evidence were reported from various caves to support microbes involved cave methane oxidation. For example, stable carbon and hydrogen isotope compositions of methane from 33 epigenic caves in the United States and 3 in New Zealand all supported that microbial methanotrophy within caves was the main methane consumption mechanism (Webster et al., 2018). Ojeda et al. (2019) also noticed methanotrophic activity of γ- and α-*Proteobacteria* in Nerja cave in Spain.

Methanotrophs have been reported since early twentieth century, and were detected at various habitats such as mud, rivers, rice paddies, sediments and sewage sludge (Whittenbury et al., 1970; Hanson and Hanson, 1996). Although atmospheric

methane oxidation rates can remain steady for more than 4 months at 1.7 ppmv of methane (Schnell and King, 1995), calculations based on the kinetic constants of isolated methanotrophic bacteria could not support such extended survival (Conrad, 1984). Studies with *Methylosinus trichosporium* and *Methylobacter albus* revealed that atmospheric methane oxidation did not supply sufficient cellular maintenance energy and reduced power for the methane monooxygenase (Roslev and King, 1994; Schnell and King, 1995). The organisms responsible for atmospheric methane uptake were unknown until Holmes et al. (1999) reported a novel group of bacteria belonging to α-*Proteobacteria*, which is distantly related to existing methane-oxidizing strains and is believed to consume atmospheric methane. Later, Knief et al. (2003) identified another novel atmospheric methane-oxidizing group belonging to γ-*Proteobacteria* through comparative sequence analysis of the *pmoA* gene, and named these two groups as "upland soil cluster α" (USC α) and "upland soil cluster γ" (USC γ), respectively. Culture-independent studies suggested that USC α is adapted to the low concentration of methane in neutral and acidic soils (Kolb et al., 2005; Martineau et al., 2014) while USC γ prefers neutral to alkalic soils (Kolb, 2009). Tveit et al. (2019) reported the first pure culture *Methylocapsa gorgona* MG08 that grows on air at atmospheric methane, and proved that the strain is closely related to uncultured members of USC α. However, the cultivation of members related to USC γ remains challenging.

The investigation of cave methanotrophic bacteria is far earlier than the discovery that caves may be important methane sink. Hutchens et al. (2004) identified strains of *Methylomonas*, *Methylococcus* and *Methylocystis*/*Methylosinus* as major methanotrophs in Movile Cave through DNA-based stable isotope probing. However, the air of Movile Cave contains 1–2% (10,000–20,000 ppmv) methane (Sarbu and Kane, 1995), which is much higher than general 1.86 ppmv atmospheric level. Zhao et al. (2018) explored the presence and diversity of methane-oxidizing bacteria in Heshang Cave, where methane concentration decreases from 1.9 ppmv at the entrance to 0.65 ppmv inside the cave. Their results provided compelling evidence that methane-oxidizing bacteria accounted for up to 20% of the whole microbial communities with the high-affinity USC γ being the dominant group. According to sequencing analysis of *pmoA* and 16S rRNA genes of weathered rock samples from three karst cave in southwest China, Cheng et al. (2021) demonstrated that USC γ group dominated the atmospheric methane-oxidizing communities, and was identified as a keystone taxon in cooccurrence networks of both methane-oxidizing and the total bacterial communities. In addition to atmospheric methane-oxidizing groups, anaerobic methane-oxidizing bacteria were also detected from some cave samples. For example, members of the phylum *Rokubacteria* were found in Pindal Cave, these organisms perform anaerobic oxidation of methane coupled to nitrite reduction (Cuezva et al., 2020).

Novel antibiotic compound producers from cave

Infectious diseases have long been threatening human society, while sprouting antibiotic-resistant pathogens are posing heavier burdens to human public health. According to the World Health Organization (WHO), there is an urgent need for investment of new antibiotics to combat antibiotic-resistant infections (World Health Organization, 2015). With a combination of unique environmental conditions and rare human intervention, more and more studies turned to caves for microorganisms producing novel antibiotics.

It has been proved that *Actinobacteria* are prolific producers of promising bioactive compounds with wide application. Approximately 45% of identified bioactive compounds are produced by *Actinobacteria*, among which 80% are derived from the *Streptomyces* genus (Bérdy, 2005). Sequencing analysis revealed the dominance of *Actinobacteria* in plenty of cave samples, such as cave soils (Wiseschart et al., 2019), cave sediments (De Mandal et al., 2015a,b), cave rocks (Zhu et al., 2019) and colonies on cave Paleolithic paintings (Stomeo et al., 2008). The isolates of *Streptomyces* genus were also obtained from many caves, such as Sigangli Cave in China (Fang et al., 2017), Altamira Cave and Tito Bustillo Cave in Spain (Groth et al., 1999), and Iron Curtain Cave in Canada (Gosse et al., 2019). Caves are not only home for various known actinobacterial taxa, but also excellent reservoir for new species of *Actinobacteria*. Forty-seven species within 30 genera belonging to *Actinobacteria* were isolated from caves and cave-related habitats from 1999 to 2018, among which seven represented novel genera (Rangseekaew and Pathom-aree, 2019). It is assumed that the extreme conditions within caves stimulated the inhabitant microorganisms to mutate their genes, making it more likely to evolve new species and novel metabolites (Tiwari and Gupta, 2013).

Isolating cave microorganisms and subsequently checking their antimicrobial activity against pathogens is one of the main approaches to identify novel antibiotics. By adopting such strategy, Herold et al. (2005) reported cervimycins, which are highly active against some Gram-positive bacteria. These compounds are produced by *Streptomyces tendae* HKI 0179, a strain isolated from a rock wall of an ancient cave in Italy. Another example is the discovery of Huanglingmycins, which are produced by *Streptomyces* sp. CB09001 from cave soil of China (Jiang et al., 2018). Noticeably, Huanglongmycin A showed not only weak activity against some Gram-negative bacteria, but also moderate cytotoxicity against A549 lung cancer cell line. Although certain bioactive compounds were not identified, some rare cave actinobacterium also showed anticancer potential. For instance, *Spirillospora albida* isolated from Phanangkhoi Cave were active against NCI-H1870 (human small lung cancer cell; Nakaew et al., 2009a); *Nonomurea roseola* isolated from Phatup Cave showed activity against human oral cavity cancer and human small lung cancer cells (Nakaew et al., 2009b). In addition, antifungal compounds were also documented from cave environment.

Antagonistic *Streptomyces*, *Micromonospora*, *Streptosporangium*, and *Dactylosporangium* isolated from five caves in Korea showed biocontrol activities against at least one of the rice pathogenic fungi (Nimaichand et al., 2015); *Streptomyces* sp. from five caves in New Mexico and the United States has been suggested to inhibit the growth of the causative fungus of white-nose syndrome in bats (Hamm et al., 2017).

Perspectives

Cave ecosystems form a huge subsurface reactor for the global biogeochemical cycle. The roles of microorganisms in both cave formation and subterranean key elements cycling are among the 50 top priority questions in subterranean biology (Mammola et al., 2020). It is now believed that many substantial mineral transformations, originally considered abiotic processes, are mediated by microbes: from microbial carbonate precipitation to the production of Fe and Mn deposits (Jones and Northup, 2021). As extremely starved environments, chemolithotrophic microbial communities driven by nitrification and sulfur oxidation have also been identified in cave ecosystems, providing valuable information on subterranean biogeochemical cycles (Jones et al., 2012; Tetu et al., 2013). These processes would not only transform minerals, change the air composition or water pH, but also lead to reshaping the cave. However, only 10% of all caves on earth have been accessed by humans, and even as many as 50% of caves in Europe and North America remain unexplored (Lee et al., 2012). As such, many more efforts are needed to explore cave microbiology, and further developments in caving technology and analytical tools are also essential to accomplish this goal.

The investigation about how microorganisms survive in nutrient-limited caves expanded our knowledge on controlling human impacts and protecting cave environments. For example, caves in north Spain contain Paleotic paintings, yet tourist activities brought in heterotrophic bacteria, threatening to damage the cultural treasures (Cañaveras et al., 2001). Furthermore, cave environment created stress for the inhabitant microorganisms at genetic level, making it a reservoir of novel microbial species and bioactive compounds. Although many cave bacterial isolates showed inhibitory properties against pathogens, only a few metabolites got identified chemical structure (Rangseekaew and Pathom-aree, 2019). The advent of genomics, transcriptomics and proteomics will facilitate the research of inter- and intra-community relationships which previously only be addressed under *in vitro* conditions. Nonetheless, to successfully isolate microorganisms that are adapted to cave environment and actively participate in element cycling is of vital importance yet remains challenging. Atmospheric methane oxidation in caves emerges as a hot research topic, although sequencing analysis proposed that USC γ played the major role, members of this group remain yet to be cultured (Cheng et al., 2021). On the one hand, a comprehensive understanding of factors affecting cave inhabitants is needed to discover ideal conditions for microbial growth; on the other hand, innovative cultivation techniques such as membrane diffusion-based cultivation, microfluidics-based cultivation and cell sorting-based cultivation are also worth applying (Lewis et al., 2020). By combining culture-dependent and sequencing-based techniques, cave microbiology explorations would lead to more exciting discoveries of subterranean environments.

Author contributions

H-ZZ: writing the original draft. C-YJ and S-JL: discussion, editing, and finalizing the manuscript. All authors contributed to the article and approved the submitted version.

Funding

This study was financially supported by the National Natural Science Foundation of China (grant no. 91951208).

Conflict of interest

The authors declare that the research was conducted in the absence of any commercial or financial relationships that could be construed as a potential conflict of interest.

Publisher's note

References

Adam, D., Maciejewska, M., Naome, A., Martinet, L., Coppieters, W., Karim, L., et al. (2018). Isolation, characterization, and antibacterial activity of hard-to-culture Actinobacteria from cave Moonmilk deposits. *Antibiotics-Basel* 7:20. doi: 10.3390/antibiotics7020028

Axenovgibanov, D. V., Voytsekhovskaya, I. V., Tokovenko, B. T., Protasov, E. S., Gamaiunov, S. V., Rebets, Y. V., et al. (2016). Actinobacteria isolated from an underground Lake and Moonmilk speleothem from the biggest conglomeratic karstic cave in Siberia as sources of novel biologically active compounds. *PLoS One* 11:e0149216. doi: 10.1371/journal.pone.0149216

Banks, E. D., Taylor, N. M., Gulley, J., Lubbers, B. R., Giarrizzo, J. G., Bullen, H. A., et al. (2010). Bacterial calcium carbonate precipitation in cave environments: a function of calcium homeostasis. *Geomicrobiol J.* 27, 444–454. doi: 10.1080/01490450903485136

Barton, H. A., and Jurado, V. (2007). "What's up down there? Microbial diversity in caves" in *Microbe*. ed. M. Schaechter (Washington, DC: ASM Press), 132–138.

Baskar, S., Baskar, R., Lee, N., Kaushik, A., and Theophilus, P. K. (2008). Precipitation of iron in microbial mats of the spring waters of Borra caves, Vishakapatnam, India: some geomicrobiological aspects. *Environ. Geol.* 56, 237–243. doi: 10.1007/s00254-007-1159-y

Baskar, S., Baskar, R., Thorseth, I. H., Ovreas, L., and Pedersen, R. B. (2012). Microbially induced iron precipitation associated with a neutrophilic spring at Borra caves, Vishakhapatnam, India. *Astrobiology* 12, 327–346. doi: 10.1089/ast.2011.0672

Beolchini, F., Fonti, V., Ozdemiroglu, S., Akcil, A., and Dell'Anno, A. (2017). Sulphur-oxidising bacteria isolated from deep caves improve the removal of arsenic from contaminated harbour sediments. *Chem. Ecol.* 33, 103–113. doi: 10.1080/02757540.2017.1281252

Bérdy, J. (2005). Bioactive microbial metabolites. *J. Antibiot. (Tokyo)* 58, 1–26. doi: 10.1038/ja.2005.1

Bindschedler, S., Cailleau, G., Braissant, O., Millière, L., Job, D., and Verrecchia, E. P. (2014). Unravelling the enigmatic origin of calcitic nanofibres in soils and caves: purely physicochemical or biogenic processes? *Biogeosciences* 11, 2809–2825. doi: 10.5194/bg-11-2809-2014

Bindschedler, S. L. M., Cailleau, G. D. J., and Verrecchia, E. (2010). Calcitic nanofibres in soils and caves: a putative fungal contribution to carbonatogenesis. *Geol. Soc. London Spec. Publ.* 336, 225–238. doi: 10.1144/SP336.11

Brannen-Donnelly, K., and Engel, A. (2015). Bacterial diversity differences along an epigenic cave stream reveal evidence of community dynamics, succession, and stability. *Front. Microbiol.* 6:729. doi: 10.3389/fmicb.2015.00729

Cañaveras, J. C., Cuezva, S., Sanchez-Moral, S., Lario, J., Laiz, L., Gonzalez, J. M., et al. (2006). On the origin of fiber calcite crystals in moonmilk deposits. *Naturwissenschaften* 93, 27–32. doi: 10.1007/s00114-005-0052-3

Cañaveras, J. C., Sanchez-Moral, S., Soler, V., and Saiz-Jimenez, J. (2001). Microorganisms and Microbially induced fabrics in cave walls. *Geomicrobiol J.* 18, 223–240. doi: 10.1080/01490450152467769

Carmichael, S. K., and Bräuer, S. L. (2015). "Microbial diversity and manganese cycling: a review of manganese-oxidizing microbial cave communities" in *Microbial Life of Cave Systems*. ed. A. S. Engel (Berlin, München, Boston, MA: De Gruyter), 137–160.

Carmichael, M. J., Carmichael, S. K., Santelli, C. M., Strom, A., and Bräuer, S. L. (2013a). Mn(II)-oxidizing bacteria are abundant and environmentally relevant members of ferromanganese deposits in caves of the upper Tennessee River basin. *Geomicrobiol J.* 30, 779–800. doi: 10.1080/01490451.2013.769651

Carmichael, S., Carmichael, M., Strom, A., Johnson, K., Roble, L., Gao, Y., et al. (2013b). Sustained anthropogenic impact in Carter saltpeter cave, Carter County, Tennessee and the potential effects on manganese cycling. *J. Cave Karst Stud.* 75, 189–204. doi: 10.4311/2012MB0267

Carmichael, S. K., Zorn, B. T., Santelli, C. M., Roble, L. A., Carmichael, M. J., and Bräuer, S. L. (2015). Nutrient input influences fungal community composition and size and can stimulate manganese (II) oxidation in caves. *Environ. Microbiol. Rep.* 7, 592–605. doi: 10.1111/1758-2229.12291

Castanier, S., Métayer-Levrel, G. L., and Perthuisot, J.-P. (2000). "Bacterial roles in the precipitation of carbonate minerals" in *Microbial Sediments*. eds. R. E. Riding and S. M. Awramik (Berlin, Heidelberg: Springer Berlin Heidelberg), 32–39.

Caumartin, V. (1963). Review of the microbiology of underground environments. *Bull. Natl. Speleol. Soc.* 25, 1–14.

Cheng, X. Y., Liu, X. Y., Wang, H. M., Su, C. T., Zhao, R., Bodelier, P. L. E., et al. (2021). USC gamma dominated community composition and Cooccurrence network of Methanotrophs and bacteria in subterranean karst caves. *Microbiol. Spectr* 9:e00820-21. doi: 10.1128/Spectrum.00820-21

Conrad, R. (1984). "Capacity of aerobic microorganisms to utilize and grow on atmospheric trace gases (H2, CO, CH4)", in *Current Perspectives in Microbial Ecology: Proceedings of the Third International Symposium on Microbial Ecology*. eds. M.J. Klug and C.A. Reddy. (Washington, DC: American Society for Microbiology).

Contos, K. A., James, J. M., Pitt, B. H. K., and Rogers, P. (2001). Morphoanalysis of bacterially precipitated subaqueous calcium carbonate from Weebubbie cave, Australia. *Geomicrobiol. J.* 18, 331–343. doi: 10.1080/01490450152467822

Cuezva, S., Martin-Pozas, T., Fernandez-Cortes, A., Canaveras, J. C., Janssens, I., and Sanchez-Moral, S. (2020). "on the role of cave-soil in the carbon cycle. A fist approach", in: EGU general assembly 2020. (online).

Cunningham, K. I., Northup, D. E., Pollastro, R. M., Wright, W. G., and Larock, E. J. (1995). Bacteria, fungi and biokarst in Lechuguilla cave, Carlsbad Caverns National Park, New Mexico. *Environ. Geol.* 25, 2–8. doi: 10.1007/BF01061824

D'Angeli, I. M., Parise, M., Vattano, M., Madonia, G., Galdenzi, S., and De Waele, J. (2019). Sulfuric acid caves of Italy: a review. *Geomorphology* 333, 105–122. doi: 10.1016/j.geomorph.2019.02.025

Danielli, H. M. C., and Edington, M. A. (1983). Bacterial calcification in limestone caves. *Geomicrobiol J.* 3, 1–16. doi: 10.1080/01490458309377780

De Mandal, S., Panda, A. K., Lalnunmawii, E., Bisht, S. S., and Kumar, N. S. (2015a). Illumina-based analysis of bacterial community in Khuangcherapuk cave of Mizoram, Northeast India. *Genom. Data* 5, 13–14. doi: 10.1016/j.gdata.2015.04.023

De Mandal, S., Sanga, Z., and Senthil Kumar, N. (2015b). Metagenome sequencing reveals Rhodococcus dominance in Farpuk cave, Mizoram, India, an Eastern Himalayan Biodiversity Hot Spot Region. *Genome Announc.* 3:e00610-15. doi: 10.1128/genomeA.00610-15

Emerson, D. (2000). "microbial oxidation of Fe(II) and Mn(II) at Circumneutral pH" in *Environmental Microbe-metal Interactions*. ed. D. R. Lovley (Washington, DC: American Society for Microbiology), 31–52.

Engel, A. S., Lee, N., Porter, M. L., Stern, L. A., Bennett, P. C., and Wagner, M. (2003). Filamentous "Epsilonproteobacteria" dominate microbial mats from sulfidic cave springs. *Appl. Environ. Microbiol.* 69, 5503–5511. doi: 10.1128/aem.69.9.5503-5511.2003

Engel, A. S., Porter, M. L., Stern, L. A., Quinlan, S., and Bennett, P. C. (2004a). Bacterial diversity and ecosystem function of filamentous microbial mats from aphotic (cave) sulfidic springs dominated by chemolithoautotrophic "Epsilonproteobacteria". *FEMS Microbiol. Ecol.* 51, 31–53. doi: 10.1016/j.femsec.2004.07.004

Engel, A. S., Stern, L. A., and Bennett, P. C. (2004b). Microbial contributions to cave formation: new insights into sulfuric acid speleogenesis. *Geology* 32, 369–372. doi: 10.1130/g20288.1

Fang, B.-Z., Salam, N., Han, M.-X., Jiao, J.-Y., Cheng, J., Wei, D.-Q., et al. (2017). Insights on the effects of heat pretreatment, pH, and calcium salts on isolation of rare Actinobacteria from karstic caves. *Front. Microbiol.* 8:1535. doi: 10.3389/fmicb.2017.01535

Fernandez-Cortes, A., Cuezva, S., Alvarez-Gallego, M., Garcia-Anton, E., Pla, C., Benavente, D., et al. (2015). Subterranean atmospheres may act as daily methane sinks. *Nat. Commun.* 6:7003. doi: 10.1038/ncomms8003

Ford, D. (2006). "Karst geomorphology, caves and cave deposits: a review of north American contributions during the past half century" in *Perspectives on Karst Geomorphology, Hydrology and Geochemistry*. eds. R. S. Harmon and C. W. Wicks (Boulder, CO: GSA Special Paper 404)

Ford, D., and Williams, P. D. (2007). *Karst Hydrogeology and Geomorphology*. West Sussex: Wiley.

Frierdich, A. J., Hasenmueller, E. A., and Catalano, J. G. (2011). Composition and structure of nanocrystalline Fe and Mn oxide cave deposits: implications for trace element mobility in karst systems. *Chem. Geol.* 284, 82–96. doi: 10.1016/j.chemgeo.2011.02.009

Gabriel, C. R., and Northup, D. E. (2013). "Microbial ecology: caves as an extreme habitat" in *Cave Microbiomes: A Novel Resource For Drug Discovery*. ed. N. Cheeptham (New York, NY: Springer), 85–108.

Galdenzi, S., and Menichetti, M. (1995). Occurrence of hypogenic caves in a karst region: examples from Central Italy. *Environ. Geol.* 26, 39–47. doi: 10.1007/BF00776030

Gonzalez, J. M., Portillo, M. C., and Saiz-Jimenez, C. (2006). Metabolically active Crenarchaeota in Altamira cave. *Naturwissenschaften* 93, 42–45. doi: 10.1007/s00114-005-0060-3

Gosse, J. T., Ghosh, S., Sproule, A., Overy, D., Cheeptham, N., and Boddy, C. N. (2019). Whole genome sequencing and Metabolomic study of cave Streptomyces isolates ICC1 and ICC4. *Front. Microbiol.* 10:1020. doi: 10.3389/fmicb.2019.01020

Groth, I., Vettermann, R., Schuetze, B., Schumann, P., and Saiz-Jimenez, C. (1999). Actinomycetes in karstic caves of northern Spain (Altamira and Tito Bustillo). *J. Microbiol. Methods* 36, 115–122. doi: 10.1016/S0167-7012(99)00016-0

Hamilton, T. L., Jones, D. S., Schaperdoth, I., and Macalady, J. L. (2015). Metagenomic insights into S(0) precipitation in a terrestrial subsurface lithoautotrophic ecosystem. *Front. Microbiol.* 5:756. doi: 10.3389/fmicb.2014.00756

Hamm, P. S., Caimi, N. A., Northup, D. E., Valdez, E. W., Buecher, D. C., Dunlap, C. A., et al. (2017). Western bats as a reservoir of novel Streptomyces species with antifungal activity. *Appl. Environ. Microbiol.* 83:e03057-16. doi: 10.1128/aem.03057-16

Hanson, R. S., and Hanson, T. E. (1996). Methanotrophic bacteria. *Microbiol. Rev.* 60, 439–471. doi: 10.1128/mr.60.2.439-471.1996

Hathaway, J. J. M., Garcia, M. G., Balasch, M. M., Spilde, M. N., Stone, F. D., Dapkevicius, M. D. L. N. E., et al. (2014). Comparison of bacterial diversity in Azorean and Hawai'ian lava cave microbial mats. *Geomicrobiol J.* 31, 205–220. doi: 10.1080/01490451.2013.777491

Hedrich, S., and Schippers, A. (2021). Distribution of acidophilic microorganisms in natural and man-made acidic environments. *Curr. Issues Mol. Biol.* 40, 25–48. doi: 10.21775/cimb.040.025

Herold, K., Gollmick, F. A., Groth, I., Roth, M., Menzel, K. D., Möllmann, U., et al. (2005). Cervimycin A-D: a polyketide glycoside complex from a cave bacterium can defeat vancomycin resistance. *Chemistry* 11, 5523–5530. doi: 10.1002/chem.200500320

Hill, C. A., and Forti, P. (1997). *Cave Minerals of the World*. Huntsville, AL: National Speleological Society.

Holmes, A. J., Roslev, P., McDonald, I. R., Iversen, N., Henriksen, K., and Murrell, J. C. (1999). Characterization of methanotrophic bacterial populations in soils showing atmospheric methane uptake. *Appl. Environ. Microbiol.* 65, 3312–3318. doi: 10.1128/aem.65.8.3312-3318.1999

Holmes, A. J., Tujula, N. A., Holley, M., Contos, A., James, J. M., Rogers, P., et al. (2001). Phylogenetic structure of unusual aquatic microbial formations in Nullarbor caves, Australia. *Environ. Microbiology* 3, 256–264. doi: 10.1046/j.1462-2920.2001.00187.x

Hose, L. D., Palmer, A. N., Palmer, M. V., Northup, D. E., Boston, P. J., and DuChene, H. R. (2000). Microbiology and geochemistry in a hydrogen-sulphide-rich karst environment. *Chem. Geol.* 169, 399–423. doi: 10.1016/S0009-2541(00)00217-5

Hubelova, D., Ulmann, V., Mikuska, P., Licbinsky, R., Alexa, L., Modra, H., et al. (2021). Nontuberculous mycobacteria prevalence in aerosol and Spiders' webs in karst caves: low risk for Speleotherapy. *Microorganisms* 9:2573. doi: 10.3390/microorganisms9122573

Hutchens, E., Radajewski, S., Dumont, M. G., McDonald, I. R., and Murrell, J. C. (2004). Analysis of methanotrophic bacteria in Movile cave by stable isotope probing. *Environ. Microbiol.* 6, 111–120. doi: 10.1046/j.1462-2920.2003.00543.x

Jagnow, D. H., Hill, C. A., Davis, D., DuChene, H., Cunningham, K. I., Northup, D., et al. (2000). History of the sulfuric acid theory of speleogenesis in the Guadalupe Mountains, New Mexico. *J. Cave Karst Stud.* 62, 54–59.

James, J. M., and Rogers, P. (1994). "The 'mysterious' calcite precipitating organism of the Nullarbor caves, Australia" in *Breakthroughs in Karst Geomicrobiology and Redox Geochemistry*. eds. I. D. Sasowsky and M. V. Palmer (Charlestown: Karst Waters Institute), 34–35.

Jiang, L., Pu, H., Xiang, J., Su, M., Yan, X., Yang, D., et al. (2018). Huanglongmycin A-C, cytotoxic polyketides biosynthesized by a putative type II polyketide synthase from Streptomyces sp. CB09001. *Front. Chem.* 6:254. doi: 10.3389/fchem.2018.00254

Johnson, J. E., Webb, S. M., Thomas, K., Ono, S., Kirschvink, J. L., and Fischer, W. W. (2013). Manganese-oxidizing photosynthesis before the rise of cyanobacteria. *Proc. Natl. Acad. Sci. U. S. A.* 110, 11238–11243. doi: 10.1073/pnas.1305530110

Jones, D. S., Albrecht, H. L., Dawson, K. S., Schaperdoth, I., Freeman, K. H., Pi, Y. D., et al. (2012). Community genomic analysis of an extremely acidophilic sulfur-oxidizing biofilm. *ISME J.* 6, 158–170. doi: 10.1038/ismej.2011.75

Jones, D. S., and Macalady, J. L. (2016). "The snotty and the stringy: energy for subsurface life in caves" in *Their World: A Diversity of Microbial Environments. Advances in Environmental Microbiology*. ed. C. J. Hurst (Switzerland: Springer), 203–224.

Jones, D. S., and Northup, D. E. (2021). Cave decorating with microbes: Geomicrobiology of caves. *Elements* 17, 107–112. doi: 10.2138/gselements.17.2.107

Jones, D. S., Schaperdoth, I., and Macalady, J. L. (2014). Metagenomic evidence for sulfide oxidation in extremely acidic cave biofilms. *Geomicrobiol J.* 31, 194–204. doi: 10.1080/01490451.2013.834008

Kimble, J. C., Winter, A. S., Spilde, M. N., Sinsabaugh, R. L., and Northup, D. E. (2018). A potential central role of Thaumarchaeota in N-cycling in a semi-arid environment, Fort Stanton cave, Snowy River passage, New Mexico, USA. *FEMS Microbiol. Ecol.* 94:fly173. doi: 10.1093/femsec/fiy173

King, G. M., and Weber, C. F. (2007). Distribution, diversity and ecology of aerobic CO-oxidizing bacteria. *Nat. Rev. Microbiol.* 5, 107–118. doi: 10.1038/nrmicro1595

Kirschke, S., Bousquet, P., Ciais, P., Saunois, M., Canadell, J. G., Dlugokencky, E. J., et al. (2013). Three decades of global methane sources and sinks. *Nat. Clim. Chang.* 6, 813–823. doi: 10.1038/ngeo1955

Knief, C., Lipski, A., and Dunfield, P. F. (2003). Diversity and activity of Methanotrophic bacteria in different upland soils. *Appl. Environ. Microbiol.* 69, 6703–6714. doi: 10.1128/AEM.69.11.6703-6714.2003

Kolb, S. (2009). The quest for atmospheric methane oxidizers in forest soils. *Environ. Microbiol. Rep.* 1, 336–346. doi: 10.1111/j.1758-2229.2009.00047.x

Kolb, S., Knief, C., Dunfield, P. F., and Conrad, R. (2005). Abundance and activity of uncultured methanotrophic bacteria involved in the consumption of atmospheric methane in two forest soils. *Environ. Microbiol.* 7, 1150–1161. doi: 10.1111/j.1462-2920.2005.00791.x

Learman, D. R., Voelker, B. M., Vazquez-Rodriguez, A. I., and Hansel, C. M. (2011). Formation of manganese oxides by bacterially generated superoxide. *Nat. Geosci.* 4, 95–98. doi: 10.1038/ngeo1055

Lee, N. M., Meisinger, D. B., Aubrecht, R., Kovacikfi, L., Porter, M. L., and Engel, A. S. (2012). "Life in caves and karst environments" in *Life at Extremes: Environments, Organisms and Strategies For Survival*. ed. E. M. Bell (Wallingford: CABI), 320–344.

Lewis, W. H., Tahon, G., Geesink, P., Sousa, D. Z., and Ettema, T. J. G. (2020). Innovations to culturing the uncultured microbial majority. *Nat. Rev. Microbiol.* 19, 225–240. doi: 10.1038/s41579-020-00458-8

Lozano, R. P., and Rossi, C. (2012). Exceptional preservation of Mn-oxidizing microbes in cave stromatolites (El Soplao, Spain). *Sediment. Geol.* 255-256, 42–55. doi: 10.1016/j.sedgeo.2012.02.003

Luther, G. W. (2010). The role of one- and two-electron transfer reactions in forming thermodynamically unstable intermediates as barriers in multi-electron redox reactions. *Aquat. Geochem.* 16, 395–420. doi: 10.1007/s10498-009-9082-3

Macalady, J. L., Dattagupta, S., Schaperdoth, I., Jones, D. S., Druschel, G. K., and Eastman, D. (2008). Niche differentiation among sulfur-oxidizing bacterial populations in cave waters. *ISME J.* 2, 590–601. doi: 10.1038/ismej.2008.25

Macalady, J. L., Jones, D. S., and Lyon, E. H. (2007). Extremely acidic, pendulous cave wall biofilms from the Frasassi cave system, Italy. *Environ. Microbiol.* 9, 1402–1414. doi: 10.1111/j.1462-2920.2007.01256.x

Macalady, J. L., Lyon, E. H., Koffman, B., Albertson, L. K., Meyer, K., Galdenzi, S., et al. (2006). Dominant microbial populations in limestone-corroding stream biofilms, Frasassi cave system, Italy. *Appl. Environ. Microbiol.* 72, 5596–5609. doi: 10.1128/aem.00715-06

Maciejewska, M., Adam, D., Naômé, A., Martinet, L., Tenconi, E., Całusińska, M., et al. (2017). Assessment of the potential role of Streptomyces in cave Moonmilk formation. *Front. Microbiol.* 8:1181. doi: 10.3389/fmicb.2017.01181

Mammola, S., Amorim, I. R., Bichuette, M. E., Borges, P. A. V., Cheeptham, N., Cooper, S. J. B., et al. (2020). Fundamental research questions in subterranean biology. *Biol. Rev.* 95, 1855–1872. doi: 10.1111/brv.12642

Marques, E. L. S., Silva, G. S., Dias, J. C. T., Gross, E., Costa, M. S., and Rezende, R. P. (2019). Cave drip water-related samples as a natural environment for aromatic hydrocarbon-degrading bacteria. *Microorganisms* 7:33. doi: 10.3390/microorganisms7020033

Martineau, C., Pan, Y., Bodrossy, L., Yergeau, E., Whyte, L. G., and Greer, C. W. (2014). Atmospheric methane oxidizers are present and active in Canadian high Arctic soils. *FEMS Microbiol. Ecol.* 89, 257–269. doi: 10.1111/1574-6941.12287

Martin-Pozas, T., Sanchez-Moral, S., Cuezva, S., Jurado, V., Saiz-Jimenez, C., Perez-Lopez, R., et al. (2020). Biologically mediated release of endogenous N(2)O and NO(2) gases in a hydrothermal, hypoxic subterranean environment. *Sci. Total Environ.* 747:141218. doi: 10.1016/j.scitotenv.2020.141218

Modra, H., Bartos, M., Hribova, P., Ulmann, V., Hubelova, D., Konecny, O., et al. (2017). Detection of mycobacteria in the environment of the Moravian karst (bull rock cave and the relevant water catchment area): the impact of water sediment, earthworm castings and bat guano. *Veterinarni Medicina* 62, 153–168. doi: 10.17221/126/2016-vetmed

Nakaew, N., Pathom-aree, W., and Lumyong, S. (2009a). First record of the isolation, identification and biological activity of a new strain of *Spirillospora albida* from Thai cave soil. *Actinomycetologica* 23, 1–7. doi: 10.3209/saj.SAJ230102

Nakaew, N., Pathom-aree, W., and Lumyong, S. (2009b). Generic diversity of rare Actinomycetes from Thai cave soils and their possible use as new bioactive compounds. *Actinomycetologica* 23, 21–26. doi: 10.3209/saj.SAJ230201

Nguyễn-Thuỳ, D., Schimmelmann, A., Nguyễn-Văn, H., Drobniak, A., Lennon, J. T., Tạ, P. H., et al. (2017). Subterranean microbial oxidation of atmospheric methane in cavernous tropical karst. *Chem. Geol.* 466, 229–238. doi: 10.1016/j.chemgeo.2017.06.014

Nimaichand, S., Devi, A. M., Tamreihao, K., Ningthoujam, D. S., and Li, W.-J. (2015). Actinobacterial diversity in limestone deposit sites in Hundung, Manipur (India) and their antimicrobial activities. *Front. Microbiol.* 6:413. doi: 10.3389/fmicb.2015.00413

Nisbet, E. G., Dlugokencky, E. J., Manning, M. R., Lowry, D., Fisher, R. E., France, J. L., et al. (2016). Rising atmospheric methane: 2007–2014 growth and isotopic shift. *Glob. Biogeochem. Cycles* 30, 1356–1370. doi: 10.1002/2016GB005406

Ojeda, L., Vadillo, I., Etiope, G., Benavente, J., Liñán, C., del Rosal, Y., et al. (2019). Methane sources and sinks in karst systems: the Nerja cave and its vadose environment (Spain). *Geochim. Cosmochim. Acta* 259, 302–315. doi: 10.1016/j.gca.2019.06.011

Ortiz, M., Legatzki, A., Neilson, J. W., Fryslie, B., Nelson, W. M., Wing, R. A., et al. (2014). Making a living while starving in the dark: metagenomic insights into the energy dynamics of a carbonate cave. *ISME J.* 8, 478–491. doi: 10.1038/ismej.2013.159

Palmer, A. N. (2007). *Cave Geology*. Dayton: Cave Books.

Palmer, A. N. (2011). Distinction between epigenic and hypogenic maze caves. *Geomorphology* 134, 9–22. doi: 10.1016/j.geomorph.2011.03.014

Pavlik, I., Ulmann, V., Modra, H., Gersl, M., Rantova, B., Zukal, J., et al. (2021). Nontuberculous mycobacteria prevalence in Bats' guano from caves and attics of buildings studied by culture and qPCR examinations. *Microorganisms* 9:2236. doi: 10.3390/microorganisms9112236

Peck, S. B. (1986). Bacterial deposition of iron and manganese oxides in north American caves. *NSS Bull.* 48, 26–30.

Perrette, Y., Poulenard, J., Saber, A.-I., Fanget, B., Guittonneau, S., Ghaleb, B., et al. (2008). Polycyclic aromatic hydrocarbons in stalagmites: occurrence and use for analyzing past environments. *Chem. Geol.* 251, 67–76. doi: 10.1016/j.chemgeo.2008.02.013

Portillo, M. C., and Gonzalez, J. M. (2011). Moonmilk deposits originate from specific bacterial communities in Altamira cave (Spain). *Microb. Ecol.* 61, 182–189. doi: 10.1007/s00248-010-9731-5

Portillo, M. C., Porca, E., Cuezva, S., Cañaveras, J. C., Sanchez-Moral, S., and Gonzalez, J. M. (2009). Is the availability of different nutrients a critical factor for the impact of bacteria on subterraneous carbon budgets? *Naturwissenschaften* 96, 1035–1042. doi: 10.1007/s00114-009-0562-5

Prather, M. J., and Holmes, C. D. (2017). Overexplaining or underexplaining methane's role in climate change. *Proc. Natl. Acad. Sci. U. S. A.* 114, 5324–5326. doi: 10.1073/pnas.1704884114

Rangseekaew, P., and Pathom-aree, W. (2019). Cave Actinobacteria as producers of bioactive metabolites. *Front. Microbiol.* 10:387. doi: 10.3389/fmicb.2019.00387

Reitschuler, C., Spötl, C., Hofmann, K., Wagner, A. O., and Illmer, P. (2016). Archaeal distribution in Moonmilk deposits from alpine caves and their Ecophysiological potential. *Microb. Ecol.* 71, 686–699. doi: 10.1007/s00248-015-0727-z

Roslev, P., and King, G. M. (1994). Survival and recovery of Methanotrophic bacteria starved under Oxic and anoxic conditions. *Appl. Environ. Microbiol.* 60, 2602–2608. doi: 10.1128/aem.60.7.2602-2608.1994

Saiz-Jimenez, C., Miller, A. Z., Martin-Sanchez, P. M., and Hernandez-Marine, M. (2012). Uncovering the origin of the black stains in Lascaux cave in France. *Environ. Microbiol.* 14, 3220–3231. doi: 10.1111/1462-2920.12008

Sarbu, S. M., Aerts, J. W., Flot, J. F., Van Spanning, R. J. M., Baciu, C., Ionescu, A., et al. (2018). Sulfur cave (Romania), an extreme environment with microbial mats in a CO_2-H_2S/O_2 gas chemocline dominated by mycobacteria. *Int. J. Speleol.* 47, 173–187. doi: 10.5038/1827-806x.47.2.2164

Sarbu, S. M., and Kane, T. C. (1995). A subterranean chemoautotrophically based ecosystem. *NSS Bull.* 57, 91–98.

Schnell, S., and King, G. M. (1995). Stability of methane oxidation capacity to variations in methane and nutrient concentrations. *FEMS Microbiol. Ecol.* 17, 285–294. doi: 10.1016/0168-6496(95)00034-8

Sendra, A., Garay, P., Ortuno, V. M., Gilgado, J. D., Teruel, S., and Reboleira, A. (2014). Hypogenic versus epigenic subterranean ecosystem: lessons from eastern Iberian Peninsula. *Int. J. Speleol.* 43, 253–264. doi: 10.5038/1827-806x.43.3.2

Stomeo, F., Portillo, M. C., Gonzalez, J. M., Laiz, L., and Saiz-Jimenez, C. (2008). Pseudonocardia in white colonizations in two caves with Paleolithic paintings. *Int. Biodeterior. Biodegradation* 62, 483–486. doi: 10.1016/j.ibiod.2007.12.011

Tebo, B. M., Johnson, H. A., McCarthy, J. K., and Templeton, A. S. (2005). Geomicrobiology of manganese(II) oxidation. *Trends Microbiol.* 13, 421–428. doi: 10.1016/j.tim.2005.07.009

Tetu, S. G., Breakwell, K., Elbourne, L. D., Holmes, A. J., Gillings, M. R., and Paulsen, I. T. (2013). Life in the dark: metagenomic evidence that a microbial slime community is driven by inorganic nitrogen metabolism. *ISME J.* 7, 1227–1236. doi: 10.1038/ismej.2013.14

Tisato, N., Torriani, S. F. F., Monteux, S., Sauro, F., De Waele, J., Tavagna, M. L., et al. (2015). Microbial mediation of complex subterranean mineral structures. *Sci. Rep.* 5:15525. doi: 10.1038/srep15525

Tiwari, K., and Gupta, R. K. (2013). Diversity and isolation of rare actinomycetes: an overview. *Crit. Rev. Microbiol.* 39, 256–294. doi: 10.3109/1040841x.2012.709819

Tveit, A. T., Hestnes, A. G., Robinson, S. L., Schintlmeister, A., Dedysh, S. N., Jehmlich, N., et al. (2019). Widespread soil bacterium that oxidizes atmospheric methane. *Proc. Natl. Acad. Sci. U. S. A.* 116, 8515–8524. doi: 10.1073/pnas.1817812116

Vanderwolf, K., Malloch, D., McAlpine, D., and Forbes, G. (2013). A world review of fungi, yeasts, and slime molds in caves. *Int. J. Speleol.* 42, 77–96. doi: 10.5038/1827-806X.42.1.9

Vlasceanu, L., Sarbu, S. M., Engel, A. S., and Kinkle, B. K. (2000). Acidic cave-wall biofilms located in the Frasassi gorge, Italy. *Geomicrobiol. J.* 17, 125–139. doi: 10.1080/01490450050023809

Webb, J. A., and James, J. M. (2006). "Karst evolution of the Nullarbor Plain, Australia" in *Karst Geomorphology, Hydrology and Geochemistry*. eds. R. S. Harmon and C. M. Wicks (Boulder, CO: Geological Society of America), 65–78.

Webster, K. D., Drobniak, A., Etiope, G., Mastalerz, M., Sauer, P. E., and Schimmelmann, A. (2018). Subterranean karst environments as a global sink for atmospheric methane. *Earth Planet. Sci. Lett.* 485, 9–18. doi: 10.1016/j.epsl.2017.12.025

Whittenbury, R., Phillips, K. C., and Wilkinson, J. F. (1970). Enrichment, isolation and some properties of methane-utilizing bacteria. *J. Gen. Microbiol.* 61, 205–218. doi: 10.1099/00221287-61-2-205

Wischer, D., Kumaresan, D., Johnston, A., El Khawand, M., Stephenson, J., Hillebrand-Voiculescu, A. M., et al. (2015). Bacterial metabolism of methylated amines and identification of novel methylotrophs in Movile cave. *ISME J.* 9, 195–206. doi: 10.1038/ismej.2014.102

Wiseschart, A., Mhuantong, W., Tangphatsornruang, S., Chantasingh, D., and Pootanakit, K. (2019). Shotgun metagenomic sequencing from Manao-pee cave, Thailand, reveals insight into the microbial community structure and its metabolic potential. *BMC Microbiol.* 19:144. doi: 10.1186/s12866-019-1521-8

World Health Organization (2015). *Global Action Plan On Antimicrobial Resistance*. Geneva: World Health Organization.

Wu, Y., Tan, L., Liu, W., Wang, B., Wang, J., Cai, Y., et al. (2015). Profiling bacterial diversity in a limestone cave of the western loess plateau of China. *Front. Microbiol.* 6:244. doi: 10.3389/fmicb.2015.00244

Yu, H., and Leadbetter, J. R. (2020). Bacterial chemolithoautotrophy via manganese oxidation. *Nature* 583, 453–458. doi: 10.1038/s41586-020-2468-5

Zhang, Z. F., Liu, F., Zhou, X., Liu, X. Z., Liu, S. J., and Cai, L. (2017). Culturable mycobiota from karst caves in China, with descriptions of 20 new species. *Persoonia* 39, 1–31. doi: 10.3767/persoonia.2017.39.01

Zhang, Z.-F., Zhou, S.-Y., Eurwilaichitr, L., Ingsriswang, S., Raza, M., Chen, Q., et al. (2021). Culturable mycobiota from karst caves in China II, with descriptions of 33 new species. *Fungal Divers.* 106, 29–136. doi: 10.1007/s13225-020-00453-7

Zhang, Y. H., and Zhu, D. H. (2012). The distribution and evolution of China's big karst caves. *J. Guilin Univ. Technol.* 32, 20–28. doi: 10.3969/j.issn.1674-9057.2012.01.003

Zhao, R., Wang, H., Cheng, X., Yun, Y., and Qiu, X. (2018). Upland soil cluster gamma dominates the methanotroph communities in the karst Heshang cave. *FEMS Microbiol. Ecol.* 94:fiy192. doi: 10.1093/femsec/fiy192

Zhao, R., Wang, H. M., Yang, H., Yun, Y., and Barton, H. A. (2017). Ammonia-oxidizing archaea dominate ammonia-oxidizing communities within alkaline cave sediments. *Geomicrobiol J.* 34, 511–523. doi: 10.1080/01490451.2016.1225861

Zhu, H.-Z., Zhang, Z.-F., Zhou, N., Jiang, C.-Y., Wang, B.-J., Cai, L., et al. (2019). Diversity, distribution and co-occurrence patterns of bacterial communities in a karst cave system. *Front. Microbiol.* 10:1726. doi: 10.3389/fmicb.2019.01726

Zhu, H.-Z., Zhang, Z.-F., Zhou, N., Jiang, C.-Y., Wang, B.-J., Cai, L., et al. (2021). Bacteria and metabolic potential in karst caves revealed by intensive bacterial cultivation and genome assembly. *Appl. Environ. Microbiol.* 87, e02440–e02420. doi: 10.1128/AEM.02440-20

frontiers | Frontiers in Microbiology

TYPE Original Research
PUBLISHED 10 November 2022
DOI 10.3389/fmicb.2022.982933

OPEN ACCESS

EDITED BY
Gorji Marzban,
University of Natural Resources and Life Sciences Vienna, Austria

REVIEWED BY
Donatella Tesei,
University of Natural Resources and Life Sciences Vienna, Austria
Nami Kartal,
İstanbul University-Cerrahpasa, Turkey

*CORRESPONDENCE
Filomena De Leo
fdeleo@unime.it

SPECIALTY SECTION
This article was submitted to Terrestrial Microbiology, a section of the journal Frontiers in Microbiology

RECEIVED 30 June 2022
ACCEPTED 17 October 2022
PUBLISHED 10 November 2022

CITATION
De Leo F, Dominguez-Moñino I, Jurado V, Bruno L, Saiz-Jimenez C and Urzì C (2022) Fungal outbreak in the Catacombs of SS. Marcellino and Pietro Rome (Italy): From diagnosis to an emergency treatment. *Front. Microbiol.* 13:982933. doi: 10.3389/fmicb.2022.982933

Fungal outbreak in the Catacombs of SS. Marcellino and Pietro Rome (Italy): From diagnosis to an emergency treatment

Filomena De Leo[1]*, Irene Dominguez-Moñino[2], Valme Jurado[2], Laura Bruno[3], Cesareo Saiz-Jimenez[2] and Clara Urzì[1]

[1]Department of ChiBioFarAm, University of Messina, Messina, Italy, [2]Institute for Natural Resources and Agrobiology, Spanish National Research Council (IRNAS-CSIC), Seville, Spain, [3]Department of Biology, University of Rome "Tor Vergata," Rome, Italy

The present study reports a sudden fungal outbreak that occurred in the corridor near the entrance of the Catacombs of SS. Marcellino and Pietro in Rome (Italy) observed after 1 year of a restoration treatment that interested the walls of the entrance of the Catacombs and some artifacts placed *in situ*. The colonization was observed on the vault at the entrance and in correspondence with the restored marble pieces displayed on the left side of the corridor. No growth was observed on the right side where similarly treated marble slabs were placed. Samples taken in correspondence with fungal biofilm were analyzed through the combined use of microscopical, cultural, and molecular tools and showed that the vault and the left side of the corridor entrance were colonized by a complex fungal biofilm consisting mainly of *Coniophora* sp. and other genera, such as *Hypomyces*, *Purpureocillium*, *Acremonium*, *Penicillium*, and *Alternaria*, many of which are well known as responsible of biodeterioration of stone surfaces. Regarding the brown-rot basidiomycete *Coniophora*, it was able to form very large colonies on the substrata with a diameter of up to 57 cm. Although the direct observation under a light microscope evidenced the presence of abundant brown fungal conidia, several attempts to cultivate the microorganism failed, therefore only through DNA sequencing analyses, it was possible to identify and characterize this fungus. There is very little literature on the genus *Coniophora* which is reported as one of the causes of wet-rot decay of wood in buildings. A connection with calcium-containing materials such as bricks and mortars was demonstrated, but no data were available about the possible role of this

species in the biodeterioration of stones. This study features the first finding of a strain related to the basidiomycetous genus of *Coniophora* in the order Boletales in association with evident phenomena of biodeterioration.

KEYWORDS

Roman Catacombs, biodeterioration, Basidiomycetes, *Coniophora* species, fungal outbreak

Introduction

Fungi are well known for their ability to colonize a plethora of substrata, both organic and inorganic due to their ubiquitous characteristics and their great adaptability to nutrient concentrations, either low or rich.

Hypogea, due to the physico-chemical characteristics of quite stable temperature, high relative humidity, and continuous availability of organic sources (derived from soil, dead animals, microorganisms, visitors, etc.) represent a favorable environment for microbial growth. However, as reported by Urzì et al. (2018), studies on fungi in hypogean environments are relatively scarce, especially in the cultural heritage context.

Vanderwolf et al. (2013) listed 1,029 fungal species in 518 genera that mainly belonged to the phylum Ascomycota found in caves and mines worldwide, underlining that the origin and ecological role of fungi in hypogean environments remain unknown although they are related to the ubiquitous, oligotrophic, and psychrotrophic characteristics of the species found.

The presence of fungi in hypogean environments has been often associated with evident phenomena of biodeterioration among which are listed white and gray alterations, black stains, and profuse mycelial growth (Dupont et al., 2007; Jurado et al., 2009, 2010; Bastian et al., 2010; Urzì et al., 2010; De Leo et al., 2012; Martin-Sanchez et al., 2012; Ma et al., 2015; Sugiyama et al., 2017; Zucconi et al., 2022). Sudden changes and/or fluctuation of microenvironmental parameters may cause spore germination with a consequent rapid, intense, and diffuse fungal colonization on plaster and frescoes (Caneva et al., 2005). These events of heavy fungal colonization were described several times in Roman hypogea and were attributed to the opening and closing of the doors to allow the entrance of visitors and/or restoration activities that boosted the dissemination of spores (Florian, 1996; Albertano et al., 2005). Similar events described as "fungal outbreak" were observed in the Lascaux Cave in France and Castañar de Ibor Cave in Spain (Dupont et al., 2007; Bastian et al., 2010; Jurado et al., 2010; Martin-Sanchez et al., 2014).

This study aimed to investigate the sudden and heavy fungal outbreak that occurred in the vault and corridor near the entrance of the Catacombs of SS. Marcellino and Pietro in Rome (Italy), observed 1 year after a restoration treatment that interested the walls of the entrance of the Catacombs and some marble artifacts placed *in situ*. This fungal growth could have compromised both the fruition by visitors due to the possible allergenic effect of airborne spores, and the state of conservation of the monument, therefore some emergency treatments were also suggested.

Materials and methods

Case study

Catacombs of SS. Marcellino and Pietro

The Catacombs of Saints Marcellino and Pietro were excavated between the third and fifth centuries A.C. and are also called the Catacombs of St. Elena or Catacombs of St. Tiburzio. They are one of the largest Catacombs situated on the third mile of the ancient *Via* Labicana, today *Via* Casilina in Rome, Italy, near the church of "SS. Marcellino and Pietro" ad Duas Lauros (at two laurels) (**Figures 1A–D**).

The Catacombs evolve in several corridors (**Figure 1A**), some of them still contain sealed niches with a skeleton inside, and in the past phototrophic biofilms as biodeteriogenic patinas have been described there (Bruno et al., 2019). Further, they contain several cubicula with high-quality frescoes (**Figure 1B**).

For this reason, they were chosen to be part of the Jubilee path of Mercy 2015–2016. Before the opening and thus to allow safer access to visitors, a new entrance was opened, and the Catacombs underwent a restoration intervention (2014–2015) for the implementation of the safety conditions of the Catacombs. At the end of Summer of 2015 on the walls and vault near the entrance, a sudden growth of black/brown colonies with a yellow halo was observed as well as the presence of smaller white/grayish colonies (**Figures 2A–C**).

Sampling areas

The fungal biofilm observed on the Catacombs surfaces appeared as very large colonies of dark brown color with a diameter varying up to 50 cm and more than 120 cm on the vault, depending on the growth stage (**Figures 2A,D**). Sometimes smaller grayish-white colonies of considerably

FIGURE 1
Overview of the SS. Marcellino and Pietro Catacombs in Rome. **(A)** Tomb excavated in the tupha; **(B)** cubicula (small room) with colorful frescoes; and **(C)** olive tree above the ground of the Catacombs.

smaller size were observed on top of the dark large colonies. Fungal growth was also observed at the edge of marble slabs displayed on the left side of the entrance corridor (**Figures 2A–C**).

Relative humidity (RH) and temperature (°C) were recorded at the different parts of the Catacombs entrance and corridor, through a portable thermohygrometer Hanna Instruments HI18564, while irradiance was measured using a radiometer (model LI-185B; LI-COR inc., USA) equipped with a quantum sensor (LI-190SB) to give a measure of the PAR (Photosynthetic active radiation) in μmol photons m^{-2} s^{-1}.

A multi-step approach consisting of airborne spores sampling, microscopy, and cultural and molecular analyses was carried out.

To assess the presence of airborne spores, adhesive tapes, commonly used for aerobiological analyses (Brighetti et al., 2014), were placed in small open Petri dishes near the contaminated areas for 24 h and then removed and observed at the light microscope Zeiss Axioscope. Experiments were performed in triplicate.

A total of 13 samples were taken from four different sites of the Catacombs indicated with numbers from 1 to 4, in correspondence of evident fungal colonization showing different pigmentation as brown (B), white (W), and yellow (Y) and morphology by using (a) the non-destructive sampling methods of adhesive tape strips (FungiTape© Did, Milan, Italy) (Urzì and De Leo, 2001) for carrying out microscopy and cultural analysis; and (b) a sterile scalpel for scraping little amounts of mycelium from lithic substrata for molecular analysis, as summarized in **Table 1**. In particular, four samples were taken from sites 1 and 2, three samples from sites 3, and two samples from site 4. Adhesive tape samples were preliminary cut

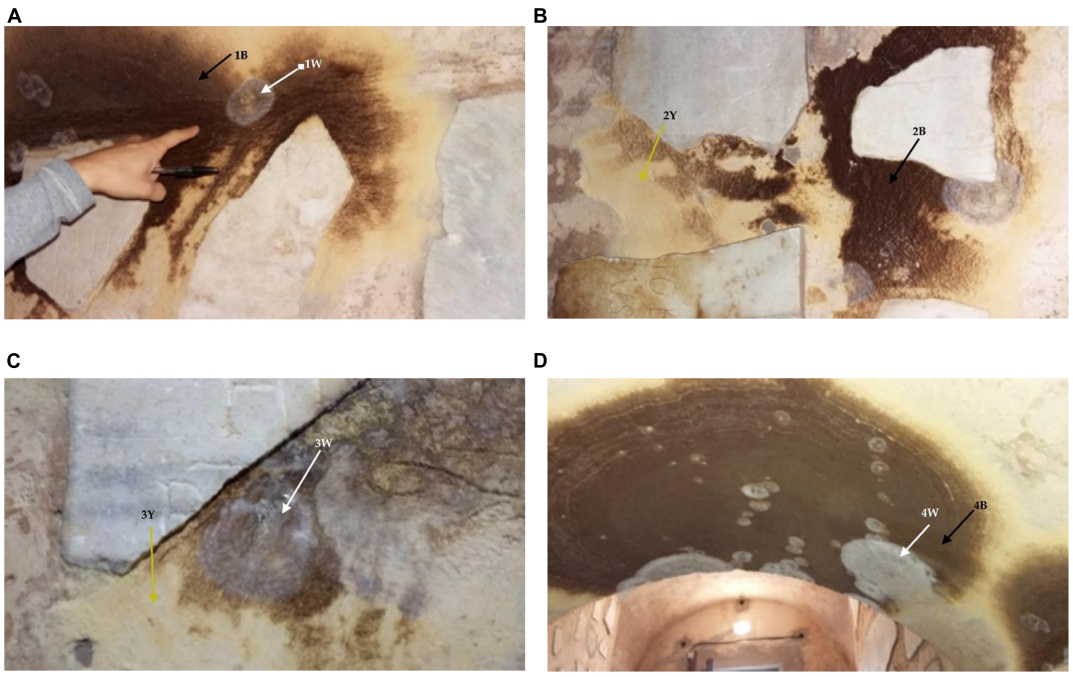

FIGURE 2
Macroscopic view of the fungal outbreak occurring on the wall and vault at the entrance of the Catacombs SS. Marcellino and Pietro. **(A)** Extensive brown and white/grayish fungal growth around a marble piece in correspondence of sampling point 1; **(B)** brown and white/grayish colonies around another marble piece in correspondence of sample 2; **(C)** brown and white/grayish fungal colonization on the sampling point 3; and **(D)** extended dark brown fungal colonization with secondary white/grayish colonies observed on the entrance vault in correspondence of sampling point 4. Arrows indicate the sampling points.

TABLE 1 Samples were taken from the fungal biofilms on the wall and vault of the Catacombs, the size of colonies, and modality of sampling.

Samples	Morphology of fungal colonies on substrata	Diameter (cm)	Adhesive tape	Scalpel
1B	Brown with abundant aerial mycelium	57	+	+
1W	White/grayish, flat	9	+	+
2Y	Yellow biofilm, no aerial mycelium	47	+	+
2B	Brown with abundant aerial mycelium	7	+	+
3W	White/grayish flat	n.d.	+	–
3Y	Yellow biofilm no aerial mycelium	n.d.	+	+
4W	White/grayish flat	34	+	–
4B	Brown colony with abundant aerial mycelium	>120	+	–

into little squares of about 0.5 cm^2 and used for microscopy and cultural analyses, while biofilm samples were analyzed through molecular methods.

Microscopy

Samples taken with adhesive tape were directly observed under Light Microscopy equipped with phase contrast (LM, Leica DMLB Wetzlar, Germany). To this purpose, little squares of adhesive tape were placed face down on a glass slide with a drop of sterile water or Amman's lactophenol solution and covered with a cover slide to keep the tape as flat as possible as described by Urzì and coworkers (Urzì and Albertano, 2001; Urzì and De Leo, 2001).

TABLE 2 Environmental parameters measured at the four sampling sites.

SITE	PARμ mol m^{-2} s^{-1}	RH%	T°
1	0.1–0.4	86	21.9
2	0.5	86.1	21.9
3	1.2	86.2	21.8
4	0.1–0.3	86.9	21.8

TABLE 3 Nearest neighbor rDNA sequences of *Coniophora marmorata* and references from NCBI databases and bibliographic references.

Sample	Representative clone	No. of clones	Closest relative sequences and % of similarity	References
1B	1B_K51	9	*Coniophora marmorata* 83.07% AJ518879	Schmidt et al., 2002; Schmidt and Moreth, 2002
	1W_K10	4	*Coniophora marmorata* 84.63% AJ518879	Schmidt et al., 2002; Schmidt and Moreth, 2002
2B	2B_K2	9	*Coniophora marmorata* 83.36% AJ518879	Schmidt et al., 2002; Schmidt and Moreth, 2002
2Y	2Y_K2	8	*Coniophora marmorata* 84.05% AJ518879	Schmidt et al., 2002; Schmidt and Moreth, 2002
3Y	3Y_K1	8	*Coniophora marmorata* 84.13% AJ518879	Schmidt et al., 2002; Schmidt and Moreth, 2002

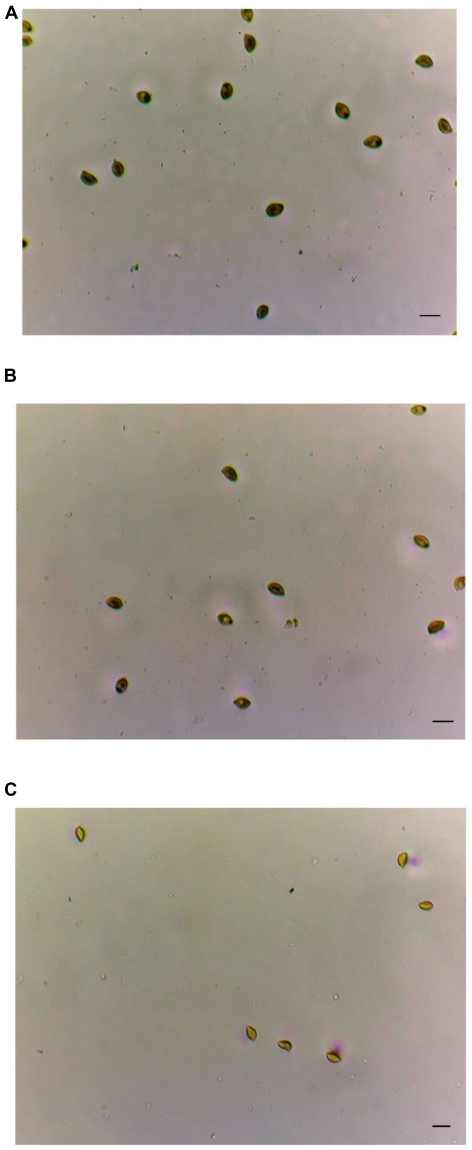

FIGURE 3
Quali/quantitative determination of airborne conidia taken after 24 h of exposure to adhesive tapes for aerobiological analysis. **(A)** At the entrance; **(B)** at the beginning of the corridor; and **(C)** toward the end of the corridor. In all the samples, the number of airborne spores/24 h was quite homogeneous in the studied environment in each microscopic area examined. Bar is 10 mm.

Cultural analyses

Cultural analyses were carried out by placing a little square of adhesive tape as above specified onto the center of agar plates of Dichlorane Rose Bengal Chloramphenicol medium (DRBC, Oxoid, Basingstoke, UK) in duplicate. Malt Extract Diclorane Agar (MYBDA), LGBA Lignin Guaiacol Benomyl agar medium with Indulin AT (1 g/L), LGBA with Humic acid (1 g/L), and LGBA with Indulin AT (1 g/L), and Humic acid (1 g/L) (Thorn et al., 1996; Thompson, 1998; Thompson et al., 2012) were used when the first attempt to grow the oval-conidia producers in DRBC failed. Incubation was carried out at 26°C for up to 1 month.

Fungal isolates identification was carried out based on the macroscopic feature of colonies grown on different cultural media and the micro-morphology of reproductive structures, according to Ellis (1971, 1976), Barnett and Hunter (1972), Fassatiovà (1986), and de Hoog et al. (2019).

Molecular analyses of samples

Molecular techniques were used for the evidence and identification of fungi from biofilm samples (1W, 1B, 2B, 2Y, and 3Y). No molecular analyses were carried out for sample 4 due to the similarity of the alteration observed and then confirmed under the microscope by the homogeneous presence of conidia comparable to those of samples 1 and 2. DNA was extracted using FastDNA SPIN Kit for Soil (MP Biomedicals, Illkirch, France). The fungal internal transcribed spacer regions were amplified by polymerase chain reaction (PCR) using the primers ITS1 (5′-TCC GTA GGT GAA CCT GCG G-3′) and ITS4 (5′-TCC TCC GCT TAT TGA TAT GC-3′) (White et al., 1990). PCR amplifications were performed in a Bio-Rad iCycler thermal cycler (Bio-Rad, Hercules, CA, USA) using the following thermal conditions: one cycle of denaturation (94°C for 2 min), followed by 35 cycles of denaturation (94°C for 1 min), annealing (50°C for 1 min), elongation (72°C for 10 min), and a terminal elongation step (72°C for 5 min) (Jurado et al., 2010). Amplification products were evaluated by electrophoresis on 1% (w/v) agarose gels, stained with SYBR Green I (Molecular

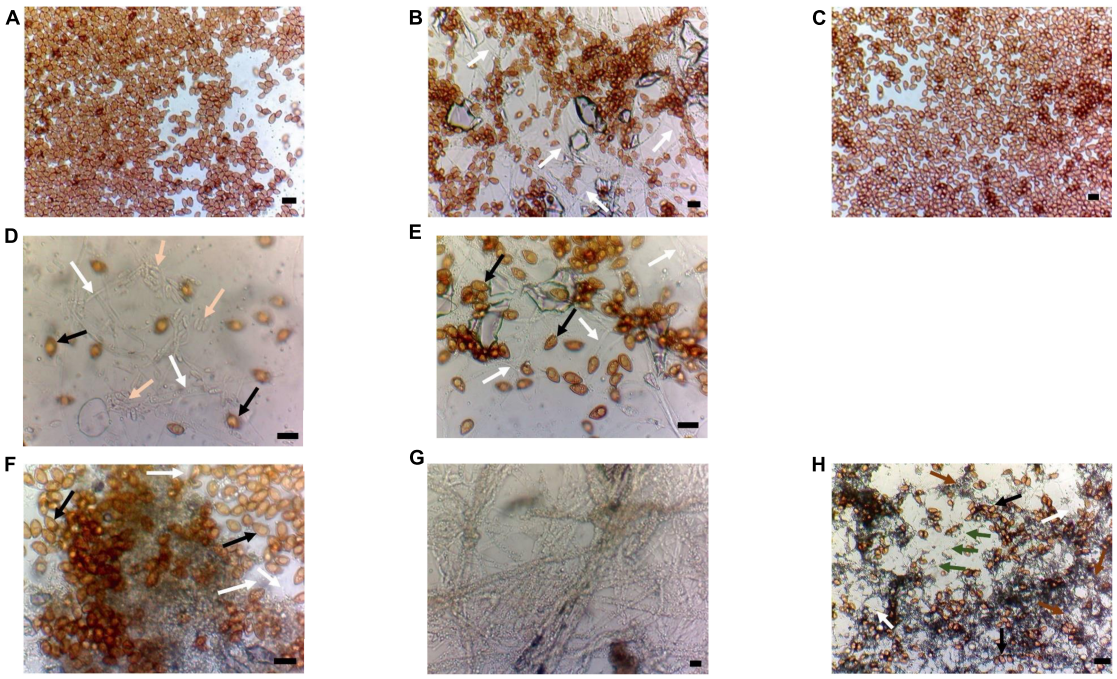

FIGURE 4
Adhesive tape samples were taken in correspondence with brown colonies and yellow and white colonies as shown in **Figure 2**. **(A–C)** Brown colonies. **(A)** Sample 1B; **(B)** sample 2B; and **(C)** sample 4B. Morphological observations suggest the presence of homogeneous oval Basidiomycetes conidia; in panel **(b)** are also visible hyaline hyphae (indicated by white arrows). **(D,E)** Yellow biofilm. **(D)** Sample 2Y; and **(E)** sample 3Y; it is observed the contemporary presence of black conidia and hyaline one (*Fusarium*-like) and hyaline hyphae (indicated by black, pink, and white arrows, respectively); **(E)** only black conidia and hyaline hyphae (indicated by black and white arrows, respectively). **(F–H)** White/grayish colonies. **(F)** The abundant presence of black ovoidal conidia and hyaline hyphae in the background (indicated by black and white arrows, respectively); **(G)** only hyaline hyphae; and **(H)** are visible two kinds of conidia (black ovoidal and roundish this latter attributable to *Aspergillus niger* indicated by black and green arrows, respectively) as well as hyaline and melanized hyphae (indicated by white and brown arrows, respectively). Bar is 10 mm.

Probes, Eugene, OR, USA), and visualized under UV light (Martin-Sanchez et al., 2014). The amplified PCR products were purified using the JetQuick PCR Purification Spin Kit (Genomed, Löhne, Germany). Purified products were cloned with a TOPO-TA Cloning Kit for Sequencing (Invitrogen, Carlsbad, CA, USA) and then were transformed into One Shot DH5α-T1 competent cells *Escherichia coli* (Invitrogen, Carlsbad, CA, USA), according to the manufacturer's instructions. Selected clones for each sample were sequenced by Macrogen Inc. (Amsterdam, Netherlands). Fungal identification was performed using the BLASTn algorithm (Altschul et al., 1990) to the non-redundant databases of sequences deposited at the National Center for Biotechnology Information (NCBI). The sequences were deposited into the GenBank database under accession numbers which are as follows: ON5101061 and ON510107-ON510111. For phylogenetic analyses, sequences were retrieved from the GenBank database that is accessible from NCBI platforms.[1] Alignments were created using the multiple sequence alignment program MUSCLE (Edgar, 2004). Molecular Evolution Genetic Analyses version 11 was employed for phylogenetic tree construction (Tamura et al., 2021). The evolutionary history using the ITS region sequences was inferred by using the máximum-likelihood method, Kimura's two-parameter model with a discrete Gamma distribution, and invariant sites (Kimura, 1980). The robustness of the tree was evaluated by bootstrap resampling (1,000 replicates).

Results and discussion

The results obtained are summarized in **Tables 2**, **3** and **Figures 3–5**.

The microclimatic parameters evidenced in all the sampling sites are quite uniform values regarding RH%, T°, and light intensity as shown in **Table 2**.

The aerobiological analyses reported a constant presence in the air of black conidia whose findings were also confirmed by the consequent contamination of the surfaces seen under the microscope observation (**Figure 3**).

1 http://www.ncbi.nlm.nih.gov, accessed on 9 May 2022 and 26 August 2022.

In particular, the slides observed for the aerobiological qualitative determination of the air quality as well as the adhesive samples taken from the brown colony (1B, 2B, 3B, and 4B) showed the almost exclusive presence, widespread and numerous, of fungal conidia with a morphology that is compatible with conidia of fungal species belonging to the phylum Basidiomycota. Microscopic observation of samples taken from the different colonies such as those described as yellow (Y) or white/grayish (W) showed the coexistence of hyaline hyphae and ovoid dark-colored spores confirming the spread of fungal spores of Basidiomycetes (**Figure 4**) as well as the presence of secondary colonization due to the ubiquitous Ascomycetous genera of *Aspergillus*, *Penicillium, Alternaria, Fusarium*, and *Paecilomyces*, as confirmed by the findings of cultural analysis (**Supplementary Figure 1** and **Supplementary Table 1**). No fungal strains associated with the black conidia observed under direct microscopy have grown in the cultural media.

Only through molecular analyses of biofilm samples, it was possible to demonstrate the dominant presence of basidiomycetous species related to the brown-rot fungal genus *Coniophora*. The sequence similarity search showed that the closest species belonged to the *Coniophora* genus with a low percentage of identity (in all cases less than 86.92%) and, in particular, the nearest sequences of *Coniophora marmorata* (AJ518879), the only *Coniophora* species known to be able to grow on rocks, mortars, and bricks, was ranging from 83.07 to 84.63% of sequence identity (**Table 3** and **Figure 5**). These low percentages are evidence that the fungal strains causing the outbreak in the Catacombs of SS. Marcellino and Pietro most likely represent a new species. However, efforts to culture the fungus in the laboratory failed, despite the wide range of culture media used. The clone 1W K2 (ON 510107) representative of five clones, resulted near to the specie of *Hypomyces chlorinigenus* (93.23% KT946843, Otto et al., 2016).

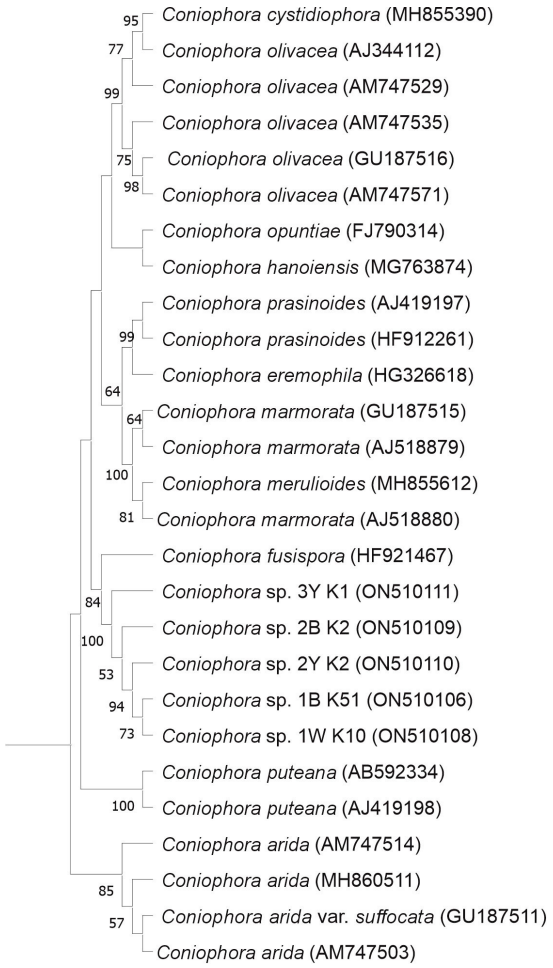

FIGURE 5
Maximum-likelihood phylogenetic tree based on ITS region sequences showing the relationship of *Coniophora* species. Bootstrap values (>50%) are expressed as percentages of 1,000 replicates. The sequence of *Actinomyces oris* (NR104896) was used as an outgroup.

Discussion

Our analysis demonstrated that the vault and the left side of the corridor at the entrance of the Catacombs of SS. Marcellino and Pietro were heavily affected by fungal colonization mainly due to a strain related to the basidiomycetous genus of *Coniophora* in the order Boletales. In further support of this attribution, the presence of the ascomycetous strains belonging to the genus *Hypomyces*, which are well-known parasites of *Boletales* species, was evidenced (Rogerson and Samuels, 1989). Members of the genus *Coniophora*, among which *C. puteana* and the less common species *C. marmorata*, *C. arida*, and *C. olivacea*, the so-called "cellar fungi" are known responsible for wood brown-rot in indoor and outdoor buildings structures (Schmidt, 2007; Gabriel and Švec, 2017). Moreover, *C. marmorata* has been associated with calcareous materials such as bricks and mortars (Singh, 1994) but to our knowledge, its biodeteriorative activity on stone monuments has never been demonstrated.

The *Coniophora* species are very difficult to distinguish from each other, and traditional cultural methods fail to grow this fungus. Thus, molecular techniques were applied to obtain a reliable method for their differentiation. However, the results obtained were not conclusive; due to the low percentage of rDNA sequence similarity, we may even suppose that the strain associated with the outbreak could belong to a not yet identified species. Further studies are in progress both to attempt the cultivation of the fungus that would allow it to deepen its physiology and taxonomy, and to investigate the possible sources of contamination. Although, no decaying wood was observed in the studied site, the presence of protruding roots of an olive tree situated above the ground in the proximity of the fungal colonization was observed (**Figure 1C**). Further

inspection of the tree did not show any apparent illness at the time of the study, but this does not exclude the tree or its roots as a possible source of contamination.

Regarding their risk potential to health, the existing literature is not vast and only a few studies (Helbling et al., 1999) have shown cases of allergic reactions due to Basidiomycetes. So, although these are not notoriously allergenic microorganisms, it is not possible to completely exclude the risk for operators and visitors. Given the extent of macrocolonies, their fast growth rate, and the spread of spores in high quantities, we suggested an emergency intervention aimed at reducing the colonization process and at the same time decreasing the risk of allergic reactions and/or asthma attacks both toward operators and visitors, especially for those subjects with reduced immune defenses, such as the elderly, children, and people with respiratory diseases.

The treatments foreseen are (a) intervention on the environment by continuous monitoring of the level of circulating spores and appearance of newly formed colonies; and (b) biocide treatments direct to the fungal colonies. Due to the fact that several causes could have created this fungal outbreak, continuous monitoring of the Catacomb's surfaces is still undergoing.

Data availability statement

The datasets presented in this study can be found in online repositories. The names of the repository/repositories and accession number(s) can be found in the article/**Supplementary material**.

Author contributions

FD, LB, CU, and CS-J: conceptualization. LB, FD, ID-M, and VJ: methodology. FD, CU, and VJ: resources. FD, LB, CU, CS-J, and VJ: data curation, writing—original draft preparation and review, and editing. All authors have read and agreed to the published version of the manuscript.

Funding

This project was supported thanks to the special funds provided by the University of Messina (approved on 21 February 2022 by the Academic Senatus) (Italy), the Spanish Ministry of Science and Innovation, and project PID2020-114978GB-I00 and project CIACCO DTC TE1 – FASE II – PROGETTI RSI8.

Acknowledgments

We are grateful to Raffaella Giuliani of the "Pontificia Commissione di Archeologia Sacra" in Rome for her open collaboration and the permission to investigate the Catacombs of SS. Marcellino and Pietro and to the center "CMA-P.Albertano" for the use of the CLSM.

Conflict of interest

The authors declare that the research was conducted in the absence of any commercial or financial relationships that could be construed as a potential conflict of interest.

Publisher's note

All claims expressed in this article are solely those of the authors and do not necessarily represent those of their affiliated organizations, or those of the publisher, the editors and the reviewers. Any product that may be evaluated in this article, or claim that may be made by its manufacturer, is not guaranteed or endorsed by the publisher.

Supplementary material

The Supplementary Material for this article can be found online at: https://www.frontiersin.org/articles/10.3389/fmicb.2022.982933/full#supplementary-material

References

Albertano, P., Urzì, C., and Caneva, G. (2005). "Tombe, catacombe e altri ipogei," in *La biologia vegetale per i beni culturali*, eds G. Caneva, M. P. Nugari, and O. Salvadori (Florence: Nardini Editore), 184–190.

Altschul, S. F., Gish, W., Miller, W., Myers, E. W., and Lipman, D. J. (1990). Basic local alignment search tool. *J. Mol. Biol.* 215, 403–410. doi: 10.1016/S0022-2836(05)80360-2

Barnett, H. L., and Hunter, B. B. (1972). *Illustrated genera of imperfect fungi*. Minneapolis, MN: Burgess Publishing Company.

Bastian, F., Jurado, V., Nováková, A., Alabouvette, C., and Saiz-Jimenez, C. (2010). The microbiology of Lascaux cave. *Microbiology* 156, 644–652. doi: 10.1099/mic.0.036160-0

Brighetti, M. A., Costa, C., Menesatti, P., Antonucci, F., Tripodi, S., and Travaglini, A. (2014). Multivariate statistical forecasting modelling to predict Poaceae pollen critical concentrations by meteoclimatic data. *Aerobiologia* 30, 25–33. doi: 10.1007/s10453-013-9305-3

Bruno, L., Rugnini, L., Spizzichino, V., Caneve, L., Canini, A., and Ellwood, N. T. W. (2019). Biodeterioration of Roman hypogea: The case study of the

Catacombs of SS. Marcellino and Pietro (Rome, Italy). *Ann. Microbiol.* 69, 1023–1032. doi: 10.1007/s13213-019-01460-z

Caneva, G., Nugari, M. P., and Salvadori, O. (2005). *La biologia vegetale per i beni culturali*, Vol. I. Florence: Nardini Editore.

de Hoog, G. S., Guarro, J., Gené, S. A., Al-Hatmi, A. M. S., Figueras, M. J., and Vitale, R. G. (2019). *Atlas of clinical fungi*, 4th Edn. Utrecht: Westerdijk Institute.

De Leo, F., Iero, A., Zammit, G., and Urzì, C. E. (2012). Chemoorganotrophic bacteria isolated from biodeteriorated surfaces in cave and catacombs. *Int. J. Speleol.* 41, 125–136. doi: 10.5038/1827-806X.41.2.1

Dupont, J., Jacquet, C., Dennetiere, B., Lacoste, S., Bousta, F., Orial, G., et al. (2007). Invasion of the French paleolithic painted cave of Lascaux by members of the *Fusarium solani* species complex. *Mycologia* 99, 526–533. doi: 10.3852/mycologia.99.4.526

Edgar, R. C. (2004). MUSCLE: Multiple sequence alignment with high accuracy and high throughput. *Nucleic Acids Res.* 32, 1792–1797. doi: 10.1093/nar/gkh340

Ellis, M. B. (1971). *Dematiaceous hyphomycetes.* Kew: CAB International Mycological Institute.

Ellis, M. B. (1976). *More dematiaceous hyphomycetes*. Kew: CAB International Mycological Institute.

Fassatiovà, O. (1986). "Moulds and filamentous fungi in technical microbiology," in *Progress in industrial microbiology*, ed. M. E. Bushell (Amsterdam: Elsevier), 22.

Florian, M. L. H. (1996). The role of the conidia of fungi in fox spots. *Stud. Conserv*. 41, 65–75.

Gabriel, J., and Švec, K. (2017). Occurrence of indoor wood decay basidiomycetes in Europe. *Fungal Biol. Rev.* 31, 212–217. doi: 10.1016/j.fbr.2017.05.002

Helbling, A., Gayer, F., and Brander, K. A. (1999). Respiratory allergy to mushroom spores: Not well recognized, but relevant. *Ann. Allergy* 83, 17–19. doi: 10.1016/S1081-1206(10)63506-5

Jurado, V., Fernández-Cortés, A., Cuezva, S., Laiz, L., Cañaveras, J. C., Sanchez-Moral, S., et al. (2009). The fungal colonization of rock art caves. *Naturwissenschaften* 96, 1027–1034. doi: 10.1007/s00114-009-0561-6

Jurado, V., Porca, E., Cuezva, S., Fernandez-Cortes, A., Sanchez-Moral, S., and Saiz-Jimenez, C. (2010). Fungal outbreak in a show cave. *Sci. Total Environ*. 408, 3632–3638. doi: 10.1016/j.scitotenv.2010.04.057

Kimura, M. (1980). A simple method for estimating evolutionary rates of base substitutions through comparative studies of nucleotide sequences. *J. Mol. Evol.* 16, 111–120. doi: 10.1007/BF01731581

Ma, Y., Zhang, H., Du, Y., Tian, T., Xiang, T., Liu, X., et al. (2015). The community distribution of bacteria and fungi on ancient wall paintings of the Mogao Grottoes. *Sci. Rep*. 5:7752. doi: 10.1038/srep07752

Martin-Sanchez, P. M., Jurado, V., Porca, E., Bastian, F., Lacanette, D., Alabouvette, C., et al. (2014). Airborne microorganisms in Lascaux Cave (France). *Int. J. Speleol.* 43, 295–303. doi: 10.5038/1827-806X.43.3.6

Martin-Sanchez, P. M., Nováková, A., Bastian, F., Alabouvette, C., and Saiz-Jimenez, C. (2012). Use of biocides for control of fungal outbreaks in subterranean environments: The case of the Lascaux cave in France. *Environ. Sci. Technol.* 46, 3762–3770. doi: 10.1021/es2040625

Otto, A., Laub, A., Wendt, L., Porzel, A., Schmidt, J., Palfner, G., et al. (2016). Chilenopeptins A and B, Peptaibols from the Chilean *Sepedonium* aff. *Chalcipori* KSH 883. *J. Nat. Prod.* 79, 929–938. doi: 10.1021/acs.jnatprod.5b01018

Rogerson, C. T., and Samuels, G. J. (1989). Boleticolous species of *Hypomyces*. *Mycologia* 81, 413–432. doi: 10.2307/3760079

Schmidt, O. (2007). Indoor wood-decay basidiomycetes: Damage, causal fungi, physiology, identification and characterization, prevention and control. *Mycol. Prog.* 6, 661–679.

Schmidt, O., Grimm, K., and Moreth, U. (2002). Molecular identity of species and isolates of *Coniophora* cellar fungi. *Holzforschung* 56, 563–571.

Schmidt, O., and Moreth, U. (2002). Data bank of rDNA-ITS sequences from building-rot fungi for their identification. *Wood Sci. Technol.* 36, 429–433. doi: 10.1007/s00226-002-0152-6

Singh, J. (1994). *Building mycology management of decay and health in buildings*. Thames: Taylor and Francis.

Sugiyama, J., Kiyuna, T., Nishijima, M., An, K. D., Nagatsuka, N., Tazato, N., et al. (2017). Polyphasic insights into the microbiomes of the Takamatsuzuka Tumulus and Kitora Tumulus. *J. Gen. Appl. Microbiol.* 63, 63–113. doi: 10.2323/jgam.2017.01.007

Tamura, K., Stecher, G., and Kumar, S. (2021). MEGA11: Molecular evolutionary genetics analysis version 11. *Mol. Biol. Evol.* 38, 3022–3027. doi: 10.1093/molbev/msab120

Thompson, T. (1998). *Development of techniques for the selective isolation of basidiomycetes from coarse woody debris and contiguous soil horizons*. MS. thesis. Durham, NH: University of New Hampshire.

Thompson, T. A., Thorn, R. G., and Smith, K. T. (2012). *Hypholoma lateritium* isolated from coarse woody debris, the forest floor, and mineral soil in a deciduous forest in New Hampshire. *Botany* 90, 457–464. doi: 10.1139/B2012-011

Thorn, R. G., Reddy, C. A., Harris, D., and Paul, E. A. (1996). Isolation of saprophytic basidiomycetes from soil. *Appl. Environ. Microbiol.* 62, 4288–4292. doi: 10.1128/aem.62.11.4288-4292.1996

Urzì, C., and Albertano, P. (2001). Studying phototrophic and heterotrophic microbial communities on stone monuments. *Methods Enzimol.* 336, 340–355. doi: 10.1016/s0076-6879(01)36600-4

Urzì, C., Bruno, L., and De Leo, F. (2018). "Biodeterioration of paintings in caves, catacombs and other hypogean sites," in *Biodeterioration and preservation in art, archeology and architecture*, eds R. Mitchell and J. Clifford (London: Archetype Publications Ltd), 114–129.

Urzì, C., and De Leo, F. (2001). Sampling with adhesive tape strips: An easy and rapid method to monitor microbial colonization on monument surfaces. *J. Microbiol. Methods* 44, 1–11. doi: 10.1016/s0167-7012(00)00227-x

Urzì, C., De Leo, F., Bruno, L., and Albertano, P. (2010). Microbial diversity in Paleolithic caves: A study case on the phototrophic biofilms of the Cave of Bats (Zuheros, Spain). *Microb. Ecol.* 60, 116–129. doi: 10.1007/s00248-010-9710-x

Vanderwolf, K. J., Malloch, D., McAlpine, D. F., and Forbes, G. J. (2013). A world review of fungi, yeasts, and slime molds in caves. *Int. J. Speleol.* 42, 77–96. doi: 10.5038/1827-806X42.1.9

White, T. J., Bruns, T., Lee, S., and Taylor, J. (1990). "Amplification and direct sequencing of fungal ribosomal RNA genes for phylogenetics," in *PCR protocols: A guide to methods and applications*, eds M. A. Innis, D. H. Gelfand, J. J. Sninsky, and T. J. White (New York, NY: Academic Press), 315–322.

Zucconi, L., Canini, F., Isola, D., and Caneva, G. (2022). Fungi affecting wall paintings of historical value: A worldwide meta-analysis of their detected diversity. *Appl. Sci*. 12:2988. doi: 10.3390/app12062988

frontiers | Frontiers in Microbiology

TYPE Original Research
PUBLISHED 21 December 2022
DOI 10.3389/fmicb.2022.1016608

OPEN ACCESS

EDITED BY
Cesareo Saiz-Jimenez,
Institute of Natural Resources and Agrobiology of Seville (CSIC), Spain

REVIEWED BY
Junaid Ali Siddiqui,
South China Agricultural University, China
Massimiliano Virgilio,
Royal Museum for Central Africa, Belgium
Wouter Hendrycks,
University of Antwerp, Belgium, in collaboration with reviewer MV

*CORRESPONDENCE
Qingbei Weng
wengqingbei@gznu.edu.cn

†These authors have contributed equally to this work

SPECIALTY SECTION
This article was submitted to Extreme Microbiology, a section of the journal Frontiers in Microbiology

RECEIVED 11 August 2022
ACCEPTED 18 November 2022
PUBLISHED 21 December 2022

CITATION
Dong Y, Chen Q, Fang Z, Wu Q, Xiang L, Niu X, Liu Q, Tan L and Weng Q (2022) Gut bacteria reflect the adaptation of *Diestrammena japanica* (Orthoptera: Rhaphidophoridae) to the cave. *Front. Microbiol.* 13:1016608. doi: 10.3389/fmicb.2022.1016608

Gut bacteria reflect the adaptation of *Diestrammena japanica* (Orthoptera: Rhaphidophoridae) to the cave

Yiyi Dong[1†], Qianquan Chen[1†], Zheng Fang[1], Qingshan Wu[1], Lan Xiang[2], Xiaojuan Niu[1], Qiuping Liu[1], Leitao Tan[1] and Qingbei Weng[1,2*]

[1]School of Life Sciences, Guizhou Normal University, Guiyang, Guizhou, China, [2]Qiannan Normal University for Nationalities, Duyun, Guizhou, China

The gut microbiota is essential for the nutrition, growth, and adaptation of the host. *Diestrammena japanica*, a scavenger that provides energy to the cave ecosystem, is a keystone species in the karst cave in China. It inhabits every region of the cave, regardless of the amount of light. However, its morphology is dependent on the intensity of light. Whether the gut bacteria reflect its adaptation to the cave environment remains unknown. In this research, *D. japanica* was collected from the light region, weak light region, and dark region of three karst caves. The gut bacterial features of these individuals, including composition, diversity, potential metabolism function, and the co-occurrence network of their gut microbiota, were investigated based on 16S rRNA gene deep sequencing assay. The residues of amino acids in the ingluvies were also evaluated. In addition, we explored the contribution of gut bacteria to the cave adaptation of *D. japanica* from three various light zones. Findings showed that gut bacteria were made up of 245 operational taxonomic units (OTUs) from nine phyla, with Firmicutes being the most common phylum. Although the composition and diversity of the gut bacterial community of *D. japanica* were not significantly different among the three light regions, bacterial groups may serve different functions for *D. japanica* in differing light strengths. *D. japanica* has a lower rate of metabolism in cave habitats than in light regions. We infer that the majority of gut bacteria are likely engaged in nutrition and supplied *D. japanica* with essential amino acids. In addition, gut bacteria may play a role in adapting *D. japanica's* body size. Unveiling the features of the gut bacterial community of *D. japanica* would shed light on exploring the roles of gut bacteria in adapting hosts to karst cave environments.

KEYWORDS

insect, gut microbiota, adaptation, cave, 16S rRNA gene sequencing, light strength, amino acid metabolism

Introduction

Microorganisms are abundant in the guts of animals, and most of them are beneficial for their hosts' health and various physiological processes (Douglas, 2011; Engel and Moran, 2013), including nutrition, development, reproduction, defense, and detoxification (Douglas, 2015). For example, they provide nutrients that hosts cannot synthesize, such as essential amino acids, B vitamins, and sterols (Douglas, 2009, 2015). In contrast to mammals, the diversity of gut microbiota in insects varies considerably among different taxa, possibly as the consequence of complex diets, variation in life span, and gut physiology (Douglas, 2011). *Apis mellifera*, for instance, harbored 14 species; however, *Reticulitermes speratus* harbored 254 operational taxonomic units (OTUs) (Colman et al., 2012).

Karst is a soluble rock that dissolves in water to form stone forests on the ground and caves under the earth. It accounts for around 20% of the land on the earth that is not covered by ice and provides water to approximately 25% of the world's population (Bystriakova et al., 2019). The karst area in southwestern China, the largest karst area in the world, is one of the 25 global biodiversity hotspots (Luo et al., 2016). The karst cave is characterized by darkness, moistness, constant temperature, poor air circulation, a high concentration of carbon dioxide, a lack of food, and low biomass (Lavoie et al., 2007). Multiple features of insect adaptations to cave environments include morphological adaptations (loss of vision and body color changes), physiological adaptations (low metabolic rate and CO_2 tolerance), and behavioral adaptations (loss of circadian rhythm and variations in mating behavior) (Howarth and Moldovan, 2018). Therefore, cave inhabitants are an ideal model for exploring the environmental adaptations of organisms.

Diestrammena japanica Blatchley (Orthoptera: Rhaphidophoridae) is the dominant insect species in karst caves and is found in all regions of caves. However, individuals from different light strength exhibit distinct morphological features. Previous reports on *D. japanica* primarily focused on its population composition (Li et al., 2001; Li, 2006), the influence of environmental factors on its population structure (Li, 2006), and the heavy metal concentration in its body in caves with heavy metal pollution (Xu et al., 2010; Ye and Li, 2011). *D. japanica* has access to different foods depending on light strength. Specifically, species in the light region consume more moss and fern, while species in weak light and dark regions feed on more animal carcasses and fungi (Li, 2007). However, the gut bacterial compositions and their roles in the adaptation of *D. japanica* to cave habitats remain unknown.

In the study, 16S rRNA gene deep sequencing was utilized to unveil the composition and structure of gut microbiota in *D. japanica* near the entrance of karst caves (light region) and in cave habitats (weak light and dark regions). Results showed that Firmicutes were the most dominant phylum, and *Lactobacillus* was the most abundant genus. The community composition and diversity indices were not influenced by light strength. Phylogenetic investigation of communities by the reconstruction of unobserved states analysis implied that many gut bacteria were involved in nutrition, such as several amino acid biosynthesis pathways. Gut bacteria of *D. japanica* exhibit low diversity but strong cooperation interactions in the dark region. These results indicated that the gut bacteria may help *D. japanica* adapt to the poor nutrient cave environment. Exploring the diversity and function of gut bacteria from cave insects can help understand species adaptation in extreme environments.

Materials and methods

Sample collection

Diestrammena japanica was collected from three karst caves in Libo county, Guizhou province, China. The locations of the caves are shown in **Supplementary Table 1**. Based on the habitat categories, light strength in the cave environment, and the presence of *D. japanica*, the zone was divided into the light region (the areas with direct sunlight are near the cave's entrance and distance from the entrance within 10 m), the weak light region (transition twilight areas distance from the entrance within 10–30 m), and the dark region (deep zones of the cave are entirely dark and distance from the entrance beyond 50 m), according to the light strength and distance from the cave entrance (Culver and Pipan, 2019). Species of *D. japanica* were caught and stored separately in sterile tubes at −20°C, and samples were subsequently transferred to the laboratory in 12 h. To quantify the individual size of *D. japanica*, a ruler with a 0.1-mm scale was used to measure trait features, including body length, hind leg length, front leg length, middle leg length, and head width, with 24 individual repetitions for each region. The least significant difference (LSD) test in *agricolae* package (de Mendiburu, 2014) was employed to examine whether there were significant differences in these morphological traits.

Amino acid titer determination in ingluvies of *Diestrammena japanica*

Ten fresh species from each light region were dissected with dissection forceps. The inclusion from the ingluvies where food was stored was extracted in a 2-ml sterile vial and then stored at −80°C. An amino acid analyzer (Sykam S433, Fürstenfeldbruck, Germany) was used to assess the concentration of amino acids in foods.

DNA extraction and 16S rRNA gene sequencing

The ethanol-treated samples were rinsed three times with enough sterile water in plates. The gut was then isolated from other tissues and placed in a sterile tube. A total of 15 guts from each light-strength region of the caves were pooled together as one biological replication. Guts were ground into a powder with a pestle. To avoid the contamination of microorganisms from the air in the laboratory, the above operations were carried out in a biosafety cabinet. DNA was extracted using the DNeasy PowerSoil Kit (Qiagen, Hilden, Germany) according to the manufacturer's protocol. The DNA quality and quantity were measured with the BioTek Epoch 2 Microplate Spectrophotometer (Agilent, Palo Alto, USA). The bacterial V3–V4 hypervariable region of the 16S rRNA gene was amplified by the universal primers 338F (ACTCCTACGGGAGGCAGCAG) and 806R (GGACTACHVGGGTWTCTAAT) using TransStart FastPfu DNA polymerase (TransGen, Beijing, China) according to the manufacturer's protocol. Each sample was amplified in triplicate, and then all polymerase chain reaction (PCR) products were checked by 2% agarose gel electrophoresis. High-quality PCR reaction products that were amplified from the same sample were pooled together and subjected to purification with AxyPrep DNA Gel Extraction Kit (Axygen Biosciences, Union City, CA, United States). Purified products were quantified with QuantiFluorTM-ST (Promega, United States) following the manufacturer's protocol. The paired-end libraries were synthesized with the TruSeqTM DNA Sample Prep Kit (Illumina, San Diego, CA, United States) following the manufacturer's protocol. Sequencing was conducted with Illumina MiSeq platform sequencing technology with a maximum read length of 2 × 300 bp at Shanghai Majorbio Bio-pharm Technology Co., Ltd.

Analysis of 16S rRNA gene sequencing data

The quality of raw reads was assessed with FASTP (version 0.19.6) (Chen S. et al., 2018). High-quality reads were assembled with Flash (version 1.2.11) (Magoc and Salzberg, 2011) and analyzed with QIIME (version 1.9.1) and Mothur (version 1.30.2) (Schloss et al., 2009; Caporaso et al., 2010; Schloss, 2020). Furthermore, bacterial operational taxonomic units (OTUs) were grouped with 97% similarity to the SILVA (version 132) and Greengenes (version 135) database with the Ribosomal Database Project Classifier (version 2.11) (DeSantis et al., 2006; Edgar, 2013; Quast et al., 2013). OTUs with more than 20 reads for all samples and distribution across three samples (at least five reads for each sample) were retained for further analysis.

Function prediction of gut bacterial communities

The function of gut bacteria was predicted by searching against the Clusters of Orthologous Groups (COGs) database with the Phylogenetic Investigation of Communities by Reconstruction of Unobserved States (PICRUSt) (Langille et al., 2013). These analyses were performed using the Majorbio Cloud Platform. [1] The Kruskal–Wallis test was used for multiple group comparisons. Differences were considered significant if the p-value was <0.05.

Analysis of network for gut bacterial communities

To compare the structure and existence pattern of the gut bacterial communities of *D. japanica*, we performed the bacterial co-occurrence network for each light-strength region separately. Each co-occurrence network was conducted based on the top 50 relative abundance genera that occurred in eight phyla in the network analysis. Only the strong correlations in these groups were visualized in the co-occurrence network. Thus, the bacterial interactions comprised only significant correlations ($p < 0.01$) of the correlative coefficient (the absolute value of $r > 0.8$) in the network. Moreover, we calculated the edge, connectance, clustering coefficient, average degree, and modularity for each co-occurrence network. We also detected that the links per species in each network were significantly different ($p < 0.001$) in the random network using the r2dtable null model. All relative network analyses were performed in R software (R Development Core Team, 2018), using the packages *igraph* (Csardi and Nepusz, 2006), *bipartite* (Dormann et al., 2008), *psych* (Revelle and Revelle, 2015), and *statnet* (Handcock et al., 2008).

Statistical analysis

First, the LSD test was conducted to assess whether there were significant differences in the morphological traits of *D. japanica* among the three light-strength regions. Mothur and R software were used to build rarefaction curves to determine if the sequencing depth (reads) was sufficient to capture the majority of gut bacteria (Schloss et al., 2009; Schloss, 2020). The top 35 abundance genera were used to generate a heatmap with ggplot2 (Ginestet, 2011), and the Kruskal–Wallis test was used to test the differences in the abundances of the 35 genera among three light regions. The Venn diagram, which exhibited the overlap of

1 www.majorbio.com

OTUs among groups, was generated with the R package *VennDiagram* (Chen and Boutros, 2011). To decipher whether the gut bacterial composition was affected by regions with different light-strength regions, the Shannon and Simpson diversity indexes were calculated with Mothur, and then the pairwise Wilcox test was used to test for significant differences in the bacterial diversity indices, with a *p*-value adjusted for false discovery rate (fdr-adjusted). Subsequently, the beta diversity of bacterial communities was compared *via* ANOSIM and permutational multivariate analysis of variance (PERMANOVA, permutation 9,999 times, based on the Bray–Curtis matrix), respectively. The analyses were conducted *via* MicrobiotaProcess (Xu et al., 2022) and Vegan (Oksanen et al., 2013) packages in R (version 4.1.2).[2] A PERMANOVA test uncovered that the compositions of gut bacteria were not significant differences among the three light regions, and then we tested the differences between two groups (light region as one group, and weak and dark regions as another group); abund_jaccard matrix (considering both OTUs' availability and abundance) was used for principal component analysis (PCA), combining with the Adonis analysis (permutation 9,999 times).

Results

Morphological adaptations of *Diestrammena japanica*

Diestrammena japanica is distributed in all regions of caves, independent of light strength. However, the LSD test showed that species from light regions were significantly larger than those from weak light and dark regions (**Figure 1A** and **Table 1**). However, the species from weak and dark regions were not significantly different in body size (**Table 1**).

The sequencing overview of gut bacteria from *Diestrammena japanica*

Sequencing was performed on a total of nine samples from three distinct light-strength regions in three caves. Following filtering, the number of high-quality reads and bases was 388,019 and 172,857,092, respectively (**Supplementary Table 2**). The average read length ranged from 442 to 449 (**Supplementary Table 2**). The minimum number of reads per sample was 32,208. The rarefaction curve verified that the depth of sequencing was sufficient to capture the majority of bacterial species (**Figure 1B**). The reads were clustered into 245 OTUs, which shared >97% sequence identity (**Supplementary Table 3**). In addition to Firmicutes, Proteobacteria, Actinobacteria, Cyanobacteria, Tenericutes, Deinococcus-Thermus, Fusobacteria, Chlamydiae, and one non-rank phylum were detected in the gut of *D. japanica* (**Figure 1C** and **Supplementary Table 3**).

Compositions and diversities of gut bacteria among different light-strength regions in *Diestrammena japanica*

Firmicutes were the most abundant in all samples, accounting for 60.87, 70.79, and 60.18% of bacterial groups of species from light, weak light, and dark regions, respectively (**Figure 1C**). Chlamydiae accounted for 8.05–23.77% of the bacterial composition from different light-strength regions. Proteobacteria accounted for 2.36–12.07% of the total bacterial sequences, of which *Rickettsiella*, including one unclassified OTU, was the most abundant genus of Proteobacteria. The top two genera of Actinobacteria were *Corynebacterium* and *Enterorhabdus*.

The top 35 abundance genera were used to generate the heatmap (**Figure 1D**). *Lactobacillus* was the most abundant genus, accounting for 37.35, 59.89, and 52.72% of bacteria found in species from light, weak light, and dark regions, respectively (**Figure 1D** and **Supplementary Table 3**). Among the 16 OTUs belonging to the genus *Lactobacillus*, *L. amylovorus* and *L. oligofermentans* were the most abundant, accounting for 66.38–85.46% and 2.43–10.41% of the abundance of the genus *Lactobacillus*. The abundance of Candidatus *Rhabdochlamydia* and *Corynebacterium* ranged from 8.05 to 23.77% and 1.43 to 11.20%, respectively.

Among the top 35 genera, *Lactococcus* (Kruskal–Wallis test, $df = 2$, $p = 0.0376$), *Weissella* (Kruskal–Wallis test, $df = 2$, $p = 0.0358$), and non-rank bacteria (Kruskal–Wallis test, $df = 2$, $p = 0.0302$) were more abundant in species from the light region than in those from weak light and dark regions (**Figure 1D**), and remailing bacterial groups were not significantly different among the three light regions.

Furthermore, the diversity analysis of bacterial community revealed that the Shannon index exhibited the following pattern: light (2.96) > weak light (2.14) > dark (1.19), and the Simpson index exhibited the opposite pattern to the Shannon index (**Figure 2A**). The two diversity indices were not significantly different among light-strength regions (all fdr-adjusted *p*-values from the pairwise Wilcox test were greater than 0.05, **Supplementary Table 4**).

Composition similarity of gut bacteria among different light-strength regions in *Diestrammena japanica*

A total of 239, 230, and 242 OTUs, respectively, were detected in the species from light, weak light, and dark regions

2 http://cran.r-project.org/

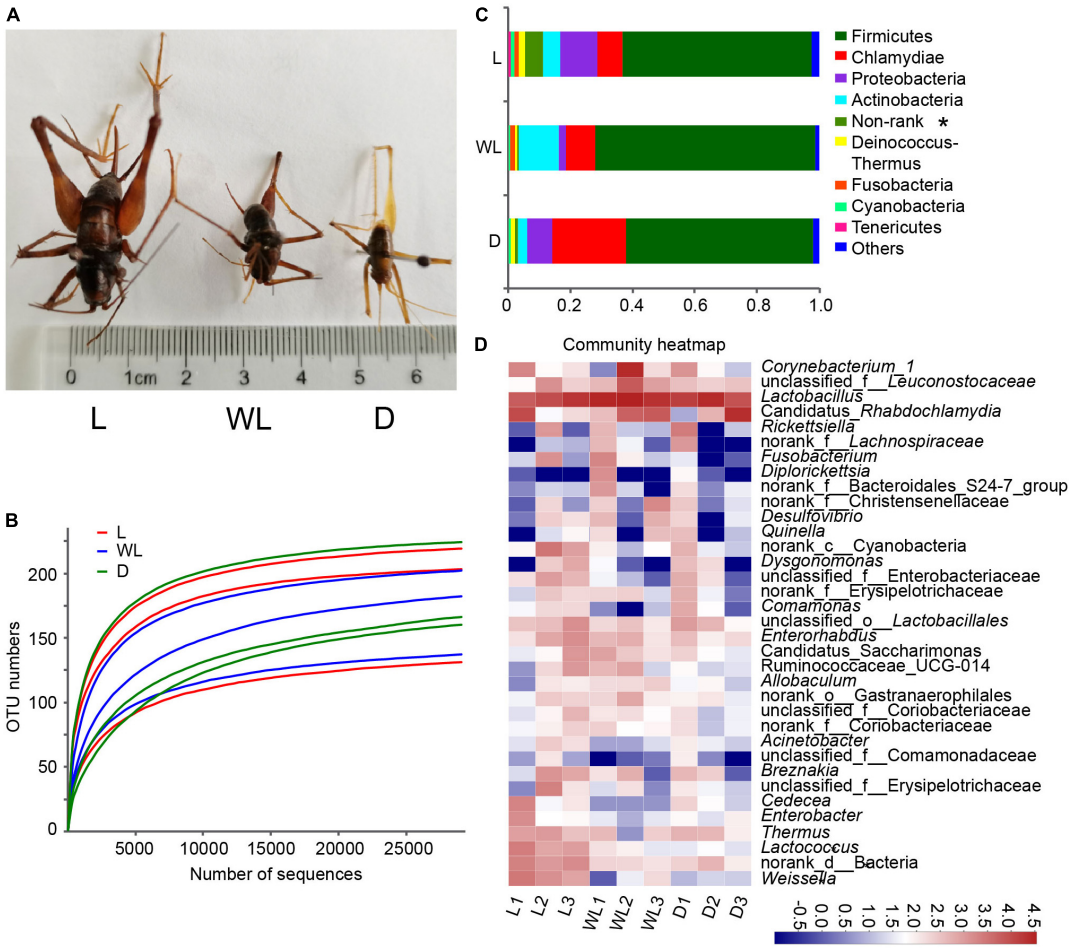

FIGURE 1
Gut bacteria dynamics among different light-strength regions in *Diestrammena japanica*. **(A)** Morphology of *D. japanica* from different light-strength regions. **(B)** Rarefaction curves generated from randomly subsampled data sets with the same number of 16S rRNA gene deep sequencing. **(C)** Relative abundance of gut bacteria at the phylum level. **(D)** Relative abundance of the top 35 abundance genera gut bacteria, the color scales display the bacterial relative abundance (log10 transformed). L, light region; WL, weak light region; D, dark region. These labels are the same as in the other figures.

(Figure 2B). The Venn diagram analysis revealed that 221 OTUs were shared by species from three regions. species from the dark and weak light regions shared six OTUs, while species from the light region shared three and 15 OTUs with species from the weak light and dark regions, respectively (Figure 2B). At bacterial species levels, the samples from three light-strength regions revealed consistent patterns (no significant differences in bacterial composition) from ANOSIM (statistic $R = 0.004$, $p = 0.43$). However, the PERMANOVA test uncovered that the bacterial community did not have significant changes in three light-strength regions (Supplementary Table 5, PERMANOVA Pseudo-F = 1.39, $R^2 = 0.32$, $p = 0.13$). Intriguingly, the PCA analysis with abund_jaccard matrix indicated that bacterial communities of species from weak light and dark regions were clustered as one group, and the remaining species from the light region were clustered as another group (Adonis test, $R = 0.3457$, $p = 0.049$; the first two axes explaining 43.60% of the total variability) (Figure 2C).

Co-occurrence network analysis of gut bacteria among different light-strength regions in *Diestrammena japanica*

A co-occurrence network analysis was carried out to unveil the interaction and structure of gut bacterial communities. Compared with gut bacteria in the species from the light region (edge: 138), the interactions among gut bacteria in the species from the weak light and dark region (edge: 363 and 385 separately) were more complex (Figure 3 and Table 2). Moreover, we observed that the network only included the positive interaction (gray line) in the dark region; the network

TABLE 1 The morphological traits of *Diestrammena japanica* in different light-strength regions (N = 24, Unit: mm).

Region	Body length	Hind leg length	Front leg length	Middle leg length	Head width
L	2.74 ± 0.09^{a}	6.71 ± 0.18^{a}	3.85 ± 0.11^{a}	3.65 ± 0.08^{a}	0.42 ± 0.02^{a}
WL	1.90 ± 0.10^{b}	5.00 ± 1.27^{b}	2.98 ± 0.18^{b}	2.84 ± 0.17^{b}	0.27 ± 0.01^{b}
D	1.89 ± 0.13^{b}	4.84 ± 1.25^{b}	2.94 ± 0.16^{b}	2.69 ± 0.15^{b}	0.30 ± 0.02^{b}

Mean ± standard error is shown. L, light region of the cave; WL, weak light region of the cave; D, dark region of the cave. Different lowercase letters in the same column are significantly different based on the least significant difference test results.

from the weak light consisted of 233 positive edges and 130 negative edges (red line). However, there were 83 positive interactions and 55 negative interactions in the gut bacterial community from the light region. In addition, the connectance and average degree of the network highlighted the pattern of dark > weak light > light, while the modularity exhibited the reverse pattern (light > weak light > dark).

Function prediction of gut bacteria among different light-strength regions in *Diestrammena japanica*

The PICRUSt prediction was conducted to reveal the role of the gut bacterial community in *D. japanica*. The results uncovered that 34.96% of gut bacteria were involved in the nutritional function of the host. Specifically, 8.40, 8.21, 5.90, 5.26, 4.04, and 3.15% of bacteria, respectively, were involved in amino acid transport and metabolism, carbohydrate transport and metabolism, inorganic ion transport and metabolism, energy production and conversion, nucleotide transport and metabolism, and lipid transport and metabolism (**Figure 4**). Moreover, 2.52% of gut microorganisms were implicated in defense.

At the same time, several pathways involved in methionine biosynthesis, including L-methionine biosynthesis I (Kruskal–Wallis test, df = 2, p = 0.0107) and L-methionine biosynthesis III (Kruskal–Wallis test, df = 2, p = 0.0107) were more abundant in species from the light region than in those from weak light and dark regions (**Figure 5A**). The titers of amino acid content in the food-storing ingluvies of *D. japanica* were further investigated. The titers of aspartic acid (Kruskal–Wallis test, df = 2, p = 0.0250) and methionine (Kruskal–Wallis test, df = 2, p = 0.0500) in the species from the light region were lower than in those from weak light and dark regions (**Figure 5B**). Moreover, the amino acid biosynthesis I (r = −0.8605, p = 0.0061) and III (r = −0.8388, p = 0.0092) pathways of gut bacteria were negatively correlated with the contents of methionine in food.

Discussion

Diverse gut bacteria are potentially involved in many physiological processes of insects, which contribute to the adaptation of the host insects to the environment. In this study, the gut bacteria character of *D. japanica* in karst caves was determined by 16S rRNA gene deep sequencing. The compositions and diversity indices of gut bacteria of *D. japanica* did not exhibit convergent patterns influenced by light-strength regions in the caves. However, bacterial groups may provide diverse functions to *D. japanica* in regions of varying light strengths. Moreover, gut bacteria may have roles in the nutritional metabolism processes (amino acids and carbohydrates) and morphological adaptation of *D. japanica* in karst caves. Altogether, this study facilitates a step forward in understanding the roles of gut bacteria in the adaptation of insects in the nutrient-poor and dark cave environment.

The overall feature of gut bacteria of *Diestrammena japanica*

In comparison to *Drosophila melanogaster* (139 OTUs), xylophagous long-horned beetles (average 103 OTUs), *Bombyx mori* (90 OTUs), and several wild mosquito species (5–71 OTUs) (Chandler et al., 2011; Engel et al., 2012; Chen B. et al., 2018; Zhao et al., 2019), *D. japanica* harbors more diverse gut bacterial composition. Each *D. japanica* sample from different light-strength regions was detected with more than 200 OTUs, covering eight bacterial phyla.

Host insects' diets can affect gut bacteria composition (Colman et al., 2012; Paoletti et al., 2013; Yun et al., 2014). As a type of omnivorous insect with complex food structures, *D. japanica* has access to different food structures depending on the different light-strength regions. For example, species in the light region consume more moss and fern, whereas those in weak light and dark regions feed on animal carcasses and fungi (Li, 2007). Previous reports have shown a positive correlation between the complexity of diet structures and the diversity of gut bacteria (Zheng et al., 2021). Therefore, it is not unexpected that more numerous bacterial taxa were observed in the gut habitat of *D. japanica* than other insect taxa previously mentioned since they contribute to the decomposition of diverse food resources.

Generally, Firmicutes and Proteobacteria are the prominent groups of gut bacteria in insects (Yun et al., 2014; Chen et al., 2016; Vilanova et al., 2016; van Schooten et al., 2018). Similar to *D. japanica* of this study, the gut bacterial communities of *Epicauta longicollis*, *Megetra cancellata*, and *Bactrocera dorsalis*

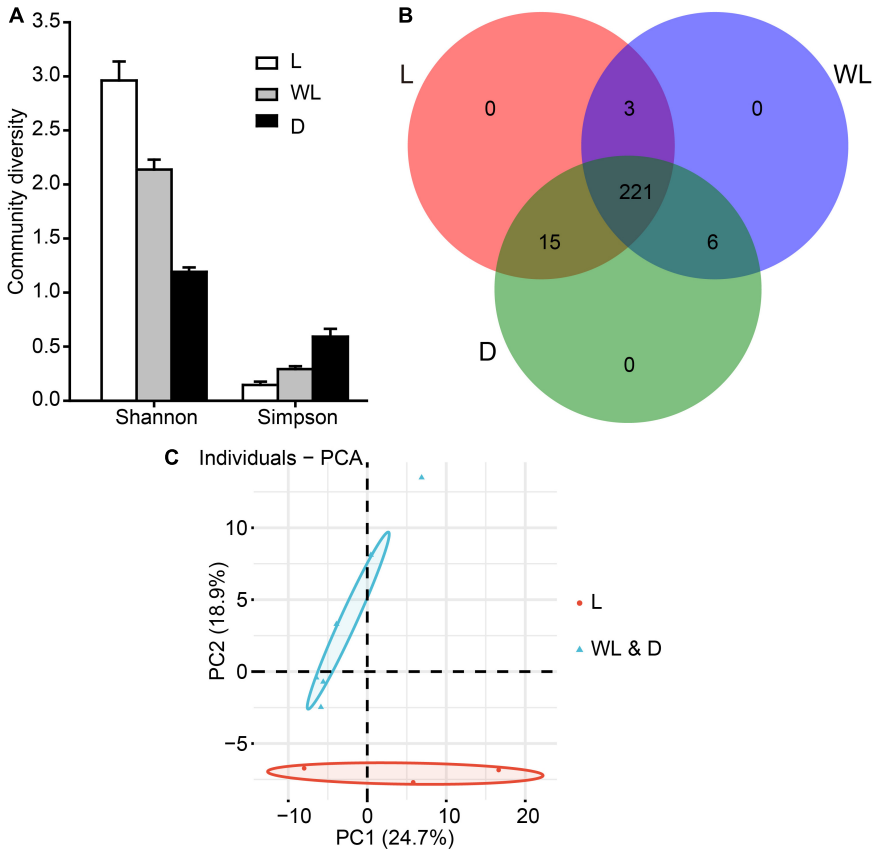

FIGURE 2
Gut bacterial community dynamics among different light-strength regions in *D. japanica*. **(A)** Community diversity measured by the Shannon index and Simpson index. **(B)** Overlap of OTUs from different light-strength regions. **(C)** Principal component analysis showed gut bacteria were clustered into two groups according to light strengths, based on the Adonis testing result (R = 0.3457, p = 0.049); the different colors show different groups with the boundaries of the 95% confidence ellipses. The red represents the species from weak light and dark regions.

were dominated by Firmicutes (Colman et al., 2012; Andongma et al., 2015). However, in the intestinal habitat of some species, such as *Bombyx mori* and *Chrysoperla sinica*, Proteobacteria was the dominating phylum (Chen B. et al., 2018; Zhao et al., 2019). Consistent with an earlier report on the gut bacterial communities of 58 insect taxa (Colman et al., 2012), these results indicated that the predominant phylum of gut bacteria varies across insect taxa.

The morphological adaptation of *Diestrammena japanica* to the cave environment

To adapt to the cave environment, cave animals are often small in bodily size. There was a strong positive correlation between oxygen concentration and insect body size. For instance, hypoxic insects exhibited smaller (Harrison et al., 2010). The bodily size of *D. japanica* in the cave regions (weak light and dark regions) was significantly smaller than that in the light regions. In addition, species of *D. japanica* in the cave consume animal feces (Li, 2007), which implies that more pathogens could be introduced by food resources (Busvine, 1980; Hassan et al., 2021). This is consistent with the high abundance of pathogenic Chlamydiae (Candidatus *Rhabdochlamydia porcellionis*) in gut bacteria of *D. japanica* in the dark regions (Busvine, 1980; Hassan et al., 2021), which could damage the digestive system of host insect (Kostanjsek and Pirc Marolt, 2015). Thus, we inferred that the small bodily size of *D. japanica* is relevant to the pathogen presence and lower oxygen concentration inside the cave.

The contribution of gut bacteria to cave adaptation of *Diestrammena japanica*

Firmicutes were the prominent group of gut bacteria of *D. japanica*, and they may play a significant role in the food digestion and energy metabolism of hosts (Chen et al., 2016), for

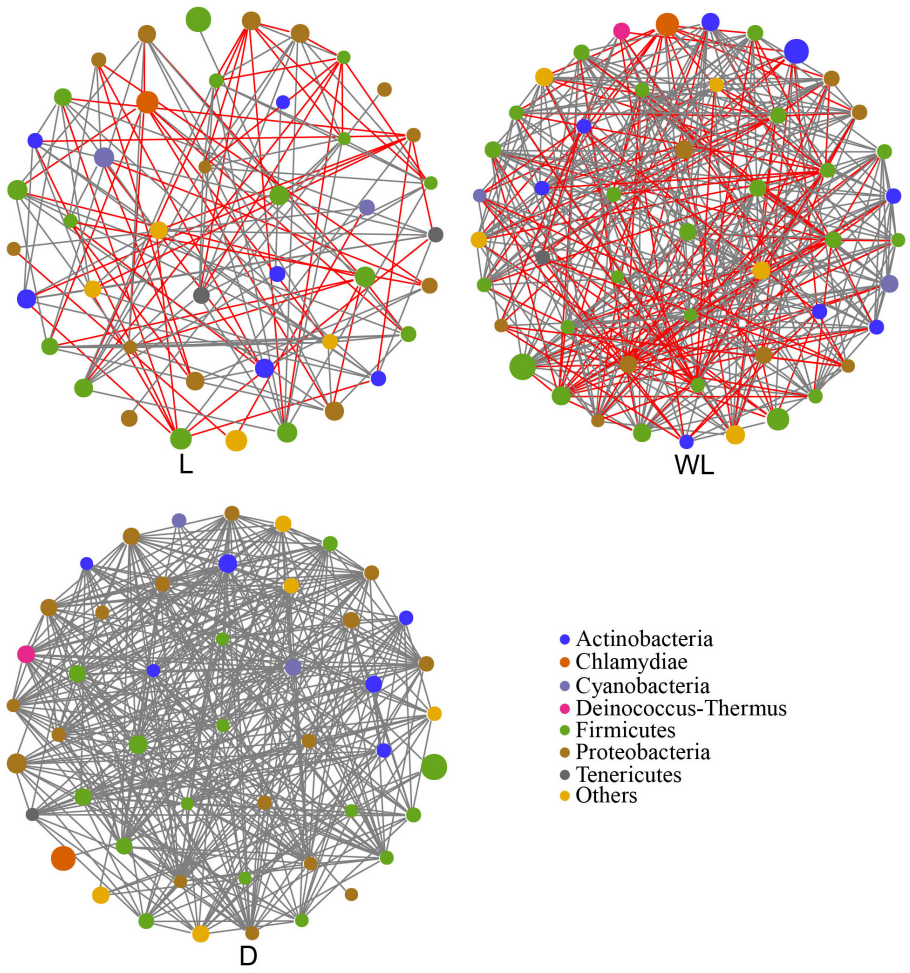

FIGURE 3
Co-occurrence network analysis of gut bacteria community in *D. japanica*. The size of the node represents the relative abundance. Positive interaction, gray line; negative interaction, red line.

TABLE 2 The co-occurrence network parameter in different light-strength regions.

Region	Edge	Connectance	Clustering coefficient	Average degree	Modularity
L	138	0.15	1.00	6.41	0.75
WL	363	0.31	1.00	14.82	0.61
D	385	0.34	1.00	16.04	0.47

L, light region of the cave; WL, weak light region of the cave; D, dark region of the cave.

instance, *Clostridia thermocellum* and *C. ljungdahlii* can degrade the cellulose and hemicellulose (Fonknechten et al., 2010). *Enterococcus* has the ability to mediate the pH of the gut environment, thereby enhancing the host'o resistance to toxins from foods (Wilson and Benoit, 1993; Xia et al., 2018). *Lactobacillus amylovorus* and *L. oligofermentans* were prevalent in our results, with the former exhibiting proteolytic activity and lactose metabolic capacity, producing lactate and carbohydrate assimilation (Mok et al., 2002; Hynönen et al., 2014; Cardarelli et al., 2016), and the latter engaging in the fermentation of xylose, ribose, and hexose (Andreevskaya et al., 2016). Thus, we have reason to believe that a high abundance of Firmicutes in gut bacteria probably supplies *D. japanica* with nutrition substrates *via* involvement in the energy-absorbing processes.

Insects have lost the capacity to independently synthesize essential amino acids throughout their evolutionary history, implying that they rely on gut bacteria or diet to apply these amino acids and nutrients (McCutcheon et al., 2009; Luan et al., 2015). For instance, the artificial diet treatment showed that *Anoplophora glabripennis* (Coleoptera: Cerambycidae) larvae

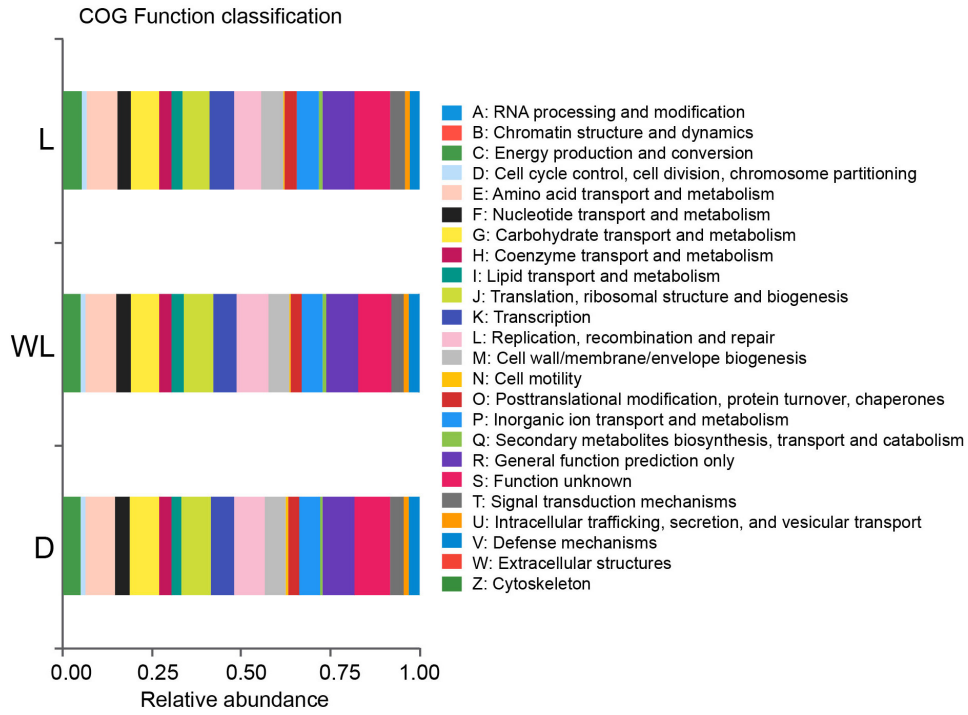

FIGURE 4
Relative abundance of gut bacterial function classification, inferred from PICRUSt analysis prediction.

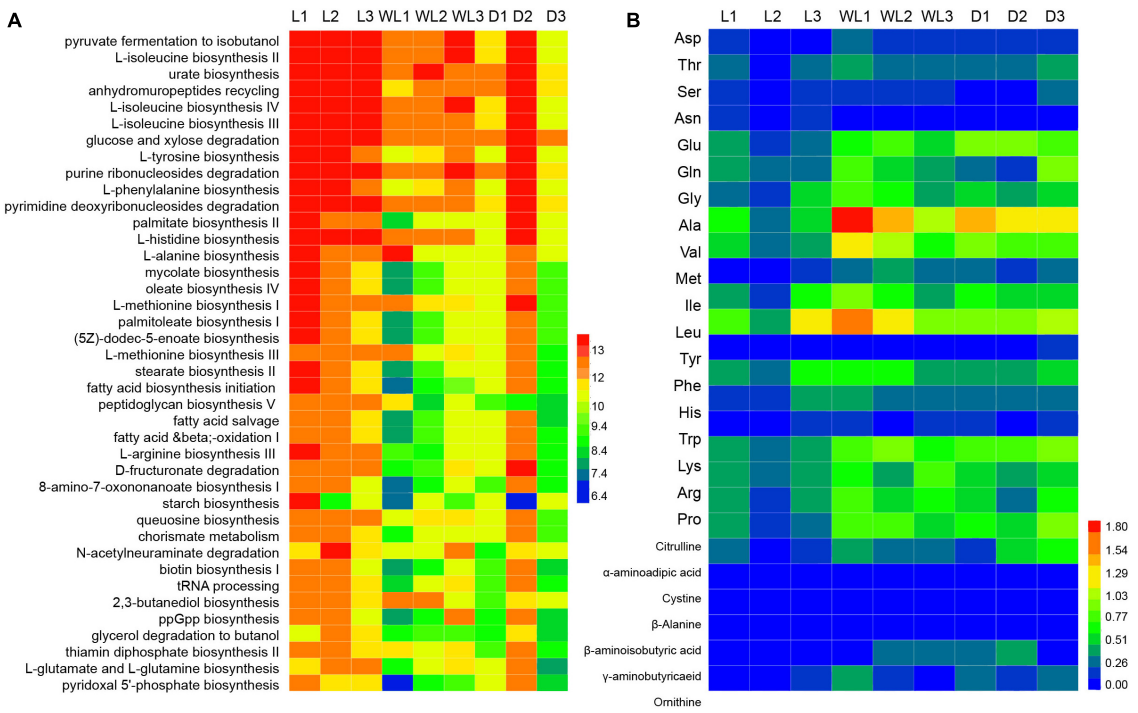

FIGURE 5
Abundance of metabolism pathway **(A)** and titer of amino acids **(B)**, the three letter codes represent the different amino acids, following the general amino acid code list, and the color scales indicate the abundances of metabolism pathways and amino acids.

rely on gut bacteria for essential amino acids (Ayayee et al., 2016). Duplais et al. demonstrated that gut bacteria are involved in the cuticular formation of turtle ants Duplais et al. (2021). In this case, the PICRUSt analysis uncovered that gut bacteria of *D. japanica* have the ability to involve in various amino acid biosynthesis and nutritional functions. Generally, compared to herbivorous insects, omnivorous *D. japanica* consume moss, animal carcasses, and fungus (Li, 2007), suggesting that they need a more diverse gut microbiota to decompose foods (Yun et al., 2014; Salcedo-Porras et al., 2020).

Moreover, in gut bacterial communities of species from cave habitats (weak light and dark regions), higher values of connectance and average degree but lower values of modularity represented that each group had more links with other species and fewer subgroups than those in light regions (Wood et al., 2017). This is also supported by the abundance of positive links in the gut bacterial community of *D. japanica*, exhibiting lots of cooperative interactions and lower efficiency of substrate transportation. Gut bacteria with a low abundance of amino acid biosynthesis pathways and more residual amino acids in the ingluvies of *D. japanica* indicated that species in cave habitats tend to have lower metabolism rates in cave habitats than in light regions. To reduce the rate of energy consumption, insects show activity, and mobility tends to be lower in cave environments than outside caves (Howarth and Moldovan, 2018), which is an adaptation of insects to the cave habitats where food and nitrogen are oligotrophic (Barton and Jurado, 2007; White and Culver, 2011).

This research aggregated 15 individual guts from each light region of each cave as a sample, which has the potential to decrease the number of species in the community with skewed compositions and to boost the convergence of patterns in bacterial compositions and network structures. Compared to the metagenomic data of bacterial communities, the 16S rRNA gene data can provide a biased similarity of bacterial communities among samples (Ellegaard et al., 2020). In addition, the identical environment acting as a filter factor can result in a convergent co-occurrence network pattern (Freilich et al., 2018). Thus, microbiome analysis with more replicates would provide more clear patterns for functional predictions of gut bacteria in insect adaptations to cave environments. In addition, more than 40% of gut bacteria may be involved in the nutrient transport and transformation, lipid metabolism, energy metabolism, and amino acid transport processes of *D. japanica,* uncovered by PICRUSt analysis. It is worth noting that these data do not indicate that the gut microbes associated with *D. japanica* do, indeed, perform various important metabolic processes, which would require further experimental studies to be demonstrated. Nevertheless, the characteristics of the gut bacterial community of *D. japanica* revealed in this study provide a basis for exploring the roles of gut bacteria in adapting hosts to caves.

Data availability statement

The datasets presented in this study can be found in online repositories. The names of the repository/repositories and accession number(s) can be found below: https://doi.org/10.6084/m9.figshare.20522079.v1.

Author contributions

YD and QC: conceptualization, data curation, and writing the original draft. ZF: visualization and investigation. QWu: formal analysis and validation. LX and XN: data curation and software. QL: methodology and visualization. LT: conceptualization and reviewing. QWe: reviewing, supervising, and funding acquisition. All authors contributed to the article and approved the submitted version.

Funding

This work was supported by the Joint Fund of the National Natural Science Foundation of China and the Karst Science Research Center of Guizhou Province (U1812401), as well as the Provincial Program on Platform and Talent Development of the Department of Science and Technology of Guizhou China (Grant Nos. [2019]5617 [2019]5655 and [2017]5726-21).

Conflict of interest

The authors declare that the research was conducted in the absence of any commercial or financial relationships that could be construed as a potential conflict of interest.

Publisher's note

Supplementary material

The Supplementary Material for this article can be found online at: https://www.frontiersin.org/articles/10.3389/fmicb.2022.1016608/full#supplementary-material

SUPPLEMENTARY TABLE 1
Detail information of sample location.

SUPPLEMENTARY TABLE 2
Statistical information of 16S rRNA gene deep sequencing.

SUPPLEMENTARY TABLE 3
OTUs table based on 97% sequence similarity.

SUPPLEMENTARY TABLE 4
The pairwise Wilcox test of alpha diversity indexes of the gut bacterial community.

SUPPLEMENTARY TABLE 5
Summary table for the PERMANOVA testing of bacterial compositions in three light-strength regions.

References

Andongma, A. A., Wan, L., Dong, Y. C., Desneux, N., White, J. A., and Niu, C. Y. (2015). Pyrosequencing reveals a shift in symbiotic bacteria populations across life stages of *Bactrocera dorsalis*. *Sci. Rep.* 5:9470. doi: 10.1038/srep09470

Andreevskaya, M., Johansson, P., Jaaskelainen, E., Ramo, T., Ritari, J., Paulin, L., et al. (2016). *Lactobacillus oligofermentans* glucose, ribose and xylose transcriptomes show higher similarity between glucose and xylose catabolism-induced responses in the early exponential growth phase. *BMC Genomics* 17:539. doi: 10.1186/s12864-016-2840-x

Ayayee, P. A., Larsen, T., Rosa, C., Felton, G. W., Ferry, J. G., and Hoover, K. (2016). Essential amino acid supplementation by gut microbes of a wood-feeding cerambycid. *Environ. Entomol.* 45, 66–73. doi: 10.1093/ee/nvv153

Barton, H. A., and Jurado, V. (2007). What's up down there? Microbial diversity in caves. *Microbiome* 2, 132–138.

Busvine, J. R. (1980). *Insects and hygiene*. New York, NY: Springer, 1–20. doi: 10.1007/978-1-4899-3198-6_1

Bystriakova, N., Alves De Melo, P. H., Moat, J., Lughadha, E. N., and Monro, A. K. (2019). A preliminary evaluation of the karst flora of Brazil using collections data. *Sci. Rep.* 9:17037. doi: 10.1038/s41598-019-53104-6

Caporaso, J. G., Kuczynski, J., Stombaugh, J., Bittinger, K., Bushman, F. D., Costello, E. K., et al. (2010). QIIME allows analysis of high-throughput community sequencing data. *Nat. Methods* 7, 335–336. doi: 10.1038/nmeth.f.303

Cardarelli, H. R., Martinez, R. C., Albrecht, S., Schols, H., Franco, B. D., Saad, S. M., et al. (2016). In vitro fermentation of prebiotic carbohydrates by intestinal microbiota in the presence of *Lactobacillus amylovorus* DSM 16998. *Benef. Microbes* 7, 119–133. doi: 10.3920/BM2014.0151

Chandler, J. A., Morgan Lang, J., Bhatnagar, S., Eisen, J. A., and Kopp, A. (2011). Bacterial communities of diverse *Drosophila* species: Ecological context of a host-microbe model system. *PLoS Genet.* 7:e1002272. doi: 10.1371/journal.pgen.1002272

Chen, B., Teh, B.-S., Sun, C., Hu, S., Lu, X., Boland, W., et al. (2016). Biodiversity and activity of the gut microbiota across the life history of the insect herbivore *Spodoptera littoralis*. *Sci. Rep.* 6:29505. doi: 10.1038/srep29505

Chen, B., Du, K. Q., Sun, C., Vimalanathan, A., Liang, X. L., Li, Y., et al. (2018). Gut bacterial and fungal communities of the domesticated silkworm (*Bombyx mori*) and wild mulberry-feeding relatives. *ISME J.* 12, 2252–2262. doi: 10.1038/s41396-018-0174-1

Chen, H., and Boutros, P. C. (2011). VennDiagram: A package for the generation of highly-customizable Venn and Euler diagrams in R. *BMC Bioinformatics* 12:35. doi: 10.1186/1471-2105-12-35

Chen, S., Zhou, Y., Chen, Y., and Gu, J. (2018). fastp: An ultra-fast all-in-one FASTQ preprocessor. *Bioinformatics* 34, i884–i890. doi: 10.1093/bioinformatics/bty560

Colman, D. R., Toolson, E. C., and Takacs-Vesbach, C. D. (2012). Do diet and taxonomy influence insect gut bacterial communities? *Mol. Ecol.* 21, 5124–5137. doi: 10.1111/j.1365-294X.2012.05752.x

Csardi, G., and Nepusz, T. (2006). The igraph software package for complex network research. *InterJournal Complex Syst.* 1695, 1–9.

Culver, D. C., and Pipan, T. (2019). *The biology of caves and other subterranean habitats*. Oxford: Oxford University Press. doi: 10.1093/oso/9780198820765.001.0001

de Mendiburu, F. (2014). *Agricolae: Statistical procedures for agricultural research. R package version, 2021.1.3-5*. Available Online at: http://CRAN.R-project.org/package=agricolae

DeSantis, T. Z., Hugenholtz, P., Larsen, N., Rojas, M., Brodie, E. L., Keller, K., et al. (2006). Greengenes, a chimera-checked 16S rRNA gene database and workbench compatible with ARB. *Appl. Environ. Microbiol.* 72, 5069–5072. doi: 10.1128/AEM.03006-05

Dormann, C. F., Gruber, B., and Fründ, J. (2008). Introducing the bipartite package: Analysing ecological networks. *R News* 8, 8–11.

Douglas, A. E. (2009). The microbial dimension in insect nutritional ecology. *Funct. Ecol.* 23, 38–47. doi: 10.1371/journal.pone.0170332

Douglas, A. E. (2011). Lessons from studying insect symbioses. *Cell Host Microbe* 10, 359–367. doi: 10.1016/j.chom.2011.09.001

Douglas, A. E. (2015). "Multiorganismal insects: Diversity and function of resident microorganisms," in *Annual review of entomology*, Vol. 60, ed. M. R. Berenbaum (Palo Alto, CA: Annual Reviews), 17–34. doi: 10.1146/annurev-ento-010814-020822

Duplais, C., Sarou-Kanian, V., Massiot, D., Hassan, A., Perrone, B., Estevez, Y., et al. (2021). Gut bacteria are essential for normal cuticle development in herbivorous turtle ants. *Nat. Commun.* 12:676. doi: 10.1038/s41467-021-21065-y

Edgar, R. C. (2013). UPARSE: Highly accurate OTU sequences from microbial amplicon reads. *Nat. Methods* 10, 996–998. doi: 10.1038/nmeth.2604

Ellegaard, K. M., Suenami, S., Miyazaki, R., and Engel, P. (2020). Vast differences in strain-level diversity in the gut microbiota of two closely related honey bee species. *Curr. Biol.* 30, 2520–2531. doi: 10.1016/j.cub.2020.04.070

Engel, P., Martinson, V. G., and Moran, N. A. (2012). Functional diversity within the simple gut microbiota of the honey bee. *Proc. Natl. Acad. Sci. U.S.A.* 109, 11002–11007. doi: 10.1073/pnas.1202970109

Engel, P., and Moran, N. A. (2013). Functional and evolutionary insights into the simple yet specific gut microbiota of the honey bee from metagenomic analysis. *Gut Microbes* 4, 60–65. doi: 10.4161/gmic.22517

Fonknechten, N., Chaussonnerie, S., Tricot, S., Lajus, A., Andreesen, J. R., Perchat, N., et al. (2010). *Clostridium sticklandii*, a specialist in amino acid degradation: Revisiting its metabolism through its genome sequence. *BMC Genomics* 11:555. doi: 10.1186/1471-2164-11-555

Freilich, M. A., Wieters, E., Broitman, B. R., Marquet, P. A., and Navarrete, S. A. (2018). Species co-occurrence networks: Can they reveal trophic and non-trophic interactions in ecological communities? *Ecology* 99, 690–699. doi: 10.1002/ecy.2142

Ginestet, C. (2011). ggplot2: Elegant graphics for data analysis. *J. R. Stat. Soc. Ser. A Stat. Soc.* 174, 245–246. doi: 10.1111/j.1467-985X.2010.00676_9.x

Handcock, M. S., Hunter, D. R., Butts, C. T., Goodreau, S. M., and Morris, M. (2008). statnet: Software tools for the representation, visualization, analysis and simulation of network data. *J. Stat. Softw.* 24, 1548–7660. doi: 10.18637/jss.v024.i01

Harrison, J. F., Kaiser, A., and VandenBrooks, J. M. (2010). Atmospheric oxygen level and the evolution of insect body size. *Proc. R. Soc. B Biol. Sci.* 277, 1937–1946. doi: 10.1098/rspb.2010.0001

Hassan, A., Uyigue, P., Akinleye, A., and Oyeromi, O. (2021). The role of common housefly as a mechanical vector of pathogenic microorganisms. *Achievers J. Sci. Res.* 3, 261–269. doi: 10.3390/microorganisms9112185

Howarth, F. G., and Moldovan, O. T. (2018). "The ecological classification of cave animals and their adaptations," in *Cave ecology. Ecological studies*, Vol. 235, eds O. Moldovan, L' Kováč, and S. Halse (Cham: Springer), 41–67. doi: 10.1007/978-3-319-98852-8_4

Hynönen, U., Kant, R., Lähteinen, T., Pietilä, T. E., Beganović, J., Smidt, H., et al. (2014). Functional characterization of probiotic surface layer protein-carrying *Lactobacillus amylovorus* strains. *BMC Microbiol.* 14:199. doi: 10.1186/1471-2180-14-199

Kostanjsek, R., and Pirc Marolt, T. (2015). Pathogenesis, tissue distribution and host response to *Rhabdochlamydia porcellionis* infection in rough woodlouse *Porcellio scaber*. *J. Invertebr. Pathol.* 125, 56–67. doi: 10.1016/j.jip.2015.01.001

Langille, M. G., Zaneveld, J., Caporaso, J. G., McDonald, D., Knights, D., Reyes, J. A., et al. (2013). Predictive functional profiling of microbial communities using 16S rRNA marker gene sequences. *Nat. Biotechnol.* 31, 814–821. doi: 10.1038/nbt.2676

Lavoie, K. H., Helf, K. L., and Poulson, T. L. (2007). The biology and ecology of North American cave crickets. *J. Cave Karst Stud.* 69, 114–134.

Li, D. (2007). Correlation between the animal community structure and environmental factors in Jialiang and Boduo caves of Guizhou Province, China. *Acta Ecol. Sin.* 27, 2167–2176.

Li, D., Rong, L., and Hu, C. (2001). Study on the animal communities in Dadongkou Cave, Guizhou Province. *Acta Ecol. Sin.* 21, 126–130.

Li, D. H. (2006). Correlation between the animal community structure and environmental factors in Dongbei Cave and Shuijiang Cave of Guizhou Province. *Zool. Res.* 27, 481–488.

Luan, J. B., Chen, W., Hasegawa, D. K., Simmons, A. M., Wintermantel, W. M., Ling, K. S., et al. (2015). Metabolic coevolution in the bacterial symbiosis of whiteflies and related plant sap-feeding insects. *Genome Biol. Evol.* 7, 2635–2647. doi: 10.1093/gbe/evv170

Luo, Z., Tang, S., Jiang, Z., Chen, J., Fang, H., and Li, C. (2016). Conservation of terrestrial vertebrates in a global hotspot of karst area in Southwestern China. *Sci. Rep.* 6:25717. doi: 10.1038/srep25717

Magoc, T., and Salzberg, S. L. (2011). FLASH: Fast length adjustment of short reads to improve genome assemblies. *Bioinformatics* 27, 2957–2963. doi: 10.1093/bioinformatics/btr507

McCutcheon, J. P., McDonald, B. R., and Moran, N. A. (2009). Convergent evolution of metabolic roles in bacterial co-symbionts of insects. *Proc. Natl. Acad. Sci. U.S.A.* 106, 15394–15399. doi: 10.1073/pnas.0906424106

Mok, J. S., Song, K. C., Kim, Y. M., and Chang, D. S. (2002). Cultural characteristics of *Lactobacillus amylovorus* IMC-1 producing antibacterial substance. *Korean J. Food Sci. Technol.* 34, 249–254.

Oksanen, J., Blanchet, F. G., Kindt, R., Legendre, P., Minchin, P. R., O'hara, R. B., et al. (2013). *Package 'vegan'. Community ecology package, version,* ***2****, 1-295*.

Paoletti, M. G., Mazzon, L., Martinez-Sañudo, I., Simonato, M., Beggio, M., Dreon, A. L., et al. (2013). A unique midgut-associated bacterial community hosted by the cave beetle *Cansiliella servadeii* (Coleoptera: Leptodirini) reveals parallel phylogenetic divergences from universal gut-specific ancestors. *BMC Microbiol.* 13:129. doi: 10.1186/1471-2180-13-129

Quast, C., Pruesse, E., Yilmaz, P., Gerken, J., Schweer, T., Yarza, P., et al. (2013). The SILVA ribosomal RNA gene database project: Improved data processing and web-based tools. *Nucleic Acids Res.* 41, D590–D596. doi: 10.1093/nar/gks1219

R Development Core Team (2018). *R: A language and environment for statistical computing*. Vienna: R foundation for statistical computing.

Revelle, W., and Revelle, M. W. (2015). Package 'psych'. *Compr. R Arch. Netw.* 337:338.

Salcedo-Porras, N., Umaña-Diaz, C., de Oliveira Barbosa Bitencourt, R., and Lowenberger, C. (2020). The role of bacterial symbionts in triatomines: An evolutionary perspective. *Microorganisms* 8:1438. doi: 10.3390/microorganisms8091438

Schloss, P. D. (2020). Reintroducing mothur: 10 years later. *Appl. Environ. Microbiol.* 86:e02343-19. doi: 10.1128/AEM.02343-19

Schloss, P. D., Westcott, S. L., Ryabin, T., Hall, J. R., Hartmann, M., Hollister, E. B., et al. (2009). Introducing mothur: Open-source, platform-independent, community-supported software for describing and comparing microbial communities. *Appl. Environ. Microbiol.* 75, 7537–7541. doi: 10.1128/AEM.01541-09

van Schooten, B., Godoy-Vitorino, F., McMillan, W. O., and Papa, R. (2018). Conserved microbiota among young *Heliconius* butterfly species. *PeerJ* 6:e5502. doi: 10.7717/peerj.5502

Vilanova, C., Baixeras, J., Latorre, A., and Porcar, M. (2016). The generalist inside the specialist: Gut bacterial communities of two insect species feeding on toxic plants are dominated by *Enterococcus* sp. *Front. Microbiol.* 7:1005. doi: 10.3389/fmicb.2016.01005

White, W. B., and Culver, D. C. (2011). *Encyclopedia of caves*. Cambridge, MA: Academic Press.

Wilson, G. R., and Benoit, T. G. (1993). Alkaline pH activates *Bacillus thuringiensis* spores. *J. Invertebr. Pathol.* 62, 87–89. doi: 10.1006/jipa.1993.1079

Wood, S. A., Gilbert, J. A., Leff, J. W., Fierer, N., D'Angelo, H., Bateman, C., et al. (2017). Consequences of tropical forest conversion to oil palm on soil bacterial community and network structure. *Soil Biol. Biochem.* 112, 258–268. doi: 10.1016/j.soilbio.2017.05.019

Xia, X., Sun, B., Gurr, G. M., Vasseur, L., Xue, M., and You, M. (2018). Gut microbiota mediate insecticide resistance in the diamondback moth, *Plutella xylostella* (L.). *Front. Microbiol.* 9:25. doi: 10.3389/fmicb.2018.00025

Xu, C., Li, D., and Me, J. (2010). Heavy metal content in animal body and its relations with soil and water in the Zhengjia small cave, Guizhou Province. *Carsologica Sin.* 29, 48–54.

Xu, S., Li, Z., Tang, W., Dai, Z., Zhou, L., Feng, T., et al. (2022). *MicrobiotaProcess: A comprehensive R package for managing and analyzing microbiome and other ecological data within the tidy framework*. Durham, NC: Research Square. doi: 10.21203/rs.3.rs-1284357/v1

Ye, Z. T., and Li, D. H. (2011). Research on enrichment of five heavy metals in cave animals from Tunshang cave of Guizhou. *Sichuan J. Zool.* 3, 372–376.

Yun, J.-H., Roh, S. W., Whon, T. W., Jung, M.-J., Kim, M.-S., Park, D.-S., et al. (2014). Insect gut bacterial diversity determined by environmental habitat, diet, developmental stage, and phylogeny of host. *Appl. Environ. Microbiol.* 80, 5254–5264. doi: 10.1128/AEM.01226-14

Zhao, C. C., Zhao, H., Zhang, S., Luo, J. Y., Zhu, X. Z., Wang, L., et al. (2019). The developmental stage symbionts of the pea aphid-feeding *Chrysoperla sinica* (Tjeder). *Front. Microbiol.* 10:2454. doi: 10.3389/fmicb.2019.02454

Zheng, X., Zhu, Q., Zhou, Z., Wu, F., Chen, L., Cao, Q., et al. (2021). Gut bacterial communities across 12 *Ensifera* (Orthoptera) at different feeding habits and its prediction for the insect with contrasting feeding habits. *PLoS One* 16:e0250675. doi: 10.1371/journal.pone.0250675

frontiers | Frontiers in Microbiology

TYPE Original Research
PUBLISHED 07 February 2023
DOI 10.3389/fmicb.2023.962452

OPEN ACCESS

EDITED BY
Diana Eleanor Northup,
University of New Mexico,
United States

REVIEWED BY
Ferenc L. Forray,
Babeş-Bolyai University,
Romania
Ilunga Kamika,
University of South Africa,
South Africa
Valme Jurado,
Institute of Natural Resources and
Agrobiology of Seville (CSIC),
Spain

*CORRESPONDENCE
Diana Felicia Bogdan
✉ diana.bogdan@ubbcluj.ro
Horia Leonard Banciu
✉ horia.banciu@ubbcluj.ro

SPECIALTY SECTION
This article was submitted to
Terrestrial Microbiology,
a section of the journal
Frontiers in Microbiology

RECEIVED 06 June 2022
ACCEPTED 17 January 2023
PUBLISHED 07 February 2023

CITATION
Bogdan DF, Baricz AI, Chiciudean I, Bulzu P-A, Cristea A, Năstase-Bucur R, Levei EA, Cadar O, Sitar C, Banciu HL and Moldovan OT (2023) Diversity, distribution and organic substrates preferences of microbial communities of a low anthropic activity cave in North-Western Romania.
Front. Microbiol. 14:962452.
doi: 10.3389/fmicb.2023.962452

Diversity, distribution and organic substrates preferences of microbial communities of a low anthropic activity cave in North-Western Romania

Diana Felicia Bogdan[1,2]*, Andreea Ionela Baricz[3], Iulia Chiciudean[3], Paul-Adrian Bulzu[4], Adorján Cristea[3], Ruxandra Năstase-Bucur[5,6], Erika Andrea Levei[7], Oana Cadar[7], Cristian Sitar[6,8], Horia Leonard Banciu[3,9]* and Oana Teodora Moldovan[5,6,10]

[1]Doctoral School of Integrative Biology, Faculty of Biology and Geology, Babeş-Bolyai University, Cluj-Napoca, Romania, [2]Institute for Research, Development and Innovation in Applied Natural Sciences, Cluj-Napoca, Romania, [3]Department of Molecular Biology and Biotechnology, Faculty of Biology and Geology, Babeş-Bolyai University, Cluj-Napoca, Romania, [4]Biology Centre CAS, Institute of Hydrobiology, Department of Aquatic Microbial Ecology, Laboratory of Microbial Ecology and Evolution, Ceske Budejovice, Czechia, [5]Emil Racovita Institute of Speleology, Cluj-Napoca Department, Cluj-Napoca, Romania, [6]Romanian Institute of Science and Technology, Cluj-Napoca, Romania, [7]INCDO-INOE 2000, Research Institute for Analytical Instrumentation, Cluj-Napoca, Romania, [8]Zoological Museum, Babeş-Bolyai University, Cluj-Napoca, Romania, [9]Centre for Systems Biology, Biodiversity and Bioresources, Faculty of Biology and Geology, Babeş-Bolyai University, Cluj-Napoca, Romania, [10]Centro Nacional de Investigación sobre la Evolución Humana, CENIEH, Burgos, Spain

Introduction: Karst caves are characterized by relatively constant temperature, lack of light, high humidity, and low nutrients availability. The diversity and functionality of the microorganisms dwelling in caves micro-habitats are yet underexplored. Therefore, in-depth investigations of these ecosystems aid in enlarging our understanding of the microbial interactions and microbially driven biogeochemical cycles. Here, we aimed at evaluating the diversity, abundance, distribution, and organic substrate preferences of microbial communities from Peştera cu Apă din Valea Leşului (Leşu Cave) located in the Apuseni Mountains (North-Western Romania).

Materials and Methods: To achieve this goal, we employed 16S rRNA gene amplicon sequencing and community-level physiological profiling (CLPP) paralleled by the assessment of environmental parameters of cave sediments and water.

Results and Discussion: *Pseudomonadota* (synonym *Proteobacteria*) was the most prevalent phylum detected across all samples whereas the abundance detected at order level varied among sites and between water and sediment samples. Despite the general similarity at the phylum-level in Leşu Cave across the sampled area, the results obtained in this study suggest that specific sites drive bacterial community at the order-level, perhaps sustaining the enrichment of unique bacterial populations due to microenvironmental conditions. For most of the dominant orders the distribution pattern showed a positive correlation with C-sources such as putrescine, γ-amino butyric acid, and D-malic acid, while particular cases were positively correlated with polymers (Tween 40, Tween 80 and α-cyclodextrin), carbohydrates (α-D-lactose, i-erythritol, D-mannitol) and most of the carboxylic and ketonic acids. Physicochemical analysis reveals that sediments are geochemically distinct, with increased concentration of Ca, Fe, Al, Mg, Na and K, whereas water showed low nitrate concentration. Our PCA indicated the clustering of different dominant orders with Mg, As, P, Fe, and Cr. This information serves as a starting point for further studies in elucidating the links between the taxonomic and functional diversity of subterranean microbial communities.

KEYWORDS

microbial communities, cave ecosystems, amplicon sequencing, karst cave, community-level physiological profiles

Introduction

Subterranean environments like caves are generally characterized by combined low temperature, high humidity, and low nutrient settings (Howarth and Moldovan, 2018). Investigations of subsurface microbial ecosystems aid in enlarging our understanding of the geomicrobial interactions of speleothems genesis and microbially driven biogeochemical cycles occurring in caves (Barton and Northup, 2007). Microorganisms adapted to cave environments feature slow metabolic and growth rates (Epure et al., 2014). Despite seemingly resource-limited condition, cave sediments could be a valuable reservoir for metabolites produced by the microbial communities inhabiting the ecosystem (Epure et al., 2014; Tomczyk-Żak and Zielenkiewicz, 2016; Rangseekaew and Pathom-Aree, 2019). Moreover, in some caves these communities could represent the primary producers that sustain the entire trophic web (Barton and Northup, 2007).

Cave microbiome generally includes *Bacteria*, *Archaea*, *Fungi* and rarely some algae and *Cyanobacteria* members. Bacterial-dominated communities are most frequently reported as colonizing the cave walls or speleothems apparently depleted in organics (Lavoie et al., 2017) and playing key roles in speleothem genesis or limestone erosion (Cuezva et al., 2009). Cave ecosystems might harbor chemotrophic-based primary production as in sulfidic Movile Cave (Sarbu et al., 1996). Microbial diversity could be shaped by geochemical composition and/or anthropic activity. Bacteria present under the oligotrophic environment of caves survive using complex metabolic pathways (Ortiz et al., 2013; De Mandal et al., 2017; Oliveira et al., 2017). Thus, despite the nutrient limitations, cave systems are inhabited by highly diverse microbial communities. Early studies revealed *Pseudomonadota*, *Acidobacteriota* (synonym *Acidobacteria*), and *Actinomycetota* (synonym *Actinobacteria*) as the most abundant phyla in addition to 'rare' (<1% of relative abundance) or unclassified prokaryotic lineages that were also detected (Addesso et al., 2021). A large number of caves, both show and pristine caves are found in the karst areas of the Romanian Carpathians (Onac and Goran, 2019). Information on microbial diversity within karst caves with restricted human access in the Romanian Carpathians is limited. Foregoing research on Carpathian caves focused on the ecophysiological groups relevant for paleoenvironmental studies, present in karstic springs (Bercea et al., 2019; Moldovan et al., 2020), air monitoring in show caves (Bercea et al., 2018), bat guano (Borda et al., 2014), and on active bacterial communities or bacterial culturable diversity within layers of an ice cave (Iţcuş et al., 2016; Paun et al., 2019).

Taxonomic diversity of microbial communities including uncultivated fraction can be directly derived from the 16S rRNA gene sequences. Furthermore, functional information could be predicted from 16S rRNA gene amplicon-sequencing datasets by computational methods such as phylogenetic investigation of communities by the reconstruction of unobserved states (PICRUSt; Koner et al., 2021). By combining these approaches with community-level physiological profiling (e.g., BIOLOG®EcoPlate™), a clearer picture of microbial diversity and metabolic potential could be drawn (Koner et al., 2021).

In this work we addressed the microbial diversity and distribution in relation to microhabitat type and carbon-source utilization patterns along Leşu Cave, a non-touristic cave located in the Romanian Carpathians. To the best of our knowledge, this is the first study to look at the relationship between taxonomic diversity and metabolic fingerprinting in low-anthropic cave environments located in the Romanian Carpathians thus contributing to a better understanding of the ecological roles of microbial communities in the trophic webs of subterranean ecosystems.

Materials and methods

Site description

Peştera cu Apă din Valea Leşului (Leşu Cave; 46.8249° N, 22.5655° E, altitude 650 m a.s.l.) located in the Apuseni Mountains (Western Carpathians of Romania) is a protected area and it is categorized as a natural reserve (category IV IUCN). The cave system consists of a main gallery of approximatively 1 km crossed by a water stream with meanders for the first 300 m, forming alluvial terraces (Figures 1A, B). The annual air temperature inside the cave averages between 8.5° and 10°C. The cave is protected for the important hibernation colony with various bat species, located predominantly near the cave entrance (Zoltan and Szántó, 2003; Bücs et al., 2012).

Sampling and sample preparation

Cave floor sediments and water samples were collected aseptically in 50 mL sterile tubes from well-established locations (Figure 1B) during February and May 2020. The six samples (Table 1) were kept at 4°C and in dark during transportation (approx. 6 h). Upon arrival in the laboratory, each sample was homogenized and subsampled for physicochemical and biological analysis. A fraction from each sample was used for metabolic fingerprinting using BIOLOG® EcoPlate™. The plates were inoculated immediately in sterile conditions and incubated (see below), while those for chemical analysis or needing further extraction of nucleic acids were frozen at −20°C until use.

Physicochemical analysis

The pH and electrical conductivity (EC) were measured in water samples and 1/5 sediment to water extracts using the Seven Excellence multiparameter (Mettler Toledo, Greifensee, Switzerland). For the measurement of elements, one gram of dried sediment sample was digested with 21 mL of 12 M HCl and 7 mL of 15.8 M HNO_3, then filtered and diluted to 100 mL with 0.5 M HNO_3. The aqua regia-extractable fraction is the maximum amount that can be extracted, and it includes both biologically available and unavailable metals. For measurement of dissolved metals and P concentration, the water samples were acidified with 15.8 M HNO_3 and filtered through

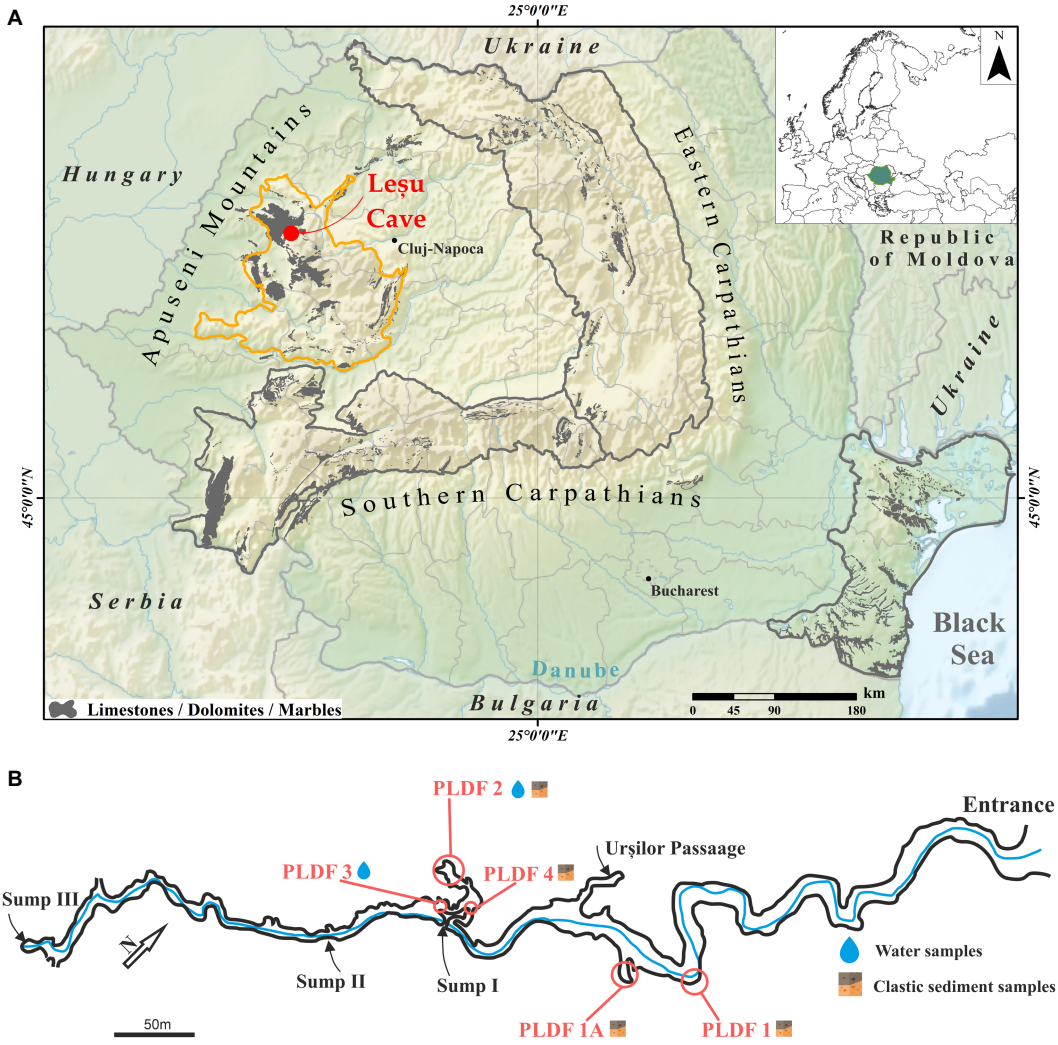

FIGURE 1
Geographical position of the Leșu Cave map (**A**; modified after Rusu, 1988) in Apuseni Mountains (NW part of Romania, maps modified in ArcGIS 10.1 from Wikipedia (https://ec.europa.eu/eurostat/web/gisco/geodata/reference-data/administrative-units-statistical-units/countries, last accessed 25th January 2023) and Eurostat (https://en.wikipedia.org/wiki/File:Relief_Map_of_Romania.png, last accessed 25th January 2023) © EuroGeographics for the administrative boundaries) with sampling sites and sample types collected **(B)**.

TABLE 1 Details and description of the cave samples analyzed in the present study.

Map ID	Sample ID	Sample type	Time of sampling
PLDF1	L1	Sand/clay from a terrace without direct water supply from the surface or the cave stream	Feb-20
PLDF1A	L1A	Sand/clay from a niche with relatively direct water supply from the surface, without known inlet	May-20
PLDF2	L2	Sand/clay from a lateral gallery without direct water supply from the surface or the cave stream	Feb-20
PLDF4	L4	Sand/clay from a lateral gallery without water	May-20
PLDF2W	L2W	Puddle on clay with percolation water which trickles down the wall	Feb-20
PLDF3W	L3W	Small lake under the rock with a sandy-clay substrate	Feb-20

0.45 µm-pore size cellulose acetate membrane filters. The concentration of Na, Mg, K, Ca, P in water and of Na, Mg, K, Ca, P, Al, Fe, S, Mn in sediments was measured by inductively coupled plasma optical emission spectrometry using an Optima 5300DV (Perkin Elmer, Waltham, MA, United States) spectrometer, while the concentration of Al, Fe, As, Cr, Mn, Co, Ni, Cu, Zn in water and of As, Cr, Co, Ni, Cu, Zn in sediments was measured by inductively coupled mass spectrometry using Elan DRC II (Perkin Elmer, Waltham, MA, United States) spectrometer. The concentration of carbon, hydrogen and nitrogen in sediments was measured with a Flash 2000 CHNS/O analyzer (ThermoFisher Scientific, Waltham, MA, United States). Total nitrogen (TN) in water was measured by catalytic combustion followed by oxidation of nitrogen monoxide to nitrogen dioxide with ozone and subsequent chemiluminescence detection using a Multi N/C 2100S Analyser (Analytik Jena, Jena, Germany). Dissolved carbon (DC) and dissolved inorganic carbon (DIC) were measured in water samples

filtered through 0.45 µm PTFE syringe filters by catalytic combustion and infrared detection of CO_2 using a Multi N/C 2100S Analyser (Analytik Jena, Jena, Germany). Dissolved organic carbon (DOC) was obtained by subtracting DIC from DC. Sulphate (SO_4^{2-}), nitrate (NO_3^-), chloride (Cl^-) and phosphate (PO_4^{3-}) were measured by ion chromatography on 761 Compact IC (Metrohm, Herisau, Switzerland).

DNA extraction and amplicon sequencing for 16S rRNA genes

Total environmental DNA (eDNA) was extracted using the protocol for the Quick-DNA Fecal/Soil Microbe Miniprep Kit (Zymo Research, Irvine, CA, United States) from approximately 250 mg of each sample. The V3-V4 hypervariable regions of the prokaryotic 16S rRNA gene were amplified *via* PCR using primers 341F (5′-CCTACGGGN GGCWGCAG-3′) and 805R (5′-GACTACHVGGGTATCTAATCC-3′), according to Illumina's 16S amplicon-based sequencing protocol. Sequencing was performed in triplicate at a commercial company (Macrogen Europe BV, Netherlands).

Sequence analysis and comparison of microbial communities

Sequencing primers from both forward and reverse reads as well as reads containing any N characters were removed using Cutadapt v2.9 (Martin, 2011). Only reads with a minimum length of 250 nt and maximum of 301, were kept for further analysis. Paired-end reads for each sample were processed using the DADA2 package (Callahan et al., 2016) implemented in R by adapting existing pipelines.[1] Following primer removal, paired reads were loaded into the DADA2 pipeline and trimmed (forward reads 3′ truncated at 280 nt, reverse reads 3′ truncated at 250 nt), filtered (max. 2 errors per read, minimum length after trimming = 200 nt) and finally merged with a minimum required overlap of 50 nt. Chimeras were removed from merged pairs. Following filtration and chimera removal, a total of 706,835 merged reads were retained (min per sample = 29,091, max per sample = 56,182, average = 44,177). The datasets presented in this study are publicly available at European Nucleotide Archive (ENA) under the BioProject ID PRJEB52949. Taxonomic classification of curated ASVs was achieved with the assignTaxonomy function within DADA2 against the SILVA 138 database (Pruesse et al., 2007).

Differences in community composition and statistics were computed using the phyloseq (McMurdie and Holmes, 2013) package in R and the XLSTAT (Addinsoft, Paris, France) Microsoft Excel extension (BASIC+, 2019.3.2).

Relative abundances were further generated at the genus, class, and phylum level, after performing taxonomic agglomeration using the tax glom function provided by phyloseq.

Venn analysis diagram of shared and unique ASVs was constructed using a web-based tool, InteractiVenn, developed by Heberle et al. (2015). It was used to indicate the distribution of the 16S related ASVs abundances between the different samples. TBtools was used for heatmap representations.

Bar plots of phyla and order-level were generated to show the community composition, and non-metric dimensional scaling (NMDS) was performed to determine the difference between prokaryotic community profiles on the distance matrix using Bray Curtis (Supplementary Figure S1). Shannon diversity and observed species indices were calculated using the estimate richness function from phyloseq. The Shannon index represents ASV abundance and estimates for both richness and evenness, whereas the observed species metric detected unique ASV's present in the samples. Functional abundances were predicted based on 16S gene rRNA sequences using the picrust2_pipeline.py provided as part of PICRUSt2 (Phylogenetic Investigation of Communities by Reconstruction of Unobserved States; Parks et al., 2014). The count table of ASVs converted to biom format[2] and ASV sequences produced with dada2 and phyloseq were used as input for the picrust2 pipeline which was run with default parameters. Full information about predicted pathways was added by employing add_descriptions.py from PICRUSt2. Statistical analyses and data representation was performed in the STAMP statistical environment (Parks et al., 2014). Microbial pathways and sample replicates were ordered by hierarchical clustering. Microbial pathways are noted by their level-2 superclasses.

Principal component analysis (PCA) of 20 physicochemical parameters with Varimax rotation and hierarchical clustering was employed using XLSTAT to interpret the structure of the principal dataset to determine which environmental variables better explain the observed bacterial community patterns in sediment samples. Due to the low number of water samples collected, and the different methods for measurements, these parameters were not included in the statistical analysis.

Community-level physiological profile

Previous research in this cave proposed a simple and relatively quick method of screening sediment for the bacterial activity that could be used in paleoenvironmental assessment (Epure et al., 2014). Here, functional diversity within the samples was assayed using BIOLOG®EcoPlate™ (Lehman et al., 1995; Garland, 2006). Prior to inoculation on the 96-well plates, the sediment was suspended in a final volume of 50 mL of 0.85% sterile NaCl solution and then stirred at 200 rpm for 30 min. One hundred microliters of the supernatant resulted from the on-the-table sedimentation was then inoculated in each of the 96 well of BIOLOG®EcoPlate™ microplate. Water samples were directly inoculated on plates. The 96-well BIOLOG®EcoPlate™ containing 31 different carbon sources in triplicate were incubated at 25°C for 200 h and color development was monitored at 12 h using a FLUOstar® Omega plate reader (BMG Labtech, Ortenberg, Germany). Parameters such as average well-color development (AWCD), substrate richness (R), Shannon-Weaver diversity index (H), and Shannon substrate evenness (E) were calculated and used to analyze the carbon source utilization pattern. For each well (i), AWCD was calculated as $\sum OD_i/31$ (Garland and Mills, 1991), R was represented as the number of metabolized substrates, $H = \sum p_i(\ln p_i)$, where $p_i = OD_i / \sum OD_i$, and E was calculated as H/lnR

1 http://benjjneb.github.io/dada2/tutorial.html; https://f1000research.com/articles/5-1492/v2

2 https://biom-format.org/

(Garland, 2006). Average absorbance values of the triplicate reads were used, after subtracting the blank and using a 0.25 threshold value for growth response, measured at OD 590 nm. Linear correlation coefficient was calculated to establish the relationship between order-level relative abundance and absorbance values, where-1 represents a negative correlation, 0 no correlation and + 1 a positive correlation.

Results

Physicochemical analysis of Leșu Cave sediments and water

Most of the sediment samples were sandy or clay with or without direct water supply with increased concentrations of Ca, Fe, Al, Mg, Na and K, whereas the substrate of water samples was either sandy-clay or puddle on clay with percolation water, both with low nitrates concentration. Major elements that may influence the community structure within sediments are revealed in the PCA plot by the clustering of different dominant orders with elements such as Mg, As, P, Fe, and Cr.

Physicochemical characteristics of sediment and water samples from Leșu Cave are given in Supplementary Tables S1, S2. The pH of the sediments was slightly alkaline (8.1–8.7). Calcium (Ca) was the major element in all sediments (5–11%), followed by Fe (1.6–2.8%), Al (0.9–2%) and Mg (0.2–3.2%). The Mg content of the L1 sediment (3.2%) was one order of magnitude higher than in the other samples (0.2–0.5%). The content of As, Cr, Co, Ni, Cu, and Zn in sediments was low (<350 mg/kg) across all samples. A higher S content in sediments without direct water supply (L1) and with a relatively direct water supply (L1A, L2) was found compared to the other sediment sample (L4). The collected water sample had a typical circumneutral pH (7.9–8.1) and low electrical conductivity (170–210 µS/cm). Similar to sediments, Ca was the major element in water (41–49 mg/L), followed by Fe, Al, Mg, Na and K. The trace metal concentrations in water were below 2 µg/L in all cases. The low concentration of DOC (<1 mg/L) compared to DIC (20–24 mg/L) suggest carbonate minerals dissolution as the main source of carbon in water.

16S rRNA gene-based taxonomic composition of bacterial community in Leșu Cave

Following quality control and the removal of mitochondrial and chloroplast DNA sequences, a data set of 16S rRNA gene fragments (V3-V4 region) containing 706,499 clean sequences was obtained, with an average number of sequences from each sample ranging from 29,091 to 56,175. These sequences were grouped into 9,314 amplicon sequence variants (ASVs), among which ~99% and ~ 1% (36 ASVs) were assigned to *Bacteria* and *Archaea* domains, respectively.

The Chao1, Shannon, and InvSimpson indices (Table 2) were used to assess the alpha diversity of cave bacterial communities. The Shannon index was higher in the sediment samples L1A and L2 than in the other two (L1, L4) and roughly similar to the water samples. Clustering of four samples (two sediments and two water samples) on NMDS plot (Supplementary Figure S1) indicates high bacterial composition.

The assessment of taxonomic composition of bacterial groups pointed a uniform distribution pattern where *Pseudomonadota* is the prevalent phylum across all samples (mean relative abundance 48.24%) followed by *Actinomycetota* (12.6%), *Acidobacteriota* (8.18%), "*Ca.* Patescibacteria" (5.68%) and *Verrucomicrobiota* (4.99%) (Figure 2). The prokaryotic communities of sediments and water in Leșu Cave were dominated by 19 bacterial orders that were prevalently present in sediment samples located closer to the cave entrance, as follows: *Chlamydiales, Diplorickettsiales*, *Xanthomonadales, Sphingomonadales*,

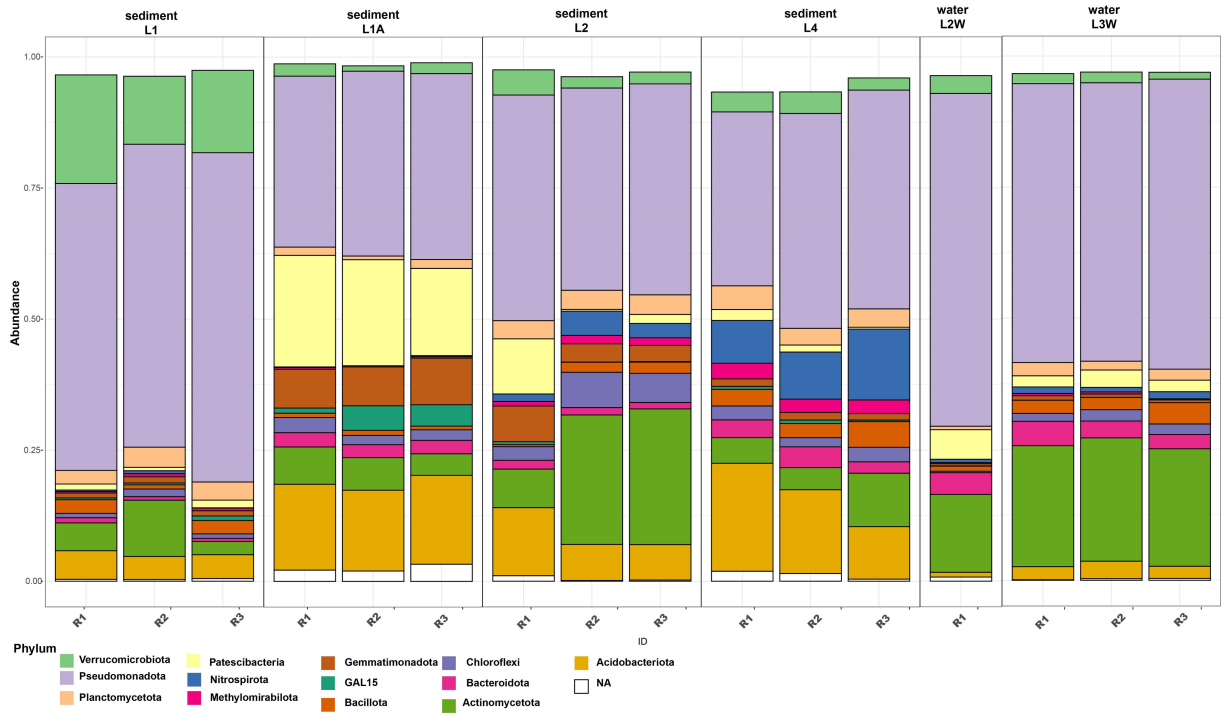

FIGURE 2
Relative abundance of dominant phyla (minimum 2% of the community) in sediments and water samples from Leșu Cave.

and *Gemmatimonadales*. *Nitrosococcales*, *Nitrospirales*, and *Burkholderiales* dominated the sediments located deeper in the cave. Water samples were less diverse compared to sediments, with *Caulobacterales*, *Propionibacterales* and *Rhizobiales* highly abundant in one sample (Figure 3), whereas *Pseudomonadales*, *Gemmatimonadales*, and *Gaiellales* were dominant in the other sample. *Gamma-and Alphaproteobacteria* were the prevailing classes with relative abundances varying from 24.15–46.07% and 5.27–27.96%. Most frequently predicted orders within *Gammaproteobacteria* included *Diplorickettsiales*, *Xanthomonadales*, "*Ca.* PLTA13," *Competibacterales* and *Burkholderiales*. "*Ca.* Patescibacteria" was found to be most abundant in L1A (19.38%) than in other samples and included "*Ca.* Saccharimonadales" and "*Ca.* Berkelbacteria" – affiliated ASVs. *Nitrospirota* was more abundant in L2 and L4 sediment samples (2.93 and 10.22%, respectively), and less abundant (below 1.2%) in water samples.

The order-level taxonomic composition (Figure 3) revealed a clumped distribution pattern where the highest abundances of *Burkholderiales* and *Pseudomonadales* were found in water samples, L2W (27.38 and 4.83% respectively) and L3W (15.16 and 26.97% respectively). In contrast, ASVs affiliated to *Gemmatimonadales, Gaiellales*, *Competibacterales*, *Nitrosococcales* and *Nitrospirales* were more abundant in sediments. Moreover, we found that "*Ca.* Saccharimonadales," *Xanthomonadales* and *Sphingomonadales* were preferentially associated with sediment (especially L1A and L1), whereas *Caulobacterales*, *Propionibacteriales* and *Rhizobiales* related ASVs were prevalent in water sample L2W. *Micrococcales* was found to be more abundant in one water sample and two sediment samples (L2, L4, L3W), whereas "*Ca.* PLTA13" was found to be slightly more abundant in sediment samples ranging from 2.01% (L4) to 4.61% (L2) and 6.06% (L1).

For the Venn analysis of shared and unique ASVs, orders with >0.1% relative abundances were considered. At order level, 23 out of 3,803 ASVs were shared among sediment samples and 56 out of 1,324 for water samples (Figure 4). The sediment shared ASVs have been mainly assigned to *Rhizobiales*, *Burkholderiales*, *Vicinamibacteriales*, *Propionibacteriales*, while other unique ASVs among sediments were assigned to *Xanthomonadales*, *Spingomonadales* (genus *Sphingosinicella*), *Nitrosococcales*, and *Micrococcales*. Several unique ASVs were unassigned to order-level but assigned to *Pseudomonadota*, "*Ca.* GAL15," and *Actinomycetota* phyla. Higher number of ASVs were shared among water samples and they were mainly classified within *Burkholderiales* (prevalent genera *Polaromonas*, *Duganella*, *Rhodoferax*), *Pseudomonadales* (predominant genera *Acinetobacter* sp. and *Pseudomonas* sp.), *Rhizobiales* (*Bradyrhizobium* sp.) and *Micrococcales* (*Arthrobacter* sp.).

Physicochemical variables shaping the community structure

Principal component analysis (PCA) of physicochemical parameters and the relative abundances of the dominant orders was performed only for sediment samples, due to the low number of water samples. PCA indicated that, except for L1 and L1A, the sediment samples are geochemically distinct, and the first two principal components explained 71.40% of the total variance. The trace elements from sediments do not represent the actual concentration in pore water nor the trace element fraction that is readily available for bacteria but the maximum amount of trace elements that could be solubilized into the pore water under certain extreme conditions. The samples L1 and L1A were similar and grouped in the 2-dimensional PCA plot defined by Mg, *Chlamydiales,*

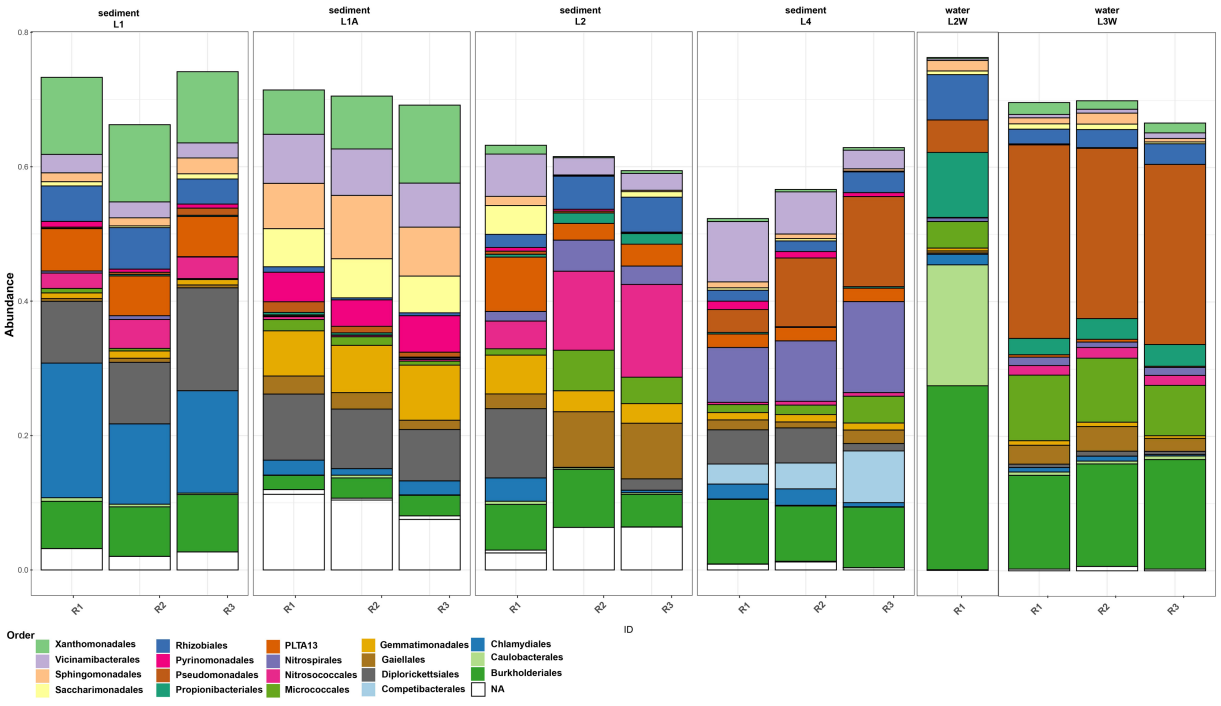

FIGURE 3
Order-level abundances of the microbial communities from sediments and water in Leșu Cave. Orders with a minimum of 5% abundance are shown.

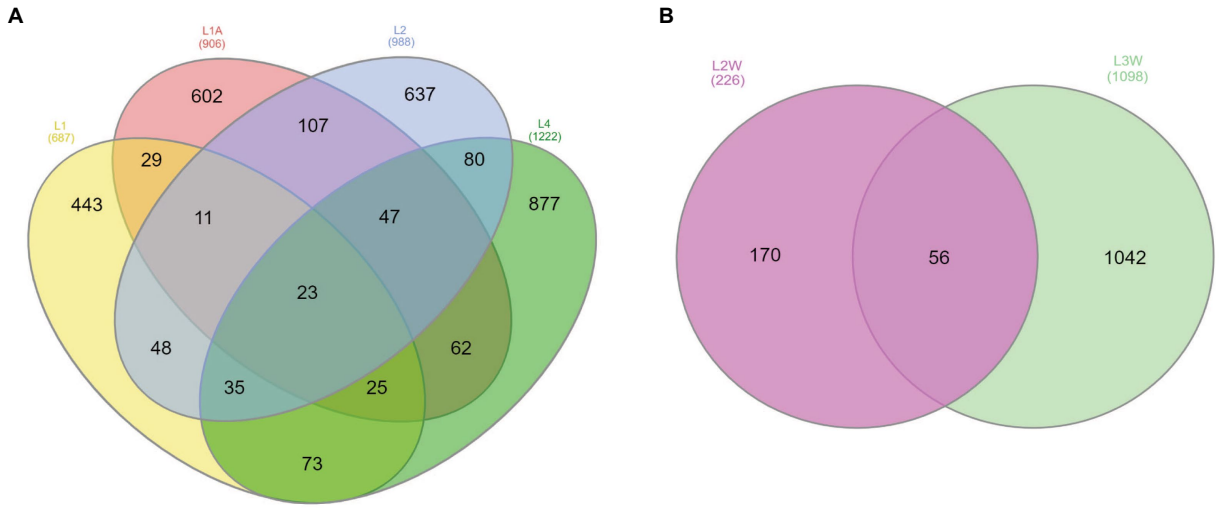

FIGURE 4
Venn diagram of the exclusive and shared ASVs at order-level with >0.1% of the community considered found among sediments **(A)** and water **(B)**.

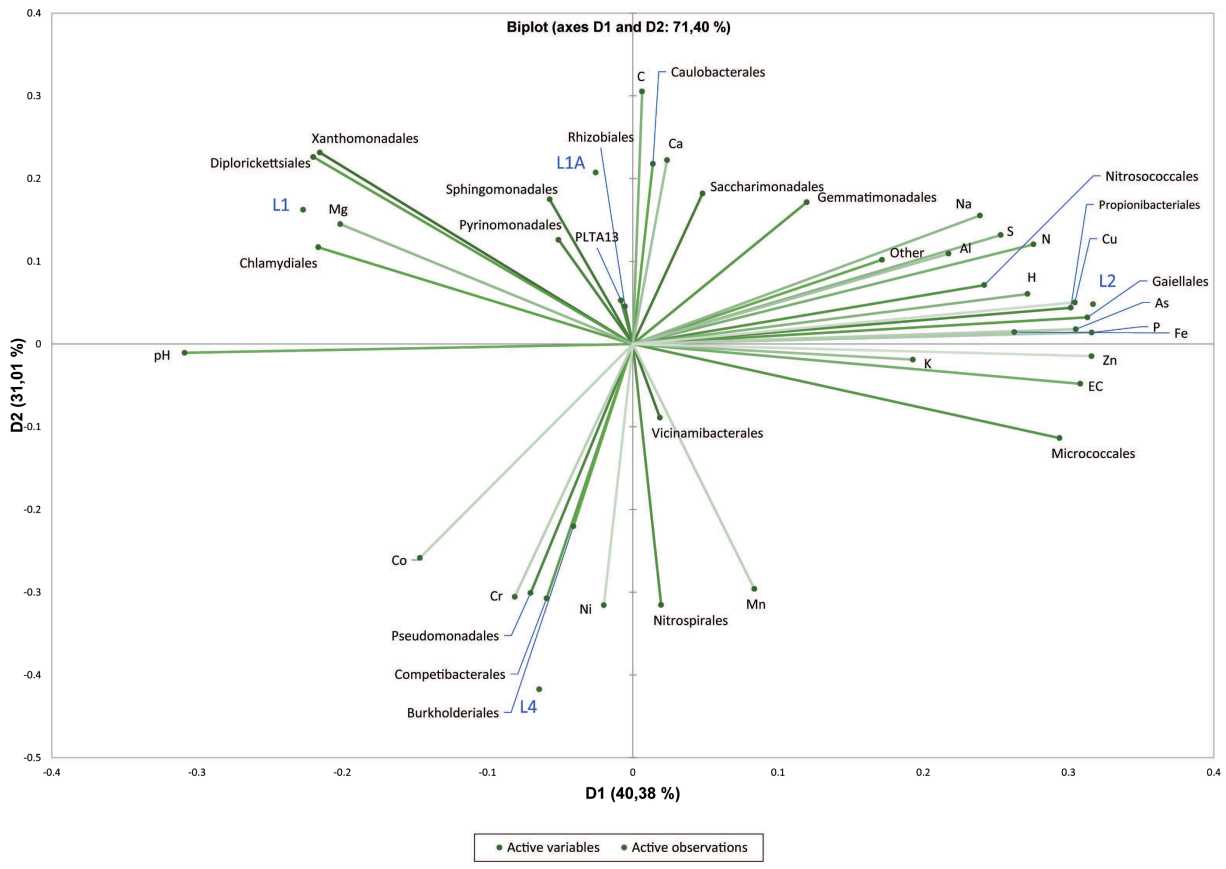

FIGURE 5
Principal Component Analysis (PCA) plot showing correlation between physicochemical factors of sediment samples with the dominant bacterial orders.

Diplorickettsiales and *Xanthomonadales* (L1), *Sphingomondales* (L1A), whereas L2 and L4 were highly different and spatially separated on the plot. L2 is defined by *Propionibacteriales, Nitrosococcales,* Cu, As, P, Fe, whereas L4 is defined by *Competibacterales* and *Pseudomonadales,* respectively Cr (Figure 5).

Community-level physiological profile and predicted functional pathways

Parameters such as average-well color development (AWCD), substrate richness (R) and diversity index H calculated after incubation

at room temperature for 200 h using BIOLOG®EcoPlate™ indicated a higher functional diversity in sediments (substantially in L2 and L1A) than in water samples (Figure 6 and Supplementary Table S3). It was overall observed that the carbon utilization rate was higher in sediments than in water (Figure 6). Interestingly, among polymers, Tween 40 and Tween 80 were consumed in all cases whereas glycogen and 2-hydroxy benzoic acid were the least degraded.

The linear correlation matrix depicting the relationship between the relative abundance of dominant order-level (minimum 5% of the community was considered) and C-source (Figure 7). With a few exceptions (*Caulobacterales*, *Rhizobiales*, *Burkholderiales*, *Propionibacteriales*, *Micrococcales*, and *Pseudomonadales*), most of the orders have a clustered distribution pattern with a positive correlation with putrescine, γ-amino butyric acid, and D-malic acid. *Sphingomonadales*, "*Ca.* Saccharimonadales," *Vicinamibacterales*, *Pyrinomonadales*, and *Gemmatimonadales* were positively correlated with polymers (Tween 40, Tween 80, α-cyclodextrin), carbohydrates (α-D-lactose, β-Methyl-D-glucoside, i-erythritol, D-mannitol), most of the carboxylic and ketonic acids, amino acids (glycyl-L-glutamic acid, and phenylethyl-amine). Similarly, *Caulobacterales*, *Rhizobiales*, *Burkholderiales*, and *Propionibacteriales* correlated positively with D-cellobiose, D, L-α-glycerol phosphate, and glycogen. *Micrococcales* and *Pseudomonadales*, on the other hand, had a negative correlation with most of the substrates. *Nitrosococcales* and *Gaiellales* are correlated particulary with Glucose-1-phosphate. The majority of the orders have a positive correlation with L-threonine amino acid and pyruvic acid methyl ester.

The PICRUSt2 analysis (Figure 8) predicted that the most abundant metabolic modules in investigated microbial communities were nucleoside and nucleotide metabolism, fatty acid and lipid metabolism, amino acid metabolism and glycolysis. The metabolic function prediction analysis also revealed enzymes involved in carbon metabolism which included alpha-amylase, pullulanase, and other carbohydrate degradation enzymes (Supplementary Tables S4–S6). Also, the analysis inferred that the enzymes involved in methane and nitrogen cycling such as methenyltetrahydrofolate cyclohydrolase (methane) and several other enzymes involved in

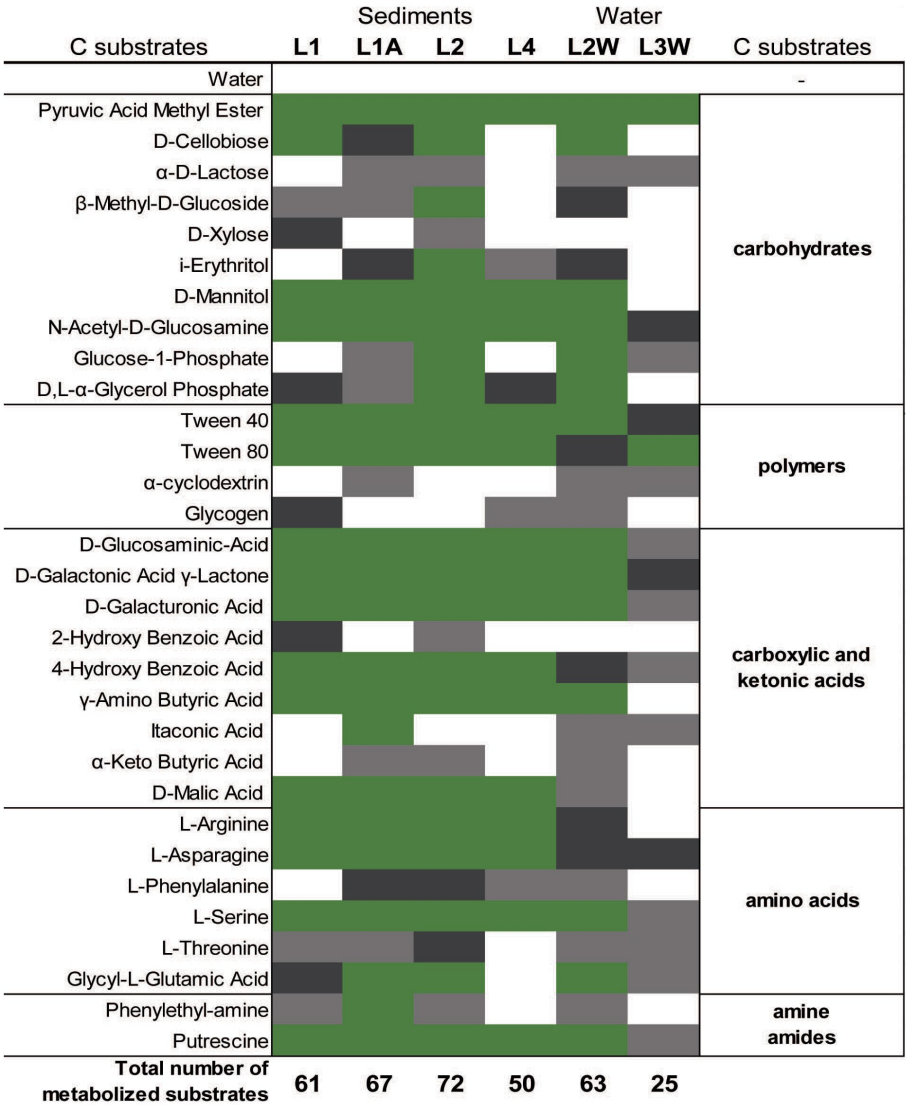

FIGURE 6
Color map of the metabolized different C-sources (substrates) among sediment and water samples collected. Substrate triplicate wells in which the color reaction occurred are marked with green (3/3 wells), dark grey (2/3 wells), light grey (1/3), and white (0/3).

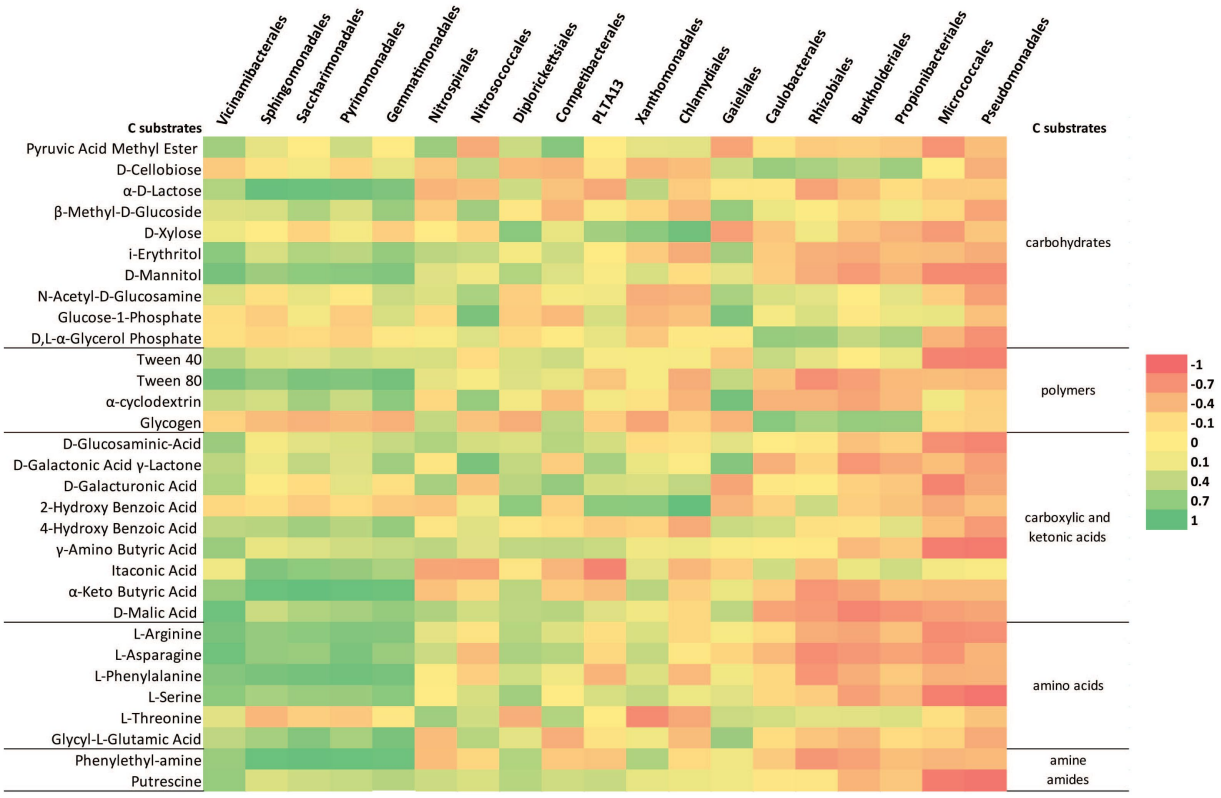

FIGURE 7
Heatmap of the correlation matrix between the relative abundance (order-level at minimum 5% of community) and C-source metabolization.

nitrification, nitrate reduction and ammonia assimilation may be present within the microbial communities (Supplementary Tables S4–S6).

Discussion

Diversity and distribution patterns of bacterial communities from Leşu Cave

In this study, we profiled the diversity, distribution, and organic substrates preferences of microbial communities in a karst cave with restricted public access located in North-Western Romania. The studied Leşu Cave in NW Romania has a low anthropic impact, and therefore, its microbial communities may resemble to those inhabiting other pristine karst caves worldwide. Previous studies on bacterial communities within caves revealed that the most abundant phyla are *Pseudomonadota*, *Actinomycetota*, *Acidobacteriota*, and *Bacillota* (synonym *Firmicutes*; Wu et al., 2015; De Mandal et al., 2017). At phyla-level the distribution pattern within the cave is uniform, whereas at order-level the differences in the relative abundances depict a spatially separated distribution between sampling sites with dominant orders among sediments and water: *Chlamydiales* (L1), *Xanthomonadales* (L1A), *Nitrosococcales* (L2), *Nitrospirales* (L4), *Burkholderiales* (L2W), and *Pseudomonadales* (L3W). Interestingly, the "*Ca.* Patescibacteria" phylum was detected in Leşu in a single sediment sample at a relative abundance exceeding 19%. This candidate bacterial group with assumedly symbiotic lifestyle was previously found in groundwater and aquifers (Chen et al., 2021) as well as in cave sediments in a relative low abundance (Addesso et al., 2021; Chen et al., 2021). The results here show that *Pseudomonadota* had the highest relative abundance in all samples. *Alphaproteobacteria* and *Gammaproteobacteria* were the dominant classes in both sediments and water, similar to findings in Pertosa-Auletta Cave (Addesso et al., 2021), Lava Beds National Monument (Lavoie et al., 2017) or Kashmir and Tiser Cave, Pakistan (Zada et al., 2021). Predominant orders of *Alphaproteobacteria* were *Rhizobiales* and *Sphingomonadales*, whereas the *Gammaproteobacteria* orders were *Pseudomonadales*, *Nitrosococcales*, *Diplorickettsiales*, *Xanthomonadales* and "*Ca.* PLTA13." *Aquicella* spp. (*Gammaproteobacteria*), abundant in Leşu sediments were previously reported in low abundance in Lascaux cave (Bastian et al., 2009) or other five caves from Mizoram, India (De Mandal et al., 2017). *Aquicella* spp. are presumed to be parasites or endosymbionts of amoebae (Bastian et al., 2009), suggesting an intricate trophic chain in Leşu Cave that deserves further exploration. Similarly, *Acinetobacter* spp. (*Pseudomonadales*, *Gammaproteobacteria*) was abundant in Leşu water samples. *Acinetobacter* sp. SC4, a strain involved in the precipitation of calcium carbonate (Li et al., 2019), was previously reported to be isolated from dripping waters from Altamira cave (Laiz et al., 1999), deep-well ground water (Stetzenbach et al., 1986), and other caves as well (Koren and Rosenberg, 2008; Adetutu et al., 2012; Tomova et al., 2013; Gan et al., 2020). It was suggested that the low concentrations of carbon may stimulate the growth of this bacterium and reflects its ability to utilize a variety of carbon sources and may in part explain its predominance in well water. "*Ca.* PLTA13," a gammaproteobacterial group previously reported in the biofilm microbial community of a Mn-rich mine from Sweden (Sjöberg et al., 2020) was found in the sediments of Leşu Cave. The little information on this elusive lineage, however, prevents us from any speculation on its ecological roles within the subterranean ecosystems.

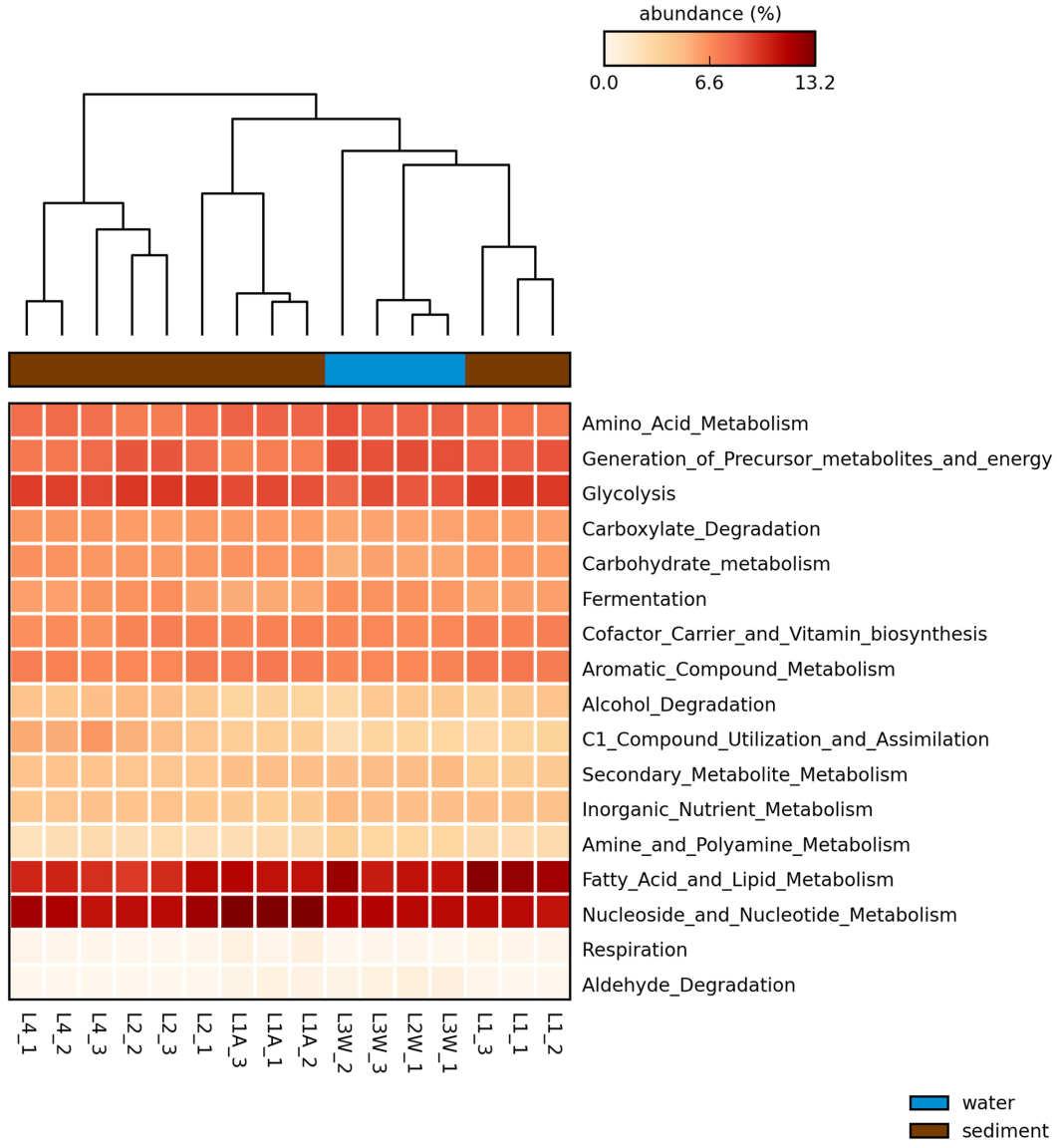

FIGURE 8
Heatmap of the proportion of sequences (5) of the predicted pathways by PICRUSt2 generated through STAMP with the average neighbor (UPGMA) method using the default parameters. Larger proportion of abundances are represented in dark red and smaller values in light yellow. Sample replicates names are included in the plot.

Actinomycetota the second most abundant phylum in this study, was frequently detected on stalactites, stalagmites, and cave walls, and as a key component of the cave soil microbiota with presumably important roles in biogeochemical cycling and weathering (Norris et al., 2011; Chen et al., 2015; Sathya et al., 2017; Zada et al., 2021). *Gaiellales* related sequences were retrieved by amplicon sequencing in this study similar to other karst (Zhu et al., 2019), and volcanic caves (Riquelme et al., 2015). The *Gaiellales* order has only one cultured representative isolated from a deep mineral water borehole that is strictly aerobic, chemoorganotrophic, being able to degrade a variety of complex substrates (Zecchin et al., 2017).

To our knowledge, this is the first evidence of *Vicinamibacterales* (*Acidobacteriota*) being reported in sediments from a karst cave with restricted access. Members of *Vicinamibacterales* are aerobic, and psychrotolerant to mesophilic chemoorganoheterotrophs, typically found in soils and growing on different simple sugars but also on complex proteinaceous compounds (Dedysh and Yilmaz, 2018). These acidobacteria are hypothesized to play an important role in soil P cycling (Wu, X. et al., 2021; Yang et al., 2022), which may explain the increased relative abundance of this *Vicinamibacteriales*-affiliated ASVs along with P concentration across a sediment sample (L2).

Gemmatimonadales-affiliated ASVs were recovered at low abundance in Leșu Cave sediments. This group include a few cultured members and it has been frequently detected in arid, low moisture soils, but also in cave vermiculation at low abundances (Hershey et al., 2018; Jurado et al., 2020).

We found that the geochemical composition of the sediment samples may influence the bacterial distribution among the sampling points in contrast to Alonso et al. (2018) who postulated that the mineral substrate is not the most significant factor determining the bacterial diversity among sediment and water samples. In the PCA plot, the distribution of *Sphingomonadales*, *Xanthomonadales* and *Diplorickettsiales* was influenced by Mg, which could be a key factor for bacterial growth (Cunrath and Bumann, 2019) or contribute to an

TABLE 2 Characteristic of diversity richness among cave sediment and water samples from Leşu Cave (R1, R2, R3 represent the number of replicates for each sample).

Sample		ASV	Chao1	Shannon	InvSimpson
L1	R1	270	271.91	4.02	25.50
	R2	283	283.60	4.13	28.71
	R3	212	212.00	3.96	22.71
L1A	R1	208	208.75	3.95	26.76
	R2	149	149.00	3.78	24.19
	R3	210	210.00	3.85	24.47
L2	R1	335	340.57	4.43	38.05
	R2	283	285.00	4.30	31.57
	R3	320	320.71	4.36	28.54
L4	R1	350	351.50	4.66	49.38
	R2	330	331.11	4.47	35.56
	R3	317	320.67	4.13	20.37
L2W	R1	216	216.00	4.06	21.69
L3W	R1	432	436.50	4.48	24.49
	R2	233	233.00	4.43	33.34
	R3	289	289.17	4.44	26.85

increase in exopolysaccharide production and biofilm stabilization, or bacterial adhesion (Song and Leff, 2006; Wang et al., 2019).

Community-level physiological profile and predicted functional pathways

By performing the community-level physiological profile (CLPP) approach, patterns of carbon-source utilization by microbial communities associated to Leşu Cave sediment and water were revealed. Simple carbon substrates, such as pyruvic acid methyl ester or diamine putrescine, a compound related to protein breakdown, were found to be the preferred forms of organic carbon degraded by the surveyed Leşu Cave microbial communities. The presence of *Sphingomonadales*, "*Ca.* Saccharimonadales," *Vicinamibacterales*, *Pyrinomonadales*, and *Gemmatimonadales*, the majority of which are uncultured or poorly described lineages, was correlated with the degradation of complex polymers such as Tween 40, Tween 80, and α-cyclodextrin. In the natural settings, complex polymers feeding cave microbial communities might originate either from terrestrial environments or from cave biofilms. The latter are usually enriched in sulfated glycosaminoglycans (sGAG), negatively charged, highly hydrophilic polymers. Recently, strong evidence was brought that sGAGs-like polymers in biofilms from Sulfur Cave (Romania) can be directly produced by prokaryotes (De Bruin et al., 2022).

Interestingly, among polymers, Tween 40 and Tween 80 were consumed in all cases whereas glycogen and 2-hydroxy benzoic acid were the least degraded. Glycogen is a highly branched polysaccharide that serves as a source of readily available glucose for many organisms. Glycogen accumulates in bacterial cells during the stationary phase or during inorganic nutrient limitation (Preiss and Romeo, 1994). Glycogen degradation may be performed by a set of extracellular enzymes (i.e., glycogen phosphorylases and glycosidases such as α-amylases) specific to bacteria that complete the degradative processes to carbohydrates (Coutinho et al., 2003), which are probably less abundant in Leşu.

"*Ca.* Saccharimonadales" ("*Ca.* Patescibacteria") was found to be a major contributing taxon in a biofilm on various polymers and particles from a headwater stream of wastewater treatment plants (Wu, H. et al., 2021), inferring their ability to degrade complex polymers. Besides, Tween 40 was metabolized by *Sphingomonas* sp. isolated from lake sediments of southern Finland (Rapala et al., 2005) and bacterial communities from cave ice layers (Iţcuş et al., 2016), Himalayan or Antarctic soils (Sanyal et al., 2018). Apparently, microbial communities from these low-temperature and oligotrophic habitats are readily exploiting chemically heterogeneous organic matter. Koner et al. (2021) noted that the non-ionic detergents were the fastest metabolized polymers by the rock microbiota. Utilization of carbon by bacterial communities is a key factor in the process of biomineralization in karst areas, and the efficiency of carbon catabolism is associated with the availability of different C-sources. Amino acid and carbohydrate consumption was predominantly linked to the outside-cave samples in the study of Koner et al. (2021), while other compounds were linked with the inside-cave samples, but in Leşu Cave we observed a positive correlation for the cave samples with most of the compounds. A study by Kenarova et al. (2014) showed that carbon substrates belonging to low molecular weight organic substances (LMWOS) are preferentially taken up by bacteria found in caves. Our results, highlighted by both BIOLOG®EcoPlate™ and PICRUSt analysis, showed that the bacterial communities are capable to have a moderate utilization of the carbon substrates belonging to LMWOS, such as fatty acid and lipid-related, amino acids and carbohydrates metabolic modules. Common metabolic pathways, e.g. carbohydrates and amino acids, within microbial communities were previously reported in a limestone cave in Southern Taiwan, similar to Leşu Cave, where dominating bacterial orders were positively correlated with the consumption of carbohydrates and amino acids (Koner et al., 2021). Our snapshot on the involvement in C and N cycles of bacterial communities inhabiting Leşu Cave predicted methenyltetrahydrofolate cyclohydrolase, an enzyme that drives reverse methanogenesis, similar to what has been reported by De Mandal et al. (2017) in caves from Mizoram, Northeast India. In the present study most of the genes involved in nitrogen cycle were inferred through PICRUSt analysis. The information about the role of bacteria in the nitrogen cycle in cave habitats is limited, but some reports point out their capacity to acquire energy through nitrogen cycling processes (De Mandal et al., 2017).

Acinetobacter sp. was one of the strains isolated from Altamira cave by Laiz et al. (1999). They further explored its ability of crystal formation when cultivated on a medium enriched with calcium and glucose. Their findings revealed that this strain is capable of producing large amounts of crystals which may help to explain why dominant orders in our study show a positive correlation with simple carbon substrates and point to the potential contribution to crystal formation inside the cave.

Conclusion

In this study, we surveyed the molecular diversity of microbial communities associated to sediments and water in a karst cave with little anthropic impact. Sediments were geochemically distinct with higher concentrations of Ca, Fe, Al, Mg, Na, K compared to water. Nitrate concentrations in water samples were low. Overall, the studied cave microbial communities were largely dominated by *Pseudomonadota* and *Actinomycetota* phyla. The calculated diversity indices revealed substantial community richness and spatial variation. These findings are at least partly explained by a few geochemical factors (e.g., Mg, As, P, Fe, and Cr) that appear to shape the structure,

composition and distribution of detected sediment and water-associated bacterial communities. The analysis of carbon substrate metabolization rates by Community-Level Physiological Profiling (CLPP) approach showed positive correlations between the most of the detected order-level taxa and the metabolization of low molecular weight C-sources such as putrescine, γ-amino butyric acid and polymers (Tween 40, Tween 80, and α-cyclodextrin). The CLPP pattern along with the predicted metabolic functions suggest that the detected bacterial communities may play key roles in the Leşu Cave trophic web by driving organic matter mineralization.

To the best of our knowledge this is the first investigation on the relationship between bacterial taxonomic diversity and organic carbon source utilization in a subterranean environment located in Eastern Europe. Nevertheless, more information on microbial activity and metabolic capabilities are yet needed to shed light on the roles of bacterial communities in the organic nutrients' degradation and biogeochemical cycles of main elements in cave ecosystems.

Data availability statement

The datasets presented in this study can be found in online repositories. The names of the repository/repositories and accession number(s) can be found in the article/Supplementary material.

Author contributions

DFB, HLB, and OTM designed the research and drafted the manuscript. DFB, AIB, IC, AC, and OTM conducted the research. AIB, IC, and P-AB analyzed the bioinformatic data. OTM performed the statistical analyses. RN-B, CS, and OTM performed the sampling. EAL and OC performed the chemical analyses. All authors contributed, verified, and approved the contents of the manuscript.

Funding

This work was supported by a grant of the Ministry of Research, Innovation and Digitization, CNCS/CCCDI – UEFISCDI, project number 2/2019 (DARKFOOD), within PNCDI III. DFB has received financial support through the project: Entrepreneurship for innovation through doctoral and postdoctoral research, POCU/380/6/13/123886 co-financed by the European Social Fund, through the Operational Program for Human Capital 2014-2020. P-AB was supported by the research grant 20-23718Y (Grant Agency of the Czech Republic).

Acknowledgments

All the authors thank to Ionuț Cornel Mirea (Institute of Speology, Bucharest) for his contribution on sampling campaigns, and map figures adaptations, Uri Gophna (Tel Aviv University, Israel) and Leah Reshef (Tel Aviv University, Israel) for their helpful advice in the predictive functional analysis.

Conflict of interest

The authors declare that the research was conducted in the absence of any commercial or financial relationships that could be construed as a potential conflict of interest.

The reviewer FF declared a shared affiliation with the authors DFB, AIB, IC, AC, CS, and HLB to the handling editor at the time of review.

Publisher's note

Supplementary material

The Supplementary material for this article can be found online at: https://www.frontiersin.org/articles/10.3389/fmicb.2023.962452/full#supplementary-material

References

Addesso, R., Gonzalez-Pimentel, J. L., D'Angeli, I. M., De Waele, J., Saiz-Jimenez, C., Jurado, V., et al. (2021). Microbial community characterizing vermiculations from karst caves and its role in their formation. *Microb. Ecol.* 81, 884–896. doi: 10.1007/s00248-020-01623-5

Adetutu, E. M., Thorpe, K., Shahsavari, E., Bourne, S., Cao, X., Fard, R. M. N., et al. (2012). Bacterial community survey of sediments at Naracoorte Caves, Australia. *Int. J. Speleol.* 41, 137–147. doi: 10.5038/1827-806X.41.2.2

Alonso, L., Creuzé-Des-Châtelliers, C., Trabac, T., Dubost, A., Moënne-Loccoz, Y., and Pommier, T. (2018). Rock substrate rather than black stain alterations drives microbial community structure in the passage of Lascaux Cave. *Microbiome* 6:216. doi: 10.1186/s40168-018-0599-9

Barton, H. A., and Northup, D. E. (2007). Geomicrobiology in cave environments: past, current and future perspectives. *J Caves Karst Stud.* 69, 163–178.

Bastian, F., Alabouvette, C., Jurado, V., and Saiz-Jimenez, C. (2009). Impact of biocide treatments on the bacterial communities of the Lascaux Cave. *Naturwissenschaften* 96, 863–868. doi: 10.1007/s00114-009-0540-y

Bercea, S., Năstase-Bucur, R., Mirea, I. C., Măntoiu, D. Ş., Kenesz, M., Petculescu, A., et al. (2018). Novel approach to microbiological air monitoring in show caves. *Aerobiologia* 34, 445–468. doi: 10.1007/s10453-018-9523-9

Bercea, S., Năstase-Bucur, R., Moldovan, O. T., Kenesz, M., and Constantin, S. (2019). Yearly microbial cycle of human exposed surfaces in show caves. *Subterr. Biol.* 31, 1–14. doi: 10.3897/subtbiol.31.34490

Borda, D. R., Năstase-Bucur, R. M., Spinu, M., Uricariu, R., and Mulec, J. (2014). Aerosolized microbes from organic rich materials: case study of bat guano from caves in Romania. *J. Caves Karst Stud.* 76, 114–126. doi: 10.4311/2013MB0116

Bücs, S. L., Jére, C., Csősz, I., Barti, L., and Szodoray-Parády, F. (2012). Distribution and conservation status of cave-dwelling bats in the Romanian Western Carpathians. *Vespertilio* 16, 97–113.

Callahan, B. J., McMurdie, P. J., Rosen, M. J., Han, A. W., Johnson, A. J. A., and Holmes, S. P. (2016). DADA2: high-resolution sample inference from Illumina amplicon data. *Nat. Methods* 13, 581–583. doi: 10.1038/nmeth.3869

Chen, R. W., He, Y. Q., Cui, L. Q., Li, C., Shi, S. B., Long, L. J., et al. (2021). Diversity and distribution of uncultured and cultured Gaiellales and Rubrobacterales in South China Sea sediments. *Front. Microbiol.* 12:657072. doi: 10.3389/fmicb.2021.657072

Chen, M., Xu, P., Zeng, G., Yang, C., Huang, D., and Zhang, J. (2015). Bioremediation of soils contaminated with polycyclic aromatic hydrocarbons, petroleum, pesticides, chlorophenols and heavy metals by composting: applications, microbes and future research needs. *Biotechnol. Adv.* 33, 745–755. doi: 10.1016/j.biotechadv.2015.05.003

Coutinho, P. M., Deleury, E., Davies, G. J., and Henrissat, B. (2003). An evolving hierarchical family classification for glycosyltransferases. *J. Mol. Biol.* 328, 307–317. doi: 10.1016/S0022-2836(03)00307-3

Cuezva, S., Sanchez-Moral, S., Saiz-Jimenez, C., and Cañaveras, J. C. (2009). Microbial communities and associated mineral fabrics in Altamira Cave, Spain. *Int. J. Speleol.* 38, 83–92. doi: 10.5038/1827-806X.38.1.9

Cunrath, O., and Bumann, D. (2019). Host resistance factor SLC11A1 restricts salmonella growth through magnesium deprivation. *Science* 366, 995–999. doi: 10.1126/science.aax7898

De Bruin, S., Vasquez-Cardenas, D., Sarbu, S. M., Meysman Sousa, D. Z., Van Loosdrecht, M. C. M., and Lin, Y. (2022). Sulfated glycosaminoglycan-like polymers are present in an acidophilic biofilm from a sulfidic cave. *Sci. Total Environ.* 829:154472. doi: 10.1016/j.scitotenv.2022.154472

De Mandal, S., Chatterjee, R., and Kumar, N. S. (2017). Dominant bacterial phyla in caves and their predicted functional roles in C and N cycle. *BMC Microbiol.* 17:90. doi: 10.1186/s12866-017-1002-x

Dedysh, S. N., and Yilmaz, P. (2018). Refining the taxonomic structure of the phylum Acidobacteria. *Int. J. Syst. Evol. Microbiol.* 68, 3796–3806. doi: 10.1099/ijsem.0.003062

Epure, L., Meleg, I. N., Munteanu, C. M., Roban, R. D., and Moldovan, O. T. (2014). Bacterial and fungal diversity of quaternary cave sediment deposits. *Geomicrobiol J.* 31, 116–127. doi: 10.1080/01490451.2013.815292

Gan, H. M., Wengert, P., Barton, H. A., Hudson, A. O., and Savka, M. A. (2020). Insight into the resistome and quorum sensing system of a divergent *Acinetobacter pittii* isolate from an untouched site of the Lechuguilla Cave. *Access Microbiol.* 2:acmi000089. doi: 10.1099/acmi.0.000089

Garland, J. L. (2006). Analysis and interpretation of community-level physiological profiles in microbial ecology. *FEMS Microbiol.* 24, 289–300. doi: 10.1111/j.1574-6941.1997.tb00446.x

Garland, M., and Mills, A. L. (1991). Classification and characterization of heterotrophic microbial communities on the basis of patterns of community-level sole-carbon-source utilization. *Appl. Environ. Microbiol.* 57, 2351–2359. doi: 10.1128/aem.57.8.2351-2359.1991

Heberle, H., Meirelles, V. G., da Silva, F. R., Telles, G. P., and Minghim, R. (2015). Interacti Venn: a web-based tool for the analysis of sets through Venn diagrams. *BMC Bioinform.* 16:169. doi: 10.1186/s12859-015-0611-3

Hershey, O. S., Kallmeyer, J., Wallace, A., Barton, M. D., and Barton, H. A. (2018). High microbial diversity despite extremely low biomass in a deep karst aquifer. *Front. Microbiol.* 9:2823. doi: 10.3389/fmicb.2018.02823

Howarth, F. G., and Moldovan, O. T. (2018). "The ecological classification of cave animals and their adaptations" in *Cave Ecology*. eds. O. T. Moldovan, L. Kovác and S. Halse (Cham: Springer), 41–67.

Iţcuş, C., Pascu, M. D., Brad, T., Perşoiu, A., and Purcarea, C. (2016). Diversity of cultured bacteria from the perennial ice block of Scărişoara Ice Cave, Romania. *Int. J. Speleol.* 45, 89–100. doi: 10.5038/1827-806x.45.1.1948

Jurado, V., Gonzalez-Pimentel, J. L., Miller, A. Z., Hermosin, B., D'Angeli, I. M., Tognini, P., et al. (2020). Microbial communities in vermiculation deposits from an Alpine Cave. *Front. Earth Sci.* 8:586248. doi: 10.3389/feart.2020.586248

Kenarova, A., Radeva, G., Traykov, I., and Boteva, S. (2014). Community level physiological profiles of bacterial communities inhabiting uranium mining impacted sites. *Ecotoxicol. Environ. Saf.* 100, 226–232. doi: 10.1016/j.ecoenv.2013.11.012

Koner, S., Chen, J. S., Hsu, B. M., Tan, C. W., Fan, C. W., Chen, T. H., et al. (2021). Assessment of carbon substrate catabolism pattern and functional metabolic pathway for microbiota of limestone caves. *Microorganisms* 9:1789. doi: 10.3390/microorganisms9081789

Koren, O., and Rosenberg, E. (2008). Bacteria associated with the bleached and cave coral *Oculina patagonica*. *Microb. Ecol.* 55, 523–529. doi: 10.1007/s00248-007-9297-z

Laiz, L., Groth, I., Gonzalez, I., and Saiz-Jimenez, C. (1999). Microbiological study of the dripping waters in Altamira Cave (Santillana del Mar, Spain). *J. Microbiol. Methods* 36, 129–138. doi: 10.1016/S0167-7012(99)00018-4

Lavoie, K. H., Winter, A. S., Read, K. J. H., Hughes, E. M., Spilde, M. N., and Northup, D. E. (2017). Comparison of bacterial communities from lava cave microbial mats to overlying surface soils from Lava Beds National Monument, USA. *PLoS One* 12:e0169339. doi: 10.1371/journal.pone.0169339

Lehman, R. M., Colwell, F. S., Ringelbergb, D. B., and White, D. C. (1995). Combined microbial community-level analyses for quality assurance of terrestrial subsurface cores. *J. Microbiol. Methods* 22, 263–281. doi: 10.1016/0167-7012(95)00012-A

Li, M., Fang, C., Kawasaki, S., Huang, M., and Achal, V. (2019). Bio-consolidation of cracks in masonry cement mortars by *Acinetobacter* sp. SC4 isolated from a karst cave. *Int. Biodeterior. Biodegradation* 141, 94–100. doi: 10.1016/j.ibiod.2018.03.008

Martin, M. (2011). Cutadapt removes adapter sequences from high-throughput sequencing reads. *EMBnet J.* 17:10. doi: 10.14806/ej.17.1.200

McMurdie, P. J., and Holmes, S. (2013). Phyloseq: an R package for reproducible interactive analysis and graphics of microbiome census data. *PLoS One* 8:e61217. doi: 10.1371/journal.pone.0061217

Moldovan, O. T., Bercea, S., Năstase-Bucur, R., Constantin, S., Kenesz, M., Mirea, I. C., et al. (2020). Management of water bodies in show caves – a microbial approach. *Tour. Manag.* 78:104037. doi: 10.1016/j.tourman.2019.104037

Norris, P. R., Davis-Belmar, C. S., Brown, C. F., and Calvo-Bado, L. A. (2011). Autotrophic, sulfur-oxidizing actinobacteria in acidic environments. *Extremophiles* 15, 155–163. doi: 10.1007/s00792-011-0358-3

Oliveira, C., Gunderman, L., Coles, C. A., Lochmann, J., Parks, M., Ballard, E., et al. (2017). 16S rRNA gene-based metagenomic analysis of Ozark cave bacteria. *Diversity* 9:31. doi: 10.3390/d9030031

Onac, B. P., and Goran, C. (2019). "Karst and Caves of Romania: A Brief Overview" in *Cave and Karst Systems of Romania*. eds. G. M. I. Ponta and B. Onac (Cham: Springer), 21–35.

Ortiz, M., Neilson, J. W., Nelson, W. M., Legatzki, A., Byrne, A., Yu, Y., et al. (2013). Profiling bacterial diversity and taxonomic composition on speleothem surfaces in Kartchner caverns, AZ. *Microb. Ecol.* 65, 371–383. doi: 10.1007/s00248-012-0143-6

Parks, D. H., Tyson, G. W., Hugenholtz, P., and Beiko, R. G. (2014). STAMP: statistical analysis of taxonomic and functional profiles. *Bioinformatics* 30, 3123–3124. doi: 10.1093/bioinformatics/btu494

Paun, V. I., Icaza, G., Lavin, P., Marin, C., Tudorache, A., Persoiu, A., et al. (2019). Total and potentially active bacterial communities entrapped in a late glacial through holocene ice core from Scarisoara Ice Cave, Romania. *Front. Microbiol.* 10:1193. doi: 10.3389/fmicb.2019.01193

Preiss, J., and Romeo, T. (1994). Molecular biology and regulatory aspects of glycogen biosynthesis in bacteria. *Prog. Nucleic Acid Res. Mol. Biol.* 47, 299–329. doi: 10.1016/S0079-6603(08)60255-X

Pruesse, E., Quast, C., Knittel, K., Fuchs, B. M., Ludwig, W., Peplies, J., et al. (2007). SILVA: a comprehensive online resource for quality checked and aligned ribosomal RNA sequence data compatible with ARB. *Nucleic Acids Res.* 35, 7188–7196. doi: 10.1093/nar/gkm864

Rangseekaew, P., and Pathom-Aree, W. (2019). Cave actinobacteria as producers of bioactive metabolites. *Front. Microbiol.* 10:387. doi: 10.3389/fmicb.2019.00387

Rapala, J., Berg, K. A., Lyra, C., Niemi, R. M., Manz, W., Suomalainen, S., et al. (2005). Paucibacter toxinivorans gen. nov., sp. nov., a bacterium that degrades cyclic cyanobacterial hepatotoxins microcystins and nodularin. *Int. J. Syst. Evol. Microbiol.* 55, 1563–1568. doi: 10.1099/ijs.0.63599-0

Riquelme, C., Hathaway, J. J. M., Dapkevicius, M. D. L. N. E., Miller, A. Z., Kooser, A., Northup, D. E., et al. (2015). Actinobacterial diversity in volcanic caves and associated geomicrobiological interactions. *Front. Microbiol.* 6:1342. doi: 10.3389/fmicb.2015.01342

Rusu, T. (1988). "Carstul din muntii padurea craiului" in *par Teodor Rusu*. eds. Dacia, Cluj-Napoca (L e karst des Monts Padurea Craiului).

Sanyal, A., Antony, R., Samui, G., and Thamban, M. (2018). Microbial communities and their potential for degradation of dissolved organic carbon in cryoconite hole environments of Himalaya and Antarctica. *Microbiol. Res.* 208, 32–42. doi: 10.1016/j.micres.2018.01.004

Sarbu, S. M., Kane, T. C., and Kinkle, B. K. (1996). A chemoautotrophically based cave ecosystem. *Science* 272, 1953–1955. doi: 10.1126/science.272.5270.1953

Sathya, A., Vijayabharathi, R., and Gopalakrishnan, S. (2017). Plant growth-promoting actinobacteria: a new strategy for enhancing sustainable production and protection of grain legumes. *3 Biotech* 7:102. doi: 10.1007/s13205-017-0736-3

Sjöberg, S., Stairs, C. W., Allard, B., Homa, F., Martin, T., Sjöberg, V., et al. (2020). Microbiomes in a manganese oxide producing ecosystem in the Ytterby mine, Sweden: impact on metal mobility. *FEMS Microbiol.* 96:fiaa169. doi: 10.1093/femsec/fiaa169

Song, B., and Leff, L. G. (2006). Influence of magnesium ions on biofilm formation by *Pseudomonas fluorescens*. *Microbiol. Res.* 161, 355–361. doi: 10.1016/j.micres.2006.01.004

Stetzenbach, L. D., Kelley, L. M., and Sinclair, N. A. (1986). Isolation, identification, and growth of well water bacteria. *Ground Water* 24, 6–10. doi: 10.1111/j.1745-6584.1986.tb01452.x

Tomczyk-Żak, K., and Zielenkiewicz, U. (2016). Microbial diversity in caves. *Geomicrobiol J.* 33, 20–38. doi: 10.1080/01490451.2014.1003341

Tomova, I., Lazarkevich, I., Tomova, A., Kambourova, M., and Vasileva-Tonkova, E. (2013). Diversity and biosynthetic potential of culturable aerobic heterotrophic bacteria isolated from Magura Cave, Bulgaria. *Int. J. Speleol.* 42, 65–76. doi: 10.5038/1827-806X.42.1.8

Wang, T., Flint, S., and Palmer, J. (2019). Magnesium and calcium ions: roles in bacterial cell attachment and biofilm structure maturation. *Biofouling* 35, 959–974. doi: 10.1080/08927014.2019.1674811

Wu, X., Peng, J., Liu, P., Bei, Q., Rensing, C., Li, Y., et al. (2021). Metagenomic insights into nitrogen and phosphorus cycling at the soil aggregate scale driven by organic material amendments. *Sci. Total Environ.* 785:147329. doi: 10.1016/j.scitotenv.2021.147329

Wu, Y., Tan, L., Liu, W., Wang, B., Wang, J., Cai, Y., et al. (2015). Profiling bacterial diversity in a limestone cave of the western Loess Plateau of China. *Front. Microbiol.* 6:244. doi: 10.3389/fmicb.2015.00244

Wu, H., Zhang, Q., Chen, X., Wang, L., Luo, W., Zhang, Z., et al. (2021). Effect of HRT and BDPs types on nitrogen removal and microbial community of solid carbon source SND process treating low carbon/nitrogen domestic wastewater. *J. Water Process Eng.* 40:101854. doi: 10.1016/j.jwpe.2020.101854

Yang, Z. N., Liu, Z. S., Wang, K. H., Liang, Z. L., Abdugheni, R., Huang, Y., et al. (2022). Soil microbiomes divergently respond to heavy metals and polycyclic aromatic hydrocarbons in contaminated industrial sites. *Environ. Sci. Ecotechnol.* 10:100169. doi: 10.1016/j.ese.2022.100169

Zada, S., Xie, J., Yang, M., Yang, X., Sajjad, W., Rafiq, M., et al. (2021). Composition and functional profiles of microbial communities in two geochemically and mineralogically different caves. *Appl. Microbiol. Biotechol.* 105, 8921–8936. doi: 10.1007/s00253-021-11658-4

Zecchin, S., Corsini, A., Martin, M., and Cavalca, L. (2017). Influence of water management on the active root-associated microbiota involved in arsenic, iron, and sulfur cycles in rice paddies. *App. Microbiol. Biotechnol.* 101, 6725–6738. doi: 10.1007/s00253-017-8382-6

Zhu, H. Z., Zhang, Z. F., Zhou, N., Jiang, C. Y., Wang, B. J., Cai, L., et al. (2019). Diversity, distribution and co-occurrence patterns of bacterial communities in a karst cave system. *Front. Microbiol.* 10:1726. doi: 10.3389/fmicb.2019.01726

Zoltan, L., and Szántó, L. (2003). Bats of the Carpathian Region. *Acta Chiropt.* 5, 155–160. doi: 10.3161/001.005.0115

frontiers | Frontiers in Microbiology

TYPE Review
PUBLISHED 20 March 2024
DOI 10.3389/fmicb.2024.1370520

OPEN ACCESS

EDITED BY
Paola Grenni,
National Research Council, Italy

REVIEWED BY
Alexandra Hillebrand-Voiculescu,
Romanian Academy, Romania
Cesareo Saiz-Jimenez,
Spanish National Research Council (CSIC), Spain

*CORRESPONDENCE
Paolo Visca
✉ paolo.visca@uniroma3.it

†These authors have contributed equally to this work and share first authorship

RECEIVED 14 January 2024
ACCEPTED 07 March 2024
PUBLISHED 20 March 2024

CITATION
Turrini P, Chebbi A, Riggio FP and Visca P (2024) The geomicrobiology of limestone, sulfuric acid speleogenetic, and volcanic caves: basic concepts and future perspectives.
Front. Microbiol. 15:1370520.
doi: 10.3389/fmicb.2024.1370520

The geomicrobiology of limestone, sulfuric acid speleogenetic, and volcanic caves: basic concepts and future perspectives

Paolo Turrini[1†], Alif Chebbi[1†], Filippo Pasquale Riggio[1] and Paolo Visca[1,2*]

[1]Department of Science, Roma Tre University, Rome, Italy, [2]National Biodiversity Future Center, Palermo, Italy

Caves are ubiquitous subterranean voids, accounting for a still largely unexplored surface of the Earth underground. Due to the absence of sunlight and physical segregation, caves are naturally colonized by microorganisms that have developed distinctive capabilities to thrive under extreme conditions of darkness and oligotrophy. Here, the microbiomes colonizing three frequently studied cave types, i.e., limestone, sulfuric acid speleogenetic (SAS), and lava tubes among volcanic caves, have comparatively been reviewed. Geological configurations, nutrient availability, and energy flows in caves are key ecological drivers shaping cave microbiomes through photic, twilight, transient, and deep cave zones. Chemoheterotrophic microbial communities, whose sustenance depends on nutrients supplied from outside, are prevalent in limestone and volcanic caves, while elevated inorganic chemical energy is available in SAS caves, enabling primary production through chemolithoautotrophy. The 16S rRNA-based metataxonomic profiles of cave microbiomes were retrieved from previous studies employing the Illumina platform for sequencing the prokaryotic V3-V4 hypervariable region to compare the microbial community structures from different cave systems and environmental samples. Limestone caves and lava tubes are colonized by largely overlapping bacterial phyla, with the prevalence of *Pseudomonadota* and *Actinomycetota*, whereas the co-dominance of *Pseudomonadota* and *Campylobacterota* members characterizes SAS caves. Most of the metataxonomic profiling data have so far been collected from the twilight and transient zones, while deep cave zones remain elusive, deserving further exploration. Integrative approaches for future geomicrobiology studies are suggested to gain comprehensive insights into the different cave types and zones. This review also poses novel research questions for unveiling the metabolic and genomic capabilities of cave microorganisms, paving the way for their potential biotechnological applications.

KEYWORDS

geomicrobiology, lava tube cave, limestone cave, microbial diversity, microbiome, sulfuric acid speleogenetic cave, volcanic cave, metataxonomic profiling

1 Introduction

Caves are defined as underground voids accessible to humans (Morgan, 1991). They are present in various lands worldwide (Ford and Williams, 2007) and represent a huge reservoir of still unexplored biodiversity. Caves also provide a huge surface for interaction with colonizing microorganisms, serving as a model habitat to study the microbial communities living in the subsurface (Gillieson, 2021). Therefore, cave microbiology has emerged as a new field of geomicrobiology, continuously improving thanks to scientific and technological advances in environmental microbiome studies. The complexity of microbial life implicated in key processes of cave ecosystems, such as nutritional and biogeochemical cycles, has recently been highlighted (Zhu et al., 2022). Microorganisms constitute the majority of rock-associated biomass in caves, capable of colonizing any cave habitat, including extremely oligotrophic environments (Reboleira et al., 2022). The high microbial diversity in these habitats represents a unique source of new genetic, metabolic, and physiological information, with a potential impact on pharmaceutical and biotechnological applications (Zada et al., 2022).

From a geochemical point of view, caves significantly differ according to the type of rock substrate and the cave formation processes (White and Culver, 2019; De Waele and Gutierrez, 2022). The main mechanism is based on rock dissolution, and sedimentary carbonate rocks constitute the prevalent fraction of soluble rocks on the Earth. Karst is the name indicating a carbonate rock landscape and karst terrains represent 15.2 % of the global ice-free continental surface (Goldscheider et al., 2020).

Among carbonate rocks, those composed of calcite ($CaCO_3$) are the prevalent substrate for limestone cave formation (Biagioli et al., 2023), as opposed to the less soluble dolomite [$CaMg(CO_3)_2$] rock. Limestone caves are often epigenic since generated by the acid rainwater actions that induce the dissolution of underlying calcite rocks (Culver and Pipan, 2009), while SAS caves are hypogenic since formed by hydrogen sulfide (H_2S)-rich water rising from the depths of the Earth (Engel et al., 2004b; D'Angeli et al., 2019a). Other caves are formed by dissolution processes of different rock types. They include evaporite rocks (gypsum, halite, anhydrite), which are relatively young with very rapid morphological evolution (D'Angeli et al., 2017), and silicate caves, which require a very long formation time since they are embedded in rocks that are poorly soluble in water, such as sandstone and quartzite (Sauro et al., 2018; Ghezzi et al., 2022; Liu et al., 2022).

Pseudokarst caves comprise underground environments generated by mechanisms other than dissolution. Among these, volcanic caves (Kempe, 2019) including lava tubes are cavities originating from lava flows and movements (Northup and Lavoie, 2015), glacial caves formed from the action of meltwater flowing through or under the glaciers (Howarth, 2021), and man-made cavities, created by human excavation (Parise et al., 2013). Early studies on cave microbiology date back to the 1960s and have been conducted on water and sediments using basic microscopy and culture-based approaches (Caumartin, 1963). It was only in the 1990s that, following the advent of molecular technologies and the use of the 16S rRNA gene as a phylogenetic marker, it became possible to study microbial communities in more detail, by gaining comprehensive taxonomic information from environmental DNA (eDNA) extracted from cave samples (Engel et al., 2004a). Although the culturability of bacteria from caves remains very low (0.02–1%), some strains endowed with biotechnological potential have been isolated under laboratory conditions (Bender et al., 2020). Microorganisms ubiquitously colonize caves, though the microbial density is much less than that of the soil. For example, a single gram of soil harbors up to 10^{10} bacterial cells and an estimated species diversity of $4x10^3$ to $5x10^4$ species (Raynaud and Nunan, 2014). The microbial density in caves is estimated at $<10^6$ microbial cells per gram of sample and varies depending on the distance from the entrance, the nutrient availability, and the rock geochemistry (Barton and Jurado, 2007; Barton, 2015).

Given the continuous improvement of next-generation sequencing (NGS) and analytical chemistry methods, various culture-independent approaches are being applied to cave microbiomes, e.g., 16S rRNA metataxonomic profiling (Biagioli et al., 2023), metagenomic shotgun sequencing (Wiseschart et al., 2019; Turrini et al., 2020), metatranscriptomics (Mondini et al., 2022) and proteomics (van Spanning et al., 2022). In parallel, high-magnification and fluorescence microscopies have contributed to unveiling biofilm-like structures on cave surfaces, identifying and quantifying specific taxa composing these communities, and studying the functional properties of individual microbial components (Jones et al., 2023). Cave microbiology has masterly been reviewed in the past, with an emphasis on geomicrobiology (Northup and Lavoie, 2001; Barton, 2006; Barton and Northup, 2007), anthropic impact (e.g., Bontemps et al., 2022), biogeochemical cycling (e.g., Zhu et al., 2022), biodiversity and functional roles of microbial communities (Engel, 2010; Kosznik-Kwaśnicka et al., 2022).

To the best of our knowledge, comparative studies of the microbial communities thriving in different types of caves (limestone, SAS, and volcanic caves) have not yet been conducted. Accordingly, here, we will *i*) describe the complexity of the cave ecosystem; *ii*) briefly overview basic concepts in cave microbiology; *iii*) describe the fundamental geological features of limestone, SAS, and volcanic caves, with a focus on the ecology and diversity of their microbial inhabitants; *iv*) compare the metataxonomic profiles of cave microbiomes retrieved from studies employing the Illumina (MiSeq) sequencing platform for sequencing the V3-V4 hypervariable regions of the prokaryotic 16S rRNA from limestone, SAS and lava tubes among volcanic caves; *v*) propose concepts and ideas for integrative cave microbiome studies, highlighting key steps of the investigation. We expect this review will also stimulate the exploitation of novel biotechnological potentials of cave microorganisms. The following three sections are intended to provide entry-level geomicrobiological information on the most common and best-studied cave ecosystems, to push forward and broaden the research interest into a still elusive component of the Earth's microbiome.

Abbreviations: ASV, amplicon sequence variant; DOM, dissolved organic matter; eDNA, environmental DNA; FISH, Fluorescence *in situ* hybridization; FTIR, Fourier Transform Infrared; iHMP, Integrative Human Microbiome Project; MAG, metagenome-assembled genome; NGS, next-generation sequencing; ppmv, parts-per-million by volume; OTU, operational taxonomic unit; POM, particulate organic matter; SAS, sulfuric acid speleogenesis; SEM, scanning electron microscopy; SRA, Sequence Read Archive; TOC, total organic carbon; VOC, volatile organic carbon.

2 The biological complexity of cave ecosystems

Caves are complex ecosystems comprising abiotic and biotic components (Culver and Pipan, 2009). All forms of life (i.e., viruses, bacteria, fungi, algae, protozoa, plants, and animals) have been described in subterranean ecosystems, including rock surfaces, groundwater pools, streams, bat guano, sediments, and others (Culver and Pipan, 2009).

The cave fauna can be divided into three categories based on adaptation and cave-related life cycle: trogloxenes, troglophiles, and troglobites (**Figure 1**). Some animals accidentally enter caves because they fall in or are transported by water flow. They are called trogloxenes due to their inability to survive in caves, while troglophiles are cave temporary resident animals. Troglophiles freely move in and out of the cave but need to use the Earth's surface environment for at least one vital function (i.e., reproduction or feeding). For instance, bats use caves as shelters during the day, and exit at night to forage for insects (Măntoiu et al., 2022). Finally, troglobites are animals permanently confined to subterranean environments, with specific physiological and morphological adaptations to cave habitats (Culver and Pipan, 2009).

In general, the cave biota distribution and adaptation depend on underground environmental conditions. Darkness is undoubtedly the hallmark of cave environments and the first ecological driver for autochthonous organisms. The only alternative to sunlight is the chemical energy deriving from the oxidation of inorganic compounds, supplied by chemolithoautotrophic microorganisms (Sogin et al., 2021). However, caves are oligotrophic environments and the chemical energy required to sustain primary production is limited, except in the case of SAS caves (Brad et al., 2021). All other caves are mostly dominated by heterotrophic organisms that consume organic matter, originating from outside the cave or generated inside by autotrophic production, as energy and carbon sources (Hershey and Barton, 2018). Organic nutrients, comprising particulate organic matter (POM), dissolved organic matter (DOM), and volatile organic carbon (VOC), enter the caves in different ways and quantities (Simon, 2019). They are transported via three main mechanisms: water, air, and animals (Culver and Pipan, 2009). Water is the primary nutrient carrier, enabling the transport of nutrients through flowing and percolation (Pronk et al., 2009). Surface streams can flow directly into void environments dragging organic material in the form of debris or large particles (POM), such as leaves and wood (Simon et al., 2007). For DOM transportation, rainwater first infiltrates through the soil and then into the rock microfractures before reaching the cave level (Simon et al., 2007). Wind and airflow inside the caves can contain spores, pollen, microorganisms, and VOCs (Porca et al., 2011). Animals can also transport nutrients through their movements in and outside the cave (e.g., feces, eggs, dead bodies).

Based on environmental parameters (light, temperature, humidity) and nutrient availability, scientists have generally subdivided caves into four zones, namely the photic, twilight, transition, and deep zones (**Figure 1**; Lee et al., 2012). The photic zone near the cave entrance mostly harbors phototrophic organisms. Flowering plants (*Spermatophyta*) are rarely found in caves, while ferns, mosses, and lichens form the bulk of the plant biomass in the cave entrance (Glime, 2022).

Progressing from the photic zone to the twilight zone, the light gradually fades depending on the daily and seasonal arc-like path of the sun (Behrendt et al., 2020). At this zone, plants can no longer grow due to low light levels and are generally replaced by algae (e.g., diatoms and green algae) (Falasco et al., 2014). This zone is also enriched with microbial species, such as fungi and bacteria, especially *Cyanobacteriota*, which produce *f* and *d* chlorophylls that allow them to absorb near-infrared (700–780 nm wavelength) radiations for oxygenic photosynthesis (Behrendt et al., 2020). Next, the transition zone is characterized by a complete absence of light, though both temperature and humidity still vary according to the climatic conditions of the Earth's surface and the seasonal changes (Kosznik-Kwaśnicka et al., 2022).

The transition zone is rich in microbial life, and the extension of this area can vary greatly depending on orography, the altitude at which the cave opens, the size and volume of the cave, and the air circulation inside the cave. Finally, the deep zone is characterized by darkness, almost constant temperature, humidity close to saturation (Badino, 2010), and oligotrophy with less than 2 mg/L of total organic carbon (Hershey and Barton, 2018). Due to its extreme conditions for life, this last zone of the cave is mainly colonized by troglobites (Novak et al., 2012), which have evolved various adaptive traits to darkness and oligotrophy, e.g., depigmentation, loss of sight sensory organs, the utmost development of touch sensory organs, lower metabolism, larger and more slender body shape (Culver and Pipan, 2009). Despite the vast knowledge of fauna caves in the deep zone, microorganisms thriving in this hidden part of the Earth remain elusive due to difficult accessibility, scarcity of biological materials, and challenges in culture-dependent and -independent approaches for the detection of cave microorganisms.

Due to their geographic location, temperate caves show remarkable differences compared with tropical caves. The most evident difference is temperature, with temperate caves typically having cooler temperatures, usually around 8–15°C, while the temperature is around 25°C in tropical caves (Mejía-Ortíz et al., 2020). Interestingly, the biodiversity is considerably higher in tropical caves than in temperate caves. This difference is linked to the greater quantity of energy permanently available in tropical caves, e.g., the abundance of guano resulting from bat colonies (Gnaspini and Trajano, 2000). However, most animals that inhabit tropical caves do not exhibit specific adaptations to cave life, different from troglobites that inhabit temperate caves, where climate is more stable and trophic resources are generally scarce (Howarth, 1980).

3 Cave microbiology: an overview

Cave microbiology is a growing research field, continuously providing novel insights into the evolution and adaptation of cave microbial inhabitants. Prominent topics in cave microbiology grossly refer to five research areas: the discovery of new species, geo-microbial interactions, microbial diversity assessment, anthropogenic impacts on cave microbiomes, mechanisms of microbial adaptation, and biotechnological potentials of cave microorganisms.

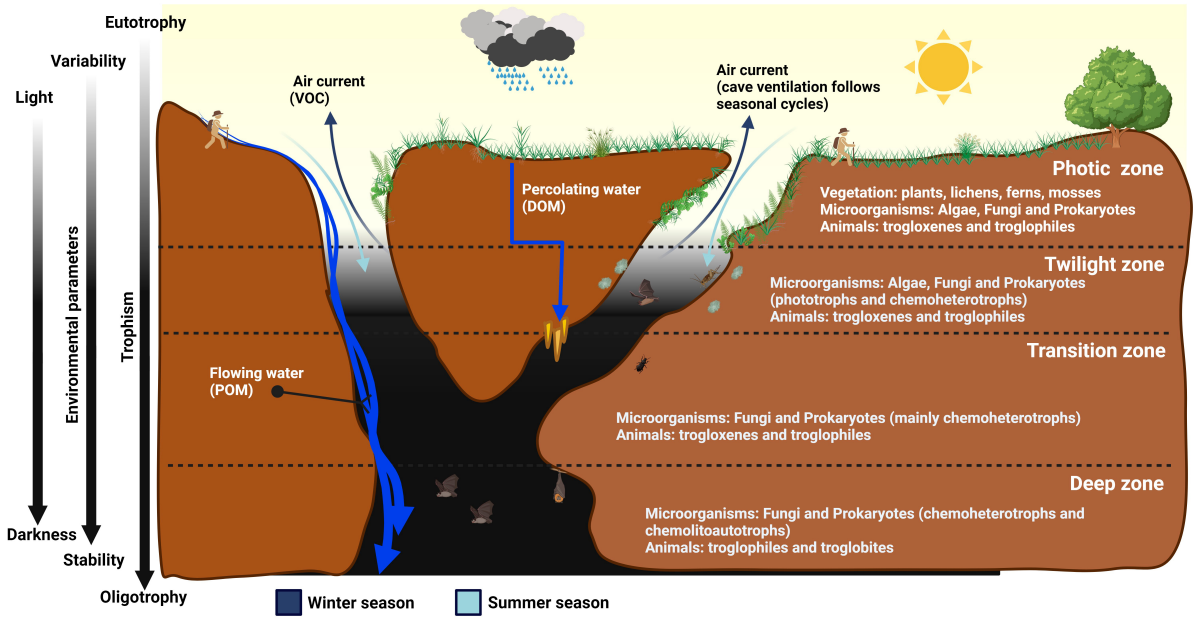

FIGURE 1
Schematic representation of the different cave zones, and their characteristics in relation to light intensity, temperature, humidity, airflow, and nutrient availability.

By analyzing research literature, out of 1,226 research papers retrieved from the Scopus database (December 2023) using "cave AND bacteria" and "cave AND microbes" as keywords, 112 described new bacterial species (nov. sp. cave bacteria as keywords) and their adaptive traits to the cave environment. Due to isolation from the Earth's surface and the selective pressure imposed by diverse habitats, cave microorganisms can accumulate genetic changes that make them distinct from their surface soil counterparts (Griebler et al., 2014).

Historically, culture-based approaches have been the main strategy for studying cave microbial species. For instance, members of the *Streptomyces* genus have been isolated from Altamira Cave and have been shown to precipitate calcium carbonate in laboratory cultures (Groth et al., 1999). By applying novel high-throughput technologies, *Candidatus* Mycobacterium methanotrophicum was isolated from an extremely acidic biofilm growing on the wall of a SAS cave in Romania (van Spanning et al., 2022). This bacterium represents the first member of *Actinomycetota* to show aerobic methanotrophic properties, previously described only in *Pseudomonadota* and *Verrucomicrobiota*. The probability of discovering new microbial species is likely to increase when different types of caves, or different cave zones, especially the very deep ones, will be explored. Another critical feature of cave microorganisms is their ability to interact with the rock surface (Jones and Northup, 2021). They can contribute to rock dissolution by releasing corrosive organic acids, e.g., oxalic acid and formic acid (Bin et al., 2008), or ligands such as metal-complexing agents, like siderophores, enabling the mobilization of mineral elements necessary for their nutrition (Duncan et al., 2021). The metabolic activity of cave microorganisms can also induce biomineralization or mineral depositions, thereby contributing to the formation of secondary mineral deposits called speleothems (Northup and Lavoie, 2001). For instance, the moonmilk formation is characterized by microcrystalline aggregates textures (i.e., calcite, aragonite, hydromagnesite) resulting from the precipitation of calcite fibers induced by certain cave bacteria, e.g., *Actinomycetota* (Cañaveras et al., 2006; Cacchio et al., 2014; Maciejewska et al., 2017). These biomineralization abilities could be useful in formulating novel bacterial-based building materials (Kosznik-Kwaśnicka et al., 2022).

Furthermore, with the advent of NGS technologies, cave microbial diversity has more intensively been investigated (Tomczyk-Żak and Zielenkiewicz, 2016). Metataxonomic profiling of the prokaryotic hypervariable regions (e.g., V3-V4) of the 16S rRNA gene, the fungal internal transcribed spacer (ITS) rRNA gene, and the eukaryotic 18S rRNA gene unraveled the great diversity of cave microbial communities, which are consortia composed of many species from multiple phyla (Hershey and Barton, 2018). With shotgun sequencing methodologies, the abundance of underexplored domains, including *Archaea*, *Eukarya*, and *Viruses* was revisited (Rossmassler et al., 2016; Kimble et al., 2018; Wiseschart et al., 2019; Turrini et al., 2020). The high species richness in oligotrophic caves remains challenging to explain (Hershey and Barton, 2018). Some authors attribute this phenomenon to competitive exclusion (Prescott et al., 2022), while others suggest interspecies interactions to exploit the scarcity of available nutrients (Barton and Jurado, 2007).

In this context, cave microbial communities are model systems for investigating bacterial relationships and even cell-to-cell communication (Ma et al., 2021). However, comparative studies on cave microbial diversity are challenging due to various factors, including rock types (e.g., limestone, quartz, basalt, gypsum), environmental matrix (wall rock surface, sediment, groundwater water), and the sampling location inside the cave (photic, twilight, transient, and deep zone). As for other extreme environments, caves have attracted researchers to study the ecological implications

of resistance to antibiotics (Bhullar et al., 2012), heavy metals (Hamedi et al., 2019), salinity (Farda et al., 2022a), UV radiation (Snider et al., 2009), radioactivity (Enyedi et al., 2019), and desiccation (Vardeh et al., 2018). For instance, in a remote zone at 400 m depth of a pristine cave in New Mexico, isolated for over 4 million years, bacteria were resistant to many antibiotics used in human medicine (Bhullar et al., 2012). Isolate LC231 belonging to *Paenibacillus* sp. was resistant to 26 of 40 antibiotics tested, including daptomycin, a relatively new antibiotic produced by *Streptomyces roseosporus* (Pawlowski et al., 2016). This finding supported the notion that antibiotic resistance mechanisms not only spread in the environment but have existed long before the selection pressure created by human use of antibiotics (Bhullar et al., 2012).

Therefore, caves constitute an excellent model to study the origins and the evolution of the mechanism of resistance in natural microbiomes, unexposed to exogenous interference. It is also clear that caves are fragile ecosystems, extremely susceptible to anthropogenic impact (Bontemps et al., 2022). For instance, show caves which attract tourists due to their beautiful speleothems or paleolithic paintings, alter their autochthonous microbial community structures due to the introduction of allochthonous species of presumptive human origin (Bontemps et al., 2022). The introduction of artificial light sources has been found to induce a progressive proliferation of greenish biofilms named "lampenflora" (Kosznik-Kwaśnicka et al., 2022). Additional factors, including a large number of visitors, and fluctuations in both environmental parameters and nutritional levels, were also associated with microbial community shifts and the appearance of alien species (Alonso et al., 2019; Rachid and Güngör, 2022). However, a dearth of information is currently available about the human impact on other types of caves, including polluted natural caves, especially those in industrial and urban areas (Qian et al., 2020; Scharping and Garey, 2021). Regarding the biotechnological potential, cave autochthonous microorganisms have extensively been investigated for their capacity to produce bioactive compounds (Ghosh et al., 2017a; Rangseekaew and Pathom-aree, 2019; Farda et al., 2022a; Zada et al., 2022). *Actinomycetota*, the main group of antibiotic-producing microorganisms (Barka et al., 2016), are generally abundant in limestone and some volcanic caves (Riquelme et al., 2017; Covington et al., 2018), and interesting antimicrobial properties have been documented for culturable *Streptomyces* strains isolated from moonmilk cave deposits (Maciejewska et al., 2016). Production of novel add-value secondary metabolites has been documented in cave isolates, including cervimycins by *Streptomyces tendae* in a limestone cave from Grotta dei Cervi, Italy (Herold et al., 2005), xiakemycin and huanglongmycin by *Streptomyces* sp. CC8-201 from karst caves in China (Jiang et al., 2018), hypogeamicins by *Nonomuraea* species from Hardin's cave system in Tennessee, USA (Derewacz et al., 2014), and curamycin by *Streptomyces benahoarensis* from a lava tube in La Palma Island (Canary Islands), Spain (Gonzalez-Pimentel et al., 2022). Recently, *Cyanobacterota* isolates from the lightened walls of the Stiffe cave in Italy were found to produce poly-β hydroxybutyrate for potential use in bioplastics production (Djebaili et al., 2022). Given the problematic culturability of cave bacteria, attempts should be made to implement culture-based strategies for better exploiting their biotechnological potential.

4 Main cave systems and microbial colonization patterns

Most studies on cave microbiology have been conducted in limestone, SAS, and volcanic caves. Considering the crucial influence of the mineral matrix on the colonizing microbial communities, hereafter we summarize the mechanisms of formation and the geological structure of limestone, SAS, and lava tubes among volcanic caves, and provide an overview of their microbial diversity.

4.1 Limestone caves

Limestone caves are natural cavities in carbonate rocks formed underneath the Earth's surface, and they can be very different from each other. Some are small, which humans can hardly penetrate, others develop complex networks, which propagate underground for up to several hundred km, reaching over one km in depth (Klusaitė et al., 2016). Most of the largest limestone caves are complex underground structures consisting of rooms, wells, meanders, and intercommunicating tunnels, which are organized to form a system or karst complex (**Figure 2A**). Mammoth Cave National Park, a World Heritage site in Kentucky, in the USA, has the world's most extended natural cave network with more than 675 km of surveyed passages. Another World Heritage site, Mulu National Park in Sarawak (Malaysia), contains the world's largest underground room - Sarawak Chamber in Nasib Bagus Cave. It covers an area of about 160,000 m^2 and has a volume of about 10 million m^3. The deepest limestone cave in the world is Verëvkina (Veryovkina) Cave in the Arabika Massif in Abkhazia (Georgia), which is 2,2 km deep (Gulden, 2019).

Dissolution of carbonate rocks requires acidic water that increases the solubility of calcite. CO_2 present in the atmosphere and soil reacts with rainwater by forming carbonic acid (H_2CO_3) (**Eq. 1**), which further dissociates, producing protons (H^+) that acidify the solution (**Eq. 2**). Acid water induces the dissolution of carbonate bedrock to release bicarbonate (HCO_3^-) and calcium (Ca^{2+}) ions (**Eq. 3**) (Ford and Williams, 2007). These simple chemical reactions can be expressed as follows:

$$CO_2 + H_2O \leftrightarrow H_2CO_3 \quad (1)$$

$$H_2CO_3 \leftrightarrow H^+ + HCO_3^- \quad (2)$$

$$Ca^{2+} + 2HCO_3^- \leftrightarrow CaCO_3 + CO_2 + H_2O \quad (3)$$

Increasing CO_2 or decreasing Ca^{2+} drives the **Eq. 3** reaction to the left, inducing calcite dissolution, while increasing Ca^{2+} or decreasing CO_2 drives the **Eq. 3** reaction to the right, precipitating calcite.

Irrespective of whether they are epigenic or hypogenic, limestone caves originate from the action of acidic water that flows through the fractures of the bedrock, thus generating subsurface voids. In epigenic caves (**Figure 2A**), water flows by gravity through the limestone massif causing subterranean drainage (groundwater circulation), and ultimately it returns to the surface at the springs. Conversely, in hypogenic caves, acidic water ascends from the depths of the Earth causing mineral dissolution, as exemplified in

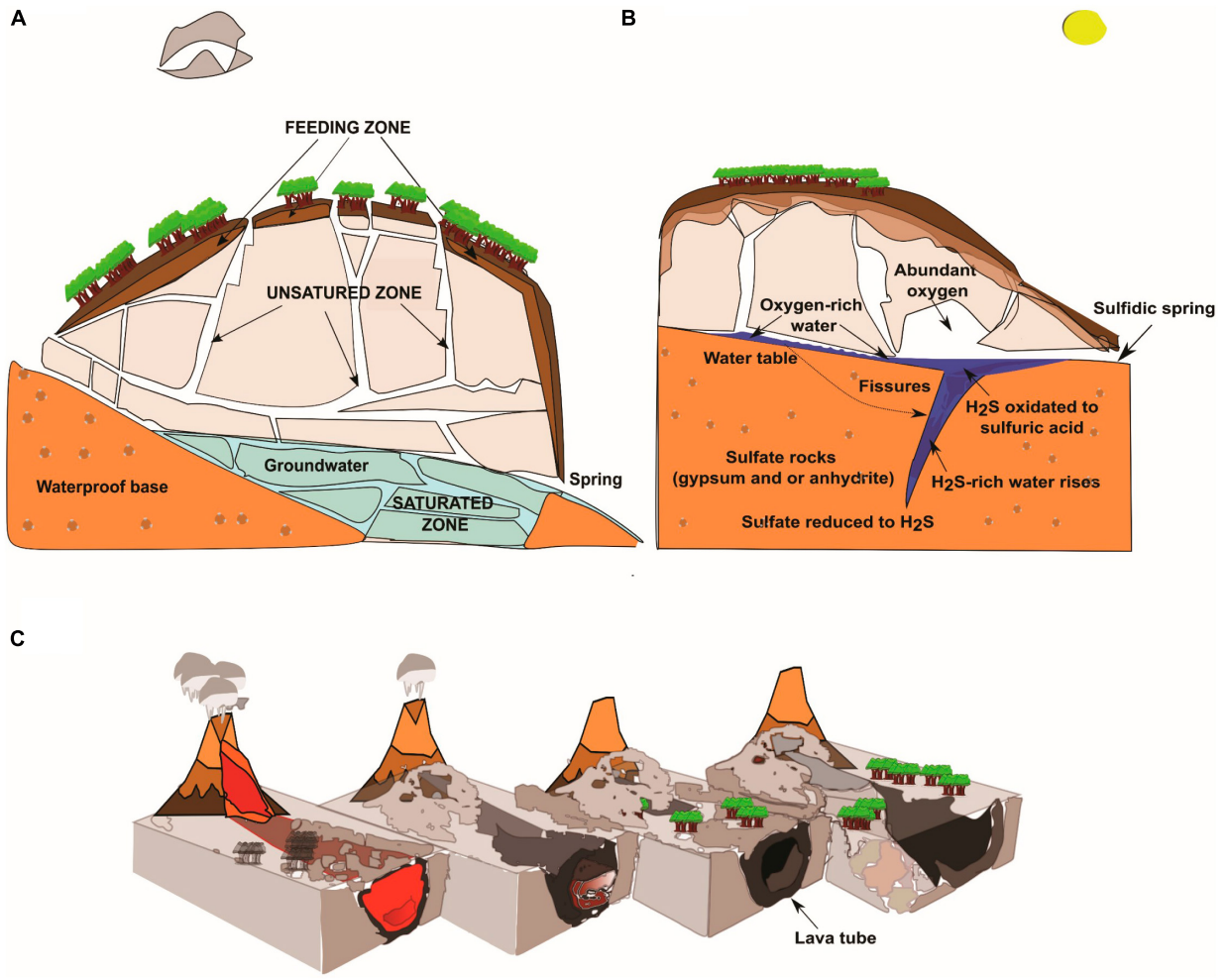

FIGURE 2
Geological characteristics of limestone, SAS, and volcanic (lava tubes) caves. **(A)** Schematic drawing of an epigenic limestone cave with the three zones of groundwater circulation. The "feeding zone" is the interface zone between the surface and caves that absorbs and collects rainwater and surface runoff waters. The "unsaturated zone" is where superficial waters flow in depth through mainly vertical paths, including wells and meanders or in correspondence with rock fractures. The "saturated zone" corresponds to totally submerged tunnels, ducts, and fractures, where the pressurized waters move in a sub-horizontal direction toward the emergency zone (spring). **(B)** Speleogenesis of hypogenic sulfuric acid caves. Ascending water from the depths of the Earth rich in aggressive substances (H_2S, CO_2) induces the dissolution of carbonate rock. **(C)** Formation of lava tubes is the consequence of cooling, emptying, and crusting in the lava flow channel.

SAS caves (**Figure 2B** and the following session 3.2). A karst system can identify three diverse zones with very different groundwater circulations: feeding, unsaturated, and saturated (Palmer, 1991; Culver and Pipan, 2009; **Figure 2A**).

The lowest zone of the karst system is an extreme oligotrophic environment made of tunnels filled with water (saturated zone) and inhabited by obligate subterranean aquatic animals (stygobionts) whose sustenance depends on chemolithoautotrophic organic matter production (Hutchins et al., 2016). The karst system is not an isolated environment; it is indeed an open system in continuous contact with the external environments by exchanging flows of matter (mainly air, water, and solutes) (**Figures 3A, B**) and energy (heat) (Waring et al., 2017).

Near the cave entrance, microbial mats overlaid by water droplets, reflecting yellow-gold or silver colored light when illuminated with an LED lamp, can be observed on the walls and ceilings (Pašić et al., 2009; Turrini et al., 2020; Martin-Pozas et al., 2023). These microbial communities are typical of limestone caves and are located predominantly in the trophic transition zone (Porca et al., 2012). Air entering the cave undergoes a decrease in temperature and an increase in relative humidity until it reaches the dew point (Mulec et al., 2015). The water vapor passes to the liquid phase, creating condensation droplets on the surface of the microbial matter (**Figures 3C, D**). These biofilm-like structures deserve more thorough studies to better understand the role played by water condensation droplets in their maintenance and functionality.

4.2 Sulfuric acid speleogenetic (SAS) caves

Some limestone caves originate from carbonate rock dissolution by H_2S- and H_2SO_4-rich water, and therefore they

FIGURE 3
Examples of the unsaturated or vadose zone in limestone caves from Lazio region, Italy. Water is transferred in the deep zone of the cave across vertical wells **(A–B)**. Biofilms colonize the walls near the cave entrance and appear overlaid by water droplets reflecting gold- or silver-colored light when illuminated with an LED lamp **(C)**. Close-up image **(D)** showing yellow microbial communities organized into similarly sized spheroidal structures (about 60 μm in diameter) retaining water droplets due to the condensation of the water vapor. Scale bar (**C**, 100 μm). Photo by P. Turrini.

are called SAS caves (Rossmassler et al., 2012; Gulecal-Pektas and Temel, 2017; de Bruin et al., 2022). Although both biotic and abiotic processes are implicated in the development of large sulfuric-acid karsts (Laurent et al., 2023), SAS caves are typically considered hypogenic since they originate from the action of water ascending from the depths of the Earth (Forti et al., 2002). This water contains high concentrations of aggressive substances, primarily H_2S, and rises through rock fissures and tectonic over-pressuring or hydraulic gradients from sediment basins of the volcanic source to the surface (**Figure 2B**). When H_2S-containing fluids get in touch with carbonate bedrock, a cave occurs (Egemeier, 1981). Indeed, H_2S-rich water meets oxygenated groundwater fed by meteoric infiltration or oxygen from the atmosphere and oxidizes to sulfuric acid (**Eq. 4**) that immediately reacts with carbonate bedrock by forming gypsum ($CaSO_4 \cdot 2H_2O$) and CO_2 (**Eq. 5**).

$$H_2S + 2O_2 \rightarrow H_2SO_4 \quad (4)$$

$$H_2SO_4 + CaCO_3 + H_2O \rightarrow CaSO_4 \cdot 2H_2O + CO_2 \quad (5)$$

Gypsum ($CaSO_4 \cdot 2H_2O$) removal through flowing meteoric water increases void spaces, enlarging the cave (Palmer, 1991; Palmer and Hill, 2019). SAS caves have been reported from many areas worldwide and occur in carbonate rocks in different climates, representing less than 10% of all known caves (Klimchouk, 2017). H_2S and elemental sulfur are toxic to most organisms, though some chemolithoautotrophic sulfur-oxidizing bacteria can use reduced sulfur compounds as energy sources and electron donors for their energetic metabolisms (Engel, 2007;

Kumaresan et al., 2014). In correspondence with the H_2S-rich rising water, chemolithoautotrophic floating filaments grow on the water surface (**Figure 4A**; Rohwerder et al., 2003; D'Angeli et al., 2019b), while biofilms thrive as streamers and sedimented filaments in the subaqueous environment (Engel et al., 2003; Jones et al., 2010; **Figure 4B**). Droplets of freshwater on the walls and ceilings of SAS caves absorb H_2S degassing from the water table, and chemolithotrophic oxidation of H_2S to sulfuric acid occurs (Hose et al., 2000). The most acidic drops accumulate on the tips of the gypsum crystals, forming characteristic highly acidic viscous peduncles called snottites (**Figure 4C**; Hose et al., 2000; Macalady et al., 2006; Jones et al., 2012). These extremely acidic (pH∼1) biofilms attached to cave walls or ceilings are sulfur-based chemosynthetic ecosystems and are observed where H_2S concentration in the cave atmosphere is 0.2–25 parts-per-million by volume (ppmv) (Jones et al., 2016).

Biovermiculations are typical formations that can be found in SAS caves, located on the surface wall rock at a certain distance from the SAS degassing water. They incorporate microbial populations forming characteristic microbial colonization patterns on the rock resembling leopard skin and appear as worm-like deposits of mud and clay (**Figure 4D**; Hose et al., 2000; Jones et al., 2008; D'Angeli et al., 2019b). Vermiculations from the Frasassi Cave were found to be composed of densely packed prokaryotic and fungal cells in a mineral-organic matrix containing 5–25% organic carbon (Jones et al., 2008).

4.3 Volcanic caves

Different from dissolution caves, volcanic caves are formed following eruption and lava outflow. Molten rock (magma) rises to the surface from depths and loses gas and aqueous vapor

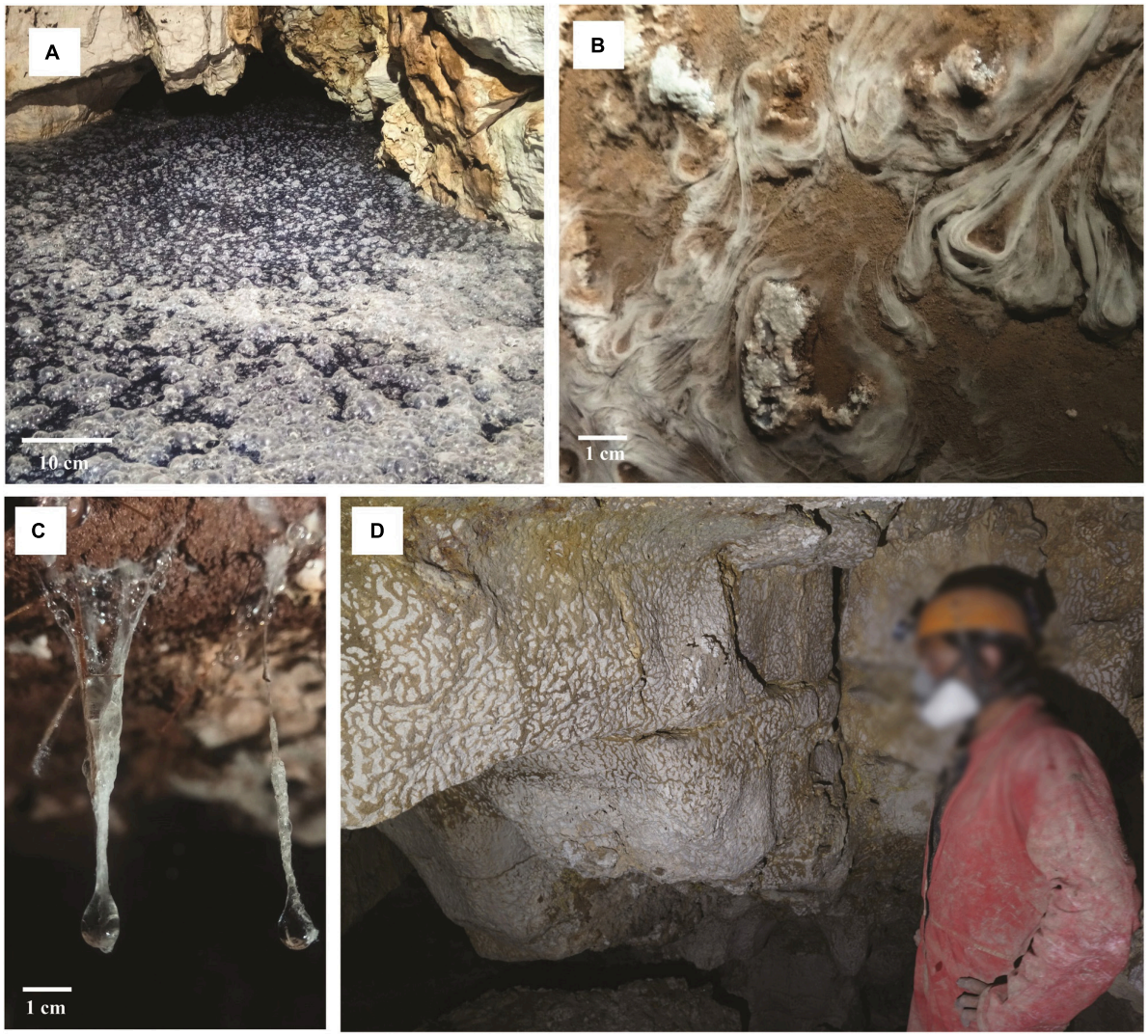

FIGURE 4
Microbial colonization patterns from a SAS cave in the Lazio region, Italy. Sulfur-oxidizing microbial communities floating on the water surface **(A)** or forming streamers and filaments in the subaqueous environment **(B)**. Microbial communities form highly acidic viscous peduncles called snottites **(C)** or vermiculations on the surface wall rock **(D)**. Scale bar (**A**, 10 cm; **B**, 1 cm; **C**, 1 cm). Photos in **(A)** and **(D)** are by P. Turrini, **(B)** and **(C)** are courtesy of A. Benassi (June 2021).

forming the so-called lava on the surface. The viscosity of the lava depends on its silica content. Low-silica basalt lava has a low viscosity and can form fast-moving narrow lava streams. Volcanic caves are indeed a large category of cavities in volcanic rocks, and they can be either primary or secondary caves, depending on their genesis (Kempe, 2019). Among primary volcanic caves, lava tubes (**Figure 2C**) are the most common caves (Palmer, 2007). They are formed as the consequence of cooling and crusting over the lava flow channel, followed by the emptying out of the molten lava leaving behind an empty conduit tube (**Figures 2C**, **5A**; Palmer, 2007; Northup and Lavoie, 2015). Lava tubes are aphotic, shallow subsurface voids that, depending on age and lava texture, can be colonized by plant roots growing through the caves' ceilings in search of water (Palmer, 2007). These roots, along with water percolating from the surface, bring carbon and nitrogen into lava tubes, creating a mosaic of nutrient availability for diverse microbial mats, mainly consisting of heterotrophic bacteria and fungi, covering the cave walls and ceilings (**Figures 5B, C**; Hathaway et al., 2014; Riquelme et al., 2015; Gonzalez-Pimentel et al., 2018; Nicolosi et al., 2023). Volcanic caves are widespread worldwide (Gulden, 2019), and contain many secondary mineral deposits with rich biological components that have gained interest as biosignatures for life, aiding the search for life on Mars (Northup et al., 2011). Microbial colonization patterns are visible in a range of colors and shades, including white, yellow, orange, blue-green, gold, and pink mats that cover the walls of lava tubes in various volcanic locations such as the Azores, Hawaii (Hathaway et al., 2014), California (Lavoie et al., 2017), and New Mexico (Northup et al., 2011). These microbial formations are closely associated with secondary mineral deposits, including amorphous copper-silicate deposits and iron-oxide formations (Northup et al., 2011). Coloring is likely to originate from pigments associated with some bacteria present in the colonization patterns, particularly *Actinomycetota* (Lavoie et al., 2017; Gonzalez-Pimentel et al., 2018).

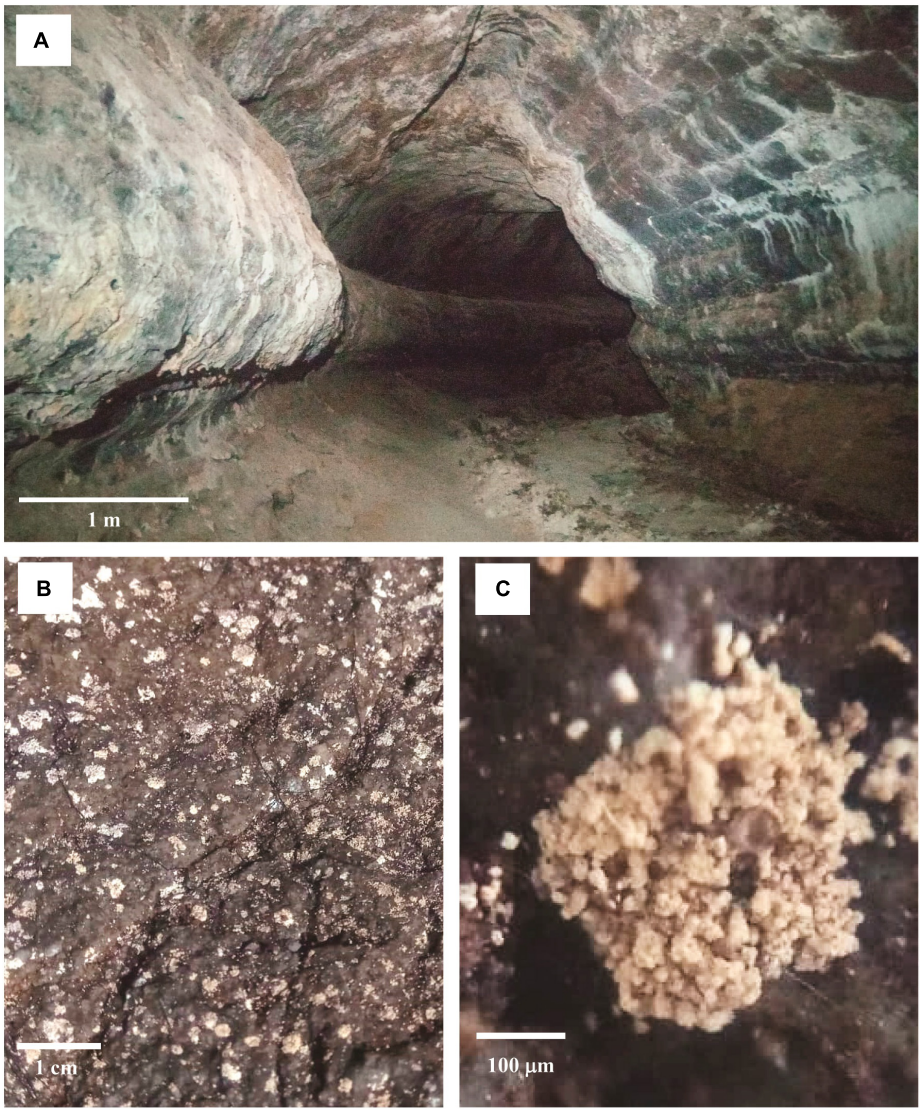

FIGURE 5
Example of a lava tube. Entrance of Montana Corona cave, Lanzarote, Canary Islands **(A)**. Microbial communities live on the basaltic rock surface **(B)**. Close-up of the microbial communities **(C)**. Scale bar (**A**, 1 m; **B**, 1 cm; **C**, 100 µm). Courtesy of A. Benassi (January 2022).

5 Microbial diversity in caves

5.1 Bacteria in caves

An extensive literature search was conducted to identify the most prevalent bacterial taxa in limestone, volcanic, and SAS caves. Out of 225 research articles screened in our literature analysis, only 20 of them, reporting metataxonomic data for 105 samples, met the inclusion criteria for a comparative assessment of bacterial diversity in caves, as determined by sequence analysis of the V3-V4 hypervariable regions of 16S rRNA using the Illumina (MiSeq) platform (**Supplementary Figure 1**). With the improvement of deep sequencing technologies, it became possible to detect extremely rare and still unclassified taxa. These are represented by taxonomic units with very low abundance together with unassigned sequences that could not be classified using currently available sequence taxonomy reference databases. Data on cave type, geographic location, and relative distribution of major bacterial taxa in the scrutinized cave samples are provided in **Supplementary Dataset 1**.

Twenty-three prevalent phyla were observed in limestone caves, with major variation in abundance depending on the sampled site and type of matrix. Based on average abundance values of 78 environmental samples from 17 limestone caves worldwide, it can be observed that *Pseudomonadota* were the most abundant phylum (40.0%), followed by *Actinomycetota* (13.5%), *Acidobacteriota* (9.5%), *Verrucomicrobiota* (5.3%), *Bacillota* (4.5%), *Chloroflexota* (4.1%), *Nitrospirota* (4.1%), *Planctomicetota* (3.5%), *Candidatus* Patescibacteria (3.0%), *Bacteroidota* (2.9%), *Gemmatimonadota* (1.7%), *Candidatus* Methylomirabilota (0.7%), *Myxococcota* (0.6%), *Bdellovibrionota* (0.5%), *Candidatus* Elusimicrobiota (0.4%), *Candidatus* Dependentiae (0.3%), *Candidatus* Latescibacteria (0.3%), *Cyanobacteriota* (0.2%), *Candidatus* Rokubacteria (0.2%), *Candidatus* GAL15 (0.1%), NB1-j (0.1%), *Fibrobacterota* (>0.1%), *Campylobacterota* (>0.1%), and others (4.5%) (**Figure 6**). The overall distribution of prevalent phyla was retained irrespective of the geographical location of the caves, and was remarkably similar to that of volcanic caves (lava tubes), even if *Actinomycetota* were more abundant in the latter cave type (**Figure 6**). Based on average abundance values of 17 environmental samples from 3 lava tubes worldwide, a predominance of *Actinomycetota* (35.0%) and *Pseudomonadota* (34.6%) was observed, followed by *Acidobacteriota* (7.4%), *Cyanobacteriota* (3.5%), *Chloroflexota* (2.8%), *Planctomycetota*

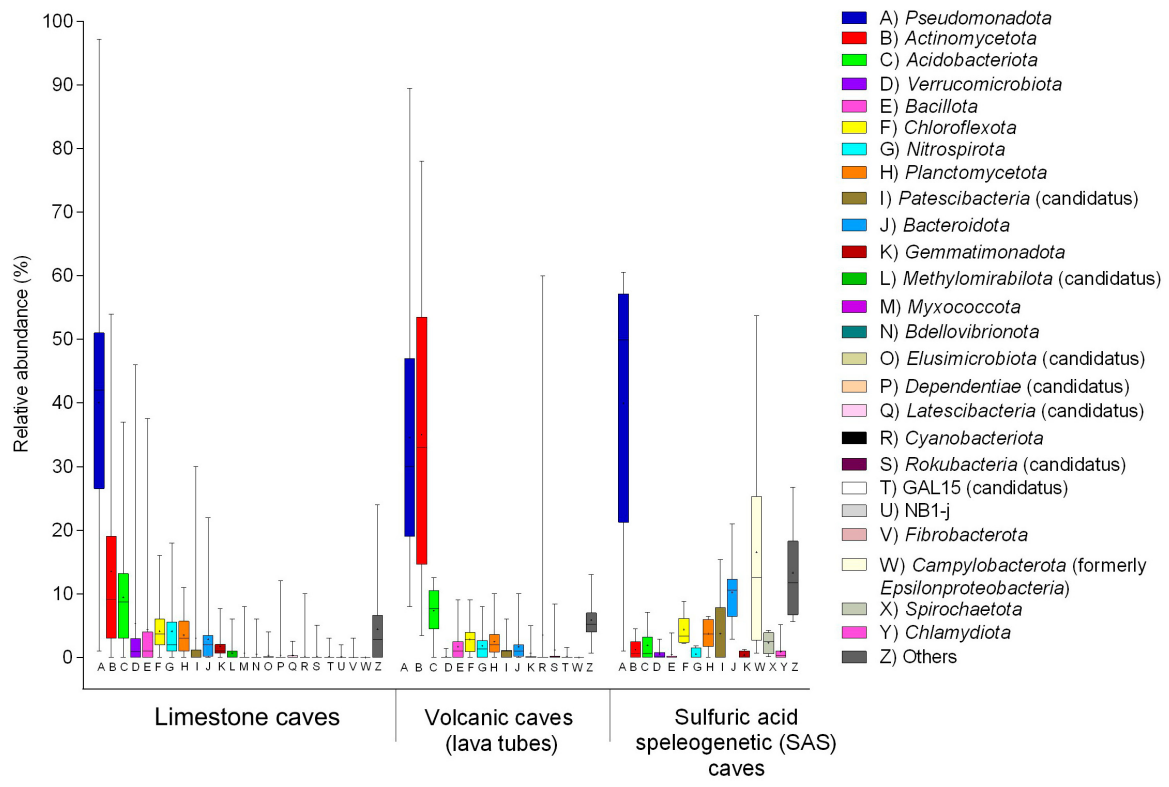

FIGURE 6
Boxplot of bacterial communities in limestone, volcanic (lava tubes), and SAS caves determined by 16S rRNA gene (V3-V4) sequencing on Illumina platform. Major phyla of pooled samples (water, sediment, biofilm) from various limestone caves retrieved from Leuko et al. (2017), Oliveira et al. (2017), Dhami et al. (2018), Alonso et al. (2019), De Kumar et al. (2019), Long et al. (2019), Dong et al. (2020), Jurado et al. (2020), Park et al. (2020), Addesso et al. (2021), Chen et al. (2021), Koner et al. (2021), Farda et al. (2022b), Bogdan et al. (2023), Martin-Pozas et al. (2023). The phyla pattern of microbial mats on the rock surface of volcanic caves (lava tubes) was obtained from Gonzalez-Pimentel et al. (2018), Gonzalez-Pimentel et al. (2021), Nicolosi et al. (2023). The phyla pattern of biofilms thriving as streamers and sedimented filaments in the water of SAS caves was obtained from D'Angeli et al. (2019a), Jurado et al. (2021). The boundaries for the first and third quartiles are shown (box length), with the centerline representing the median, the symbol (†) indicating the average, and the whiskers representing the maximum/minimum values. Raw data are provided in **Supplementary Dataset 1**.

(2.5%), *Nitrospirota* (1.8%), *Bacteroidota* (1.7%), *Bacillota* (1.7%), *Candidatus* Rokubacteria (1.2%), *Candidatus* Patescibacteria (1.1%), *Gemmatimonadota* (0.7%), *Verrucomicrobiota* (0.2%) and others (5.9%) (**Figure 6**).

The average phyla distribution in 10 environmental samples from two SAS caves showed the dominance of *Pseudomonadota* (40.0%) and *Campylobacterota* (16.5%), followed by *Bacteroidota* (10.2%), *Chloroflexota* (4.4%), *Candidatus* Patescibacteria (3.8%), *Planctomicetota* (3.7%), *Spirochaetota* (2.3%), *Acidobacteriota* (1.9%), *Actinomycetota* (1.2%), *Chlamydiota* (0.9%), *Verrucomicrobiota* (0.6%), *Nitrospirota* (0.5%), *Bacillota* (0.5%), *Gemmatimonadota* (0.4%) and others (13.3%) (**Figure 6**).

Following the updated taxonomic revision of bacterial phyla (Oren and Garrity, 2021), the class-level distribution of the *Pseudomonadota* members (*Alpha-*, *Beta-*, *Gamma-*, and *Delta-proteobacteria*) and the *Campylobacterota* phylum (formerly *Epsilonproteobacteria*) were compared for the three types of caves. A remarkably different distribution of taxa was observed in the three cave types; *Gammaproteobacteria* predominated in limestone and volcanic caves, whereas the phylum *Campylobacterota* (heterotypic synonym *Epsilonproteobacteria*) dominated in SAS caves (**Figure 7**). In addition to the Fetida Cave, Italy (**Figure 7**), also the Lower Kane Cave, USA (Engel et al., 2003), the Frasassi Cave, Italy (Macalady et al., 2008; Zerkle et al., 2016) and the Acquasanta Terme Cave, Italy (Jones et al., 2010) showed *Campylobacterota* as the major contributor to microbial mats.

According to the selected literature (**Supplementary Dataset 1**), the taxonomic data of bacterial communities from volcanic (lava tubes) and SAS caves are mainly referred to biofilms and microbial aggregates collected from the rock surfaces and H_2S-rich groundwater, respectively (**Figure 6** and **Supplementary Dataset 1**).

Three different types of matrices, namely biofilms, sediments, and water, are commonly investigated at the microbiological level in limestone caves. **Figure 8** illustrates pooled data on the relative abundance of bacterial phyla in biofilm, sediment, and groundwater samples (33, 34 and 11 samples, respectively) taken from 17 limestone caves worldwide. The most abundant phyla in biofilm and sediment samples were (respectively) *Pseudomonadota* (45.1–40.9%) followed by *Actinomycetota* (15.0–15.3%), *Acidobacteriota* (9.0–11.6%), *Verrucomicrobiota* (0.6–2.4%), *Bacillota* (4.0–6.1%), *Chloroflexota* (3.6–5.2%), *Nitrospirota* (5.0–3.0%), *Planctomycetota* (4.6–3.1%), *Bacteroidota* (2.3–2.9%), *Gemmatimonadota* (1.9–2.0%), and others (5.7–4.3%). Differently, the abundance of phyla in water samples was *Verrucomicrobiota* (28.3%), *Pseudomonadota* (22.3%), *Candidatus* Patescibacteria (16.9%), *Bacteroidota* (4.4%), *Acidobacteriota* (4.2%), *Nitrospirota* (3.7%), *Myxococcota* (3.5%), *Bdellovibrionota* (3.5%), *Actinomycetota* (3.4%), *Chloroflexota* (2.5%), *Candidatus* Elusimicrobiota (2.1%), *Planctomicetota* (1.5%), *Candidatus* Methylomirabilota (1.2%), *Bacillota* (0.4%), *Fibrobacterota* (0.4%), *Gemmatimonadota* (0.3%), *Cyanobacteriota* (0.2%), and others (1.0%).

It was interesting to notice the very similar distribution of bacterial phyla in biofilms and sediments, both showing remarkable differences from water samples taken from the same cave. Sediments are likely to serve as a reservoir and source of bacteria which can spread on cave wall surfaces giving rise to biofilm formations on suitable rock matrices under permissive environmental conditions (Martin-Pozas et al., 2023). Overall, one major difference between groundwater samples and both biofilm and sediment samples was the prevalence of *Verrucomicrobiota* and *Candidatus* Patescibacteria, and the relative scarcity of *Actinomycetota*. This is not surprising, given that *Verrucomicrobiota* and *Candidatus* Patescibacteria are prominently aquatic taxa, as opposed to the ubiquitous *Actinomycetota* that can thrive in both terrestrial and aquatic environments (Dhami et al., 2018). Indeed, *Verrucomicrobiota* were detected with high abundance in cave drip water, whereas they were rare in sediments and biofilms (Bogdan et al., 2023; Martin-Pozas et al., 2023).

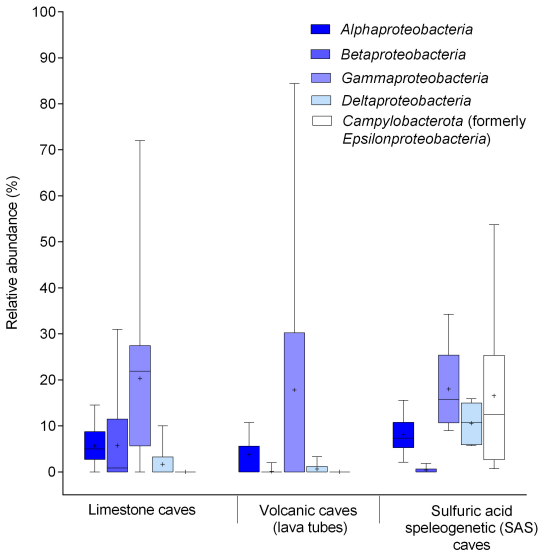

FIGURE 7
Boxplot of bacterial communities in limestone, volcanic (lava tube), and SAS caves determined by 16S rRNA gene (V3-V4) sequencing on Illumina platform. Relative composition of *Pseudomonadota* at the class level and *Campylobacterota* (heterotypic synonym *Epsilonproteobacteria*) phylum. Major classes of pooled samples (water, sediment, biofilm) from various limestone caves retrieved from Leuko et al. (2017), Oliveira et al. (2017), De Kumar et al. (2019), Jurado et al. (2020), Park et al. (2020), Addesso et al. (2021), Farda et al. (2022b), Martin-Pozas et al. (2023). The class pattern of microbial mats from volcanic caves (lava tubes) was obtained from Gonzalez-Pimentel et al. (2018), Gonzalez-Pimentel et al. (2021), Nicolosi et al. (2023). The class pattern of biofilms thriving as streamers and sedimented filaments in the water of SAS caves was obtained from D'Angeli et al. (2019a), Jurado et al. (2021). The boundaries for the first and third quartiles are shown (box length), with the centerline representing the median, the symbol (†) indicating the average, and the whiskers representing the maximum/minimum values. Raw data are provided in **Supplementary Dataset 1**.

5.2 Functional roles of bacteria in limestone and volcanic caves

The success of *Pseudomonadota* in colonizing cave environments may partly be attributed to their involvement in sulfur cycling, and their ability to degrade a wide range of organic compounds, fix atmospheric carbon, and transform nitrogen (Tomczyk-Żak and Zielenkiewicz, 2016). Among *Gammaproteobacteria*, the prevalent orders in caves are

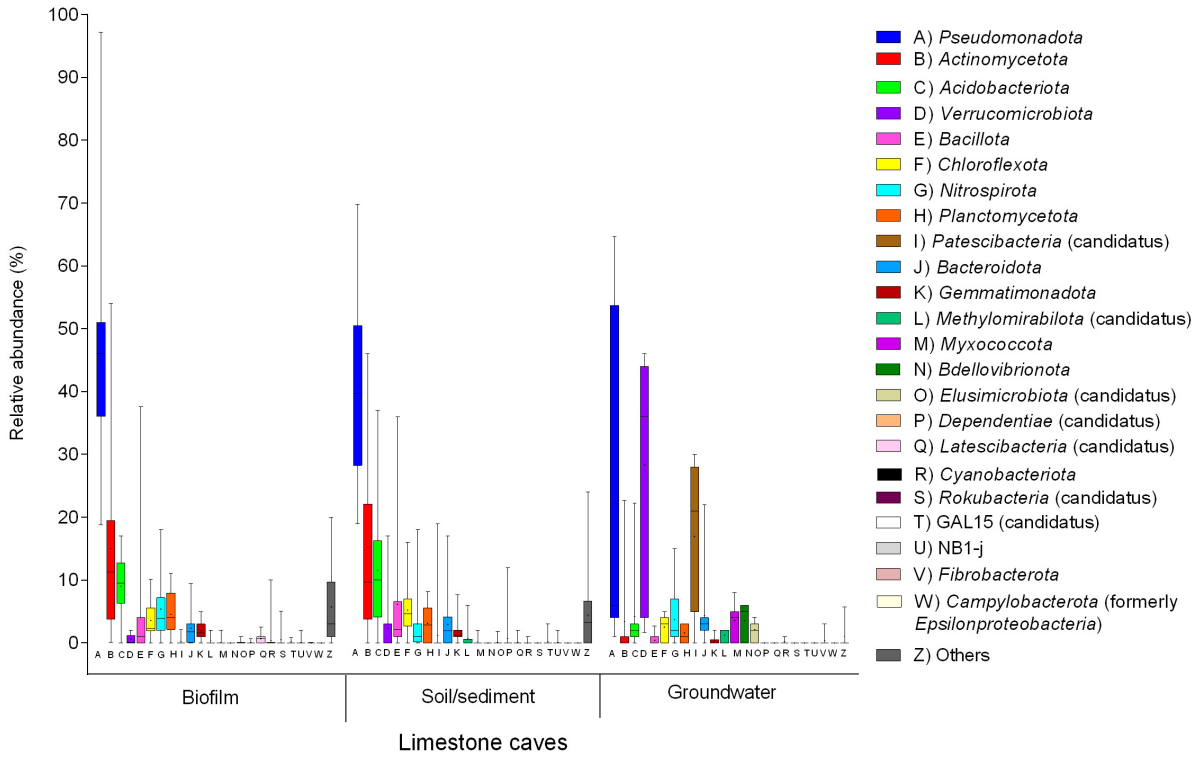

FIGURE 8
Distribution of the main bacterial phyla in three types of matrices (water, biofilm from wall surfaces, and sediment) from limestone caves determined by 16S rRNA gene (V3-V4) sequencing on Illumina platform. Phyla distributions of the biofilm samples were obtained from Leuko et al. (2017), Alonso et al. (2019), De Kumar et al. (2019), Long et al. (2019), Dong et al. (2020), Jurado et al. (2020), Addesso et al. (2021), Chen et al. (2021), Koner et al. (2021), Martin-Pozas et al. (2023). Phyla distributions of the sediment samples were obtained from Oliveira et al. (2017), Dhami et al. (2018), Dong et al. (2020), Park et al. (2020), Koner et al. (2021), Farda et al. (2022b), Bogdan et al. (2023), Martin-Pozas et al. (2023). Phyla distribution of the water samples was obtained from Chen et al. (2021), Bogdan et al. (2023), Martin-Pozas et al. (2023). The boundaries for the first and third quartiles are shown (box length), with the centerline representing the median, the symbol (†) indicating the average, and the whiskers representing the maximum/minimum values. Raw data are provided in **Supplementary Dataset 1**.

Pseudomonadales, *Xanthomonadales,* and *Chromatiales*, which are generally associated with freshwater (Porca et al., 2012; Hershey et al., 2018). In the *Alphaproteobacteria* class, *Rhizobiales* are typically associated with nitrogen fixation (Carvalho et al., 2010), and are generally found near the cave entrance, their tropism being influenced by the nearby rhizosphere community and the availability of nutrients from root exudates (Michail et al., 2021). *Sphingomonadales* can degrade aromatic compounds (Marques et al., 2019). *Caulobacterales* (e.g., members of the *Brevundimonas* genus) are often isolated from caves (Ghosh et al., 2017b; Zhu et al., 2021). Within the class *Betaproteobacteria*, the dominant order is *Nitrosomonadales* (including *Nitrosomonas* and *Nitrosospira*) which are ammonia-oxidizing bacteria (Zhao et al., 2017; Kimble et al., 2018; Jurado et al., 2020). *Actinomycetota* colonize both limestone and volcanic caves, mainly due to their broad adaptive abilities. For instance, they can produce degradative enzymes for numerous natural macromolecules (Riquelme et al., 2017; Hamedi et al., 2019), and release secondary metabolites such as antibiotics to prevent nutrient withholding by competitors under oligotrophic conditions (Barka et al., 2016; Maciejewska et al., 2016). *Crossiella* (*Pseudonocardiales*) is a common inhabitant of both limestone and volcanic caves and is often isolated from moonmilk deposits, where it plays a critical role in calcite precipitation through urease activity-dependent alkalinization (Gonzalez-Pimentel et al., 2021). *Crossiella* also provided a new model of bacterial proliferation and dispersion in caves, since free *Crossiella* cells from surface and underground sediments can attach to cave walls and form the first filaments that subsequently evolve into mature biofilms (Martin-Pozas et al., 2023). The family *Euzebyaceae* has been reported to be abundant in microbial mats of lava tubes (Riquelme et al., 2015; Gonzalez-Pimentel et al., 2018) and limestone caves (Ma et al., 2021).

Bacteria of the genus *Streptomyces* (Maciejewska et al., 2017; Oliveira et al., 2017; Long et al., 2019) are the most abundant producers of antimicrobials and play a role in maintaining the microbial community by inhibiting the growth of surrounding microorganisms (Park et al., 2020). Bacteria belonging to the phylum *Acidobacteriota* are ubiquitous in various terrestrial environments (Kalam et al., 2020) and relatively abundant in caves (**Figure 6** and **Supplementary Dataset 1**). Although acidobacterial sequences are preponderant in soil samples and account for a significant fraction of cave microbiomes, the ecological role and metabolic function(s) of these bacteria remain elusive due to their recalcitrance to laboratory cultivation. Some *Acidobacteriota* members have been classified as k-strategists, in that they have oligotrophic metabolism which enables them to thrive in settings with limited nutritional availability with slow growth rates (Kalam et al., 2020). These features are likely to contribute to the

environmental fitness of *Acidobacteriota* in caves (Fierer et al., 2007). *Bacillota* is a phylum frequently found in caves due to their resistance to desiccation and nutrient stress (Dong et al., 2020). Both anaerobic (e.g., *Clostridium* spp.) and aerobic (e.g., *Bacillus* spp.) spore-formers were detected in caves (Oliveira et al., 2017). The *Chloroflexota* are CO_2-fixing autotrophic green non-sulfur bacteria that frequently colonize volcanic caves, where they represent one of the most abundant phyla (Riquelme et al., 2015).

While nitrogen is a limiting nutrient in caves (Anda et al., 2020), the chemolithoautotrophic members of phylum *Nitrospirota* are relatively abundant and ubiquitous in subterranean environments, where they play a role in primary production by assimilating inorganic carbon (Lücker et al., 2010; Mueller et al., 2023). The ammonia-oxidizing *Nitrosospira* and nitrite-oxidizing *Nitrospira* complete the entire nitrification cycle and support primary production in oligotrophic environments (Lavoie et al., 2017; Leuko et al., 2017). *Nitrospirota* members were detected in a variety of subterranean environments, e.g., on a cave wall in the western Loess Plateau of China (Anda et al., 2020), in the Su Bentu limestone cave in Sardinia (Leuko et al., 2017) and the limestone Pindal Cave in Spain (Martin-Pozas et al., 2023), but also in speleothems of a silicate cave in Guiana (Liu et al., 2022) and in the lava tubes of Lava Beds National Monument, USA (Lavoie et al., 2017). Members of *Thermodesulfovibrionia*, a class of *Nitrospirota* characterized by hydrogen oxidation, sulfate reduction, nitrate reduction, and sulfur disproportionation, are rare in surface environments but are frequent in marine and terrestrial subsurface aquifers (D'Angelo et al., 2023).

Bacteroidota are common inhabitants of caves (**Figure 6** and **Supplementary Dataset 1**) and have been proposed as bioindicators of human disturbance since their relative abundance significantly increased in a cave open to tourists (Alonso et al., 2019). Indeed, the most convincing alteration of the microbiota caused by touristic visits to show caves is the occasional introduction of human commensal microorganisms, like *Staphylococcus* spp. or *Enterobacteriaceae* (Espino del Castillo et al., 2018; Bontemps et al., 2022). Seemingly, the overall distribution of microbial phyla in caves reflects what is observed in the soil (Hershey and Barton, 2018). It should be considered that microorganisms can constantly gain access to the caves through entrances, underground streams, air currents, and percolating water, continuously modifying the native cave microbial communities (Wu et al., 2015). However, at lower taxonomic levels, only 16 % overlap of OTUs was observed between the cave and external microbiomes in the limestone Kartchner Caverns, Arizona (Ortiz et al., 2014), and 11.2 % between surface soil and microbial mats collected from lava tubes of Lava Beds National Monument, California (Lavoie et al., 2017). These data support the hypothesis that cave-indigenous microbial populations differ from surface soil populations. Indeed, Earth's surface microorganisms can migrate into the caves, but once there, environmental, and chemical factors determine a selective pressure that selects those microorganisms that better adapt to the harsh conditions dictated by the caves.

Most cave microbiology studies have been performed in easily accessible shallow caves or near cave entrances, while limited information is available in the deep zone. In the Krubera-Voronja Cave, one of the deepest limestone caves in the world, high microbial diversity was observed at the phylum and genus levels (Kieraite-Aleksandrova et al., 2015). *Pseudomonadota* were most abundant in the lower parts of the cave, while *Actinomycetota* dominated in the upper parts, presumably due to differences in organic carbon availability between these two zones (Kieraite-Aleksandrova et al., 2015). In the case of limestone caves, there is some evidence of the presence of cave-adapted bacteria. Indeed, a core microbiome was observed in the golden droplet-forming microbial communities inhabiting three geographically separate limestone caves, namely Altamira Cave in Spain, Sloup-sosuvka caves in the Czech Republic, and Pajsarjeva Jama in Slovenia (Porca et al., 2012). About 60% of the 16S rRNA full-length gene sequences formed three core OTUs common to all three sampling sites. These were referred to *Pseudonocardinae* (30–50% of sequences), *Chromatiales* (6–25% of sequences), and *Xanthomonadales* (0.5–2.0% of sequences). Interestingly, the bacterial communities inhabiting the rock surfaces in a limestone cave located on the western Loess Plateau of China (Wu et al., 2015) and the moonmilk samples collected from a limestone cave in South Korea (Park et al., 2020) were dominated by some phylotypes showing high similarity with phylotypes identified in geographically distinct European caves (Porca et al., 2012).

Furthermore, a robust core microbiome of shared ASVs (15.1%) between five limestone caves located in different regions of Italy (Biagioli et al., 2023) supported the high degree of adaptation and specialization for microbial communities in limestone caves. Different from limestone caves, studies on volcanic caves from geographically distant areas highlighted a low number of shared OTUs among microbial communities, suggesting that slight differences in lava chemistry or other microenvironmental factors may affect the microbial community structure of volcanic caves (Hathaway et al., 2014; Gonzalez-Pimentel et al., 2018; Prescott et al., 2022). In particular, differences in mineral composition and the high porosity of volcanic rocks could favor the diversification of the endemic microbial communities. In this context, the microbial community can vary because of the interaction with different mineral components of volcanic rocks (Jones and Bennett, 2014). In contrast, limestone caves comprise less porous and mineral-poor carbonate rocks. This makes limestone caves more similar to each other, even if located in geographically distant karst areas. The uniform nature of the carbonate rock could therefore select specific taxa, well adapted to limestone subterranean substrates.

5.3 Functional roles of bacteria in SAS caves

Campylobacterota (Waite et al., 2017), are the most abundant bacteria in SAS caves (**Figure 7**; Engel et al., 2003; Macalady et al., 2006). Members of *Campylobacterota* are prominently associated with sulfur metabolism, causing both sulfide oxidation and sulfate reduction, thereby completing the sulfur cycle (Barton and Luiszer, 2005). Microbial communities associated with SAS caves include stream biofilms, snottites, and biovermiculations (**Figure 4**). In correspondence with the H_2S-rich rising water, chemolithoautotrophic biofilms thrive as streamers and sedimented filaments in the subaqueous environment (Engel et al., 2003, 2004a; Macalady et al., 2006; Jones et al., 2010), while floating filaments grow on the water surface (Rohwerder et al., 2003;

D'Angeli et al., 2019b). Studies on water streamer communities in Lower Kane Cave and Frasassi Cave have confirmed the prevalence of sulfur-oxidizing microorganisms, particularly *Campylobacterota* which dominate in waters with high H_2S and low oxygen, while *Thiothrix* (*Thiotrichales, Gammaproteobacteria*) dominate in waters with low H_2S and high oxygen levels (Engel et al., 2004a; Macalady et al., 2008). *Beggiatoa* (*Thiotrichales, Gammaproteobacteria*) was the dominant group in locations where the shear stress caused by the flowing water is low enough to allow fine sediment accumulation, regardless of sulfide and oxygen concentration (Macalady et al., 2008). In the sulfidic spring of Fetida Cave, Italy, the microbial biomass of water filaments was dominated by the genus *Arcobacter* within the phylum *Campylobacterota* (Jurado et al., 2021). Notably, *Arcobacter* species are primary producers because capable of fixing CO_2 and growing chemolithotrophically via sulfur oxidation. *Desulfocapsa* (Jurado et al., 2021) are anaerobic sulfate-reducing bacteria that produce H_2S useful for sulfur-oxidizing bacteria (Macalady et al., 2006, 2008; Keeler and Lusk, 2021). Snottites are extremely acidic (pH∼1) biofilms growing on the walls and ceilings of caves where sulfide-rich springs degas H_2S into the cave atmosphere (**Figure 4C**; Jones et al., 2012). In Frasassi Cave, snottites are dominated by *Acidithiobacillus* (*Gammaproteobacteria,* 71.4–75.4%), *Thermoplasmatales* (15.6–20.0%), and *Acidimicrobiaceae* (*Actinomycetota*, 5.7–7.0%), in addition to several low-abundance taxa (Macalady et al., 2007). *Acidithiobacillus* are sulfide-oxidizing chemolithoautotrophic bacteria, while *Acidimicrobiaceae* and *Thermoplasmatales* are capable of organotrophic or mixotrophic growth via sulfide and organic carbon oxidation (Macalady et al., 2007).

Biovermiculations are organic-rich sediment formations, showing a typical deposition pattern, found on the walls of some SAS caves (**Figure 4D**). The diversity of biovermiculation patterns has been studied in Fetida Cave and Frasassi Cave, both located in Italy (Jones et al., 2008; D'Angeli et al., 2019b), and Cueva de Villa Luz Cave in Mexico (D'Auria et al., 2018). Biovermiculations are mainly composed of bacteria belonging to the *Betaproteobacteria*, *Gammaproteobacteria*, *Acidobacteriota*, *Nitrospirota*, and *Planctomycetetota*. Members of *Hydrogenophilales* (*Hydrogenophilia*) and *Acidiferrobacterales* (*Gammaproteobacteria*) obtain energy from sulfur and iron oxidation, and perform carbon fixation (D'Angeli et al., 2019b). In biovemiculations, the presence of *Nitrospirota* suggests an energetic metabolism based on the oxidation of reduced nitrogen compounds, together with chemoheterotrophy, as inferred by the presence of hydrocarbon-degrading bacteria (*Hydrocarboniphaga*, *Gammaproteobacteria*), and members of *Acidobacteriota* and *Actinmycetota* (Jones et al., 2008).

5.4 Fungi in caves

Fungi are important components of cave microbiotas, particularly *Ascomycota* which are the predominant phylum. Genus *Candida* (class *Saccharomycetes*) was found abundant in caves open to tourists where visitors may act as a primary vector of human commensal fungi (Biagioli et al., 2023). Other fungal phyla found in caves are *Basidiomycota, Zygomycota,* and *Mycetozoa* (Vanderwolf et al., 2013; Carmichael et al., 2015). Fungal taxa so far recognized in caves are those commonly found on the Earth's surface, and air currents entering and circulating within caves can distribute spores from the outside environment. It has also been suggested that the presence of fungi in caves is an indirect consequence of the entry of organic matter vehicled by cave animals, human visitors, and airborne spores from outside (Martin-Pozas et al., 2022). Fungi are not distributed evenly throughout caves, being commonly associated with organic debris and cave fauna. The genus *Mortierella*, a psychrotolerant cellulose-degrading fungus belonging to *Mortierellomycota*, was found particularly abundant in wild natural caves, primarily associated with the macro-fauna components, i.e., rodents and bats (Biagioli et al., 2023). Fungi in caves generally act as decomposers or parasites, and several fungal species in caves are known to parasitize cave insects (Benoit et al., 2004). Mycorrhizal fungi can also be found in association with plant roots that penetrate shallow caves, such as lava tubes.

Bats can be vectors for fungal spores in and out of the cave environments. Bat guano is the most common source of organic matter where several fungal species grow (Vanderwolf et al., 2013). Among these, *Histoplasma capsulatum* is the most widely studied fungus in caves, being the etiological agent of histoplasmosis, a potentially fatal disease acquired by the inhalation of spores vehicle by bats, endemic to Southeast Asia, Australia, Africa, and parts of South and North America (Taylor et al., 2022).

5.5 *Archaea* in caves

Archaea are generally found in caves, and their abundance in microbial communities seems to be quite small (<2%) (Hershey and Barton, 2018), although their population size can increase especially under oligotrophic conditions (Cheng et al., 2023). *Archaea* play a key role in the nitrogen cycle (Kimble et al., 2018), the predominance of the phylum *Thaumarchaeota* in archaeal cave populations is mainly attributed to its ability to oxidize nitrogen compounds (e.g., ammonia and nitrites) even under low nitrogen conditions, and autotrophically generate organic molecules for growth (Ortiz et al., 2014; Wiseschart et al., 2019). Other archaeal taxa in cave communities are *Euryarchaeota, Crenarchaeota,* and *Woesearchaeota* phyla (Alonso et al., 2019; Biagioli et al., 2023). The role and activity of *Archaea* in cave ecosystems remain enigmatic (Hershey and Barton, 2018; Alonso et al., 2019). Their composition in caves revealed similar patterns as those found on plants, suggesting that some *Archaea* could originate from plants' rhizosphere growing above caves and transported inside caves by water infiltration (Bontemps et al., 2022). This hypothesis is reasonable for microbial communities thriving near the cave entrances (photic, twilight, and transient zones) where matter transfer from the external environment occurs.

6 Good practices in future cave microbiome studies

While most natural and man-made caves are still unexplored from a microbiological perspective, the fascinating idea is

gaining ground that caves are not only model ecosystems to investigate microbial adaptation to extreme conditions (pH, temperature, oligotrophy, darkness, presence of potential growth inhibitors, etc.) but also valuable reservoirs of microbial diversity and potential sources of biotechnologically relevant microbial species. Literature analysis has evidenced some methodological heterogeneity in the design and conduction of studies aimed to characterize cave microbial communities, complicating the comparison of results, data processing, and the proposal of prototypical microbiomes for different types of caves and/or environmental samples. Microbiological investigation of caves requires careful planning and standardization of methodological approaches, to make data from different studies comparable. Hereafter we shall briefly discuss some methodological approaches to cave microbiome investigations, encompassing "in-cave", "in-lab", and "in-silico" studies.

It is advisable for microbiologists to join regional/international speleological groups to obtain permission and assistance for access to caves. Conventions with the local authorities should be signed whenever caves are in a protected natural area or signatory countries of the Nagoya Protocol agreement (McCluskey et al., 2017).

For in-situ studies, the map, GPS coordinates, and elevation above sea level of the cave entrance should be determined. Sampling sites along the four cave trophic zones (i.e., photic, twilight, transient, and deep zones) should be mapped and reported in data repositories and/or research papers. To define these zone borders, environmental parameters including light intensity (i.e., photosynthetic active radiation PAR, λ = 400–700 nm), temperature (°C), humidity (%), and TOC (mg/L, mg/Kg) should be measured at each sampling site and, preferably, monitored during the time using *in situ* dataloggers (Mejía-Ortíz et al., 2020). The TOC concentration determines the nutrient availability across the cave zones, and it should be determined in the groundwater and sediments. Standard physicochemical characterization of the environmental matrices (e.g., groundwater, rock, air, sediment) would aid in understanding the metabolic activity of microbial inhabitants and the local biogeochemical cycling (D'Angeli et al., 2019b; Zada et al., 2022; Zhu et al., 2022). For instance, portable spectrophotometers and Fourier Transform Infrared (FTIR) spectroscopes can detect the presence of some organic and inorganic compounds (e.g., heavy metals) potentially involved in microbial metabolism (Macalady et al., 2008).

Recent advances in imaging and camera resolutions make it possible to take high-resolution photographs of microbial colonization patterns. Macro-photography can be carried out whether using *in situ* optical microscopy lenses (with appropriate adapters) or employing in-lab optical microscopy on environmental matrix samples. It is recommended to change the focal plane during the picture collection to reconstruct the focused three-dimensional object (e.g., with Helicon focus software). Scanning electron microscopy (SEM) is a powerful tool for imaging and analyzing cave microbiome morphologies, generating images with very high magnifications (He et al., 2021). It can also provide elemental analysis. However, SEM requires *ex-situ* preparation steps (fixation, dehydration, and coating) that can alter the native structure of the sample. Whenever possible, samples should be kept refrigerated (4°C) or frozen (<20°C) during transportation to the laboratory.

For in-lab studies, cell count is also a key parameter to estimate the microbial population size in different cave matrices (e.g., biofilm, air, sediment, and groundwater). Several methods have been proposed for the quantification of bacteria in water (Hershey et al., 2019) and soil (Lee et al., 2021). Fluorescence *in situ* hybridization (FISH) can identify and quantify specific microbial taxa in environmental samples, allowing for direct microscopic observation using epifluorescence or confocal laser scanning microscopies (Jones et al., 2023).

Metagenomic analysis of environmental samples can provide a comprehensive view of the structure and dynamics of microbial communities thriving in caves. To analyze eDNA samples, two approaches could be used. In one case, biological replicates (≥2 from the same cave site and matrix) could be extracted, sequenced, and analyzed separately [e.g., (D'Angeli et al., 2019b)]. Otherwise, samples from multiple homogeneous sites can be collected and pooled before eDNA extraction, to capture the full range of microbial diversity in a specific cave site (Biagioli et al., 2023). Sample pooling increases the quantity and diversity of eDNA and ensures statistical robustness, though it affects the alpha and beta diversity indices and reduces the sensitivity required for the detection of rare taxa (Beng and Corlett, 2020; Weinroth et al., 2022). Following the extraction of eDNA, the microbial community structure can be determined by amplicon metataxonomic profiling (e.g., 16S rRNA, ITS, 18S rRNA) using appropriate primers for specific domains of life (e.g., Archaea, Bacteria, Eucaryotes, Fungi, Viruses), in combination with NGS technologies. Recent portable NGS platforms (e.g., MinION) can apply to cave microbiome studies due to low cost and rapid workflow (Latorre-Pérez et al., 2020; Wang et al., 2021). This approach offers acceptable accuracy when combined with novel algorithms of error corrections and other NGS technologies (e.g., Illumina) (Nygaard et al., 2020; Kovaka et al., 2023). The shotgun metagenomic approach involves the untargeted sequencing of all microbial genomes in the eDNA sample. This approach provides a more accurate taxonomic profile of the entire microbial community and can substantiate metabarcoding results. Recovering whole genome sequences can also provide essential information about the functional properties of the microbial community through the reconstruction of metabolic pathways (Quince et al., 2017; Chiciudean et al., 2022). *De novo* assembly of metagenome samples has been applied to studying cave microbial communities (Rossmassler et al., 2016; Kimble et al., 2018; Wiseschart et al., 2019; Turrini et al., 2020) and constructing microbial genomes, known as MAGs (van Spanning et al., 2022).

MAGs provide comprehensive coverage of the genetic diversity in a microbial community (Asnicar et al., 2020; Kashaf et al., 2021), and predict the involvement of individual components in nutrient cycling (Bendia et al., 2022) and symbiotic relationships (Wang et al., 2022). Metatranscriptomics consists of sequencing and quantifying the relative abundance of mRNAs in a sample to determine the functional activities of a given microbiome (Bashiardes et al., 2016). Although crucial for understanding the regulation of gene expression in microbial communities (Zhang et al., 2021), this technique has occasionally been applied to cave microbiome research (Mondini et al., 2022). It could be combined with proteomics and metabolomics (Idle and Gonzalez, 2007; Roldán et al., 2018) to systematically quantify protein expression and identify metabolites from cave samples. It is worth noting

that despite the great number of metataxonomic profiling studies from caves, only a few of them have employed high throughput metabolite characterization on pure bacterial strains from caves (Gosse et al., 2019; Zhu et al., 2021).

Culture-dependent approaches make it possible to obtain pure cultures of cave microorganisms and to gain insights into the role played by individual components of the community. However, only a very low fraction, as less as ca. 1% of cave bacteria, will grow on standard laboratory media (Bodor et al., 2020). To increase the recovery of microbial species, one possibility is to move cultivation from the lab into the cave environment. To this purpose, a diffusion chamber (called "isolation chip" or "ichip") in which cells from environmental samples are diluted in agar and posed between two membranes with 20- to 30-nm pore size, can be used. Once the chamber is returned to the original environment (e.g., water, sediment), naturally occurring nutrients and growth factors diffuse into the chamber, fulfilling the growth requirements of individual components of the microbial community, ultimately increasing their recovery rate. In contrast, the movement of bacteria into/out of the chamber is prevented (Nichols et al., 2010). Microcosm experiments can also provide useful information on the ecology of cave microorganisms, as they allow systematic manipulation of environmental parameters to examine their impact on microbial communities (Vos et al., 2013). Enrichment cultures using definite nutrients and energy sources can also allow the selection of taxa endowed with specific metabolic properties from the microbial pool.

In the age of big data, integrative microbiome-based research is expected to provide a comprehensive understanding of microbiome changes and interactions by the assembly of datasets from the same ecological niche or sample type (Wood-Charlson et al., 2020). Different from human microbiome-based initiatives (e.g., The Integrative Hmp (iHMP) Research Network Consortium, 2019), no attempts have so far been made to apply integrative microbiomics to cave microbiology. Caves are diverse but relatively stable ecosystems, so they could be suited to integrative studies. Physicochemical characterization datasets and multi-omics studies from a variety of cave types could be integrated into a standardized database and made accessible to cave scientists (e.g., microbiologists, geologists, physicists, climatologists, etc.) (**Figure 9**). Various strategies can be used, including a number of statistical tests for microbiome differential abundance analyses (Lin and Peddada, 2020), spectral clustering (Imangaliyev et al., 2015), and network analyses (Jiang et al., 2019). Bioinformatic tools have also been proposed for the integrative analysis of microbiome datasets, which could well apply to cave microbiome research

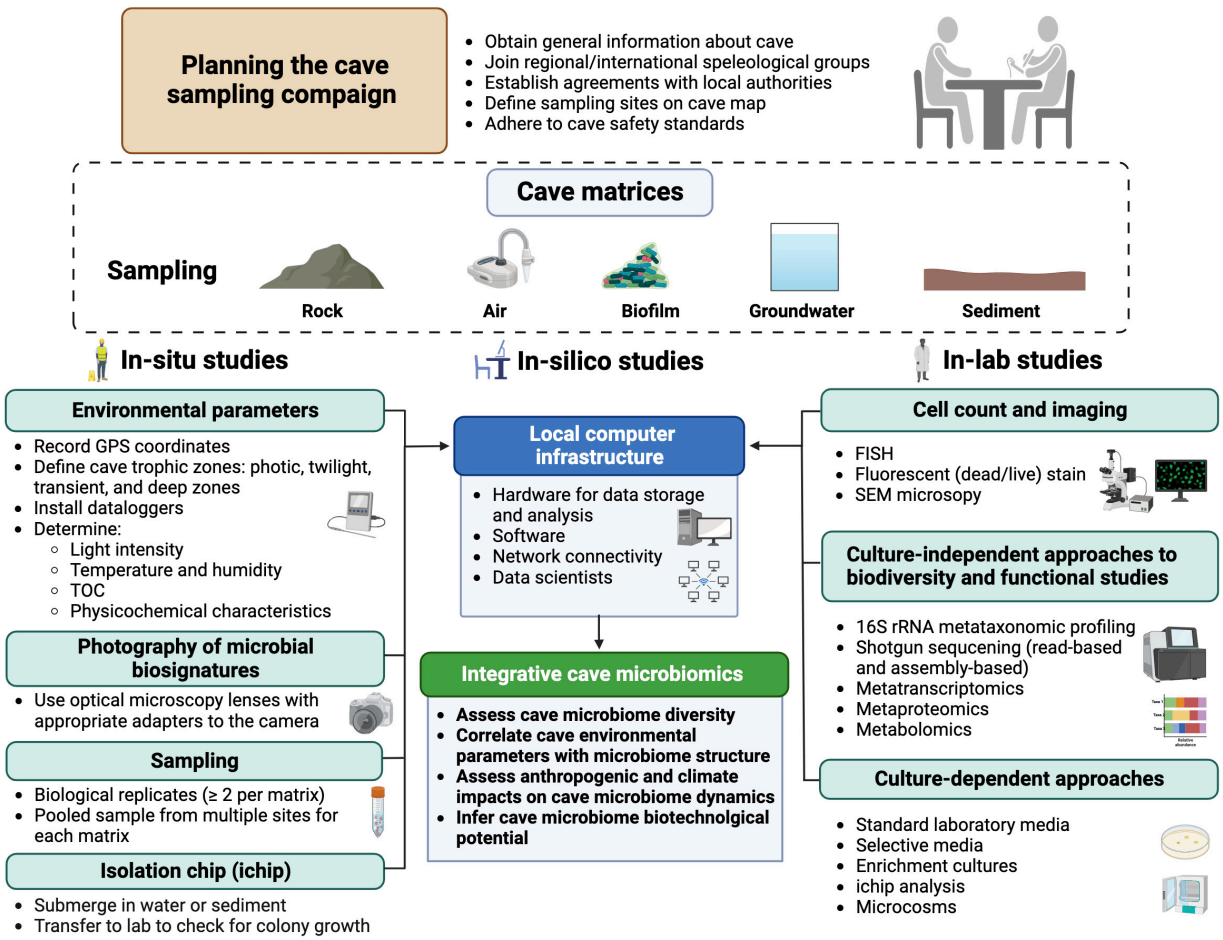

FIGURE 9
Integrated methodological workflow for cave microbiology research.

(The Integrative Hmp (iHMP) Research Network Consortium, 2019; Buza et al., 2019). This concept can also be useful for monitoring cave microbiome biodiversity over time and detecting the effects of climate change and the anthropogenic impact, in addition to predicting potential biotechnological applications of cave microorganisms. A connection between cave microbiomes and surface climatic conditions was inferred from the analysis of various terrestrial caves across the globe, highlighting the sensitivity of cave microbial communities to changes in external environmental conditions (Biagioli et al., 2024). In the future, combining environmental and microbial genomics data with machine learning algorithms will improve biomonitoring (Cordier et al., 2019), and provide new insights into the microbial ecology of cave systems. Noteworthy, machine learning tackled fundamental problems in the ecology of complex microbial communities (Wang et al., 2024), and machine-learning algorithms have already been used in the prediction of cave entrances on the Earth and on Mars (Character et al., 2023; Watson and Baldini, 2024).

7 Conclusion

Caves are increasingly attractive to microbiological investigation, as they represent geologically diverse environments unified by extreme conditions for life. Microbial communities composed of bacteria, archaea, fungi, and micro-eukaryotes are the living backbone of cave biota and play a key role in sustaining trophic networks. Studies of cave microbiomes have mostly been focused on the geomicrobiological interactions with different rock matrices, microbial diversity, mechanisms of microbial resistance and adaptation, anthropogenic impact on the cave ecosystem, and the biotechnological potential of cave microorganisms. Limestone, SAS, and volcanic caves have different genesis, textures of the rock matrix, and chemical composition, which determine different patterns of microbial colonization. Sulfidic caves provide an energetically exploitable ecosystem to chemolithoautotrophic metabolism due to the presence of H_2S-rich groundwater, determining the predominance of sulfur-oxidizing *Campylobacterota*. Limestone caves are typically oligotrophic environments, while volcanic caves are shallow subsurface voids easily accessible by nutrients, and both cave types are primarily colonized by *Pseudomonadota* and *Actinomycetota*.

Actinomycetota are particularly abundant in volcanic caves and are endowed with great biotechnological potential. These bacteria could be isolated as pure cultures, and their ability to produce added-value secondary metabolites such as antibiotics and enzymes could be exploited under laboratory conditions. Yet, a significant portion of cave microbiomes is composed of still unclassified and uncharacterized taxa which deserve more focused investigation in search of new species and new metabolic functions or pathways.

Caves are difficult-to-access sites for untrained microbiologists, so it is not surprising that most studies have focused on microbial communities sampled near entrances or in caves with sub-horizontal development, in the so-called "transition zone", where the environmental parameters vary depending on external climatic conditions. Conversely, the deepest cave zones are largely unexplored, although they account for a huge surface of underground voids. Stable environmental conditions and nutrient scarcity make deep zones an attractive model to study life under conditions of extreme oligotrophy and may also provide useful hints on how life functioned on the early Earth or how microorganisms might live beneath the surface of Mars or other planets.

The rock texture and chemical composition certainly contribute to inter-cave microbiome variability, being affected by the compactness and porosity properties of limestone and volcanic rocks, respectively. Attempts to define a core microbiome for geologically similar cave types have been successful for limestone caves (Biagioli et al., 2023), but not for volcanic caves (Gonzalez-Pimentel et al., 2018). However, genuinely autochthonous cave microorganisms can hardly be defined without robust comparative studies that differentiate them from allochthonous ones, i.e., those driven from outside through infiltrating water, bat guano, soil, air, etc. Meta-analysis of microbial community structures from different cave types could therefore help better define shared taxa between different types of caves, but this approach is challenging. For instance, Sequence Read Archive (SRA) data and accessory metadata (e.g., cave type, cave zones, environmental matrix, etc.) are unavailable in major sequence repositories (e.g., NCBI) for many studies. Moreover, eDNA extraction methods, 16S rRNA regions used as taxonomic markers, and sequencing technologies greatly vary among studies, complicating the assembly of a reliable dataset for comparative analysis. It should also be emphasized that the 16S rRNA-barcoding approach can only determine the taxonomic composition of the cave microbiome, but it does not provide information on its functional capabilities, with some arguing that a taxonomic approach is no longer useful and that a core functional microbiome should be prioritized (Neu et al., 2021).

Due to the high inter-cave variability and the complex dynamics of cave microbiomes, several key considerations are crucial for conducting statistically robust comparative studies at lower taxonomic levels, including sample size, replication, data compositionality, and cohorts' population. Future comparative studies should also address the taxonomic and potentially functional characteristics of cave microbial communities by utilizing a statistically significant number of shotgun sequencing samples obtained from caves. Additional efforts should therefore be directed to the harmonization of cave microbiome studies, encompassing all steps of the investigation, from the sampling campaign to downstream data analyses.

Author contributions

PT: Conceptualization, Data curation, Formal analysis, Investigation, Methodology, Validation, Visualization, Writing – original draft, Writing – review and editing. AC: Conceptualization, Data curation, Formal analysis, Investigation, Methodology, Validation, Visualization, Writing – original draft, Writing – review and editing. FPR: Data curation, Formal analysis, Investigation, Writing – review and editing. PV: Conceptualization, Formal analysis, Investigation, Funding acquisition, Methodology, Project administration, Resources, Supervision, Validation, Visualization, Writing – original draft, Writing – review and editing.

Funding

The author(s) declare financial support was received for the research, authorship, and/or publication of this article. This work was supported by the "Excellence Departments 2023–2027" grant from the Italian Ministry of University and Research (MUR-Italy) (Art. 1, commi 314-337 Legge 232/2016) to the Department of Science, Roma Tre University, and a research contract (999900 PON RTD A7-G-15023; PON 240/2010 D.M. MUR 1062/2021) to AC. The authors acknowledge the financial support of NBFC to Roma Tre University– Department of Science, funded by the Italian Ministry of University and Research, PNRR, Missione 4 Componente 2, 'Dalla ricerca all'impresa', Investimento 1.4, Project CN00000033.

Acknowledgments

We thank Dr. Andrea Benassi for kindly providing the photos assembled in **Figures 4B, C**, **5A–C**. **Figures 1**, **9** were created by using BioRender (Agreement numbers: XA25BPWZZY, MU25BTR2FY), while **Figures 6–8** were drawn with GraphPad version 9 (Trial version). We acknowledge the constructive criticism provided by Dr. Martina Cappelletti. We also acknowledge with great respect the work of very many researchers who have contributed to understanding in this field, and that for reasons of space, we were not able to directly reference here.

Conflict of interest

The authors declare that the research was conducted in the absence of any commercial or financial relationships that could be construed as a potential conflict of interest.

Publisher's note

All claims expressed in this article are solely those of the authors and do not necessarily represent those of their affiliated organizations, or those of the publisher, the editors and the reviewers. Any product that may be evaluated in this article, or claim that may be made by its manufacturer, is not guaranteed or endorsed by the publisher.

Supplementary material

The Supplementary Material for this article can be found online at: https://www.frontiersin.org/articles/10.3389/fmicb.2024.1370520/full#supplementary-material

References

Addesso, R., Gonzalez-Pimentel, J. L., D'Angeli, I. M., De Waele, J., Saiz-Jimenez, C., Jurado, V., et al. (2021). Microbial community characterizing vermiculations from karst caves and its role in their formation. *Microb. Ecol.* 81, 884–896. doi: 10.1007/s00248-020-01623-5

Alonso, L., Pommier, T., Kaufmann, B., Dubost, A., Chapulliot, D., Doré, J., et al. (2019). Anthropization level of Lascaux Cave microbiome shown by regional-scale comparisons of pristine and anthropized caves. *Mol. Ecol.* 28, 3383–3394. doi: 10.1111/mec.15144

Anda, D., Szabó, A., Kovács-Bodor, P., Makk, J., Felföldi, T., Ács, É, et al. (2020). In situ modelling of biofilm formation in a hydrothermal spring cave. *Sci. Rep.* 10:21733. doi: 10.1038/s41598-020-78759-4

Asnicar, F., Thomas, A. M., Beghini, F., Mengoni, C., Manara, S., Manghi, P., et al. (2020). Precise phylogenetic analysis of microbial isolates and genomes from metagenomes using PhyloPhlAn 3.0. *Nat. Commun.* 11:2500. doi: 10.1038/s41467-020-16366-7

Badino, G. (2010). Underground meteorology– "What's the weather underground?". *Acta Carsol.* 39, 427–448. doi: 10.3986/ac.v39i3.74

Barka, E. A., Vatsa, P., Sanchez, L., Gaveau-Vaillant, N., Jacquard, C., Meier-Kolthoff, J. P., et al. (2016). Taxonomy, physiology, and natural products of Actinobacteria. *Microbiol. Mol. Biol. Rev.* 80, 1–43. doi: 10.1128/mmbr.00019-15

Barton, H. (2015). "Starving artists: Bacterial oligotrophic heterotrophy in caves," in *Microbial life of cave systems*, ed. A. S. Engel (Boston, MA: De Gruyter), 79–104.

Barton, H. A. (2006). Introduction to cave microbiology: A review for the non-specialist. *J. Cave Karst Stud.* 68, 43–54.

Barton, H. A., and Jurado, V. (2007). What's up down there? Microbial diversity in caves. *Microbe* 2, 132–138.

Barton, H. A., and Luiszer, F. (2005). Microbial metabolic structure in a sulfidic cave hot spring: Potential mechanisms of biospeleogenesis. *J. Cave Karst Stud.* 67, 28–38.

Barton, H. A., and Northup, D. E. (2007). Geomicrobiology in cave environments: Past, current and future perspectives. *J. Cave Karst Stud.* 69, 163–178.

Bashiardes, S., Zilberman-Schapira, G., and Elinav, E. (2016). Use of metatranscriptomics in microbiome research. *Bioinform. Biol. Insights* 10, 19–25. doi: 10.4137/BBI.S34610

Behrendt, L., Trampe, E. L., Nord, N. B., Nguyen, J., Kühl, M., Lonco, D., et al. (2020). Life in the dark: Far-red absorbing cyanobacteria extend photic zones deep into terrestrial caves. *Environ. Microbiol.* 22, 952–963. doi: 10.1111/1462-2920.14774

Bender, K. E., Glover, K., Archey, A., and Barton, H. A. (2020). The impact of sample processing and media chemistry on the culturable diversity of bacteria isolated from a cave. *Int. J. Speleol.* 49, 209–220. doi: 10.5038/1827-806X.49.3.2337

Bendia, A. G., Callefo, F., Araújo, M. N., Sanchez, E., Teixeira, V. C., Vasconcelos, A., et al. (2022). Metagenome-assembled genomes from Monte Cristo cave (Diamantina, Brazil) reveal prokaryotic lineages as functional models for life on Mars. *Astrobiology* 22, 293–312. doi: 10.1089/ast.2021.0016

Beng, K. C., and Corlett, R. T. (2020). Applications of environmental DNA (eDNA) in ecology and conservation: Opportunities, challenges and prospects. *Biodivers. Conserv.* 29, 2089–2121. doi: 10.1007/s10531-020-01980-0

Benoit, J. B., Yoder, J. A., Zettler, L. W., and Hobbs, H. H. (2004). Mycoflora of a trogloxenic cave cricket, *Hadenoecus cumberlandicus* (Orthoptera: Rhaphidophoridae), from two small caves in northeastern Kentucky. *Ann. Entomol. Soc. Am.* 97, 989–993. doi: 10.1603/0013-87462004097[0989:MOATCC]2.0.CO;2

Bhullar, K., Waglechner, N., Pawlowski, A., Koteva, K., Banks, E. D., Johnston, M. D., et al. (2012). Antibiotic resistance is prevalent in an isolated cave microbiome. *PLoS One* 7:e34953. doi: 10.1371/journal.pone.0034953

Biagioli, F., Coleine, C., Delgado-Baquerizo, M., Feng, Y., Saiz-Jimenez, C., and Selbmann, L. (2024). Outdoor climate drives diversity patterns of dominant microbial taxa in caves worldwide. *Sci. Total Environ.* 906:167674. doi: 10.1016/j.scitotenv.2023.167674

Biagioli, F., Coleine, C., Piano, E., Nicolosi, G., Poli, A., Prigione, V., et al. (2023). Microbial diversity and proxy species for human impact in Italian karst caves. *Sci. Rep.* 13:689. doi: 10.1038/s41598-022-26511-5

Bin, L., Ye, C., Lijun, Z., and Ruidong, Y. (2008). Effect of microbial weathering on carbonate rocks. *Earth Sci. Front.* 15, 90–99. doi: 10.1016/S1872-5791(09)60009-9

Bodor, A., Bounedjoum, N., Vincze, G. E., Erdeiné Kis, Á, Laczi, K., Szilágyi, G., et al. (2020). Challenges of unculturable bacteria: Environmental perspectives. *Rev. Environ. Sci. Biotechnol.* 9, 1–22. doi: 10.1007/s11157-020-09522-4

Bogdan, D. F., Baricz, A. I., Chiciudean, I., Bulzu, P. A., Cristea, A., Năstase-Bucur, R., et al. (2023). Diversity, distribution and organic substrates preferences of microbial communities of a low anthropic activity cave in North-Western Romania. *Front. Microbiol.* 14:962452. doi: 10.3389/fmicb.2023.962452

Bontemps, Z., Alonso, L., Pommier, T., Hugoni, M., and Moënne-Loccoz, Y. (2022). Microbial ecology of tourist Paleolithic caves. *Sci. Total Environ.* 816:151492. doi: 10.1016/j.scitotenv.2021.151492

Brad, T., Iepure, S., and Sarbu, S. M. (2021). The chemoautotrophically based Movile Cave groundwater ecosystem, a hotspot of subterranean biodiversity. *Diversity* 13:128. doi: 10.3390/d13030128

Buza, T. M., Tonui, T., Stomeo, F., Tiambo, C., Katani, R., Schilling, M., et al. (2019). iMAP: An integrated bioinformatics and visualization pipeline for microbiome data analysis. *BMC Bioinformatics* 20:374. doi: 10.1186/s12859-019-2965-4

Cacchio, P., Ferrini, G., Ercole, C., Del Gallo, M., and Lepidi, A. (2014). Biogenicity and characterization of moonmilk in the Grotta Nera (Majella National Park, Abruzzi, Central Italy). *J Cave Karst Stud.* 76, 88–103. doi: 10.4311/2012MB0275

Cañaveras, J. C., Cuezva, S., Sanchez-Moral, S., Lario, J., Laiz, L., Gonzalez, J. M., et al. (2006). On the origin of fiber calcite crystals in moonmilk deposits. *Naturwissenschaften* 93, 27–32. doi: 10.1007/s00114-005-0052-3

Carmichael, S. K., Zorn, B. T., Santelli, C. M., Roble, L. A., Carmichael, M. J., and Bräuer, S. L. (2015). Nutrient input influences fungal community composition and size and can stimulate manganese (II) oxidation in caves. *Environ. Microbiol. Rep.* 7, 592–605. doi: 10.1111/1758-2229.12291

Carvalho, F. M., Souza, R. C., Barcellos, F. G., Hungria, M., and Vasconcelos, A. T. R. (2010). Genomic and evolutionary comparisons of diazotrophic and pathogenic bacteria of the order Rhizobiales. *BMC Microbiol.* 10:37. doi: 10.1186/1471-2180-10-37

Caumartin, V. (1963). Review of the microbiology of underground environments. *Natl. Speleol. Soc. Bull.* 25, 1–14.

Character, L. D., Beach, T., Luzzadder-Beach, S., Cook, D., Schank, C., Valdez, F. Jr., et al. (2023). Machine learning for cave entrance detection in a Maya archaeological area. *Phys. Geogr.* doi: 10.1080/02723646.2023.2261182

Chen, J. S., Tsai, H. C., Hsu, B. M., Fan, C. W., Fang, C. Y., Huang, T. Y., et al. (2021). The role of bacterial community in the formation of a stalactite in coral limestone areas of Taiwan by 16S rRNA gene amplicon surveys. *Environ. Earth Sci.* 80:665. doi: 10.1007/s12665-021-09969-w

Cheng, X., Xiang, X., Yun, Y., Wang, W., Wang, H., and Bodelier, P. L. (2023). Archaea and their interactions with bacteria in a karst ecosystem. *Front. Microbiol.* 14:1068595. doi: 10.3389/fmicb.2023.1068595

Chiciudean, I., Russo, G., Bogdan, D. F., Levei, E. A., Faur, L., Hillebrand-Voiculescu, A., et al. (2022). Competition-cooperation in the chemoautotrophic ecosystem of Movile Cave: First metagenomic approach on sediments. *Environ. Microbiome* 17:44. doi: 10.1186/s40793-022-00438-w

Cordier, T., Lanzén, A., Apothéloz-Perret-Gentil, L., Stoeck, T., and Pawlowski, J. (2019). Embracing environmental genomics and machine learning for routine biomonitoring. *Trends Microbiol.* 27, 387–397. doi: 10.1016/j.tim.2018.10.012

Covington, B. C., Spraggins, J. M., Ynigez-Gutierrez, A. E., Hylton, Z. B., and Bachmann, B. O. (2018). Response of secondary metabolism of hypogean actinobacterial genera to chemical and biological stimuli. *Appl. Environ. Microbiol.* 84, e01125-18. doi: 10.1128/AEM.01125-18

Culver, D. C., and Pipan, T. (2009). *The biology of caves and other subterranean habitats*. Oxford: Oxford University Press.

D'Angeli, I. M., Ghezzi, D., Leuko, S., Firrincieli, A., Parise, M., Fiorucci, A., et al. (2019a). Geomicrobiology of a seawater-influenced active sulfuric acid cave. *PLoS One* 14:e0220706. doi: 10.1371/journal.pone.0220706

D'Angeli, I. M., Parise, M., Vattano, M., Madonia, G., Galdenzi, S., and De Waele, J. (2019b). Sulfuric acid caves of Italy: A review. *Geomorphology* 333, 105–122. doi: 10.1016/j.geomorph.2019.02.025

D'Angeli, I. M., Serrazanetti, D. I., Montanari, C., Vannini, L., Gardini, F., and De Waele, J. (2017). Geochemistry and microbial diversity of cave waters in the gypsum karst aquifers of Emilia-Romagna region, Italy. *Sci. Total Environ.* 598, 538–552. doi: 10.1016/j.scitotenv.2017.03.270

D'Auria, G., Artacho, A., Rojas, R. A., Bautista, J. S., Méndez, R., Gamboa, M. T., et al. (2018). Metagenomics of bacterial diversity in villa Luz caves with sulfur water springs. *Genes* 9:55. doi: 10.3390/genes9010055

D'Angelo, T., Goordial, J., Lindsay, M. R., McGonigle, J., Booker, A., Moser, D., et al. (2023). Replicated life-history patterns and subsurface origins of the bacterial sister phyla Nitrospirota and Nitrospinota. *ISME J.* 17, 891–902. doi: 10.1038/s41396-023-01397-x

de Bruin, S., Vasquez-Cardenas, D., Sarbu, S. M., Meysman, F. J. R., Sousa, D. Z., van Loosdrecht, M. C. M., et al. (2022).). Sulfated glycosaminoglycan-like polymers are present in an acidophilic biofilm from a sulfidic cave. *Sci. Total Environ.* 829:154472. doi: 10.1016/j.scitotenv.2022.154472

De Kumar, A., Muthiyan, R., Sunder, J., Bhattacharya, D., Kundu, A., and Roy, S. (2019). Profiling bacterial diversity of B2 cave, a limestone cave of Baratang, Andaman and Nicobar Islands, India. *Proc. Indian Natl. Sci. Acad.* 85, 853–862. doi: 10.16943/ptinsa/2019/49589

De Waele, J., and Gutierrez, F. (2022). *Karst hydrogeology, geomorphology and caves*. Chichester: Wiley Blackwell.

Derewacz, D. K., McNees, C. R., Scalmani, G., Covington, C. L., Shanmugam, G., Marnett, L. J., et al. (2014). Structure and stereochemical determination of hypogeamicins from a cave-derived actinomycete. *J. Nat. Prod.* 77, 1759–1763. doi: 10.1021/np400742p

Dhami, N. K., Mukherjee, A., and Watkin, E. L. (2018). Microbial diversity and mineralogical-mechanical properties of calcitic cave speleothems in natural and in vitro biomineralization conditions. *Front. Microbiol.* 9:40. doi: 10.3389/fmicb.2018.00040

Djebaili, R., Mignini, A., Vaccarelli, I., Pellegrini, M., Spera, D. M., Del Gallo, M., et al. (2022). Polyhydroxybutyrate-producing cyanobacteria from lampenflora: The case study of the "Stiffe" caves in Italy. *Front. Microbiol.* 13:933398. doi: 10.3389/fmicb.2022.933398

Dong, Y., Gao, J., Wu, Q., Ai, Y., Huang, Y., Wei, W., et al. (2020). Co-occurrence pattern and function prediction of bacterial community in karst cave. *BMC Microbiol.* 20:137. doi: 10.1186/s12866-020-01806-7

Duncan, T. R., Werner-Washburne, M., and Northup, D. E. (2021). Diversity of siderophore-producing bacterial cultures from Carlsbad Caverns national park caves, Carlsbad, New Mexico. *J. Cave Karst Stud.* 83, 29–43. doi: 10.4311/2019ES0118

Egemeier, S. J. (1981). Cavern development by thermal waters. *Natl. Speleol. Soc. Bull.* 43, 31–51.

Engel, A. S. (2007). Observations on the biodiversity of sulfidic karst habitats. *J. Cave Karst Stud.* 69, 187–206.

Engel, A. S. (2010). "Microbial diversity of cave ecosystems," in *Geomicrobiology: Molecular and environmental perspective*, eds L. Barton, M. Mandl, and A. Loy (Dordrecht: Springer), 219–238.

Engel, A. S., Lee, N., Porter, M. L., Stern, L. A., Bennett, P. C., and Wagner, M. (2003). Filamentous "Epsilonproteobacteria" dominate microbial mats from sulfidic cave springs. *Appl. Environ. Microbiol.* 69, 5503–5511. doi: 10.1128/AEM.69.9.5503-5511.2003

Engel, A. S., Stern, L. A., and Bennett, P. C. (2004b). Microbial contributions to cave formation: New insights into sulfuric acid speleogenesis. *Geology* 32, 369–372. doi: 10.1130/G20288.1

Engel, A. S., Porter, M. L., Stern, L. A., Quinlan, S., and Bennett, P. C. (2004a). Bacterial diversity and ecosystem function of filamentous microbial mats from aphotic (cave) sulfidic springs dominated by chemolithoautotrophic "Epsilonproteobacteria". *FEMS Microbiol. Ecol.* 51, 31–53. doi: 10.1016/j.femsec.2004.07.004

Enyedi, N. T., Anda, D., Borsodi, A. K., Szabó, A., Pál, S. E., Óvári, M., et al. (2019). Radioactive environment adapted bacterial communities constituting the biofilms of hydrothermal spring caves (Budapest, Hungary). *J. Environ. Radioact.* 203, 8–17. doi: 10.1016/j.jenvrad.2019.02.010

Espino del Castillo, A., Beraldi-Campesi, H., Amador-Lemus, P., Beltrán, H. I., and Le Borgne, S. (2018). Bacterial diversity associated with mineral substrates and hot springs from caves and tunnels of the Naica underground system (Chihuahua, Mexico). *Int. J. Speleol.* 47, 213–227. doi: 10.5038/1827-806X.47.2.2161

Falasco, E., Ector, L., Isaia, M., Wetzel, C. E., Hoffmann, L., and Bona, F. (2014). Diatom flora in subterranean ecosystems: A review. *Internat. J. Speleol.* 43, 231–251. doi: 10.5038/1827-806X.43.3.1

Farda, B., Djebaili, R., Vaccarelli, I., Del Gallo, M., and Pellegrini, M. (2022a). Actinomycetes from caves: An overview of their diversity, biotechnological properties, and insights for their use in soil environments. *Microorganisms* 10:453. doi: 10.3390/microorganisms10020453

Farda, B., Vaccarelli, I., Ercole, C., Djebaili, R., Del Gallo, M., and Pellegrini, M. (2022b). Exploring structure, microbiota, and metagenome functions of epigean and hypogean black deposits by microscopic, molecular and bioinformatic approaches. *Sci. Rep.* 12:19405. doi: 10.1038/s41598-022-24159-9

Fierer, N., Bradford, M. A., and Jackson, R. B. (2007). Toward an ecological classification of soil bacteria. *Ecology* 88, 1354–1364. doi: 10.1890/05-1839

Ford, D. C., and Williams, P. (2007). *Karst hydrogeology and geomorphology*. Chichester: Wiley.

Forti, P., Galdenzi, S., and Sarbu, S. M. (2002). The hypogenic caves: A powerful tool for the study of seeps and their environmental effects. *Cont. Shelf Res.* 22, 2373–2386. doi: 10.1016/S0278-4343(02)00062-6

Ghezzi, D., Foschi, L., Firrincieli, A., Hong, P. Y., Vergara, F., De Waele, J., et al. (2022). Insights into the microbial life in silica-rich subterranean environments: Microbial communities and ecological interactions in an orthoquartzite cave (Imawarì Yeuta, Auyan Tepui, Venezuela). *Front. Microbiol.* 13:930302. doi: 10.3389/fmicb.2022.930302

Ghosh, S., Kuisiene, N., and Cheeptham, N. (2017a). The cave microbiome as a source for drug discovery: Reality or pipe dream? *Biochem. Pharmacol.* 134, 18–34. doi: 10.1016/j.bcp.2016.11.018

Ghosh, S., Paine, E., Wall, R., Kam, G., Lauriente, T., Sa-Ngarmangkang, P. C., et al. (2017b). In situ cultured bacterial diversity from iron curtain cave, Chilliwack, British Columbia, Canada. *Diversity* 9:36. doi: 10.3390/d9030036

Gillieson, D. S. (2021). *Caves: Processes, development, and management*. Hoboken, NJ: Wiley-Blackwell.

Glime, J. M. (2022). *"Caves," bryophyte ecology: Habitat and role*. Houghton, MI: Michigan Technological University.

Gnaspini, P., and Trajano, E. (2000). "Guano communities in tropical caves," in *Ecosystems of the world*, eds H. Wilkens, D. C. Culver, and W. F. Humphreys (Amsterdam: Elsevier), 251–268.

Goldscheider, N., Chen, Z., Auler, A. S., Bakalowicz, M., Broda, S., Drew, D., et al. (2020). Global distribution of carbonate rocks and karst water resources. *Hydrogeol. J.* 28, 1661–1677. doi: 10.1007/s10040-020-02139-5

Gonzalez-Pimentel, J. L., Hermosin, B., Saiz-Jimenez, C., and Jurado, V. (2022). *Streptomyces benahoarensis* sp. nov. isolated from a lava tube of la Palma, Canary Islands, Spain. *Front. Microbiol.* 13:907816. doi: 10.3389/fmicb.2022.907816

Gonzalez-Pimentel, J. L., Martin-Pozas, T., Jurado, V., Miller, A. Z., Caldeira, A. T., Fernandez-Lorenzo, O., et al. (2021). Prokaryotic communities from a lava tube cave in La Palma Island (Spain) are involved in the biogeochemical cycle of major elements. *Peer J.* 9:e11386. doi: 10.7717/peerj.11386

Gonzalez-Pimentel, J. L., Miller, A. Z., Jurado, V., Laiz, L., Pereira, M. F., and Saiz-Jimenez, C. (2018). Yellow coloured mats from lava tubes of La Palma (Canary Islands, Spain) are dominated by metabolically active Actinobacteria. *Sci. Rep.* 8:1944. doi: 10.1038/s41598-018-20393-2

Gosse, J. T., Ghosh, S., Sproule, A., Overy, D., Cheeptham, N., and Boddy, C. N. (2019). Whole genome sequencing and metabolomic study of cave streptomyces isolates ICC1 and ICC4. *Front. Microbiol.* 10:1020. doi: 10.3389/fmicb.2019.01020

Griebler, C., Malard, F., and Lefébure, T. (2014). Current developments in groundwater ecology from biodiversity to ecosystem function and services. *Curr. Opin. Biotechnol.* 27, 159–167. doi: 10.1016/j.copbio.2014.01.018

Groth, I., Vettermann, R., Schuetze, B., Schumann, P., and Sáiz-Jiménez, C. (1999). Actinomycetes in karstic caves of northern Spain (Altamira and Tito Bustillo). *J. Microbiol. Methods* 36, 115–122. doi: 10.1016/S0167-7012(99)00016-0

Gulden, B. (2019). *USA long cave list*. Available online at: https://cave-exploring.com/index.php/long-and-deep-caves-of-the-world/usa-long-cave-list/ (accessed December 15, 2023).

Gulecal-Pektas, Y., and Temel, M. (2017). A Window to the subsurface: Microbial diversity in hot springs of a sulfidic cave (Kaklik, Turkey). *Geomicrobiol. J.* 34, 374–384. doi: 10.1080/01490451.2016.1204374

Hamedi, J., Kafshnouchi, M., and Ranjbaran, M. (2019). A study on actinobacterial diversity of Hampoeil cave and screening of their biological activities. *Saudi J. Biol. Sci.* 26, 1587–1595. doi: 10.1016/j.sjbs.2018.10.010

Hathaway, J. J. M., Garcia, M. G., Balasch, M. M., Spilde, M. N., Stone, F. D., Dapkevicius, M. D. L. N., et al. (2014). Comparison of bacterial diversity in Azorean and Hawai'ian lava cave microbial mats. *Geomicrobiol. J.* 31, 205–220. doi: 10.1080/01490451.2013.777491

He, D., Wu, F., Ma, W., Zhang, Y., Gu, J. D., Duan, Y., et al. (2021). Insights into the bacterial and fungal communities and microbiome that causes a microbe outbreak on ancient wall paintings in the Maijishan Grottoes. *Int. Biodeter. Biodegr.* 163:105250. doi: 10.1016/j.ibiod.2021.105250

Herold, K., Gollmick, F. A., Growth, I., Roth, M., Menzel, K. D., Mollmann, U., et al. (2005). Cervimycin A-D: A polyketide glycoside complex from a cave bacterium can defeat vancomycin resistance. *Chem. Eur. J.* 11, 5523–5530. doi: 10.1002/chem.200500320

Hershey, O. S., and Barton, H. A. (2018). "The microbial diversity of caves," in *Ecological studies*, eds O. Moldovan, L. Kováč, and S. Halse (Cham: Springer), 69–90.

Hershey, O. S., Kallmeyer, J., and Barton, H. A. (2019). "A practical guide to studying the microbiology of karst aquifers," in *Karst water environment: Advances in research, management and policy*, eds T. Younos, M. Schreiber, and K. Kosič Ficco (Cham: Springer), 191–207.

Hershey, O. S., Kallmeyer, J., Wallace, A., Barton, M. D., and Barton, H. A. (2018). High microbial diversity despite extremely low biomass in a deep karst aquifer. *Front. Microbiol.* 9:2823. doi: 10.3389/fmicb.2018.02823

Hose, L. D., Palmer, A. N., Palmer, M. V., Northup, D. E., Boston, P. J., and DuChene, H. R. (2000). Microbiology and geochemistry in a hydrogen-sulphide-rich karst environment. *Chem. Geol.* 169, 399–423. doi: 10.1016/S0009-2541(00)00217-5

Howarth, F. G. (1980). The zoogeography of specialized cave animals: A bioclimatic model. *Evolution* 34, 394–406. doi: 10.2307/2407402

Howarth, F. G. (2021). Glacier caves: A globally threatened subterranean biome. *J. Cave Karst Stud.* 83, 66–70. doi: 10.4311/2019LSC0132

Hutchins, B. T., Engel, A. S., Nowlin, W. H., and Schwartz, B. F. (2016). Chemolithoautotrophy supports macroinvertebrate food webs and affects diversity and stability in groundwater communities. *Ecology* 97, 1530–1542. doi: 10.1890/15-1129.1

Idle, J. R., and Gonzalez, F. J. (2007). Metabolomics. *Cell Metab.* 6, 348–351. doi: 10.1016/j.cmet.2007.10.005

Imangaliyev, S., Keijser, B., Crielaard, W., and Tsivtsivadze, E. (2015). Personalized microbial network inference via co-regularized spectral clustering. *Methods* 83, 28–35. doi: 10.1016/j.ymeth.2015.03.017

Jiang, D., Armour, C. R., Hu, C., Mei, M., Tian, C., Sharpton, T. J., et al. (2019). Microbiome multi-omics network analysis: Statistical considerations, limitations, and opportunities. *Front. Genet.* 10:995. doi: 10.3389/fgene.2019.00995

Jiang, L., Pu, H., Xiang, J., Su, M., Yan, X., Yang, D., et al. (2018). Huanglongmycin A-C, cytotoxic polyketides biosynthesized by a putative type II polyketide synthase from *Streptomyces* sp. *Front. Chem.* 6:254. doi: 10.3389/fchem.2018.00254

Jones, A. A., and Bennett, P. C. (2014). Mineral microniches control the diversity of subsurface microbial populations. *Geomicrobiol. J.* 31, 246–261. doi: 10.1080/01490451.2013.809174

Jones, D. S., Albrecht, H. L., Dawson, K. S., Schaperdoth, I., Freeman, K. H., Pi, Y., et al. (2012). Community genomic analysis of an extremely acidophilic sulfur-oxidizing biofilm. *ISME J.* 6, 158–170. doi: 10.1038/ismej.2011.75

Jones, D. S., and Northup, D. E. (2021). Cave decorating with microbes: Geomicrobiology of caves. *Elements* 17, 107–112. doi: 10.2138/gselements.17.2.107

Jones, D. S., Lyon, E. H., and Macalady, J. L. (2008). Geomicrobiology of biovermiculations from the Frasassi cave system. *Italy. J. Cave Karst Stud.* 70, 78–93.

Jones, D. S., Schaperdoth, I., and Macalady, J. L. (2016). Biogeography of sulfur-oxidizing Acidithiobacillus populations in extremely acidic cave biofilms. *ISME J.* 10, 2879–2891. doi: 10.1038/ismej.2016.74

Jones, D. S., Schaperdoth, I., Northup, D. E., Gómez-Cruz, R., and Macalady, J. L. (2023). Convergent community assembly among globally separated acidic cave biofilms. *Appl. Environ. Microbiol.* 89:e0157522. doi: 10.1128/aem.01575-22

Jones, D. S., Tobler, D. J., Schaperdoth, I., Mainiero, M., and Macalady, J. L. (2010). Community structure of subsurface biofilms in the thermal sulfidic caves of Acquasanta Terme, Italy. *Appl. Environ. Microbiol.* 76, 5902–5910. doi: 10.1128/AEM.00647-10

Jurado, V., D'Angeli, I., Martin-Pozas, T., Cappelletti, M., Ghezzi, D., Gonzalez-Pimentel, J. L., et al. (2021). Dominance of *Arcobacter* in the white filaments from the thermal sulfidic spring of Fetida Cave (Apulia, southern Italy). *Sci. Total Environ.* 800:149465. doi: 10.1016/j.scitotenv.2021.149465

Jurado, V., Gonzalez-Pimentel, J. L., Miller, A. Z., Hermosin, B., D'Angeli, I. M., Tognini, P., et al. (2020). Microbial communities in vermiculation deposits from an Alpine cave. *Front. Earth Sci.* 8:586248. doi: 10.3389/feart.2020.586248

Kalam, S., Basu, A., Ahmad, I., Sayyed, R. Z., El-Enshasy, H. A., Dailin, D. J., et al. (2020). Recent understanding of soil Acidobacteria and their ecological significance: A critical review. *Front. Microbiol.* 11:580024. doi: 10.3389/fmicb.2020.580024

Kashaf, S. S., Almeida, A., Segre, J. A., and Finn, R. D. (2021). Recovering prokaryotic genomes from host-associated, short-read shotgun metagenomic sequencing data. *Nat. Protoc.* 16, 2520–2541. doi: 10.1038/s41596-021-00508-2

Keeler, R., and Lusk, B. (2021). Microbiome of Grand Canyon caverns, a dry sulfuric karst cave in Arizona, supports diverse extremophilic bacterial and archaeal communities. *J. Cave Karst Stud.* 83, 44–56. doi: 10.4311/2019MB0126

Kempe, S. (2019). "Volcanic rock caves," in *Encyclopedia of caves*, 3rd Edn, eds W. B. White, D. C. Culver, and T. Pipan (Amsterdam: Academic Press), 118–1127.

Kieraite-Aleksandrova, I., Aleksandrovas, V., and Kuisiene, N. (2015). Down into the earth: Microbial diversity of the deepest cave of the world. *Biologia* 70, 989–1002. doi: 10.1515/biolog-2015-0127

Kimble, J. C., Winter, A. S., Spilde, M. N., Sinsabaugh, R. L., and Northup, D. E. (2018). A potential central role of *Thaumarchaeota* in N-cycling in a semi-arid environment, fort Stanton cave, snowy river passage, New Mexico, USA. *FEMS Microbiol. Ecol.* 94:173. doi: 10.1093/femsec/fiy173

Klimchouk, A. (2017). "Types and settings of Hypogene karst," in *Hypogene karst regions and caves of the world*, Vol. 1, eds A. Klimchouk, A. N. Palmer, J. D. Waele, A. S. Auler, and P. Audra (Cham: Springer), 1–39.

Klusaitė, A., Vičkačkaitė, V., Vaitkevičienė, B., Karnickaitė, R., Bukelskis, D., Kieraitė-Aleksandrova, I., et al. (2016). Characterization of antimicrobial activity of culturable bacteria isolated from Krubera-Voronja Cave. *Int. J. Speleol.* 45, 275–287.

Koner, S., Chen, J. S., Hsu, B. M., Tan, C. W., Fan, C. W., Chen, T. H., et al. (2021). Assessment of carbon substrate catabolism pattern and functional metabolic pathway for microbiota of limestone caves. *Microorganisms* 9:1789. doi: 10.3390/microorganisms9081789

Kosznik-Kwaśnicka, K., Golec, P., Jaroszewicz, W., Lubomska, D., and Piechowicz, L. (2022). Into the unknown: Microbial communities in caves, their role, and potential use. *Microorganisms* 10:222. doi: 10.3390/microorganisms10020222

Kovaka, S., Ou, S., Jenike, K. M., and Schatz, M. C. (2023). Approaching complete genomes, transcriptomes and epi-omes with accurate long-read sequencing. *Nat. Methods* 20, 12–16. doi: 10.1038/s41592-022-01716-8

Kumaresan, D., Wischer, D., Stephenson, J., Hillebrand-Voiculescu, A., and Murrell, J. C. (2014). Microbiology of movile cave-a chemolithoautotrophic ecosystem. *Geomicrobiol. J.* 31, 186–193. doi: 10.1080/01490451.2013.839764

Latorre-Pérez, A., Pascual, J., Porcar, M., and Vilanova, C. (2020). A lab in the field: Applications of real-time, in situ metagenomic sequencing. *Biol. Methods Protoc.* 5:baa016. doi: 10.1093/biomethods/bpaa016

Laurent, D., Barré, G., Durlet, C., Cartigny, P., Carpentier, C., Paris, G., et al. (2023). Unravelling biotic versus abiotic processes in the development of large sulfuric-acid karsts. *Geology* 51, 262–267. doi: 10.1130/G50658.1

Lavoie, K. H., Winter, A. S., Read, K. J. H., Hughes, E. M., Spilde, M. N., and Northup, D. E. (2017). Comparison of bacterial communities from lava cave microbial mats to overlying surface soils from lava beds national monument, USA. *PLoS One* 12:e0169339. doi: 10.1371/journal.pone.0169339

Lee, J., Kim, H. S., Jo, H. Y., and Kwon, M. J. (2021). Revisiting soil bacterial counting methods: Optimal soil storage and pretreatment methods and comparison of culture-dependent and-independent methods. *PLoS One* 16:e0246142. doi: 10.1371/journal.pone.0246142

Lee, N. M., Meisinger, D. B., Aubrecht, R., Kovacik, L., Saiz-Jimenez, C., Baskar, S., et al. (2012). "Caves and karst environments," in *Life at extremes: Environments, organisms and strategies for survival*, ed. E. M. Bell (Wallingford: CAB International), 320–344.

Leuko, S., Koskinen, K., Sanna, L., D'Angeli, I. M., De Waele, J., Marcia, P., et al. (2017). The influence of human exploration on the microbial community structure and ammonia-oxidizing potential of the Su Bentu limestone cave in Sardinia, Italy. *PLoS One* 12:e0180700. doi: 10.1371/journal.pone.0180700

Lin, H., and Peddada, S. D. (2020). Analysis of microbial compositions: A review of normalization and differential abundance analysis. *NPJ Biofilms Microbiomes* 6:60. doi: 10.1038/s41522-020-00160-w

Liu, Q., He, Z., Naganuma, T., Nakai, R., Rodríguez, L. M., Carreño, R., et al. (2022). Phylotypic diversity of bacteria associated with speleothems of a silicate cave in a Guiana Shield tepui. *Microorganisms* 10:1395. doi: 10.3390/microorganisms10071395

Long, Y., Jiang, J., Hu, X., Zhou, J., Hu, J., and Zhou, S. (2019). Actinobacterial community in Shuanghe cave using culture-dependent and-independent approaches. *World J. Microbiol. Biotechnol.* 35:153. doi: 10.1007/s11274-019-2713-y

Lücker, S., Wagner, M., Maixner, F., Pelletier, E., Koch, H., Vacherie, B., et al. (2010). A Nitrospira metagenome illuminates the physiology and evolution of globally important nitrite-oxidizing bacteria. *Proc. Natl. Acad. Sci. U.S.A.* 107, 13479–13484. doi: 10.1073/pnas.1003860107

Ma, L., Huang, X., Wang, H., Yun, Y., Cheng, X., Liu, D., et al. (2021). Microbial interactions drive distinct taxonomic and potential metabolic responses to habitats in karst cave ecosystem. *Microbiol. Spectr.* 9:e0115221. doi: 10.1128/Spectrum.01152-21

Macalady, J. L., Dattagupta, S., Schaperdoth, I., Jones, D. S., Druschel, G. K., and Eastman, D. (2008). Niche differentiation among sulfur-oxidizing bacterial populations in cave waters. *ISME J.* 2, 590–601. doi: 10.1038/ismej.2008.25

Macalady, J. L., Jones, D. S., and Lyon, E. H. (2007). Extremely acidic, pendulous cave wall biofilms from the Frasassi cave system, Italy. *Environ. Microbiol.* 9, 1402–1414. doi: 10.1111/j.1462-2920.2007.01256.x

Macalady, J. L., Lyon, E. H., Koffman, B., Albertson, L. K., Meyer, K., Galdenzi, S., et al. (2006). Dominant microbial populations in limestone-corroding stream biofilms, Frasassi cave system, Italy. *Appl. Environ. Microbiol.* 72, 5596–5609. doi: 10.1128/AEM.00715-06

Maciejewska, M., Adam, D., Martinet, L., Naômé, A., Całusińska, M., Delfosse, P., et al. (2016). A phenotypic and genotypic analysis of the antimicrobial potential of cultivable Streptomyces isolated from cave moonmilk deposits. *Front. Microbiol.* 7:1455. doi: 10.3389/fmicb.2016.01455

Maciejewska, M., Adam, D., Naômé, A., Martinet, L., Tenconi, E., Całusińska, M., et al. (2017). Assessment of the potential role of streptomyces in cave moonmilk formation. *Front. Microbiol.* 8:1181. doi: 10.3389/fmicb.2017.01181

Măntoiu, D. Ş, Mirea, I. C., Şandric, I. C., Cîşlariu, A. G., Gherghel, I., Constantin, S., et al. (2022). Bat dynamics modelling as a tool for conservation management in subterranean environments. *PLoS One* 17:e0275984. doi: 10.1371/journal.pone.0275984

Marques, E. L. S., Silva, G. S., Dias, J. C. T., Gross, E., Costa, M. S., and Rezende, R. P. (2019). Cave drip water related samples as a natural environment for aromatic hydrocarbon-degrading bacteria. *Microorganisms* 7:33. doi: 10.3390/microorganisms7020033

Martin-Pozas, T., Fernandez-Cortes, A., Cuezva, S., Cañaveras, J. C., Benavente, D., Duarte, E., et al. (2023). New insights into the structure, microbial diversity and ecology of yellow biofilms in a Paleolithic rock art cave (Pindal Cave, Asturias, Spain). *Sci. Total. Environ.* 897:165218. doi: 10.1016/j.scitotenv.2023.165218

Martin-Pozas, T., Nováková, A., Jurado, V., Fernandez-Cortes, A., Cuezva, S., Saiz-Jimenez, C., et al. (2022). Diversity of Microfungi in a high radon cave ecosystem. *Front. Microbiol.* 13:869661. doi: 10.3389/fmicb.2022.869661

McCluskey, K., Barker, K. B., Barton, H. A., Boundy-Mills, K., Brown, D. R., Coddington, J. A., et al. (2017). The US culture collection network responding to the requirements of the Nagoya protocol on access and benefit sharing. *mBio* 8, e00982-17. doi: 10.1128/mBio.00982-17

Mejía-Ortíz, L., Christman, M. C., Pipan, T., and Culver, D. C. (2020). What's the temperature in tropical caves? *PLoS One.* 15:e0237051. doi: 10.1371/journal.pone.0237051

Michail, G., Karapetsi, L., Madesis, P., Reizopoulou, A., and Vagelas, I. (2021). Metataxonomic analysis of bacteria entrapped in a stalactite's core and their possible environmental origins. *Microorganisms* 9:2411. doi: 10.3390/microorganisms9122411

Mondini, A., Anwar, M. Z., Ellegaard-Jensen, L., Lavin, P., Jacobsen, C. S., and Purcarea, C. (2022). Heat shock response of the active microbiome from perennial cave ice. *Front. Microbiol.* 12:4370. doi: 10.3389/fmicb.2021.809076

Morgan, I. M. (1991). *Geology of caves*. Washington, DC: U.S. Government Printing Office, doi: 10.3133/7000072

Mueller, A. J., Daebeler, A., Herbold, C. W., Kirkegaard, R. H., and Daims, H. (2023). Cultivation and genomic characterization of novel and ubiquitous marine nitrite-oxidizing bacteria from the Nitrospirales. *ISME J.* 17, 2123–2133. doi: 10.1038/s41396-023-01518-6

Mulec, J., Oarga-Mulec, A., Tomazin, R., and Matos, T. (2015). Characterization and fluorescence of yellow biofilms in karst caves, southwest Slovenia. *Int. J. Speleol.* 44, 107–114.

Neu, A. T., Allen, E. E., and Roy, K. (2021). Defining and quantifying the core microbiome: Challenges and prospects. *Proc. Natl. Acad. Sci. U.S.A.* 118:e2104429118. doi: 10.1073/pnas.2104429118

Nichols, D., Cahoon, N., Trakhtenberg, E. M., Pham, L., Mehta, A., Belanger, A., et al. (2010). Use of ichip for high throughput in situ cultivation of "uncultivable" microbial species. *Appl. Environ. Microbiol.* 76, 2445–2450. doi: 10.1128/AEM.01754-09

Nicolosi, G., Gonzalez-Pimentel, J. L., Piano, E., Isaia, M., and Miller, A. Z. (2023). First Insights into the bacterial diversity of Mount Etna volcanic caves. *Microb. Ecol.* 86, 1632–1645. doi: 10.1007/s00248-023-02181-2

Northup, D. E., and Lavoie, K. H. (2001). Geomicrobiology of caves: A review. *Geomicrobiol. J.* 18, 199–222. doi: 10.1080/01490450152467750

Northup, D. E., Melim, L. A., Spilde, M. N., Hathaway, J. J., Garcia, M. G., Moya, M., et al. (2011). Lava cave microbial communities within mats and secondary mineral deposits: Implications for life detection on other planets. *Astrobiology* 11, 601–618. doi: 10.1089/ast.2010.0562

Northup, D., and Lavoie, K. (2015). "Microbial Diversity and ecology of lava caves," in *Microbial life of cave systems*, ed. A. S. Engel (Boston, MA: De Gruyter), 161–192.

Novak, T., Perc, M., Lipovšek, S., and Janžekovič, F. (2012). Duality of terrestrial subterranean fauna. *Int. J. Speleol.* 41, 181–188. doi: 10.5038/1827-806X.41.2.5

Nygaard, A. B., Tunsjø, H. S., Meisal, R., and Charnock, C. (2020). A preliminary study on the potential of Nanopore MinION and illumina MiSeq 16S rRNA gene sequencing to characterize building-dust microbiomes. *Sci. Rep.* 10:3209. doi: 10.1038/s41598-020-59771-0

Oliveira, C., Gunderman, L., Coles, C. A., Lochmann, J., Parks, M., Ballard, E., et al. (2017). 16S rRNA gene-based metagenomic analysis of Ozark cave bacteria. *Diversity* 9:31. doi: 10.3390/d9030031

Oren, A., and Garrity, G. M. (2021). Valid publication of the names of forty-two phyla of prokaryotes. *Int. J. Syst. Evol. Microbiol.* 71:005056. doi: 10.1099/ijsem.0.005056

Ortiz, M., Legatzki, A., Neilson, J. W., Fryslie, B., Nelson, W. M., Wing, R. A., et al. (2014). Making a living while starving in the dark: Metagenomic insights into the energy dynamics of a carbonate cave. *ISME J.* 8, 478–491. doi: 10.1038/ismej.2013.159

Palmer, A. N. (1991). Origin and morphology of limestone caves. *Geol. Soc. Am. Bull.* 103, 1–21. doi: 10.1130/0016-76061991103<0001:OAMOLC<2.3.CO;2

Palmer, A. N. (2007). *Cave geology*. Dayton, OH: Cave Books.

Palmer, A. N., and Hill, C. A. (2019). "Sulfuric acid caves," in *Encyclopedia of caves*, eds W. B. White, D. C. Culver, and T. Pipan (Cambridge, MA: Academic Press), 1053–1062.

Parise, M., Galeazzi, C., Bixio, R., and Dixon, M. (2013). "Classification of artificial cavities: A first contribution by the UIS Commission," in *Proceedings of the 16th international congress of speleology BRNO*, (Prague: Czech Speleological Society), 230–235.

Park, S., Cho, Y. J., Jung, D. Y., Jo, K. N., Lee, E. J., and Lee, J. S. (2020). Microbial diversity in moonmilk of Baeg-nyong cave, Korean CZO. *Front. Microbiol.* 11:613. doi: 10.3389/fmicb.2020.00613

Pašić, L., Kovče, B., Sket, B., and Herzog-Velikonja, B. (2009). Diversity of microbial communities colonizing the walls of a Karstic cave in Slovenia. *FEMS Microbiol. Ecol.* 71, 50–60. doi: 10.1111/j.1574-6941.2009.00789.x

Pawlowski, A. C., Wang, W., Koteva, K., Barton, H. A., McArthur, A. G., and Wright, G. D. (2016). A diverse intrinsic antibiotic resistome from a cave bacterium. *Nat. Commun.* 7:13803. doi: 10.1038/ncomms13803

Porca, E., Jurado, V., Martin-Sanchez, P. M., Hermosin, B., Bastian, F., Alabouvette, C., et al. (2011). Aerobiology: An ecological indicator for early detection and control of fungal outbreaks in caves. *Ecol. Indic.* 11, 1594–1598. doi: 10.1016/j.ecolind.2011.04.003

Porca, E., Jurado, V., Žgur-Bertok, D., Saiz-Jimenez, C., and Pašić, L. (2012). Comparative analysis of yellow microbial communities growing on the walls of geographically distinct caves indicates a common core of microorganisms involved in their formation. *FEMS Microbiol. Ecol.* 81, 255–266. doi: 10.1111/j.1574-6941.2012.01383.x

Prescott, R. D., Zamkovaya, T., Donachie, S. P., Northup, D. E., Medley, J. J., Monsalve, N., et al. (2022). Islands within islands: Bacterial phylogenetic structure and consortia in Hawaiian lava caves and fumaroles. *Front. Microbiol.* 13:934708. doi: 10.3389/fmicb.2022.934708

Pronk, M., Goldscheider, N., Zopfi, J., and Zwahlen, F. (2009). Percolation and particle transport in the unsaturated zone of a karst aquifer. *Groundwater* 47, 361–369. doi: 10.1111/j.1745-6584.2008.00509.x

Qian, Z., Mao, Y., Xiong, S., Peng, B., Liu, W., Liu, H., et al. (2020). Historical residues of organochlorine pesticides (OCPs) and polycyclic aromatic hydrocarbons (PAHs) in a flood sediment profile from the Longwang Cave in Yichang, China. *Ecotoxicol. Environ. Saf.* 196:110542. doi: 10.1016/j.ecoenv.2020.110542

Quince, C., Walker, A. W., Simpson, J. T., Loman, N. J., and Segata, N. (2017). Shotgun metagenomics, from sampling to analysis. *Nat. Biotechnol.* 35, 833–844. doi: 10.1038/nbt.3935

Rachid, A. N., and Güngör, N. D. (2022). Screening of bioactive compounds for biomedical and industrial uses from Actinobacteria isolated from the Parsik Cave (Turkey). *Johnson Matthey Technol. Rev.* 67, 159–170. doi: 10.1595/205651322X16482034395036

Rangseekaew, P., and Pathom-aree, W. (2019). Cave Actinobacteria as producers of bioactive metabolites. *Front. Microbiol.* 10:387. doi: 10.3389/fmicb.2019.00387

Raynaud, X., and Nunan, N. (2014). Spatial ecology of bacteria at the microscale in soil. *PLoS One* 9:e87217. doi: 10.1371/journal.pone.0087217

Reboleira, A. S., Bodawatta, K. H., Ravn, N. M. R., Lauritzen, S. E., Skoglund, R. Ø, Poulsen, M., et al. (2022). Nutrient-limited subarctic caves harbour more diverse and complex bacterial communities than their surface soil. *Environ. Microbiome* 17:41. doi: 10.1186/s40793-022-00435-z

Riquelme, C., Dapkevicius, M., Miller, A., Charlop-Powers, Z., Brady, S., Mason, C., et al. (2017). Biotechnological potential of Actinobacteria from Canadian and Azorean volcanic caves. *Appl. Microbiol. Biotechnol.* 101, 843–857. doi: 10.1007/s00253-016-7932-7

Riquelme, C., Marshall Hathaway, J. J., Enes Dapkevicius, M. L., Miller, A. Z., Kooser, A., Northup, D. E., et al. (2015). Actinobacterial diversity in volcanic caves and associated geomicrobiological interactions. *Front. Microbiol.* 6:1342. doi: 10.3389/fmicb.2015.01342

Rohwerder, T., Sand, W., and Lascu, C. (2003). Preliminary evidence for a sulphur cycle in Movile Cave, Romania. *Acta Biotechnol.* 23, 101–107. doi: 10.1002/abio.200390000

Roldán, C., Murcia-Mascarós, S., López-Montalvo, E., Vilanova, C., and Porcar, M. (2018). Proteomic and metagenomic insights into prehistoric Spanish Levantine rock art. *Sci Rep.* 8:10011. doi: 10.1038/s41598-018-28121-6

Rossmassler, K., Engel, A. S., Twing, K. I., Hanson, T. E., and Campbell, B. J. (2012). Drivers of epsilonproteobacterial community composition in sulfidic caves and springs. *FEMS Microbiol. Ecol.* 79, 421–432. doi: 10.1111/j.1574-6941.2011.01231.x

Rossmassler, K., Hanson, T. E., and Campbell, B. J. (2016). Diverse sulfur metabolisms from two subterranean sulfidic spring systems. *FEMS Microbiol. Lett.* 363, fnw162. doi: 10.1093/femsle/fnw162

Sauro, F., Cappelletti, M., Ghezzi, D., Columbu, A., Hong, P. Y., Zowawi, H. M., et al. (2018). Microbial diversity and biosignatures of amorphous silica deposits in orthoquartzite caves. *Sci. Rep.* 8:17569. doi: 10.1038/s41598-018-35532-y

Scharping, R. J., and Garey, J. R. (2021). Relationship between aquifer biofilms and unattached microbial indicators of urban groundwater contamination. *Mol. Ecol.* 30, 324–342. doi: 10.1111/mec.15713

Simon, K. S. (2019). "Cave ecosystems," in *Encyclopedia of caves*, 3rd Edn, eds W. B. White, D. C. Culver, and T. Pipan (Cambridge, MA: Academic Press), 223–226.

Simon, K. S., Pipan, T., and Culver, D. C. (2007). A conceptual model of the flow and distribution of organic carbon in caves. *J. Cave Karst Stud.* 69, 279–284.

Snider, J. R., Goin, C., Miller, R. V., Boston, P. J., and Northup, D. E. (2009). Ultraviolet radiation sensitivity in cave bacteria: Evidence of adaptation to the subsurface? *Int. J. Speleol.* 38, 11–22. doi: 10.5038/1827-806X.38.1.2

Sogin, E. M., Kleiner, M., Borowski, C., Gruber-Vodicka, H. R., and Dubilier, N. (2021). Life in the dark: Phylogenetic and physiological diversity of chemosynthetic symbioses. *Annu. Rev. Microbiol.* 75, 695–718. doi: 10.1146/annurev-micro-051021-123130

Taylor, M. L., Reyes-Montes, M. D. R., Estrada-Bárcenas, D. A., Zancopé-Oliveira, R. M., Rodríguez-Arellanes, G., and Ramírez, J. A. (2022). Considerations about the geographic distribution of Histoplasma species. *Appl. Environ. Microbiol.* 88:e0201021. doi: 10.1128/aem.02010-21

The Integrative Hmp (iHMP) Research Network Consortium (2019). The integrative human microbiome project. *Nature* 569, 641–648. doi: 10.1038/s41586-019-1238-8

Tomczyk-Żak, K., and Zielenkiewicz, U. (2016). Microbial diversity in caves. *Geomicrobiol. J.* 33, 20–38. doi: 10.1080/01490451.2014.1003341

Turrini, P., Tescari, M., Visaggio, D., Pirolo, M., Lugli, G. A., Ventura, M., et al. (2020). The microbial community of a biofilm lining the wall of a pristine cave in Western New Guinea. *Microbiol. Res.* 241:126584. doi: 10.1016/j.micres.2020.126584

van Spanning, R. J., Guan, Q., Melkonian, C., Gallant, J., Polerecky, L., Flot, J. F., et al. (2022). Methanotrophy by a *Mycobacterium* species that dominates a cave microbial ecosystem. *Nat. Microbiol.* 7, 2089–2100. doi: 10.1038/s41564-022-01252-3

Vanderwolf, K. J., Malloch, D., McAlpine, D. F., and Forbes, G. J. (2013). A world review of fungi, yeasts, and slime molds in caves. *Int. J. Speleol.* 42, 77–96. doi: 10.5038/1827-806X.42.1.9

Vardeh, D. P., Woodhouse, J. N., and Neilan, B. A. (2018). Microbial diversity of speleothems in two Southeast Australian limestone cave arches. *J. Cave Karst Stud.* 80, 121–132. doi: 10.4311/2017MB0119

Vos, M., Wolf, A. B., Jennings, S. J., and Kowalchuk, G. A. (2013). Micro-scale determinants of bacterial diversity in soil. *FEMS Microbiol. Rev.* 37, 936–954. doi: 10.1111/1574-6976.12023

Waite, D. W., Vanwonterghem, I., Rinke, C., Parks, D. H., Zhang, Y., Takai, K., et al. (2017). Comparative genomic analysis of the class Epsilonproteobacteria and proposed reclassification to Epsilonproteobacteria (phyl. nov.). *Front. Microbiol.* 8:682. doi: 10.3389/fmicb.2017.00682

Wang, D., Wang, Y., Liu, L., Chen, Y., Wang, C., Xu, X., et al. (2022). Niche differentiation and symbiotic association among ammonia/nitrite oxidizers in a full-scale rotating biological contactor. *Water Res.* 225:119137. doi: 10.1016/j.watres.2022.119137

Wang, X. W., Sun, Z., Jia, H., Michel-Mata, S., Angulo, M. T., Dai, L., et al. (2024). Identifying keystone species in microbial communities using deep learning. *Nat Ecol Evol.* 8, 22–31. doi: 10.1038/s41559-023-02250-2

Wang, Y., Zhao, Y., Bollas, A., Wang, Y., and Au, K. F. (2021). Nanopore sequencing technology, bioinformatics and applications. *Nat. Biotechnol.* 39, 1348–1365. doi: 10.1038/s41587-021-01108-x

Waring, C. L., Hankin, S. I., Griffith, D. W., Kertesz, M. A., Kobylski, V., Wilson, N. L., et al. (2017). Seasonal total methane depletion in limestone caves. *Sci. Rep.* 7:8314. doi: 10.1038/s41598-017-07769-6

Watson, T. H., and Baldini, J. U. L. (2024). Martian cave detection via machine learning coupled with visible light imagery. *Icarus* 411:115952. doi: 10.1016/j.icarus.2024.115952

Weinroth, M. D., Belk, A. D., Dean, C., Noyes, N., Dittoe, D. K., Rothrock, M. J., et al. (2022). Considerations and best practices in animal science 16S ribosomal RNA gene sequencing microbiome studies. *J. Anim. Sci.* 100:skab346. doi: 10.1093/jas/skab346

White, W. B., and Culver, D. C. (2019). "Cave, definition of," in *Encyclopedia of caves*, 3rd Edn, eds W. B. White, D. C. Culver, and T. Pipan (Cambridge, MA: Academic Press), 255–259.

Wiseschart, A., Mhuantong, W., Tangphatsornruang, S., Chantasingh, D., and Pootanakit, K. (2019). Shotgun metagenomic sequencing from Manao-Pee cave, Thailand, reveals insight into the microbial community structure and its metabolic potential. *BMC Microbiol.* 19:144. doi: 10.1186/s12866-019-1521-8

Wood-Charlson, E. M., Anubhav, K., Auberry, D., Blanco, H., Borkum, M. I., Corilo, Y. E., et al. (2020). The national microbiome data collaborative: Enabling microbiome science. *Nat. Rev. Microbiol.* 18, 313–314. doi: 10.1038/s41579-020-0377-0

Wu, Y., Tan, L., Liu, W., Wang, B., Wang, J., Cai, Y., et al. (2015). Profiling bacterial diversity in a limestone cave of the western Loess Plateau of China. *Front. Microbiol.* 6:244. doi: 10.3389/fmicb.2015.00244

Zada, S., Sajjad, W., Rafiq, M., Ali, S., Hu, Z., Wang, H., et al. (2022). Cave Microbes as a Potential Source of Drugs Development in the Modern Era. *Microb. Ecol.* 84, 676–687. doi: 10.1007/s00248-021-01889-3

Zerkle, A. L., Jones, D. S., Farquhar, J., and Macalady, J. L. (2016). Sulfur isotope values in the sulfidic Frasassi cave system, central Italy: A case study of a chemolithotrophic S-based ecosystem. *Geochim. Cosmochim. Acta* 173, 373–386. doi: 10.1016/j.gca.2015.10.028

Zhang, Y., Thompson, K. N., Branck, T., Yan, Y., Nguyen, L. H., Franzosa, E. A., et al. (2021). Metatranscriptomics for the human microbiome and microbial community functional profiling. *Annu. Rev. Biomed. Data Sci.* 4, 279–311. doi: 10.1146/annurev-biodatasci-031121-103035

Zhao, R., Wang, H., Yang, H., Yun, Y., and Barton, H. A. (2017). Ammonia-oxidizing *Archaea* dominate ammonia-oxidizing communities within alkaline cave sediments. *Geomicrobiol. J.* 34, 511–523. doi: 10.1080/01490451.2016.1225861

Zhu, H. Z., Jiang, C. Y., and Liu, S. J. (2022). Microbial roles in cave biogeochemical cycling. *Front. Microbiol.* 13:950005. doi: 10.3389/fmicb.2022.950005

Zhu, H. Z., Zhang, Z. F., Zhou, N., Jiang, C. Y., Wang, B. J., Cai, L., et al. (2021). Bacteria and metabolic potential in karst caves revealed by intensive bacterial cultivation and genome assembly. *Appl. Environ. Microbiol.* 87, e02440-20. doi: 10.1128/AEM.02440-20

Frontiers in Microbiology

Explores the habitable world and the potential of microbial life

The largest and most cited microbiology journal which advances our understanding of the role microbes play in addressing global challenges such as healthcare, food security, and climate change.

Discover the latest Research Topics

See more →

Frontiers

Avenue du Tribunal-Fédéral 34
1005 Lausanne, Switzerland
frontiersin.org

Contact us

+41 (0)21 510 17 00
frontiersin.org/about/contact